

Copyright Warning & Restrictions

The copyright law of the United States (Title 17, United States Code) governs the making of photocopies or other reproductions of copyrighted material.

Under certain conditions specified in the law, libraries and archives are authorized to furnish a photocopy or other reproduction. One of these specified conditions is that the photocopy or reproduction is not to be “used for any purpose other than private study, scholarship, or research.” If a user makes a request for, or later uses, a photocopy or reproduction for purposes in excess of “fair use” that user may be liable for copyright infringement,

This institution reserves the right to refuse to accept a copying order if, in its judgment, fulfillment of the order would involve violation of copyright law.

Please Note: The author retains the copyright while the New Jersey Institute of Technology reserves the right to distribute this thesis or dissertation

Printing note: If you do not wish to print this page, then select “Pages from: first page # to: last page #” on the print dialog screen

The Van Houten library has removed some of the personal information and all signatures from the approval page and biographical sketches of theses and dissertations in order to protect the identity of NJIT graduates and faculty.

BOND AND FATIGUE CHARACTERISTICS OF
HIGH STRENGTH CEMENT-BASED COMPOSITES

by

Somboon Chimamphant

Dissertation submitted to the Faculty of the Graduate School
of the New Jersey Institute of Technology in partial fulfillment
of the requirements for the degree of
Doctor of Engineering Science

1989

VITA

Name: Somboon Chimamphant

Degree and date to be conferred: D. Eng. Sc., 1989

<u>Collegiate institutions attended</u>	<u>Dates</u>	<u>Degree</u>	<u>Date of Degree</u>
New Jersey Institute of Technology	1985-1988	D.E.S.	1989
Asian Institute of Technology	1977-1978	M.Eng.	1978
Kasetsart University	1973-1976	B.S.C.E.	1976

Major: Civil Engineering

Positions held: 1985-1986 Research Assistant

1986-1988 Teaching Assistant

New Jersey Institute of Technology

Newark, New Jersey 07102

Publications:

1. S. Chimamphant, "Stress Analysis of the Anchorage Zone of the prestress concrete box girder by finite prism method", Master Thesis, Asian Institute of Technology, 1978.

2. M. Wecharatana and S. Chimamphant, "Bond Strength of Deformed Bars and Steel Fibers in High Strength Concrete", Materials Research Society, Symposium Proceedings, Vol.114, Bond in Cementitious Composites, Editors S. Mindess and S.P. Shah, Dec. 1987, pp. 245-254.

3. S. Chimamphant and M. Wecharatana, "Fatigue Characteristics of High Strength Cementitious Composites", The Second East Asia-Pacific Conference on Structural Engineering and Construction, Jan. 1989.

4. S. Chimamphant and M. Wecharatana, "Bond-Slip Characteristics of Reinforcement in High Strength Concrete", The Second East Asia-Pacific Conference on Structural Engineering and Construction, Jan. 1989.

5. M. Wecharatana, S. Chimamphant and C.C. Lin, "New Polymer Concrete for Marine Structures", The Second East Asia-Pacific Conference on Structural Engineering and Construction, Jan. 1989.

6. S. Chimamphant and M. Wecharatana, "Bond-Slip Characteristics of High Strength Fibrous Concrete", To be submitted for possible publication in Apr. 1989, ACI Journal.

ABSTRACT

Title of Dissertation: Bond and Fatigue Characteristics of
High Strength Cement-Based Composites

Somboon Chimamphant, Doctor of Engineering Science, 1989

Dissertation directed by: Dr. Methi Wecharatana, Associate Professor
of Civil Engineering

The results of a series of tests on a variety of high strength cementitious composites yield a model from which an empirical equation of general normalized pull-out stress vs. pull-out displacement relationship is developed. A new variable named the "Brittleness Index" is defined and used in the proposed equation. Additionally, the concept of maximum strain is used to predict the fatigue life of high strength concrete.

Three sizes of deformed bars and two types of steel fibers with four different volume fractions were used to observe bond-slip and pull-out characteristics of high strength concrete. The results indicate that the maximum slippage of deformed bars is only about 10 % of that observed in normal concrete. Consequently, the required development length may have to be longer for high strength concrete members as compared to normal concrete. For the fatigue characteristics study, standard 3x6 in. cylinders were tested at the rates of 6 and 12 Hz. in a closed-loop load-controlled system. The results show that as the compressive strength of the composites increases from 4000 to 11000 psi., the fatigue strength increases by 17 percents. The rate of loading does not significantly affect the S-N relationship, fatigue strength and fatigue limit of the high strength cement-based composites. The S-N curves of high strength concrete shows a faster decay rate than those of normal concrete. The maximum strain at any cycle under cyclic loading is always less than the maximum strain at failure under monotonic loading. Also observed is that the maximum strain-cycle relationship is linear. These results indicate that the design code for flexure of normal concrete cannot be applied to high strength concrete.

Blank Page

ACKNOWLEDGMENT

I like to express my deepest gratitude to my wife and friends for their support through this very difficult endeavor. I must make special thanks to my friend, Allyn Luke, who proofread this manuscript. I would also like to thank Prof. C.T. Thomas Hsu, Dr. F. Ansari, Dr. N. Meegoda, and Dr. S. Nanthavani, who served as members of the dissertation committee for their advice and criticism. Most of all, I would like to thank my advisor Dr. Methi Wecharatana for his vital counseling.

CONTENTS

I.	INTRODUCTION	1
1.1	General	1
1.2	Research Significance	3
II.	LITERATURE REVIEW	6
2.1	High Strength Concrete	6
2.2	Bond Characteristics	10
2.2.1	Steel Reinforced Concrete	10
2.2.2	Fiber Reinforced Concrete	13
2.3	Fatigue Characteristics	22
2.3.1	Cyclic Compression	23
2.3.2	Cyclic Tension	25
2.3.3	Reverse Loading	29
2.3.4	Factors Affecting Fatigue Characteristics	29
2.3.5	Fatigue on High Strength Concrete	33
III.	OBJECTIVE AND SCOPE OF WORK	36
3.1	Objective	36
3.1.1	Experimental Program	36
3.1.2	Empirical Modelling	43
3.2	Scope of Work	45
IV.	TESTING PROCEDURE	48
4.1	Material Compositions	48
4.2	Mix Proportions	48
4.3	Specimens	49
4.4	Specimen Casting	51
4.5	Test Setup and Procedure	52
4.5.1	Compression Test	52
4.5.2	Tension Test	53
4.5.3	Beam Test	54
4.5.4	Bond Strength Test	54
4.5.4.1	Bond Strength of Reinforced High Strength Concrete	54

4.5.4.2	Pull-Out Stress of High Strength Fibrous Concrete	55
4.5.5	Fatigue Test	55
V.	RESULTS AND DISCUSSION	60
5.1	Basic Properties of High Strength Concrete	60
5.1.1	Compressive Strength	60
5.1.2	Mode of Failure	64
5.1.3	Flexural Properties	66
5.1.4	Tensile Strength	69
5.2	Bond Strength-Slip Relationship	71
5.2.1	Reinforced High Strength Concrete	71
5.2.2	Fiber Reinforced High Strength Concrete	74
5.2.2.1	Load Displacement Relationship	74
5.2.2.2	Normalized Load Displacement Relationship ..	78
5.3	Fatigue Characteristics	80
5.3.1	S-N Curve	80
5.3.2	Fatigue Strength	82
5.3.3	Strain-Cycle Relationship	86
VI.	EMPIRICAL MODEL	89
6.1	Bond Strength Characteristic	89
6.1.1	Normalized Pull-Out Stress-Displacement Relationships	89
6.1.2	Brittleness Index	97
6.1.2.1	Brittleness Index Model	98
6.1.2.2	Statistical Analysis	99
6.2	Fatigue Characteristics	102
6.2.1	S-N Curve	102
6.2.2	Maximum Strain Concept	103
VII.	CONCLUSIONS	105
	FUTURE RESEARCH	108
	APPLICATIONS OF THE OBSERVED BEHAVIORS	109

BIBLIOGRAPHY	110
APPENDIX A	Uniaxial Compressive Stress vs. Strain Curves118
APPENDIX B	Flexural Stress vs. Deflection Curves155
APPENDIX C	Bond Strength vs. Slip Curves165
APPENDIX D	Pull-Out Stress vs. Displacement Curves of Concrete172
APPENDIX E	Bond Strength vs. Pull-Out Displacement Curves of High Strength fibrous Concrete178
APPENDIX F	Normalized Pull-Out Stress vs. Normalized Displace ment Curves of Concrete192
APPENDIX G	Normalized Bond Strength vs. Normalized Pull-Out Displacement Curves of HS. Fibrous Concrete197
APPENDIX H	Cyclic Compressive Stress vs. Strain Curves211
APPENDIX I	Normalized Cyclic Compressive Stress vs. Strain Curves240
APPENDIX J	Monotonic vs. Cyclic Compression Relationship265
APPENDIX K	Strain vs. Number of Loading Cycle Relationship	...271
APPENDIX L	Experimental Results290

LIST OF TABLES

Table	Page
II.1 Fatigue Load Spectrum	23
III.1 Bond Strength Test	46
III.2 Fatigue Test due to the Effect of Max. Stress Level	47
III.3 Fatigue Test due to the Effect of Rate of Loading	47
V.1 Compression Properties	62
V.2 Flexural Properties of High Strength Concrete	67
V.3 Direct Tension Properties of Cement-Based Composites	69
V.4 Bond Strength Properties of Reinforced High Strength Concrete	72
V.5 Bond Strength Properties of High Strength Fibrous Concrete	75
V.6 Number of Cycles to Failure under Repeated Load	83
VI.1 Brittleness Index of the Materials	92
VI.2 Brittleness Index (m) of the specimen from the Proposed Model	100
VI.3 Two-Factor Analysis of Variance	101
VI.4 Coefficients of A and B	102

LIST OF CHART

Chart	Page
I Scheme of Work	38

LIST OF FIGURES

Figure	Page
1.1 Stress vs. Strain Curve of High Strength Concrete	5
3.1 Direct Tension, Dog-Bone Specimen	37
3.2 Tapered Specimen	40
3.3 Dog-Bone Specimen	40
4.1 Friction Grips (T. Cintora [90])	50
4.2 Compression and Fatigue Test	57
4.3 Direct Tension Test, Tapered Specimen	57
4.4 Beam Test	58
4.5 Pull-Out Test (Bars #3, #4)	58
4.6 Pull-Out Test of Deformed Bar #6.....	59
5.1 Typical Stress vs. Strain Curves of Different High Strength Concrete compare with Normal Concrete	63
5.2 Stress vs. Strain Curves of Polymer Concrete due to the Effect of Curing Period	63
5.3 Comparison of Stress vs. Strain Curves of HSC between Closed-Loop Axial and Circumferential Strain Control	65
5.4 Comparison of Flexural Stress vs. Deflection of Different Beam Sizes of High Strength Concrete	68
5.5 Typical Tensile Stress vs. Displacement by Splitting Test Method	68
5.6 Comparison of Pull-Out Stress vs. Displacement Relationship of Cement-Based Composites	70
5.7 Bond-Slip Relationships of Deformed Bars under Pull-Out Test	73
5.8 Typical Pull-Out Stress vs. Displacement of High Strength Fibrous Concrete (Straight-End Fiber)	76
5.9 Typical Pull-Out Stress vs. Displacement of High Strength Fibrous Concrete (Hooked-End Fiber)	76

Figure	Page
5.10 Pull-Out Stress vs. Displacement of Different High Strength Concrete and High Strength Fibrous Concrete	77
5.11 Comparison of Normalized Pull-Out Stress vs. Displacement of Cement-Based Composites (Straight-End Fiber)	79
5.12 Comparison of Normalized Pull-Out Stress vs. Displacement of Cement-Based Composites (Hooked-End Fiber)	79
5.13 Comparison of the S-N Curves of different High Strength Concrete with Normal Concrete	81
5.14 Typical Stress vs. Strain Curve under Cyclic Compression Test of Superplasticizer Concrete	84
5.15 Typical Stress vs. Strain Curve under Cyclic Compression Test of Microsilica Concrete (6 Hz)	84
5.16 Typical Stress vs. Strain Curve under Cyclic Compression Test of Microsilica Concrete (12 Hz)	85
5.17 Typical Stress vs. Strain Curve under Cyclic Compression Test of Polymer Concrete	85
5.18 Typical Peak Strain vs. No. of Cycles of different High Strength Cement-Based Composites	88
5.19 Typical Monotonic vs. Cyclic Loading Relationship of High Strength Concrete	88
6.1 Maximum Pull-Out Displacement vs. Average Grain Size of sand	91
6.2 Comparison of the Proposed Equation with Normal Concrete Data (T. Cintora [90])	93
6.3 Comparison of the Proposed Equation with High Strength Concrete Data (Present Study)	93
6.4 Comparison of the Proposed Equation with Polymer Concrete Data (Present Study)	94
6.5 Comparison of the Proposed Equation with Normal Fibrous Concrete Data (Shah et.al. and Naaman et.al.) . . .	94
6.6 Comparison of the Proposed Equation with Normal Fibrous Concrete Equation (M. Wecharatana [19])	95
6.7 Comparison of the Proposed Equation with High Strength Fibrous Concrete (Straight-End Fiber)	95

Figure	Page
6.8 Comparison of the Proposed Equation with High Strength Fibrous Concrete (Hooked-End Fiber)	96
6.9 Normalized Pull-Out Stress vs. Displacement Curves of Cement-Based Composites from the Proposed Equation	96
6.10 Brittleness Index Model	98
6.11 Typical Peak Strain vs. No. of Loading Cycles Curve of Superplasticizer Concrete	104
6.12 Typical Peak Strain vs. No. of Loading Cycles Curve of Microsilica Concrete	104

CHAPTER I

INTRODUCTION

1.1 General

High strength concrete has gradually been developed over many years. Recently the method of making high strength concrete has been simplified by the simple addition of microsilica, fly ash, polymer and other types of additives. This has made production of high strength concrete less expensive and easier, therefore the applications of high strength concrete have increased.

Definitions of high strength concrete have been made by many investigators [1-5]. The definition is generally accepted and adopted by ACI Committee 363-High Strength Concrete which defined high strength concrete with specified compressive strength for design of 6,000 psi (41 MPa) or greater. A typical stress-strain curve of high strength concrete reported by Shah, et.al. [6] is shown in Fig.1.1. As the use of high strength concrete increases, the need to clearly understand its properties is obvious. Some properties of high strength concrete such as compressive strength (f'_c), modulus of elasticity (E_c) and modulus of rupture (f_r) have been investigated and reported recently, many remain unspecified.

Bond strength between concrete and reinforcing bar and the bond stress-slip relationship are among the most fundamental properties of reinforced concrete needed for design. One of the purposes of understanding bond strength properties of reinforced concrete is to properly specify the required embedment length of steel and the concrete cover. Most investigations [7-11] which study the bond-slip characteristics were mostly conducted on normal reinforced concrete. None of them is on reinforced high strength cementitious composites. Although a lot of bond stress-slip tests have been conducted, no statistically dependable curve has ever been developed because of large scatter of data. These variations are primarily due to many factors

such as concrete mix proportions, consistency of the mix, type of steel bars, testing machine, method of testing and slippage measurement, etc.

The pull-out stress characteristic of steel fiber in cement matrix is also an important property of fiber reinforced concrete. It determines the deformability, strength and toughness of the composite. The pull-out stress properties of fiber reinforced concrete are influenced by numerous factors, such as, fiber aspect ratio, strength and shape of the fibers, fiber length and the mix proportion of the matrix. Many investigators have studied the pull-out stress-slip relationship of steel fiber reinforced concrete [12-19]. All of these studies were on normal fibrous concrete, none of them was on high strength fibrous concrete. From the pull-out studies of normal fibrous concrete, Visalvanich and Naaman [17] and Wecharatana and Shah [19] found an interesting unique normalized stress-pull-out displacement relationship. This relationship can predict the pull-out stress or the pull-out displacement of the composite independent of the fiber volume fraction and aspect ratio (dia./length) in the composite.

Another important material property of high strength concrete that needs to be investigated is the fatigue characteristic. The process of progressive and irreversible deterioration in a material subjected to repetitive stresses is called fatigue. Fatigue is always described by a parameter termed fatigue life which essentially represents the number of cycles needed to fail the material under a given repetitive load. It is generally agreed that the relative magnitude of the stress change under load is the most important variable that influences fatigue life. Other factors such as maximum stress level, rate of loading, etc. also affect the fatigue life. Fatigue properties are essential to the design of structures under cyclic loading. These structures are railway and highway bridges, airport pavements, marine structures and mass transit system. There are three different types of fatigue behavior; cyclic compression, cyclic tension and reverse loading. Many researchers [20-35] have studied the fatigue properties of cyclic compression [20-27], cyclic tension [28-34] and a few on reversed loading [35]. Most of these studies [20-35] are conducted on normal concrete, the

fatigue behavior on high strength concrete has never been cited in the literature.

It is the objective of this investigation to provide experimental data on these needed and unavailable material properties such as bond and fatigue characteristics of high strength cement-based composite. Empirical modelling of these observed behaviors will also be developed during the course of this studies.

1.2 Research Significance

The significance of this research can be categorized into seven different areas as follows :

1. At present high strength concrete is a new and useful material widely used in many countries. Basic properties such as compressive strength (f'_c), tensile strength, modulus of elasticity (E_c) and modulus of rupture (f_r) of high strength concrete have been investigated by many investigators while some other properties like bond strength of reinforcing bars, fibers and aggregate in high strength concrete as well as fatigue characteristics have not yet been studied. For structures using high strength concrete, these two properties, bond and fatigue, play an important role in engineering design in defining the steel embedment length, concrete cover and load factor for fatigue design. These needed properties will be experimentally observed in this study.

2. The use of high strength concrete together with refined design procedures have resulted in slender structures. Thus the bond strength between reinforcing steel and high strength concrete and the amount of concrete cover are critical. When the structure is slender, the dead load represents a smaller part of the total load, thus the fatigue problem will play an important role in the structure design. As high strength concrete is more widely used, these properties need to be clarified.

3. Marine structures are frequently subjected to fatigue and dynamic loadings. Use of high strength impervious polymer concrete and other high strength cementitious composites is often encountered. There is a need to understand the fatigue characteristics of these new high strength materials so that these marine structures can be properly designed.

4. For a general cementitious composites, there is a brittleness number which can be used to predict the properties of a cement-based composites. The more brittle the material is, the lower the value of the brittleness index. In this study, the brittleness index is proposed in the general normalized pull-out stress-displacement relationship. This brittleness index can be used to predict the softening response of a cementitious composite without conducting the direct tension test.

5. A general, unique normalized post-peak pull-out stress - displacement equation of the cemented composites is proposed in terms of the brittleness index as follows:

$$\left[\frac{\tau}{\tau_{\max}} \right]^m + \left[\frac{\delta}{\delta_{\max}} \right]^{2m} = 1 \quad (1.1)$$

where :

- τ = Post-peak pull-out stress
- τ_{\max} = Maximum pull-out stress of the cemented composite
(Max. post-peak pull-out stress for fibrous conc.)
- δ = Post-peak pull-out displacement
- δ_{\max} = Maximum pull-out displacement of the cemented composite (Half the fiber length for fibrous concrete)
- m = Brittleness index of the composite

6. The S-N curve of high strength concrete which is one of the most important properties for fatigue design is investigated. These S-N curves are used to predict the serviceability of structures.

Stress vs. Strain Curve

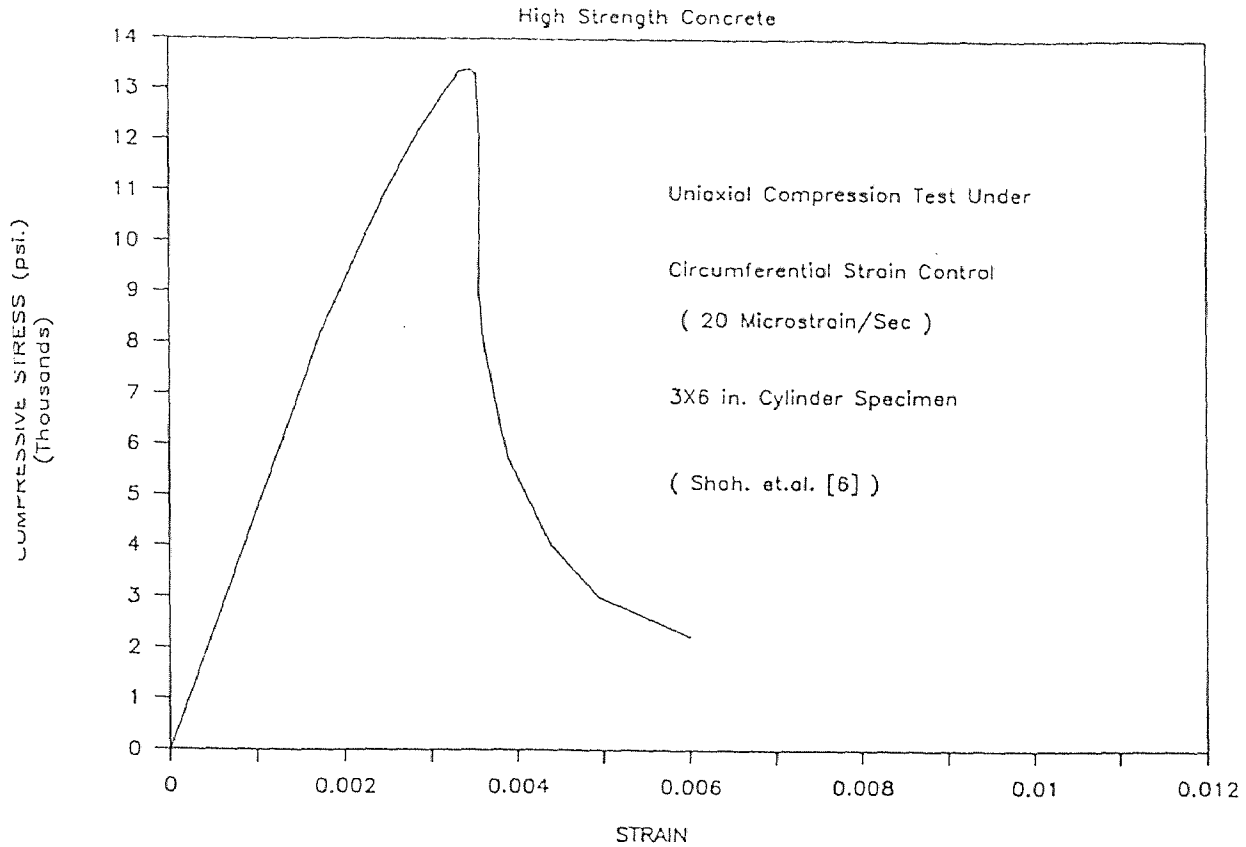


Fig. 1.1 Stress vs. Strain Curve of High Strength Concrete

7. The Maximum strain concept of high strength cementitious composite is developed to predict the fatigue life. It is believed that for any cementitious materials under different loading conditions, the material can sustain only up to a given magnitude of strain. Beyond that abrupt failure may occur. Knowing the maximum strain of the concrete used together with the existing condition, the fatigue life can then be predicted.

CHAPTER II

LITERATURE REVIEW

2.1 High Strength Concrete

High strength concrete has gradually been developed over the past few decades. As the development continues, the definition of high strength concrete has changed. In recent years, the applications of high strength concrete have increased and is presently used in many countries all over the world.

The definition of high strength concrete was given by many investigators [1-5]. V.V. Bertero [1] defined the definition of high strength concrete as concrete with compressive strength higher than 6,000 psi for normal weight concrete and higher than 4,000 psi for light weight concrete. John Albinger and Jaime Moreno [2] also defined high strength concrete as concrete with compressive strength between 6,000-11,000 psi for normal weight concrete and from 5,000-8,000 psi for light weight concrete at 56 days. Merlin D. Copen [3] assumed high strength concrete to be concrete with compressive strength of 10,000 psi (700 kgf/cm^2) or greater at 1 year of age. Saucier [4] classified high strength concrete into three categories, (1) the present range of 5,000-10,000 psi ($35-70 \text{ MN/m}^2$), (2) the available range of 10,000-15,000 psi ($70-105 \text{ MN/m}^2$) and (3) the exotic area of 15,000 psi (105 MN/m^2). These definitions and categories are generally accepted and have been adopted by ACI Committee 363-High Strength Concrete [5] which defined high strength concrete as concrete with specified compressive strength for design of 6,000 psi (41 MPa) or greater.

Many attempts to make and to properly proportion the matrix compositions and admixtures in order to achieve high strength concrete by many researchers have been successfully made in recent year [36-43]. Katharine Mather [37] produced high strength concrete by using high density materials. She used magnetite aggregate and ilmenite aggregate

whose unit weight is about 230 lb per cu.ft. instead of normal crushed limestone aggregate. The compressive strength gained was 9,000 psi at 7 days and 11,000 psi at 28 days. Cameron Macinnis and Donald V. Thomson [40] have proposed special technique for achieving high compressive strength concrete by using high speed slurry mixing, seeding and revibration together with two addition admixtures (fly ash and lignosulfonic acid water reducing agent). The compressive strength gained was in the range of 6,000-11000 psi (420-770 ksc.). Another method to produce high compressive strength concrete is to use ultra fine cement as studied by Ramnath N. Swamy [41]. By using ultra fine cement and limestone aggregate with the mix proportion of 1 : 1 : 3 (ultra cement : sand : aggregate) and water/cement = 0.35, the compressive strength was reported to be 12,600 psi in 28 days.

The most common practice for making high strength concrete is the addition of microsilica, fly ash, and superplasticizer to normal concrete. These methods were investigated by E.J. Sellevold and F.F. Radjy [42], and G. Carrette and V.M. Malhotra [43]. They reported that the efficiency of the microsilica in producing compressive strength was 2 to 4 times greater than cement. Adding 10 % of silicafume with sufficient water reducing agent to make water/cement ratio equal 0.42 in the mix, increased concrete strength by 50 %.

Due to the increasing use of high strength concrete, it is necessary to know the material properties and structural behavior of high strength concrete. Most basic properties needed for structural design such as compressive strength (f'_c), tensile strength, modulus of elasticity (E_c), modulus of rupture (f_r), creep, shrinkage, shear stress, deflection, porosity and stress-strain curve of high strength concrete have already been reported in the literatures [44-56], but some have yet to be thoroughly investigated. The bond strength of steel and fiber in high strength concrete as well as fatigue characteristics have not yet been studied.

The mode of failure of high strength concrete is totally different from normal concrete. Normal concrete will gradually fail after it

reaches the peak load while high strength concrete will suddenly explode at the peak load. Possibly because high strength concrete is more brittle than normal concrete and the descending part of the stress-strain curve is very steep. Therefore the descending part of the stress-strain curve of high strength concrete under uniaxial compression can not be ascertained from a conventional testing system (except for polymer high strength concrete of which the descending part can be obtained due to its plasticity). Both the ascending and the descending parts of the stress-strain curve are very important and necessary for engineering analysis and design. So far only one report on the complete stress-strain curve of the high strength concrete by S.P. Shah, Ulker Gokoz and Farhad Ansari [6] has been cited in the literature. They conducted the uniaxial compression test on three specimen sizes; 3x6, 4x8, 3x9 in. (75x150, 100x200 and 75x225 mm) at two strain rates. Instead of using a highly stiffened testing machine to get the complete stress-strain curve as mentioned by Hudson, J.A., Crouch, S.L., and Fairhurst, C. [57], they used a servo-controlled closed-looped testing machine and controlled the test by circumferential strain. With this method, they obtained the complete stress-strain curve as shown in Fig.1.1.

Another type of well known high strength concrete is polymer concrete. Polymer concrete is a new material which has been developed over the last few decades. The general properties of polymer concrete are different from normal concrete and other types of high strength concrete. Deformations and deflections of polymer concrete under load are much larger than normal concrete and high strength concrete while its modulus of elasticity is less. The mode of failure of polymer concrete is the same as normal concrete but different from high strength concrete which tends to explode at the peak load.

There are many methods of making polymer concrete. The properties of polymer concrete differ according to the mix proportion, materials used, curing condition, ages, etc. So far there is no standard mix proportion for polymer concrete.

Polymer concrete is normally made by adding plastic chemicals such as monomer and catalyst or hardener to normal concrete. These chemicals form plastic links binding coarse and fine aggregates together. This chemical process so-called polymerization creates a stronger bond and results in a stronger matrix than conventional concrete. Depending on the amount of polymer added, the strength of polymer concrete is partly generated from polymerization process and partially from the hydration process of cement.

Although there are many mix proportions of polymer concrete, the mechanical properties of these polymer concrete are effected by the same factors such as temperature, curing condition, type of polymer, etc. The compressive and flexural strength of dry-cured specimen are higher than the wet-cured one. Similar improvements are also observed for sulfate resisting properties as well. The durability and energy absorption of the dry-cured polymer concrete is higher than for wet-cured. However, the compressive strength, flexural strength and modulus of elasticity decreased when the testing temperature increased as mentioned by M.U. Haddad, D.W. Fowler and D.R. Paul [58] and S.A. Trondistou-Yannas and S.P. Shah [59].

Applications of polymer concrete so far have been limited to small projects like pavement and bridge deck repairs and overlays. This is mainly because polymer concrete is too expensive to be used in construction projects. The cost of polymer concrete is directly proportional to the amount of polymer added. In general, the cost of polymer concrete is ranging between \$ 1.50 to \$ 2.00 per pound.

In order to expand the applications of polymer concrete, Wecharatana M. and Lin C.C. [60] studied and developed a new polymer concrete, especially for marine structures. Many trial mix proportions were made in order to achieve a high compressive strength, flexural strength, and chemical resistance at a lesser cost.

Because marine structures are frequently subjected not only to static load and chemical attack from sulphates and chlorides in the sea

water, but also dynamic and fatigue loadings. Therefore in this paper, an attempt will be made to study the flexural strength as well as fatigue characteristics of this new polymer concrete.

2.2 Bond Characteristics

2.2.1 Steel Reinforced Concrete

The bond strength between concrete and the reinforcing steel and the bond stress-slip relationships are among the most fundamental problems of steel reinforced concrete. In the past, many researchers [7-11] investigated the bond-slip characteristic. Most of these investigations were on normal reinforced concrete. None of them were on reinforced high strength concrete. Although a lot of bond stress-slip tests were conducted no statistically dependable curves have been developed because of large scatter of data. These variations were the effects of many factors such as concrete mix proportion, consistency of the mix, steel bar, testing machine, method of testing and slippage measurement, etc.

The pull-out test, mentioned by Martin [7], Windisch [8] and recommended by RILEM/CEB/FIP [9], is one of the most simplest reproducible instructive bond test. In studying the bond performance of Ribbed Bars with different water cement ratios, consistencies and grading curves, Martin [7] found that the bond strength of Ribbed Bars could differ by more than 100 %. The relation between tensile splitting strength and cube compressive strength was $f_{c,t} = 0.222 (f_{\text{cube}})^{2/3}$, whereas the relation between tensile bending strength and compressive strength was $f_{c,t} = 0.35 (f_{\text{cube}})^{2/3}$. The maximum bond factor (bond stress/cube strength) was about 0.55 with bond slip between 1-2 mm.

From pull-out tests, Windisch [8] found that the loaded end slips were significantly greater than the slip measured at the unloaded end of the bond length, primarily in the case of larger diameters (\emptyset 16mm) with greater relative rib areas. The unloaded end slip alone did not give the proper slip-distribution along the bond length. He also

observed that the bond stress-slip diagrams derived from the pull-out test and the beam test could not be the same, even if all other influencing factors were similar.

A.D. Edwards and P.J. Yannopoulos [10] studied the bond stress-slip characteristics in reinforced concrete by using 16 mm. diameter hot rolled deformed bars and mild steel plain bars with 32 and 25 mm. concrete cover and 4 times the welbond deformed bar slug spacing which is 38 mm. for embedment. Concrete cube strength at 28 days was 6293 psi (43.4 N/mm²). Two types of test were conducted , one with the bottom end of the reinforcing bar free, and the other with a constant back load applied at the bottom end of the bar. He found that maximum bond stress developed by plain bars (600 psi) was about 35-50 % of that of the corresponding deformed bar (1500 psi) and the slips at maximum stress were 0.01-0.06 mm. for plain bars and 0.10-0.30 mm. for deformed bars. The maximum bond stress increased with increasing concrete cover and the direction of bar pulled to the direction of concrete casting. He also reported that the maximum bond stress was not significantly affected by the bar back load.

Saeed M. Mirza and Jules Houde [11] conducted the bond stress-slip tests on 62 concentric tension specimens with different bar sizes, some of the specimens were internally instrumented. They observed that the slip increased linearly with stress in the steel, specimen dimensions up to a certain size, and the ratio of concrete to steel area (A_c/A_s) up to a value of 45 to 60. Concrete strength between 3,000 and 5,000 psi had an insignificant effect on the slip value which averaged 28.6×10^{-4} in. The steel stress at the end face was almost equal to the free bar stress. From this experiment they proposed the following slip vs. steel stress equation :

$$\text{Slip} = k_1 f_s^{k_2} \left(\frac{A_c}{A_s} \right)^{k_3} \quad (2.1)$$

where : k_1, k_2, k_3 are constants. ($k_2=1$)

And the bond stress-slip equation is

$$U = 1.95 \times 10^6 d - 2.35 \times 10^9 d^2 + 1.39 \times 10^{12} d^3 - 0.33 \times 10^{15} d^4 \quad (2.2)$$

where :

U = bond stress

d = local slip

There are also other factors that affect the bond strength of reinforced concrete, most of which have already been studied. For example, the effects of high range water reducers on bond strength was studied by Barie B. Brettman, David Darwin, and Rex C. Donahey [61]. The effects of temperature [62-65], cyclic, impact and sustained loadings [66-70] have also been investigated.

The effects of cyclic loading was studied by N.M. Hawkin, I.J. Lin and F.L. Jeang [66]. They conducted tests on 30 reinforced concrete blocks with different types and sizes of bars, under monotonic and cyclic loadings. They observed that the maximum bond stress was affected by the embedment length, and it increased almost proportionally to the concrete compressive strength until upto 4900 psi (34 N/mm²) for monotonic loading. For cyclic loading, the bond effectiveness at the maximum capacity is less than for monotonic loading with the decrease in capacity being greater for fully reversed cyclic loading than for zero to a maximum cyclic loading. To model the bond stress-slip of reinforced concrete, they found that it comprised of 3 steps, i.e., uncracked response stage, internal cracked response stage and sliding shear response stage. They also proposed the bond stress-slip equations for both monotonic and cyclic loading.

To analyse the bond stress-slip relationships of reinforced concrete by finite element method, a special element between steel and concrete is required. Many investigators have proposed different approaches about this element. Ngo and Scordeles proposed this element as the bond-link that had no physical dimensions. Hoshiro and Schafer gave a continuous connection between two elements by using a linear or higher-order displacement field. Dinges modified and gave a more general version of this element by taking into account normal stresses

between concrete and reinforcement. To obtain an accurate model of bond-stress slip relationship of reinforced concrete, Manfred Keuser and Gerhard Mehlhorn [71] not only considered these general functions mentioned above but also local factors such as position of bar during casting of concrete, direction of casting and slip.

In developing the design criteria of bond in reinforced concrete, Emory L. Kemp [72] tested 157 stub cantilever specimens. From the test results and the assumptions that the entire tensile force in the bar was transferred to concrete through the lugs, the radial bursting stress (P_r) was proportional to the bond stress. And the splitting of the concrete was caused by the radial bursting stress. He then developed the ultimate bond strength equation as :

$$(F_b)_{ult} = 232 + 2.72\left(\frac{C_{bs}}{Dia}\right)\sqrt{f'_c} + 0.201\left(\frac{A_{sst} \cdot f_{yst}}{S_p \cdot Dia}\right) + 195(I_{aux}) - 21.2(F_d N)^{0.66} \quad (2.3)$$

where :

- $(F_b)_{ult}$ = ultimate bond stress
- A_{sst} = area of transverse reinforcement (in^2)
- C_{bs} = the smallest of clear bottom cover, clear side cover and half the clear spacing between two adjacent bars (in.)
- Dia = diameter of the test bars (in.)
- f'_c = concrete cylinder compressive strength (psi)
- F_d = dowel force per bar (kip/bar)
- f_y = yield strength for test bars (psi)
- f_{yst} = yield strength for transverse reinforcement (psi)
- I_{aux} = parameter for auxilliary reinforcement
- S_p = center to center spacing between two adjacent transverse reinforcement (in.)
- N = number of bars

2.2.2 Fiber Reinforced Concrete

Fiber reinforced concrete is a new material which has developed

over the past few decades into one of the most useful materials in civil engineering. The added fibers are generally known to arrest cracks, increase ductility and energy absorption. Many researchers [12-19] have experimentally studied as well as analytically modeled the pull-out stress-slip relationship of steel fiber reinforced concrete. Most of these studies only emphasized on normal concrete, none of them were on high strength concrete. The steel fiber makes up for the weakness of the concrete under tensile stresses. The stresses at the interface are transmitted from matrix to the individual fibers or vice-versa, through the bond at the interface.

The fiber-matrix interfacial bond is one of the basic factors deciding the deformability, strength and toughness of a composite material. The bond strength properties of fiber reinforced concrete are generally influenced by many parameters, such as fiber diameter, strength and shape of the fibers, fiber length, aspect ratio, the mix proportions, curing conditions, age of the specimens and etc. [12-17].

A.E. Naaman and S.P. Shah [12] studied the pull-out behavior of steel fiber reinforced concrete with different inclination of fibers, the loading condition, the number of fibers, and the efficiency of the random orientation. They conducted three series of pull-out tests using different fiber diameters of 0.016 in. (0.4 mm.), 0.01 in. (0.25 mm.), and 0.006 in. (0.15 mm.). Each pull-out test consisted of pulling out two fibers symmetrically oriented with respect to the loading direction at angles of orientation of 0, 15, 30, 45, 60, 75 degrees. The fibers had a smooth surface and the embedment length was set for 0.5 in. (13 mm.). The fibers with the diameter of 0.01 in. was a brass coated surface while the other two were high strength music wires. They found that the bond efficiency of inclined fibers was essentially the same or better than that of parallel fibers. The final load (the load prior to the complete pull-out test) was zero for the parallel fibers while the final load for the inclined fibers increased with the angle of inclination and could be as high as the corresponding peak load. The final pull-out distance was equal to the embedment length for the parallel fibers while it might be less than the embedment length for

the inclined fibers. The work required to completely pull-out an inclined fiber was higher than that for a parallel fiber. The final pull-out load was zero for parallel fibers while for inclined fibers, the final load increased with the increasing angle of orientation. No significant effect on the peak pull-out load or the final pull-out distance was observed for an increase in number of fibers from 2 sq in. - 36 sq in. when fibers aligned parallel to the direction of loading. But for the inclined fibers, the peak pull-out load, the final load, the final pull-out distance and the total pull-out work decreased with an increasing number of fibers. The efficiency ratio, defined as the ratio of modulus of rupture of the randomly oriented fibers to that of parallel fibers decreased when the volume fraction of fibers increased.

The bond strength properties due to the effect of vibration, shape of fibers, strength of the matrix and the fiber volume fraction were studied by A. Burakiewicz [13]. He used mortar with water/cement ratio of 0.55, hooked end ($\emptyset 0.4 \times 30$ mm.) and round straight fibers ($\emptyset 0.38 \times 25$ and $\emptyset 0.30 \times 25$ mm.). He conducted the pull-out tests on a single fiber as well as groups of fibers embeded in the matrix. He observed that the shape of the load-displacement curve depended on the fiber type. The pull-out of hooked end indented fibers required more energy than plain fibers. The bond strength increased with the strength of the matrix and the fiber volume content in the matrix which was different from Naaman and Shah [12]. He also concluded that there was no significant influence on the bond strength due to the vibration and orientation of fibers during setting and hardening of the matrix.

To develop the bond stress of steel fiber reinforced matrix, D.J. Pinchin and D. Tabor [14] tested cylinder specimens of 3.42 cm. diameter and 3.05 cm. in length with a centrally embedded wire while applying a radial compressive force on a specimen. The wire was loaded with no pressure applied to the specimen until debonding. Pressure was applied either immediately subsequent to the debonding of the embedded wire or after a cross head movement of 1.00 mm. The pressure was applied in 4 stages , 7.5, 14.5, 21.5, and 28.5 N/mm^2 . From this tests,

they observed that the radial compressive force produced an increase in fiber-matrix contact pressure and fractional stress transfer. The compaction of the concrete near the wire would increase the frictional bond. The pull-out load increased linearly with the confinement. The pull-out load in the wire was found to be relative to the geometry and material properties of the specimen and also to the wire-matrix misfit. The wire-matrix misfit was the difference between the radius of the wire and the radius of the hole in the matrix in the absence of wire. This misfit, he said, could be produced by shrinkage of the matrix or an applied pressure on the specimen.

R.J. Gray and C.D. Johnson [15] studied the interfacial bond strength in steel-reinforced cementitious composites by pulling a single concentric fiber from a block of matrix immersed in water. They found that the direction of casting affected the bond strength. Horizontally cast specimens developed lower bond strength than vertically cast specimens. The average interfacial bond strength increased slightly with an increase in the rate the fiber is withdrawn. An increase in the sand cement ratio of the mortar matrix has contrasting effects on the strength of the interfacial bond in both vertically and horizontally cast specimens. The interfacial bond strength decreased for the vertically cast specimens while it increased for the horizontally cast specimens.

Magne Maage [16] observed that the bond properties between steel fibers and cement based matrices were of a mechanical nature where the anchoring effect was more important than the adhesive effect. He also stated that the mean pull-out load per fiber was unaffected by the number of fibers, which is in agreement with similar tests reported by A.E. Naaman and S.P. Shah [12].

The fracture characteristics of steel fiber reinforced cementitious composites was investigated by K. Visalvanich and A.E. Naaman [17]. They conducted tests on the 32 double cantilever beam specimens and 80 tensile prisms of fiber reinforced mortar, concrete and asbestos cement. Straight cut, brass-coated steel fibers were used

with three different lengths of 0.25, 0.50 and 0.75 in. and the corresponding aspect ratio (length/diameter) of 42, 83 and 47. Three different volume fractions of fibers of 0.5, 1.0 and 2.0 % were used to study the effect of fiber content. By conducting direct tensile test, they found that the maximum post cracking stress of steel fiber reinforced mortar could be expressed in terms of the fiber reinforcing index ($V_f l / \phi$) as $\bar{\sigma} = \alpha \tau V_f l / \phi$. From this analytical relationship, they proposed the normalized σ - δ law which is independent of the steel volume fraction, aspect ratio, and length of the steel fiber in the polynomial form as :

$$\frac{\sigma}{\alpha \tau V_f (l/\phi)} = \left[0.1 \left[\frac{2\delta}{l} \right] + 1 \right] \left[\left[\frac{2\delta}{l} \right] - 1 \right]^2 \quad (2.4)$$

where :

σ = post-cracking stress

δ = displacement

τ = interfacial bond strength

α = efficiency factor ($\alpha \tau = 660$ psi)

l = fiber length

V_f = percent fiber volume fraction of cement

ϕ = fiber diameter

Whereas the proposed normalized σ - δ law for plain concrete is

$$\sigma = \bar{\sigma} \left[\frac{\delta}{\bar{\delta}} - 1 \right]^2 \left[5 \left(\frac{\delta}{\bar{\delta}} \right)^2 - 4 \left(\frac{\delta}{\bar{\delta}} \right) + 1 \right] \quad (2.5)$$

where :

$\bar{\sigma}$ = maximum post-cracking stress

$\bar{\delta}$ = maximum displacement (half fiber length)

These two equations can predict any stress-displacement response of fiber reinforced mortar and plain concrete under uniaxial tension.

Base on these σ - δ laws, they proposed the fracture energy of the steel fiber reinforced mortar as

$$G_a = \alpha \tau V_f \cdot \frac{1}{\phi} \cdot \beta C^n \left[1 - 1.9 \left(\frac{\beta C^n}{1} \right) + 1.067 \left(\frac{\beta C^n}{1} \right)^2 + 0.2 \left(\frac{\beta C^n}{1} \right)^3 \right] \leq G_c \quad (2.6)$$

where :

$$G_c = 0.171 \alpha \tau V_f \frac{1}{\phi} l^2$$

G_a = energy per unit crack extension during the slow crack growth process

G_c = steady state fracture energy

Vellore S. Gopalaratnum and S.P. Shah [18] studied and proposed a theoretical model for the stress distribution in fiber reinforced concrete. They conducted experiments with several mixes of concrete, mortar and paste. Fiber reinforced mortar with 3/16 in. (5.0 mm.) maximum aggregate size and three fiber volume fractions of 0.5, 1.0 and 1.5 % were selected. Smooth brass-coated steel fibers of 1.0 in. long and 0.016 in. diameter (25x0.44 mm.) with the aspect ratio of 62.5 were used. The tension specimen were 3 in. wide (76 mm.), 12 in. long (305 mm.) and 3/4 in. (19 mm.) thick. The direct tension test were conducted with the loading rate of 1 μ strain/sec. and tested up to a maximum displacement of 7,000 μ in (178 μ m).

Concrete, mortar and paste specimens exhibited linear elastic behavior up to about 50 % of their tensile strengths. Increase in composite strength was linearly related to the fiber content. Fibrous composites absorbed 500 % more fracture energy than a plain concrete matrix.

By the assumptions that all nonlinearities in the composite occurred along two localized zones of cracking, namely interfacial debonding process and transverse matrix crack, the fiber and the matrix behaved elastically and the interface transferred the load through the matrix without yielding or slip, they proposed the theoretical model to predict the load on fibers under pull-out condition as :

$$P = \left[\frac{\frac{2\pi r \tau_s}{\beta} \sinh \frac{\beta m l}{2} + \pi r l_i \tau (1-m) \cosh \frac{\beta m l}{2}}{(1 - \alpha) \cosh \frac{\beta m l}{2} + \alpha} \right] \quad (2.7)$$

and the fiber slip Δ as :

$$\Delta = U_f\left(\frac{1}{2}\right) = \left[\frac{\int_0^{m_{cr} \frac{1}{2}} F(x) dx + \int_{m_{cr} \frac{1}{2}}^{\frac{1}{2}} F(x) dx}{A_f \cdot E_f} \right] \quad (2.8)$$

The proposed effective crack width, ω was

$$\omega = 2 \left[\Delta - \frac{l \sigma_p e^{-k\omega^\lambda}}{2E_m} \right] \quad (2.9)$$

and the matrix stress could be determined from :

$$\sigma_c = \sigma (1 - NA_f) + PN \quad (2.10)$$

This theoretical model gave favorite results when compared with the experimental data.

M. Wecharatana and S.P. Shah [19] studied the fracture toughness of fiber reinforced concrete and proposed a theoretical model based on the concept of nonlinear fracture mechanics to predict resistance provided by the fiber against the fracture of matrix. The matrix mix-proportion used in their study was 1 : 2 : 0.5 (cement:sand:water). Straight cut brass coated steel fiber with specific gravity of 490 lb/ft³ were used. Three different volume fraction of fibers, 0.5, 1.0 and 2.0 % were selected. Two different sizes of fibers, 0.25 in. long with 0.006 in. diameter and 0.75 in. long with 0.016 in. diameter were used. With the assumption that the maximum post-cracking strength

occurs at the end of the matrix process zone or the beginning of the fiber bridging zone, and smoothly decreases to zero as the crack surfaces displacement reaches half of the fiber length, they proposed the normalized stress-displacement relationships as :

$$\frac{\sigma}{\sigma_{\max}} = \left[1 - \frac{\eta}{\eta_{\max}^f} \right]^2 \quad (2.11)$$

where :

- σ is the post cracking strength
- σ_{\max} is the maximum post-cracking strength
- η is the post-peak pull-out displacement
- η_{\max}^f is the maximum pull-out displacement of fibers

They also proposed stress-displacement relationship for other types of fiber reinforced composites as :

$$\frac{\sigma}{\sigma_{\max}} = \left[1 - \frac{\eta}{\eta_{\max}^f} \right]^2 e^{-m \left\{ \frac{\eta}{\eta_{\max}^f} \right\}^n} \quad (2.12)$$

Where m and n are constants which depend on the type and the pull-out behavior of fiber. This proposed equation is matched very well with the experiment data reported by other researchers (S.P. Shah, A.E. Naaman and K. Visavanich).

To analyse the theoretical model of bond at the interface between steel fibers and cementitious composites, George Nammur Jr. and A.E. Naaman [73] assumed that the fibers are aligned squarely within the specimen. Each individual fiber along with its share of matrix acts and behaves independently of other fibers and the rest of the matrix body. They also assumed that the bond slip relationship is a material property (location independent). In the pre-cracking stage, the maximum shear stress occurred at both ends of the fibers when the

elastic shear bond was intact. The stresses were transferred from the matrix to the fibers. In the post-cracking stage, the fibers will transmit the stresses into the uncracked part of the matrix. From these assumptions, they proposed a bond stress model equation in a differential equation form as :

$$\frac{d^2S}{dx^2} = \frac{4}{dE_f} \left[1 + n \frac{V_f}{1-V_f} \right] k.S(x) \quad (2.13)$$

where :

- $S(x)$ = slip at any point on the fiber
- E_f = modulus of elasticity of the fiber
- V_f = fiber volume fraction
- E_m = modulus of elasticity of the matrix in tension
- k = bond modulus
- n = E_f/E_m

With the boundary conditions at the center of the fiber (as origin) as:

$$X = 0 , S = 0 \quad \text{and} \quad X = l/2 , F = xF_o$$

The shearing-stress equation at the interface at any section is

$$\tau(x) = \frac{x F_o}{kl} k \sinh(kx) + \tau_o \quad (2.14)$$

$$\pi d \cosh\left(\frac{x}{2}\right)$$

where :

- τ_o = basic adhesion
- F_o = end fiber force

$$k = \frac{4}{E_f} \left[1 + n \frac{V_f}{1-V_f} \right] \frac{k}{d} \quad (2.15)$$

This equation is valid if the bond stress does not exceed the bond capacity of the interface. The equation can predict the bond shear stresses at the interface, as well as the normal tensile stress in the fibers and the matrix.

All these bond strength properties, both for reinforced concrete and fibrous concrete reported were on normal concrete. For high strength concrete no investigations have yet been made.

2.3 Fatigue Characteristics

Fatigue characteristics is one of the most important properties of concrete. Much of our present knowledge of the fatigue of concrete in compression is derived from test performed over fifty years ago. Most of these test were on normal concrete, very few were on high strength concrete. Fatigue strength basically depends on the range of cycle stress, maximum stress level, rate of loading, mix-proportion, etc.

Van Ornum [74-75] was the first researcher to study fatigue of concrete. From his experiment, he observed that brittle engineering materials, of which cement mixtures were a fair type, possessed the properties of progressive failure or gradual fracture which became complete under the repetition of load well within the ultimate strength of the material. He also stated that the stress-strain curve varied with the number of load repetitions. The convex upward curve gradually straightened under repeated load and finally became concave upward near failure. A similar reduction in modulus of elasticity of concrete was observed. Also introduced in his study was the S-N curve. These conclusions were later confirmed by other researcher [76]. Mehmel found that elastic strain and remaining strain (permanent deformation) increased with the number of repetitions as long as a certain critical stress (endurance limit) was not exceed and that the ratio (remaining strain/elastic strain) grew larger with the number of cycle. Heim indicated that the remaining deformation was greater than elastic deformation after a period of repetitive loading and the remaining deformation did not become constant even after 1,000,000 cycle. Yoshida

TABLE II.1 FATIGUE LOAD SPECTRUM

LOW CYCLE FATIGUE	HIGH CYCLE FATIGUE		SUPER HIGH CYCLE FATIGUE	
Structures Subjected to Earthquake	Airport Pavements and Bridges	Highway and Railway Bridge, Highway Pavement Concrete Railroad Ties	Rapid Mass Transit Structures	Sea Structures
0	10 ³	10 ⁵	10 ⁷	5x10 ⁸
Number of Cycles				

examined the change in Poisson's ratio, μ , with repeated loads. He found that if $m = 1/\mu$, m was about 7-8 after 140,000 cycle and increases to 11-12 in the stage close to failure.

The range of cyclic loading is different according to the type of structure, for example railroad bridge, highway bridge, airport pavement, sea structures, mass rapid transit system, etc. T.C. Hsu [77] has classified the range of cyclic loading into a spectrum of cycles; low-cycle fatigue, high-cycle fatigue and super-high-cycle fatigue as shown in Table II.1.

Fatigue of concrete has been studied and mostly directed toward the compression, flexure, tension, and reverse loading which is reviewed as follows.

2.3.1 Cyclic Compression

The effect of the minimum stress and the stress range on the fatigue strength was first determined by Graf and Brenner [20]. They

established a Modified Goodman Diagram for the repeated compressive loading. Both maximum stress and minimum stress level are expressed in terms of the percentage of the static strength. The fatigue failure is based on 2 million cycles of loading.

Aas-Jakobsen [21] studied the effect of the minimum stress (f_{\min}). From Modified Goodman Diagram, he observed that the relationship between f_{\max}/f'_c and f_{\min}/f'_c was linear for fatigue failure at 2 million cycles of loads. Thus the relationship between f_{\max}/f'_c and R (stress range) was also linear. With these properties, he derived a general f-N-R relationship as shown below :

$$\frac{f_{\max}}{f'_c} = 1 - \beta(1-R)\log N \quad (2.16)$$

where :

β = slope of the f-N curve when R = 0 ($\beta = 0.064$)

R = stress range (f_{\min}/f_{\max})

This equation is valid only for $0 \leq R \leq 1$.

Ralejs Tepfers and Thomas Kutti [22] studied the fatigue strength of plain, ordinary and lightweight concrete by experiment and their results were then compared with the equation proposed by Aas-Jakobsen [21]. Base on their test data, they found that $\beta = 0.0679$ for ordinary concrete and $\beta = 0.0694$ for lightweight concrete when $R < 0.8$. But they recommended use of the mean value of β which was equal to 0.0685, for estimating the fatigue life for both ordinary and lightweight concrete. By comparing the Wöhler curves, they observed that the different strength of concrete had no effect on the fatigue results when they were set out in nondimensional form as the ratio $f_{r\max}/f'_r$. This equation is not only valid for compression but for tension as well.

Although Tepfers and Kutti's equation is widely accepted, it has two limitations as pointed out by T.C. Hsu [77]. First, when $R = 1$, the

equation becomes $f_{\max}'/f_c' = 1$ and f_{\max}' equals to a constant which is not correct. This is because when R approaches unity, a repeated load approaches a sustained load which is time dependent as mentioned by Rusch [23]. The long time strength may approaches 75 percent of the short time static strength of concrete if tested under the ASTM loading rate. Second, the equation does not include the rate of loading as variable. This equation was developed for the range of high-cycle fatigue for which the effect of strain rate is small as observed by many investigators [20, 24-26]. But for low-cycle fatigue, the effect of strain rate was found to be very significant [26-28]. Therefore Hsu introduced the element of time (T) into the f-N-R-relationship, where T is the period of the repetitive loads expressed in sec/cycle. He proposed two equations, one for high-cycle fatigue and the other for low-cycle fatigue.

For high-cycle fatigue :

$$\frac{f_{\max}'}{f_c'} = 1 - 0.0662(1 - 0.556R)\log N - 0.0294\log T \quad (2.17)$$

For low-cycle fatigue :

$$\frac{f_{\max}'}{f_c'} = 1.20 - 0.2R - 0.133(1 - 0.779R)\log N - 0.0530(1 - 0.445R)\log T \quad (2.18)$$

These two equations are valid for :

1. Normal weight concrete with $f_c' < 8000$ psi.
2. When stress range value (R) is between 0 and 1
3. Frequency from 0 - 150 cycle/sec
- 4 Number of cycle from 1 - 20 million cycles
5. Compression and flexure test

2.3.2 Cyclic Tension

The tensile fatigue of concrete has not been widely studied. One reason is the difficulties in applying the direct tensile load to the specimen and holding the specimens in such a way that avoids

eccentricity of loading. Thus most of the fatigue test in tension were conducted by indirect tension tests such as splitting test or flexure test. But these indirect tension tests gave some problems as mentioned by M. Saito and S. Imai [28].

For direct tension fatigue test, M. Saito and S. Imai [28] used friction grip to conduct the test on 2.8x2.8x29 in. (7x7x74 cm) prismatic specimens with enlarged ends. Sinusoidal pulsating loads were applied to the specimens at a constant speed of 240 cpm. (cycles/minute). Maximum stress levels varied from 75 to 87.5 % of static strength while minimum stress level maintained at 8 %. The ratio of minimum to maximum stress (R) was in the range of 0.09 to 0.11. The surfaces of all specimens were coated with parafin wax to prevent drying during fatigue test. From the test, they proposed the S-N relationship for a 50 % probability of failure as :

$$S = 98.73 - 4.12 \log N \quad (2.19)$$

Where :

- S - Maximum applied stress level (percent of f'_c)
- N - Number of cycle to failure

According to their equation, the fatigue strength for 2 million cycles under direct tensile loading was 72.8 % of the static strength. This fatigue strength was considerably higher than fatigue strength under indirect tension test and compression test. They also observed that plain concrete exhibited no fatigue limit in tensile fatigue at less than 2 million cycles.

For indirect tensile fatigue test, Ralejs Tepfers [29] performed splitting fatigue tests on 6 in. (15 cm) cubes specimen. Two types of concrete with ultimate strength of 5,900 psi and 8,200 psi were used in this study. The maximum stress range ($R = f_{\min} / f_{\max}$) of 0.20, 0.30 and 0.40 were selected. He observed that the same fatigue strength equation for compression which is :

$$\frac{f_c^{\max}}{f_c} = 1 - \beta(1-R)\log N \quad (2.20)$$

can also be used to determine the number of load pulse to fatigue failure for tension. He also found that the concrete strength had no effect on fatigue strength when they were set out in nondimensional form as the ratio of f_r^{\max}/f_c' .

Tepfers, Garlin and Samuelsson [30] observed that there was no differences in the fatigue stress levels on normal concrete and lightweight concrete. And the same fatigue strength equation for compression colud also be used for splitting tensile fatigue on normal and lightweight concrete.

For the flexure test, W. Murdock and Clyde E. Kesler [31], conducted an experiments on beam 6x6x60 in. The specimen was loaded at the third points in order to avoid shear stress at the middle span. Three different stress ranges R ($R = f_r^{\min}/f_r^{\max}$) of 0.25, 0.5 and 0.75 were used for this test. From this test, they observed that there was no fatigue limit for plain concrete made with sand and aggregate subjected to repeated flexure loading of at least 10 million repetitions of stress. The results agreed very well with Kesler [25] and H.A. Williams [32] but disagreed with thosed reported by Clemmer [33]. Kesler [25] found no fatigue limit but established fatigue strength at 10 million repetitions of stress ranging from a small value in tension to some maximum value. The fatigue limits were approximately 62 % of the static ultimate flexural strength. Williams [32] found that for lightweight aggregate beams, there was no fatigue limit. But Clemmer's [33] results indicated that the fatigue limit for plain concrete was 55 % of the static ultimate flexural strength. Murdock and Kesler also found that the stress ranges have a significant influence on the fatigue strength. They proposed a fatigue strength equation in terms of stress range at ten million cycles as :

$$F_{10} = 0.56 + 0.44M \quad \text{or} \quad F_{10} = 1.3 / (2.3 - R) \quad (2.21)$$

where :

$$M = f_r^{\min} / f_r'$$

$$R = f_r^{\min} / f_r^{\max}$$

for value of M and R between 0 and 1

For stress reversal :

$$-0.56 < M < 0 \quad \text{and} \quad -1 < R < 0$$

$$F_{10} = 0.56 \quad (2.22)$$

To include probability of failure in fatigue analysis, T. John and Mc. call [34] conducted the test on air-entrained concrete beams 3x3x14.5 in. with natural sand and crush-limestone with maximum size of 3/4 in. They performed the test with the speed of 1,800 cpm until failure or 20 million cycles with the different maximum flexure stress which varied from 47-70 % of modulus of rupture. From this test, they proposed the mathematical model of fatigue strength in terms of stress range, number of cycle and probability of survival as :

$$L = 10^{-0.0957R^{3.32}(\log N)^{3.17}} \quad (2.23)$$

where :

- L = probability of survival = 1-P
- P = probability of failure
- R = S/S_{rp}
- N = number of cycle
- S = stress used in the test
- S_{rp} = mean static strength

They observed that the S-N curves for concrete did not become asymptotic to a particular stress level in a range up to 20 million cycles. The probability of failure at 20 million cycles was slightly less than one half for concrete tested at a stress level of 50 % of modulus of rupture.

2.3.3 Reverse Loading

There are very few experimental investigations reported on concrete exposed to cyclic compression-tension stress.

R. Tepfers [35] studied the fatigue of plain concrete subjected to stress reversals. He conducted experiments on two different types of samples. One was on transversely compressed cubes with a pulsating splitting load and the other a concrete prism with axial pulsating compressive loads and central splitting line loads. He observed that stress reversal between tension and compression caused a slight reduction in the fatigue strength of concrete in compression. The fatigue strength of concrete was obtained from the absolute maximum static strength ratio and zero minimum stress. But this reduction may have been due to the difficulties in loading the specimens precisely on the tensile side of the pulse. Thus he concluded that the fatigue strength due to stress reversal could be predicted by the fatigue strength equation which proposed by other investigators [21-22, 29] as:

$$\frac{f_c^{\max}}{f_c} = 1 - 0.0685(1-R)\log N \quad (2.24)$$

where :

- f_c' = static strength of concrete
- f_c^{\max} = upper stress limit for pulsating load
- $R = f_c^{\min}/f_c^{\max}$
- f_c^{\min} = lower stress limit for pulsating load
- N = number of load pulse to fatigue failure

2.3.4 Factors Affecting Fatigue Characteristics

There are many other factors that affect the fatigue strength of concrete which have been investigated by many researchers [26, 78-83]. These factors are rate of loading, stress range, stress gradient, moisture condition, loading waveform, rest period, etc.

P.R. Sparks and J.B. Menzies [78] studied the effect of the loading rate on the static and fatigue strength of plain concrete in compression by conducting experiments on concrete prisms made with gravel, limestone and lytag aggregate. The specimens were loaded at a rate between 10^{-3} and $10 \text{ N/mm}^2\text{s}$ for static test. For fatigue test, a triangular wave form was employed with constant loading and unloading. The rate of loading used in these fatigue tests were 0.5 and $50 \text{ N/mm}^2\text{s}$. The maximum load was between $0.90 f'_c$ and $0.70 f'_c$ whereas the minimum load was $0.33 f'_c$. They found that the stiffness and the strength for both static and fatigue of these three types of concrete tested were enhanced by increases in the rate of application of load. They also found that the strain in the concrete loaded at the slowest rate was about 25 % greater than that loaded at the faster rate, these results compared favorably with Spooner's work [79]. They concluded that the relation between the rate of increase of secondary strain per cycle and the endurance, irrespective of the rate of loading, was linear.

Based on tests of 300 prismatic specimens M.E. Award and H.K. Hilsdorf [26] observed that both longitudinal and lateral strain increased with increasing number of cycles. The strains at failure were larger with lower applied maximum stress levels or the longer the time to failure. The effect of frequency of loading was likely to diminish with decreasing maximum stress level. An increase in the stress rate by one order of magnitude led to an increase in the number of cycles to failure by almost one order of magnitude especially for a small stress range. They also found that damage caused by high repeated loads depended on both the number of applied cycles and the total time that concrete had to sustain high stress.

Clyde E. Kesler [25] studied the effect of speed of testing on 100 concrete beams specimens of two different concrete strength ($f'_c = 3,600$ and $4,600 \text{ psi}$) with three speeds of loading (70, 230 and 440 cpm). The results indicated that the speed of testing for this range of investigation had little or no effect on the fatigue strength. This was also confirmed by W.H. Gray, J.F. Mc Laughlin and J.D. Antrim [80]. This conclusion was limited to concrete made of round aggregate. He

also observed that no specimen failed at a stress less than 55 % of static strength at 10 million cycles.

The stress range R (f_c^{\min}/f_c^{\max}) of a fatigue test significantly effects the fatigue strength. The lower the stress range, the shorter the fatigue life of the specimen is. This has been investigated and reported by many investigators [26,31].

The effect of stress gradient on fatigue life of plain concrete was studied by F.S. Ople Jr., and C.L. Hulsbos [81]. The experiment was conducted on 4x6x12 in. prism specimens under repeated compression. The specimens were tested at the rate of 500 cpm (cycle/minute) with three different eccentricities (= 0, 1/3 and 1 in.). The tests were performed until the specimens failed or sustained upto 2 million cycles. The maximum stress level used in this test varied from 65 to 95 % of static strength while minimum stress kept constant at 10 % of static strength for all test. When $e = 0$ (concentricity), the load produced uniform stress throughout the cross section, and when $e > 0$, the load produced nonuniform stress. He also observed that the mean S-N curves of both concentrically loaded and eccentrically loaded samples were parallel and the slopes of these curves were flat. The fatigue strengths due to concentrically and eccentrically loads were quite different. The fatigue strength of nonuniformly stressed specimens was higher than that of uniformly stressed specimen by about 17 % of static ultimate strength. They also reported that the fatigue life of both concentrically and eccentrically loaded samples was highly sensitive to small changes in maximum stress levels. A change in stress of about 5-75 % could cause the fatigue change from 40,000 to 1,000,000 cycles.

K.D. Raithby and J.W. Galloway [82] studied the effects of moisture condition, age and rate of loading on fatigue of plain concrete. They conducted an experiment on 102x102x510 mm beams with third-point loading. A sinusoidal load was applied to the specimen with the frequency between 20 Hz and 4 Hz. He observed that the moisture condition significantly affected both modulus of rupture and fatigue performance in a consistent pattern. Oven-dried specimens showed the

longest fatigue life while the partially dried specimen gave the shortest and the fully saturated specimen exhibited intermediate fatigue life. This difference in fatigue performance was probably due to different strain generated by moisture gradient within the specimens. They also found that the fatigue endurance increased with the age of the specimens, the type of concrete and the stress range. The mean fatigue life of 2 years old beams was 2000 times the fatigue life of beams at 4 weeks old.

Based on 185 6x6x60 in. plain concrete beam specimens, H.K. Hilsdorf and C.E. Kesler [83] investigated the fatigue strength of concrete under varying flexure stresses. The specimens were loaded at one-third points of 60 in. span with the rate of 450 cpm. The ratio of the minimum to the maximum load was 0.17. The specimens were loaded until failed or reaching one million cycles with 5 different rest periods of 1, 5, 10, 20 and 27 minutes. The results indicated that a periodic rest period increased the fatigue strength for a specified fatigue life and it became more pronounce when the length of rest period increased up to 5 minutes. From 5-27 minutes of rest period, the fatigue strength did not further increase. Hilsdorf and Kesler also studied the fatigue strength varying the maximum stress level. Two different types of maximum stress were selected. In the first, the maximum stress level was changed only once during the test, while in the second study, the maximum stress level was changed periodically. They found that the fatigue strength and life of concrete was influenced by the sequence in which these loads were applied. The fatigue life of the specimens in which the maximum stress level was changed only once in the test was linear if the higher stress level had been applied first. For the specimens in which the upper stress level was varied between two values continuously while the lower value was kept constant, the fatigue life would decrease with an increasing magnitude of the higher stress level.

S.S. Takhar, I.J. Jordaan and B.R. Gamble [84] investigated the fatigue behavior of concrete under lateral confining pressure. 96 cylinders were tested with three different confining pressures of 0,

1000 and 2000 psi under a sinusoidal load at a rate of 60 cpm. The maximum axial fatigue loadings used in this study were 80, 85 and 90 percent of the corresponding static ultimate compressive strength while the minimum stress level was kept constant at $0.2 f'_c$. From this test they observed that the confining pressure significantly affected the S-N curve of the specimens and it prolonged the fatigue life. The effect of the lateral confining pressure was dependent on the maximum stress level of the fatigue load. For a maximum stress level of $0.90 f'_c$, the difference in fatigue behavior with or without the lateral confining pressure was not significant while for a maximum stress level of $0.8 f'_c$, the difference was quite pronounced.

R. Tepfers, J. Gorlin and T. Samuelsson [85] studied the effect on the fatigue strength due to different loading waveforms. Three different waveforms, sinusoidal, triangular and rectangular were used in this study. Their experiment concluded that the triangular waveform was less damaging than the sinusoidal, while the rectangular waveform did the most damage and gave the shortest fatigue life. This might be because of different waveforms caused different rates of loading. Thus they recommended to use triangular waveform on fatigue test for the earthquake design in which the effect of loading rate is an important factor.

2.3.5 Fatigue on High Strength Concrete

Very few investigators have studied fatigue properties on high strength concrete. W.H. Gray, J.F. Mc Laughlin and J.D. Antrim [80] studied the fatigue properties of high strength lightweight aggregate by repeated compression on 150 3x6 in. cylinders. Different maximum stress levels of 40, 50, 60, 70, and 80 % of static compressive strength and minimum stress level of 70 and 170 psi were selected. Two speeds of testing, 500 cpm and 1,000 cpm were used to study the effect of rate of loading. All specimens, after 28 days of water curing, were placed in an oven for 4 to 5 days to prevent further hydration during fatigue test. The test results indicated that there was no difference in the fatigue properties between low strength and high strength

lightweight concrete and normal concrete. The rate of loading between 500-1000 cpm. had no effect on the fatigue properties. They also found that there was no fatigue limit up to 10 million repetitions of loading.

E.W. Bennett and S.E. St. J. Muir [86] conducted an experiment under repeated compression load on 8x3x3 in. prism specimen with four different capping methods. The compressive strength was between 6000-8500 psi. The specimens were loaded at the rates of 240 and 480 cpm. with maximum stress level starting from 80 % of the static prism strength and gradually reduced to the limit that specimens could resist up to 1 million cycles. The minimum stress level was kept constant at 5 tons or 1250 psi for all tests. The test concluded that high-alumina-cement compound gave the highest ratio of prism strength to cube strength. The mean fatigue strength was 67 % of static cube strength or 60 % when the minimum stress level was zero which was almost the same as normal concrete. The elastic strain (immediately recoverable on removal of the load) became stable after 300,000 repetitions. Both the elastic strain and the remaining strain were linearly proportional to the upper limit of the maximum stress level of loading for both strengths of concrete except for the remaining strain which was less for high strength concrete after one million repetitions of loading. Therefore the relationship between upper limit of fluctuating stress and the remaining strain was probably not linear for lower stress level. Rest periods were also found to have an influence upon the value of the remaining strain. A recover of 50 % of the remaining strain was observed during the rest period of 24 hr. after 190,000 repetitions of load in one test. In another test the recover of 7 % was found in a rest period of 5 days after 3,400,000 loadings at 66 % maximum stress level.

High strength concrete is now generally accepted and used in practice. The strength of concrete used is up to 15,000 psi. But most structures which used high strength concrete are not only subjected to static loads but also to fatigue loads. These structures are high rise building, bridge, pavements, marine structures. Since the fatigue

behavior plays an important role in the analysis and design of these structures, thus fatigue characteristics of high strength concrete need further investigation.

CHAPTER III

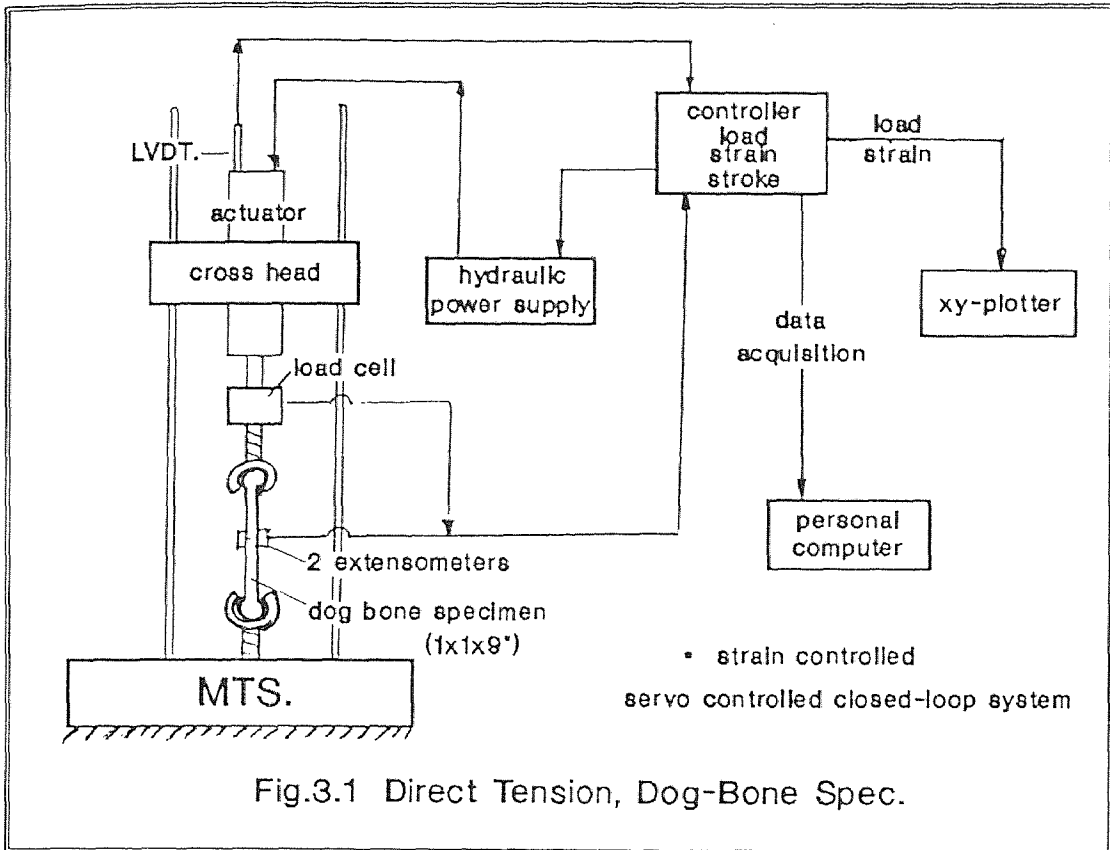
OBJECTIVE AND SCOPE OF WORK

3.1 Objective

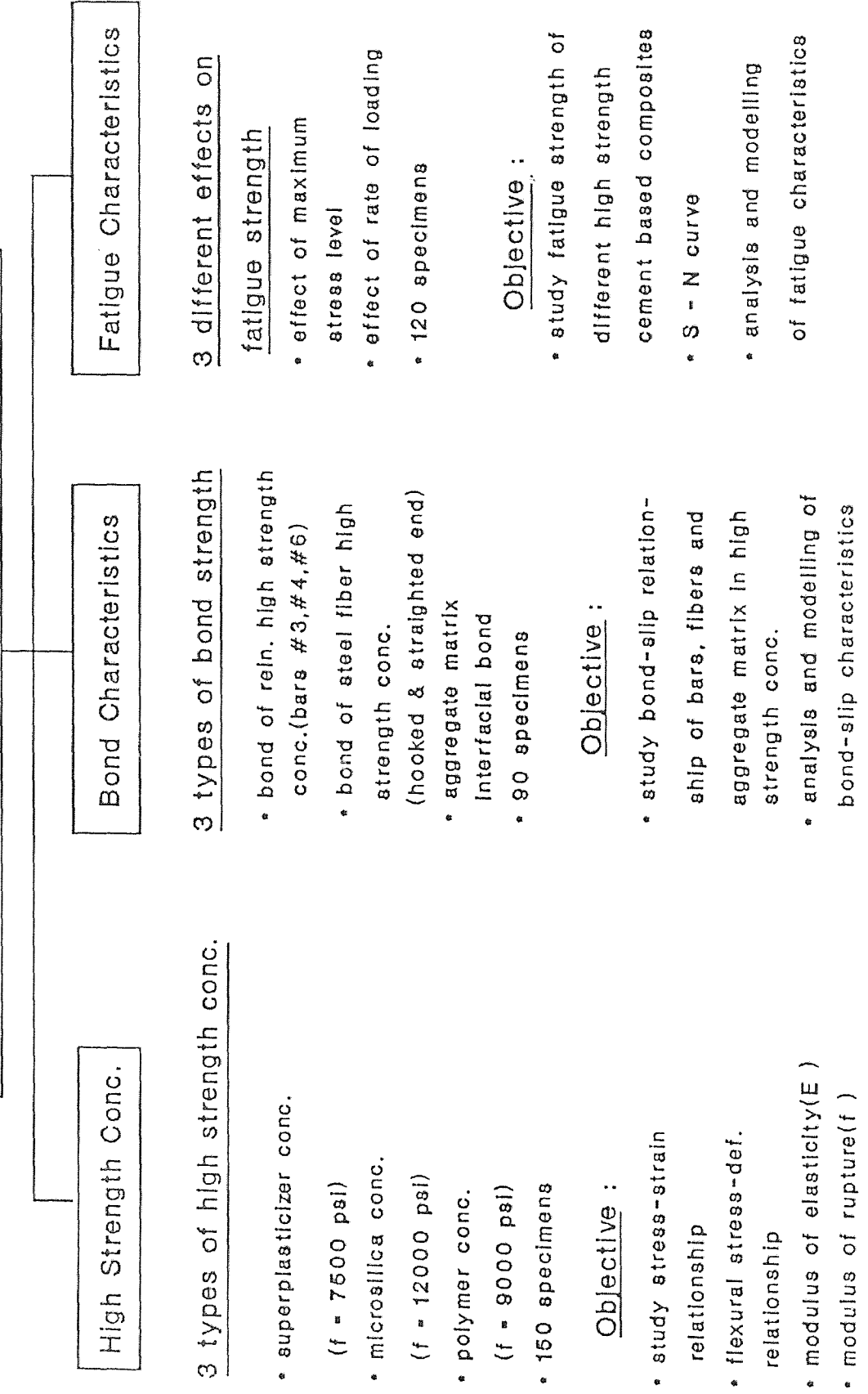
Recently, due to the widely use of different high strength cement based composites in engineering construction, it has become necessary to better understand their properties. Many researchers have investigated the basic properties such as compressive strength (f'_c), tensile strength and modulus of elasticity (E_c). Other properties such as bond and fatigue characteristics of high strength cement-based composites are unaccounted for. In this study, attempts were made to investigate these properties of high strength cement-based composite which can be divided into two major aspects; experimental program and empirical modelling. Three different types of high strength cement-based composites, superplasticizer concrete, microsilica concrete and polymer concrete and one type of normal concrete are used in this study. About 440 specimens were tested in this study.

3.1.1 Experimental Program

The experimental program can be divided into 5 different tests, compression test (3x6 in. cylinder specimen), direct tension test (dog-bone specimen), indirect tension test (beam), bond strength test (tapered and cubed specimens) and fatigue test (3x6 in. cylinder specimen). All tests were conducted in a MTS hydraulic closed-loop testing system as shown in Fig.3.1. All specimens were cured in water at least 56 days before testing with the exception of polymer concrete specimen which were cured in the air for 3 days prior to testing. All cylinder specimens were capped with sulphur based-capping compound before testing. The brief scheme of work on both experimental and modelling is shown in CHART I.



BOND AND FATIGUE CHARACTERISTICS OF HIGH STRENGTH CEMENT BASED COMPOSITES



3.1.1.1. Compression Test

About 120 of 3x6 in. cylinder specimens were tested in uniaxial compression under the closed-loop strain control. The objectives of these tests were as follows :

1. To study the stress-strain relationship and the modulus of elasticity of these three different high strength cement-based composites.
2. To differentiate the type of high strength concrete.
3. To use the results of the compression test to predetermine the maximum and minimum strength for the fatigue test.
4. To determine the bond factor of the bond strength in reinforced high strength cement-based composite.

3.1.1.2 Tension Test

The 1x3x12 in. tapered specimens (Fig.3.2) and the 1x1x9 in dog-bone specimens (Fig.3.3) of high strength cement-based composites were tested under MTS closed-loop strain control. The objectives of these tests were :

1. To study the post peak stress-displacement relationship of high strength cementitious matrices.
2. To evaluate the tensile strength of a high strength matrix and compare with normal concrete.
3. To observe the effect of the specimen size on the tensile strength of high strength cement-based composite.

Also six standard 3x6 in. cylinder specimens of polymer concrete were tested in split tension in order to find the tensile stress of the matrix.

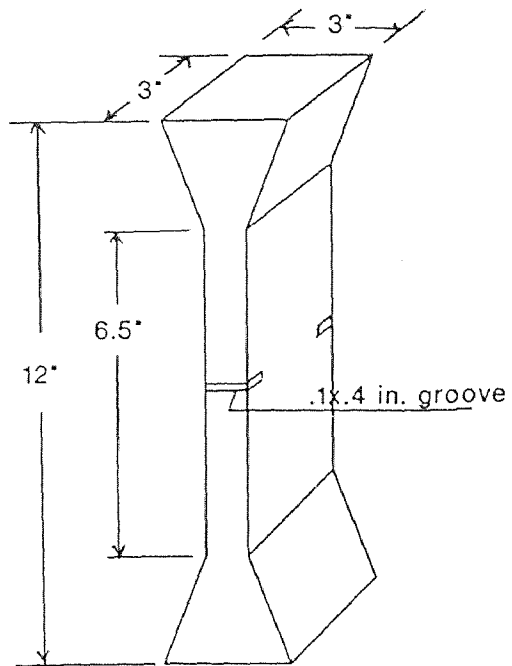


Fig. 3.2 Tapered Specimen

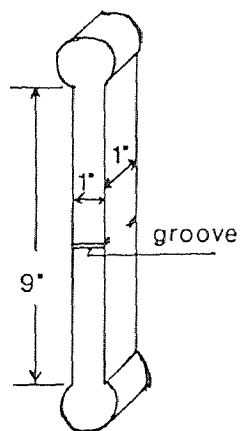


Fig. 3.3 Dog-Bone Specimen

3.1.1.3 Beam Test

Five different sizes of microsilica beams 1x2x12, 2x4x12, 2x5x24, 4x6x30, and 6x6x30 in. and two sizes of polymer beams 1x2x12 and 2x4x12 in. were tested under the closed-loop strain control (deflection control). The objectives of these tests were :

1. To obtain the flexural strength - deflection relationship of different high strength cement-based composites.
2. To evaluate the modulus of rupture (f_r) of high strength concrete and compare with normal concrete.

3.1.1.4 Bond Strength Test

The bond strength test in this study is divided into 2 areas, bond strength of reinforced high strength concrete and pull-out stress of high strength fibrous concrete.

Bond strength of Reinforced High Strength Concrete

Three different deformed bar sizes, #3, #4, and #6 were reinforced in a high strength concrete cubes of 5x5x5, 5x5x5, and 8x8x8 in. respectively. The pull-out tests were conducted under the closed-loop displacement control. The purposes of these tests were as follow :

1. To study the bond-slip relationship of high strength concrete and compare with normal concrete.
2. To observe the bond strength of the matrix due to different sizes of deformed bars.
3. To determine the proper embedment length of reinforcing bar in high strength concrete structures.

Pull-Out Stress of High Strength Fibrous Concrete

Two types of steel fibers, one with hooked-end and the other straight were selected to study the high strength fibrous concrete.

Both types of steel fibers have a density of 490 lb/ft^3 , an average of one inch length, and an approximate aspect ratio (l/d) of 60. Four different fiber volume fractions of 0.5, 1.0, 1.5, and 2.0 % were used to study the effect of fiber content. The specimen was tested under the closed-loop strain control. The number of specimens used in this study is shown in Table III.1. The objectives of these tests were :

1. To study the post-peak pull-out stress vs. displacement relationship of high strength fibrous concrete.
2. To observe the post-peak pull-out stress vs. displacement relationship for different types of steel fibers (straight-end and hooked-end) and various fiber volume fractions (0.5, 1.0, 1.5, 2.0 %).
3. To obtain the normalized post-peak pull-out stress vs. displacement relationship of high strength fibrous concrete and compare with normal fibrous concrete.

3.1.1.5 Fatigue Test

Three different high strength cement based composites; superplasticizer concrete, microsilica concrete and polymer concrete, were used to study the fatigue characteristics. The fatigue behavior due to the effect of maximum stress level was observed. The specimens used in this study were standard 3x6 in. cylinders. The tests were conducted under closed-loop load control with two different rates of loading; 6, and 12 Hz (cycles/sec). The minimum stress level was kept constant at $0.1 f'_c$, whereas, the maximum stress level was varied for seven different stress levels of 0.40, 0.50, 0.60, 0.70, 0.75, 0.80, and 0.90 of f'_c . All the specimens were tested until failure or until reaching one million cycles, and some up to three million cycles. The number of specimens used in this study is shown in Tables III.2-III.3. The objectives of these tests were :

1. To study the fatigue strength of these three different high strength cementitious composites (superplasticizer concrete, microsilica concrete, and polymer concrete).

2. To obtain the S-N curves of these high strength concretes and compare with normal concrete.
3. To observe the fatigue behavior due to the effect of maximum stress level (0.4 to 0.9 f'_c), and rate of loading (6, and 12 Hz).

3.1.2 Empirical Modelling

With the aid of experimental results of bond and fatigue characteristics of high strength cement based composites, the bond-slip relationship and fatigue strength can be modelled and predicted. Attempts were made to generate a constitutive law and a general equation for the normalized pull-out stress-displacement relationship of brittle materials (normal concrete, high strength concrete, and other cement-based composites). Also, the general equations for the fatigue characteristics of high strength cement-based composites was generated in order to predict the fatigue strength.

Normalized Stress-Displacement Relationship :

A general unique normalized post-peak pull-out stress vs. displacement equation of the cement-based composite has been proposed. This general equation can be applied to different types of cement-based matrices. The equation varies with the single term of "brittleness index" of each matrix. This equation can be used to predict the post-peak response of the composite matrix. The proposed equation is as follows :

$$\left[\frac{\tau}{\tau_{\max}} \right]^m + \left[\frac{\delta}{\delta_{\max}} \right]^{2m} = 1 \quad (3.1)$$

where :

- τ = Post-peak pull-out stress
- τ_{\max} = Maximum pull-out stress of the cemented composite
- δ = Post-peak pull-out displacement
- δ_{\max} = Maximum pull-out displacement of the cemented composites (Half fiber length for fibrous concrete)

m = Brittleness Index of the composite

Brittleness Index :

During the course of this study, a term called the "Brittleness Index" has been proposed as defined in Equation 3.1. For a general cementitious composites; there is a brittleness number which can be used to predict the basic properties of a cement-based composite. The lower the value of the brittleness index, the more brittle the material is. The brittleness index can be used to predict the softening response of a cementitious composite without conducting the direct tension test. The brittleness index may also be used to predict the S-N curves of high strength cement-based composites.

Maximum Strain Concept :

For a given cementitious material, there is a certain amount of maximum strain that the material can sustain. This maximum strain property may be used to predict other basic properties such as compressive strength, tensile strength, etc. In this study, attempts were made to develop the maximum strain concept to predict the fatigue behavior of high strength cement-based composites.

S-N Curve :

The fatigue strength characteristic of a material subjected to repeated stress of constant magnitude is known as the S-N curve, in which N is the number of cycles of stress (S), which would cause failure. Each material has its own unique S-N curve equation. In this study, an attempt was made to develop the general S-N equation for cement-based composites, especially for high strength concrete, by using the maximum strain concept.

3.2 Scope of Work

In order to study the complete properties of high strength cement-based composites, both experimental and empirical studies were performed. For experimental study five different tests, namely, compression test (3x6 in. cylinder specimen), direct tension test (dog-bone specimen), indirect tension test (beams), bond strength test (tapered and cube specimens) and fatigue test (3x6 in. cylinder specimen) were conducted as mentioned earlier. At least three specimens were tested in each test. About 100 cylinder specimens and 30 beam specimens were tested for studying the basic properties of high strength cement-based composites. For bond-slip characteristic study, 51 tapered specimens with 5 different fiber volume fractions and 18 cube specimens with 3 different bar sizes were used. Table III.1 details the specimens used for the bond strength tests. Two types of steel fibers, straight-end and hooked-end were used. One hundred and twenty standard 3x6 in. cylinders were tested to study fatigue characteristics of high strength cement-based composites. Tables III.2-III.3 show the details of cylinder specimens used in the fatigue test. All cylinder specimens were capped with sulphur based-capping compound before testing.

TABLE III.1 BOND STRENGTH TEST

TYPE OF SPECIMEN	NUMBER OF FIBER									
	NORMAL CONCRETE	HIGH STRENGTH CONCRETE								
		Fiber Volume Fractions (V_f)					Deformed Bar (ϕ)			
		0	0.5	1.0	1.5	2.0	#3	#4	#6	
Cylinder 3"x6"	3	-	-	-	-	-	3	3	3	
Dog-Bone Spec.	6*	10*	-	-	-	-	-	-	-	
Tapered Spec.	-	3	12**	12**	12**	12**	-	-	-	
Pull-out Spec. (cube)	-	-	-	-	-	-	12	6	6	

Notes : * Dog Bone Specimen with a single 3/4" aggregate.

** 6 Specimens with straight end fiber and 6 specimens with hooked-end fiber.

TABLE III.2 FATIGUE TEST DUE TO THE EFFECT OF MAX. STRESS LEVEL

TYPE OF CONCRETE	$\frac{f_{max}}{f_c}$	$\frac{f_{min}}{f_c}$	Number of Specimens	
			Controlled Strength	Fatigue
Super Plasticizer Conc.	0.90	0.10	9	9
	0.80	0.10	6	9
Microsilica Conc.	0.75	0.10	6	9
	0.70	0.10	6	9
Polymer Conc.	0.60	0.10	6	9
	0.55	0.10	6	9
	0.50	0.10	3	9
	0.45	0.10	3	3
	0.40	0.10	3	3

TABLE III.3 FATIGUE TEST DUE TO THE EFFECT OF RATE OF LOADING

TYPE OF CONCRETE	$\frac{f_{max}}{f_c}$	$\frac{f_{min}}{f_c}$	Number of Specimens			
			6 Hz		12 Hz	
			Control	Fatigue	Control	Fatigue
Microsilica Concrete	0.9	0.1	4	4	6	6
	0.8	0.1	4	4	4	6
	0.7	0.1	4	4	4	6
	0.6	0.1	4	4	4	6

CHAPTER IV

TESTING PROCEDURE

4.1 Material Compositions

The process of producing high strength cement-based composite varies with geographical location. This is due to the fact that the strength of high strength cement-based composite depends on the type of aggregate and additive. Guidelines in selecting materials and mix proportions are presented in the following literatures [36-43].

The material used for the three types of high strength cement-based composites in this study are Portland Cement Type I, local siliceous sand passing sieve No.4, river gravel with maximum size of 3/8 in. as aggregate, microsilica (1-5 μm), high range water reducing admixture (Daracem 100), Linmix and unsaturated polyester resin solution. Microsilica used in this study is in the powdered form with 96 % of SiO_2 . Three sizes of deformed bars, No.3, No.4, and No.6 (9, 12, and 18 mm) were selected to evaluate the size effect on bond-slip characteristics. One-inch, hooked-end and straight, steel fibers were used for the high strength fibrous concrete to study the effect of end types. Both types of fibers have approximately the same aspect ratio (l/d) of 60. Four different fiber volume fractions of 0.5, 1.0, 1.5, and 2.0 % of cement were used to study the effect of fiber content. The fiber had a density of 490 lb/ft³.

4.2 Mix Proportions

Many trial mix proportions were tried in order to achieve higher compressive strength at lesser cost. Especially for polymer concrete in which the compressive strength depends on the amount of polymer added to the mix. The proper mix proportion for superplasticizer concrete used in this study was 1 : 1.87 : 2.50 (cement : sand : aggregate) with 0.30 water/cement ratio. A 15 fl.oz/100 lb cement dosage of Daracem 100

superplasticizer was added to provide workability. The range of compressive strength obtained from this mix was 7,500 to 8,000 psi. at 56 days For microsilica concrete, the mix proportion was 1 : 1.72 : 2.5 : 0.15 (cement : sand : aggregate : silica fume) with 0.35 water/cement ratio. A 30 fl.oz/100 lb cement dosage of superplasticizer was added. The range of compressive strength obtained was between 11,000 to 13,000 psi at 56 days lime water curing. The mix proportion of polymer concrete used was 1 : 3 : 0.1 : 0.8 : 0.1 (cement : sand : linmix : resin : water) which gave a compressive strength of approximately 10,000 psi at 35 days after casting.

4.3 Specimens

According to the ASTM (American Society for Testing and Materials) and RILEM (Materials and Structures) recommendations, different types and sizes of specimens were used because of the high compressive strength of high strength cement based composites and maximum capacity of the testing machine. A 3x6 in. standard cylinder specimen was selected for the present fatigue characteristic study. The maximum capacity of the MTS testing system used is 100 kip with the expected maximum force on the tested 3x6 in. cylinder specimen of 85 kip for a 12,000 psi. concrete. If a bigger size of cylinder is used, the maximum force will be higher and thus exceeds the maximum capacity of the MTS testing system.

For a direct tension tests, 1x3x12 in. tapered (Fig.3.2) and 1x1x9 in. dog-bone (Fig.3.3) specimens were used. Teresa Cintora [90] developed a tapered specimens of 1x3x12 in. to investigate the softening response of concrete in direct tension. The steel box-shaped grip with the dimension of 6x4x5 in. was fabricated. Its consisted of 3 steel plates (one 6x5 and 3x6 in.) and two 3/2x3/2x1/8 in. angles. The two 3x6 in. plates were connected to the edges of the 6x5 in. plate, using 6 1/2 in. bolts, which in turn were linked to each other using the two steel angles. Within this box were the two PVC wedges, with angle complementing those of the specimen, which would secure the specimen in place (Fig.4.1; Ref [90]).

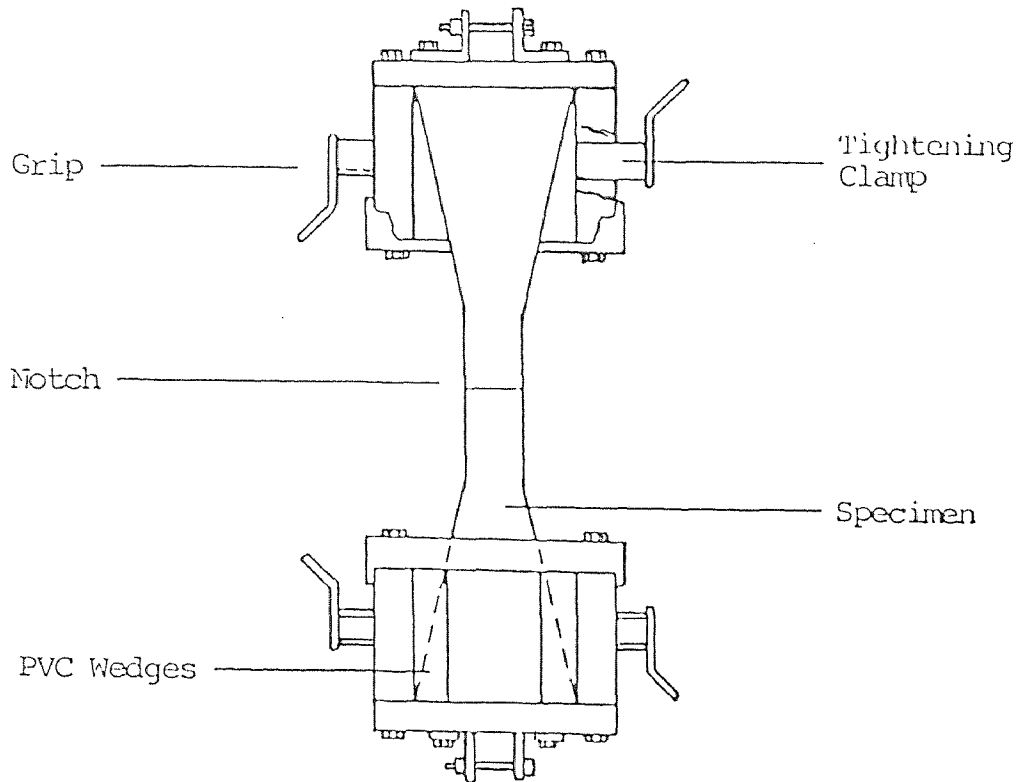


Fig. 4.1 Friction Grips (T. Cintora [90])

For testing bond strength, cube and tapered specimens were used. Many investigators have observed that the amount of concrete cover affects the bond strength of reinforced concrete. According to the RILEM recommendation [9], the proper dimension for a cube specimen of reinforced concrete is 10 times the bar diameter. In this study, the deformed bars No.3, No.4, and No.6 were used in order to study the effect of bar size. Therefore, a 5x5x5 in. concrete cube specimen was used for bar sizes No.3 and No.4 and a 8x8x8 in. specimen for the No.6 bar. The embedment length of five times the bar diameter was selected for the expected bond factor (f_r^{\max}/f'_c), which could be as low as 0.2, and the ratio of f_y/f'_c is only equal to 4 for high strength concrete. For the pull-out stress vs. displacement of high strength fibrous concrete, 1x3x12 in. tapered specimens with the same dimension as those used in the tension test were used. Two type of 1 in. steel fibers,

straight-end and hooked-end, were used with four different fiber volume fractions of 0.5, 1.0, 1.5 and 2.0 % to study the effect of end fabrication and the fiber content.

For the flexural test, five different sizes of beams 1x2x12, 2x4x12, 2x5x24, 4x6x30 and 6x6x30 of microsilica and two sizes of polymer concrete were tested under mid-span point load in order to study the flexural characteristics and the effect of beam size.

4.4 Specimen Casting

Four different concrete types, normal concrete, superplasticizer concrete, microsilica concrete, and polymer concrete were used in this study. The materials used were Portland Cement Type I, local siliceous sand passing sieve #4, river gravel, microsilica, admixture, linmix and unsaturated polyester resin solution. All concrete were prepared by in a mechanical mixer. For each test specimen casted three controlled compression cylinders were casted. The molds were prepared and lubricated with oil before concrete was poured. The mixing procedure for these high strength concretes were similar to the general method used for conventional concrete. After the mix was poured into the molds, it was vibrated on a vibrating table to expell the air in order to obtain a well compacted specimen. For the 4x6x30 in. and 6x6x30 in. beam specimens, a portable vibrator was used instead of vibrating table because the specimens were too big for the vibrating table. After 24 hours, the molds were stripped and the specimens were placed in a lime saturated water solution and left to cure for a period of at least 56 days. The testing age of the specimens varied from 56 days to a year. For polymer concrete, cement and aggregate were mixed in a conventional concrete mixture. Latex was then added to the mix to form the plastic mixture. The mixture was mixed for about 5 minutes before being poured into the molds and formworks. Setting time of polymer concrete is approximately 20 to 30 minutes. After 24 hours, the specimens were removed from their molds and allowed to air dry rather than curing in water. This is because the presence of water tends to slow down the polymerization process and thus reduces the strength of polymer

concrete. The testing age of the specimens varied from 3 to 35 days to evaluate the high early strength property of polymer concrete..

For reinforced high strength concrete specimen, the reinforcing bar was fixed in the mold. The concrete was then poured into the mold perpendicular to the reinforcing bar in order to have the same condition as the reinforced concrete beams in actual structures.

4.5 Test Setup and Procedure

Test setup and procedure of testing can be categorized into 5 different types, compression test (3x6 in. cylinder specimen), direct tension test (tapered and dog-bone specimens), indirect tension test (beam), bond strength test (tapered and cube specimens) and fatigue test (3x6 in. cylinder specimen). All tests were conducted on a MTS hydraulic closed-loop testing system as shown in Fig.3.1. All cylinder specimens were capped with sulphur based capping compound before testing.

4.5.1 Compression Test

The 3x6 in. cylinder specimens were tested in uniaxial compression under closed-loop strain control to study the stress-strain behavior, the compressive strength (f'_c), and the modulus of elasticity (E_c) of different high strength cement-based composites. The tests were conducted at the strain rate of $1 \times 10^{-4} \text{ sec}^{-1}$. The specimen broke between 3 to 5 minutes. Two strain gages (0.20 in.) were mounted to the specimen, as shown in the test set up Fig.4.2, in order to record the average axial displacements. The signals from the two strain gages were averaged and fed back to the controller to constantly adjust the applied load. All signals of load, strain, and stroke were recorded directly onto the computer disk where data manipulation and plotting could later be done. These cylinder tests were also used to determine strength parameters for the bond and fatigue tests.

4.5.2 Tension Test

The 1x3x12 in. tapered specimens and the 1x1x9 in. dog-bone specimens of high strength cement-based composites were tested under MTS closed-loop strain control in order to obtain the complete stress-strain and stress-displacement curves under uniaxial tension. The specimens were saw cut in the middle, creating notches on both sides. The notches provide an exact critical section for crack initiation, where two extensometers with 5 mm. maximum travel distance were placed over the two notches to measure the average crack opening displacement. In order to avoid creating the moment which may occur during testing, the lower end of the steel grip was held fixed to the base of MTS testing machine while the upper end was hinge. Due to the brittle nature of concrete especially high strength concrete, the rate of loading was set at a very slow rate. In this study, the starting strain rate of loading is $2.5 \times 10^{-7} \text{ sec}^{-1}$ in order to obtain the peak stress. After the load reached the peak, the loading rate was gradually increased to speed up the experiment. This step was necessary in order to reduce the creep effect. The signals from the two extensometers were averaged and fed back to the controller to constantly adjust the applied load. The closed-loop strain controlled test allows monitoring of the whole stable post-peak response. Two AC-LVDTs were also placed over the critical section on the remaining two faces of the specimen to monitor large deformation. All signals of load, strain, and LVDT were recorded directly onto the computer disk where data manipulation and plotting could later be done. The total time of testing a specimen was about 4 hrs. The test set up is shown in Figs.3.1 & 4.3 for dog-bone and tapered specimen respectively.

Six standard 3x6 in. cylinders of polymer concrete were also tested in split tension in order to find the tensile stress of the matrix. The indirect tensile strength was used as a reference for comparing with the direct tensile results.

4.5.3 Beam Test

Five different sizes of beams 1x2x12, 2x4x12, 2x5x24, 4x6x30, and 6x6x30 in. of microsilica and polymer concrete were tested in order to study the flexural characteristics of high strength concrete. These observed behaviors were then compared with those from normal concrete. The three-point-load testing method was used for these beam tests. Fig.4.4 shows the test set up for the beam test. The test was conducted under the closed-loop deflection control. Because high strength polymer concrete is more ductile than high strength microsilica concrete due to the plastic like component in polymer concrete, the rate of loading used were different. For microsilica concrete, the strain rate of loading was $4.440 \times 10^{-5} \text{ sec.}^{-1}$ whereas for polymer concrete the strain rate was $1.786 \times 10^{-4} \text{ sec.}^{-1}$. The average deflection of the beam was recorded by the two extensometers mounted at the middle of the beam. And again, the signals from the two extensometers were averaged and fed back to the controller and all the signals of load, strain, stroke were recorded onto the computer disk. About 30 beam specimens were used in this study.

4.5.4 Bond Strength Test

The bond strength test in this study was divided into 2 parts; bond strength of reinforced high strength concrete and bond strength of high strength fibrous concrete.

4.5.4.1 Bond strength of Reinforced High Strength Concrete

Three different deformed bar sizes, #3, #4, and #6 were reinforced in high strength concrete cubes of 5x5x5, 5x5x5, and 8x8x8 in. respectively. In this study, the embedment length of five times the bar diameter was used for the expected bond factor (f_r^{\max}/f_c'), which could be as low as 0.2, and the ratio of f_y/f_c' was about equal to only 4 for high strength concrete. The test was carried out under displacement control. Two AC-LVDTs were attached on both sides of the specimen measured the average pull-out slip of the reinforcing bar. The test

were performed at the rate of 7.143×10^{-4} in./sec. The detail of the test set up is shown in Fig.4.5. For large bars (#6), pushing instead pulling was used to observe the bond-slip behavior because the total pull-out strength exceeded the yield strength of the steel grips shown in Fig.4.6. All the signals of load, strain, and stroke were recorded directly onto the computer disk. It should be noted that for both pull-out test setups the slip must be measured on the side where the bars is moving out of the concrete specimen. Otherwise, the observed results are incomparable.

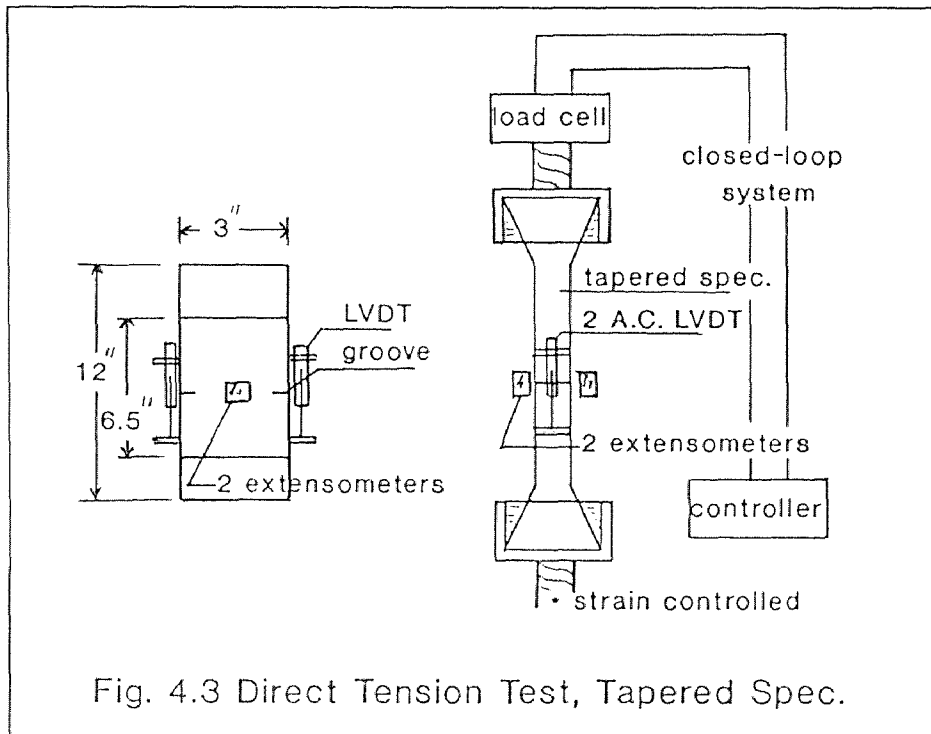
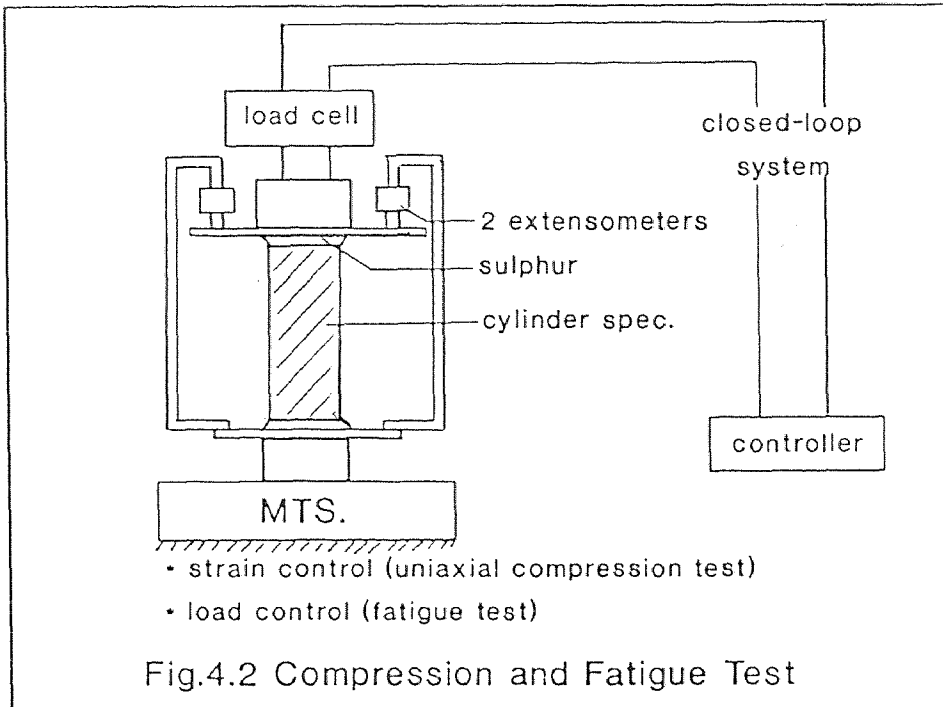
4.5.4.2 Pull-Out Stress of High Strength Fibrous Concrete

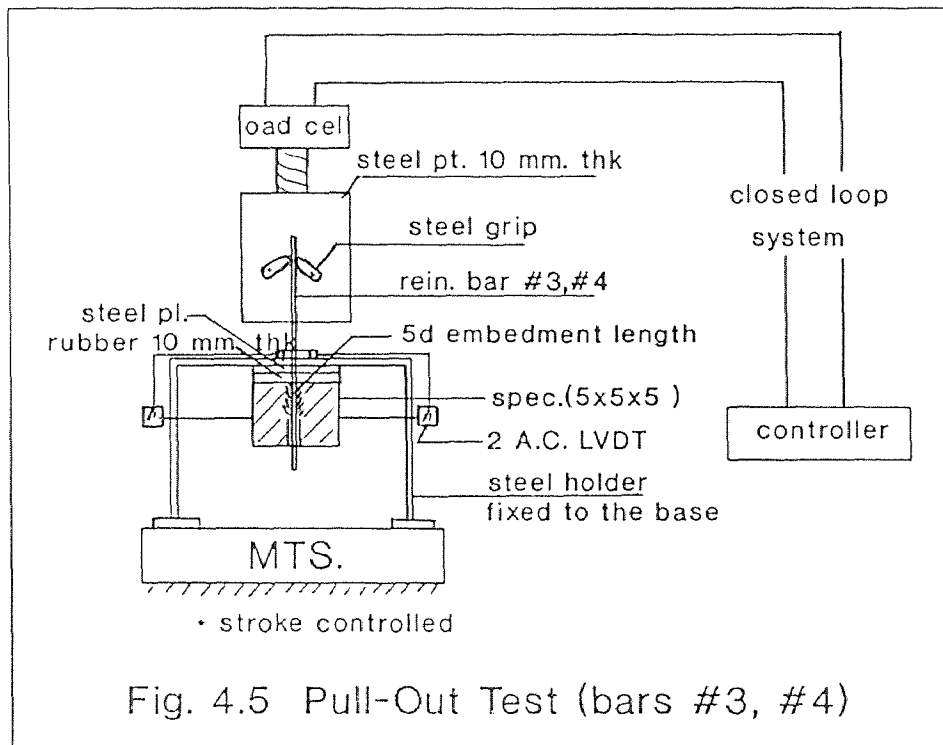
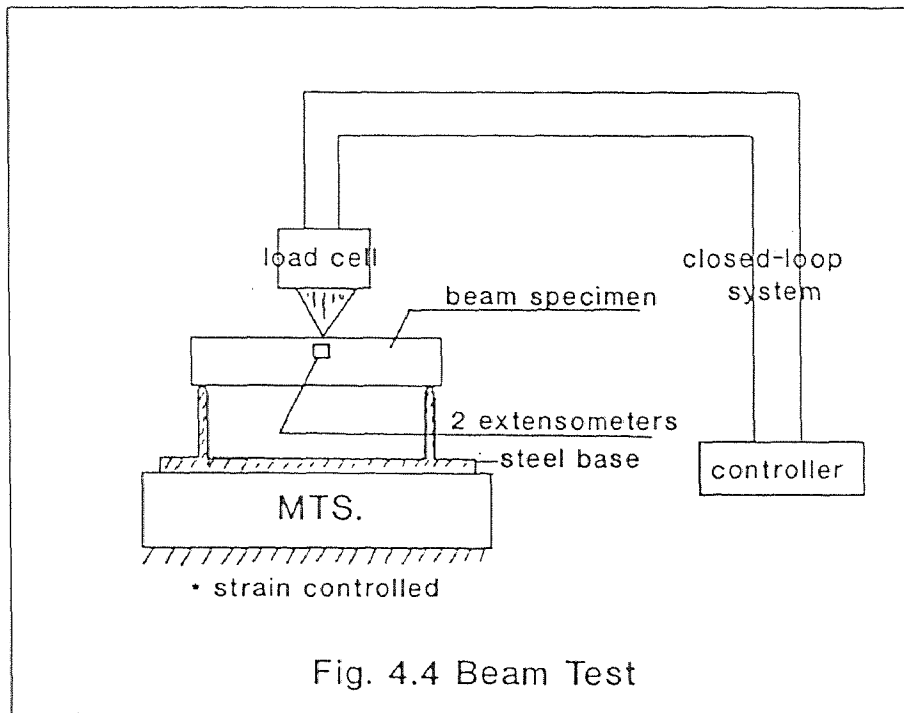
Two types of steel fibers, one with hooked-end and the other straight were used to study the pull-out stress-slip behavior of high strength fibrous concrete. Four different fiber volume fractions of 0.5, 1.0, 1.5, and 2.0 percent of cement were used to study the effect of fiber content. The specimens were tested under the closed-loop strain control. The detail of specimen, test set up and data recording are the same as explained in Section 4.5.2-Tension Test. The number of specimens used in this study is shown in Table III.1.

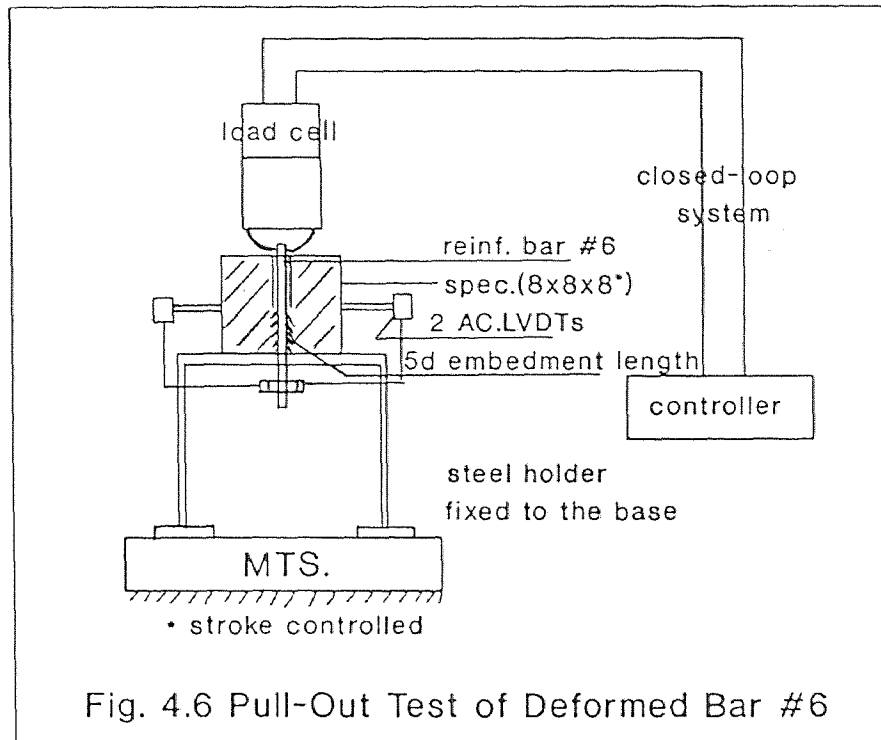
4.5.5 Fatigue Test

The standard 3x6 in. cylinder specimens were used to study the fatigue characteristics of three different high strength cement-based composites, superplasticizer concrete, microsilica concrete, and polymer concrete. The effect of maximum stress level of 0.40, 0.50, 0.60, 0.70, 0.75, 0.80 and 0.90 of f'_c were observed. The minimum stress of $0.10 f'_c$ were kept constant. Two different rates of loading of 6, and 12 Hz (cycle/sec) were conducted to study the effect of rate of loading. All the specimens were tested until failure or until one million cycle, some up to three million. Generally for all the test, the specimen was tested under the closed-loop strain control in order to control the strain of the specimen during the test and more safer than other closed-loop control. But for fatigue testing, it is necessary to use closed-loop load control in order to maintain the same

maximum stress level at each loading cycle during the test. The load was applied to the specimen with the low starting rate of 0.05 cycle/sec. for the first 100 cycles and then gradually increased until the loading rate reaches the required rate of 6 or 12 Hz. at about 1000 cycles. Then the rate was kept constant throughout the rest of the test until the specimen failed or one million cycles was reached. The average strain at different intervals during the fatigue test was recorded with the corresponding number of loading cycles by the 2 extensometers mounted to the specimen as shown in Fig.4.2. Due to the maximum recording speed of MTS testing machine, only one data point per second was record. Thus while recording the load and strain in each loading cycle, the loading rate was slowed down to 0.05 cycle/sec in order to obtain at least 20 data points per cycle. The average testing time was about 2 days per specimen. The details of specimens used in this study is shown in Tables III.2 & III.3.







CHAPTER V

RESULTS AND DISCUSSION

5.1 Basic Properties of High Strength Concrete

5.1.1 Compressive Strength

The compressive strength of cement-based composites varies according to the materials used and mix proportion. The highest compressive strength, specified by manufacturer, obtained from superplasticizer concrete is between 7000 to 7500 psi. In this study three different high strength cement-based composites are used, superplasticizer concrete, microsilica concrete and polymer concrete. Table V.1 shows the average compression properties of different high strength concretes as compared to normal concrete. The minimum curing time for high strength concrete is at least 56 days before test. Longer curing period (58-400 days) did not significantly affect the compressive strength, the maximum strain at peak load, nor the modulus of elasticity of either superplasticizer concrete or microsilica concrete. Dry cured polymer concrete gives higher compressive strength than wet cured one. On the contrary, superplasticizer and microsilica concrete exhibit a lower strength with dry cured condition. This is because the polymerization process of polymer concrete is dictated by the temperature and moisture. The higher the temperature the faster the rate of polymerization which results in a stronger polymer concrete. The curing period of polymer concrete (3 to 35 days air cured) significantly affects the compressive strength, peak strain, and modulus of elasticity as also shown in Table V.1. The average compressive strengths of superplasticizer concrete, microsilica concrete and polymer concrete are 7371, 9526, and 9755 psi respectively. Fig.5.1 shows the typical stress versus strain curves of different high strength concrete as compared with normal concrete. It can be seen that polymer concrete is likely to absorb more energy than other brittle concrete. This may be attributed to the strength of the

aggregate-matrix bonding of polymerization in polymer concrete as compared to normal bonding of cement gel. The effect of the curing period on the compressive strength versus strain of polymer concrete is presented in Fig. 5.2. The older the polymer concrete, the more brittle it behaves. The faster curing process makes polymer concrete a suitable material for quick repair projects such as underwater structures, etc.

The average strain at the peak load of both superplasticizer and microsilica concrete are 0.00206 and 0.00218 respectively which is about one third less than normal concrete (0.00356). While for polymer concrete, the average strain at peak load is 0.01282 at 35 days dry cured which is about 4 times of normal concrete. Details of all compressive stress-strain curves of high strength concrete tested in this studies are summarized in Appendix A.

TABLE V.1 COMPRESSION PROPERTIES

Type of Concrete	* Curing (days)	Max Compr. Strength (psi)	Strain at Max. Load $\times 10^{-3}$	Modulus of Elasticity $\times 10^6$ psi	Remarks
Normal Concrete	21	5142	3.560	2.044	
Superplasticizer Concrete	58-70	7371	2.059	3.705	
	65-76	7793	2.020	4.190	**
Microsilica Concrete	62-406	9526	2.058	4.524	
	66-630	10121	2.222	4.797	**
Polymer Concrete	3-6	4704	16.69	0.754	
	13	6696	12.37	1.084	
	35	9755	12.82	1.570	
	23-27	8413	9.69	1.575	***

Remarks :

- * Normal Concrete, superplasticizer concrete and microsilica concrete were cured in lime water, while polymer concrete was cured in the laboratory environment.
- ** Prefatigue load at least 1,000,000 cycles at the load of $\leq 0.70 f'_c$
- *** Prefatigue load at least 1,000,000 cycles at the load of $\leq 0.40 f'_c$

STRESS VS STRAIN CURVE

HIGH STRENGTH CONCRETE (COM-COMP)

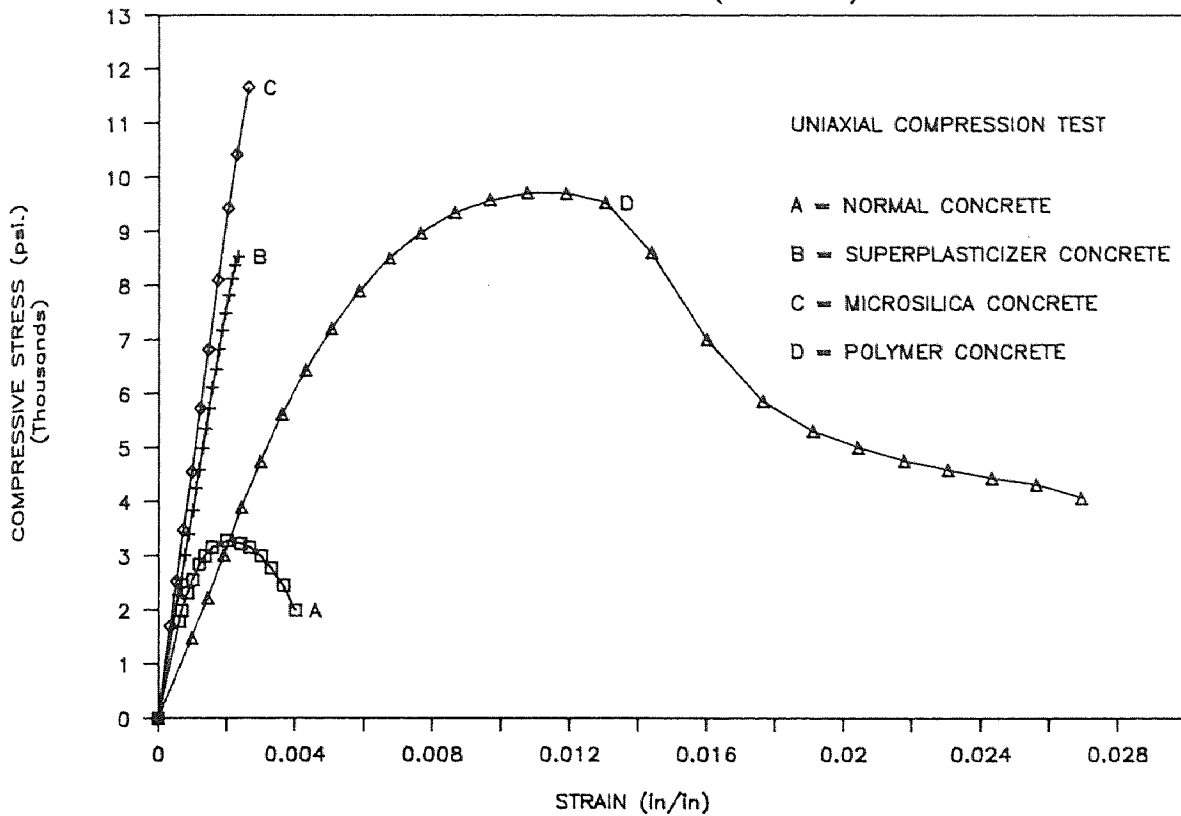


Fig. 5.1 Typical Stress vs. Strain Curves of Different High Strength Concrete compare with Normal Concrete

STRESS VS. STRAIN CURVE

POLYMER CONCRETE (POC21-6)

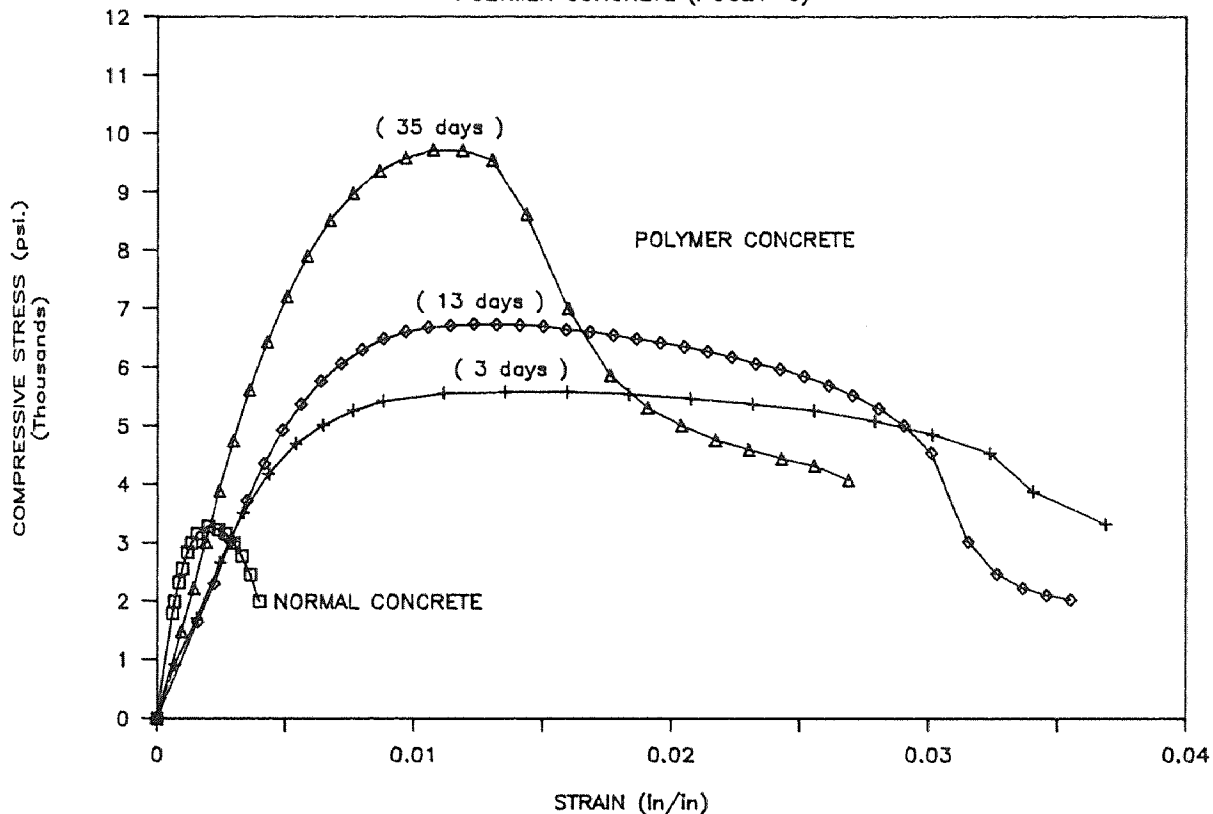


Fig. 5.2 Stress vs. Strain Curve of Polymer Concrete due to the Effect of Curing Period

5.1.2 Mode of Failure

The mode of failure of high strength concrete observed during testing was clearly different from normal concrete. In general, normal concrete will gradually fail after it reaches the peak load while high strength concrete suddenly explodes at the peak load. Possibly because high strength concrete is more brittle than normal concrete and the descending part of the stress versus strain curve is very steep indicating low ductile behavior. Therefore the descending part of the stress versus strain curve of high strength concrete under uniaxial compression can not be ascertained using a conventional testing system. Both the ascending and descending part of the stress versus strain curves of concrete are very important and necessary for engineering analysis and design. Thus, the test set-up and testing procedure for this study were carefully designed. MTS closed-loop axial strain control is used to test the specimen. Fig.5.3 shows the comparison of stress versus strain curves of microsilica concrete from this present study as compared to Shah et.al.'s [6]. They conducted the test by using circumferential closed-loop strain control. The results indicate that the behavior of stress strain relationship of high strength concrete obtained from closed-loop axial strain control is the same as those from closed-loop circumferential strain control. However, due to the abrupt bursting failure of high strength concrete, closed-loop circumferential strain control provides a more accurate and faster response of strain increment over the post-peak region. As a result, a more stable softening response can be observed even for very brittle material like high strength concrete.

STRESS VS. STRAIN CURVE

HIGH STRENGTH CONCRETE (COMP-COM)

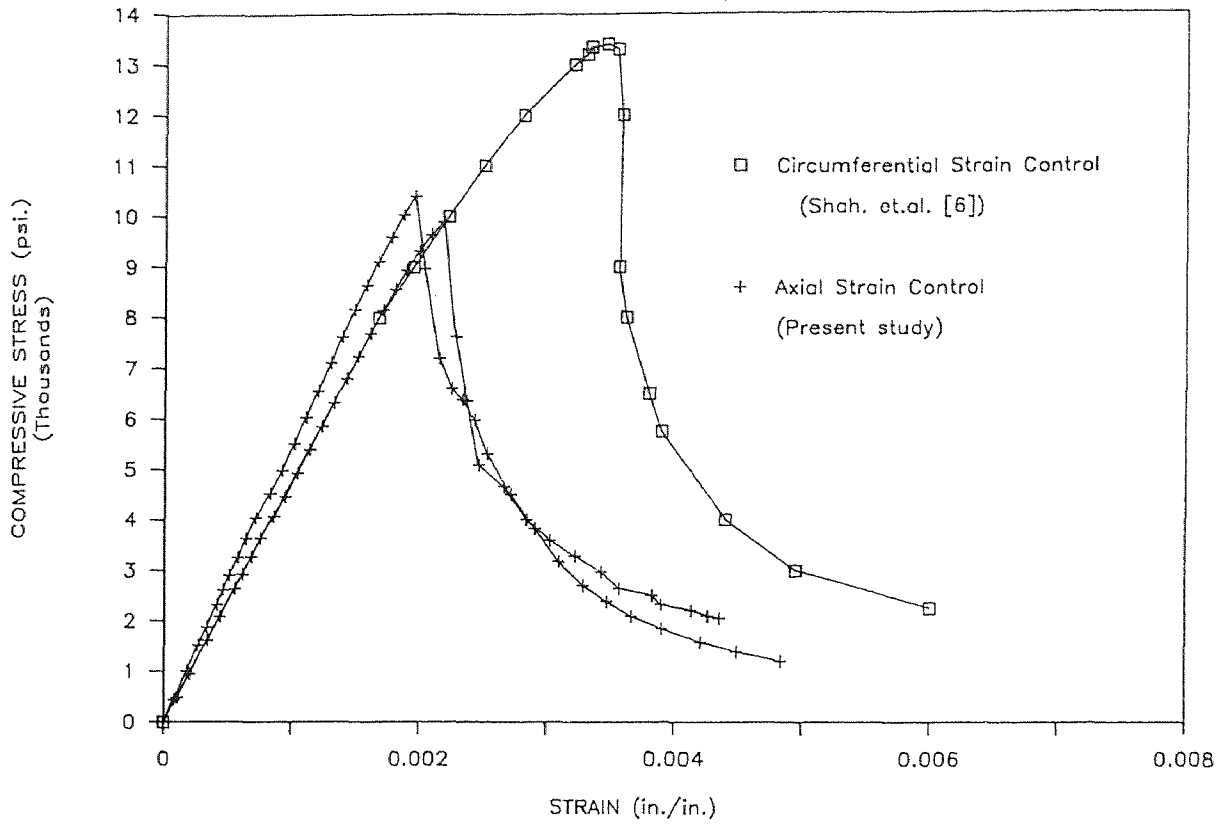


Fig. 5.3 Comparison of Stress vs. Strain Curves of HSC between Closed-Loop Axial and Circumferential Strain Control

5.1.3 Flexural Properties

Table V.2 presents the average flexural properties of five different sizes of beams 1x2x12, 2x4x12, 2x5x24, 4x6x30, and 6x6x30 in. of both microsilica and polymer concrete and compare with values from ACI flexural strength equation ($f_r = 7.5(f'_c)^{0.5}$). The modulus of rupture decreases with the increase of beam sizes for microsilica concrete whereas for polymer concrete, the modulus of rupture increases with the increase of beam size. The modulus of rupture of 6x6x30 in. beam size decreases about 16 % when compared to a smaller (2x4x12 in.) beam size of microsilica concrete while it increases 18.5 % for a 2x4x12 in. beam size when compared to a smaller (1x2x12 in.) beam size of polymer concrete. The flexural strength of both high strength microsilica and polymer concrete are higher than the calculated values from the ACI flexural strength equation. The flexural strength of high strength concrete is about 41 % higher than the ACI recommendation for microsilica concrete and 281 % for polymer concrete. Thus the ACI flexural equation is very conservative and may be inaccurate for high strength cement-based composites. Fig.5.4 shows the typical flexural stress versus deflection curves of different beam sizes of both microsilica and polymer concrete.

A typical splitting test result is presented in Fig.5.5. The average tensile stress of polymer concrete from the six 3x6 in. cylinder splitting test was 696.70 psi. This tensile stress was about 1.12 times higher than the ACI flexural stress (613.69 psi.) and 0.298 times the flexural test. Details of all other flexural stress - deflection curves are compiled in Appendix B.

TABLE V.2 FLEXURAL PROPERTIES OF
HIGH STRENGTH CONCRETE

Type of HSC	Size of Beam	Curing (day)	Max. P (lb.)	f'_r (psi.)	Max. Def $\times 10^{-2}$ in	Modulus of Elasticity $\times 10^6$ psi	$\frac{f_{r \text{ test}}}{f_{r \text{ ACI}}}$
Microsilica Concrete	2x4x12	155	2241	1049	1.290	0.306	1.537
	2x5x24	155	1428	942	1.004	1.532	1.380
	4x6x30	155	3355	980	2.762	2.440	1.436
	6x6x30	155	4527	880	1.898	1.075	1.289
Polymer Concrete	1x2x12	9	644	2098	4.360	0.728	3.419
	2x4x12	9	5361	2573	7.278	0.201	4.139

Remarks :

* ACI flexural equation, $f'_r = 7.5 \sqrt{f'_c}$
 For microsilica conc. $f'_r = 682.56$ psi.
 For polymer conc. $f'_r = 613.69$ psi.

FLEXURAL STRESS VS. DEFLECTION

MICROSILICA CONC. and POLYMER CONC.

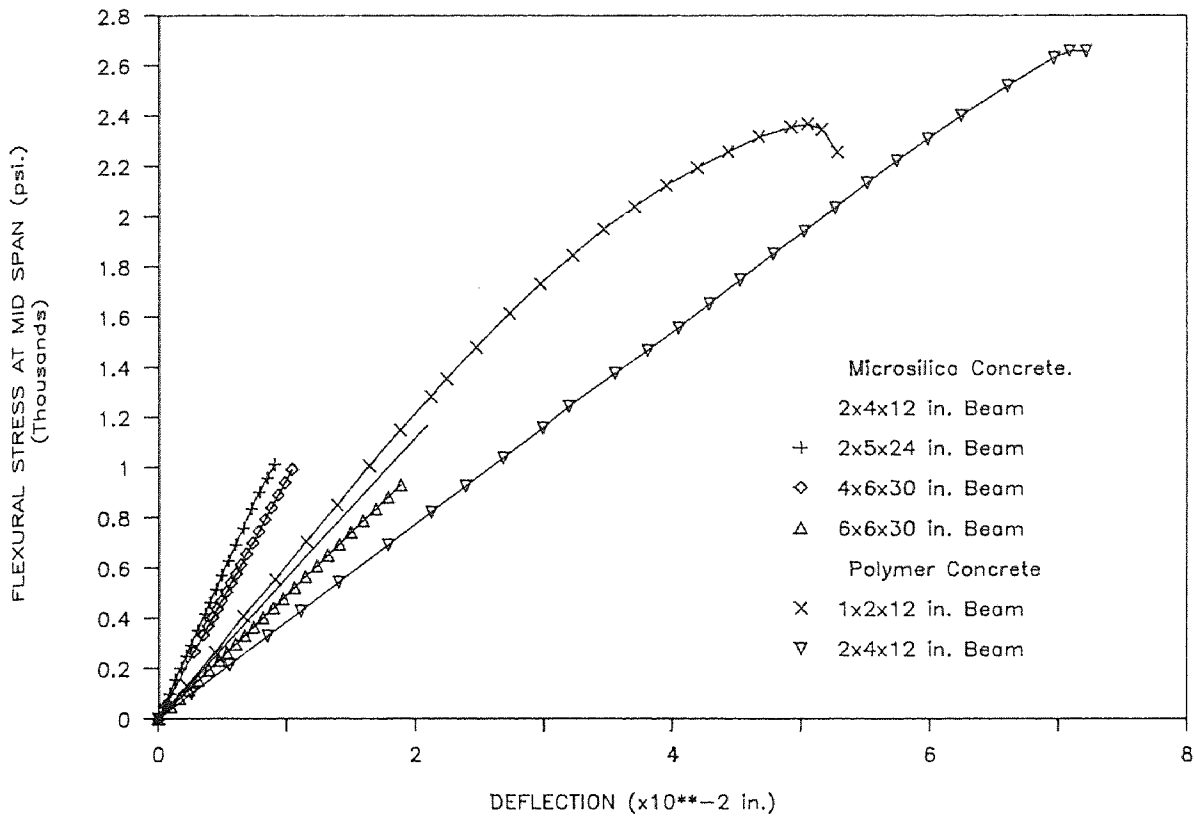


Fig. 5.4 Comparison of Flexural Stress vs. Deflection of Different Beam Sizes of High Strength Concrete

SPLITTING TEST

POLYMER CONCRETE (PS5)

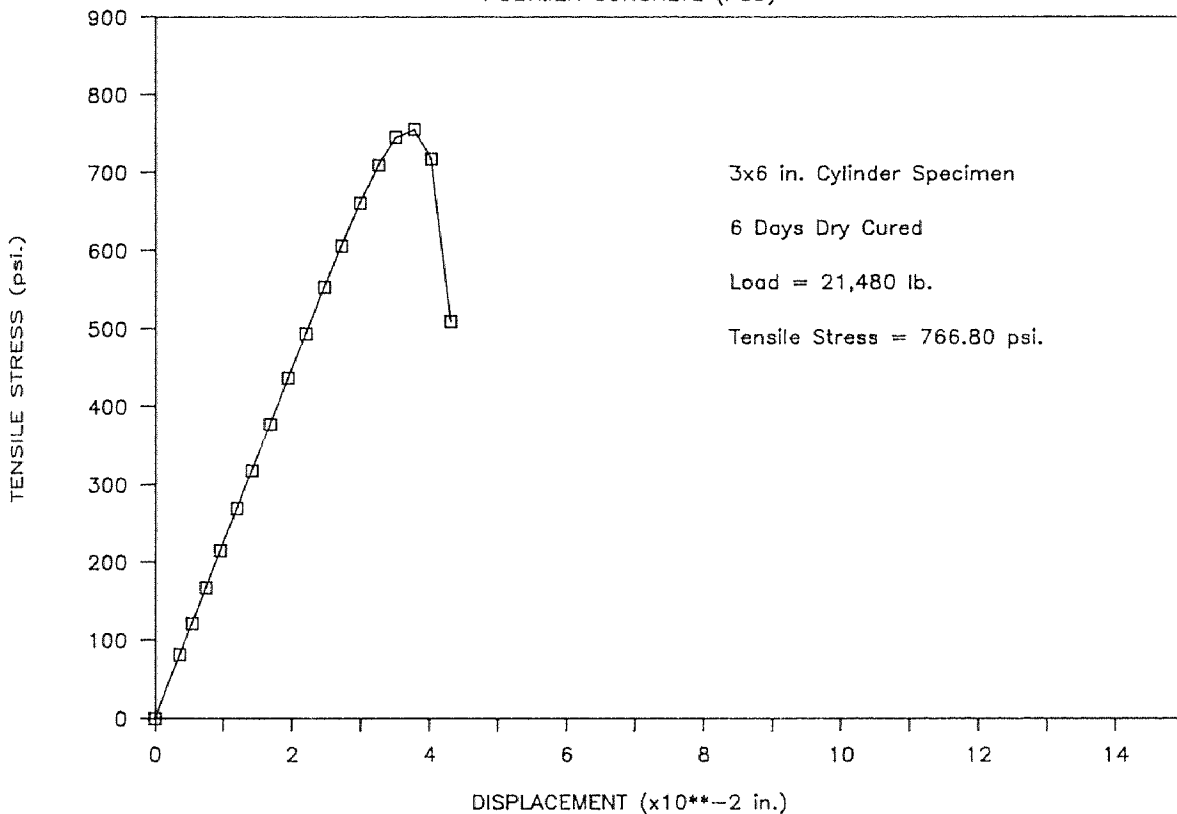


Fig. 5.5 Typical Tensile Stress vs. Displacement by Splitting Test Method

5.1.4 Tensile Strength

Two types of specimens, tapered and dog-bone specimens, were used in tension tests for this study. Tapered specimens were used for microsilica concrete, and dog-bone specimens were used for polymer concrete to study the post-peak stress displacement relationships. Table V.3 presents the average tension properties of different cement-based composites. The results indicate that normal concrete has lower tensile strength and peak displacement than high strength concrete. Polymer concrete shows the highest peak tensile stress (617.50 psi.) and peak displacement (0.141×10^{-2} in.). The average peak tensile stress of microsilica and polymer concrete are about 61 % and 154 % higher than normal concrete respectively. The energy absorption of high strength concrete is also higher than normal concrete. Polymer concrete absorbed the highest energy because of its plastic property as shown in Fig.5.6. Also observed is that the pull-out displacements of these high strength concretes differed from each other as well as from normal concrete. The pull-out displacement at the peak-load of normal concrete is about 66 % higher than microsilica concrete and 200 % lower than polymer concrete. Appendix C summarizes all the direct tension test results of both normal and high strength concrete.

TABLE V.3 DIRECT TENSION PROPERTIES
OF CEMENT-BASED COMPOSITES

Type of Concrete	Peak Stress (psi.)	Peak Displ. ($\times 10^{-2}$ in.)	Type of Specimen
Normal Concrete	243.14	0.044	Tapered Spec.
Microsilica Conc.	391.50	0.015	Tapered Spec.
Polymer Concrete	617.50	0.141	Dog-Bone Spec.

DIRECT-TENSION TEST

CEMENT BASED COMPOSITES (N-M-P)

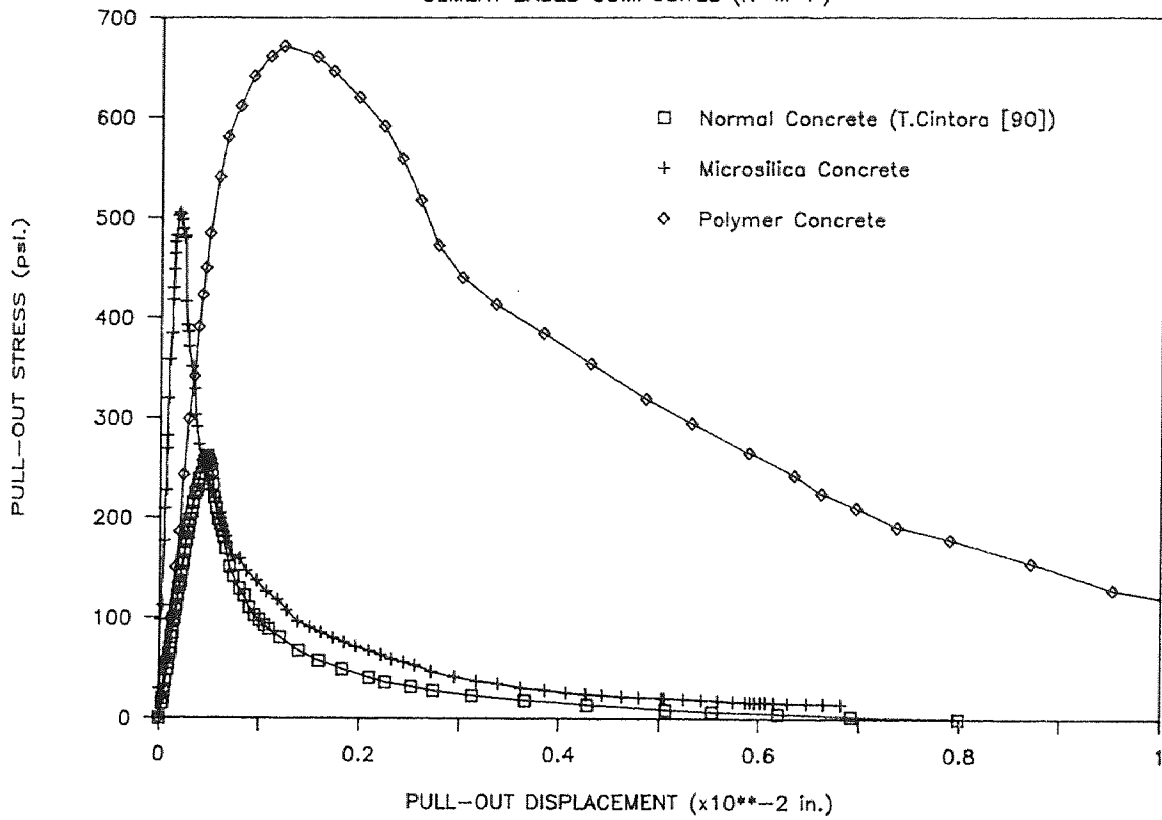


Fig. 5.6 Comparison of Pull-Out Stress vs. Displacement Relationship of Cement-Based Composites

5.2 Bond Strength-Slip Relationship

The bond strength-slip behaviors reported for normal concrete [7, 10] are widely scattered. These variations were attributed to many factors, such as loading rate, lateral confinement, monotonic or cyclic loading, size of specimen and concrete cover, and the embedment length. In this study, the bond strength properties can be divided into 2 parts, bond strength of reinforced high strength concrete and pull-out stress of high strength fibrous concrete. Two types of fibers, straight-end and hooked-end fibers are used.

5.2.1 Reinforced High Strength Concrete

Three different deformed bar sizes, #3, #4, and #6 were reinforced in a microsilica concrete cubes of 5x5x5, 5x5x5 and 8x8x8 in. respectively. Embedment length was five times the bar diameter. The average bond strength properties of reinforced high strength concrete are detailed in Table V.4. The results indicate that the larger the bar diameter used the lower the bond strength, bond factor (f_r^{\max}/f'_c) and slip obtained. The bond factor and slip per embedment length of reinforced microsilica concrete are ranging between 0.170 to 0.276 and 1.213 to 3.068 respectively. The average maximum bond strength observed from all three deformed bar sizes was 2518 psi. and the average maximum slip of 0.00767 in. This slip is only 10 % of those reported for normal concrete of 0.06 to 0.08 in. by Martin [7] and about 77 % if compared to the value of 0.01 in. given by Edward [10]. A 10-fold decrease in slippage of high strength matrix may cause some concerns over the required development length if the present design code is followed. Fig.5.7 presents the bond-slip relationship of deformed bars in high strength concrete as compared to normal concrete.

Another interesting parameter studied here is the bond factor, a ratio defined as the maximum bond strength (f_r^{\max}) over the ultimate compressive strength (f'_c). The average bond factor obtained for high strength concrete in this study was about 0.212 while most reported values for normal concrete are ranging from 0.15 and 0.26 [10,11]

TABLE V.4 BOND STRENGTH PROPERTIES OF
REINFORCED HIGH STRENGTH CONCRETE

Bar Sizes	f'_c (psi.)	f_r^{\max} (psi.)	Slip $\times 10^{-3}$ in	Bond Fac. f_r^{\max}/f'_c	Slip/ L_d ($\times 10^{-3}$)
# 3	9113	2518	7.67	0.276	3.068
# 4	8816	1672	6.99	0.189	2.796
# 6	11134	1893	4.55	0.170	1.213

Remarks :

f'_c - Compressive Stress (psi.)

f_r^{\max} - Modulus of Rupture (psi.)

f_r^{\max}/f'_c - Bond Factor

respectively to 0.60 [10,62,66]. Bond factors as high as 1.0 has also been reported by Hawkin [66]. These high values mostly resulted from the effect of confinement provided in the test specimens.

Since high strength concrete is generally more brittle than normal concrete and usually exhibits lesser extent of microcracks, the pull-out slip in high strength matrix should then be less than those in normal concrete This behavior was observed and confirmed in the present study. However, the results in this study also indicate that bond strength in both high strength concrete and normal concrete are essentially the same. The present findings may lead to the conclusion that if high strength concrete is used, sufficient development length should be provided to ensure proper bonding and to avoid catastrophic failure.

PULL-OUT TEST

REINF. HIGH STRENGTH CONC. (BAR #3,4,6)

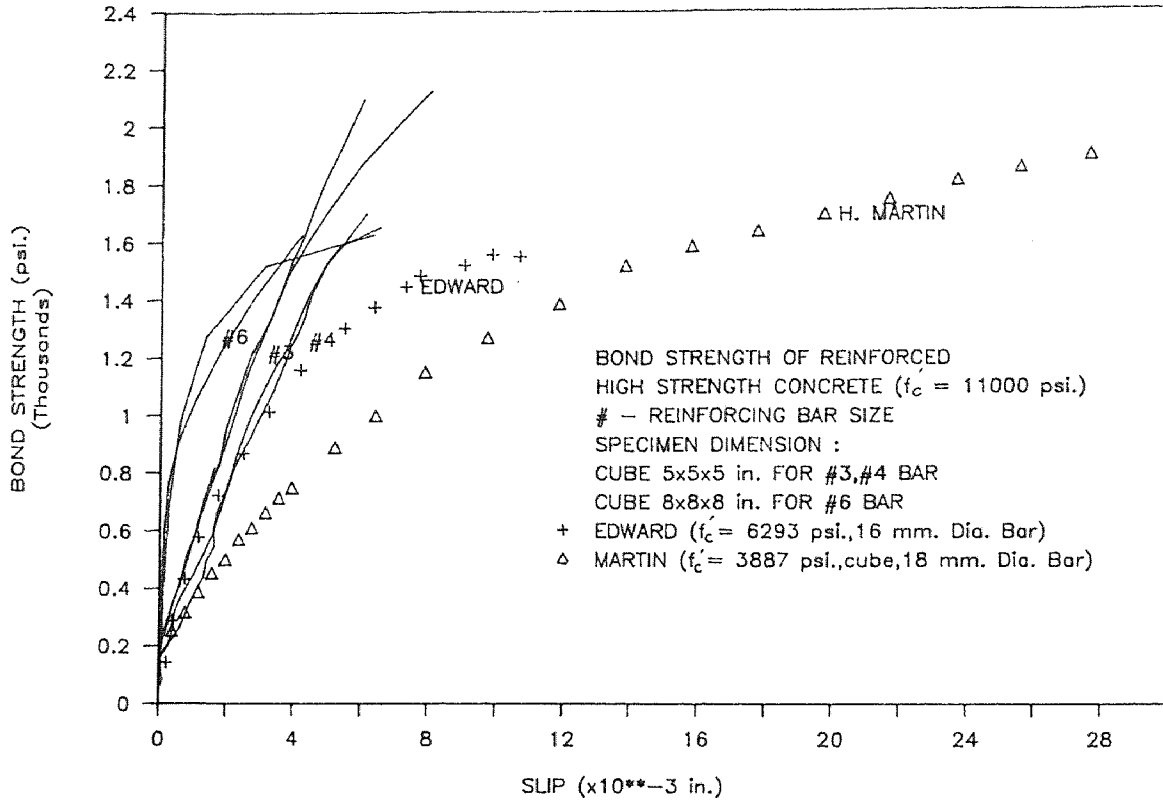


Fig. 5.7 Bond-Slip Relationships of Deformed Bars under Pull-Out Test

5.2.2 Fiber Reinforced High Strength Concrete

In brittle materials like concrete, the addition of steel fiber greatly improves the resistance to crack growth, enhanced ductility, impact resistance, and energy absorption capacity of the unreinforced matrix. Since these small fibers are, in practice, randomly distributed in the matrix during the mixing process, thus such random distribution of fibers was maintained in this study. The tapered fiber reinforced concrete specimens were tested in direct tension to study the fiber pulled-out behavior. Table V.5 presents the average pull-out stress properties of different type of high strength concrete and high strength fibrous concrete as compared to normal concrete. Included in the table are the peak stress, peak displacement and the steel fiber volume fraction used in the mix.

5.2.2.1 Load Displacement Relationship

The typical pull-out stress and displacement relationship of straight-end steel fiber and hooked-end steel fiber with five different fiber volume fractions of 0, 0.50, 1.00, 1.50, and 2.00 % are shown in Figs.5.8 & 5.9. It is quite obvious that the presence of fiber has significant effect on the pull-out behavior. The higher the fiber volume fraction, the larger are the peak stress and the amount of energy absorption. More importantly, the post-cracking energy is the dominating portion of fiber reinforced composites. Depending on the volume fraction, the length and type of fibers, this post cracking energy varies. Also interesting is the concept of maximum crack width where all fibers are completely pulled-out. This critical crack width is believe to equal half the fiber length. Fig.5.10 shows the typical pull-out stress versus displacement of different high strength concrete and high strength fibrous concrete with a 2.0 % steel fiber volume fraction. The results indicate that high strength fibrous concrete with both straight-end fiber and hooked-end fiber absorbs more energy than unreinforced high strength concrete and polymer concrete. Also showed is the effect of end type of the fiber. For straight-end fiber, the post peak pull-out stress versus displacement is gradually and smoothly

TABLE V.5 BOND STRENGTH PROPERTIES OF
HIGH STRENGTH FIBROUS CONCRETE

Type of Concrete	V_f (%)	Peak Load-lb	Peak Stress-psi	Peak Displ. ($\times 10^{-2}$ in)
Normal Concrete	0.0	523	243.14	0.044
Microsilica Conc.	0.0	905	391.50	0.015
Polymer Concrete	0.0	411	617.75	0.141
HSFC(Straight End)	0.5	1068	535.26	0.029
	1.0	775	355.73	0.018
	1.5	1136	544.04	0.034
	2.0	1342	640.09	0.116
HSFC (Hooked-End)	0.5	1103	516.50	0.021
	1.0	1128	521.50	0.025
	1.5	1335	602.67	0.021
	2.0	1385	665.10	0.066

Remarks :

V_f - Fiber volume fraction (%)

drops to zero, while for hooked-end fibers, the post-peak pull-out stress drops in a series of envelopes down the post-peak portion of the curve because of the slip at the end of the hooked-end fiber. The maximum pull-out displacements presented here are 25 times longer than those reported by Gopalaratnam and Shah [18]. Details of all other pull-out stress versus displacement curves of normal, and high strength concrete and high strength fibrous concrete are summarized in Appendices D and E respectively.

PULL-OUT STRESS VS. DISPLACEMENT CURVE

HSFC (STRAIGHT END FIBER)

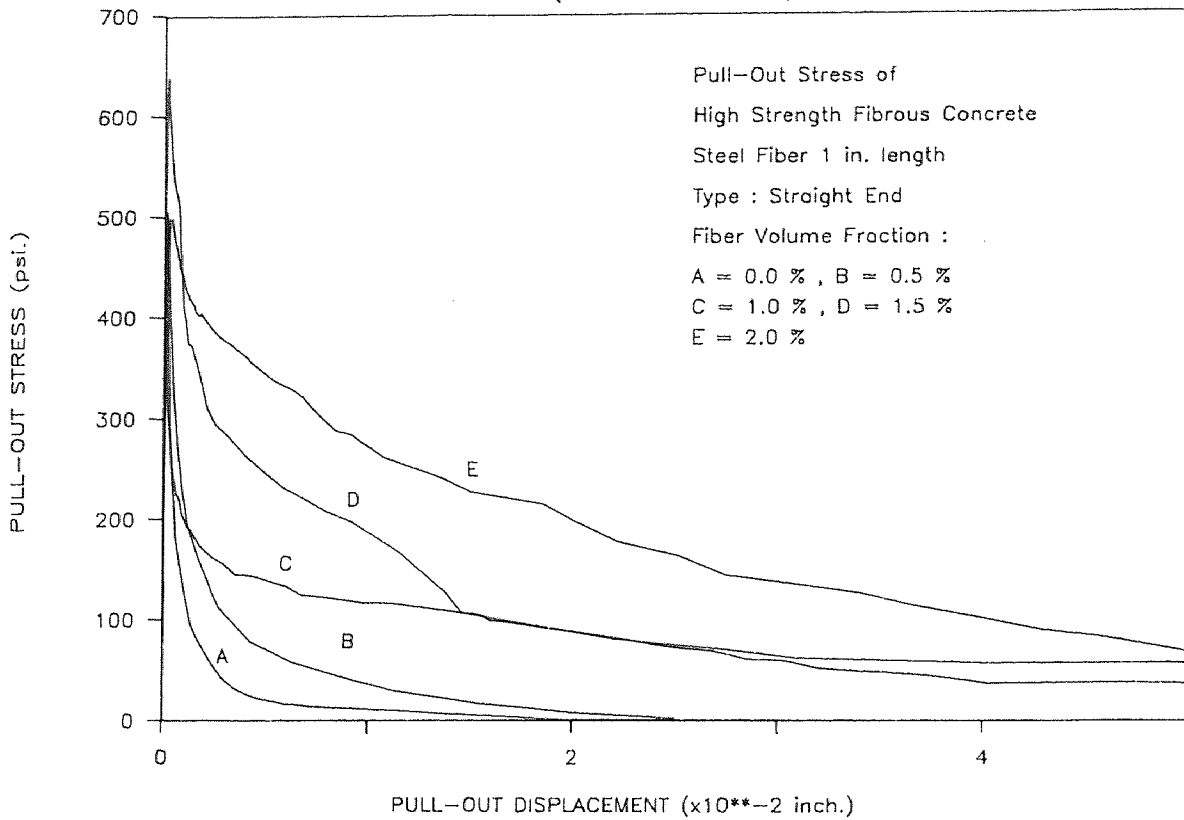


Fig. 5.8 Typical Pull-Out Stress vs. Displacement of High Strength Fibrous Concrete (Straight-End Fiber)

PULL-OUT STRESS VS. DISPLACEMENT CURVE

HSFC (HOOKED END FIBER)

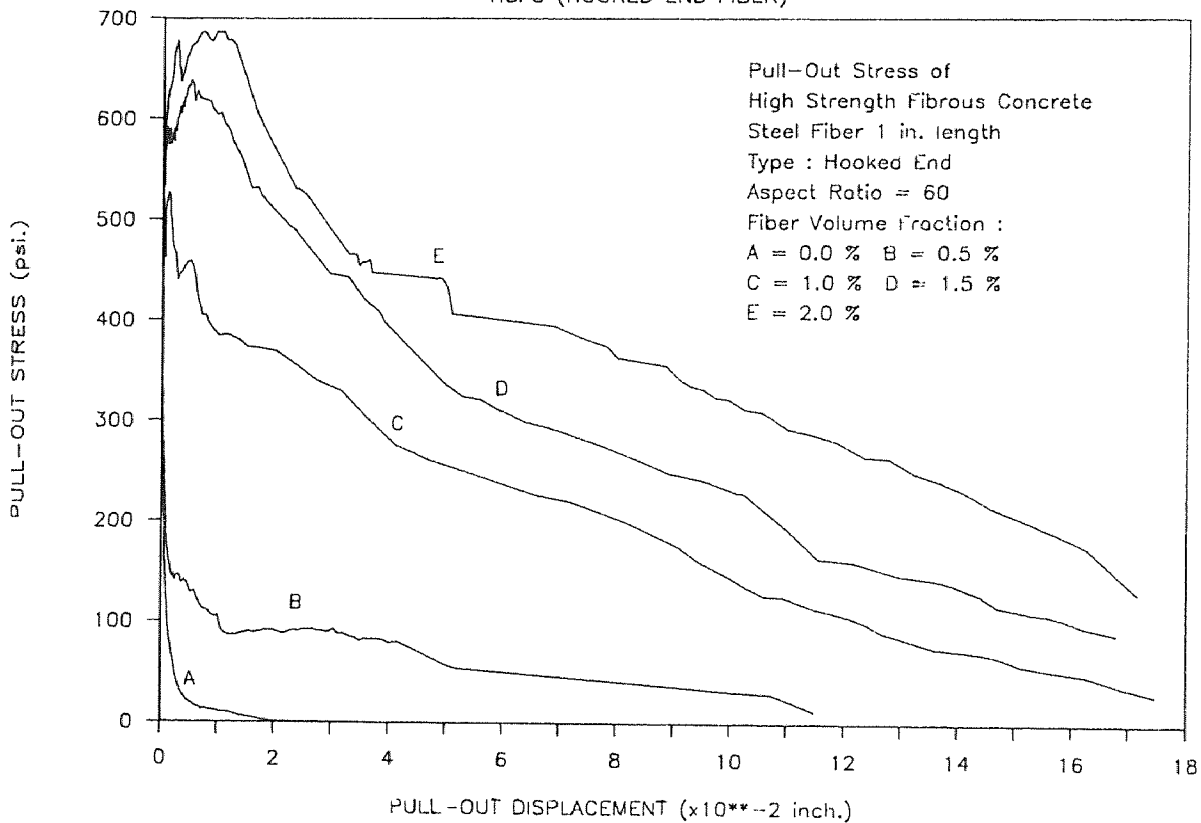


Fig. 5.9 Typical Pull-Out Stress vs. Displacement of High Strength Fibrous Concrete (Hooked-End Fiber)

PULL-OUT STRESS VS. DISPLACEMENT

HSC and HSFC

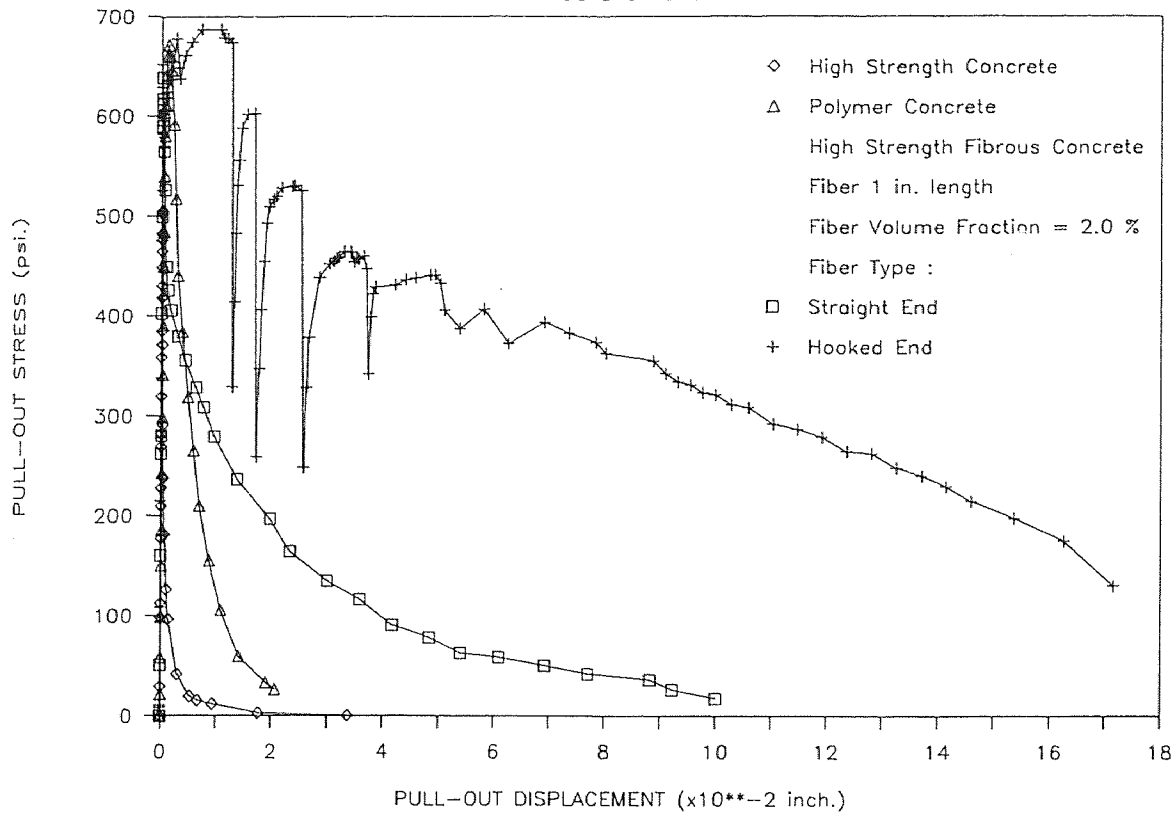


Fig. 5.10 Pull-Out Stress vs. Displacement of Different High Strength Concrete and High Strength Fibrous Concrete

5.2.2.2 Normalized Load-Displacement Relationship

It was anticipated that there would be a unique relationship of the load versus the displacement for cementitious materials. However due to different mix proportions, different amounts of fiber volume fractions, and the varying strength of the tested specimens, it was necessary to normalize the results obtained. The load was normalized with respect to the peak load and the displacement with respect to the maximum post-peak displacement. For high strength fibrous concrete, the maximum pull-out displacement was observed to be about half of the fiber length. Thus the displacement of high strength fibrous concrete was normalized with respect to the half fiber length.

The normalized post-peak pull-out stress versus pull-out displacement relationship for high strength concrete, normal concrete [90,92], high strength fibrous concrete, and normal fibrous concrete [17,19] are compared in Figs.5.11 & 5.12. The results show that such a normalized relationship is unique for both normal concrete [17,19,90,92] and high strength concrete. The shape of the unique normalized curves is associated with the brittle nature of the cement-based composites. The lower the curve, the more brittle is the material. Figs.5.11 & 5.12 also confirm that high strength composites are generally more brittle than normal cemented materials. Similar conclusions are observed in both the straight-end and the hooked-end fibers reinforce high strength concrete. Appendices F and G summarize all the normalized pull-out stress versus displacement curves of both normal and high strength concrete and high strength fibrous concrete respectively.

NORMALIZED PULL-OUT STRESS VS. DISPL.

CEMENT-BASED COMPOSITES (BFSS520)

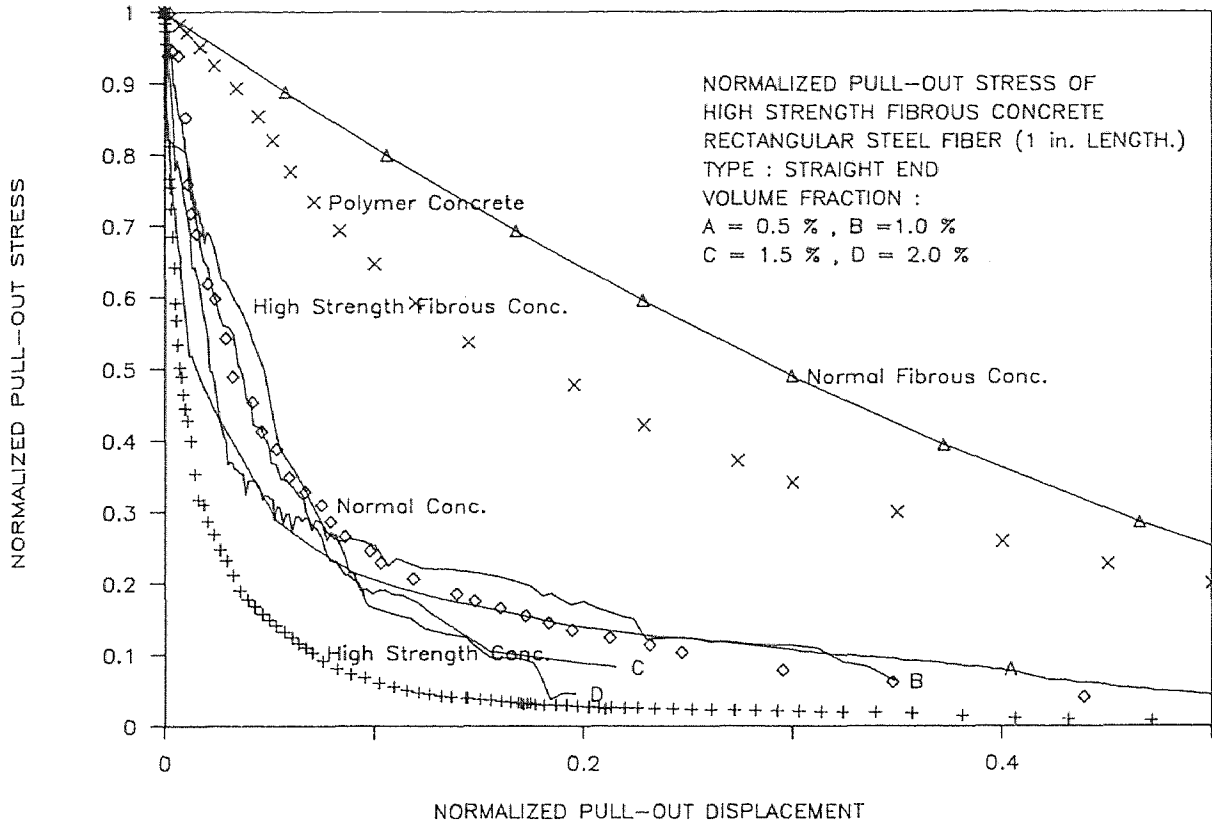


Fig. 5.11 Comparison of Normalized Pull-Out Stress vs. Displ. of Cement-Based Composites (Straight-End Fiber)

NORMALIZED PULL-OUT STRESS VS. DISPL.

CEMENT-BASED COMPOSITES (BFH520)

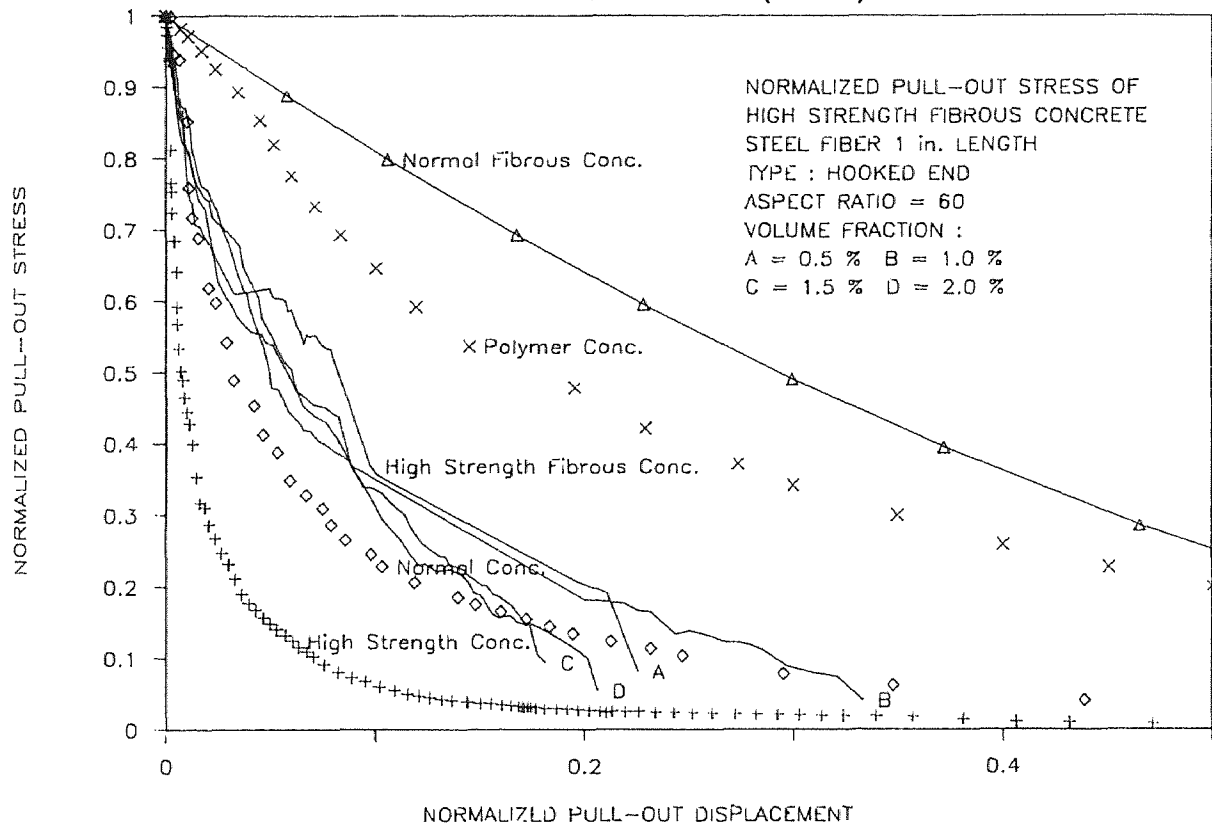


Fig. 5.12 Comparison of Normalized Pull-Out Stress vs. Displ. of Cement-Based Composites (Hooked-End Fiber) 79

5.3 Fatigue Characteristics

The fatigue characteristics are among the most important properties of the cement-based composites, especially for high strength concrete. It is generally agreed that the relative magnitude of the stress change under repeated load is the most important variable that influences fatigue life. The reported fatigue strength of normal concrete is about 60-65 % of f'_c . In this study, series of experiments on uniaxial cyclic compression test were conducted on three types of high strength concrete; superplasticizer concrete, microsilica concrete and polymer concrete. Maximum stress level varied from $0.4 f'_c$ to $0.9 f'_c$ while minimum stress level was kept constant at $0.10 f'_c$ in order to prevent stress reversal as well as to minimize the effect of capping and seating of the test fixture. Two different rates of loading, 6 Hz. and 12 Hz., were used to examine the effect of loading rate.

5.3.1 S-N Curve

The fatigue characteristics of a material subjected to repeated stress of constant magnitude is known as the S-N curve, where N is the number of cycles of stress (S), which would cause failure. Each material has its own unique S-N curve. With the S-N relationship, we can predict the fatigue life for a given maximum stress level. Fig.5.13 presents the S-N curves of the high strength cement-based composites as compared to that of normal concrete. The results indicate that the S-N curve for high strength concretes are not significantly different from normal concrete, except for polymer concrete because of the extensive plasticity.

The S-N curve of normal concrete was reported to be bilinear [77] whereas for high strength concrete, the reported S-N behavior is linear. The results observed from this study also indicates that the S-N curve of high strength concrete is linear.

S-N CURVE

HIGH STRENGTH CONCRETE (COM S-N)

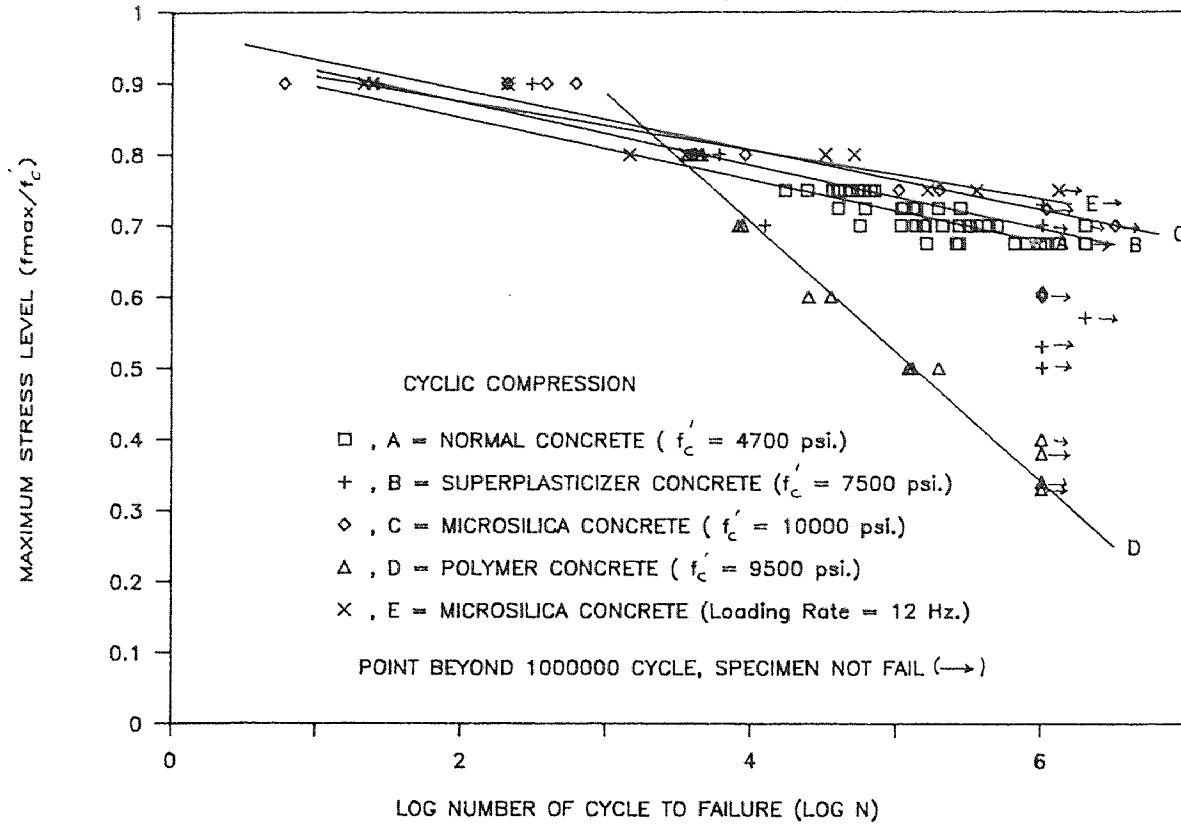


Fig. 5.13 Comparison of the S-N Curves of Different High Strength Concrete with Normal Concrete

5.3.2 Fatigue Strength

The term fatigue strength is generally defined as the strength that fails a specimen after one million cycle of repeated loading. For normal concrete, the fatigue strength is between 60-65 % of f'_c . Table V.6 presents the number of repeated stress to failure of different high strength concrete. The effect of loading rate is also included. The results indicate that the fatigue strength of high strength superplasticizer concrete and microsilica concrete are not significant different. Also observed was that there was little effect on the fatigue strength of microsilica concrete when the loading rate was changed from 6 to 12 Hz. The fatigue strength of superplasticizer concrete and microsilica concrete is between 70 - 75 % of f'_c . The fatigue limit (stress which specimen fails at 10 million cycles) of high strength concrete is about 66 % of f'_c compared to about 55 % of f'_c [25] for normal concrete. Apparently there is no fatigue limit for polymer concrete. Figs. 5.14-5.16 show typical fatigue tests for different high strength concrete with maximum stress level of $0.80 f'_c$.

For polymer concrete, fatigue characteristics are rather different from normal concrete and high strength concrete. Due to the plasticity of the matrix, large excessive deformations can easily be visualized during fatigue tests. Fig.5.17 presents one of the fatigue curves of polymer concrete sample loaded under a maximum stress range of $0.70 f'_c$. It can be seen that the strain increment over the first 8011 cycles was only 0.017 whereas the plastic strain from 8011 to 8051 cycles was 0.023. It was observed that most of the plastic strain in polymer concrete occurred during the later stages just prior to failure. The S-N curve of polymer concrete indicates the fatigue strength to be as low as 45 % of f'_c compared to 70-75 % for high strength concrete and 60-65 % for normal concrete. The results from this study seem to indicate that for non-plastic brittle concrete, the higher the compressive strength, the higher is the fatigue strength. Other details of the compressive stress-strain curves and normalized stress-strain curves of each fatigue test specimen of different high strength concrete and rate of loading can be found in Appendices H and I respectively.

TABLE V.6 NUMBER OF CYCLES TO FAILURE
UNDER REPEATED LOAD

Type of Concrete	Maximum stress level (f_{\max}/f'_c)						
	0.90	0.80	0.75	0.70	0.60	0.50	0.40
* Superplasti- cizer Conc.	26	5,875	430,510	M	M	M	-
	300	4,096	-	M	M	M	-
	F	4,566	-	12,299	-	-	-
	F	-	-	-	-	-	-
* Microsilica Concrete	380	4,014	102,200	M	M	-	-
	204	8,937	196,546	M	M	-	-
	6	-	-	-	-	-	-
	608	-	-	-	-	-	-
	F	-	-	-	-	-	-
	F	-	-	-	-	-	-
* Polymer Concrete	-	3,608	-	8,650	24,789	121,431	M
	-	4,476	-	8,052	35,034	127,800	M
	-	-	-	-	-	196,800	M
	-	-	-	-	-	-	M
** Microsilica Concrete	24	3,470	161,210	M	-	-	-
	21	1,431	353,502	M	-	-	-
	204	31,683	1291,367	-	-	-	-
	-	50,277	-	-	-	-	-

Remarks :

- M - Specimen not fail at N = 1,000,000 load cycles
- F - Specimen failed
- * - Rate of loading = 6 Hz.
- ** - Rate of loading = 12 Hz.

FATIGUE TEST

SUPERPLASTICIZER CONC., R=6 Hz.(S1F108)

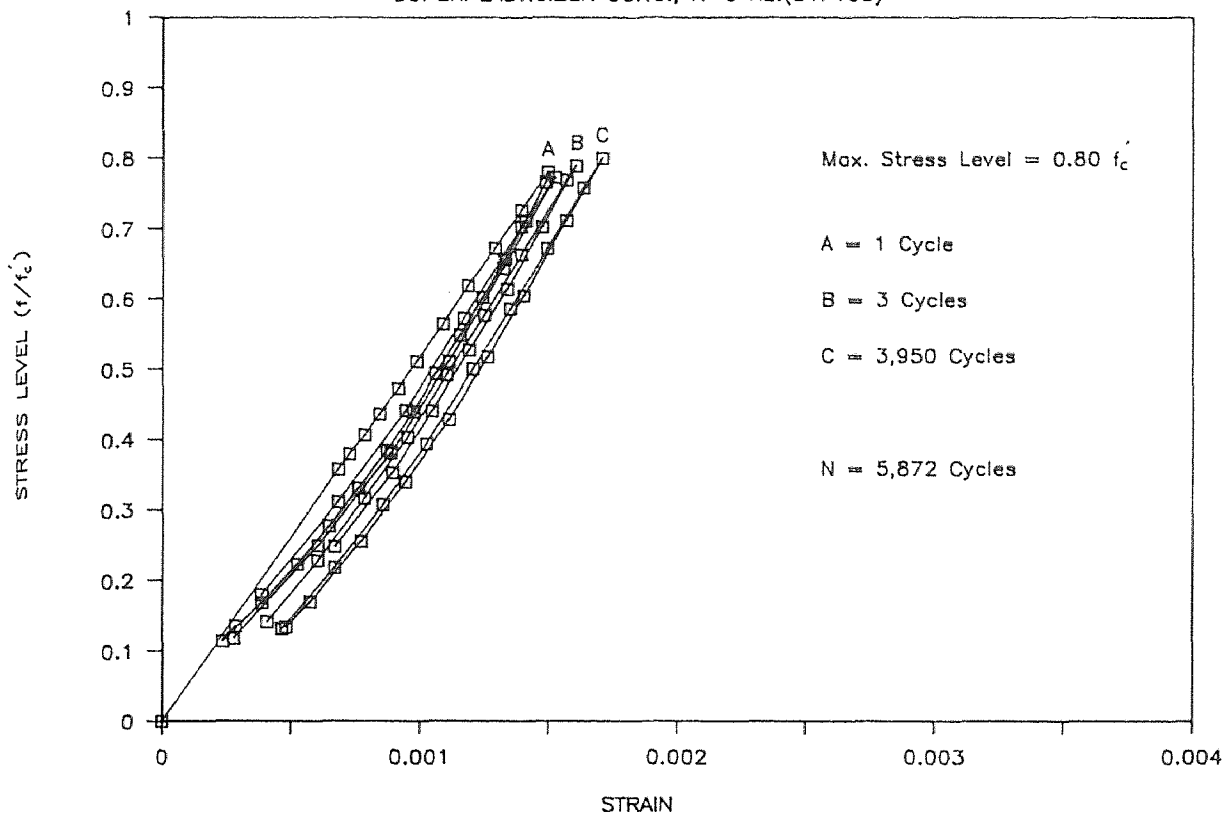


Fig. 5.14 Typical Stress vs. Strain Curve under Cyclic Compression Test of Superplasticizer Concrete

FATIGUE TEST

MICROSILICA CONC., RATE = 6 Hz.(M2F208)

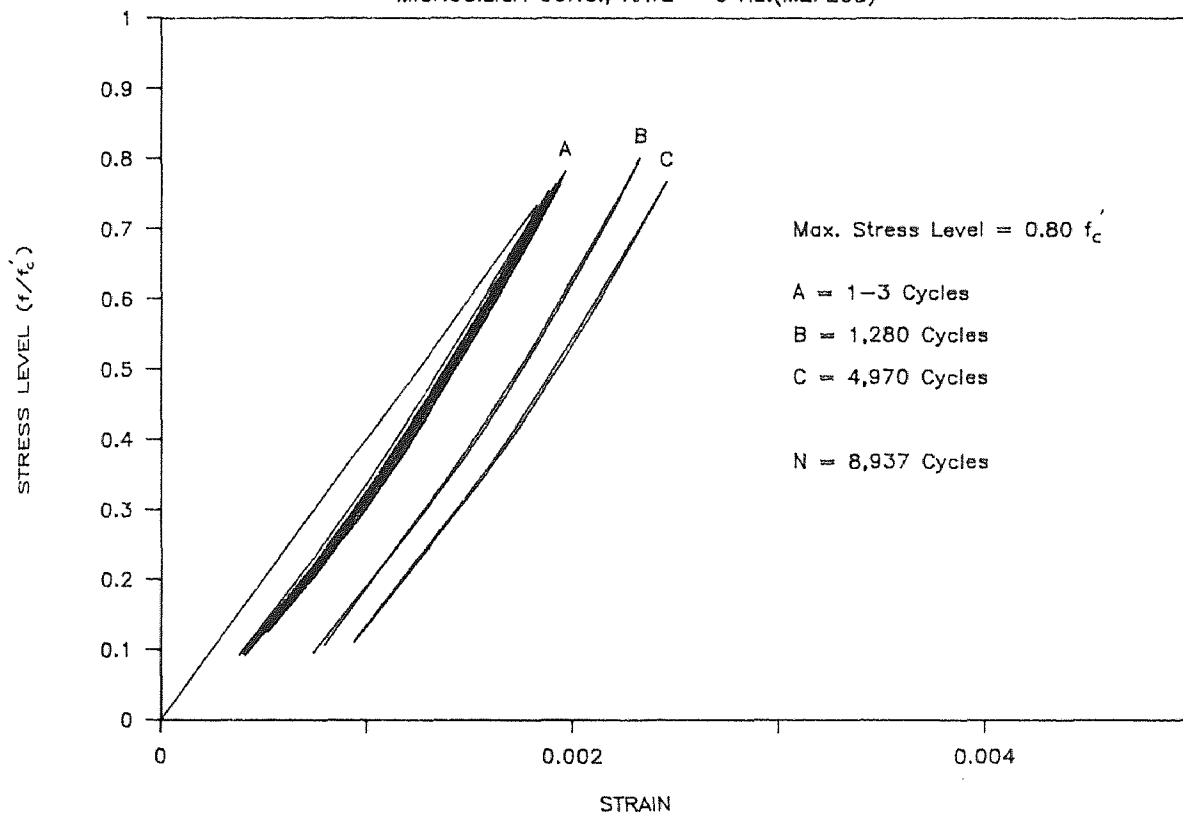


Fig. 5.15 Typical Stress vs. Strain Curve under Cyclic Compression Test of Microsilica Concrete (6 Hz)

FATIGUE TEST

MICROSILICA CONC., RATE = 12 Hz.(M3TF6)

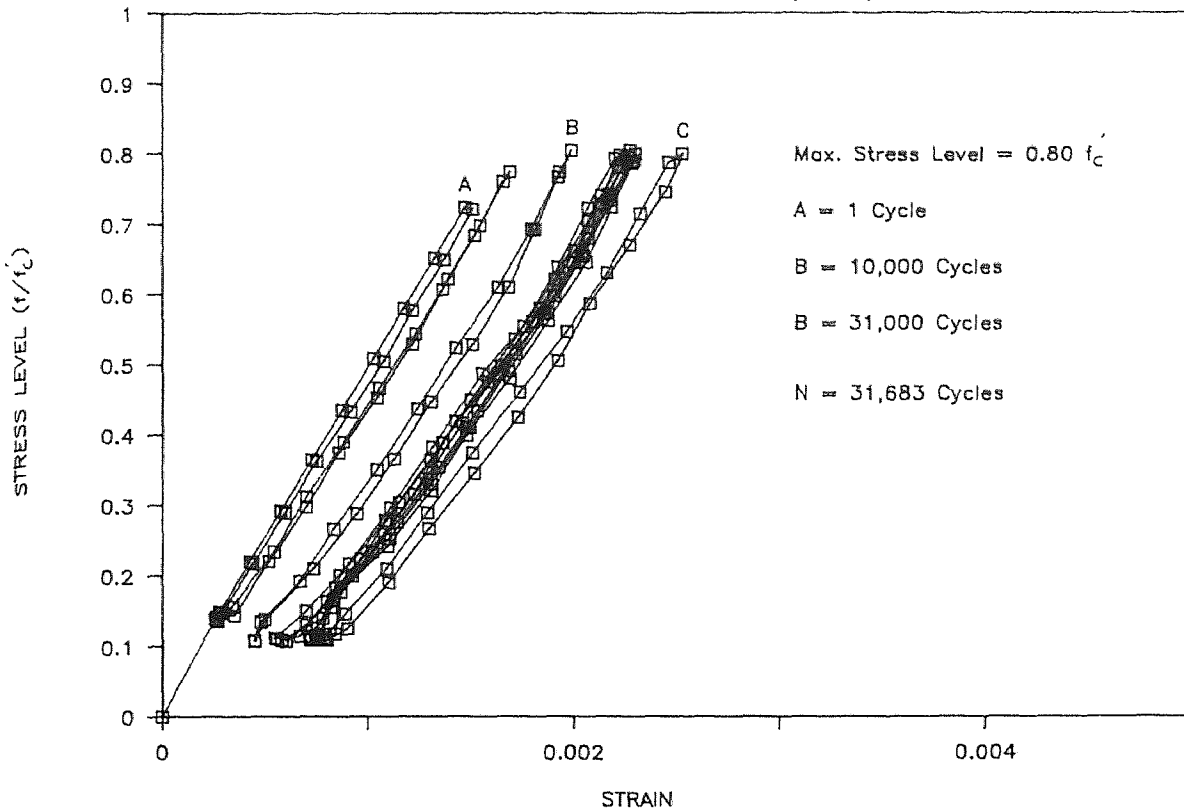


Fig. 5.16 Typical Stress vs. Strain Curve under Cyclic Compression Test of Microsilica Concrete (12 Hz)

FATIGUE TEST

POLYMER CONCRETE , RATE = 6 Hz. (PF207)

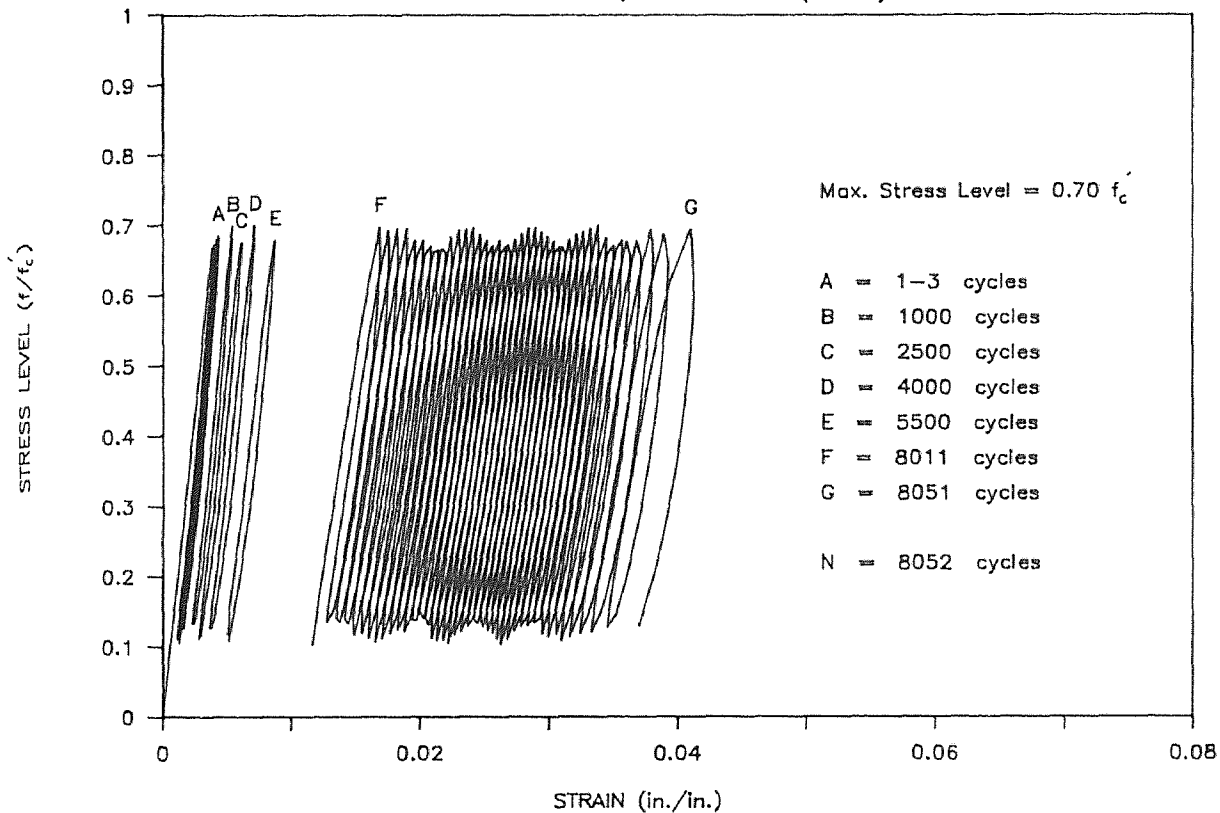


Fig. 5.17 Typical Stress vs. Strain Curve under Cyclic Compression Test of Polymer Concrete

5.3.3 Strain-Cycle Relationship

The recorded peak strains at different cycles of loading of the fatigue test were plotted in Fig.5.18. It was observed that the fatigue failure of high strength concrete generally occurred in three stages of strain rate. At low and high cycles of loading, strain rate is usually high whereas in the middle range (between 500-7500 cycles) the strain rate is rather constant. The same behaviors were also reported for normal concrete [78]. In general, for normal concrete and high strength brittle concrete, the middle portion represents up to 85 % of the whole fatigue response. For polymer concrete, The middle range can not be clearly defined. This is probably due to the plastic content added to the concrete. The strain rate concept which may be used to predict the fatigue strength of the matrix can only be applied to brittle concrete matrices such as normal concrete, superplasticizer concrete and microsilica concrete. For plastic materials like polymer concrete, the constant strain rate concept is not valid. This may be attributed to differences in the matrix formation process. In brittle matrices (normal concrete and high strength concrete), bonding is developed through the hydration process whereas in polymer concrete, a polymerization process develops plastic links which provide the strength to the composites. In addition, it is believed that the formations of microcracks in these two types of high strength (brittle and plastic) concretes are also different.

Fig.5.19 shows a comparison of the stress versus number of loading cycles of high strength superplasticizer concrete under monotonic and cyclic loading. The maximum and minimum stress levels for this test were 0.60 and 0.10 of f'_c . The specimen can sustain the load more than 2,000,000 cycles. It should be noted that the peak strain at any cycle under the cyclic load is usually less than the maximum strain of the monotonic load. The same behaviors were also observed in other applied ranges. This suggests that monotonic load curve may serve as the failure envelop of the fatigue behaviors. The fatigue behavior of microsilica concrete also exhibits similar responses as those reported for superplasticizer concrete. Appendix J summarizes all the

compressive stress versus strain curves under monotonic and cyclic loading of superplasticizer, microsilica and polymer concrete.

STRAIN VS. CYCLE CURVE

HIGH STRENGTH CONCRETE (COM S-C)

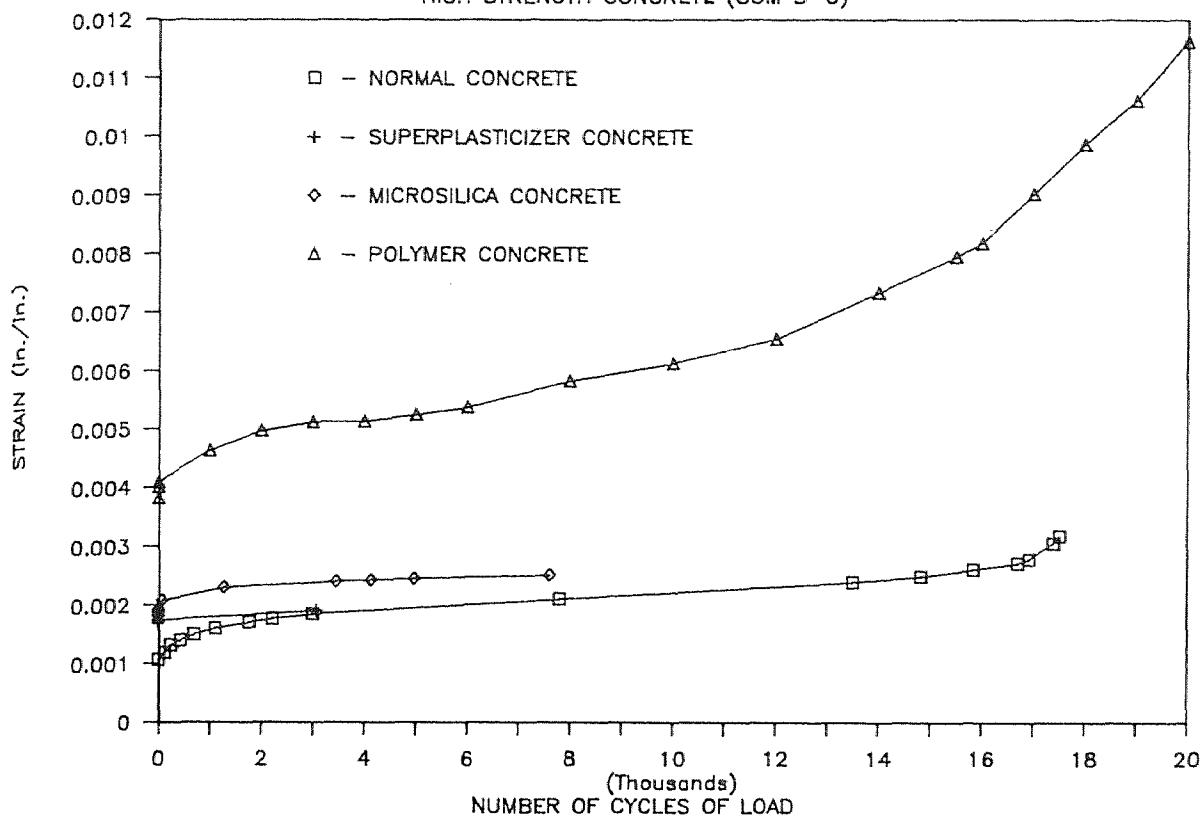


Fig. 5.18 Typical Peak Strain vs. No. of Cycles of Different High Strength Cement-Based Composites

MONOTONIC VS. CYCLIC CURVE

SUPERPLASTICIZER CONCRETE (S1F175)

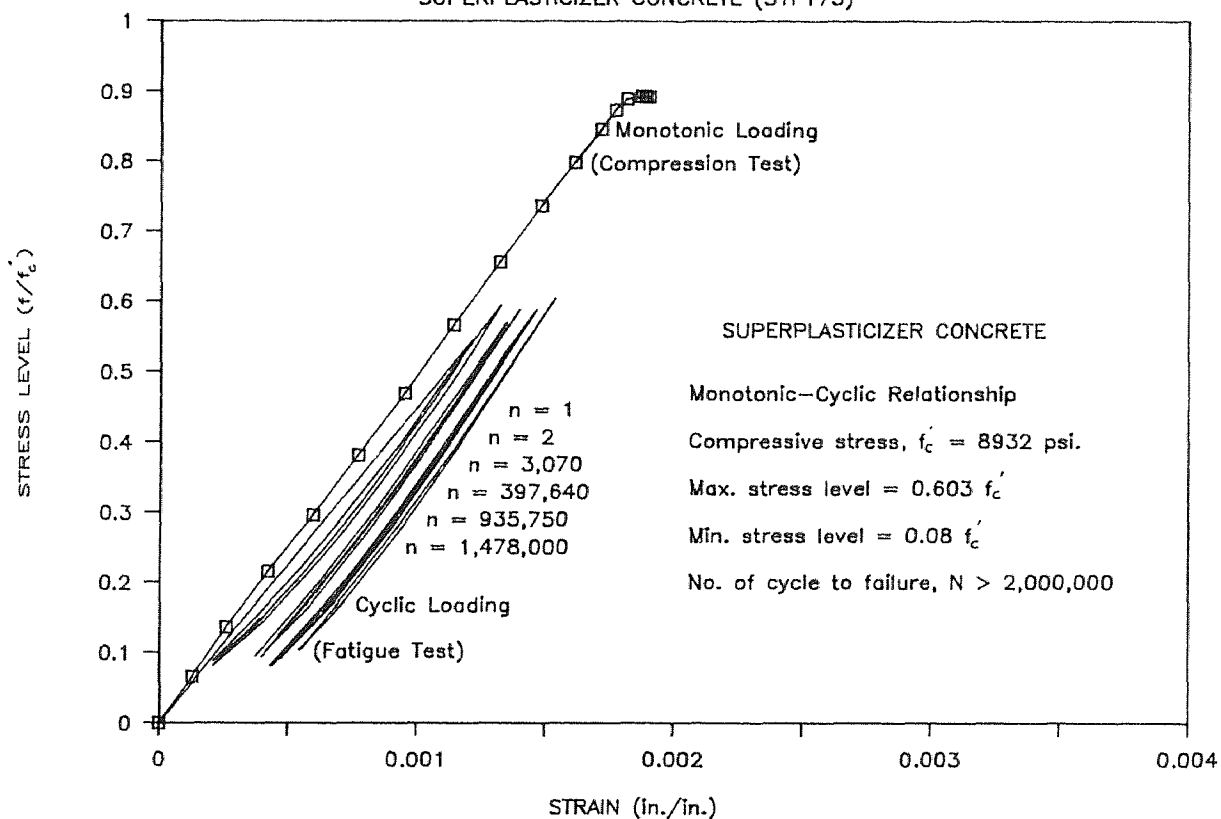


Fig. 5.19 Typical Monotonic vs. Cyclic Loading Relationship of High Strength Concrete

CHAPTER VI

EMPIRICAL MODEL

6.1 Bond Strength Characteristics

A empirical model of tension softening of concrete is necessary for analysis and design because to carry out direct tension tests in brittle material like concrete is very difficult.

6.1.1 Normalized Pull-Out Stress-Displacement Relationships

Since tension softening in brittle composites cannot easily be obtained from conventional testing machines. Closed-loop testing machines and very stiff testing machines are the only two means of obtaining the post-peak tensile responses of concrete. Since these machines are not commonly available, it is necessary to develop a means of predicting the tension softening of concrete. The concept of the normalized stress-displacement law recently developed by Wecharatana and Shah [19] is revised here to account for post-peak stress-displacement relationship for cement-based composites as follows:

$$\left[\frac{\tau}{\tau_{\max}} \right]^m + \left[\frac{\delta}{\delta_{\max}} \right]^{2m} = 1 \quad (6.1)$$

Where :

- τ - Post-peak pull-out stress
- τ_{\max} - Maximum pull-out stress of the cemented composite
(Max. post-peak pull-out stress for fibrous concrete)
- δ - Post-peak pull-out displacement
- δ_{\max} - Maximum pull-out displacement of the cemented composite (Half the fiber length for fibrous conc.)
- m - Brittleness Index of the composite

For Cemented Composite :

- τ_{\max} - Obtained from the normal testing (pull-out test)
- δ_{\max} - Obtained from the average grain size of sand as shown in Fig.6.1 [90].

For Fibrous Concrete :

Visalvanich [17] found that the maximum pull-out stress of steel fiber reinforced mortar can be expressed in terms of the fiber reinforcing index ($V_f l / \phi$) as :

$$\tau_{\max} = \alpha \sigma V_f \cdot \frac{1}{\phi} \quad (6.2)$$

Where :

- α = Efficiency factor
- σ = Interfacial bond strength
- and $\delta_{\max} =$ Half of the fiber length ($l/2$)

Since τ_{\max} and δ_{\max} can be obtained from normal testing methods and the size of the fiber respectively, the only variable in the proposed equation is the "BRITTLINESS INDEX". Table VI.1 presents the values of brittleness index for different types of cement-based composite, i.e., normal concrete, normal fibrous concrete, high strength concrete, high strength fibrous concrete with straight-end fiber, high strength fibrous concrete with hooked-end fiber, and polymer concrete. Among them, high strength concrete is the most brittle material and has the lowest brittleness index of 0.20. For normal concrete, the brittleness index is 0.265.

Figs. 6.2 to 6.8 show comparisons of the proposed equation with data from the present study and other researchers. The data from present study are for high strength concrete, high strength fibrous concrete (straight-end and hooked-end fibers) and polymer concrete. The data obtained from other researchers are for normal concrete [90], and normal fibrous concrete [12,17,19]. The results agree closely with the

MAXIMUM DISPLACEMENT VS. GRAIN SIZE

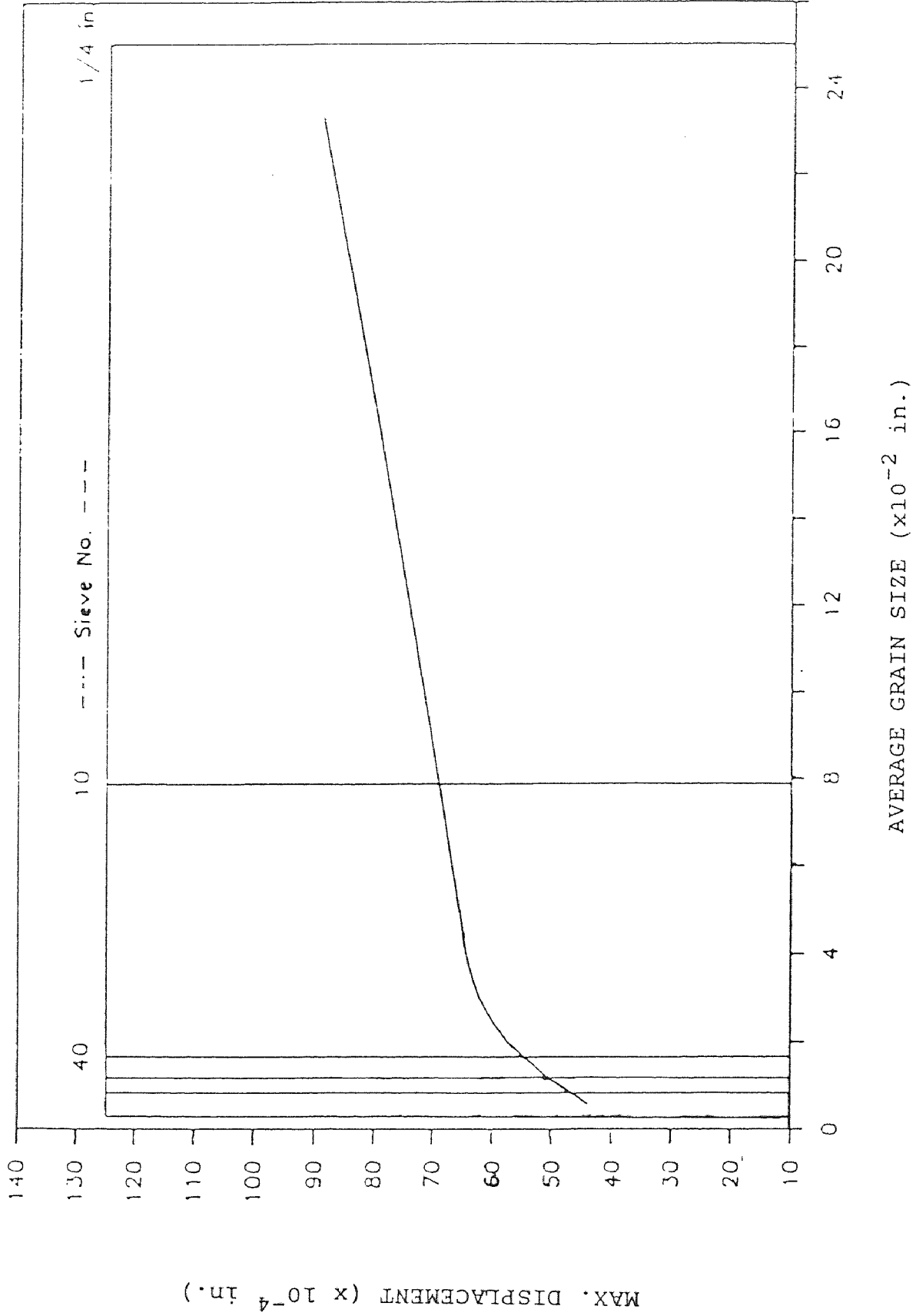


Fig. 6.1 Maximum Pull-Out Displacement vs. Average Grain Size of Sand

value predicted from Equation (6.1) with the different brittleness index of the composites. The standard errors between the experimental data and proposed equation are between 0.04 to 0.08 which is very small. Therefore, the predicted normalized pull-out stress versus pull-out displacement relationships of the composites obtained from the proposed equation as shown in Fig.6.8 can then be applied. These relationships can be used to predict not only the tension softening of the matrix but also fracture resistance, and energy absorption.

TABLE VI.1 BRITTLINESS INDEX OF THE MATERIALS

Type of Materials	Brittleness Index
High Strength Concrete	0.200
High Strength Fibrous Concrete (Straight End Fiber)	0.259
Normal Concrete	0.265
High Strength Fibrous Concrete (Hooked End Fiber)	0.290
Polymer Concrete	0.400
Normal Fibrous Concrete	0.500

NORMALIZED STRESS-DISPLACEMENT CURVE

NORMAL CONCRETE

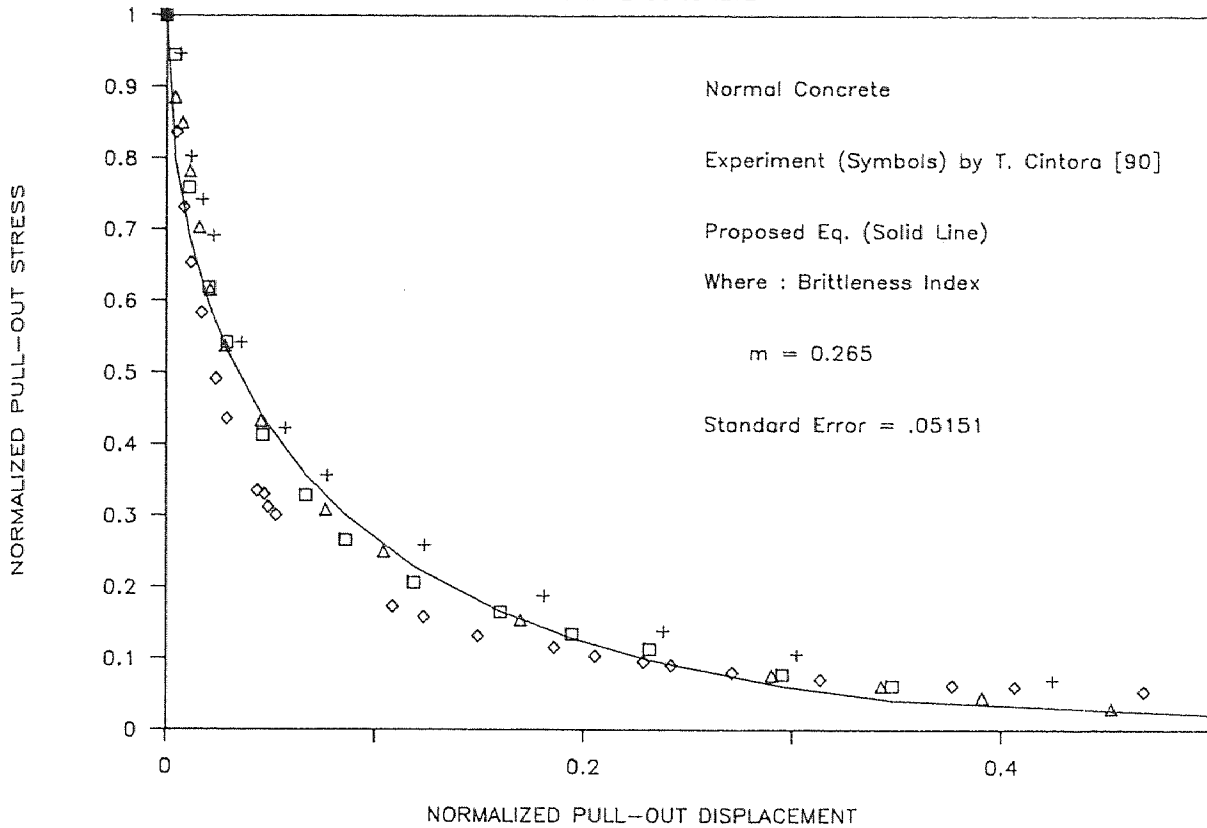


Fig. 6.2 Comparison of the Proposed Equation with Normal Concrete Data (T. Cintora [90])

NORMALIZED STRESS-DISPLACEMENT CURVE

HIGH STRENGTH CONCRETE

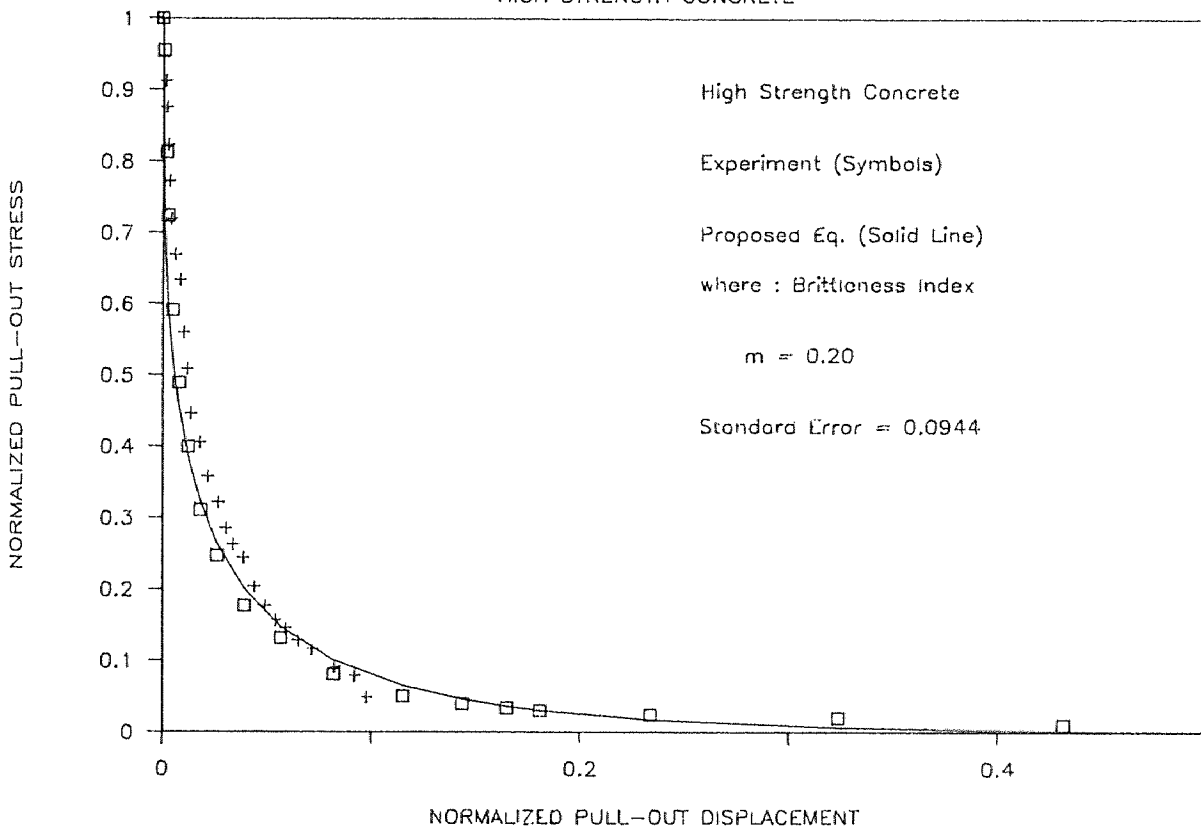


Fig. 6.32 Comparison of the Proposed Equation with High Strength Concrete Data (Present Study)

NORMALIZED STRESS-DISPLACEMENT CURVE

POLYMER CONCRETE

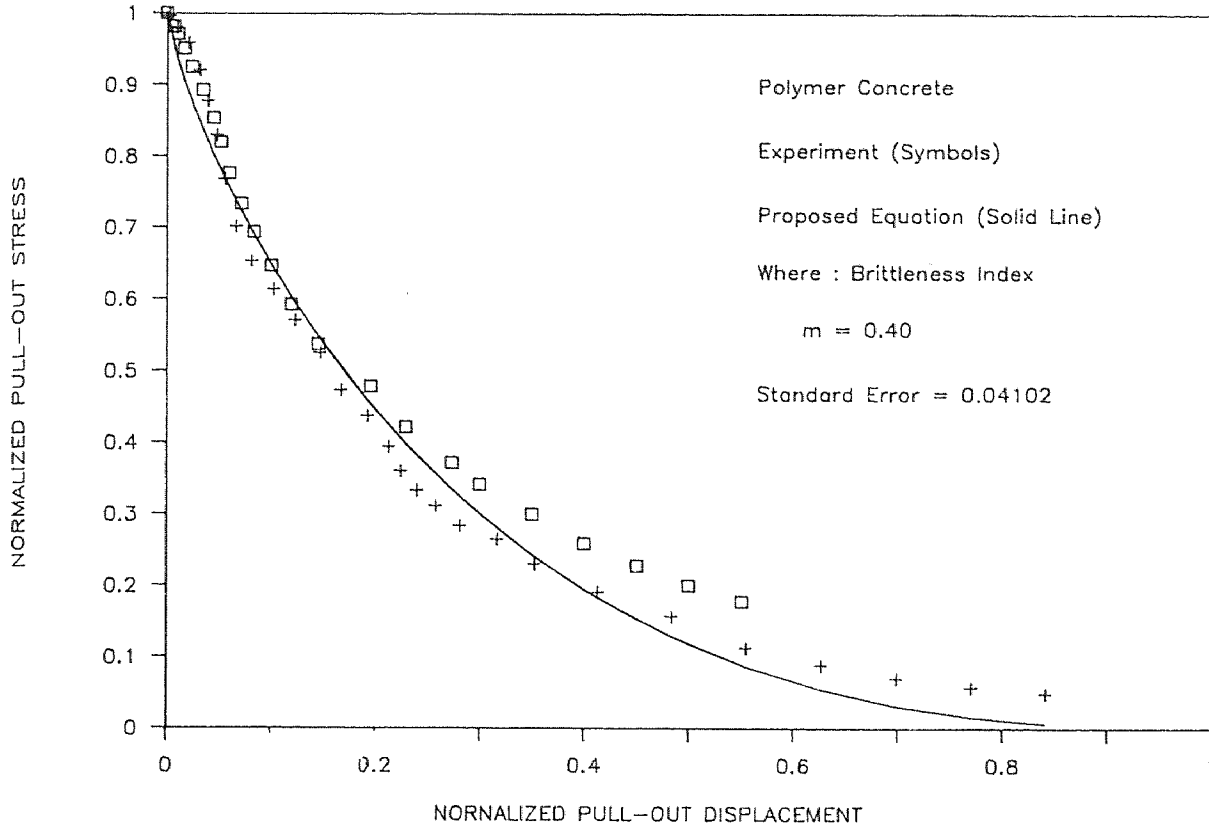


Fig. 6.4 Comparison of the Proposed Equation with Polymer Concrete Data (Present Study)

NORMALIZED STRESS-DISPLACEMENT CURVE

NORMAL FIBROUS CONCRETE

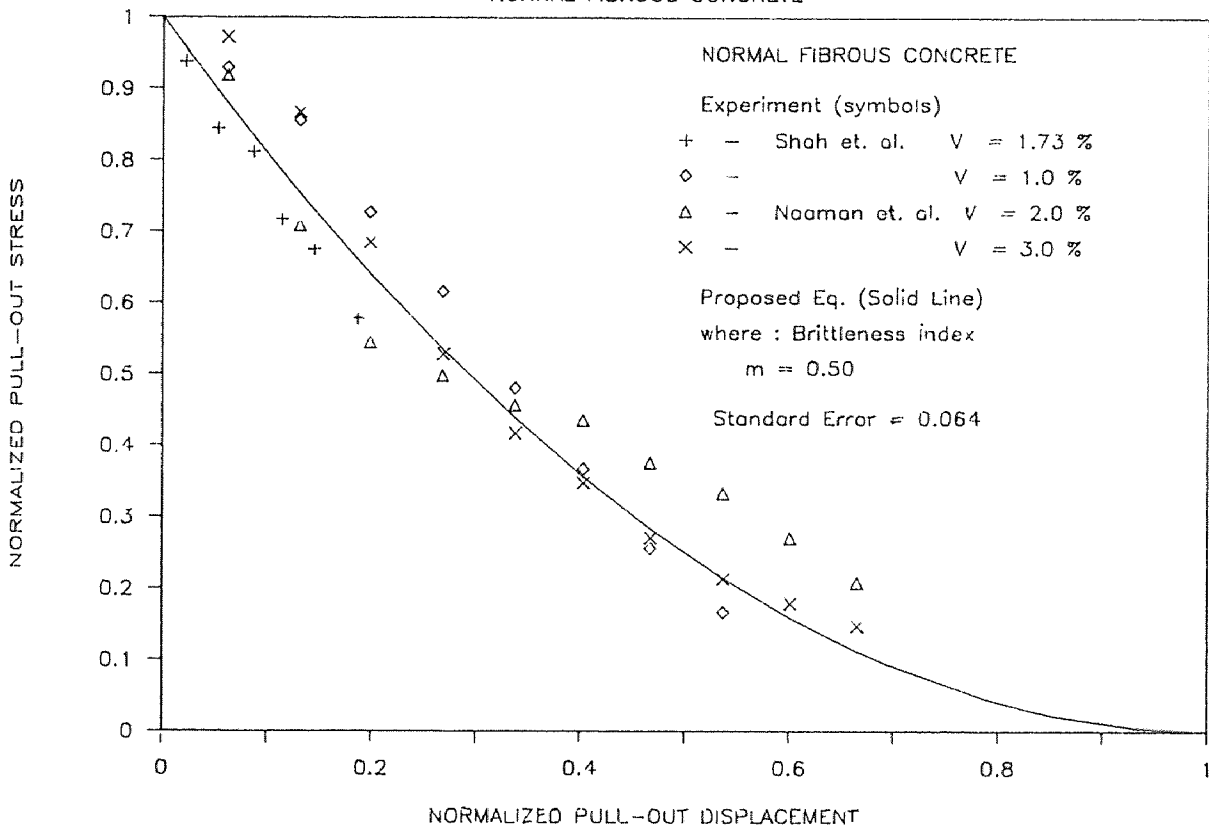


Fig. 6.5 Comparison of the Proposed Equation with Normal Fibrous Concrete Data (Shah et.al. and Naaman et.al.)

NORMALIZED STRESS-DISPLACEMENT CURVE

NORMAL FIBROUS CONCRETE

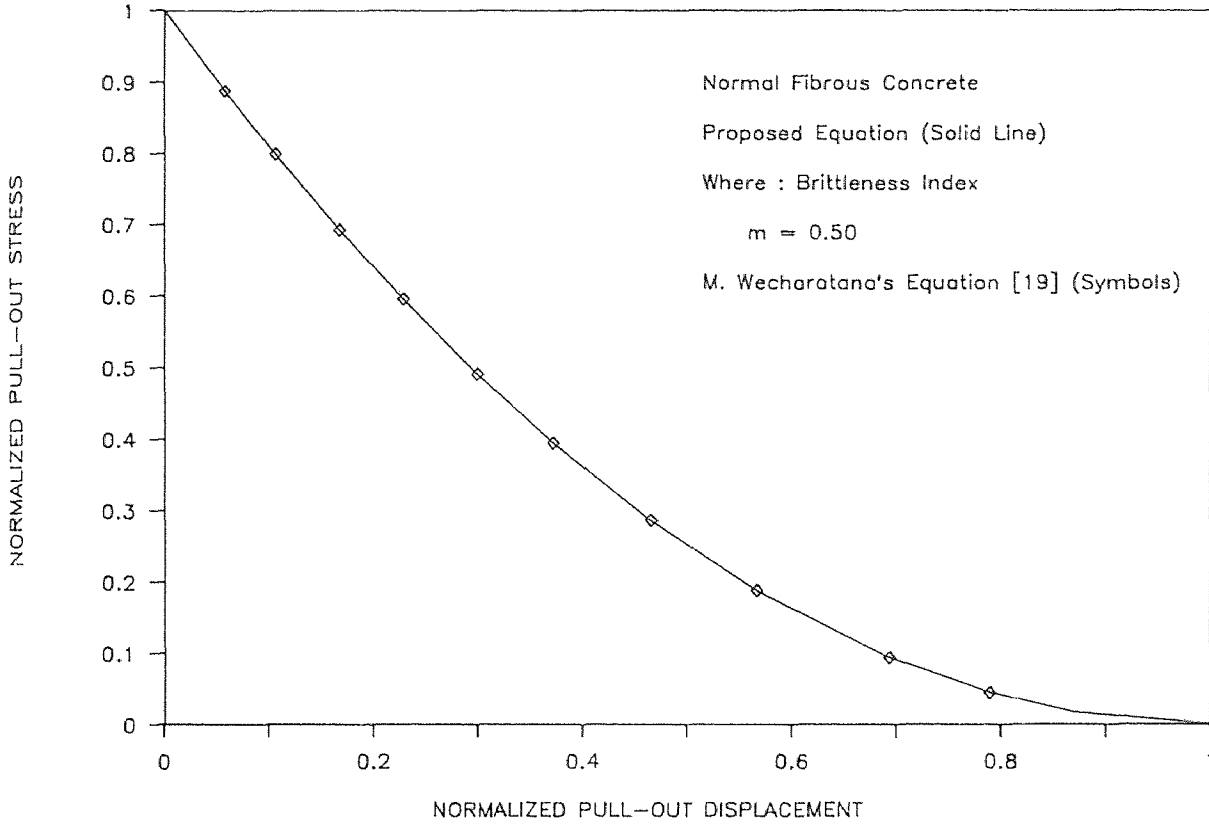


Fig. 6.6 Comparison of the Proposed Equation with Normal Fibrous Concrete Equation (M. Wecharatana [19])

NORMALIZED STRESS-DISPLACEMENT CURVE

HSFC (STRAIGHT END FIBER)

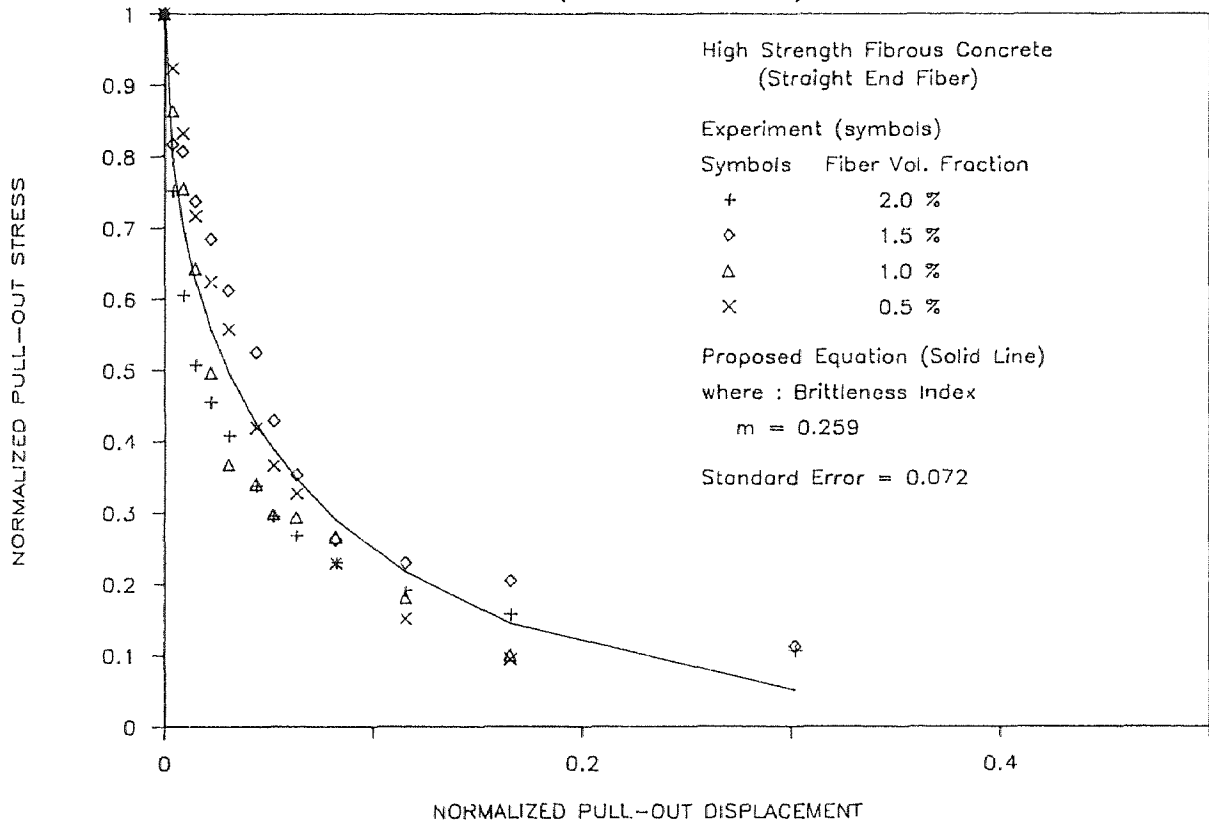


Fig. 6.7 Comparison of the Proposed Equation with High Strength Fibrous Concrete (Straight-End Fiber)

NORMALIZED STRESS-DISPLACEMENT CURVE

HSFC (HOOKED END FIBER)

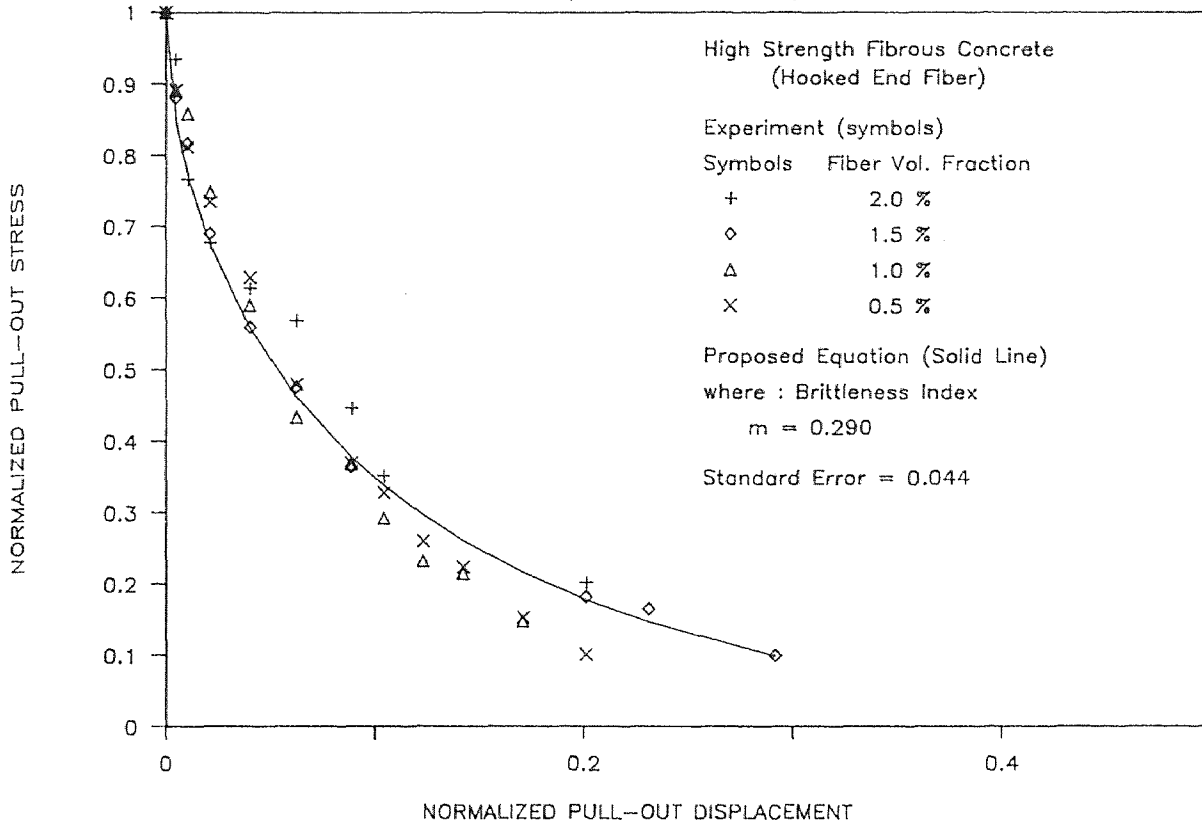


Fig. 6.8 Comparison of the Proposed Equation with High Strength Fibrous Concrete (Hooked-End Fiber)

NORMALIZED STRESS-DISPLACEMENT CURVE

POST-CRACKING (PROPOSED EQUATION)

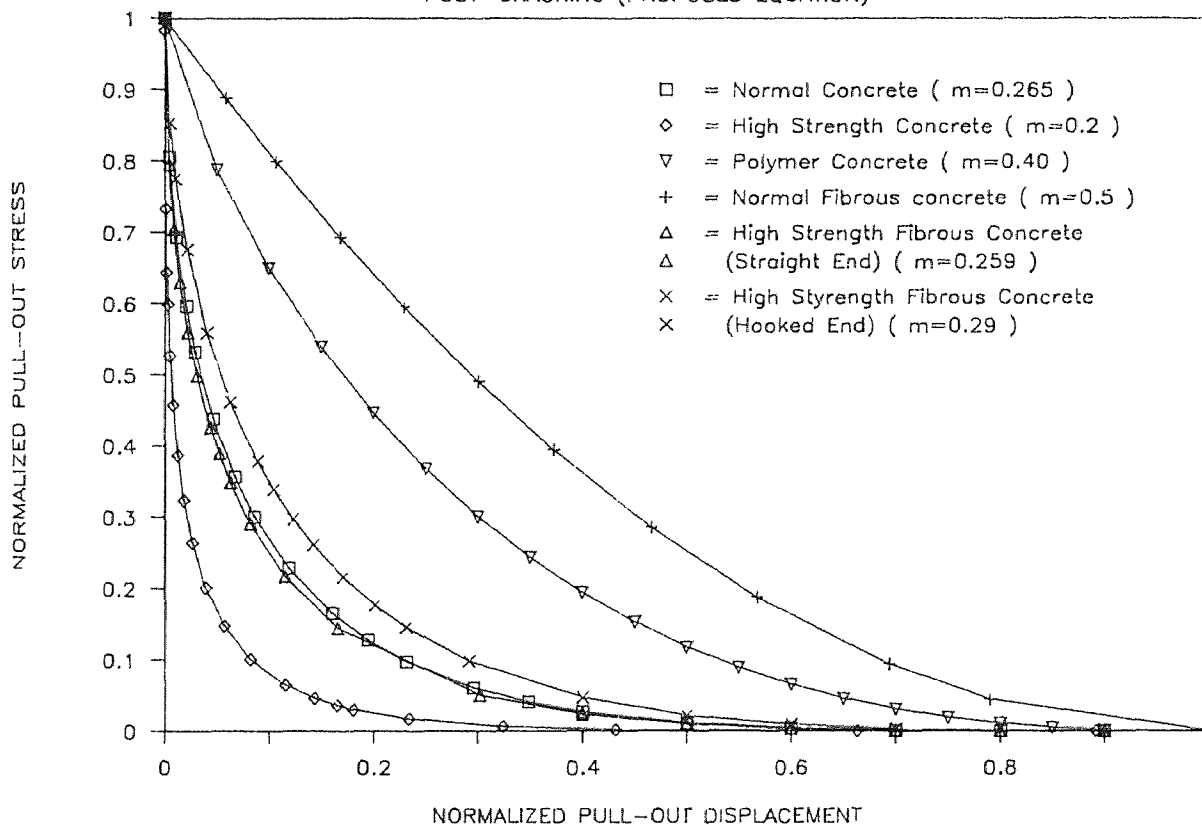


Fig. 6.9 Normalized Pull-Out Stress vs. Displacement Curves of Cement-Based Composites from the Proposed Equation

6.1.2 Brittleness Index

For a general cementitious composites, there is a brittleness number which can be used to predict the basic properties of a cement-based composite. The lower the value of the brittleness index, the more brittle the material is. In this study, the brittleness index (m) has been proposed in the general normalized pull-out stress displacement relationship. This brittleness index can be used to predict the softening response of a cementitious composite without conducting the direct tension test.

In this study, many attempts have been made to define the brittleness index of the cementitious material. Both compression and tension behavior (stress and displacement) were evaluated. The more brittle the material is, the smaller the observed brittleness number. The stress-strain relationship in compression of brittle material is quite linear. For the more brittle material, the more linear and steeper is the compressive stress-strain curve. Thus the brittleness index cannot be defined from compressive stress-strain relationship. Furthermore, the direction of the compressive stress is normally parallel to cracking and therefore not considered to be the direct crack causing stress.

For tension behavior, many trials were also made on the load-displacement relationship to evaluate the brittleness index. The proper definition of the brittleness index found from this present study is the ratio of the energy absorption at the proportional limit (U_1) to the elastic energy absorption at the peak load (U_p) of a direct tension load-displacement curve (see Fig.6.10).

6.1.2.1 BRITTLENESS INDEX MODEL

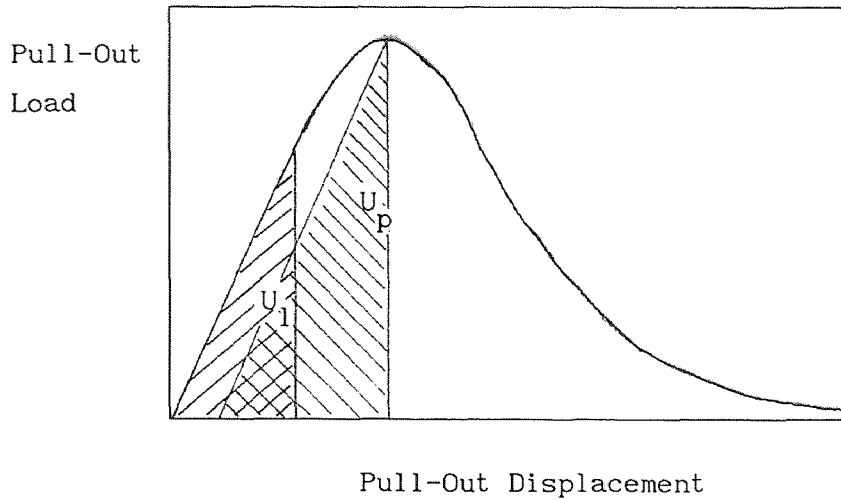


Fig. 6.10 Pull-Out Test

$$\text{Brittleness Index, } m = \frac{U_1}{U_p} \quad (6.3)$$

Where : U_1 = Energy absorption at the proportional limit
 U_p = Elastic energy absorption at the peak load

Energy absorption at the proportional limit (U_1) is the area under the pull-out load-displacement curve of the pull-out test. The elastic energy absorption at peak load (U_p) is the area under the curve when the load is released from the peak load to zero. The unloading curve is assume to be parallel to the initial slope of the load-displacement curve.

Table VI.2 presents the brittleness index values of all the pull-out test specimens compared to those from the proposed equation. The absolute difference between the brittleness index obtained from the proposed model and equation is between 2 to 8 %, and can be considered negligible. High strength concrete showed the highest difference in brittleness index (8.0 %) while high strength fibrous concrete (straight-end) was the lowest (2.32 %).

6.1.2.2 Statistical Analysis

In order to analyse whether the brittleness index of high strength fibrous concrete is a function of steel fiber volume fraction and/or fiber type, the two-factor analysis of variance method is employed. The brittleness index values from different types of fiber and volume fractions as determined from the proposed model were used in the analysis (see Table VI.2). The results shown in Table VI.3 indicate that the brittleness index values are significantly different when compared among the two fiber types ($p < 0.0001$) and the four fiber volume fractions ($p < 0.0001$). Therefore, it can be stated that the brittleness index of the high strength fibrous concrete depends on both the fiber type (Hooked-end and Straight-end) and fiber volume fraction for the range studied. Thus the normalized pull-out stress-displacement of high strength fibrous concrete is different according to the fiber type and fiber volume fraction. However, it should be noted that the amount of data on which this analysis was performed was relatively small and could be insufficient to fully justify this conclusion. Thus the effects of different types of fiber and their volume fractions on the brittleness index of high strength fibrous concrete still need further investigation. For normal fibrous concrete, Visalvanich and Naaman [17] and Wecharatana and Shah [19] stated that the normalized pull-out stress displacement is unique and independent of fiber volume fraction. Their conclusions were not, however, confirmed by any statistical analysis. It is possible that the normalized pull-out stress displacement may depend on fiber volume fraction and not be unique if normalized stress-displacement data was statistically analysed.

From Table VI.2, we can observe that the average values of brittleness index (m) from the proposed model of high strength fibrous concrete are very close to the values obtained from the proposed equation. Since the differences between the brittleness index values derived from the proposed equation and those obtained from the model are small (2-8 %), it can be concluded that the values of the brittleness index established from the model can be used in the

proposed normalized pull-out stress-displacement equation.

TABLE VI.2 BRITTLENESS INDEX (m) OF THE SPECIMEN
FROM THE PROPOSED MODEL

Type of Materials	m (from proposed model) Fiber Volume Fraction (%)						m (from prop. Eq.)	m Diff. (%)	
	0.0	0.5	1.0	1.5	2.0	Ave. m			
Normal Concrete	.256								
	.308								
	.279								
	Ave.	.281	-	-	-	-	.281	.265	6.04
Microsilica Conc.	.206								
	.226								
	Ave.	.216	-	-	-	-	.216	.200	8.0
Polymer Concrete	.347								
	.409								
	.365								
	Ave.	.374	-	-	-	-	.374	.400	6.5
High Strength Fibrous Concrete (Straight End)		.260	.262	.269	.281				
		.284	.289	.306	.306				
		.252	.263	.264	.285				
		.248	-	-	.273				
	Ave.	.251	.262	.268	.275	.264	.259	2.32	
% Diff. From Prop. Eq.		3.09	1.16	3.47	6.18			3.47	
High Strength Fibrous Concrete (Hooked End)		.278	.319	.305	.315				
		.284	.289	.306	.306				
		.280	-	.311	.320				
		.282	-	-	-				
	Ave.	.281	.304	.307	.314	.301	.290	3.80	
% Diff. From Prop. Eq.		3.10	4.83	5.86	8.28			5.52	

Anova table for a 2-factor Analysis of Variance on Y1: Brittleness Index

Source:	df:	Sum of Squares:	Mean Square:	F-test:	P value:
Fiber Type (A)	1	.009	.009	142.166	.0001
% Fiber (B)	3	.003	.001	17.488	.0001
AB	3	1.562E-4	5.207E-5	.853	.4833
Error	18	.001	6.106E-5		

1

There were no missing cells found.

Table VI.3 Two-Factor Analysis of Variance

6.2 Fatigue Characteristics

A theoretical model of fatigue in concrete is desirable in order to obtain the S-N curve, one of the most important material properties of concrete, because carrying out fatigue test is difficult and time consuming.

6.2.1 S-N Curve

Design for fatigue is normally facilitated by the used of a Modified Goodman diagram or the S-N curve. Fig.5.13 compares the S-N curves of normal concrete, superplasticizer concrete, microsilica concrete and polymer concrete. The regression lines shown were obtained from empirical data and the typical linear equation can be written as follows :

$$\log N = A \left[\frac{f_{\max}}{f'_c} \right] + B \quad (6.3)$$

Where :

- N = Number of cycle
- f_{\max} = Maximum stress level
- f'_c = Ultimate compressive strength
- A, B = Constant coefficients

For different cementitious matrices, these two constants are listed in Table VI.4

TABLE VI.4 COEFFICIENTS OF A AND B

Type of Concretes	A	B
Normal Concrete	-22.86	21.49
Superplasticizer Concrete	-22.40	21.60
Microsilica Concrete	-23.66	23.11
Polymer Concrete	-5.51	7.87

With this proposed S-N equation, we can predict the fatigue life of the material under a given repeated load.

6.2.2 Maximum Strain Concept

For a given cementitious material, there is a certain amount of maximum strain that the material can sustain. This maximum strain property will be used to predict the fatigue behavior of high strength cement-based composites, namely superplasticizer concrete and microsilica concrete. For polymer concrete, this maximum strain concept can not be applied because of the extensive plasticity.

For a cyclic compression test, the maximum strain of the material is obtained from the uniaxial compression test. In the present study, the average maximum strain for superplasticizer concrete and microsilica concrete are 0.00206 and 0.0022 respectively. With these maximum strain values, we can predict the fatigue life of the specimen. Figs. 6.11 & 6.12 present the typical peak strain versus number of cycles of loading which show that the specimens fail within the maximum strain values. The horizontal dotted lines in these figures are the maximum strain of the composites obtained from the monotonic compression test. To predict the number of cycle to failure, the maximum strain-cycle curve is extrapolated until it intercepts the horizontal dotted line. The number of load cycle reading at this point represents the predicted failure cycle of the tested specimen. Figs. 6.11 and 6.12 show that the predicted number of cycle to failure are 4200 and 6 cycles for superplasticizer concrete and microsilica concrete while the actual number of cycle to failure observed from the experiments were 4096 and 6 cycles respectively. These relatively good agreements imply that the concept of maximum strain criteria may be used to predict the fatigue life of high strength composites. Details of all other peak strain and number of loading cycles relationships of superplasticizer, microsilica and polymer concrete are summarized in Appendix K.

STRAIN VS. CYCLE CURVE

SUPERPLASTICIZER CONCRETE (S1F208)

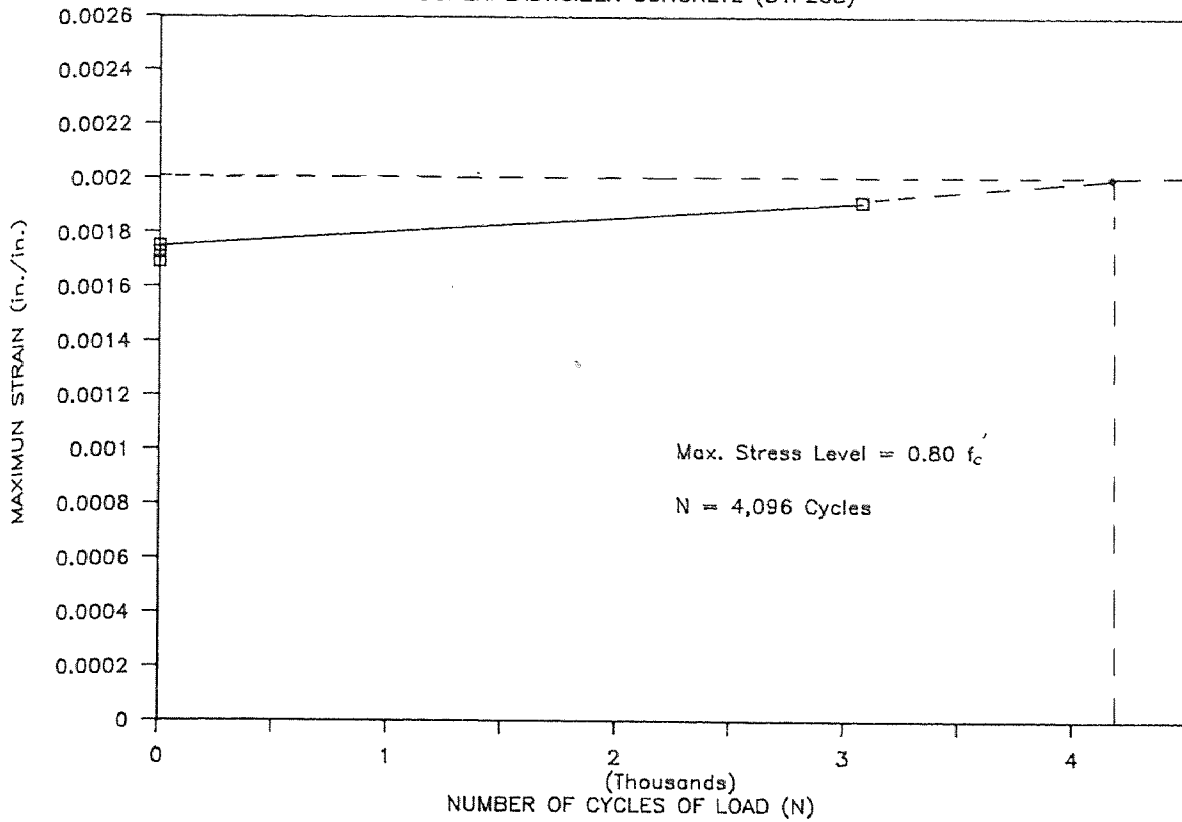


Fig. 6.11 Typical Peak Strain vs. No. of Loading Cycles Curve of Superplasticizer Concrete

STRAIN VS. CYCLE CURVE

MICROSILICA CONCRETE (M2F209)

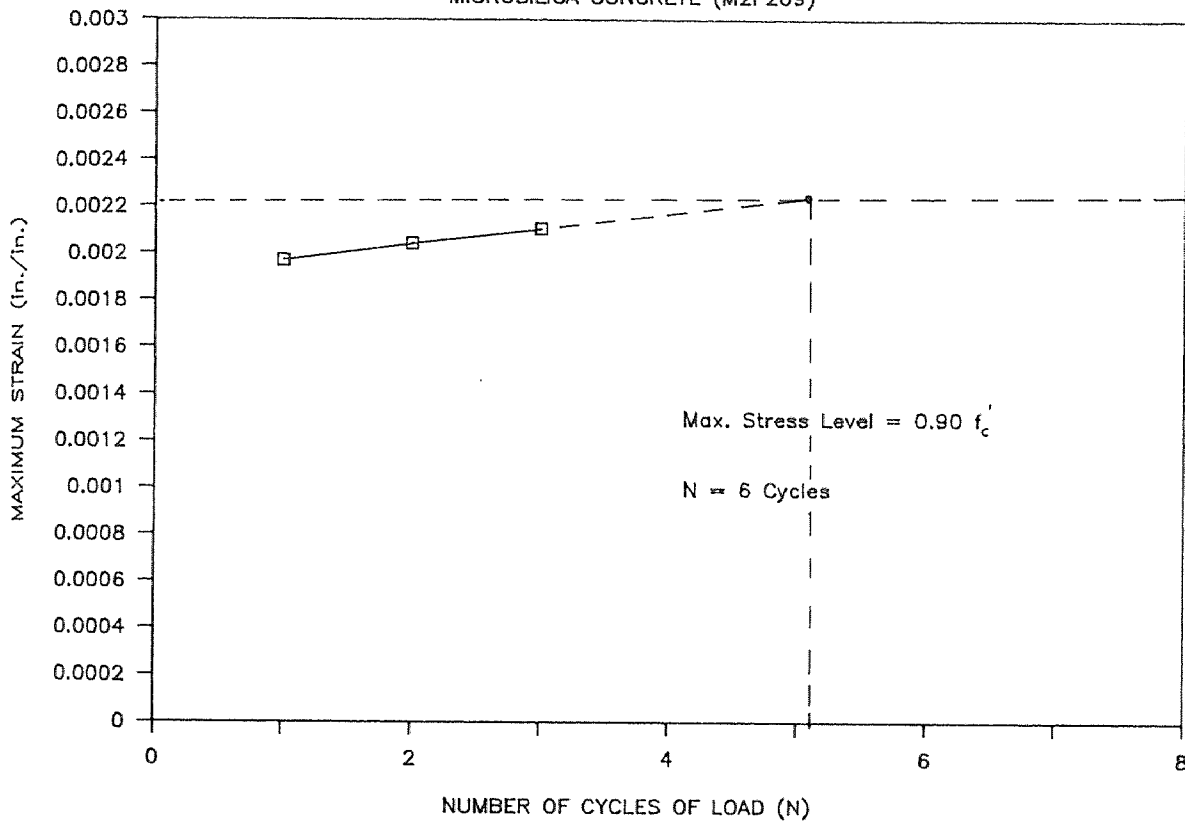


Fig. 6.12 Typical Peak Strain vs. No. of Loading Cycles Curve of Microsilica Concrete

CHAPTER VII

CONCLUSIONS

This investigation yielded a large amount of data on the compression, tension, and flexural properties as well as the bond strength-slip relationships and fatigue characteristics of high strength cement-based composites. The high strength concretes used in this study were superplasticizer concrete, microsilica concrete and polymer concrete.

The results from compression tests clearly showed that dry cured specimens of polymer concrete provided higher strength than wet cured whereas the same conditions provided lower strength to superplasticizer and microsilica concrete. This is because the presence of water interferes with the polymerization process of polymer concrete. Curing period from 58 to 400 days did not significantly affect the compressive strength, maximum strain at the peak load, or the modulus of elasticity of superplasticizer or microsilica concrete. There were, however, significant differences on these properties for polymer concrete when tested at 3 and 35 days. The average strain at the peak load of high strength concrete is about one third less than normal concrete, except for polymer concrete which is about 4 times higher.

The mode of failure of high strength concrete is different from normal concrete. High strength concrete will suddenly burst when the load reaches the peak while for normal concrete the failure process occurs gradually.

The specimen size affects the flexural strength of high strength concrete. The ACI flexural equation is very conservative and should be modified for high strength concrete, especially for polymer concrete.

The tensile strength and energy absorption of high strength concrete in direct tension tests were 2-3 and 2-7 times higher than

normal concrete respectively. Among the high strength concrete, polymer concrete absorbed the most energy. The pull-out displacement at the peak load of normal concrete is about 66 % higher than microsilica concrete but about 200 % lower than polymer concrete.

The results of bond strength in reinforced high strength concrete study indicated that the larger the bar diameter the lower the bond strength, bond factor and slip. The bond factor for high strength concrete was 0.212 which is low when compared to normal concrete (0.15-0.60). The bond slip of these high strength concretes was also low, about 10 % of normal concrete. Therefore, if high strength concrete is used, additional development length should be considered.

The results from high strength fibrous concrete tests clearly indicated that the bond stress-displacement relationship was affected by the fiber type and fiber content. The higher the fiber volume fraction, the larger are the peak stress and the amount of energy absorption. The post-peak pull-out stress versus displacement relationship gradually drops to zero for straight-end fiber while for hooked-end fiber it drops in a series of envelopes down the post-peak portion of the curve. This is probably because of the slip at the end of the hooked-end fiber.

The unique normalized pull-out stress versus pull-out displacement of high strength concrete and high strength fibrous concrete (both straight-end and hooked-end fiber) were obtained. These unique normalized relationships were statistically found to be dependent of both the fiber type and the fiber volume fraction.

The normalized post-peak pull-out stress versus normalized pull-out displacement equation for cementitious composites, contains only one single material parameter called **Brittleness Index**, is proposed. The brittleness index varies with the type of cementitious composites. The more brittle the material, the lower the brittleness index is. The proposed brittleness index is defined as the ratio of the energy absorption at the proportional limit (U_1) to the elastic energy

absorption at the peak load (U_p) of the direct tension load-displacement curve. This relationship determines the brittleness value of the material without conducting the post-peak direct tension test. The normalized post-peak stress displacement equation can be used to predict not only the tension softening but also fracture resistance and energy absorption of cementitious materials.

The fatigue strength of superplasticizer and microsilica concrete is between 70-75 % of f'_c compared to 60-65 % of f'_c for normal concrete and 45 % of f'_c for polymer concrete. The fatigue limit of high strength concrete is about 66 % of f'_c compared to 55 % of f'_c [25] for normal concrete. There was no fatigue limit for polymer concrete. The results in this study indicate that the higher the compressive strength, the higher the fatigue strength of non-plastic concrete is likely to be.

The peak strain at any cycle under the cyclic loading is always less than the maximum strain of the monotonic load. Therefore the maximum strain concept may be used to predict the fatigue life. This maximum strain concept is not valid for polymer concrete because of its plasticity.

The linear regression equations of S-N curves for different high strength concrete were proposed in terms of loading stress and number of cycles. This equation can be used to predict the fatigue life of high strength cement-based materials.

FUTURE RESEARCH

For future investigation on bond and fatigue characteristics of high strength concrete, the author would like to suggest as follows :

1. Different high strength cement-based composites should be used.
2. For bond strength of reinforced high strength concrete study, strain gauges should be attached to the reinforcing bar in order to examine the bond-slip relationship and bond stress distribution.
3. For high strength fibrous concrete study, other sizes and shapes (rectangular, dog-bone, notched and unnotched and etc.) of the direct tension specimen should be tested in order to take into account the possible effects due to geometry and size. The results should then be compared to the proposed general equation in this dissertation. Different types and sizes of fiber should also be studied.
4. For fatigue characteristics, the effect due to different stress range of cyclic compression should be studied. Also, cyclic tension and reverse loading of high strength concrete need more investigation.

APPLICATIONS OF THE OBSERVED BEHAVIORS

The applications of the observed behaviors on bond and fatigue characteristics of high strength cement-based composites in this study can be summarized as follows :

1. In recent years nonlinear finite element analysis and other numerical methods have proved to be efficient and highly accurate. Thus information on the softening response of cementitious composites (complete stress-displacement curve) is necessary to develop an accurate crack model. Due to the brittle nature of cementitious composites and the unavailability of equipment stiff enough to control the cracking process, it is difficult to obtain the complete stress-displacement curve. Therefore, in this study, attempts to use the brittleness index to predict direct tension post-peak responses of cementitious material will be carried out.

2. From the bond characteristics study, the bond stress-slip relationship is developed to define the proper embedment length for steel reinforced high strength concrete.

3. The S-N curve is the most fundamental property of the fatigue characteristics of the material. In order to determine the S-N curve, a time consuming fatigue test has to be conducted. In this study, attempts were made to use the value of brittleness index or the maximum strain concept of the material to obtain the S-N curve.

4. The S-N curve developed from a compression test may be used to predict the fatigue life of beam.

BIBLIOGRAPHY

- [1] V.V. Bertero, "Proc. of High Strength Concrete", Workshop, S.P. Shah, Editor, University of Illinois at Chicago, Circle, Dec. 2-4, 1979, pp. 96-167.
- [2] John Albinger and Jaime Moreno, S.E., "High Strength Concrete", Chicago Style., Concrete Construction, Vol.26, March 1981, pp. 241-245.
- [3] Merlin D. Copen, "Problems Attending Use of High Strength Concrete in Thin Arch Dams", ACI Journal, Vol.75, No.4, April 1975, pp. 138-140.
- [4] Saucier K.L., "High-Strength Concrete, Past, Present, Future"., Paper presented at the 1979 Annual Convention. American Concrete Institute, Milwaukee, Wisconsin, March 18-23, 1979, 11 p.
- [5] ACI Committee 363, "State-of-the-Art Report on High Strength Concrete" ACI Journal, July-August 1984, pp. 364-411.
- [6] S.P. Shah, Ulker Gokoz and Fahad Ansari, "An Experimental Technique for Obtaining Complete Stress-Strain Curves for High Strength Concrete, Cement, Concrete and Aggregates", CCAGDP, Vol.3, No.1, Summer 1981, pp. 21-27.
- [7] H. Martin, Proc. Inter. Conf. on "Bond in Concrete", Paisley, Scotland, June 1982, pp. 289-299.
- [8] A. Windisch, "A Modified Pull-Out Test and New Evaluation Methods for a More Real Local Bond Slip Relationship", Material and Structure (RILEM) 1985.
- [9] RILEM / CEB / FIP RECOMMENDATION. "Bond test reinforcing steel, Materials and Structures, Vol.6, No.32, 1973, pp. 97-105.
- [10] A.D. Edwards and P.J. Yannopoulos, "Local Bond-Stress to Slip Relationship for Hot Rolled Deformed bars and Mild Steel Plain Bars", ACI Journal, March 1979, pp. 405-420.
- [11] Saeed M. Mirza and Jules Houde, "Study of Bond Stress-Slip Relationships in Reinforced Concrete", ACI Journal, January 1979, pp. 19-46.
- [12] A.E. Naaman and S.P. Shah, "Pull-Out Mechanism in Steel Fiber-Reinforced Concrete", ACI Journal, August 1976, pp.

1537-1547.

- [13] A. Burakiewicz, "Testing of Fiber Bond Strength in Cement matrix", Proceedings, RILEM Symposium on Testing and Test Methods of Fibre Cement Composites, Edited by R.N. Swamy, The Construction Press, 1978, pp. 355-365.
- [14] D.J. Pinchin and D. Tabor, "Interfacial Contact Pressure and Frictional Stress Transfer in Steel Fiber", Proceedings, RILEM Symposium on Testing and Test Methods of Fibre Cement Composites, Edited by R.N. Swamy, The Construction Press, 1978, pp. 337-344.
- [15] R.J. Gray and C.D. Johnson, "The Measurement of Fibre-Matrix Interfacial Bond Strength in Steel Fibre-Reinforced Cementitious Composites", Proceedings, RILEM Symposium on Testing and Test Methods of Fibre cement Composites, Edited by R.N. Swamy, The Construction Press, 1978, pp. 317-328.
- [16] Magne Maage, "Fibre Bond and Friction in Cement and Concrete", Proceedings, RILEM Symposium on Testing and Test Methods of Fibre Cement Composites, Edited by R.N. Swamy, The Construction Press, 1978, pp. 329-336.
- [17] K. Visalvanich and A.E. Naaman, "Fracture Model for Fiber Reinforced Concrete", ACI Journal, No. 80-14, March-April 1983, pp. 128-138.
- [18] V.S. Gopalaratnum and S.P. Shah, "Tensile Failure of Steel Fiber-Reinforced Mortar, Journal of Engineering Mechanics, Vol.113, No.5, May 1987.
- [19] M. Wecharatana and S.P. Shah, "A Progress Report on Fracture Toughness of Fiber Reinforced Concrete", Department of Civil Engineering, Northwestern University, June 1983.
- [20] O. Graf and E. Brenner, "Experiments for Investigating the Resistance of Concrete Under Often Repeated Loads", (Versuche Zur Ermittlung der Widerstandsfahigkeit Von Beton gegen oftmals Wiederholte Druckbelastung), Bulletins No.76 and No.83, Deutscher Ausschuss fur Eisenbeton, 1934, 1936.
- [21] K. Aas-Jakobsen, "Fatigue of Concrete Beams and Columns", Bulletin No. 70-1, NTH Institute of Betonkonstruksjoner, Trondheim, Sep. 1970, pp.148.
- [22] R. Tepfers and T. Kutti, "Fatigue Strength of Plain, Ordinary, and Lightweight Concrete", ACI Journal, Title No.76-29, May 1979, pp. 635-653.
- [23] H. Rusch, "Researches Toward a General Flexural Theory for

Structural Concrete", ACI Journal, Proceedings, Vol.57, No.1, July 1960, pp. 1-28.

- [24] J.W. Galloway and K.D. Raithby, "Effect of Rate of Loading on Flexural Strength and Fatigue Performance of Concrete", TRRL Report, No. LR547, Transport and Road Research Laboratory, Crownthorne, Berkshire, 1972, 18 p.
- [25] C.E. Kesley, "Effect of Speed of Testing on Flexural Fatigue Strength of Plain Concrete", Proceedings, Highway Research Board, Vol.32, 1953, pp. 251-258.
- [26] M.E. Awad and H.K. Hilsdorf, "Strength and Deformation Characteristics of Plain Concrete Subjected to High Repeated and Sustained Loads", ACI Journal, SP 41-1, 1974, pp. 1-13.
- [27] P.R. Spark, "The Influence of Rate of Loading and Material Variability on the Fatigue Characteristics of 'Concrete'", American Concrete Institute Publication, SP-75, Fatigue of Concrete Structure, 1982 pp. 331-341.
- [28] M. Saito and S. Imai, "Direct Tensile Fatigue of Concrete by the use of friction grips", ACI Journal, Title No. 80-42, Sep-Oct 1983, pp. 431-438.
- [29] R. Tepfers, "Tensile Fatigue Strength of Plain Concrete", ACI Journal, Title No.76-39, August 1979, pp. 919-933.
- [30] R.Tepfers, J. Garlin and T. Samuelsson, "Concrete subjected to Pulsating Load and Pulsating Deformation of Different Pulse Waveforms", Nordisk Betong, No.4, 1973, pp. 27-36.
- [31] John W. Murdock and Clyde E. Kesler, "Effect of Range of Stress on Fatigue Strength of Plain Concrete Beams", ACI Journal, Aug. 1958, pp. 221-231.
- [32] H.A. Williams, "Fatigue Tests of Lightweight Aggregate Concrete Beams", ACI Journal, April 1943, Proceeding Vol.39, pp. 441-448.
- [33] H.E. Clemmer, "Fatigue of Concrete", Proceeding, ASTM Vol. 22, Part II, 1922, pp. 408-419.
- [34] John T. Mc.Call, "Probability of Fatigue Failure of Plain Concrete", ACI Journal, Aug 1958, pp. 233-244.
- [35] R. Tepfers, "Fatigue of Plain Concrete subjected to Stress Reversals", ACI Publication, SP-75-9, 1986, pp. 195-215.

- [36] FIP Commission, "Methods of Achieving High Strength Concrete", ACI Journal, Vol.64, No.1, January 1967, pp. 45-48.
- [37] Katharine Mather, "High Strength, High Density Concrete", ACI Journal, Vol 62, No.8, Aug. 1965, pp.951-962.
- [38] A.J. Harris, "High Strength Concrete : Manufacture and Properties", The Structural Engineer, November 1969, Vol.47, No.11, pp. 441-446.
- [39] J.J. Beaudoin and R.F. Feldman, "High-Strength Cement Paste-A Critical Appraisal", Cement and Concrete Research, Vol.15, 1985, pp. 105-116.
- [40] Cameron Macinnis and Donald V. Thomson, "Special Techniques for Producing High Strength Concrete", ACI Journal, Dec. 1970, pp. 996-1002.
- [41] Ramnath N. Swamy, "Properties of High Strength Concrete, American Society for Testing and Material, 1986.
- [42] E.J. Sellevold and F.F. Radjy, "Condensed Silica Fume (Microsilica) in Concrete : Water Demand and Strength Development", ACI. SP.79-35, June 5, 1986.
- [43] G. Carette and V.M. Malhotra, "Early-Age Strength Development of Concrete-Incorporation Fly Ash and Condensed Silica Fume", ACI, SP.79-35, June 5, 1986.
- [44] ACI, "High Strength Concrete Seminar Course Manual/SCM-15(87)", 1987, pp. 765-784.
- [45] R.L. Carrasquillo, Mater. Res. Soc. Proc. 42 Nov.,1984, pp. 151-168.
- [46] S.H. Ahmad, and S.P. Shah, Mat. Res. Soc. Sym. Proc. 42, pp. 169-181.
- [47] R.N. Swamy, ASTM, "Cement, Concrete and Aggregates", CCAGDP, 8, No.1, Summer 1986, pp. 33-41.
- [48] R.N. Swamy and K.L. Anand, "Shrinkage and Creep Properties of High Strength Structural Concrete", Civil Engineering and Public Works and Review, Vol.68, No.807, Oct. 1973, pp. 859-868.
- [49] Pierre-Claude Aictin, pierre Laplante and claude Benard, "Development and Experimental use of a 90 MPa(13,000 psi) Field Concrete", ACI. SP.-87-5, 1986.

- [50] Arthur H. Nilson (FACI), "Design Implications of Current Research on High Strength Concrete", ACI, SP.-87-7, 1986.
- [51] R.N. Swamy and A.B. Ibrahim, "Shrinkage and Creep Properties of High Early Strength Structural Lightweight Concrete", Institute of Civil Engineers, Proceedings, Vol.55, Sept 1973, pp. 635-646.
- [52] Seven Thaulow, "Tensile Splitting Test and High Strength Concrete Test Cylinders", ACI, Vol.53, No.7, Jan. 1957, pp. 699-706.
- [53] R.N. Swamy, "High Strength Concrete-Material Properties and Structural Behavior", ACI, SP-87-8, 1986.
- [54] S.E. Swartz, A. Nikaren, H.D. Narayan Baber, N. Perigakaruppan, T.M.E. Refai, "Structural Bending Properties of high Strength Concrete", ACI, SP-87-9, 1986.
- [55] Andrew G.Mphonde, Gregory C. Frantz, "Shear Test of High and Low strength concrete with Stirrups", ACI, SP-87-10, 1986.
- [56] Robert C. Chen, Ramon L. Carrasquillo, David W. Power, "Behavior of High Strength Concrete Under Uniaxial and Bending Compression", ACI, SP-87-14, 1986.
- [57] Hudson, J.A., Crouch, S.L., and Fairhurst, C., "Soft, Stiff and Servo-Controlled Testing Machines : A Review with Reference to Rock Failure", Engineering Geology, Vol.6, No.3, 1972, pp. 155-189.
- [58] M.U. Haddad, D.W. Fowler, and D.R. Paul, "Factors Affecting the Curing and Strength of Polymer Concrete", ACI Journal, Sep.-Oct. 1983, pp. 396-402.
- [59] S.A. Frondistou-Yannas and S.P. Shah, "Polymer Latex Modified Mortar", ACI Journal, January 1972, pp. 61-65.
- [60] Wecharatana, M., and Lin, C.C., "New Polymer Concrete for Marine Structures", Final Report, Submitted to the New Jersey Marine Sciences Consortium, New Jersey Sea Grant, Grant No. R/N-10, September 1988.
- [61] Barie B. Brettmann, David Darwin, and Rex c. Donahey, "Bond of Reinforcement to Superplasticizer Concrete, ACI Journal, Jan.-Feb., 1986, pp. 98-107.
- [62] T.S. Shih, G.C. Lee, and K.C. Chang, "Local Concrete-Steel Bond Behavior at Low Temperature", Journal of Structural Engineering, Vol. 113, No.11, Nov 1987.

- [63] H. Sagar and F.S. Rostasy, "The Effect of Elevated Temperature on the Bond Behavior of Embedded Reinforcing Bars", Proc. Inter. Conf. on Bond in Concrete, Paisley, Scotland, June 1982, pp. 206-216.
- [64] R. Rayles, P.D. Morley and M.R. Khan, "The Behavior of Reinforced Concrete at Elevated Temperatures with Particular Reference to Bond Strength", Proc. Inter. Conf. on Bond in Concrete, Paisley, Scotland, June 1982, pp. 217-228.
- [65] U. Diederiches and U. Schneider, "Changes in Bond Behavior due to Elevated Temperatures" , Proc. Inter. conf. on Bond in Concrete, Paisley, Scotland, June 1982, pp. 229-238.
- [66] Neil M. Hawkins, I.J. Lin and F.L. Jeang, "Local Bond Strength of Concrete for Cyclic Reverse Loading", proc. Inter. Conf. on Bond in Concrete, Paisley, Scotland, June, pp. 151-161.
- [67] M. Arnaud, M. Bourabrab and M. Lorrain, "On the Reversibility Properties of Bond in Concrete", Proc. Inter. Conf. on Bond in Concrete, Paisley, Scotlant, June 1982, pp. 162-172.
- [68] E. Vas and H.W. Reinhardt, "Bond Stress-Slip Behavior of Deformed Bars, Plain Bars and Strands under Impact Loading", Proc. Inter. Conf. on Bond in Concrete, Paisley, Scotlant, June 1982, pp. 173-182.
- [69] F.S. Rostasy and B. kepp, "Time-Dependence of Bond", Proc. Inter. Conf. on Bond in Concrete, Paisley, Scotland, June 1982, pp. 183-192.
- [70] P. Plaines, T. Tassios and E. Vintzileou, "Bond Relaxation and Bond Slip Creep under Monotonic and Cyclic Actions", Proc. Inter. Conf. on Bond in Concrete, Paisley, Scotland, June 1982, pp. 193-205.
- [71] Manfred Keuser and Gerhard Mehlhorn, "Finite Element Models for Bond Problems", possible publication on ASCE, Oct. 9, 1988.
- [72] Emory L. Kemp, "Bond in Reinforced Concrete : Behavior and Design Criteria", ACI Journal, No.-83-7, Jan.-Feb., 1986, pp. 50-57.
- [73] G. Nammur Jr. and A.E. Naaman, "A Bond Stress Model For Fiber Reinforced Concrete Based on Bond Stress-Relationship".
- [74] Van Ornum, J.L., "Fatigue of Cement Products", Transactions, ASCE, Vol.51, 1903, pp. 443.

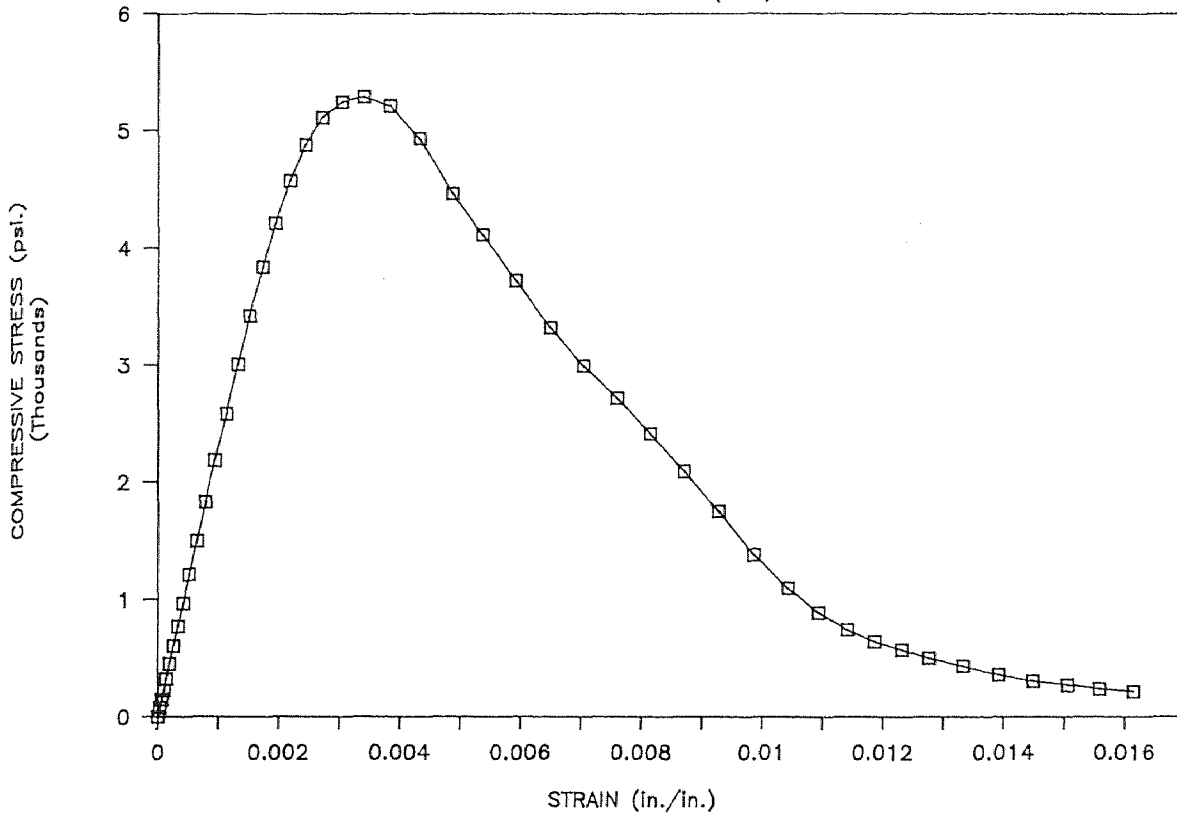
- [75] Van Ornum, J.L., "Fatigue of Concrete", Transactions, ASCE, Vol. 58, 1907, pp. 294-320.
- [76] Gene M. Nordby, "Fatigue of Concrete-A Review of Research", ACI Journal, Aug. 1958, pp. 191-217.
- [77] Thomas T.C. Hsu, "Fatigue of Plain Concrete", ACI Journal, Title No. 78-27, July-August 1981, pp. 292-305.
- [78] P.R. Sparks and J.B. Menzies, "The effect of Rate of Loading upon the Static and Fatigue Strengths of Plain Concrete in Compression", Magazine of Concrete Research, Vol. 25, No. 83, June 1973, pp. 73-80.
- [79] D.C. Spooner, "Stress-Strain-Time relationships for Concrete", Magazine of Concrete Research, Vol. 23, No. 75-76, June-September 1971, pp. 127-131.
- [80] W.H. Gray, J.F. Mc Laughlin and J.D. Antrim, "Fatigue Properties of Lightweight Aggregate Concrete", ACI Journal, Title no. 58-6, August 1961, pp. 149-161.
- [81] F.S. Ople, Jr. and C.L. Hulsbos, "Probable Fatigue life of Plain Concrete with Stress Gradient", Research Report, ACI Journal, Title No. 63-2, January 1966, pp. 59-81.
- [82] K.D. Raithby and J.W. Galloway, "Effects of Moisture Condition, Age, and Rate of Loading on Fatigue of Plain Concrete", ACI Publication, SP-41-2, 1974, pp. 15-34.
- [83] H.K. Hildorf and Clyde E. Kesler, "Fatigue Strength of Concrete Under Varying Flexural Stresses", ACI Journal, Title NO. 63-50, Oct. 1966, pp. 1059-1076.
- [84] S.S. Takhar, I.J. Jordaan and B.R. Gamble, "Fatigue of Concrete Under Lateral Confining Pressure", ACI Publication, SP.-41-4, 1974, pp. 59-69.
- [85] R. Tepfers, J. Gorlin and T. Samuelsson, "Concrete Subjected to Pulsating Load and Pulsating Deformation of Different Pulse Wave-Form", Nordisk Betong, No. 4, 1973, pp. 27-36.
- [86] E.W. Bennett and S.E. St. J. Muir, "Some Fatigue Tests on High Strength Concrete in Axial Compression", Magazine of Concrete Research, Vol. 19, No. 59, June 1967, pp. 113-117.
- [87] C.M. Eric and Thomas T.C. Hsu, "Biaxial Compression Fatigue of

- Concrete", Research Report UHCE 86-17, University of Houston, Dept. of Civil Engineering, Dec. 1986.
- [88] Wecharatana, M., and Lin, C.C., "New Polymer Concrete for Shore Protection and Marine Structures", Progress Report, submitted to the New Jersey Sciences Consortium, New Jersey Sea Grant, Grant No. R/N-10, September 1986, 11 p.
- [89] "Polymer Concrete", ACI SP-89, J.T. Dikeou and D.W. Fowler, Editors, American Concrete Institute, 1985, 346 p.
- [90] T. Cintora, "Softening Response of Concrete in Direct Tension", Master Thesis, New Jersey Institute of Technology, Nov. 12, 1987, 79 p.
- [91] "Polymer Modified Concrete", ACI SP-99, D.W. Fowler, Editor, American Concrete Institute, 1987, 214 p.
- [92] M. Wecharatana, and W.J. Chiou, Proc. 1986 SEM, Spring Conf., June 1986, pp. 23-30.
- [93] M. Wecharatana and S. Chimamphant, "Bond Strength of Deformed Bars and Steel Fibers in High Strength Concrete", Materials Research Society, Symposium Proceedings, Vol.114, Bond in Cementitious Composites, Editors S. Mindess and S.P. Shah, Dec. 1987, pp. 245-254.
- [94] S. Chimamphant and M. Wecharatana, "Fatigue Characteristics of High Strength Cementitious Composites", The Second East Asia-Pacific Conference on Structural Engineering and Construction, Jan. 1989.
- [95] S. Chimamphant and M. Wecharatana, "Bond-Slip Characteristics of Reinforcement in High Strength Concrete", The Second East Asia-Pacific Conference on Structural Engineering and Construction, Jan. 1989.
- [96] M. Wecharatana, S. Chimamphant and C.C. Lin, "New Polymer Concrete for Marine Structures", The Second East Asia-Pacific Conference on Structural Engineering and Construction, Jan. 1989.
- [97] S. Chimamphant and M. Wecharatana, "Bond-Slip Characteristics of High Strength Fibrous Concrete", To be submitted for possible publication in Apr. 1989, ACI Journal.

APPENDIX A

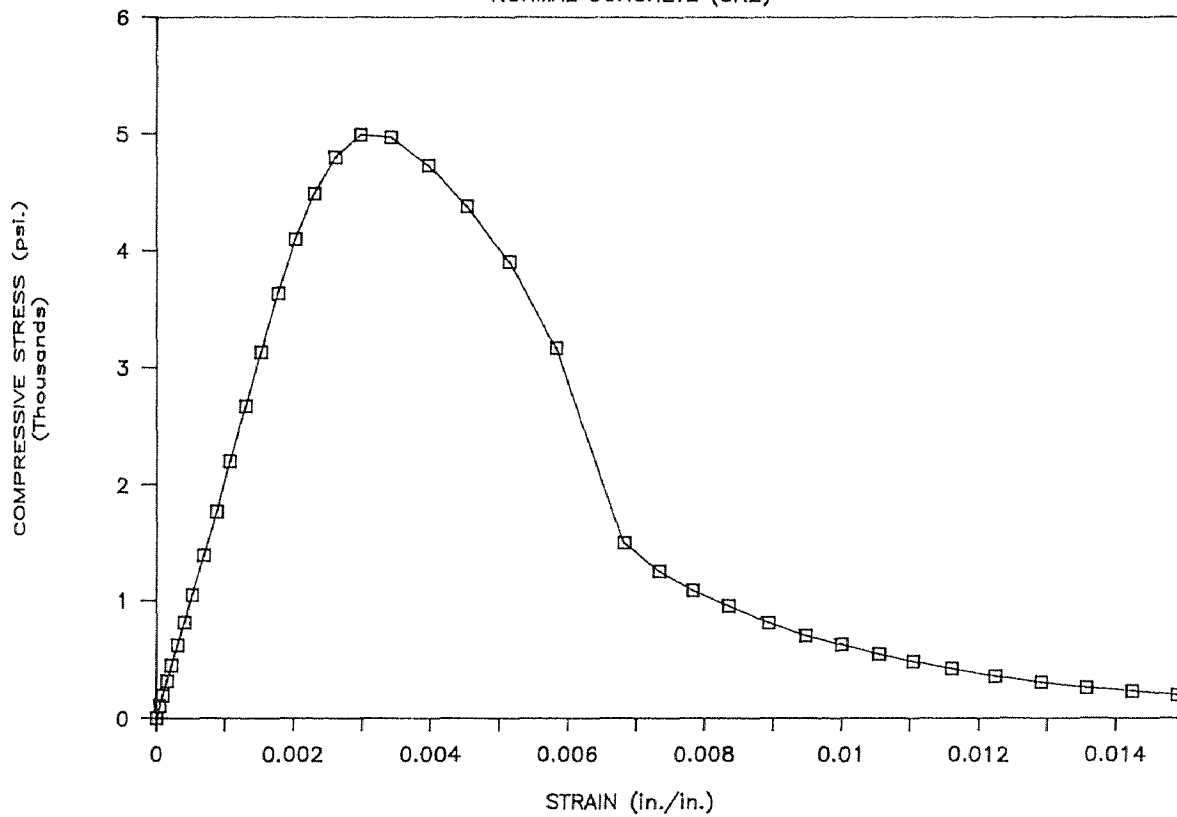
STRESS VS. STRAIN CURVE

NORMAL CONCRETE (SN1)



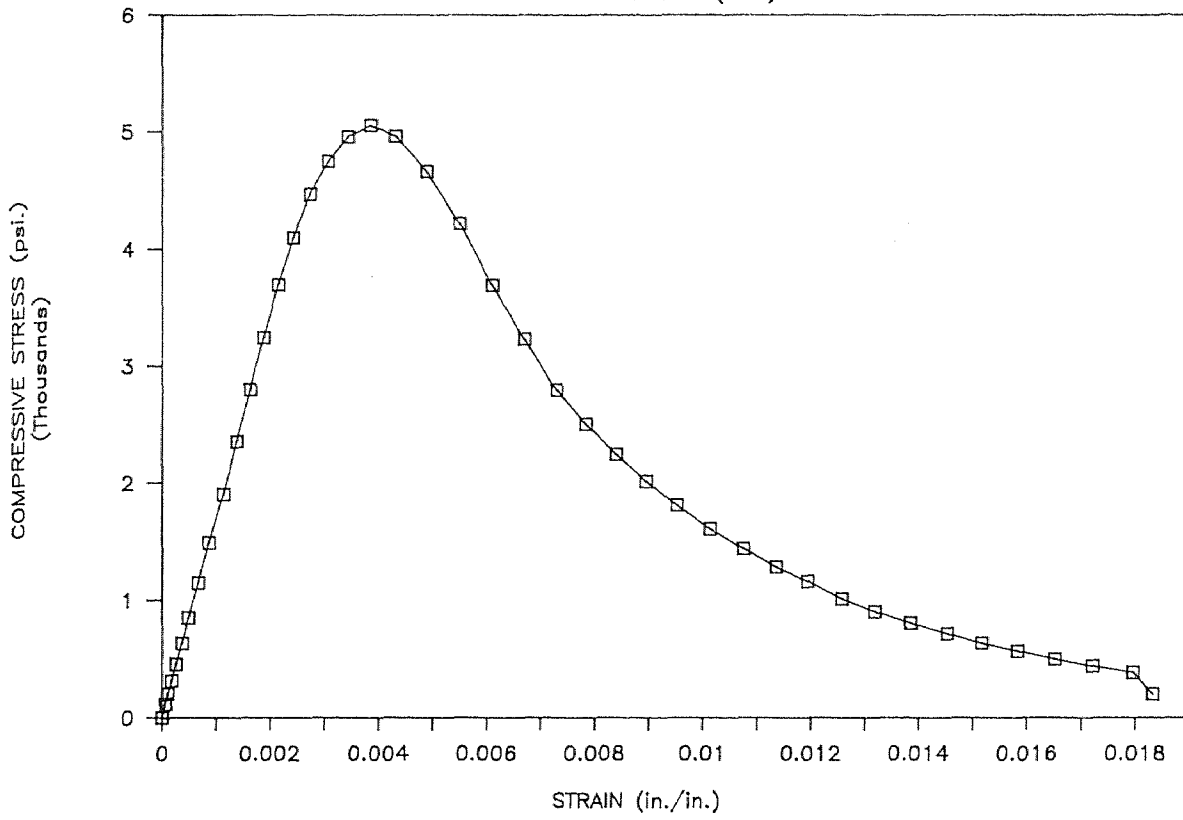
STRESS VS. STRAIN CURVE

NORMAL CONCRETE (SN2)



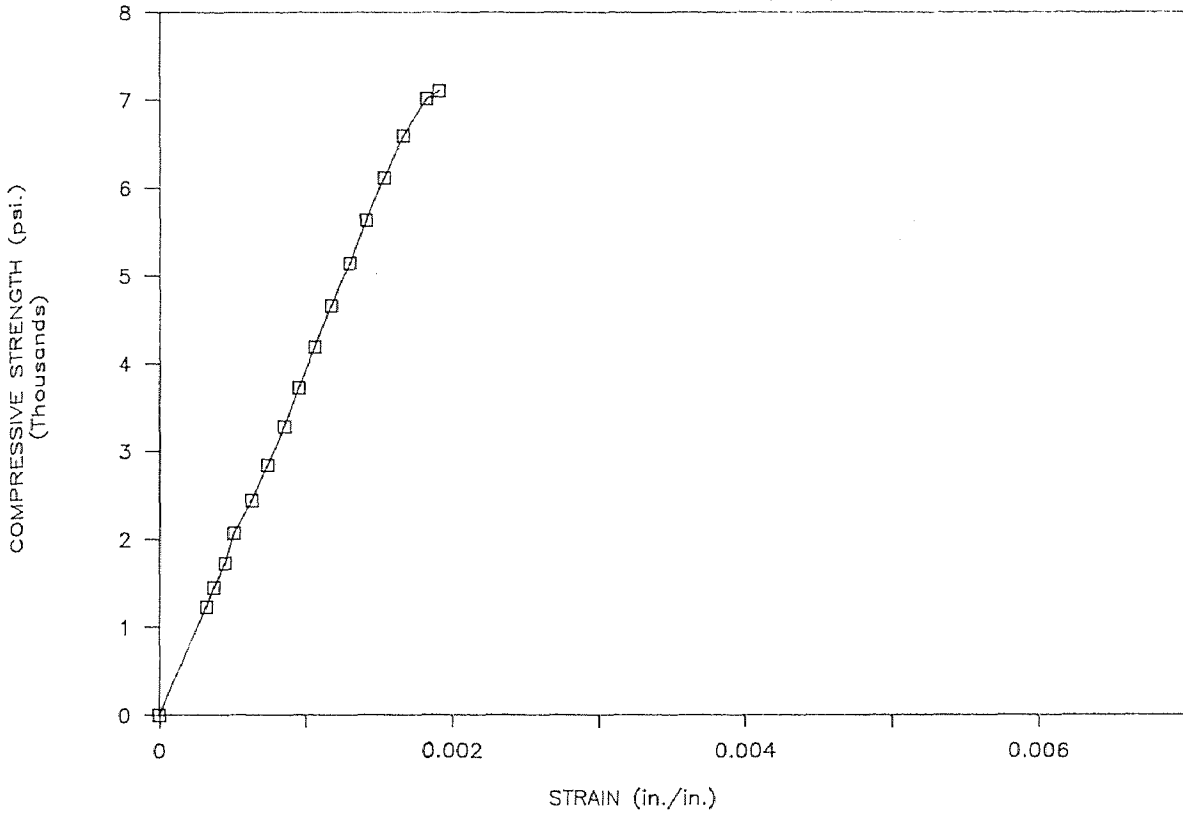
STRESS VS. STRAIN CURVE

NORMAL CONCRETE (SN3)



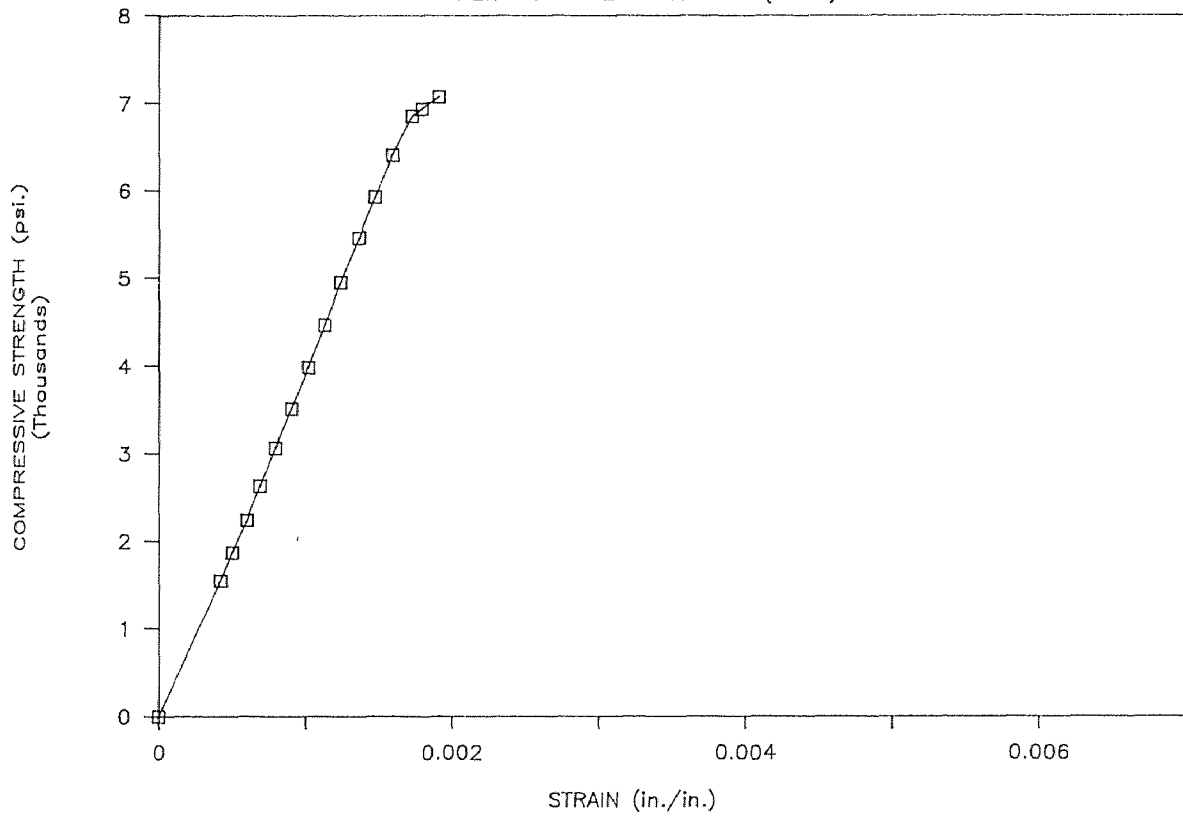
STRESS VS. STRAIN CURVE

SUPERPLASTICIZER CONCRETE (S1S1)

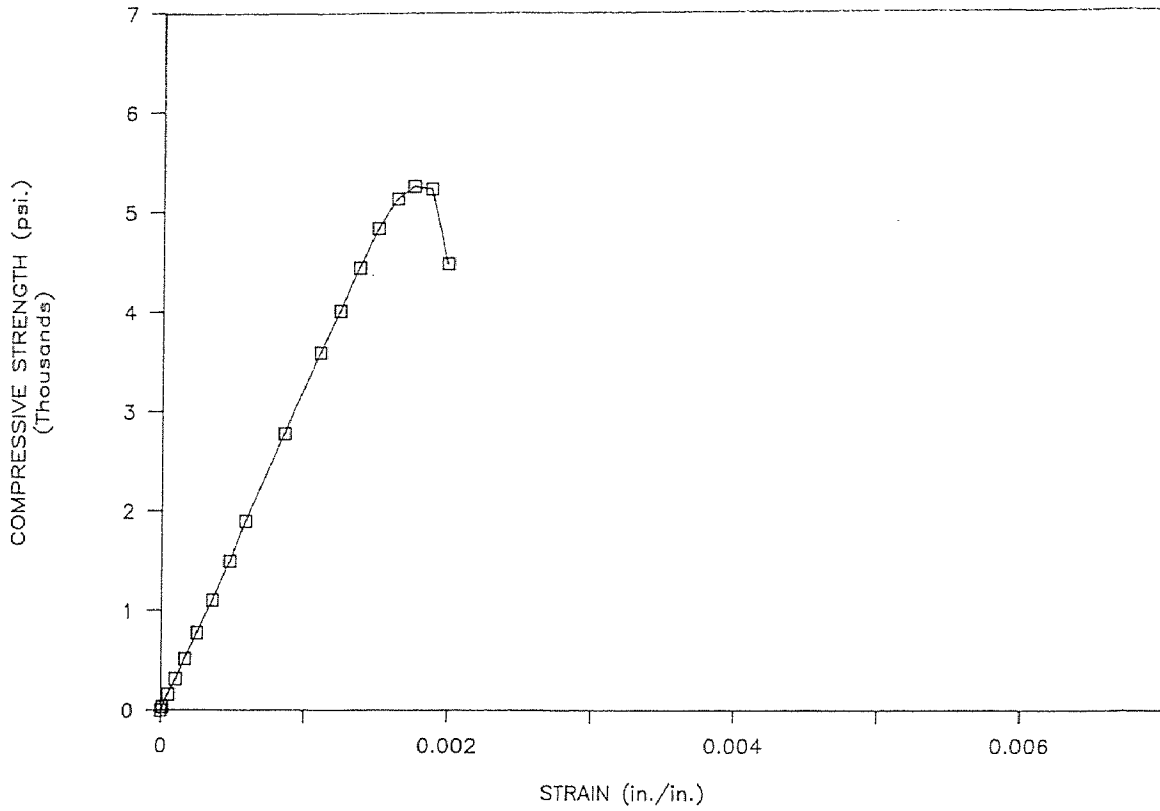


STRESS VS. STRAIN CURVE

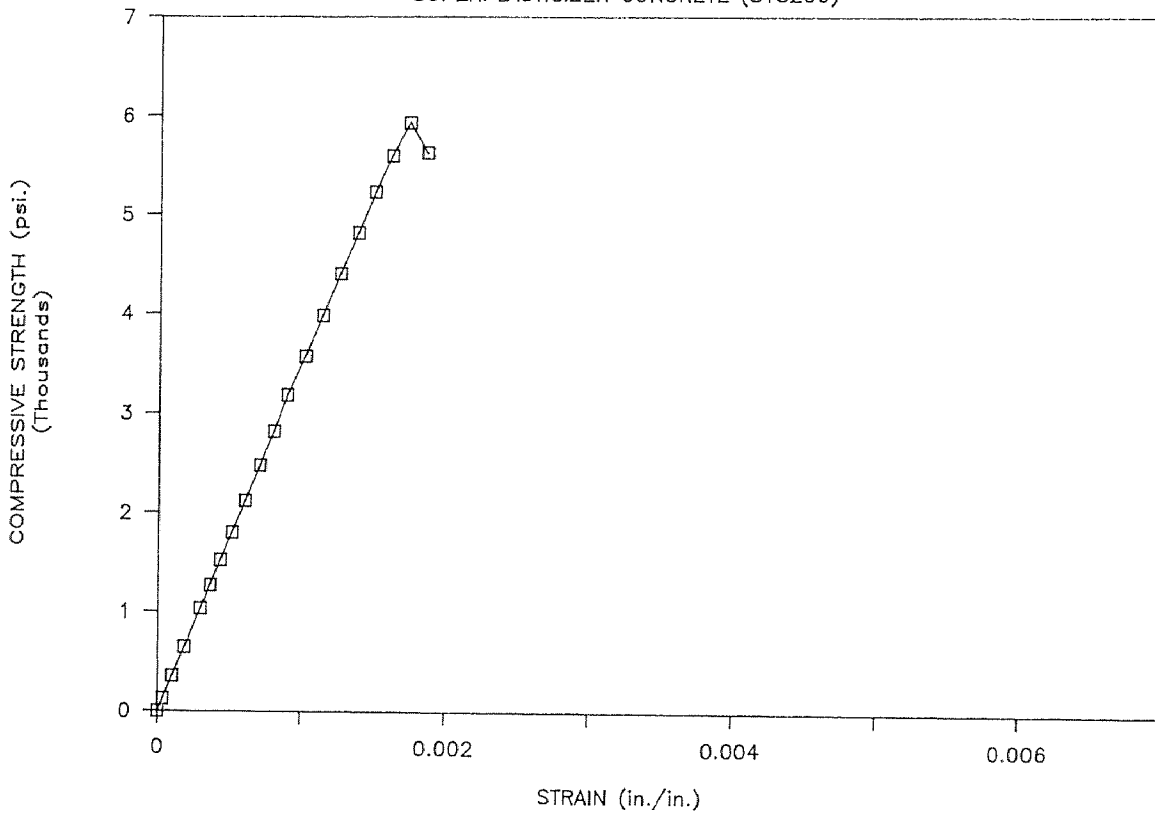
SUPERPLASTICIZER CONCRETE (S1S2)



STRESS VS. STRAIN CURVE
SUPERPLASTICIZER CONCRETE (S1S106)

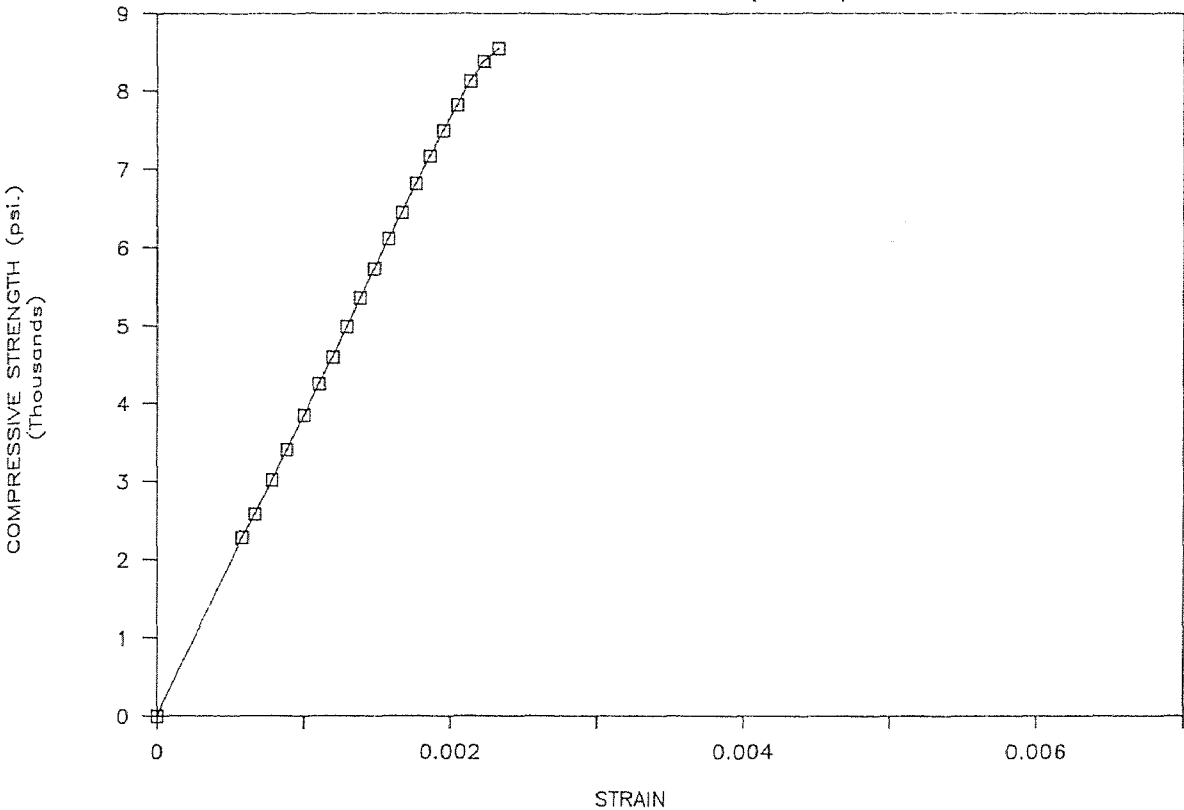


STRESS VS. STRAIN CURVE
SUPERPLASTICIZER CONCRETE (S1S206)



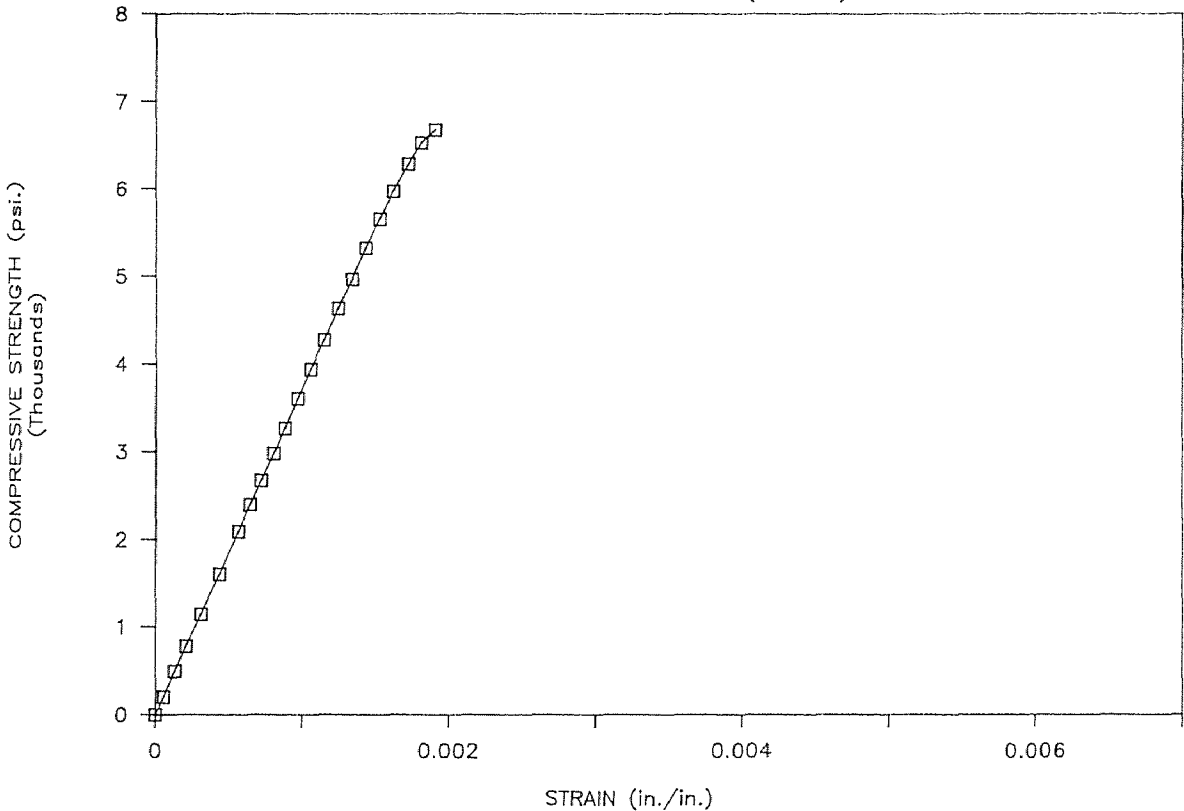
STRESS VS. STRAIN CURVE

SUPERPLASTICIZER CONCRETE (S1S306)



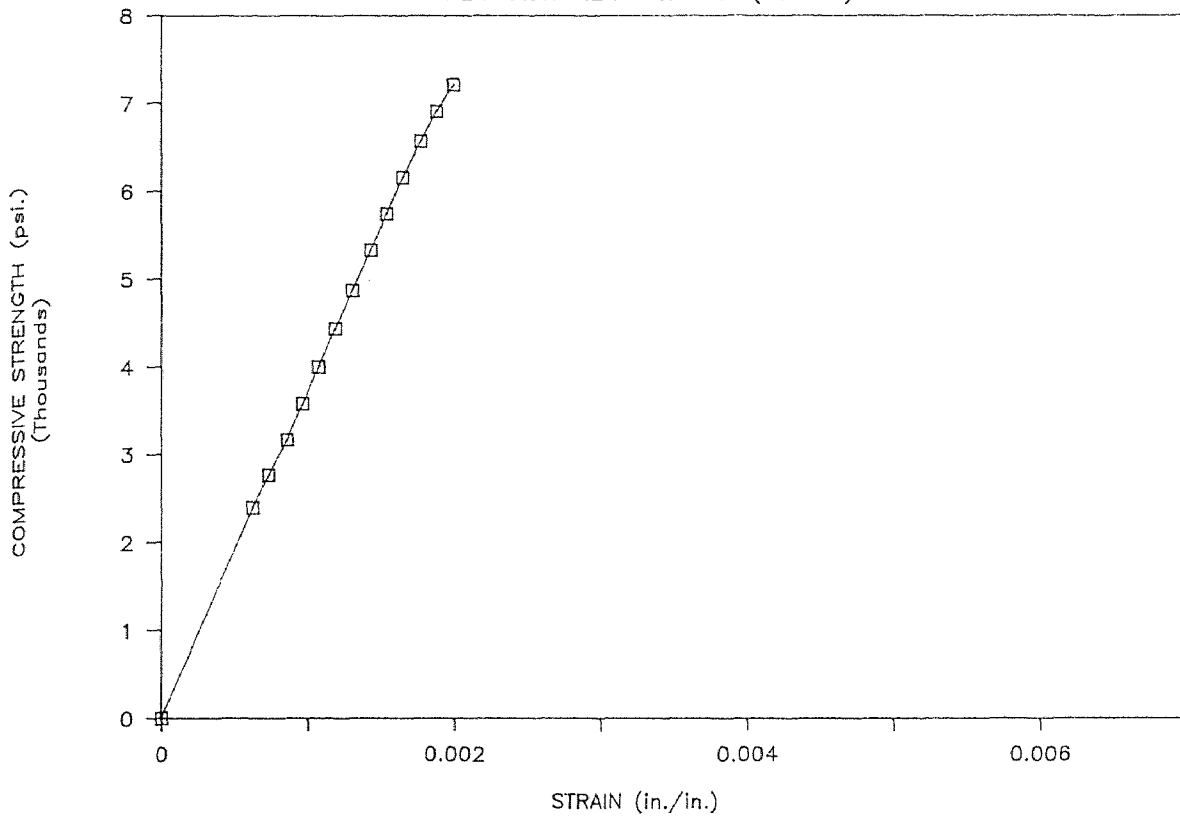
STRESS VS. STRAIN CURVE

SUPERPLASTICIZER CONCRETE (S1S406)



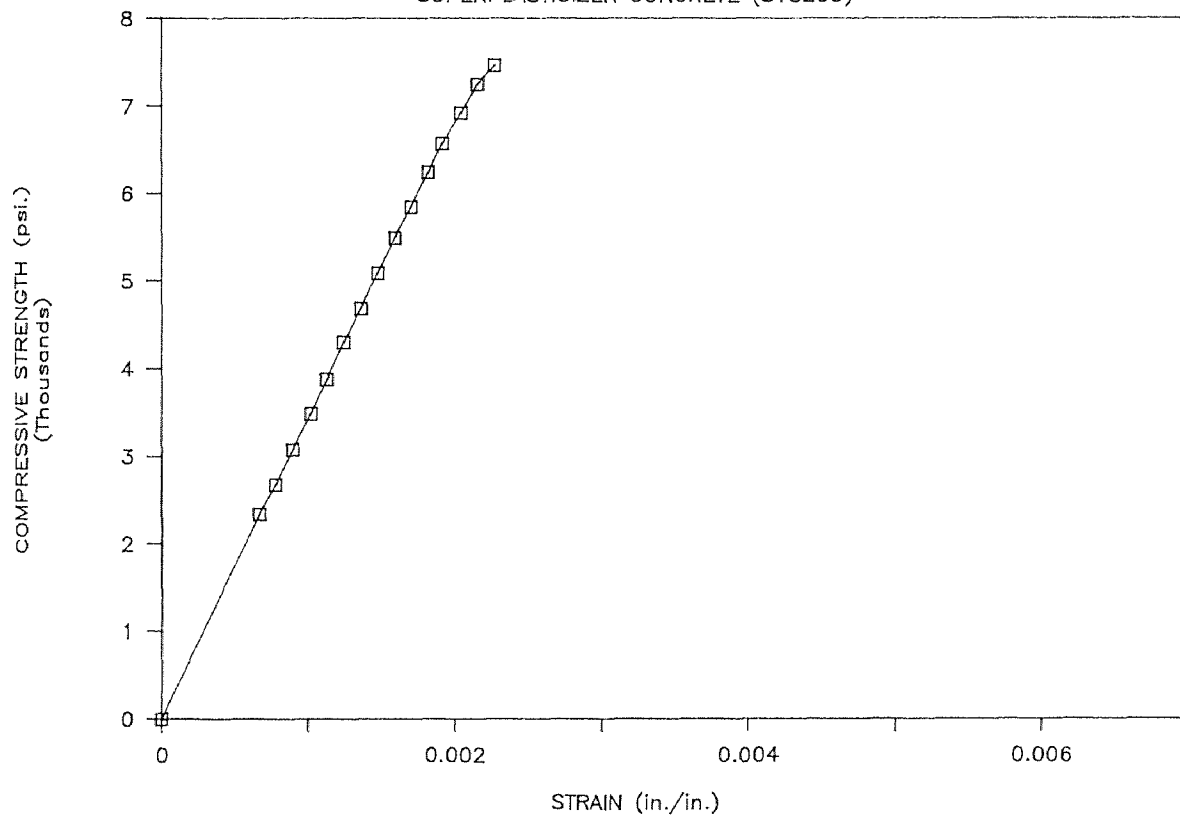
STRESS VS. STRAIN CURVE

SUPERPLASTICIZER CONCRETE (S1S109)



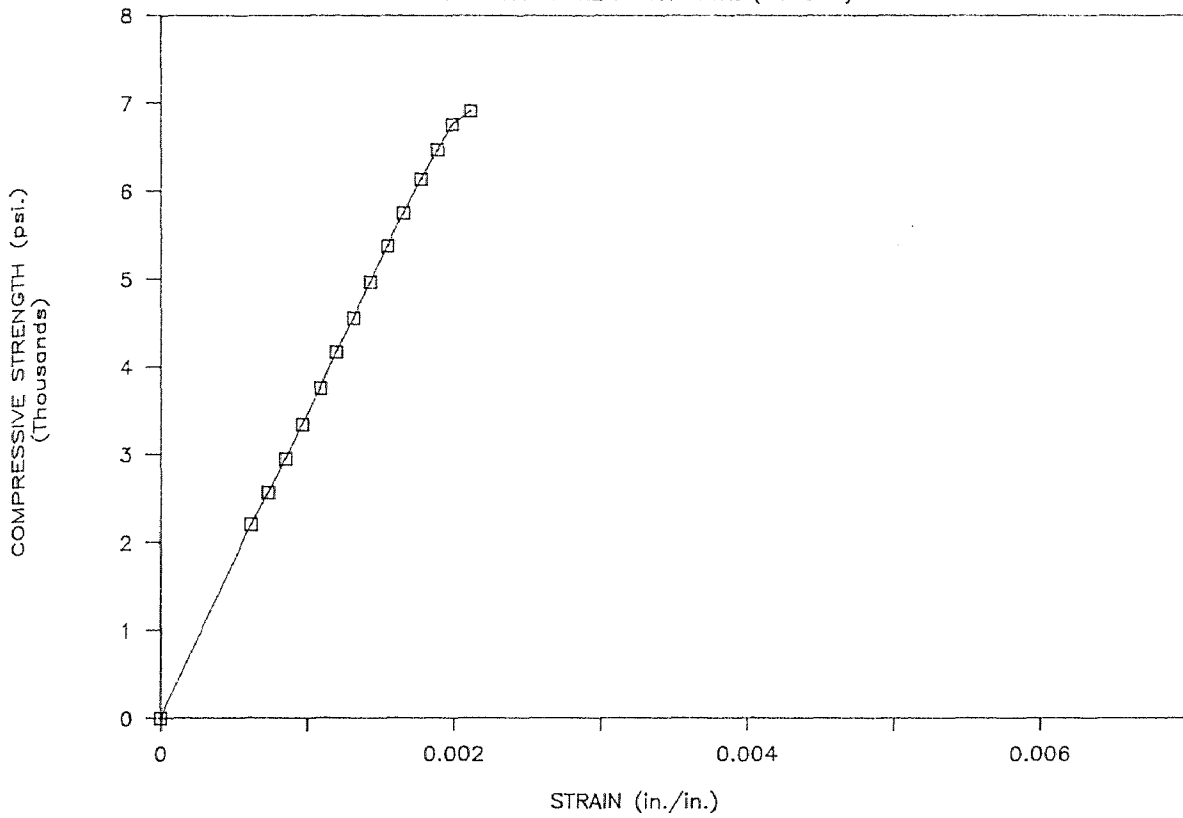
STRESS VS. STRAIN CURVE

SUPERPLASTICIZER CONCRETE (S1S209)



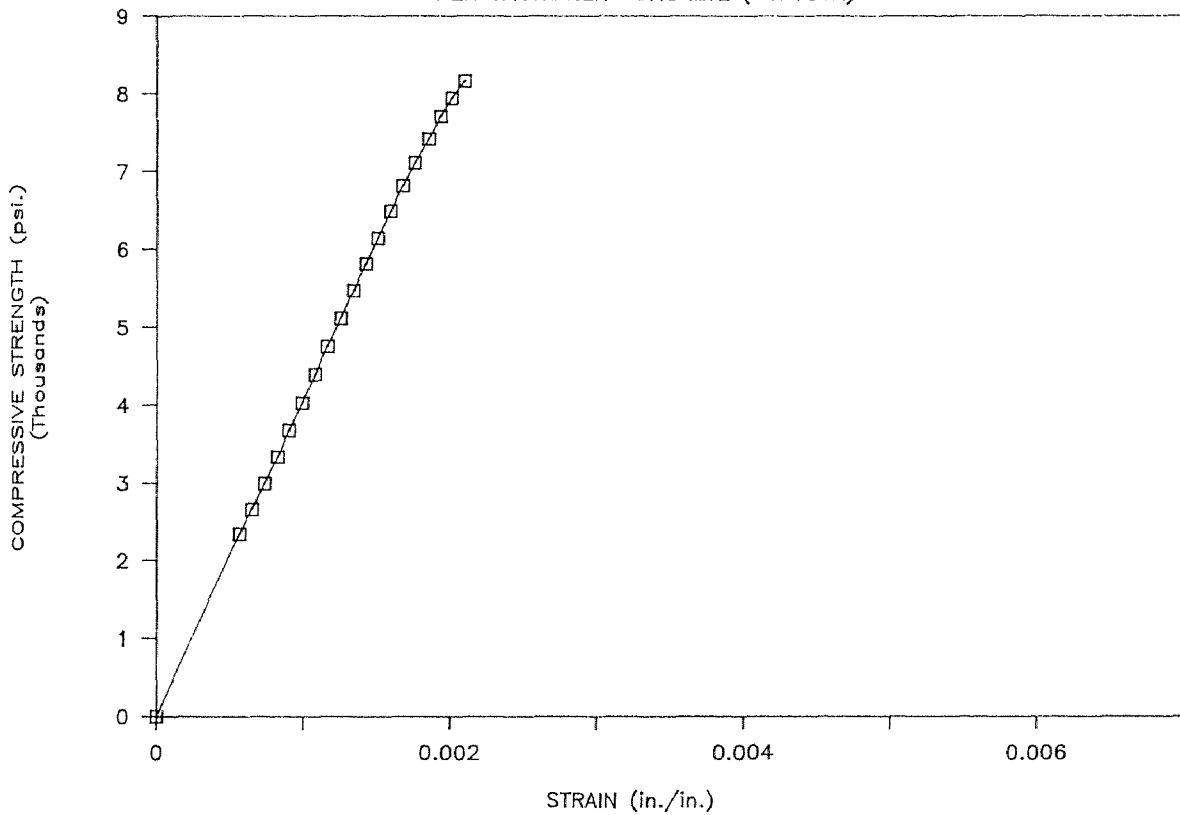
STRESS VS. STRAIN CURVE

SUPERPLASTICIZER CONCRETE (S1S309)



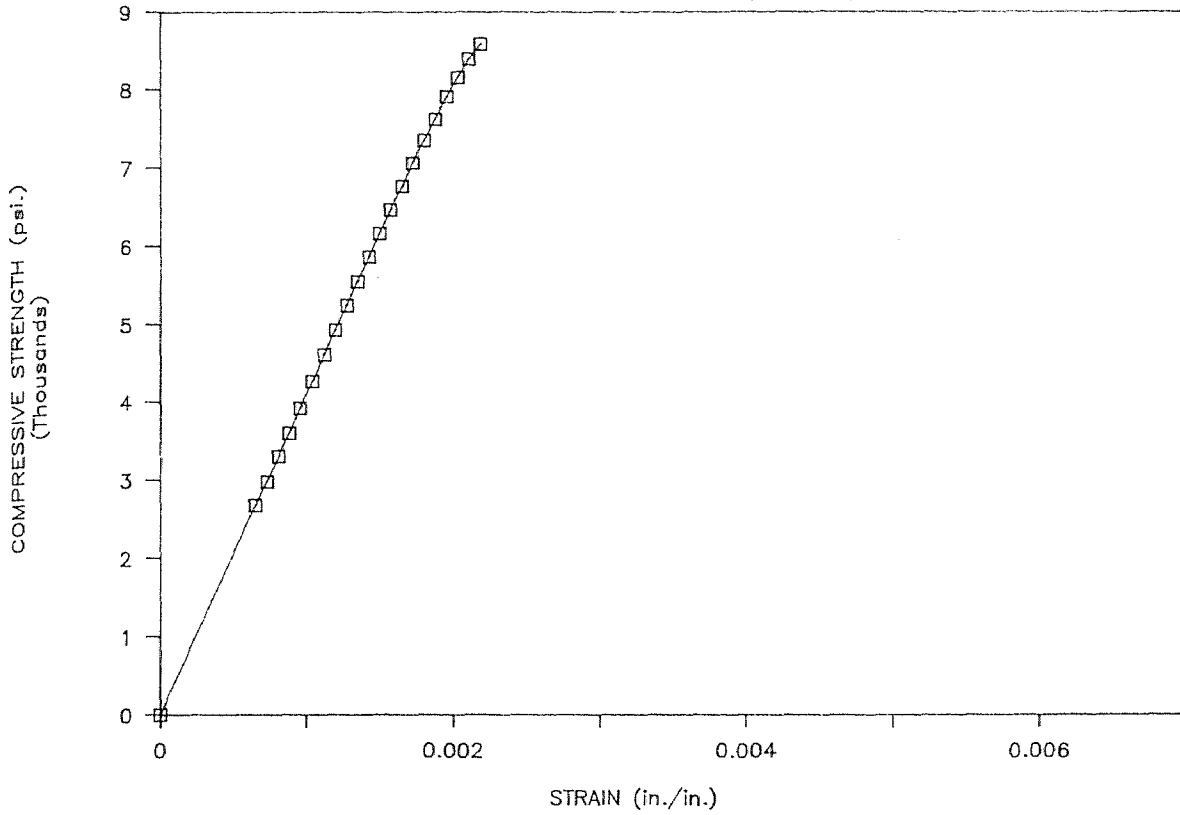
STRESS VS. STRAIN CURVE

SUPERPLASTICIZER CONCRETE (S1F106A)



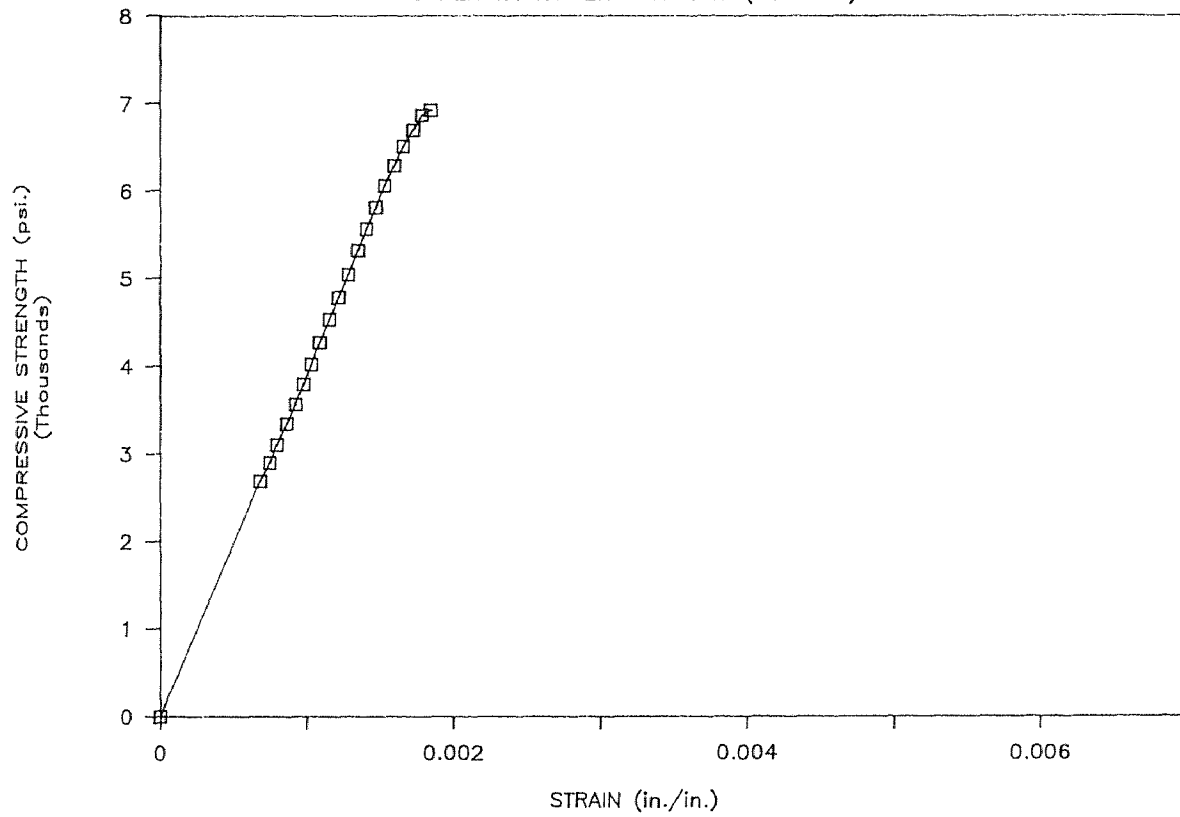
STRESS VS. STRAIN CURVE

SUPERPLASTICIZER CONCRETE (S1F206A)



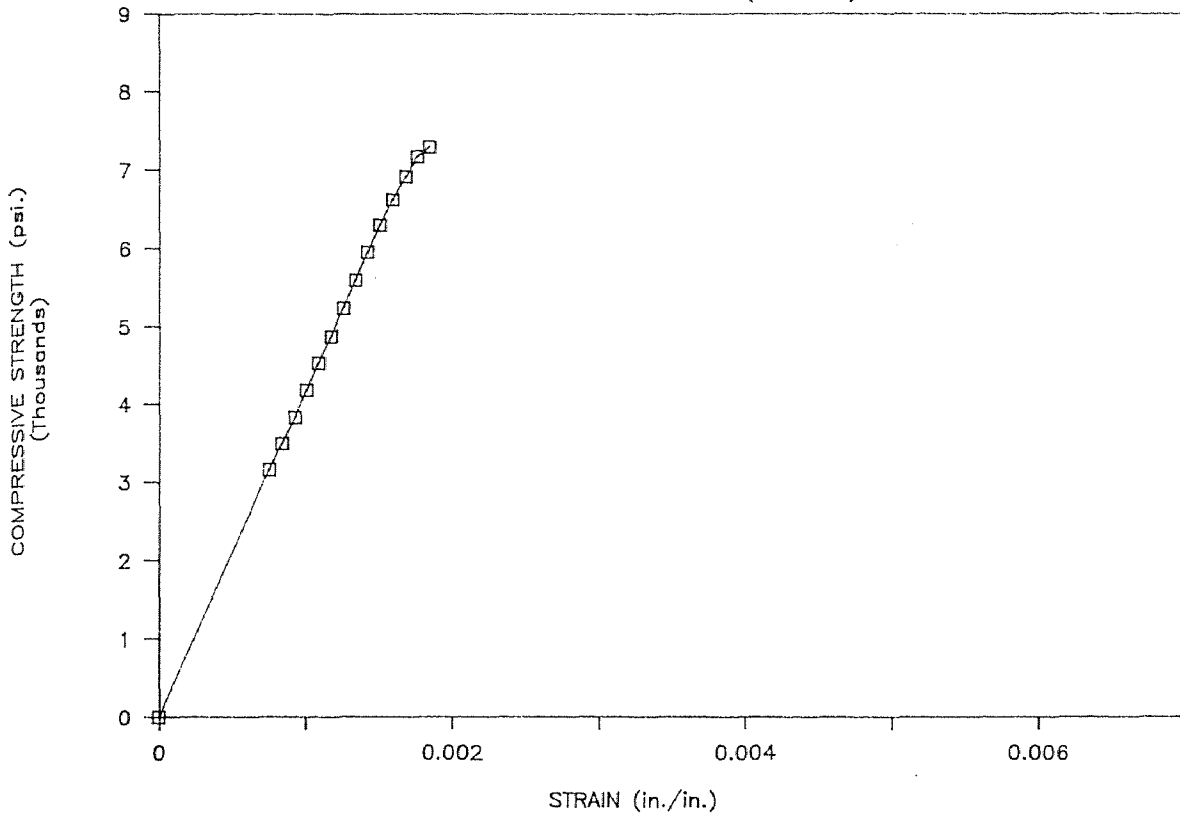
STRESS VS. STRAIN CURVE

SUPERPLASTICIZER CONCRETE (S1F207A)



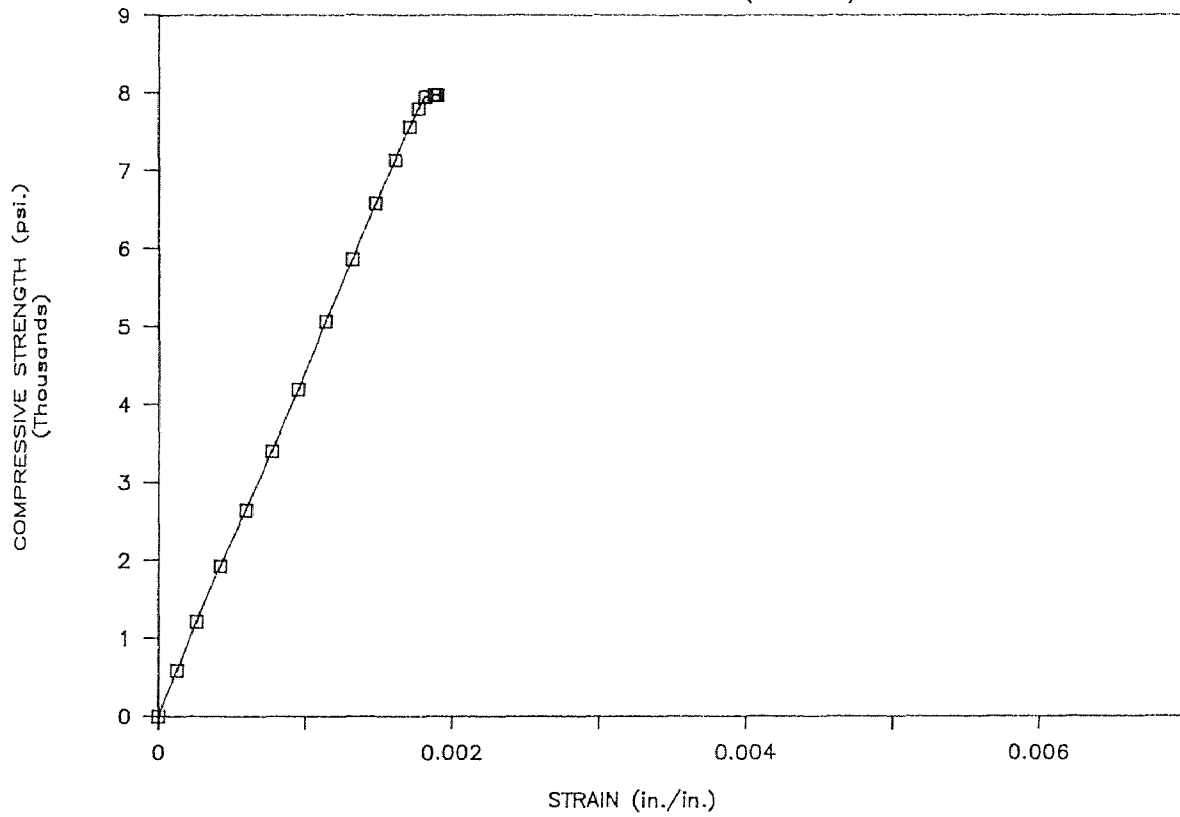
STRESS VS. STRAIN CURVE

SUPERPLASTICIZER CONCRETE (S1F307A)



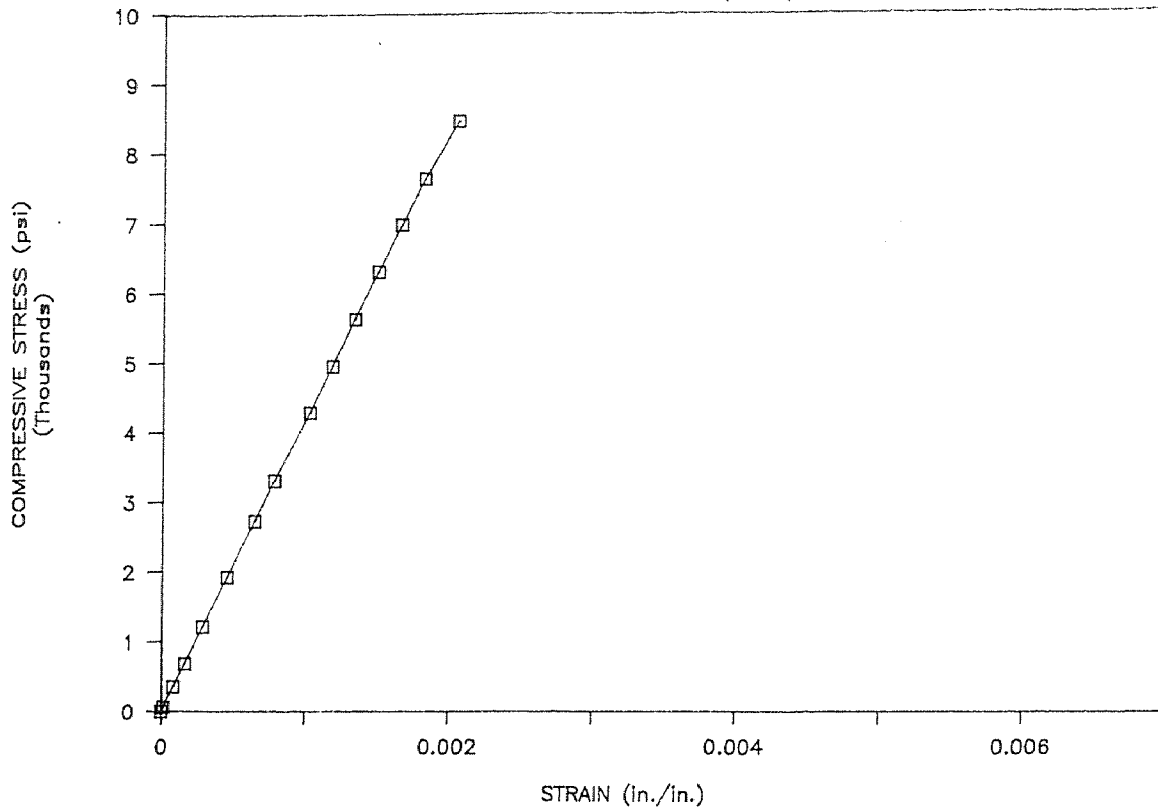
STRESS VS. STRAIN CURVE

SUPERPLASTICIZER CONCRETE (S1F175A)



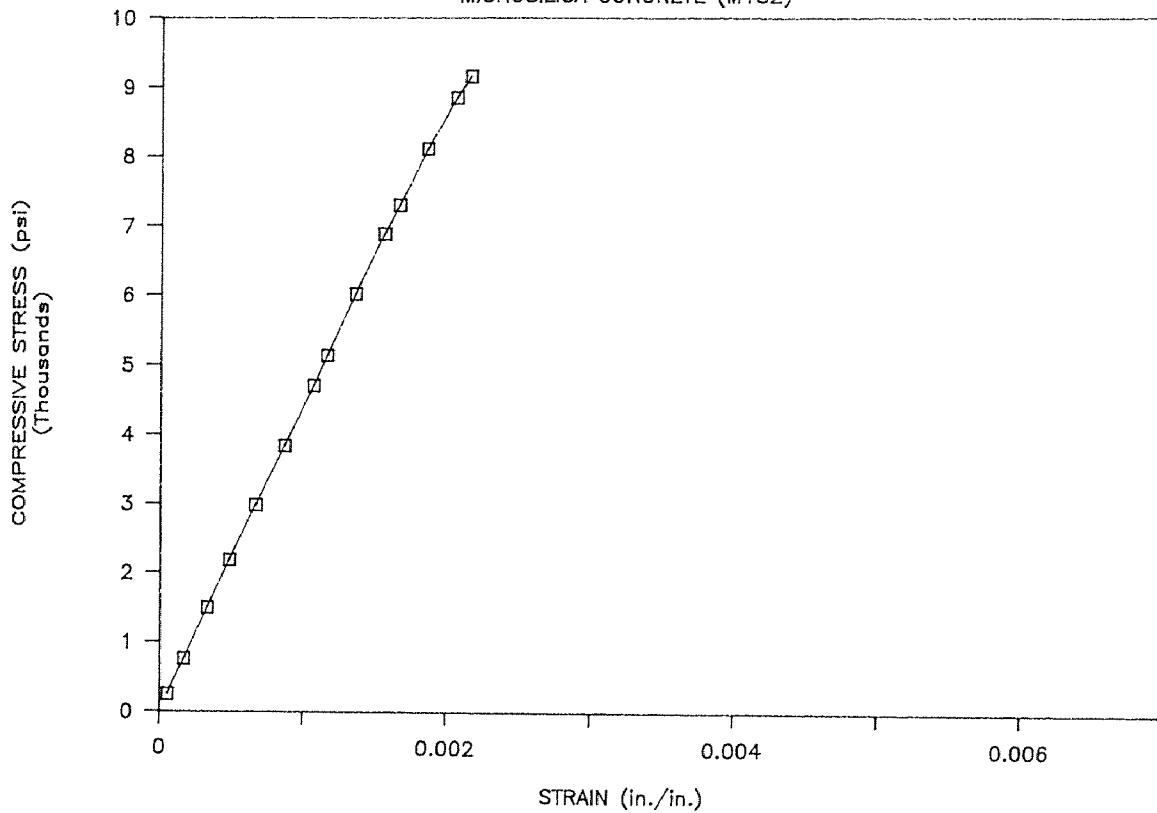
STRESS VS. STRAIN CURVE

MICROSILICA CONCRETE (M1S1)



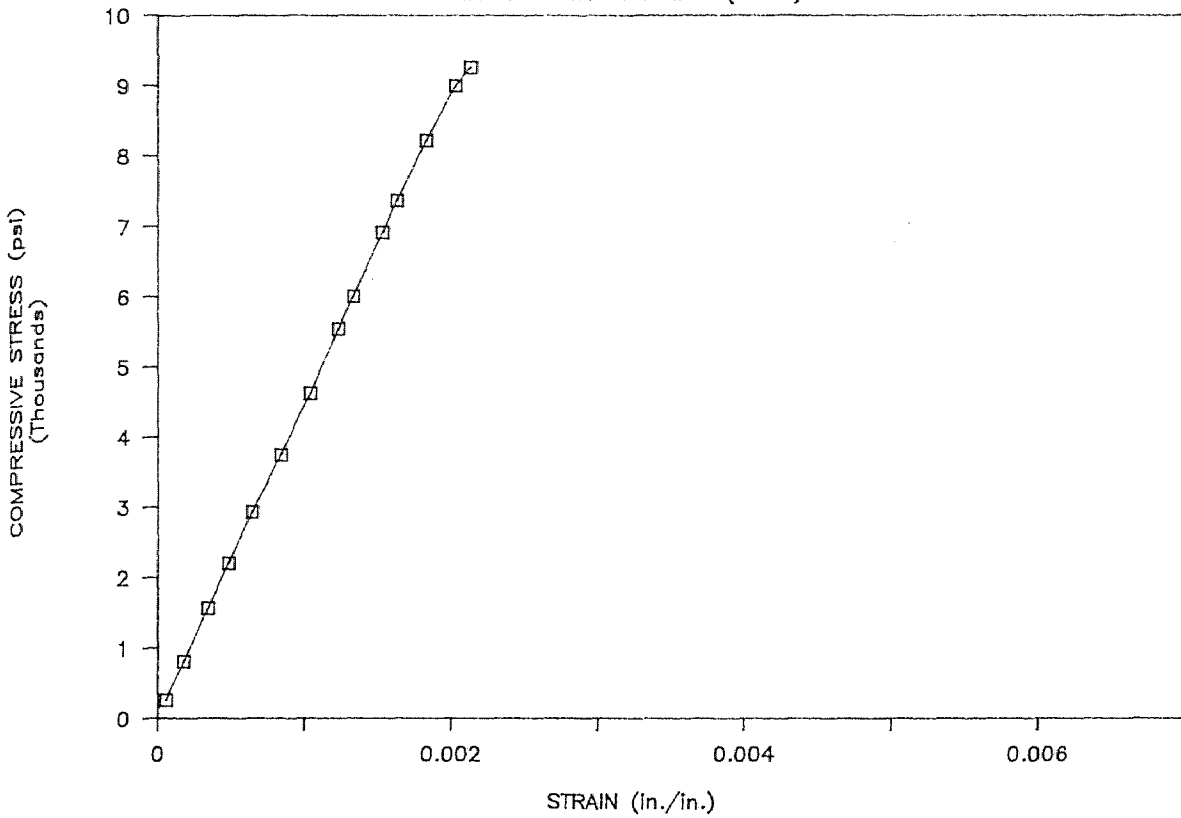
STRESS VS. STRAIN CURVE

MICROSILICA CONCRETE (M1S2)



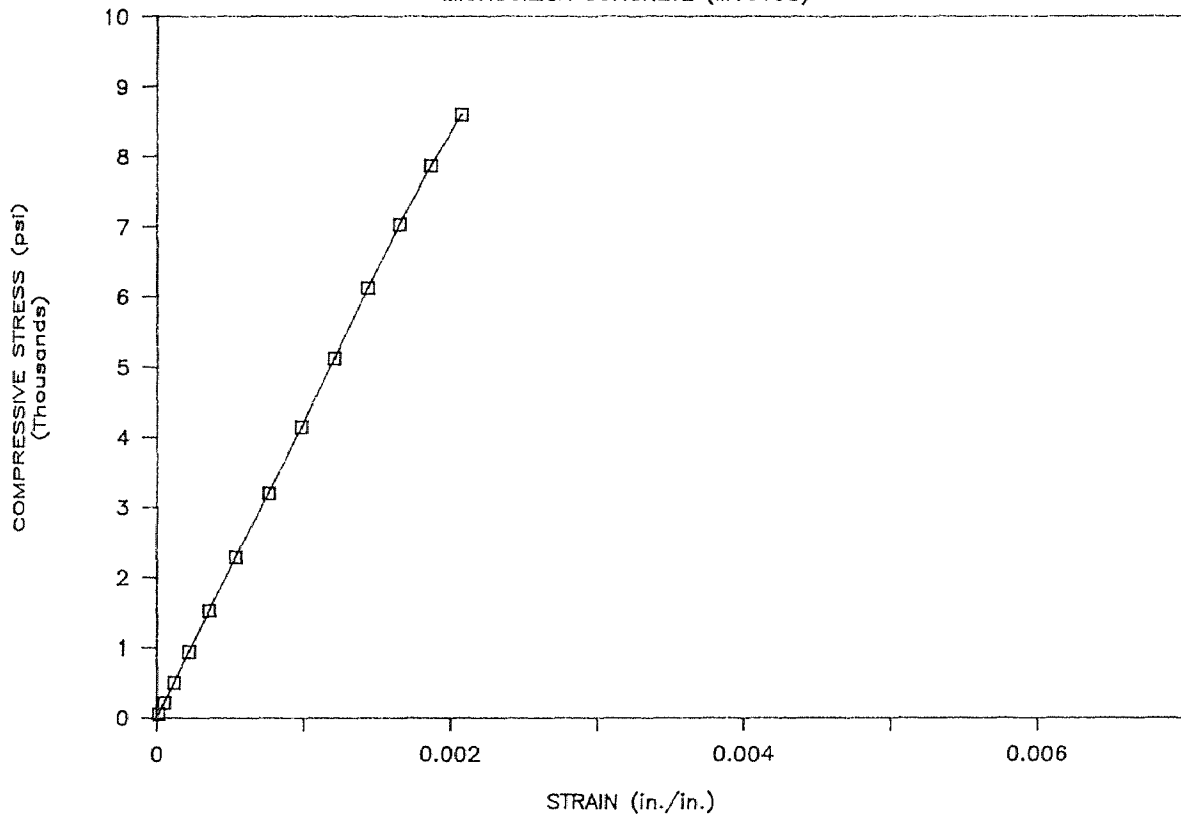
STRESS VS. STRAIN CURVE

MICROSILICA CONCRETE (M1S3)



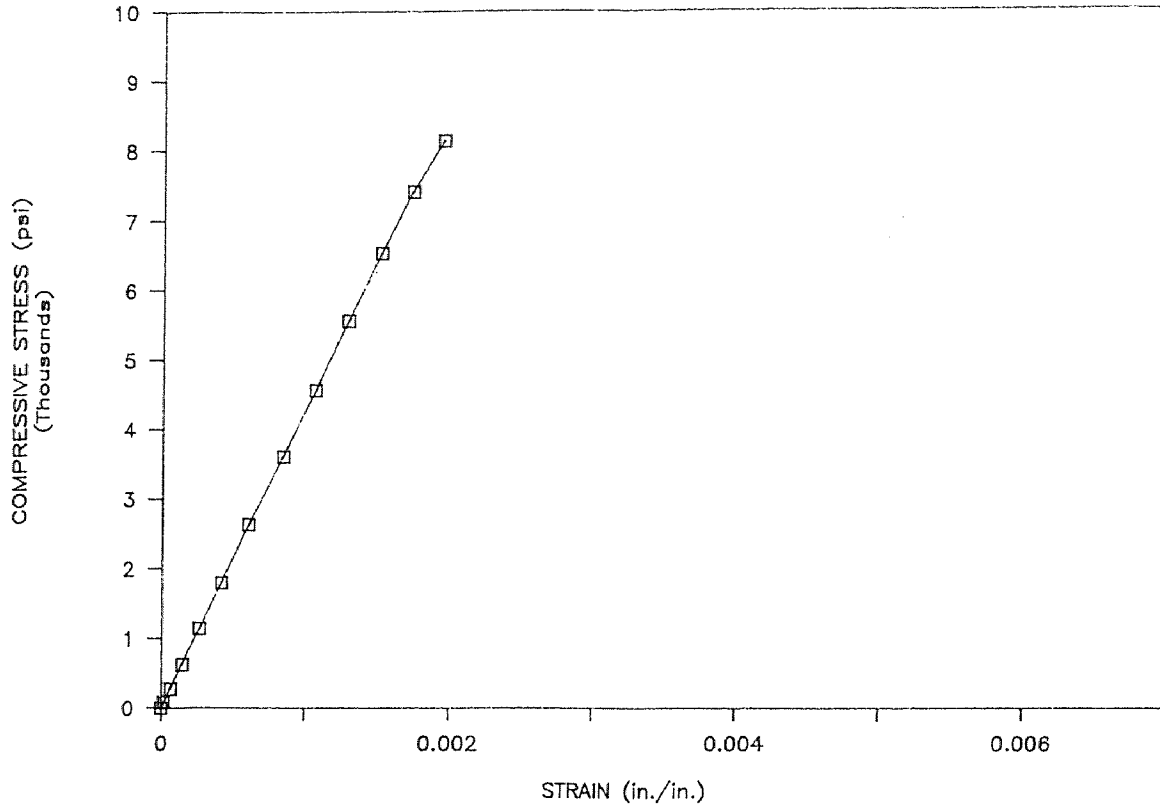
STRESS VS. STRAIN CURVE

MICROSILICA CONCRETE (M1S108)



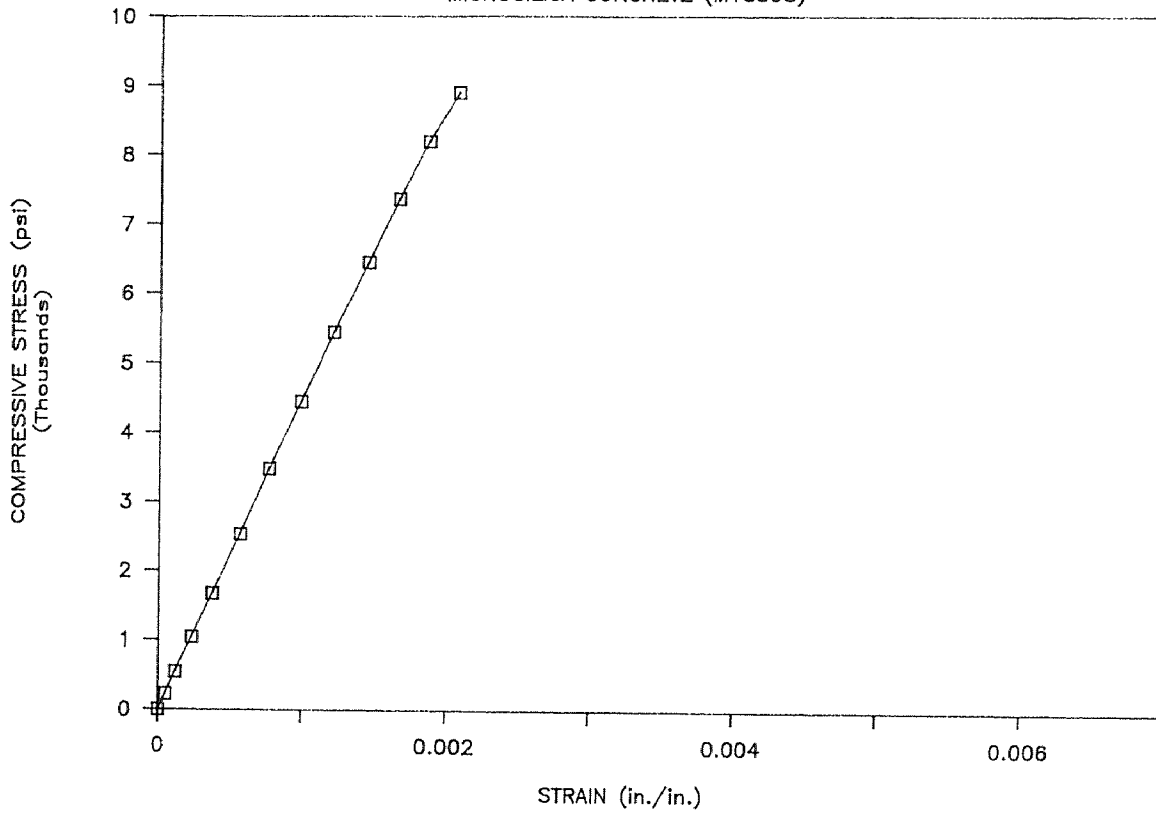
STRESS VS. STRAIN CURVE

MICROSILICA CONCRETE (M1S208)



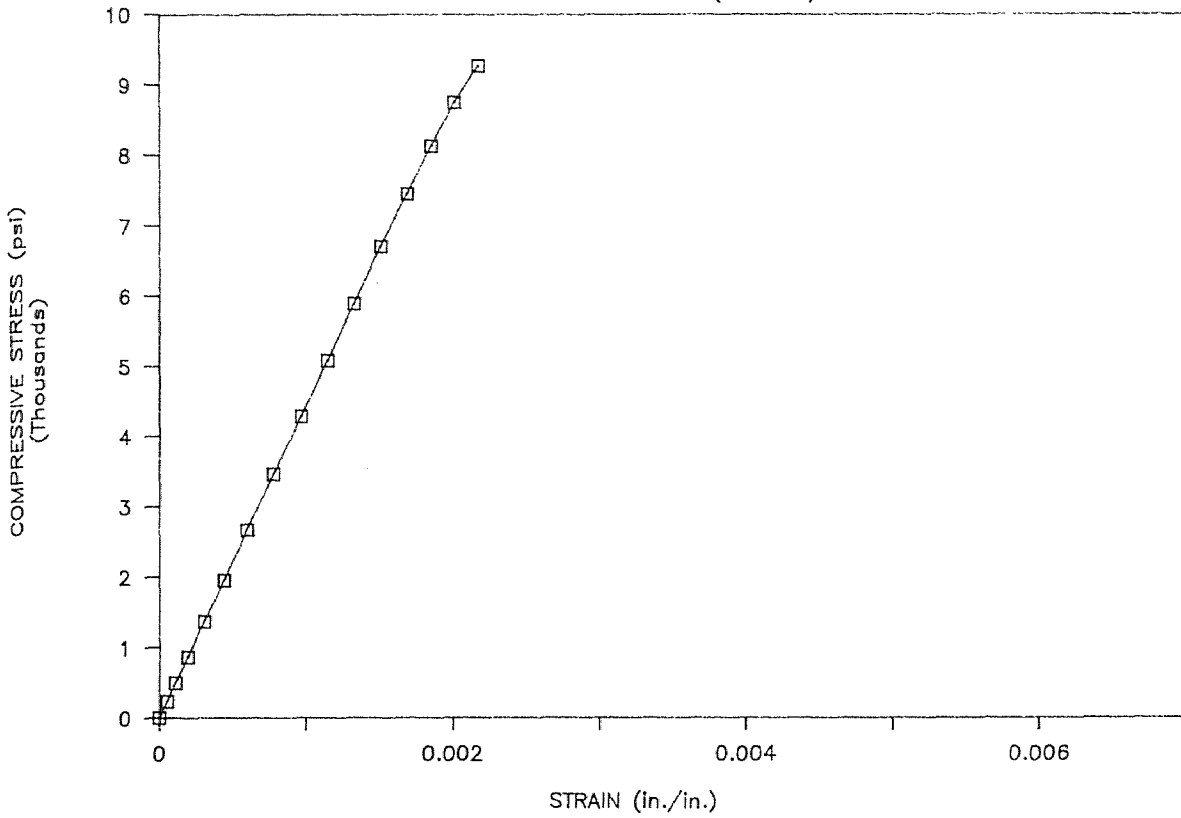
STRESS VS. STRAIN CURVE

MICROSILICA CONCRETE (M1S308)



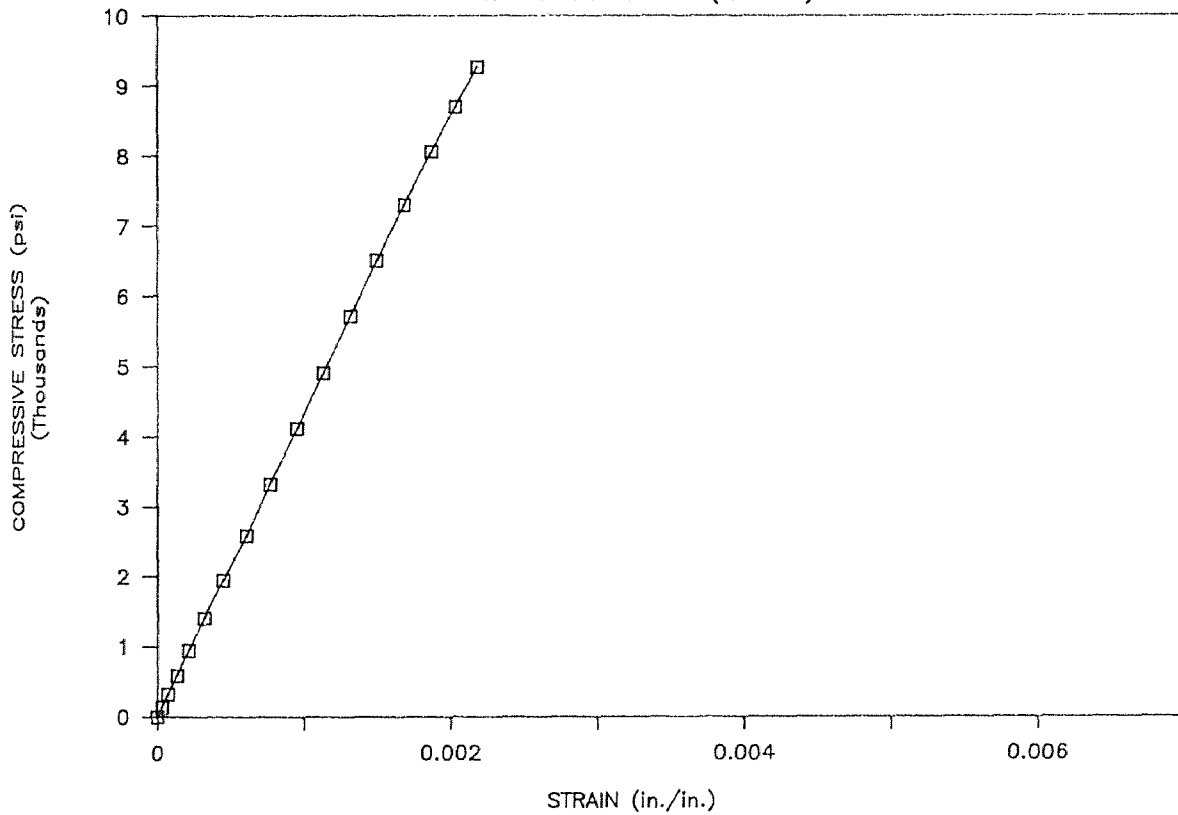
STRESS VS. STRAIN CURVE

MICROSILICA CONCRETE (M1S109)



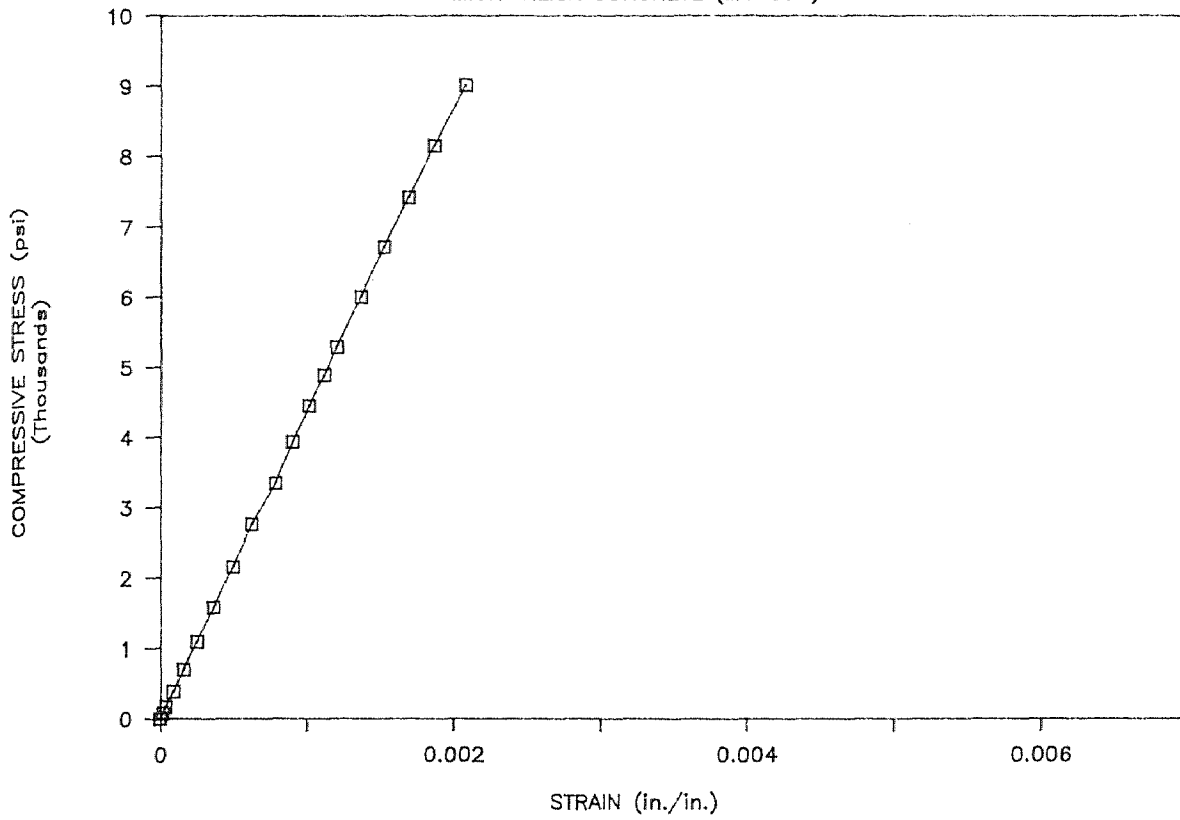
STRESS VS. STRAIN CURVE

MICROSILICA CONCRETE (M1S209)



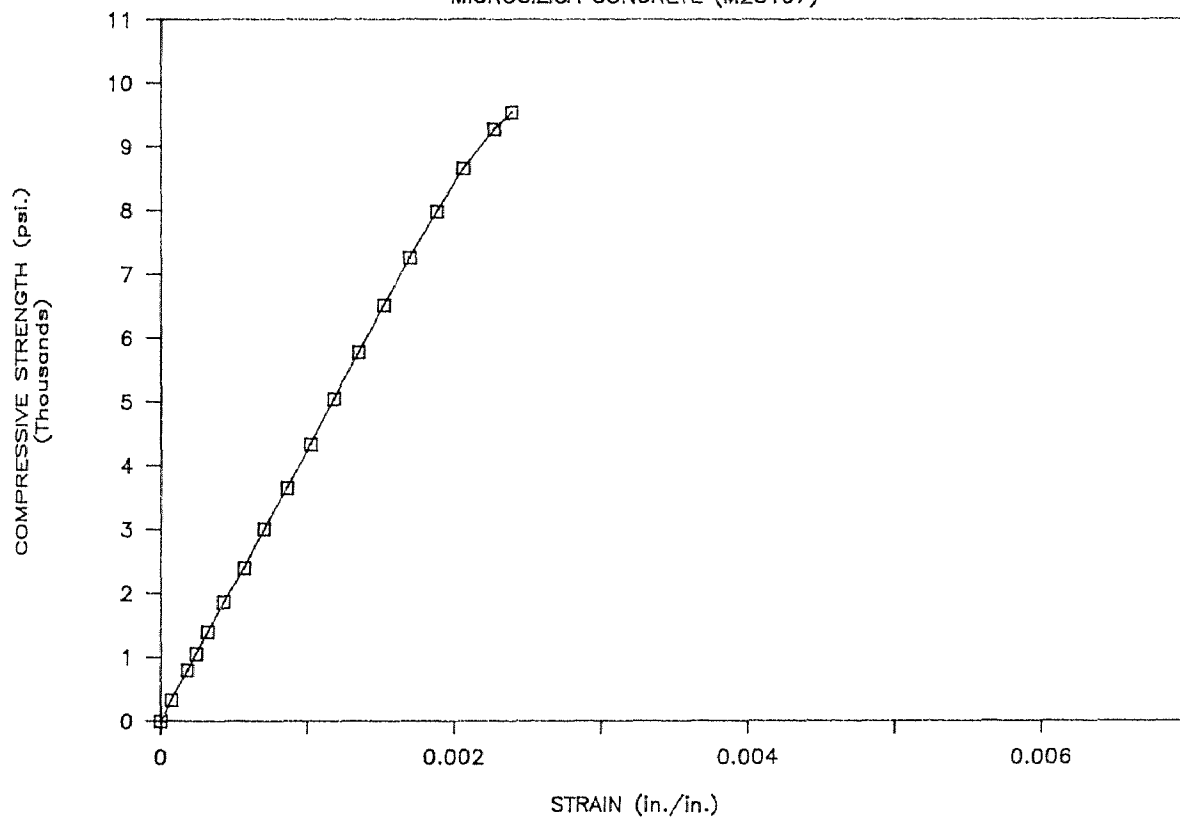
STRESS VS. STRAIN CURVE

MICROSILICA CONCRETE (M1S309)



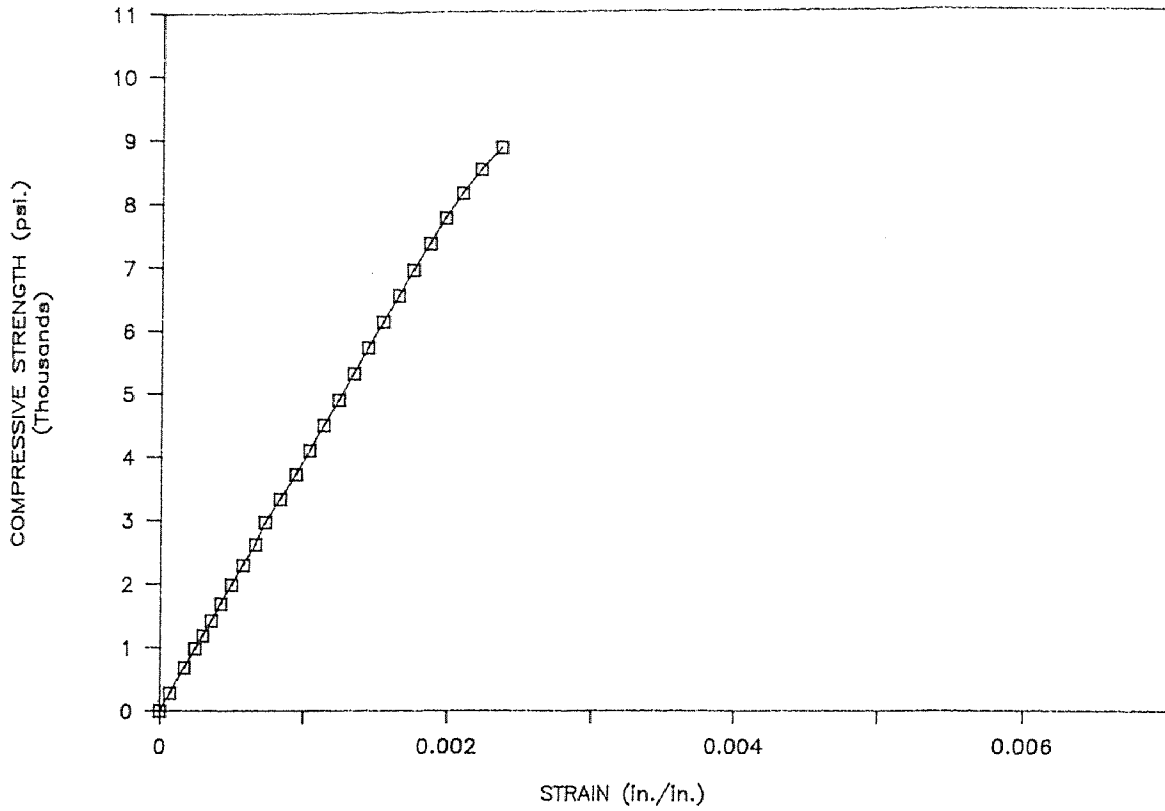
STRESS VS. STRAIN CURVE

MICROSILICA CONCRETE (M2S107)



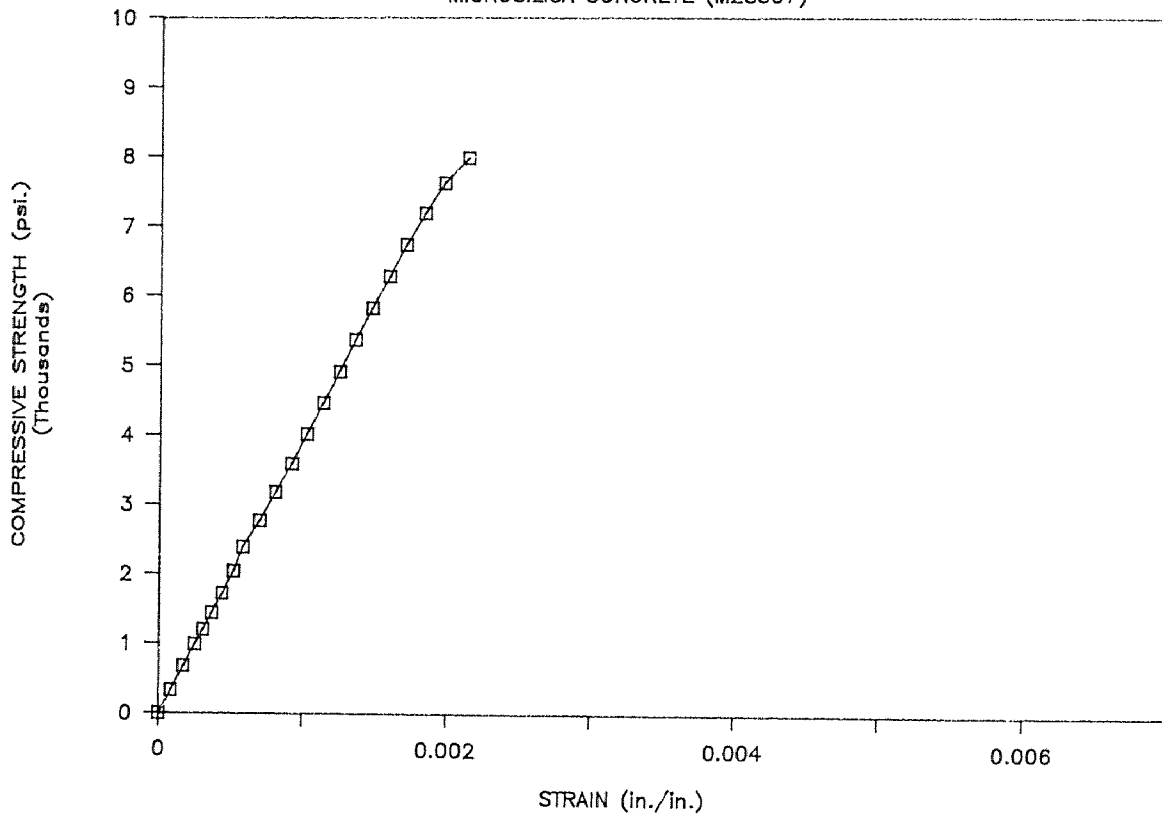
STRESS VS. STRAIN CURVE

MICROSILICA CONCRETE (M2S207)



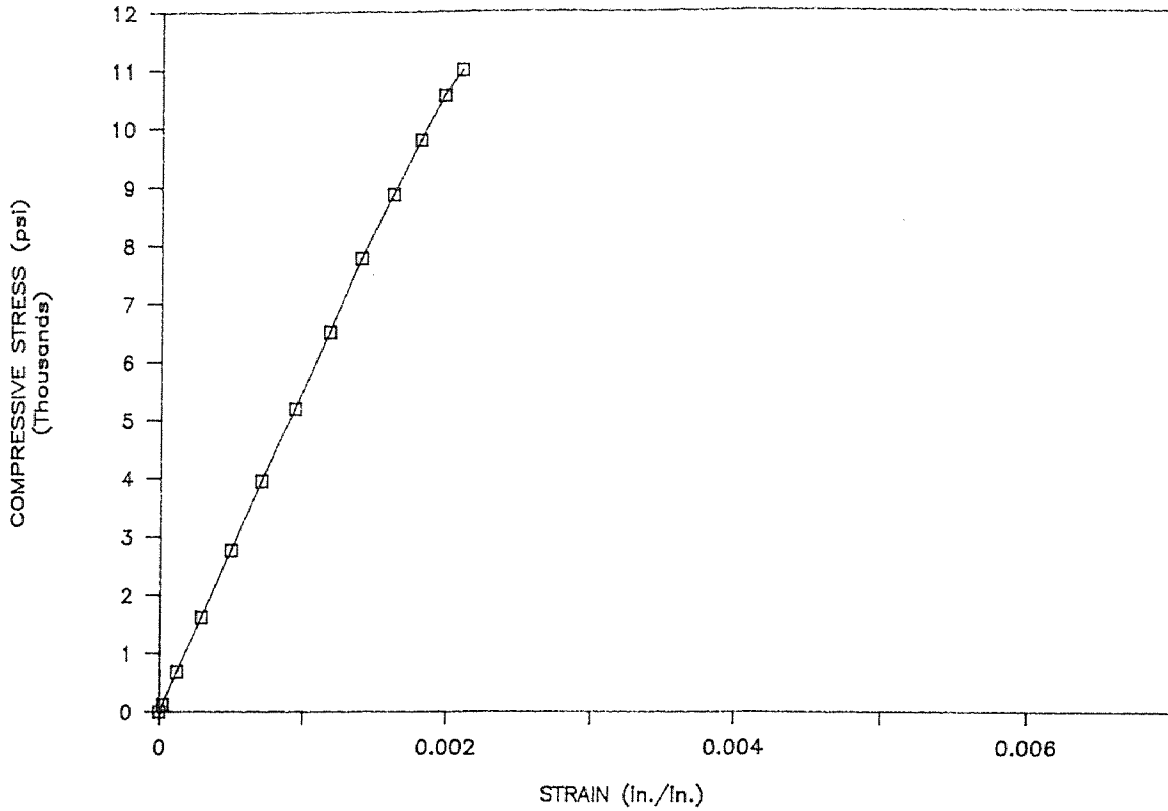
STRESS VS. STRAIN CURVE

MICROSILICA CONCRETE (M2S307)



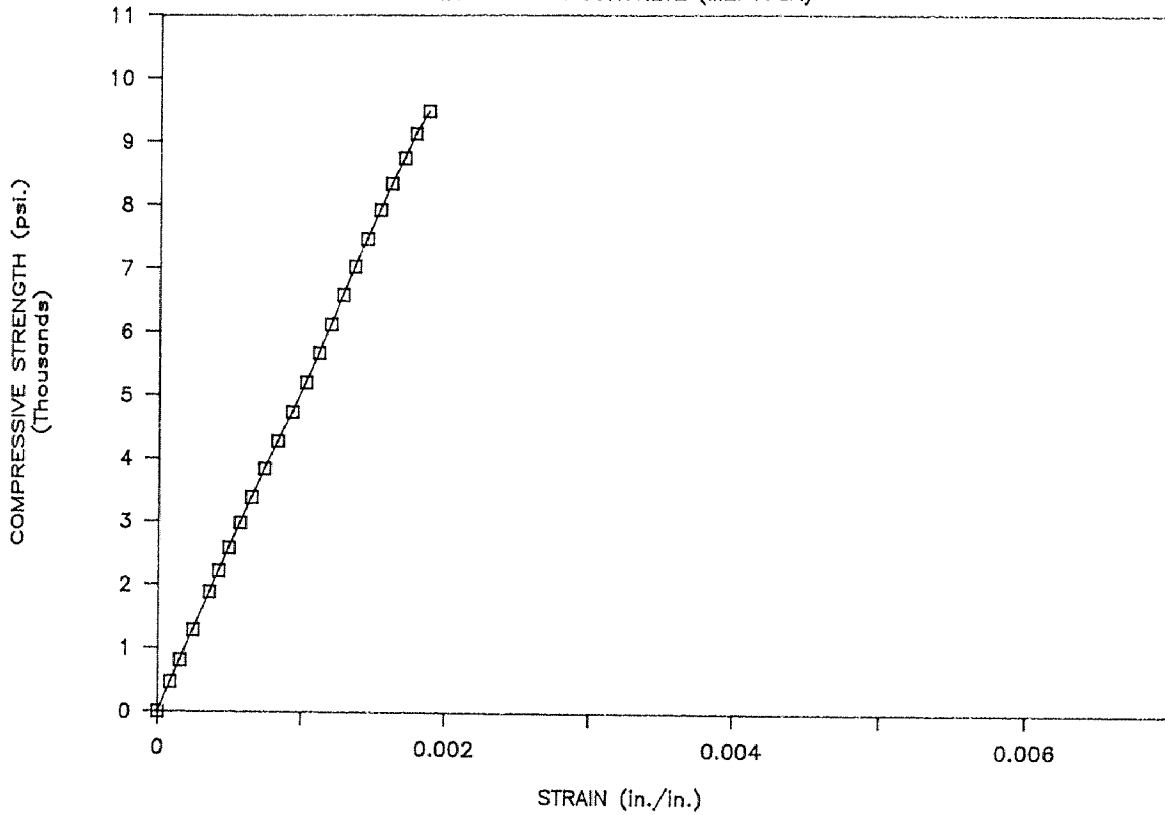
STRESS VS. STRAIN CURVE

MICROSILICA CONCRETE (M1F207A)



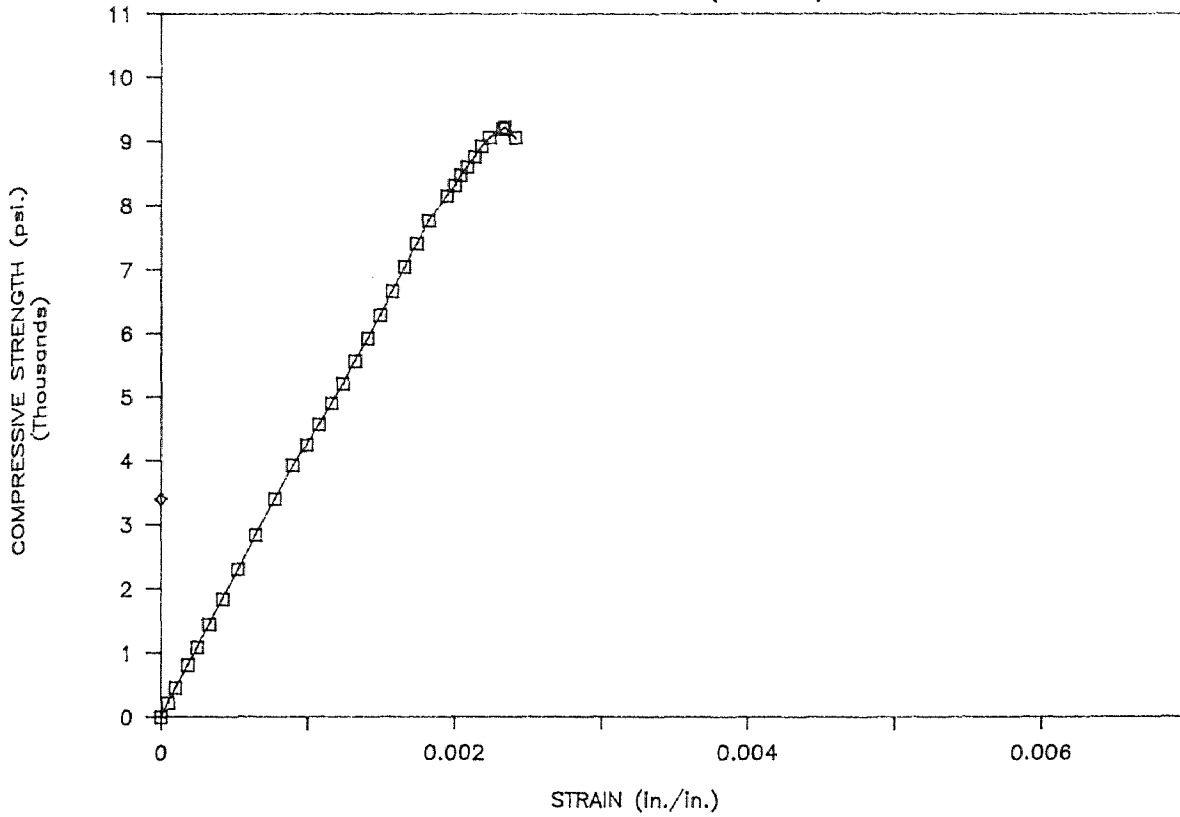
STRESS VS. STRAIN CURVE

MICROSILICA CONCRETE (M2F175A)



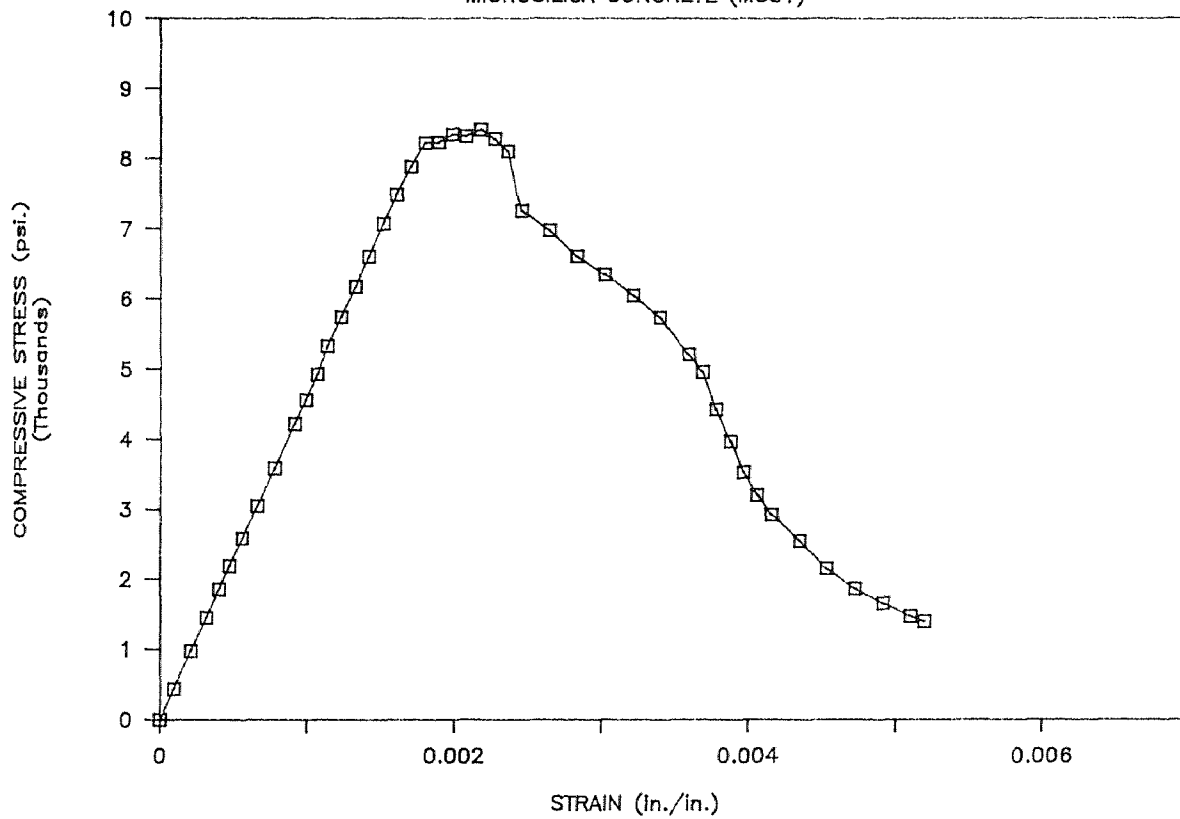
STRESS VS. STRAIN CURVE

MICROSILICA CONCRETE (M2F475A)



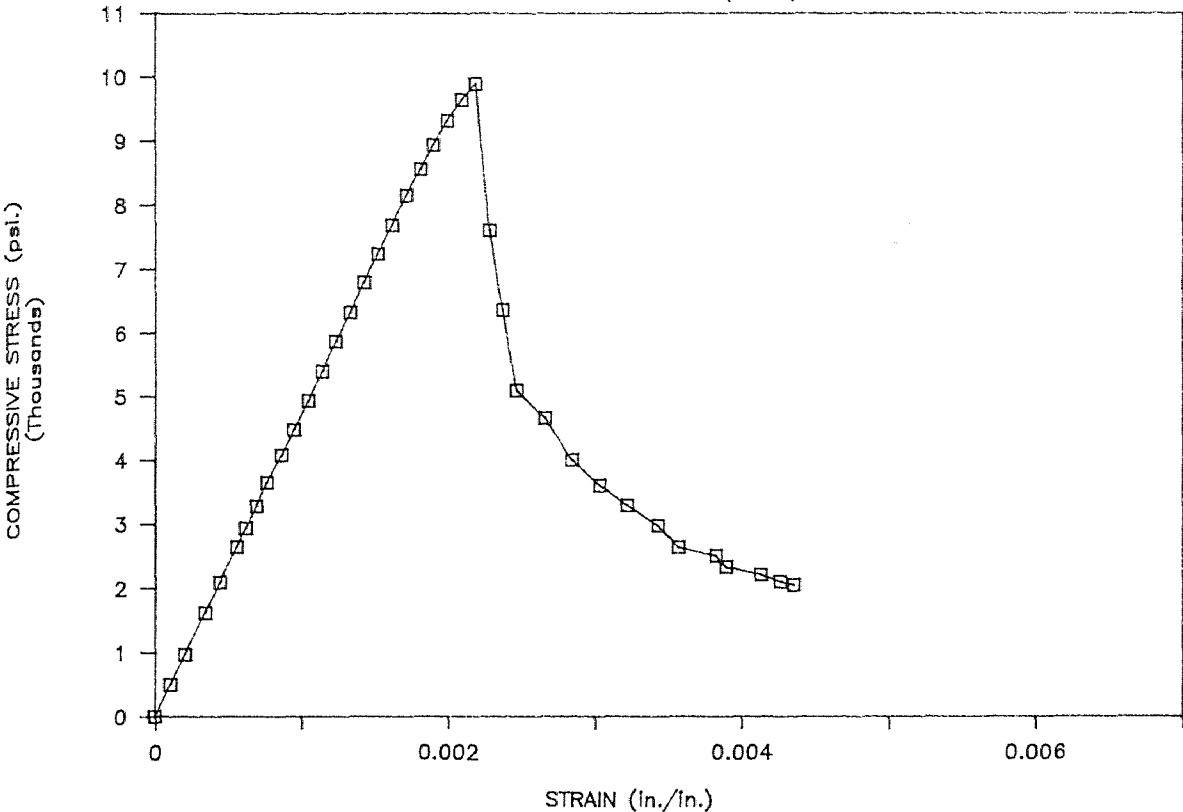
STRESS VS. STRAIN CURVE

MICROSILICA CONCRETE (M3S1)



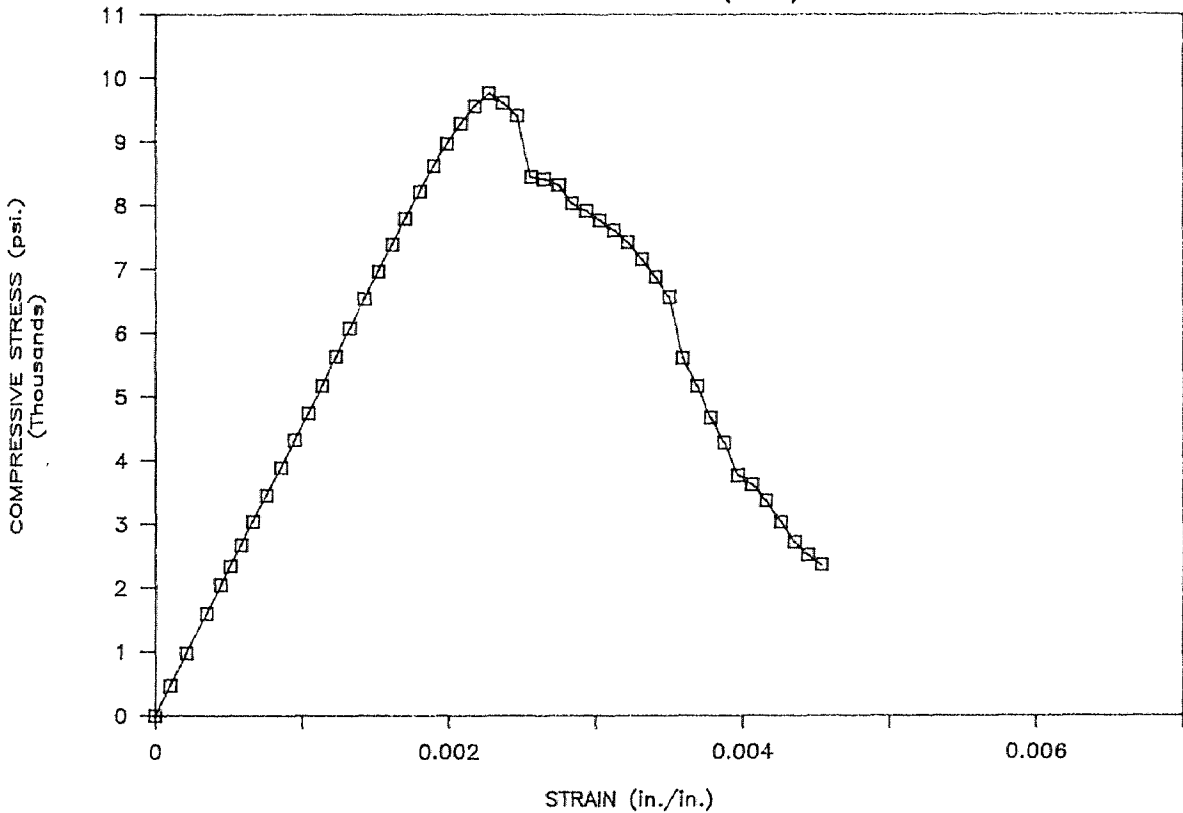
STRESS VS. STRAIN CURVE

MICROSILICA CONCRETE (M3S3)

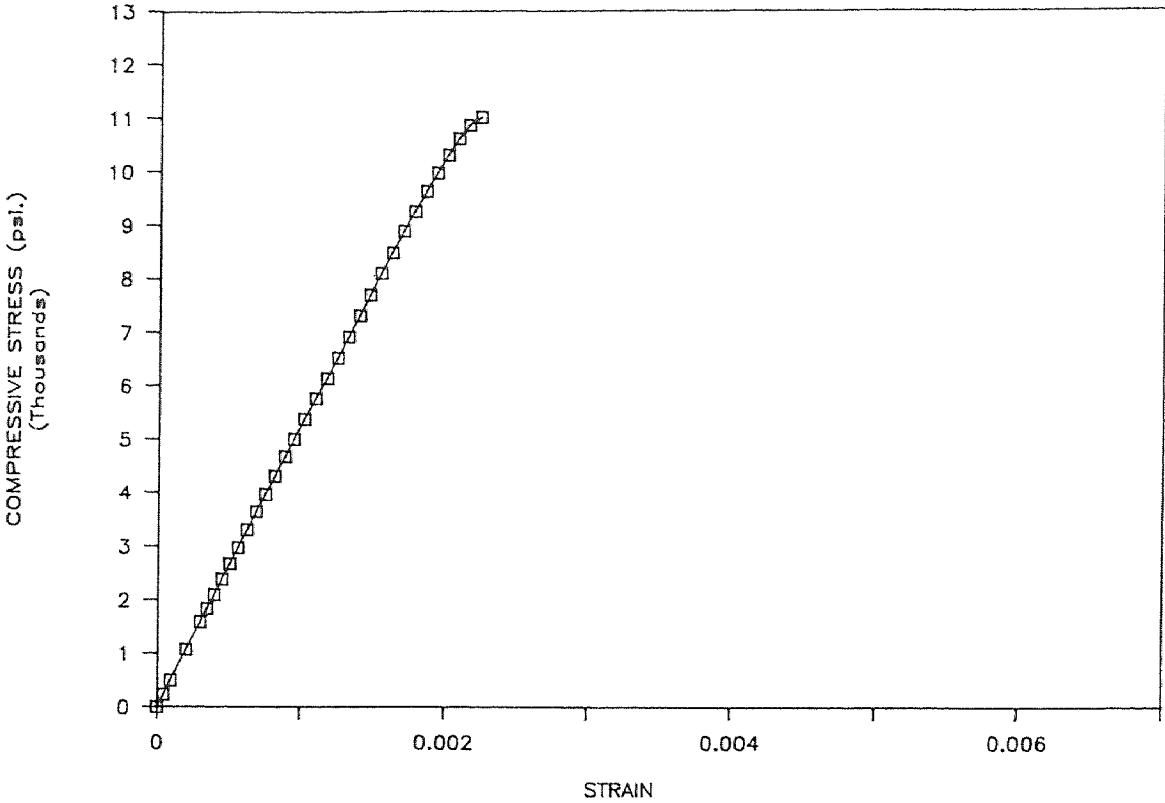


STRESS VS. STRAIN CURVE

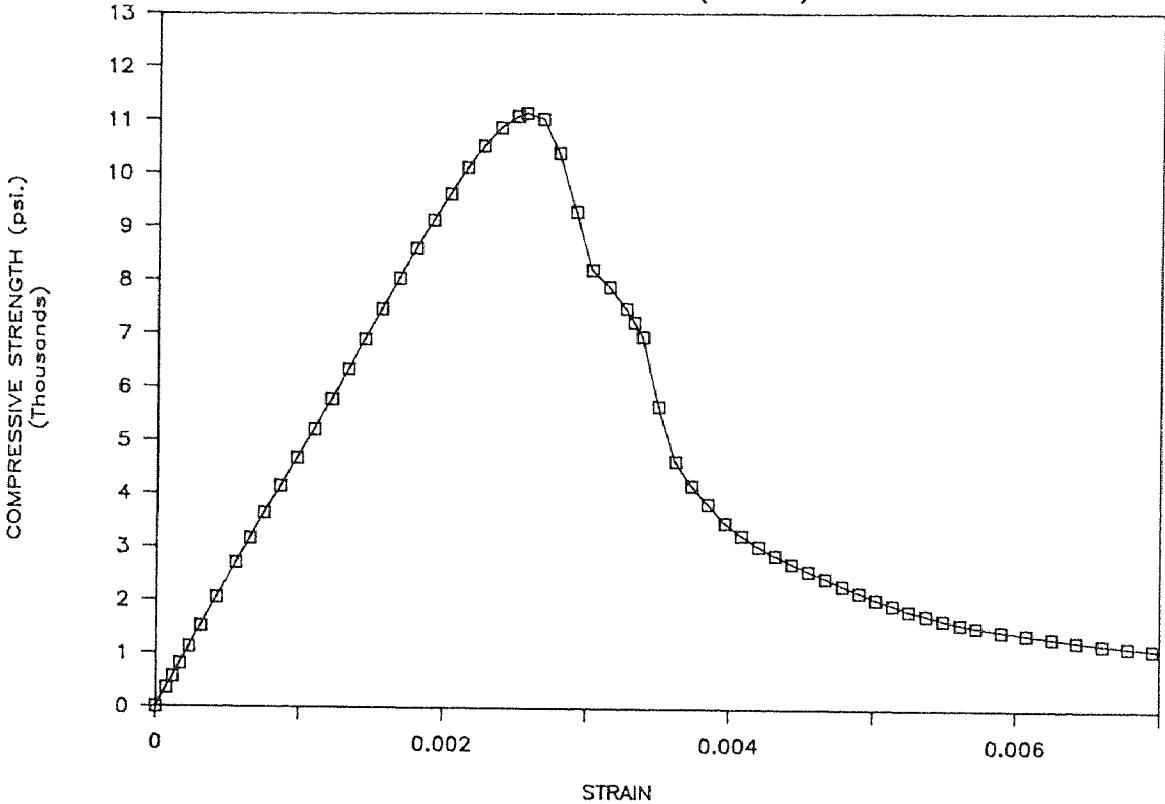
MICROSILICA CONCRETE (M3S4)



STRESS VS. STRAIN CURVE MICROSILICA CONCRETE (M3TF11A)

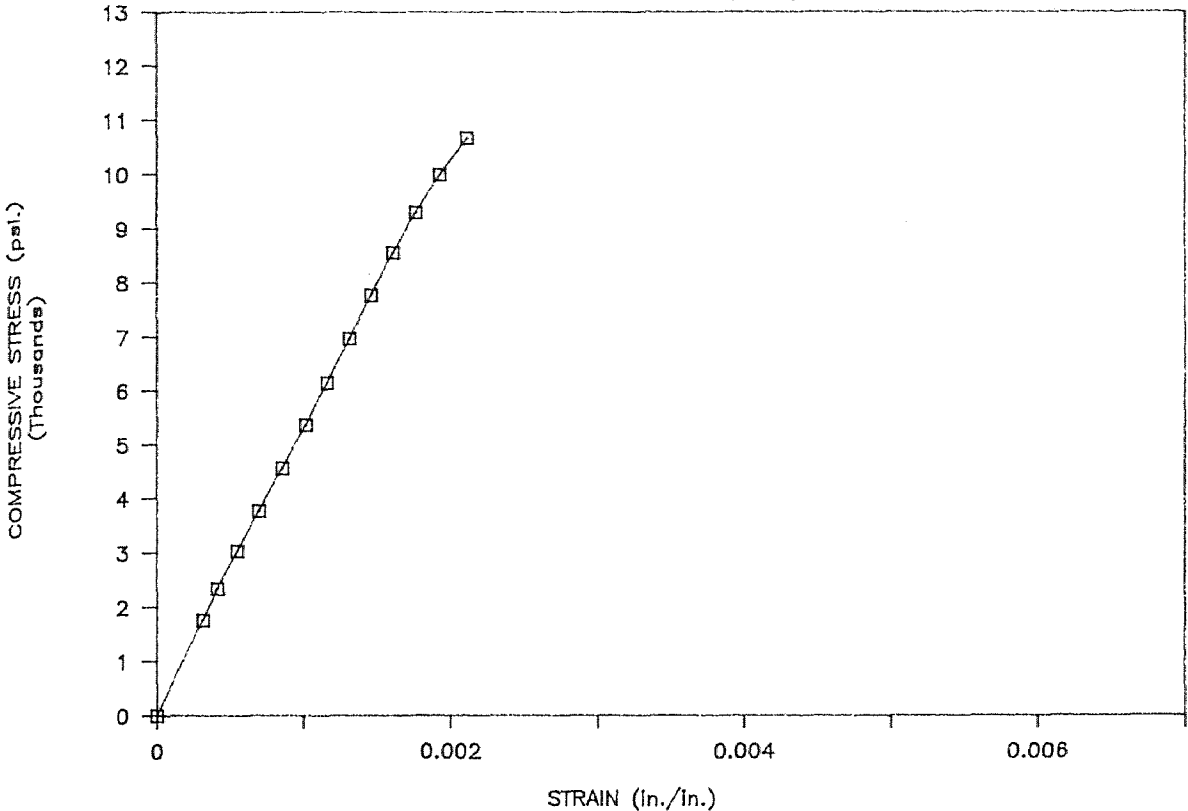


STRESS VS. STRAIN CURVE MICROSILICA CONCRETE (M3TF12A)



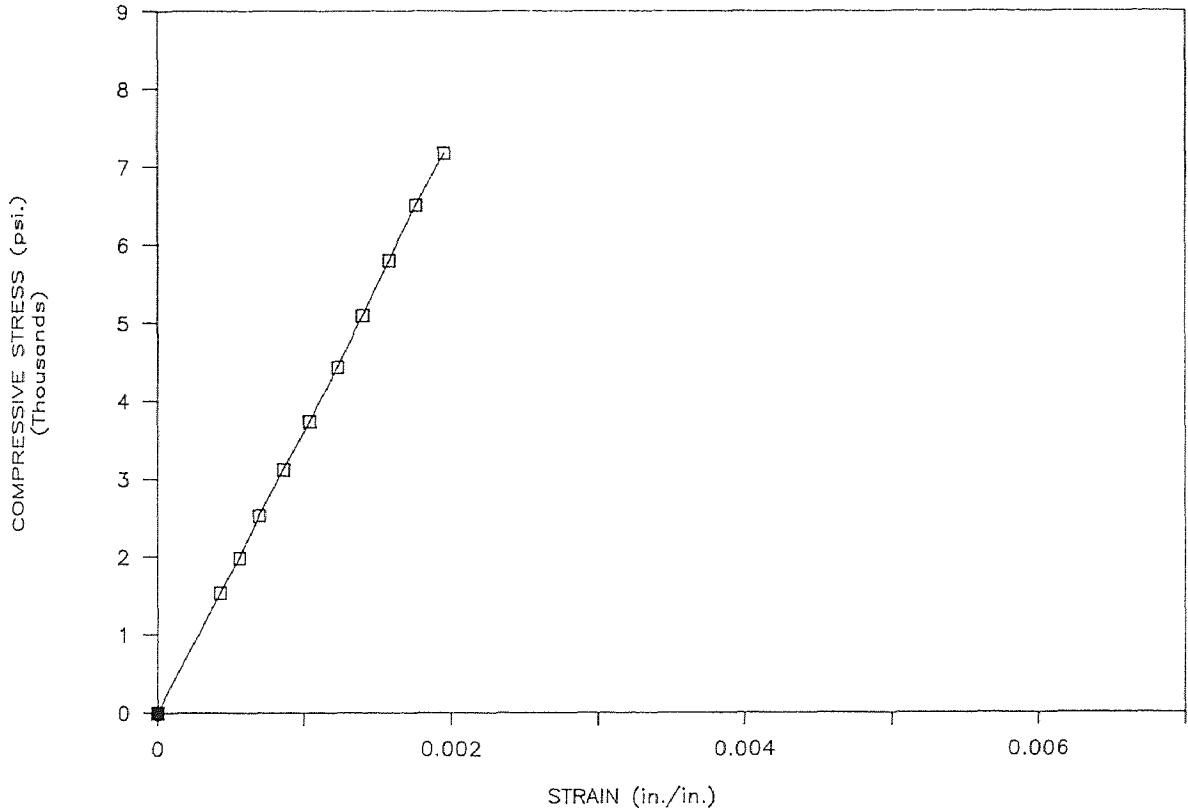
STRESS VS. STRAIN CURVE

MICROSILICA CONCRETE (SS31)



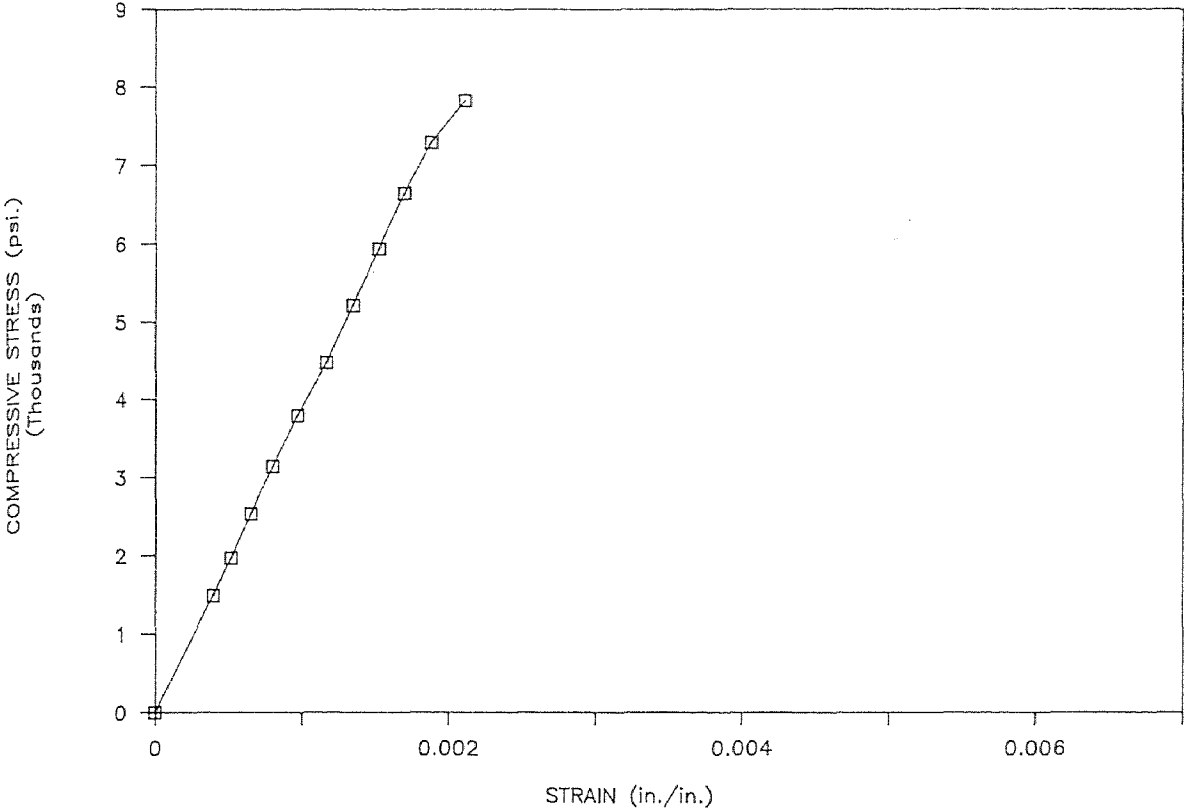
STRESS VS. STRAIN CURVE

MICROSILICA CONCRETE (SS32)



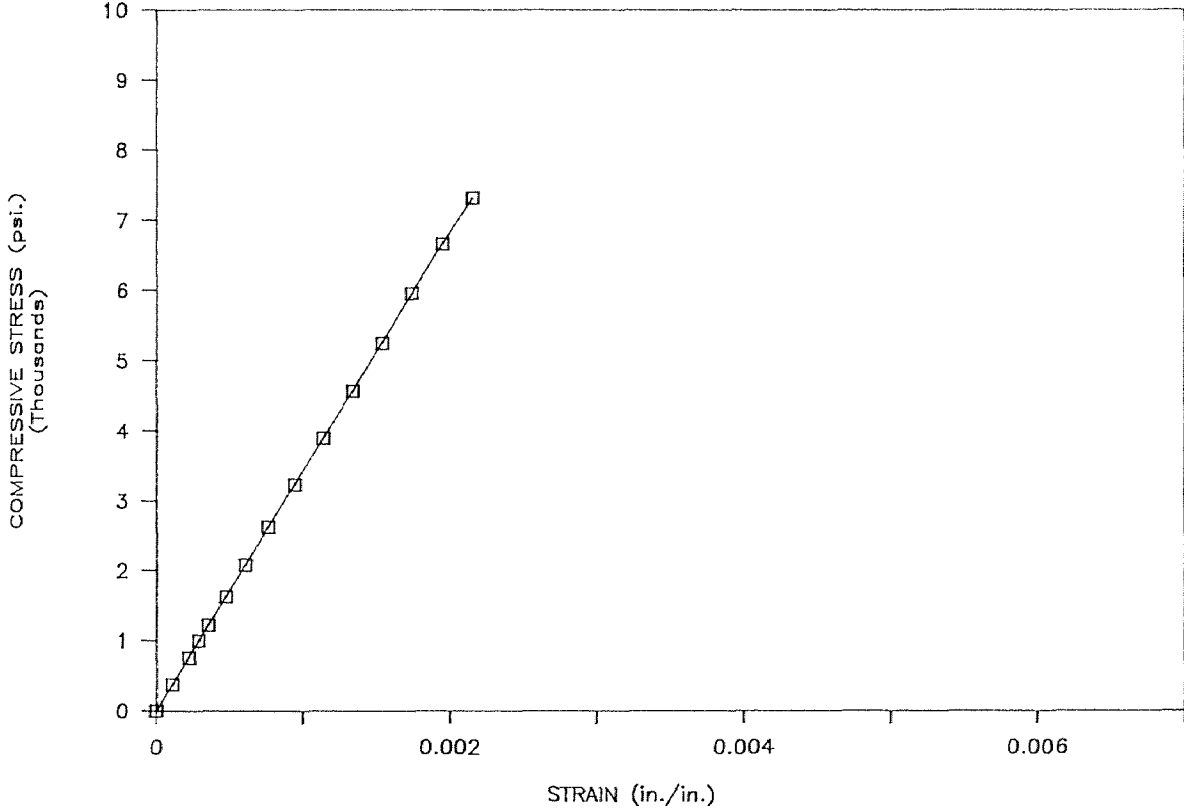
STRESS VS. STRAIN CURVE

MICROSILICA CONCRETE (SS33)



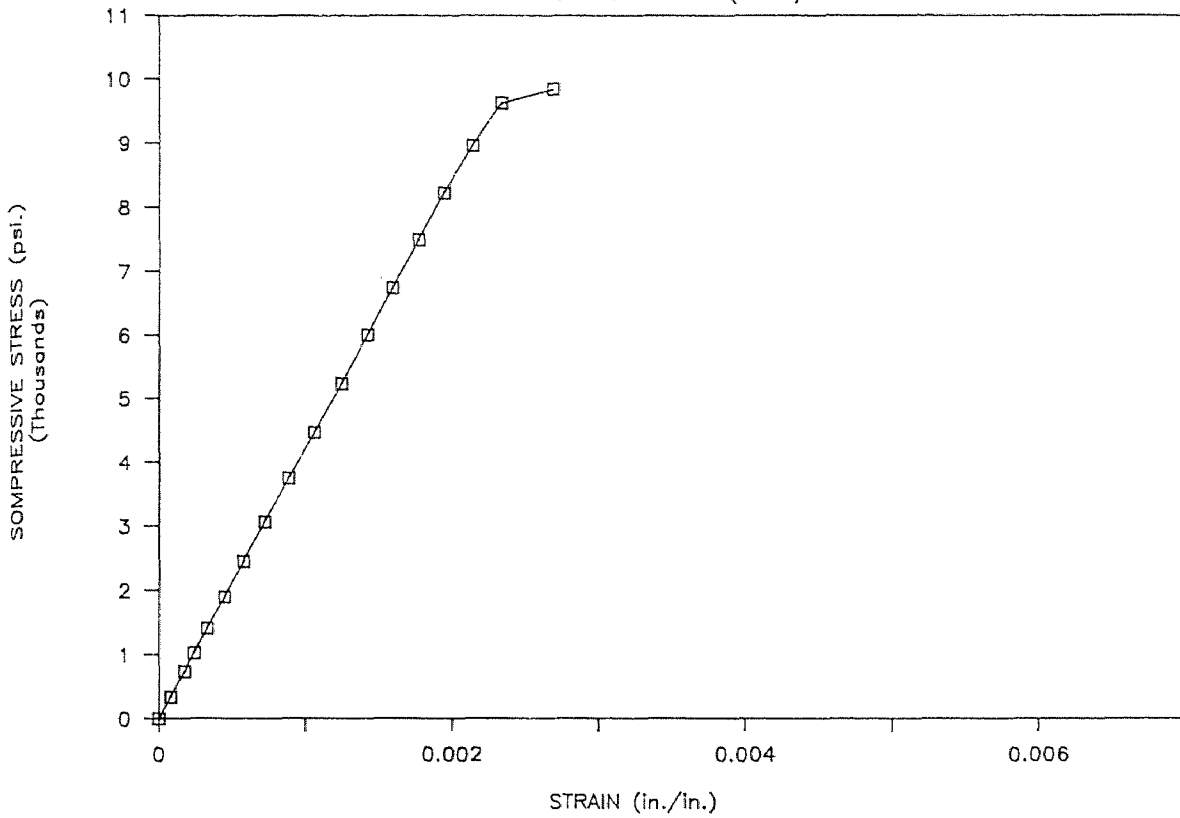
STRESS VS. STRAIN CURVE

MICROSILICA CONCRETE (SS41)



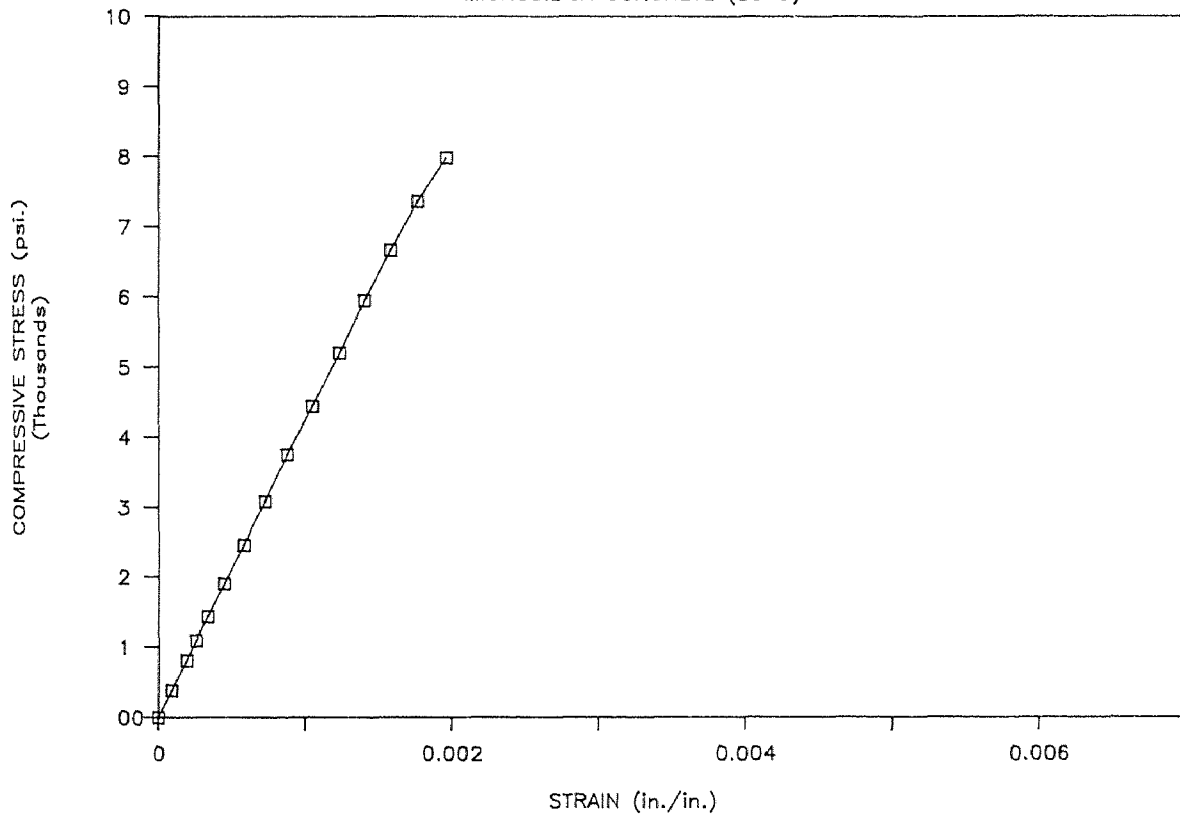
STRESS VS. STRAIN CURVE

MICROSILICA CONCRETE (SS42)



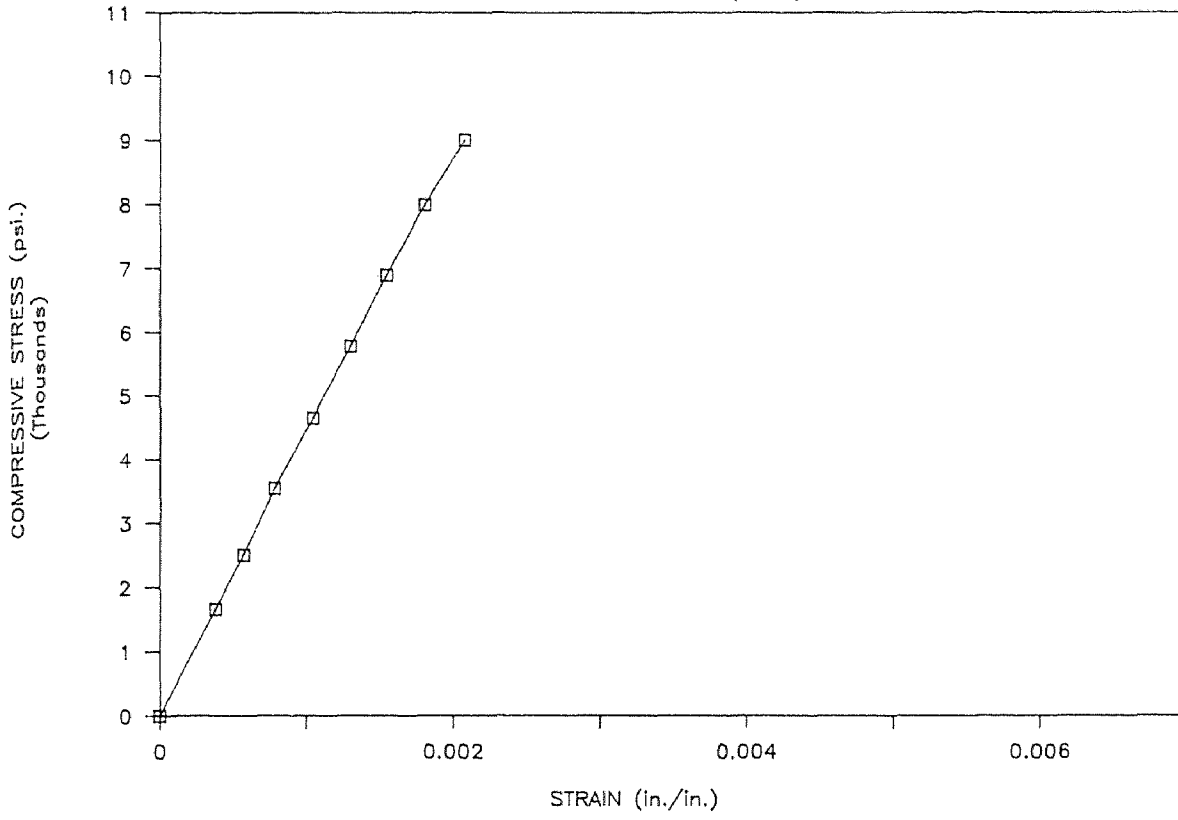
STRESS VS. STRAIN CURVE

MICROSILICA CONCRETE (SS43)



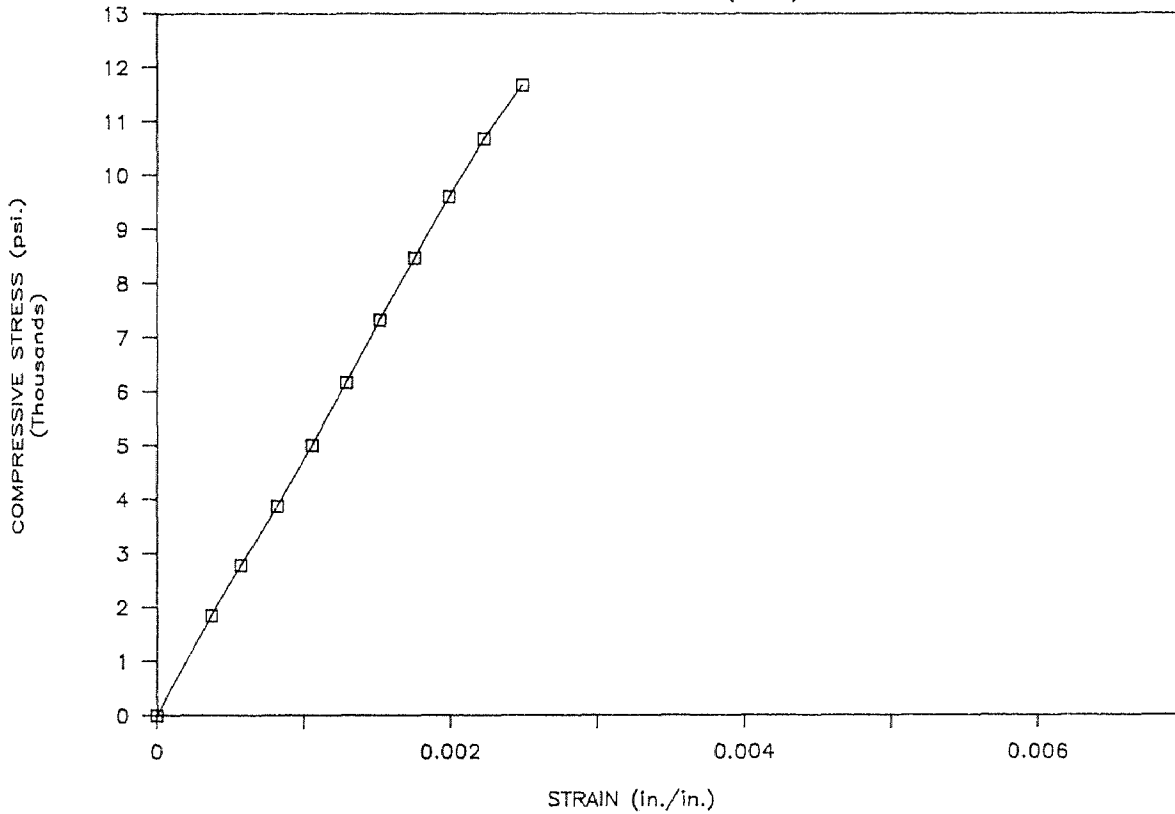
STRESS VS. STRAIN CURVE

MICROSILICA CONCRETE (SS61)



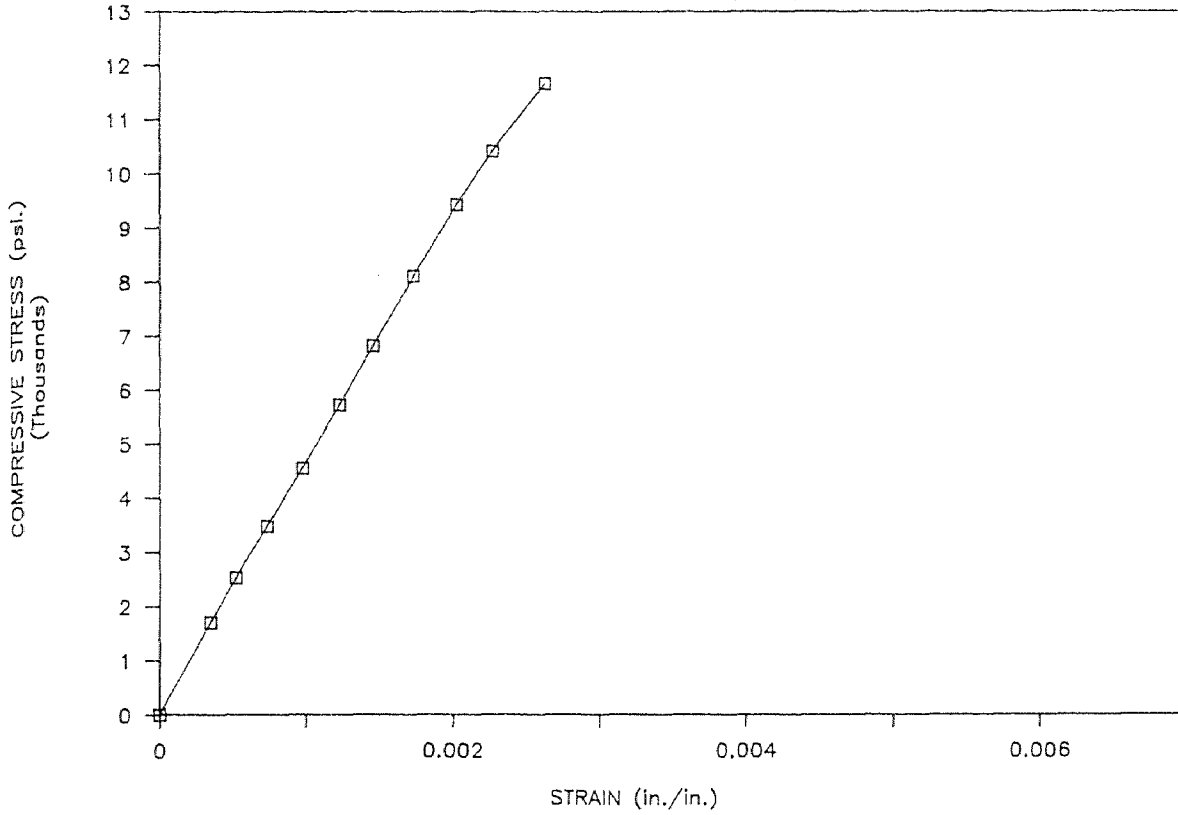
STRESS VS. STRAIN CURVE

MICROSILICA CONCRETE (SS62)



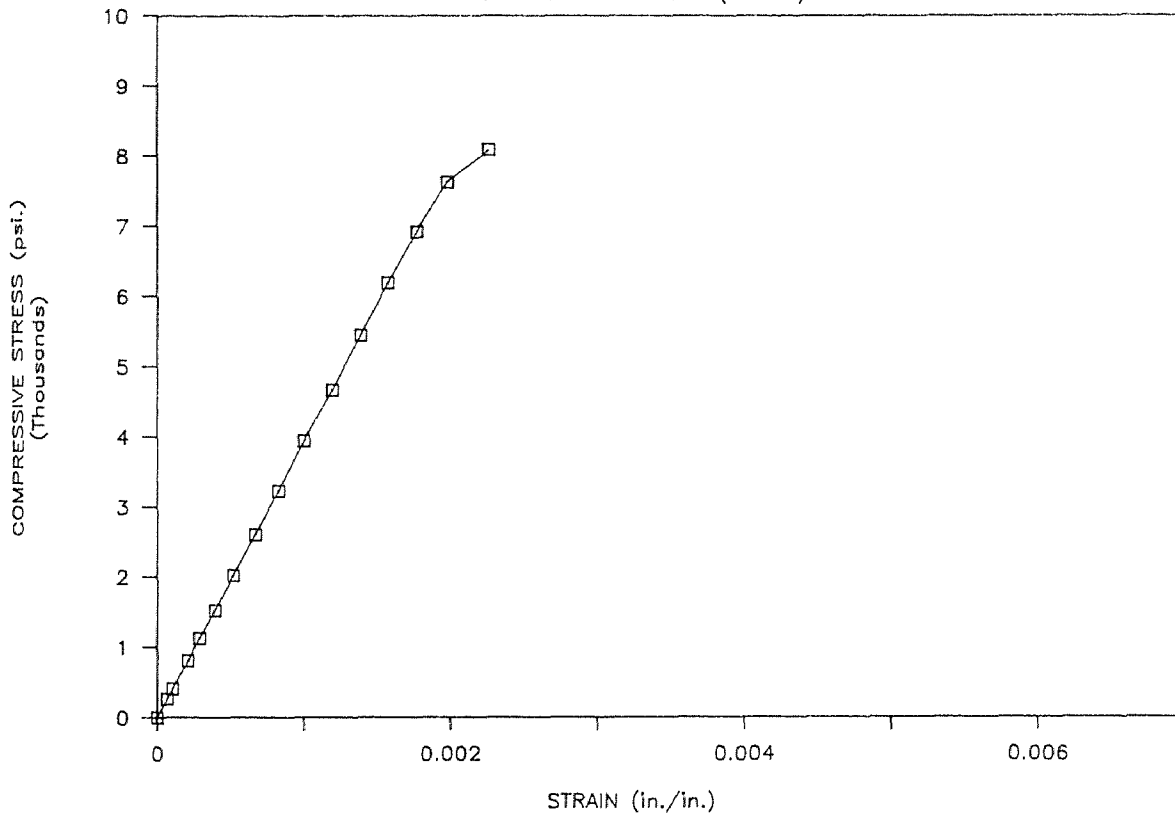
STRESS VS. STRAIN CURVE

MICROSILICA CONCRETE (SS63)



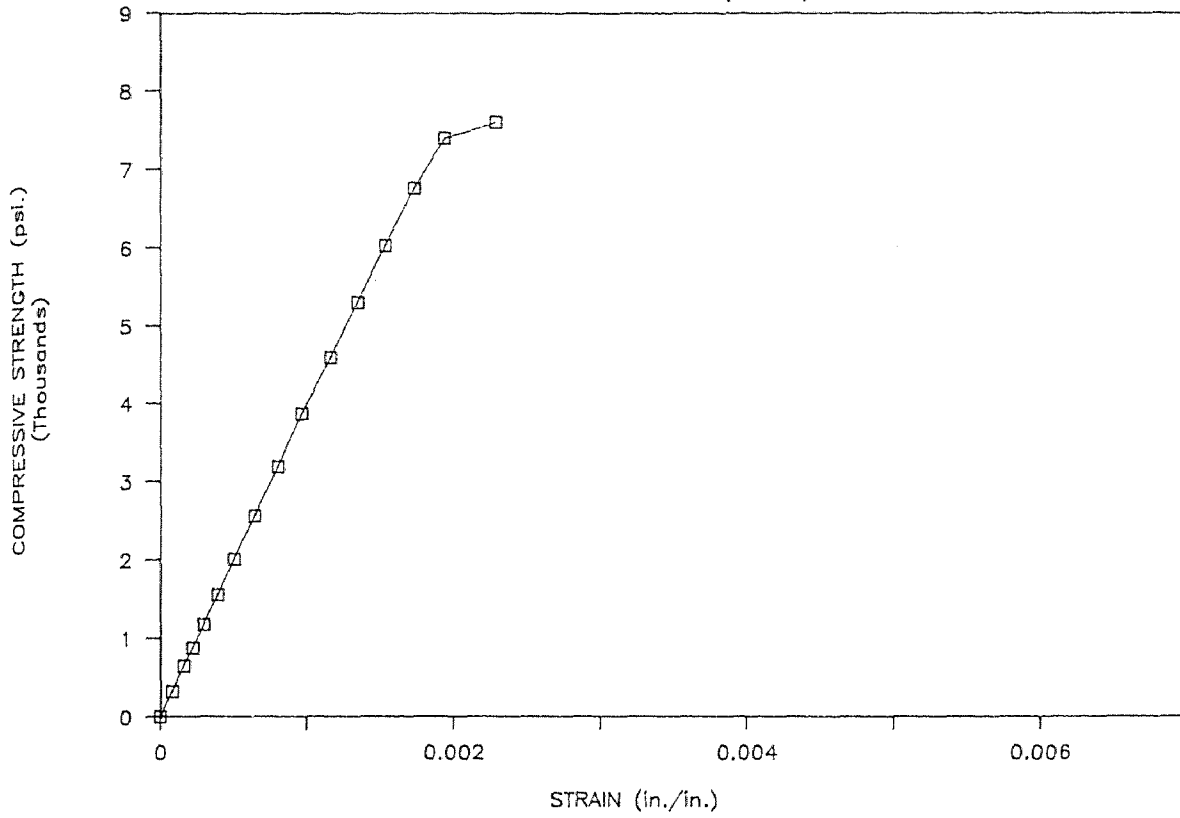
STRESS VS. STRAIN CURVE

MICROSILICA CONCRETE (SS321)



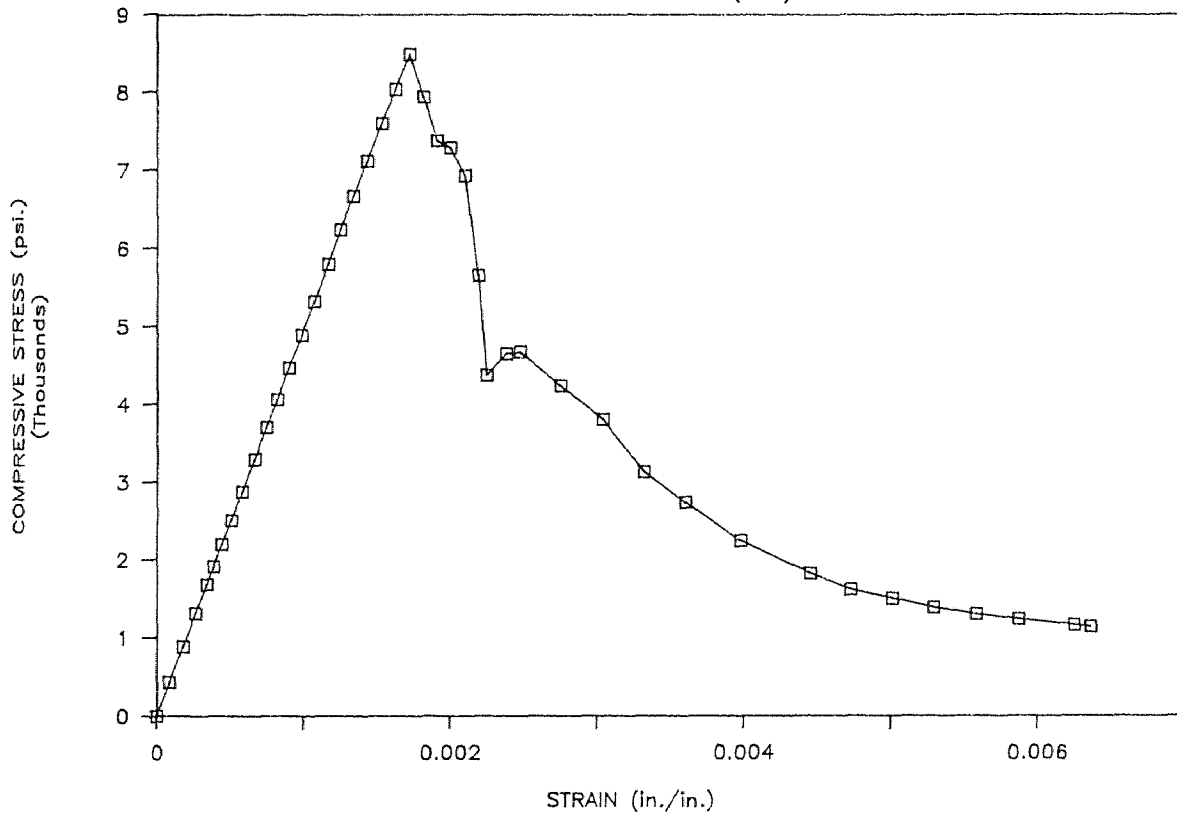
STRESS VS. STRAIN CURVE

MICROSILICA CONCRETE (SS331)



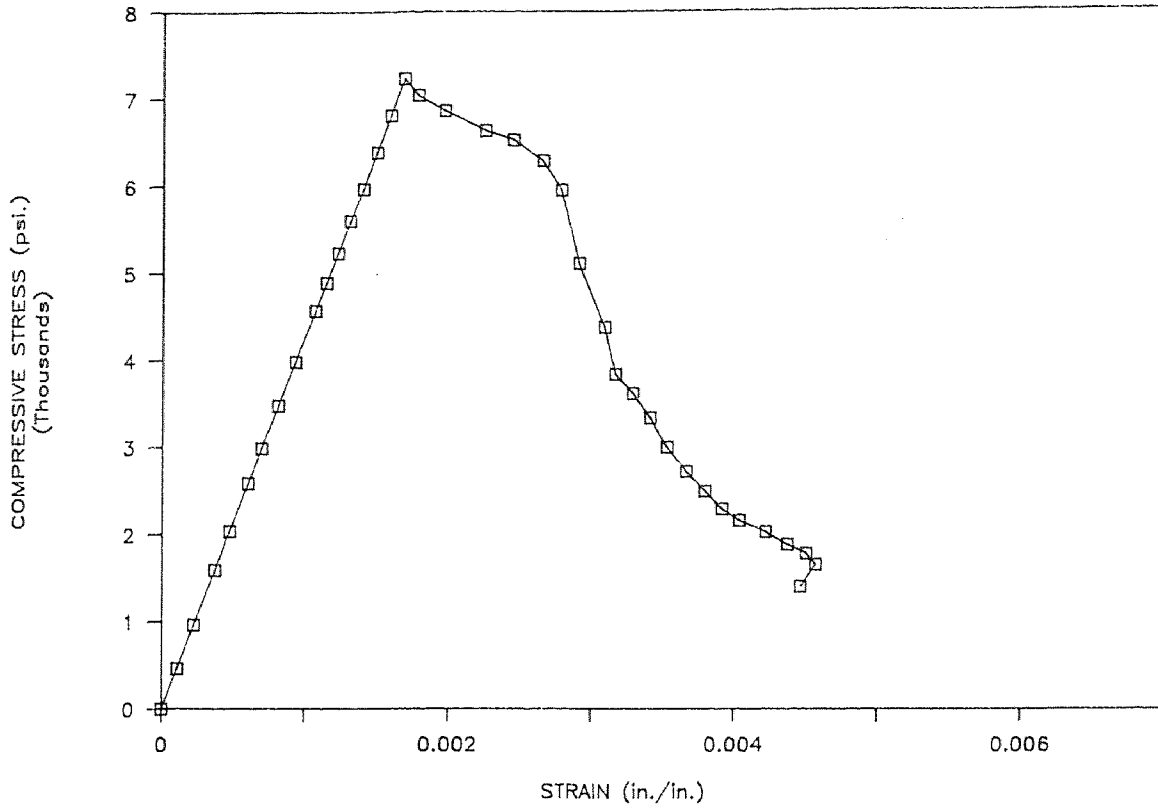
STRESS VS. STRAIN CURVE

MICROSILICA CONCRETE (S11)



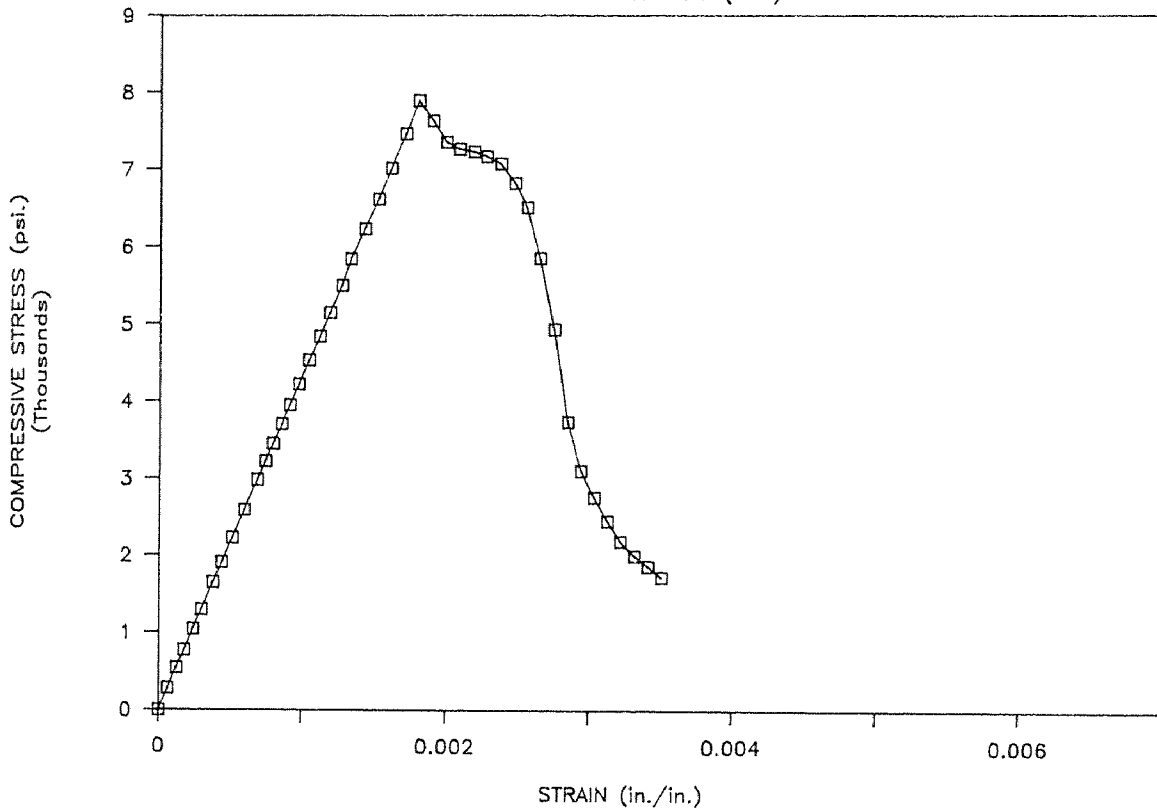
STRESS VS. STRAIN CURVE

MICROSILICA CONCRETE (S12)



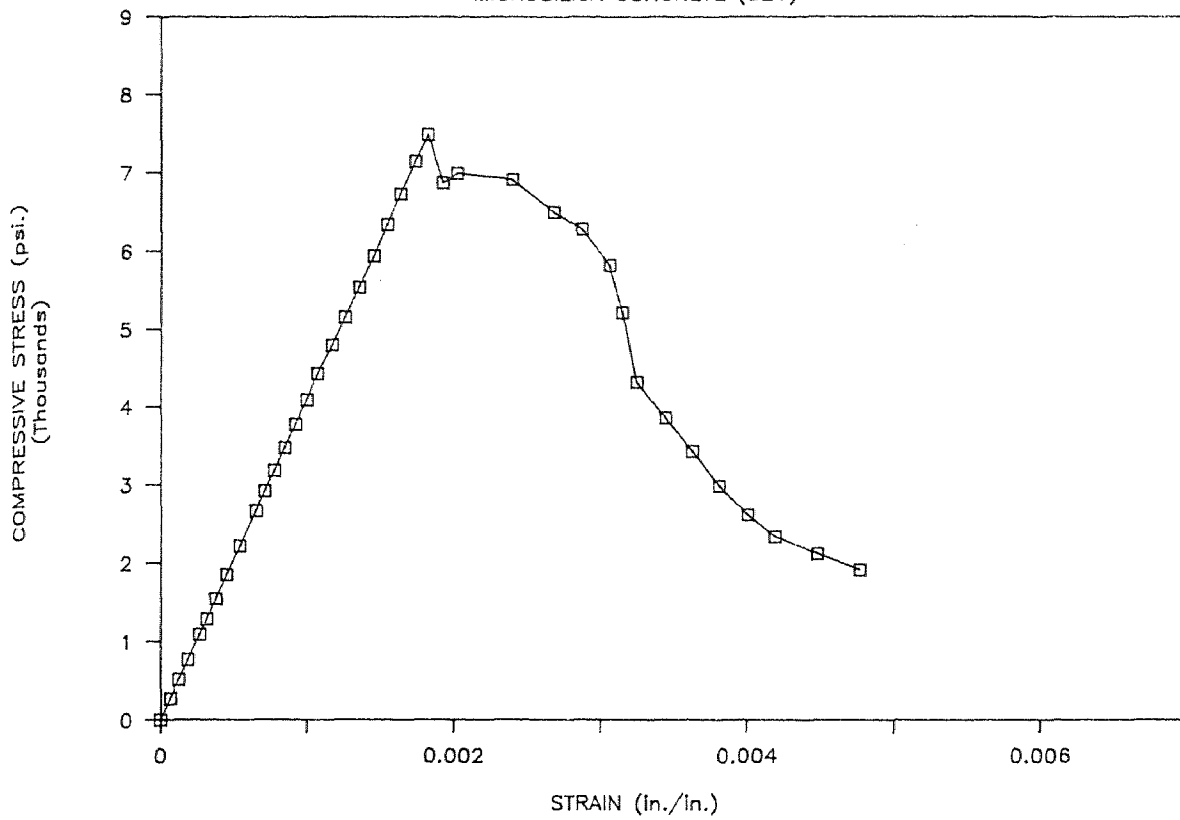
STRESS VS. STRAIN CURVE

MICROSILICA CONCRETE (S13)



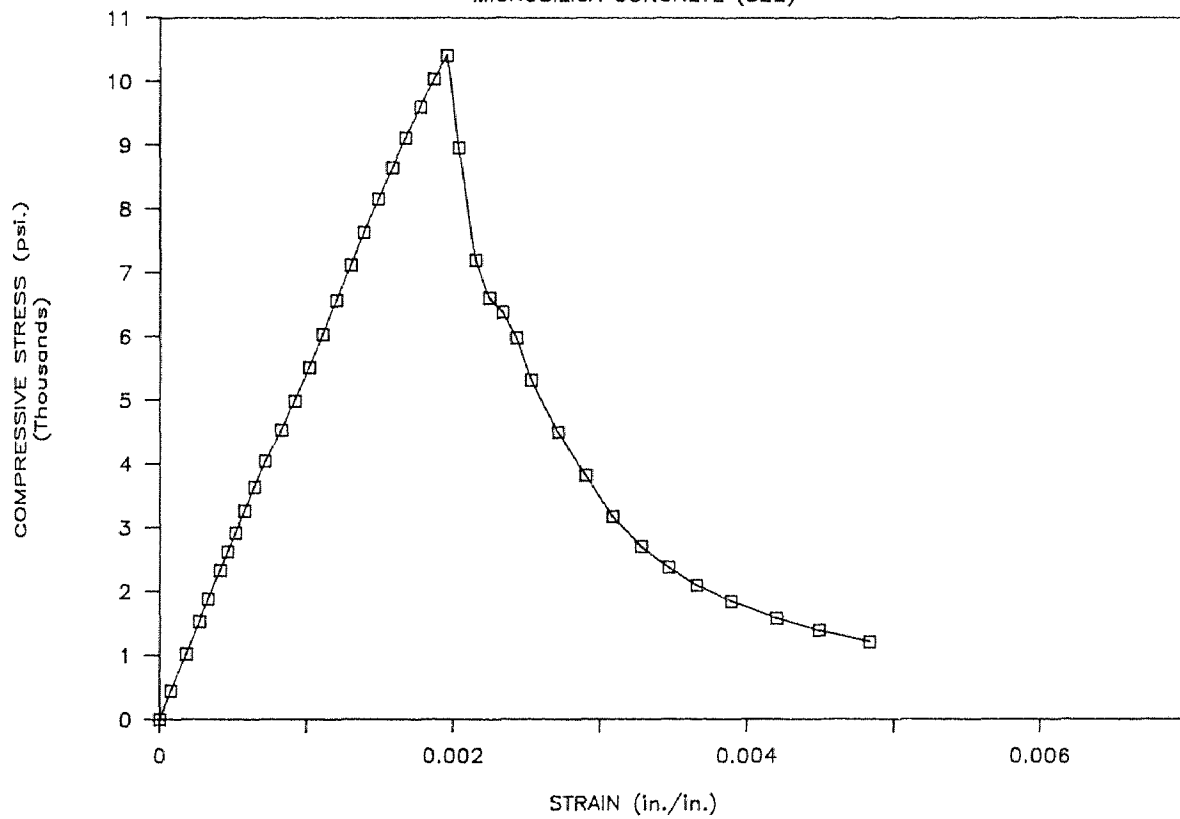
STRESS VS. STRAIN CURVE

MICROSILICA CONCRETE (S21)



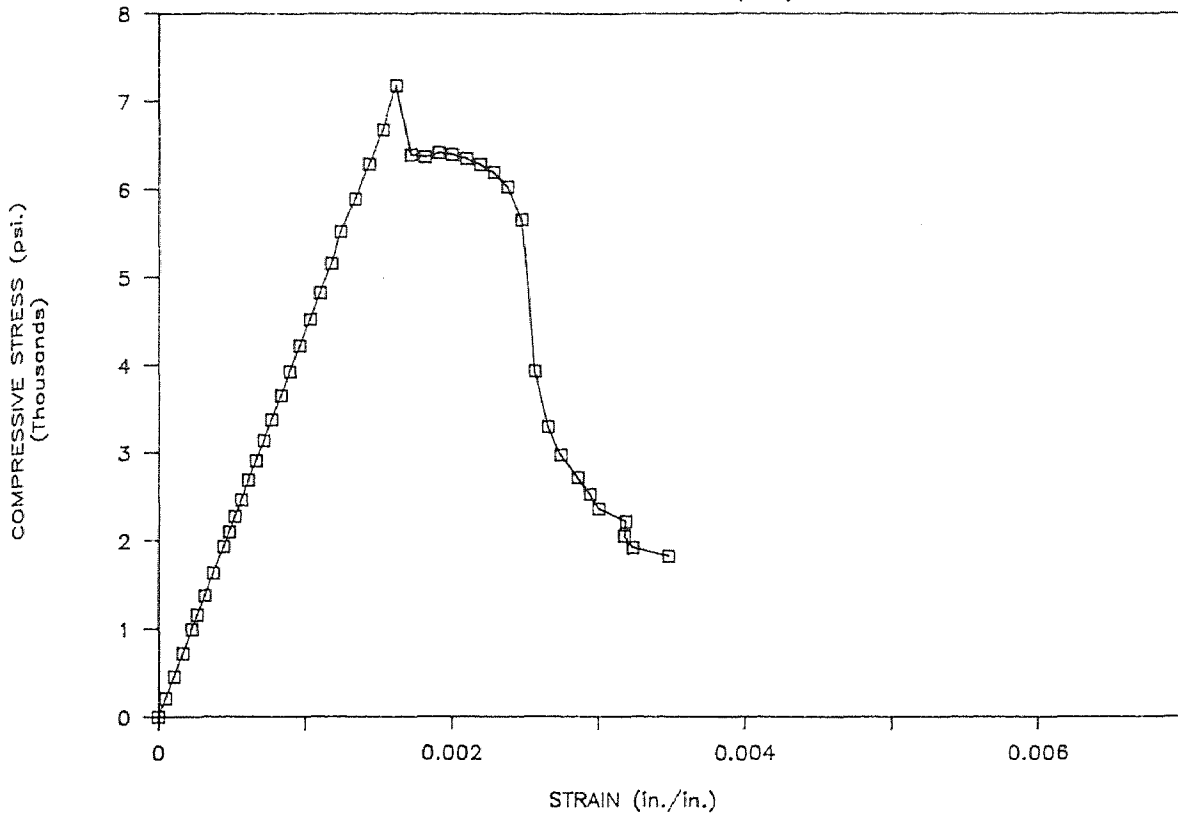
STRESS VS. STRAIN CURVE

MICROSILICA CONCRETE (S22)



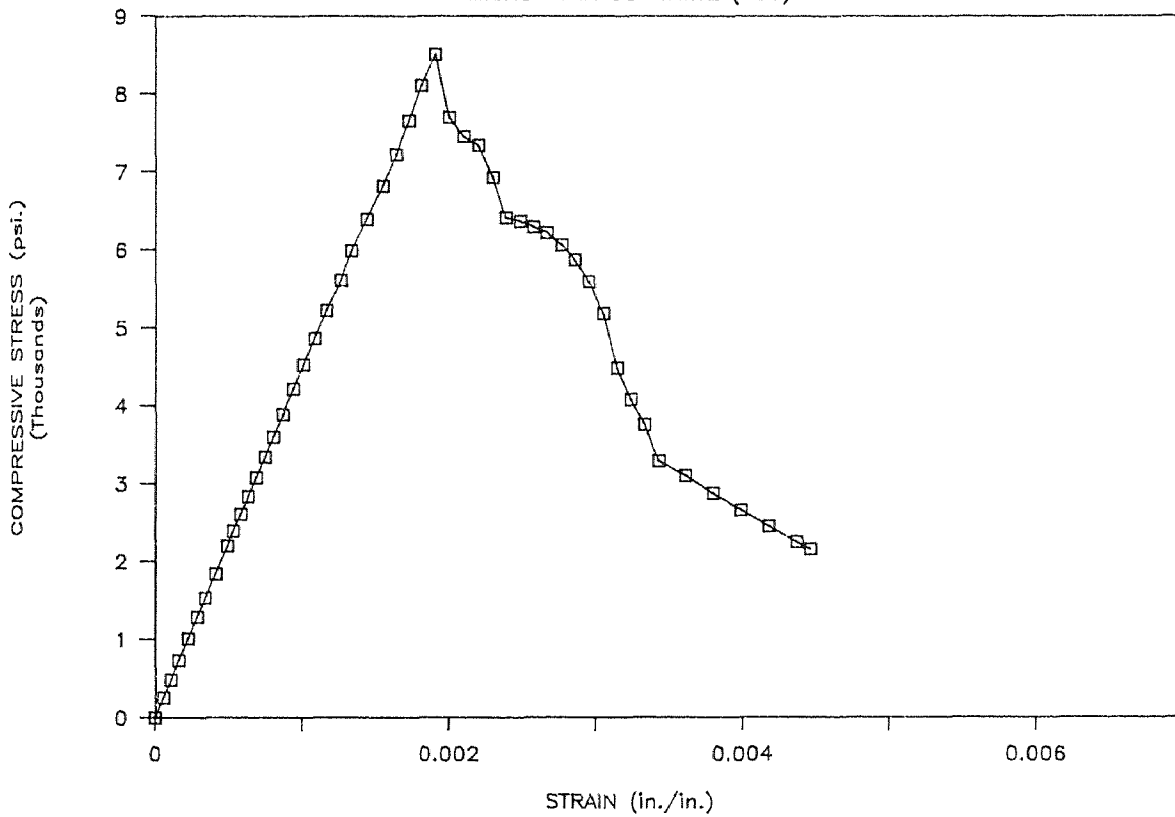
STRESS VS. STRAIN CURVE

MICROSILICA CONCRETE (S23)



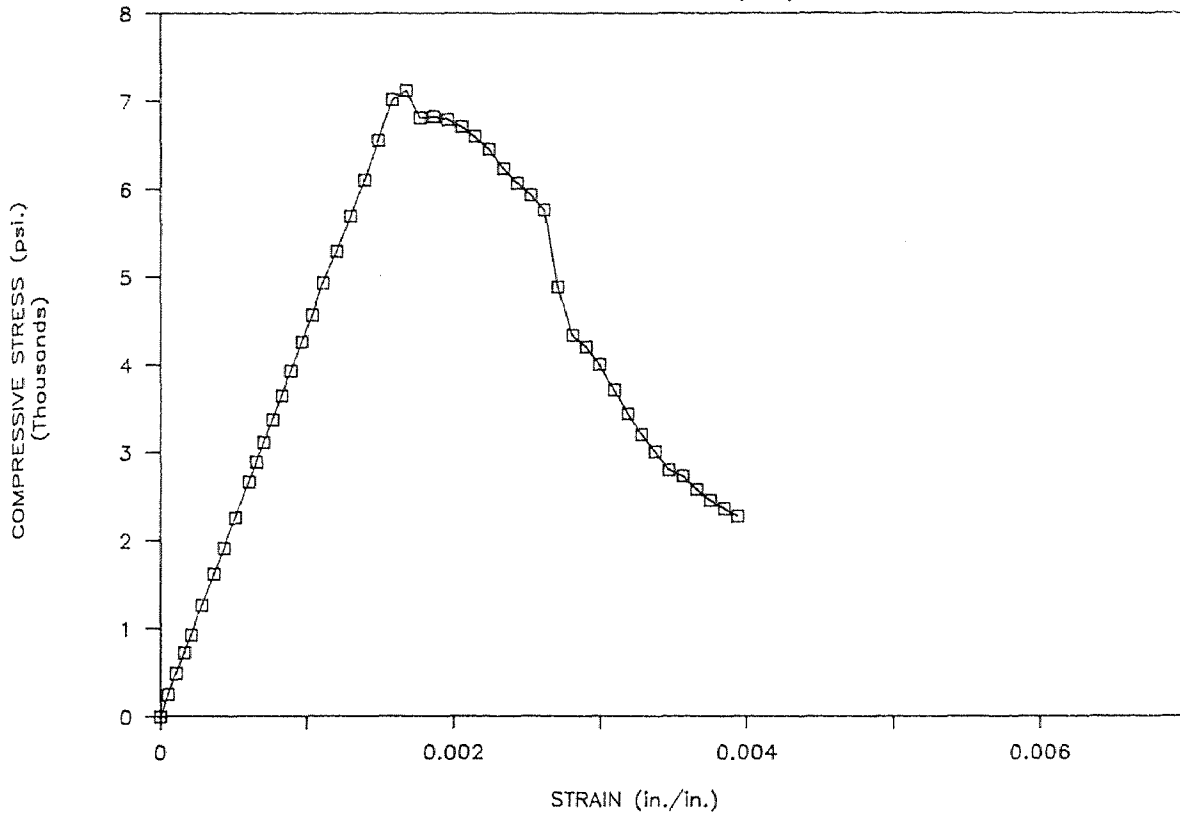
STRESS VS. STRAIN CURVE

MICROSILICA CONCRETE (S31)



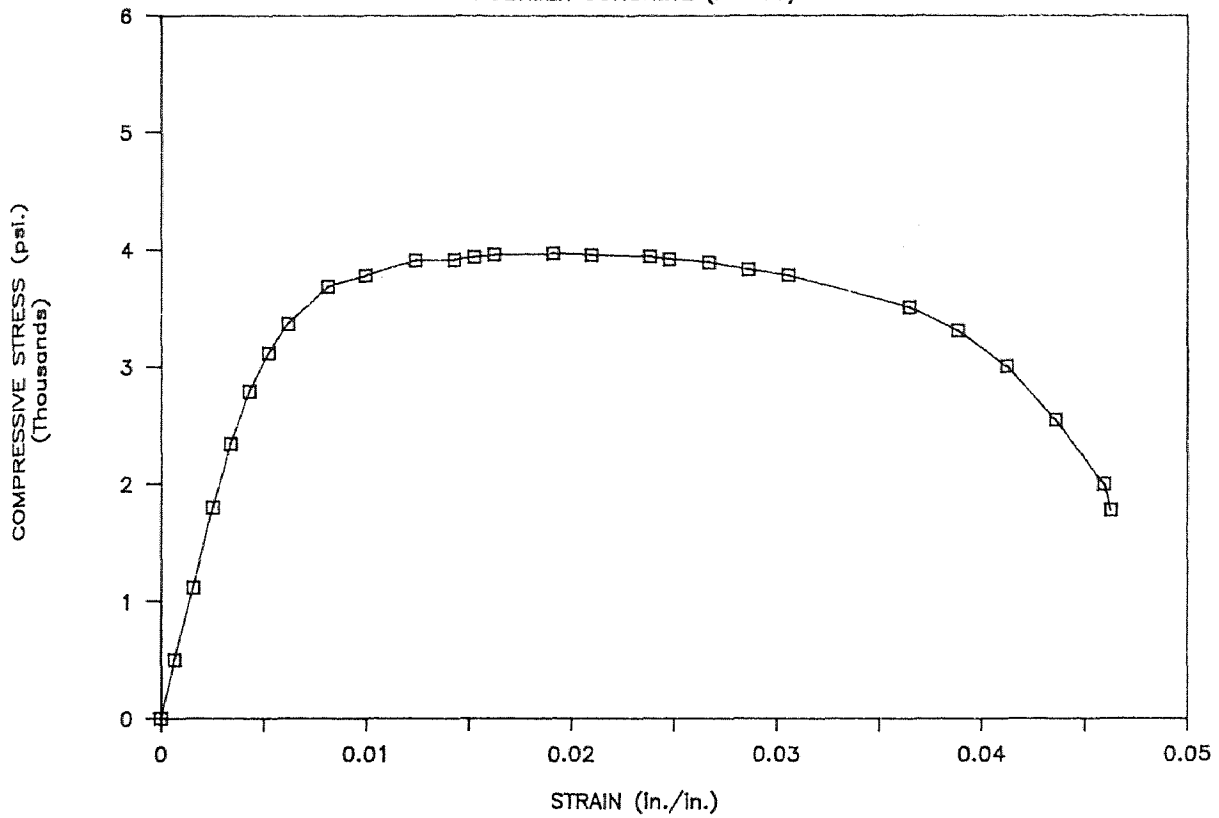
STRESS VS. STRAIN CURVE

MICROSILICA CONCRETE (S32)



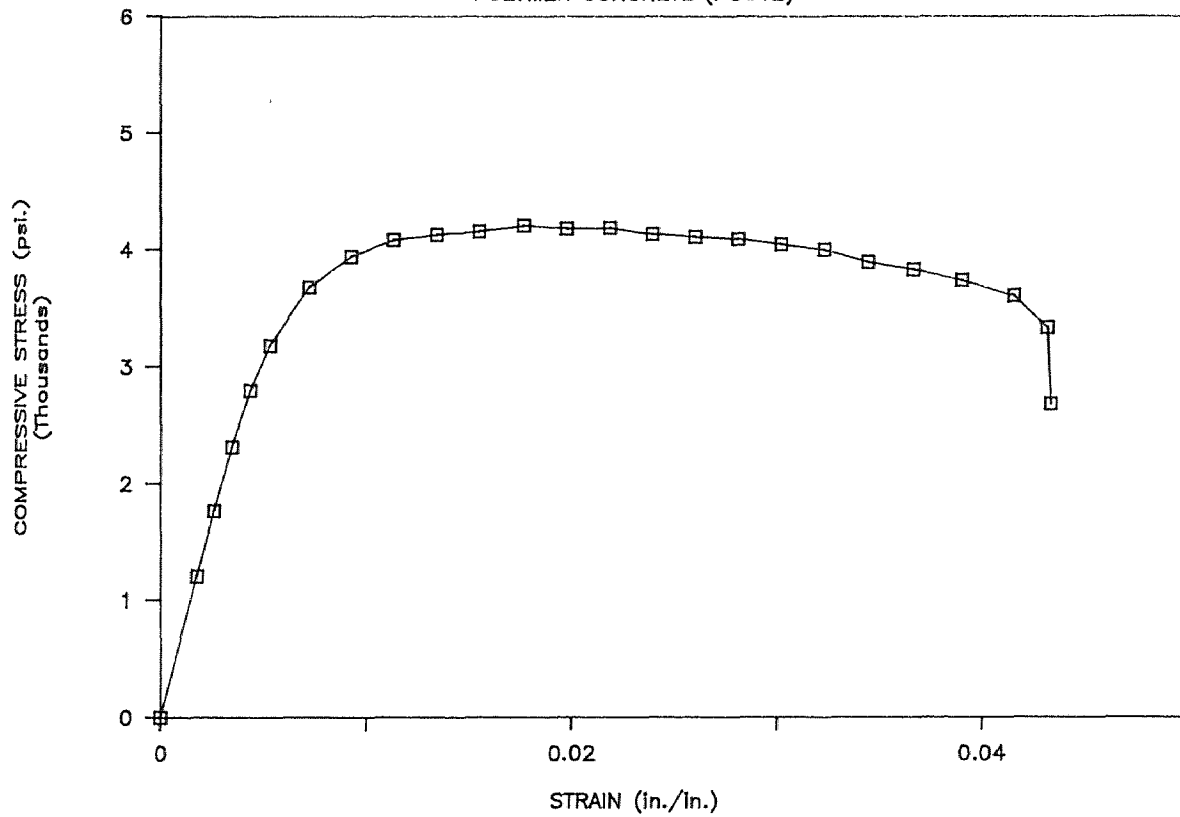
STRESS VS. STRAIN CURVE

POLYMER CONCRETE (POC11)



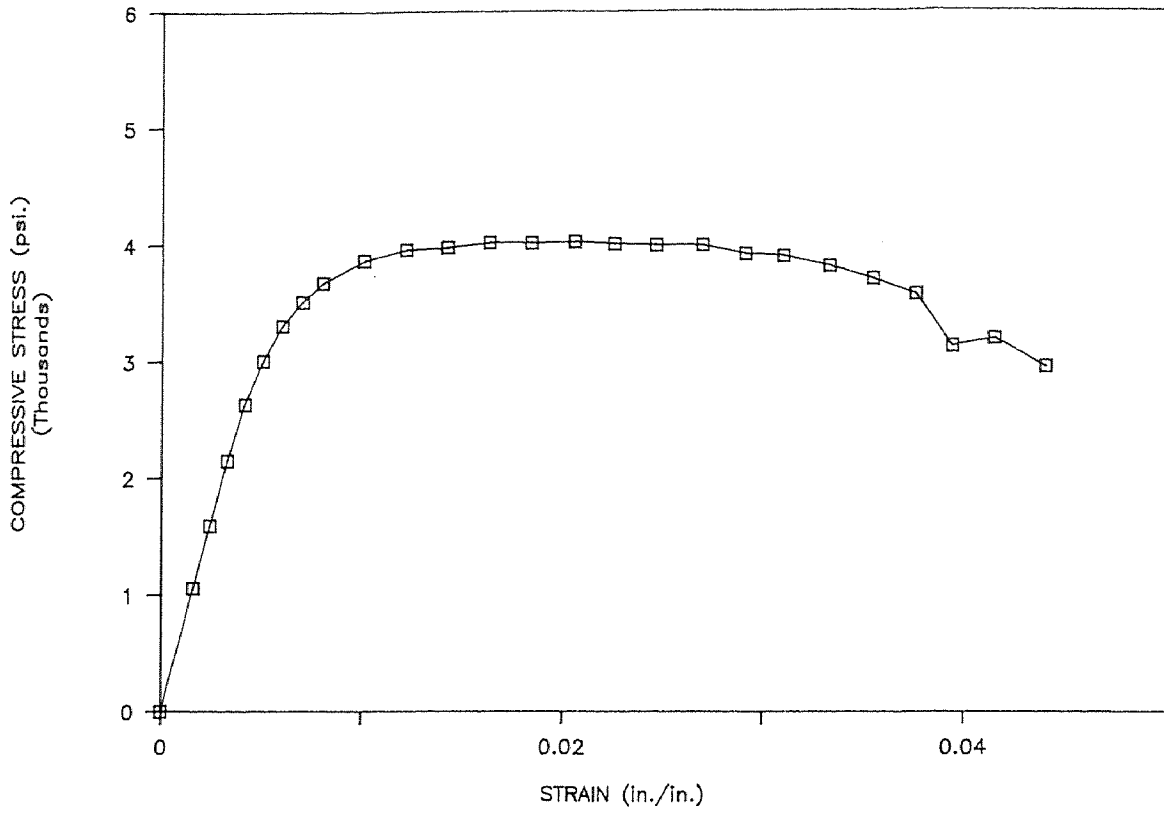
STRESS VS. STRAIN CURVE

POLYMER CONCRETE (POC12)



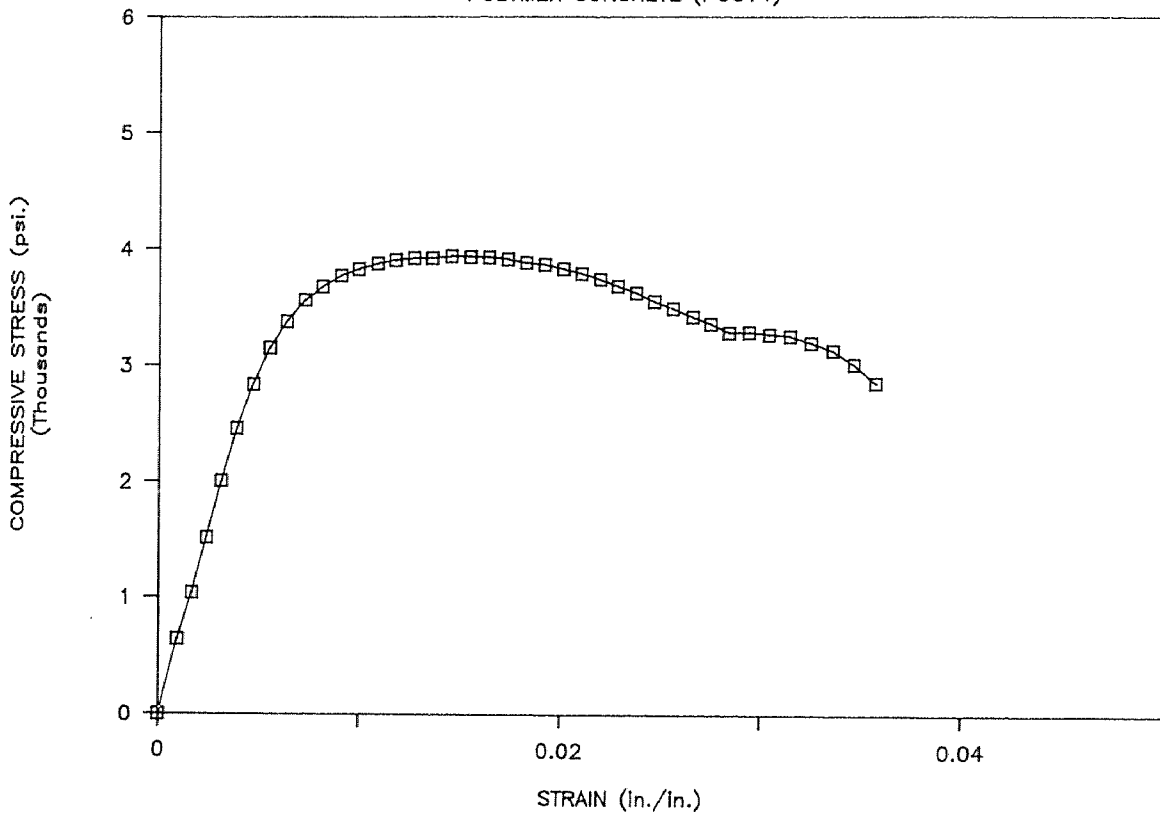
STRESS VS. STRAIN CURVE

POLYMER CONCRETE (POC13)



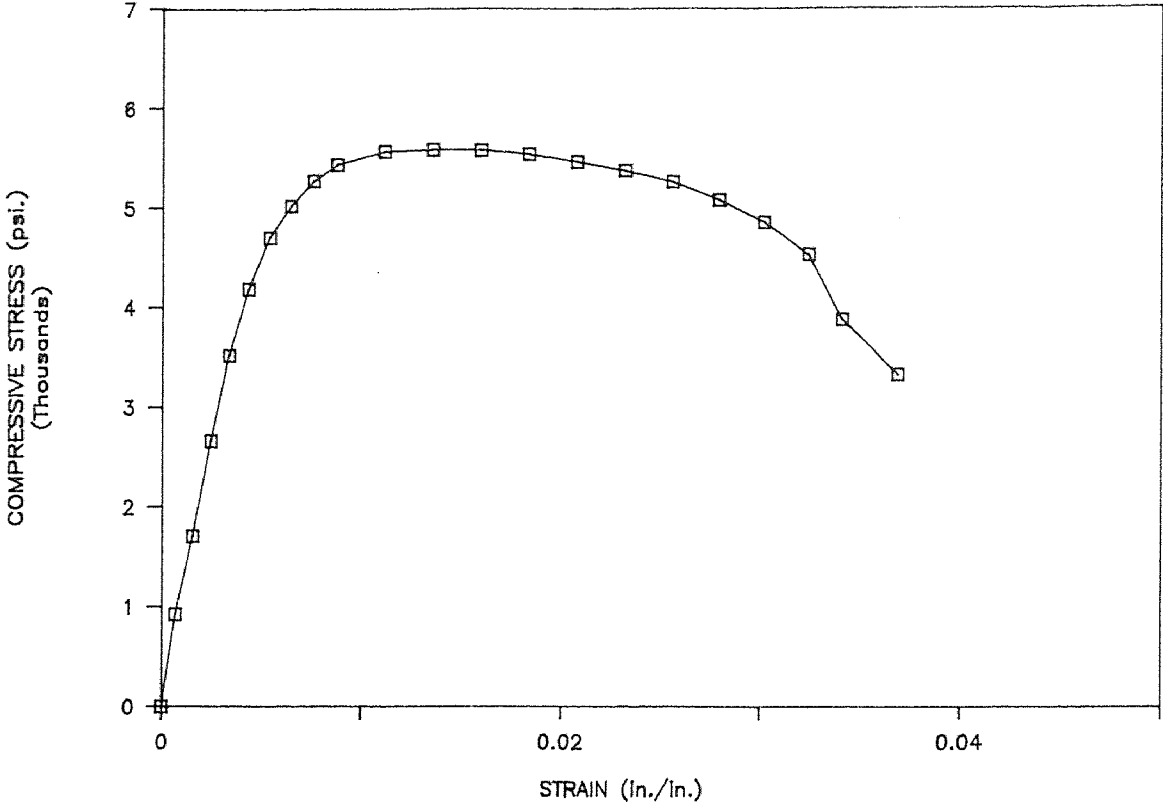
STRESS VS. STRAIN CURVE

POLYMER CONCRETE (POC14)



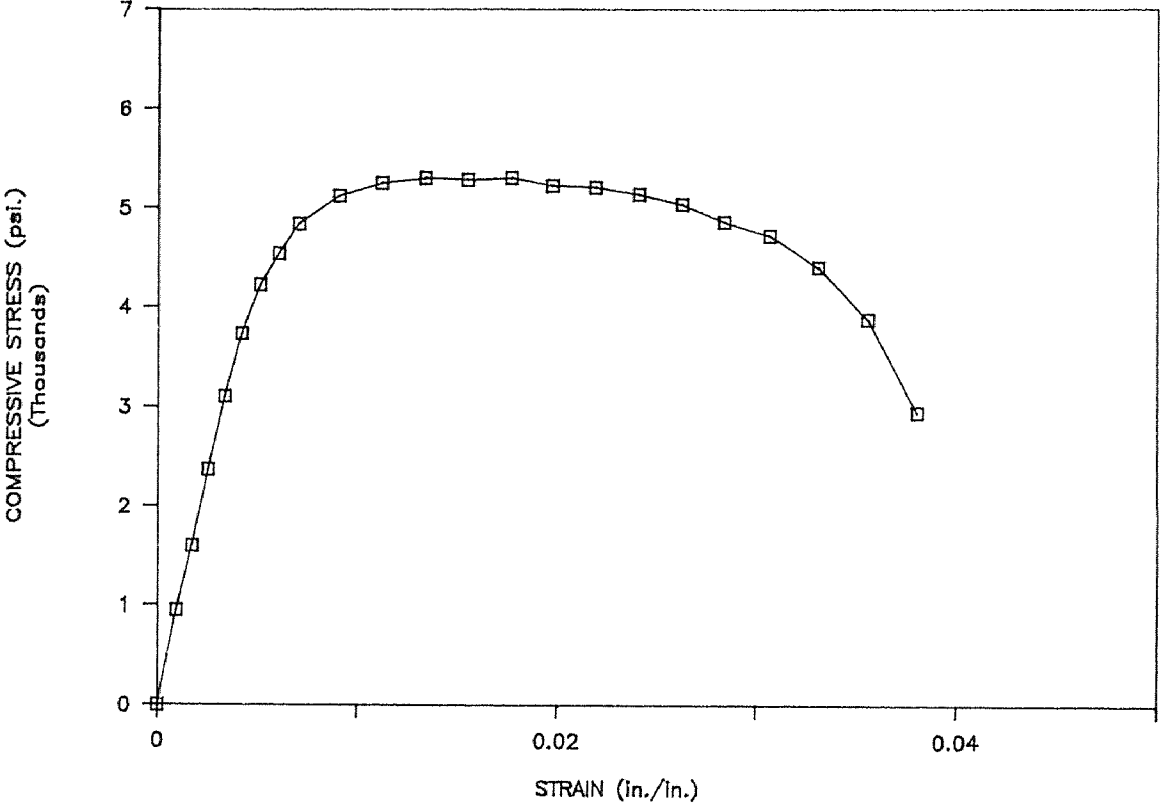
STRESS VS. STRAIN CURVE

POLYMER CONCRETE (POC21)



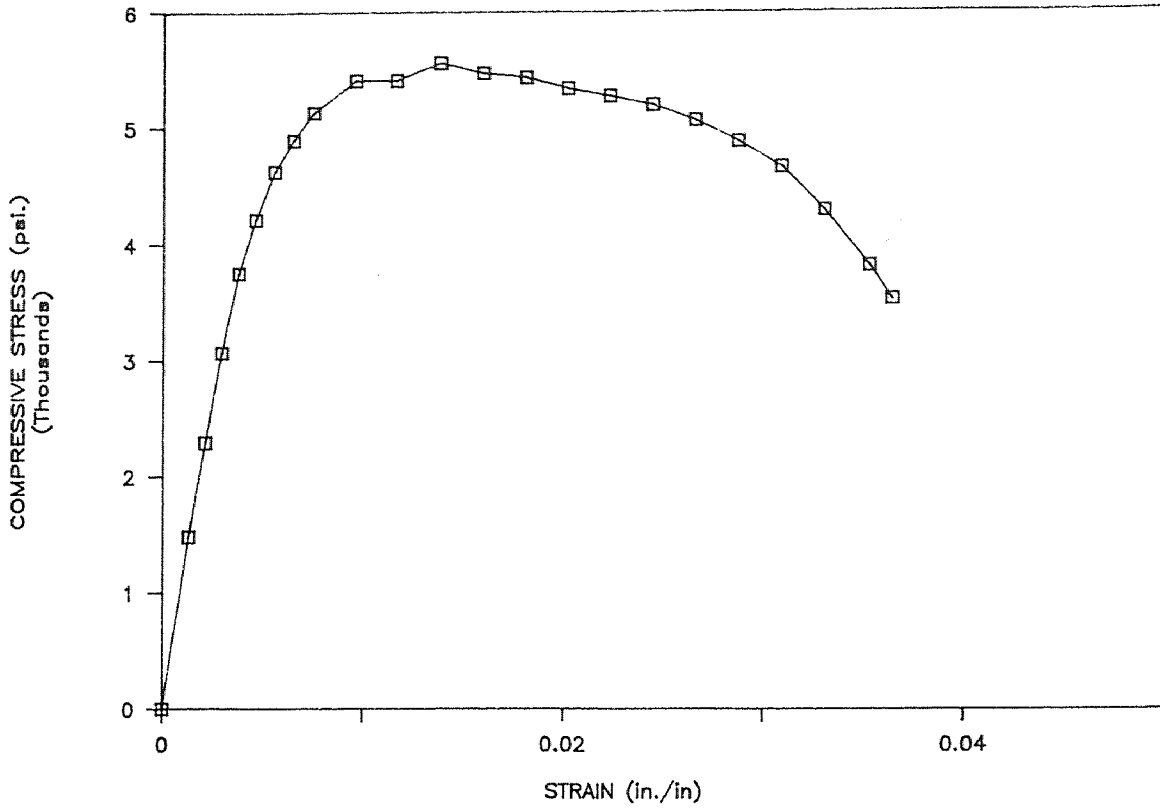
STRESS VS. STRAIN CURVE

POLYMER CONCRETE (POC22)



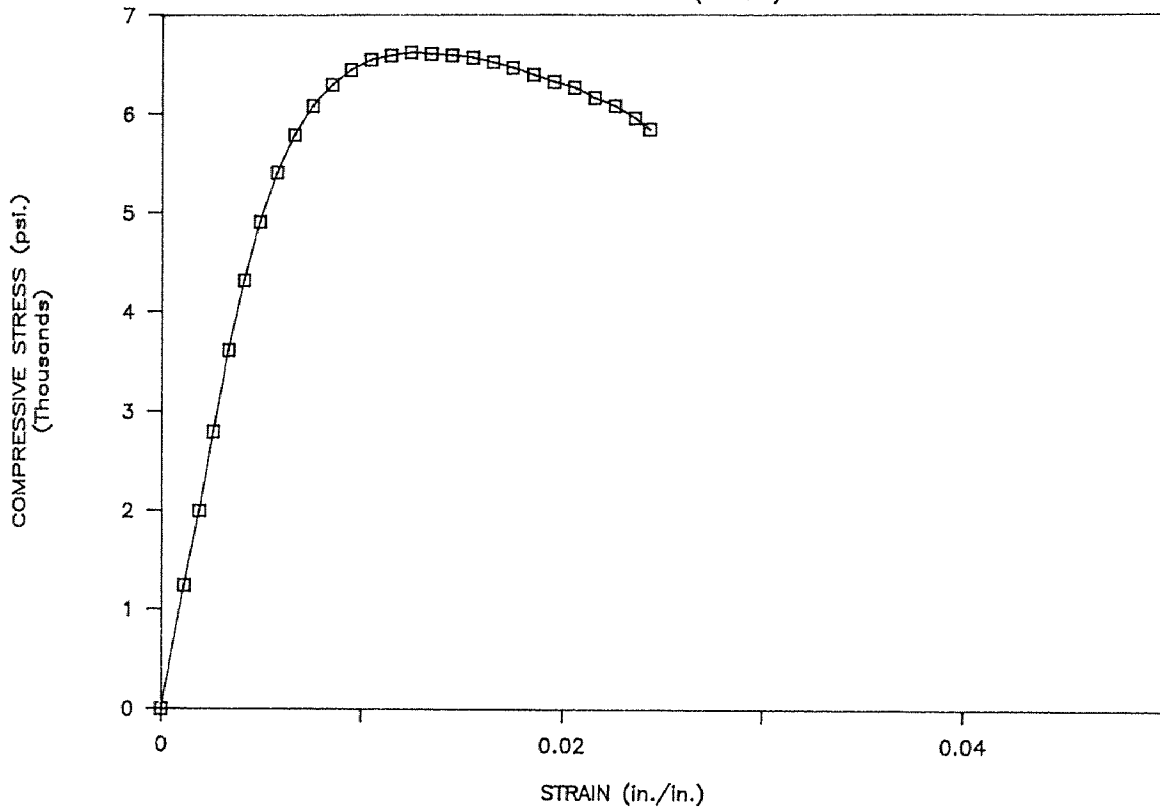
STRESS VS. STRAIN CURVE

POLYMER CONCRETE (POC23)



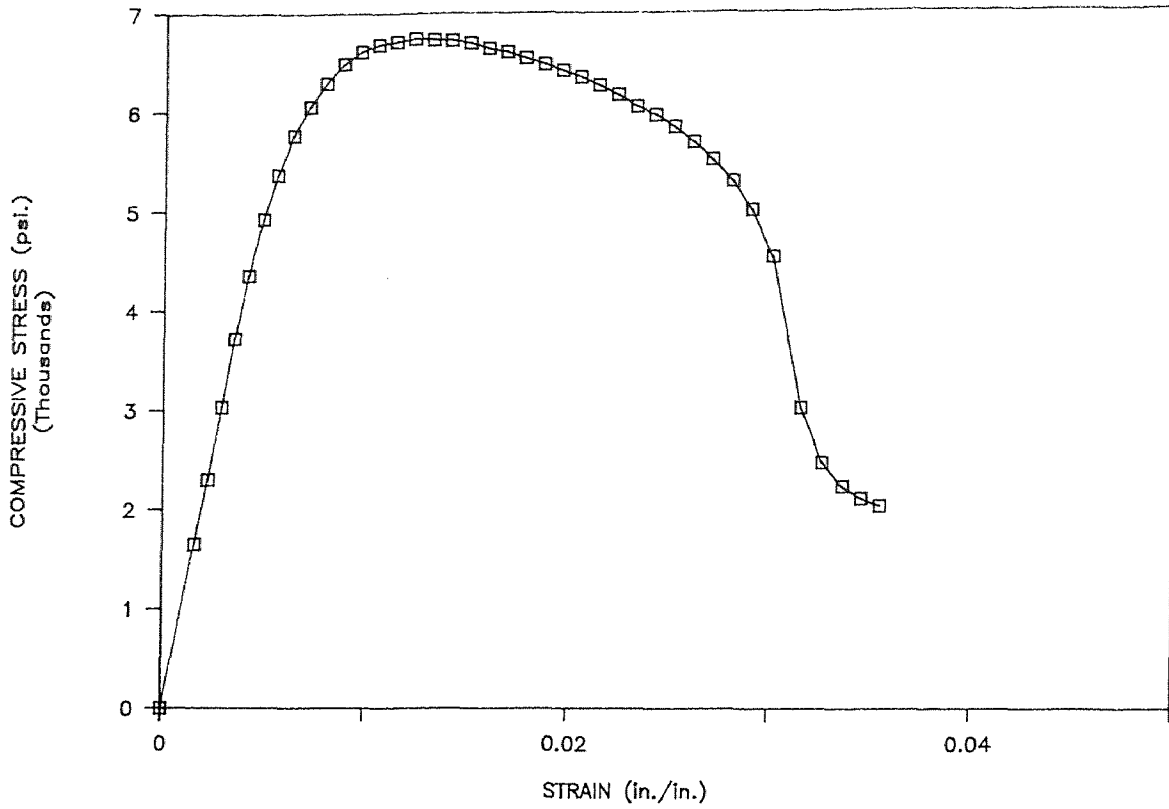
STRESS VS. STRAIN CURVE

POLYMER CONCRETE (POC24)



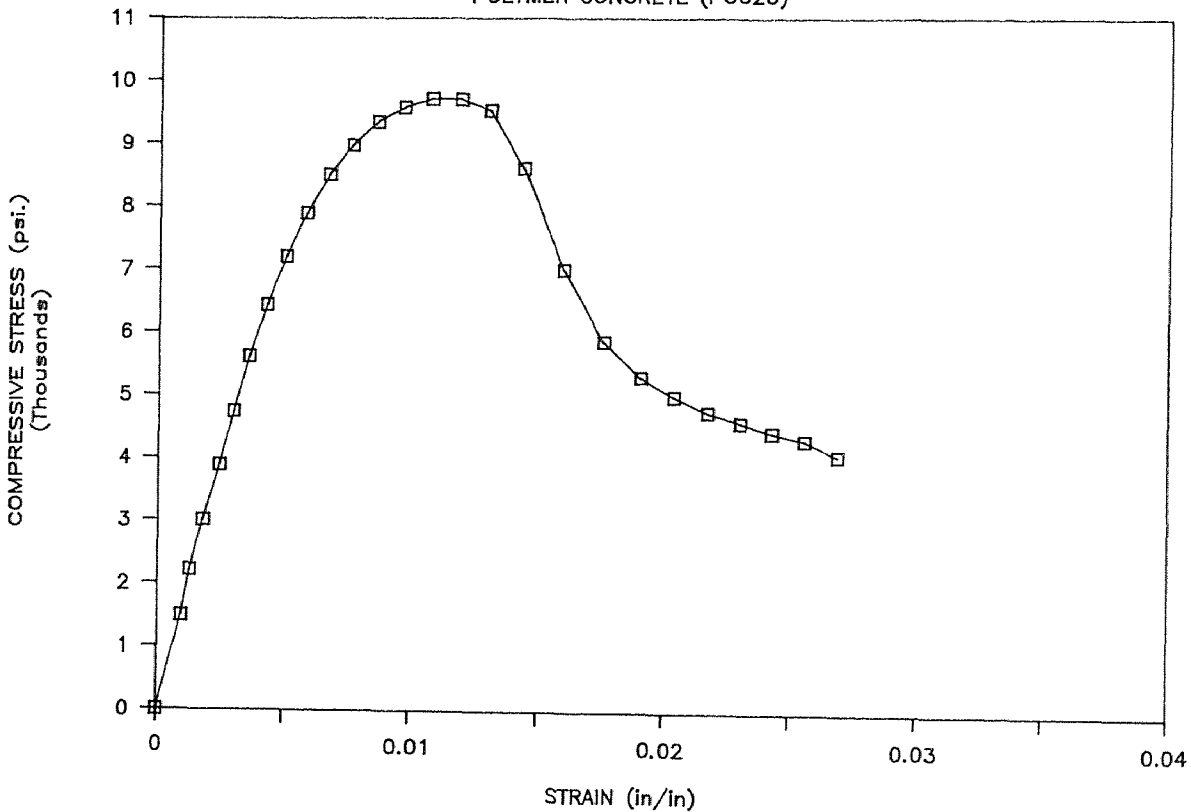
STRESS VS. STRAIN CURVE

POLYMER CONCRETE (POC25)



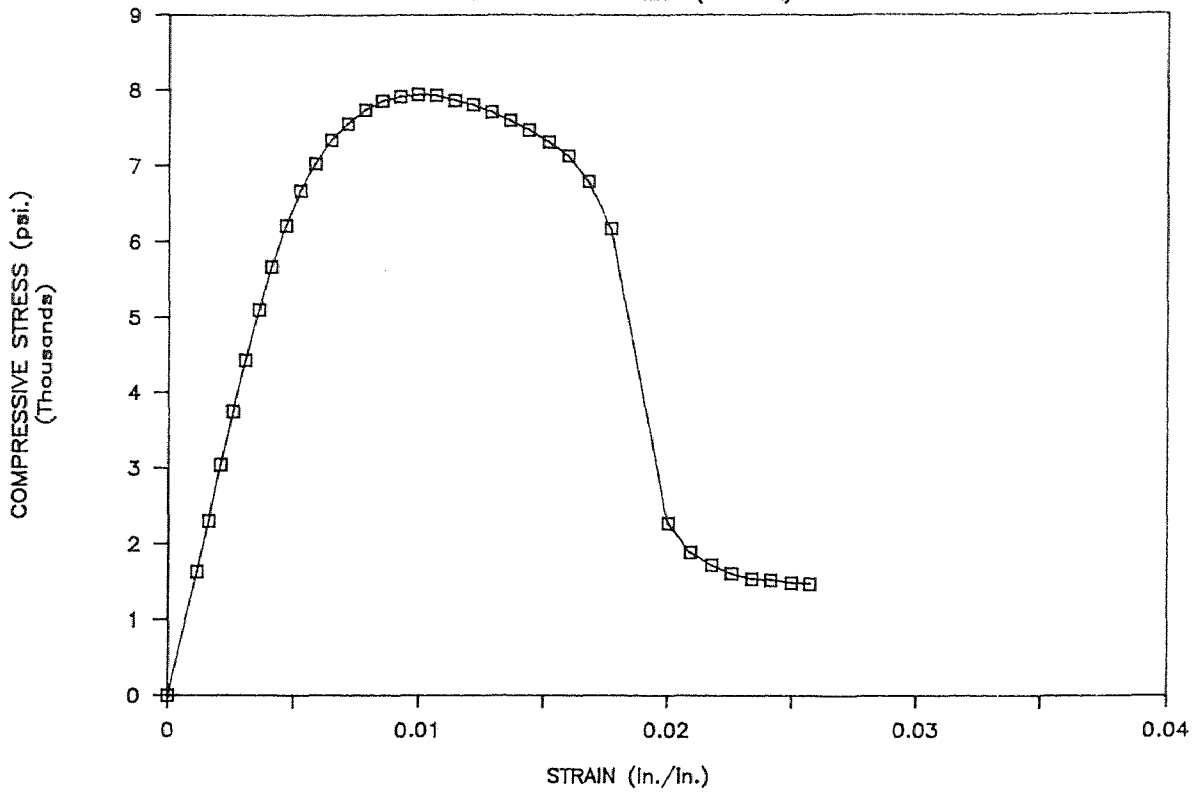
STRESS VS. STRAIN CURVE

POLYMER CONCRETE (POC26)



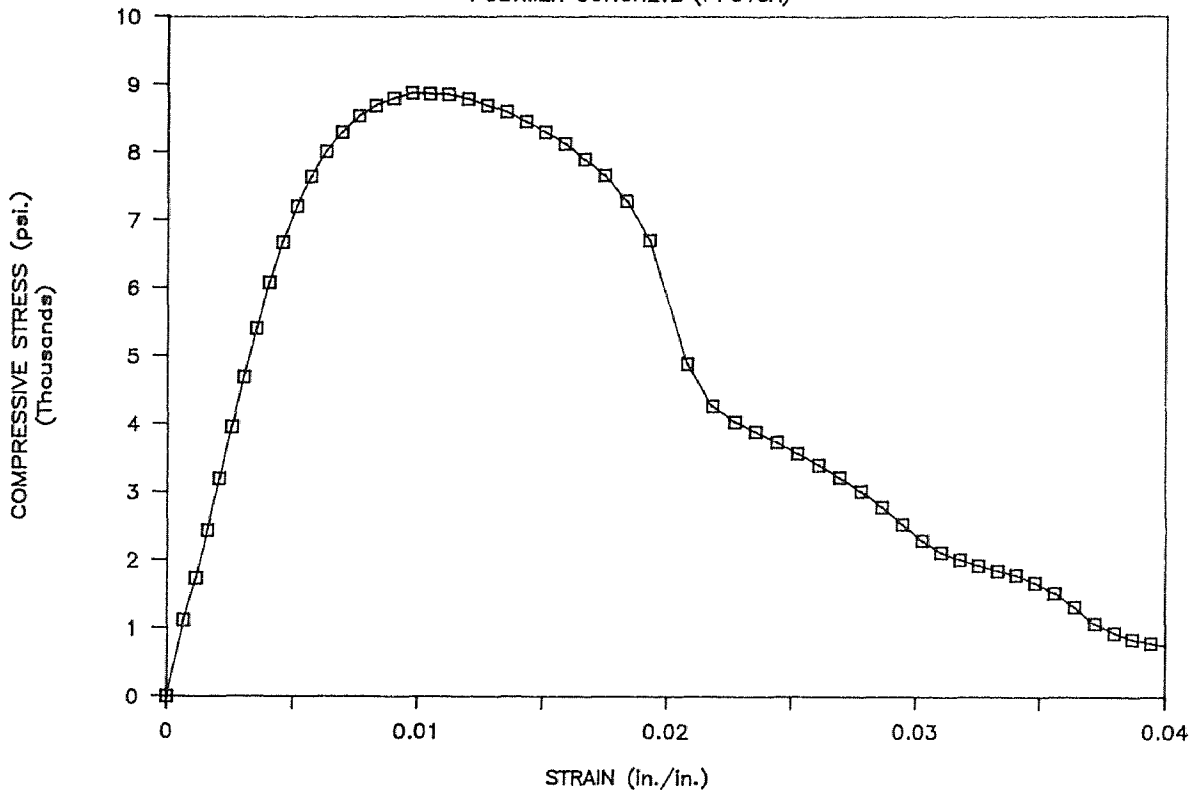
STRESS VS. STRAIN CURVE

POLYMER CONCRETE (PFC13A)



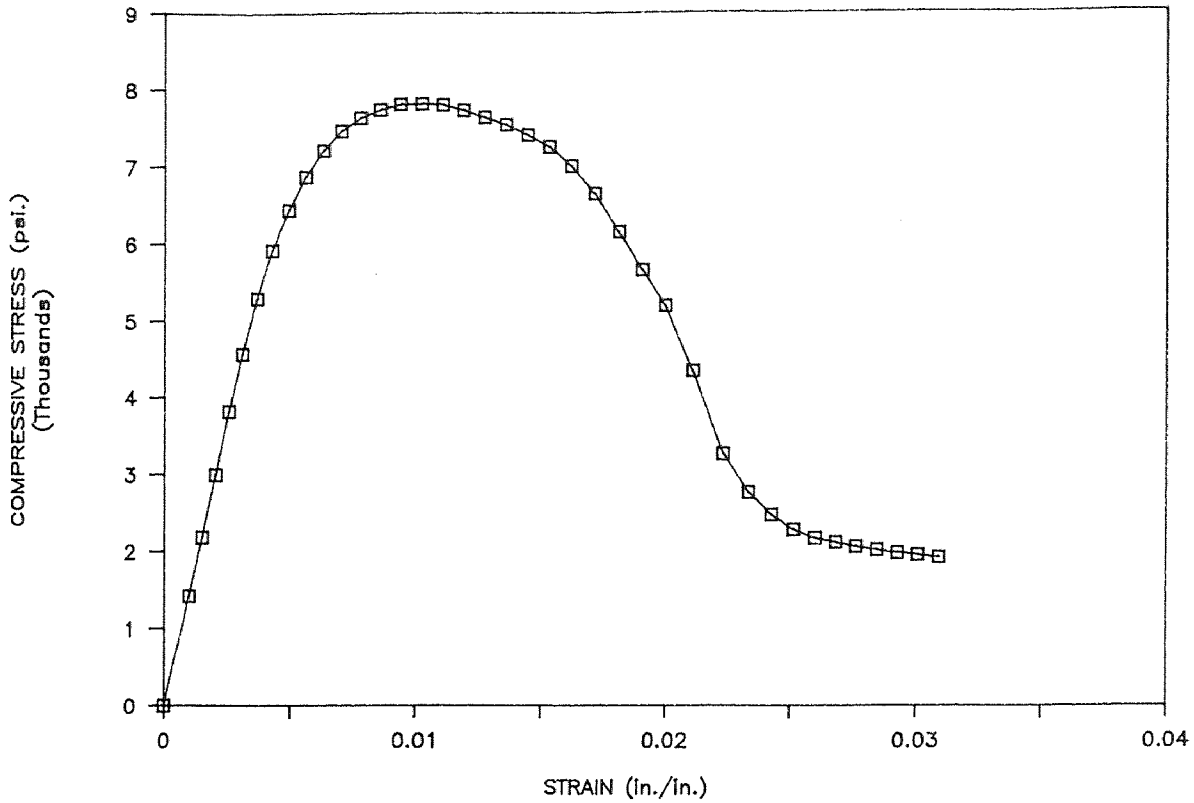
STRESS VS. STRAIN CURVE

POLYMER CONCRETE (PFC15A)



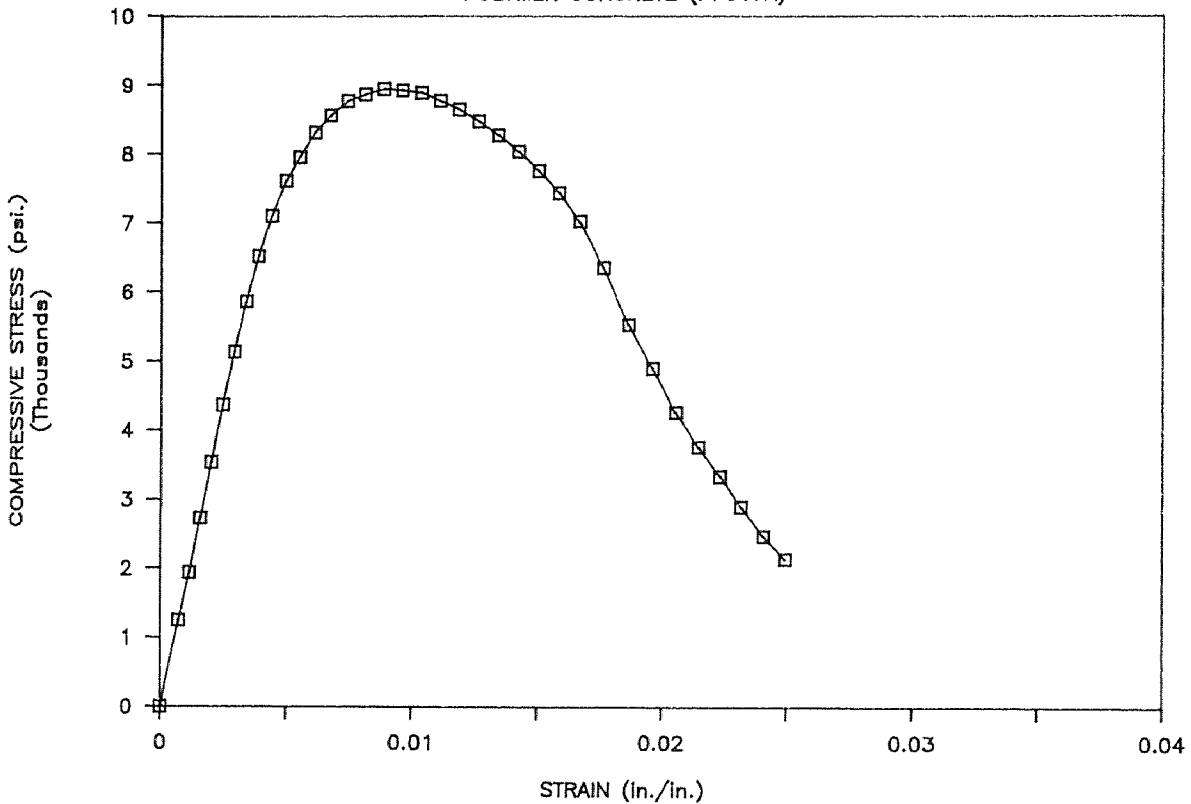
STRESS VS. STRAIN CURVE

POLYMER CONCRETE (PFC16A)



STRESS VS. STRAIN CURVE

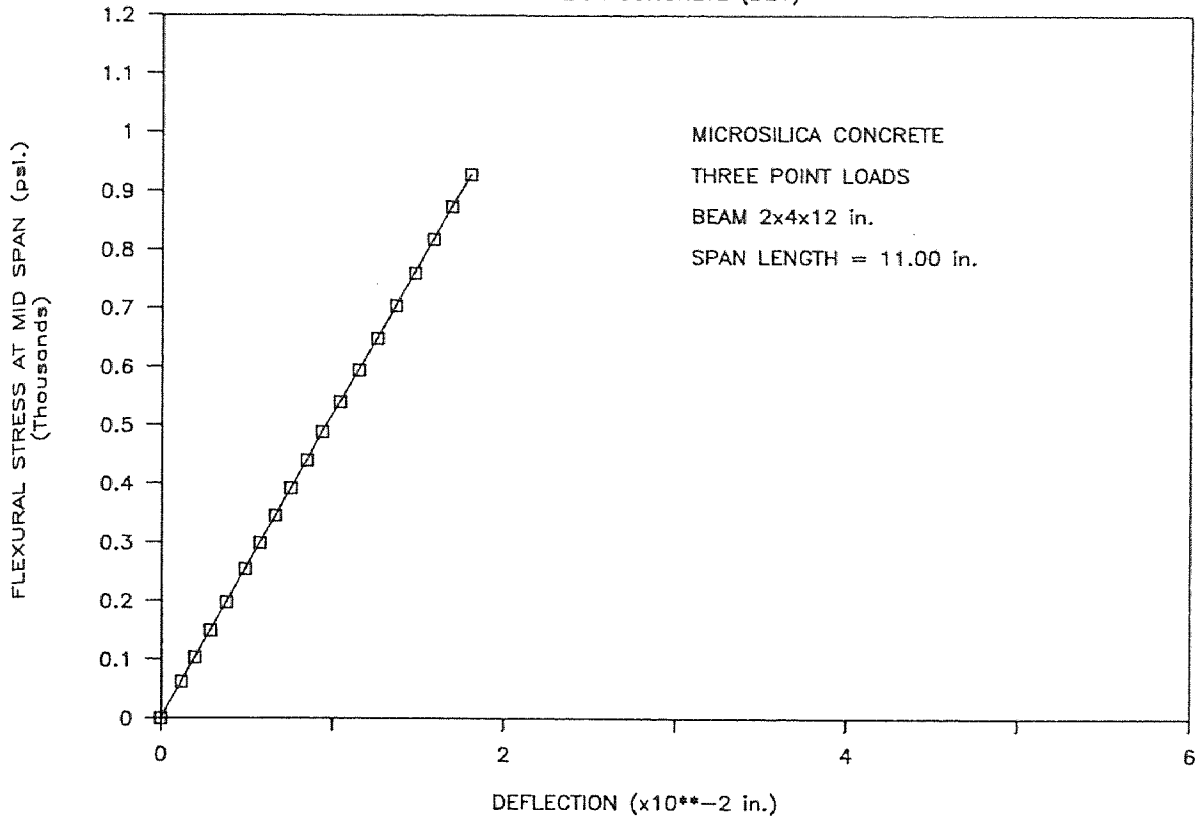
POLYMER CONCRETE (PFC17A)



APPENDIX B

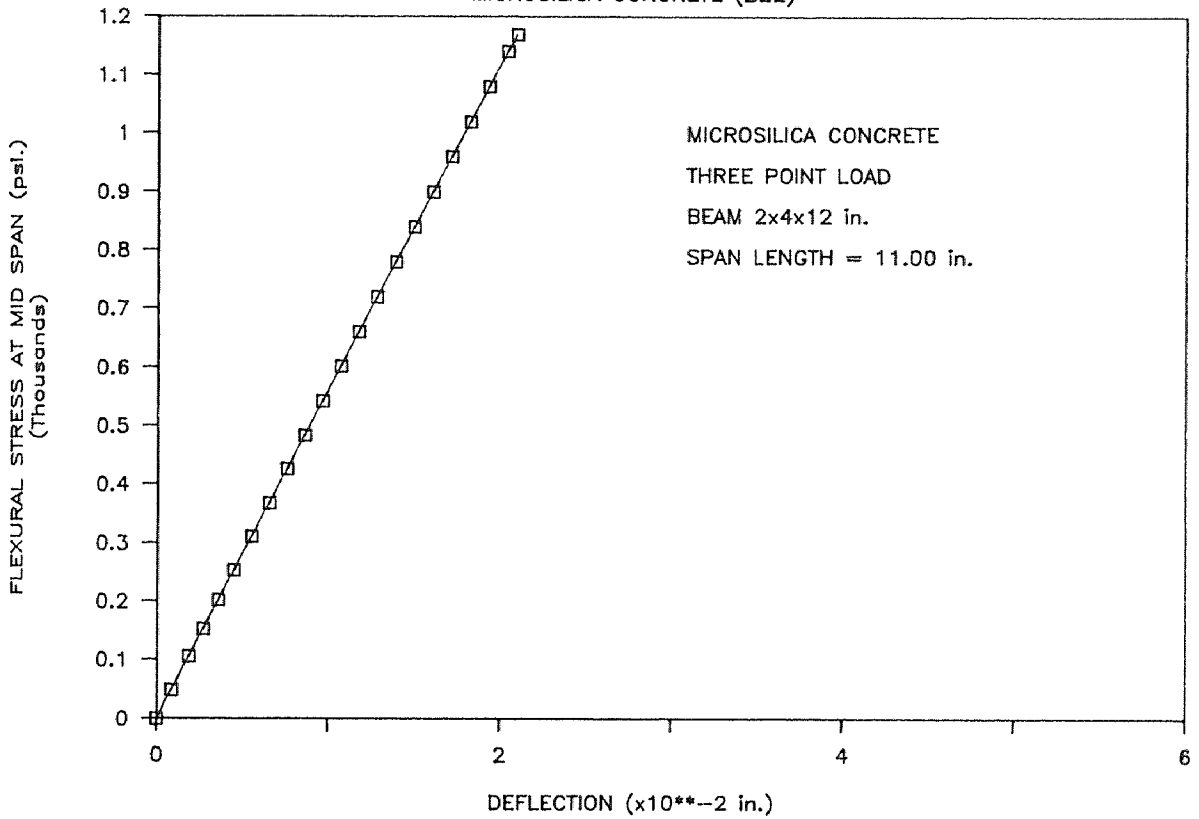
FLEXURAL STRESS VS. DEFLECTION

MICROSILICA CONCRETE (B21)



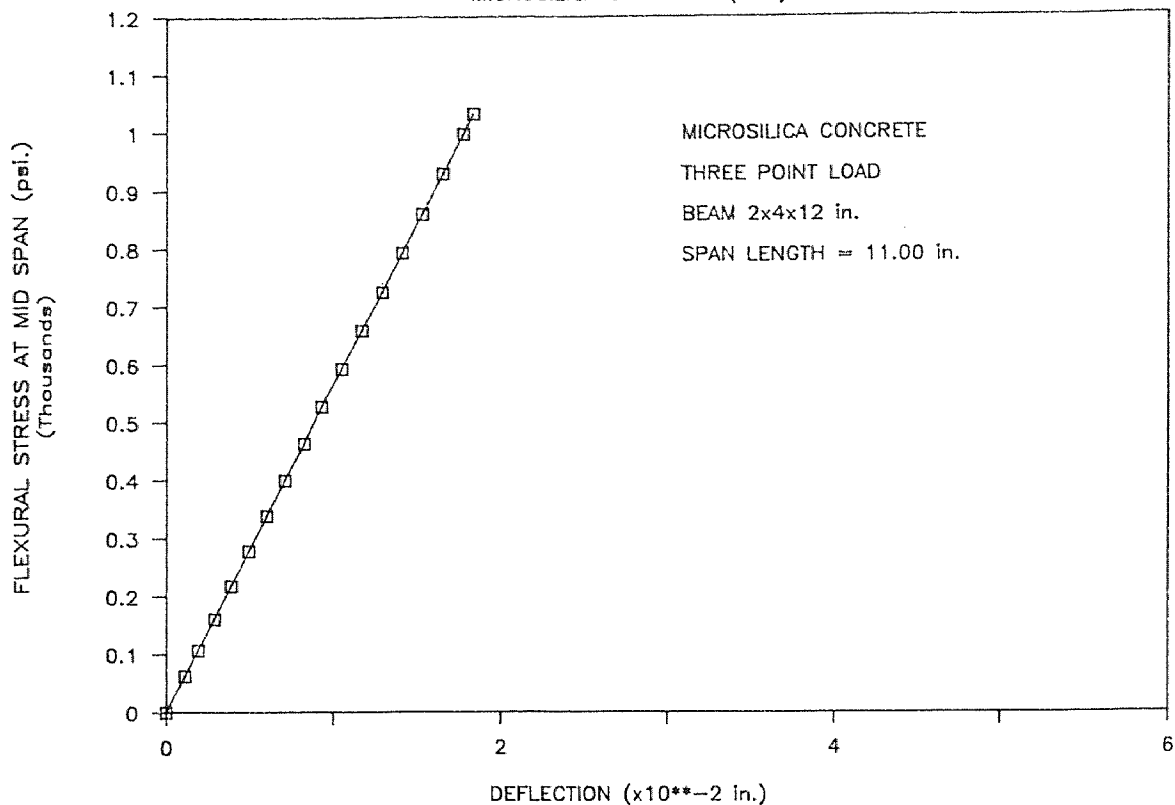
FLEXURAL STRESS VS. DEFLECTION

MICROSILICA CONCRETE (B22)



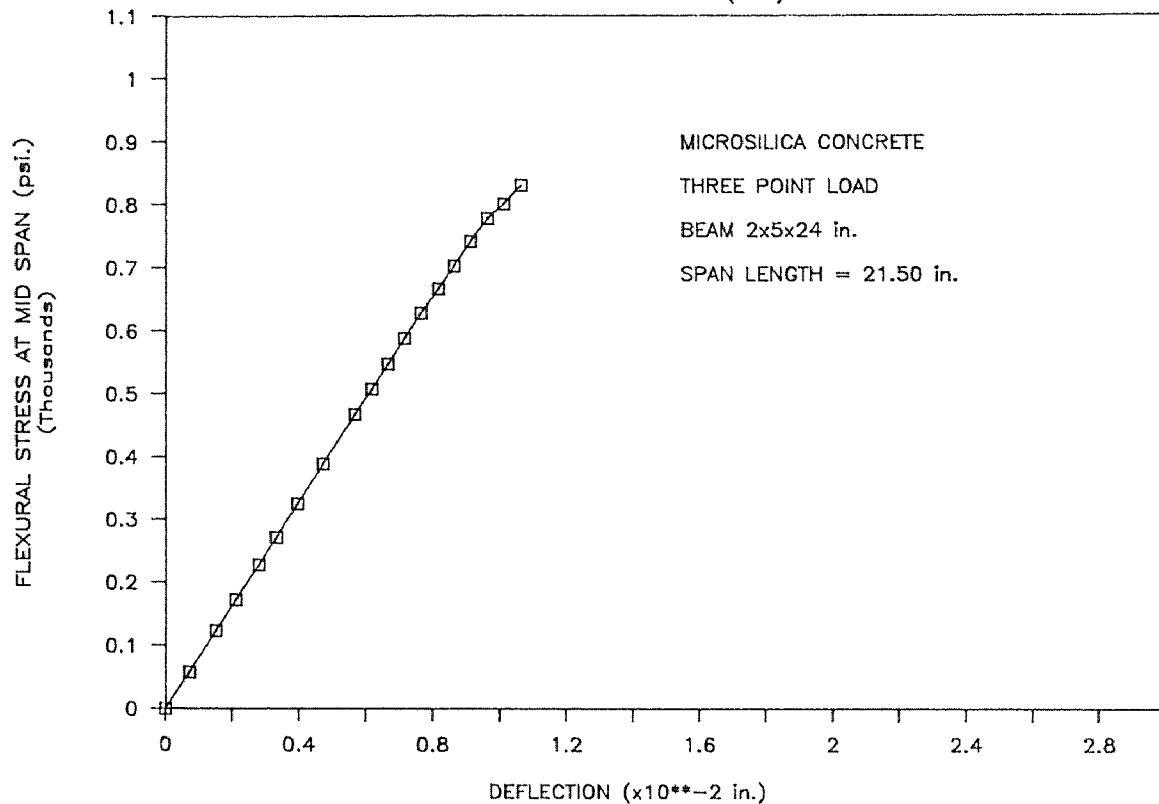
FLEXURAL STRESS VS. DEFLECTION

MICROSILICA CONCRETE (B23)



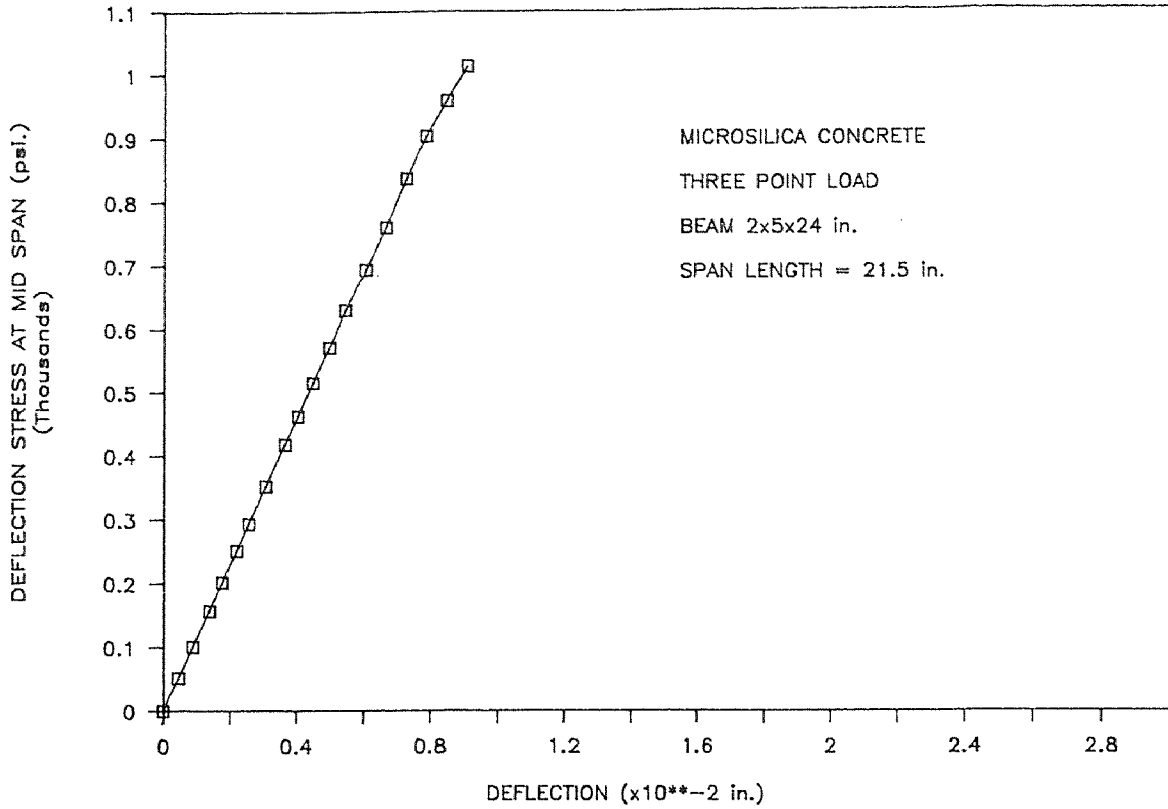
FLEXURAL STRESS VS. DEFLECTION

MICROSILICA CONCRETE (B51)



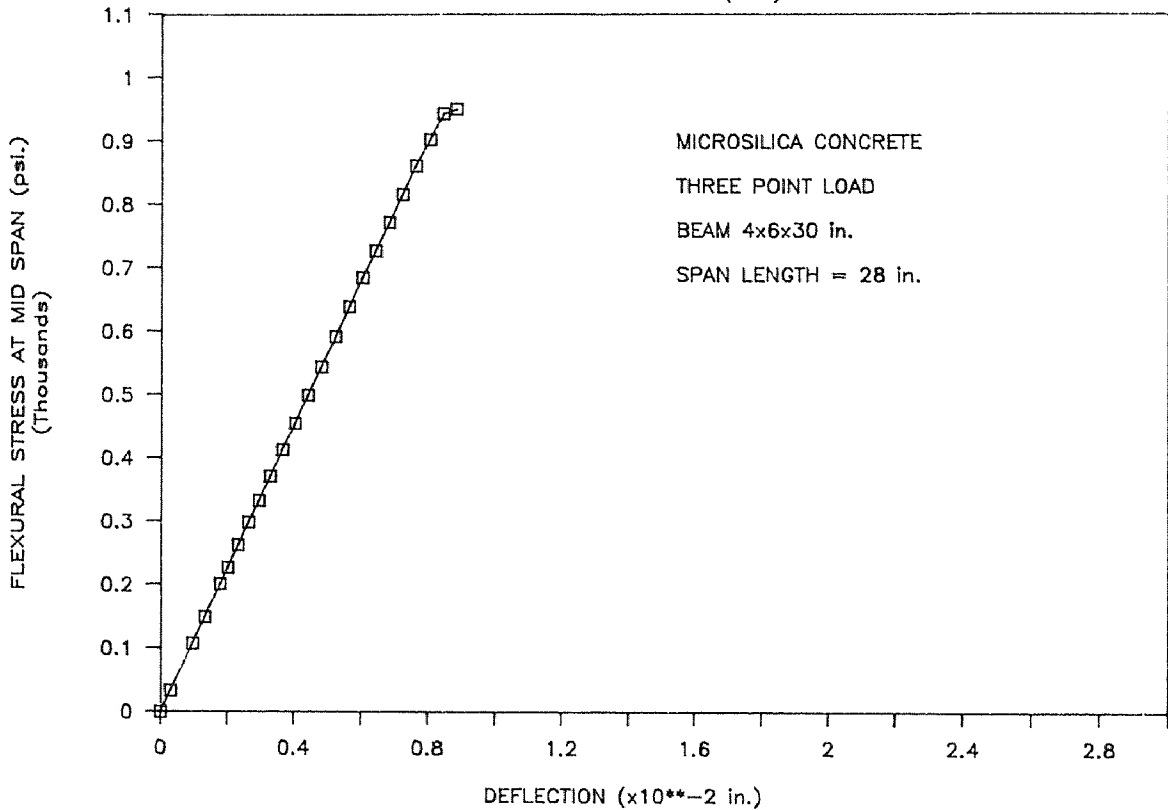
FLEXURAL STRESS VS. DEFLECTION

MICROSILICA CONCRETE (B52)



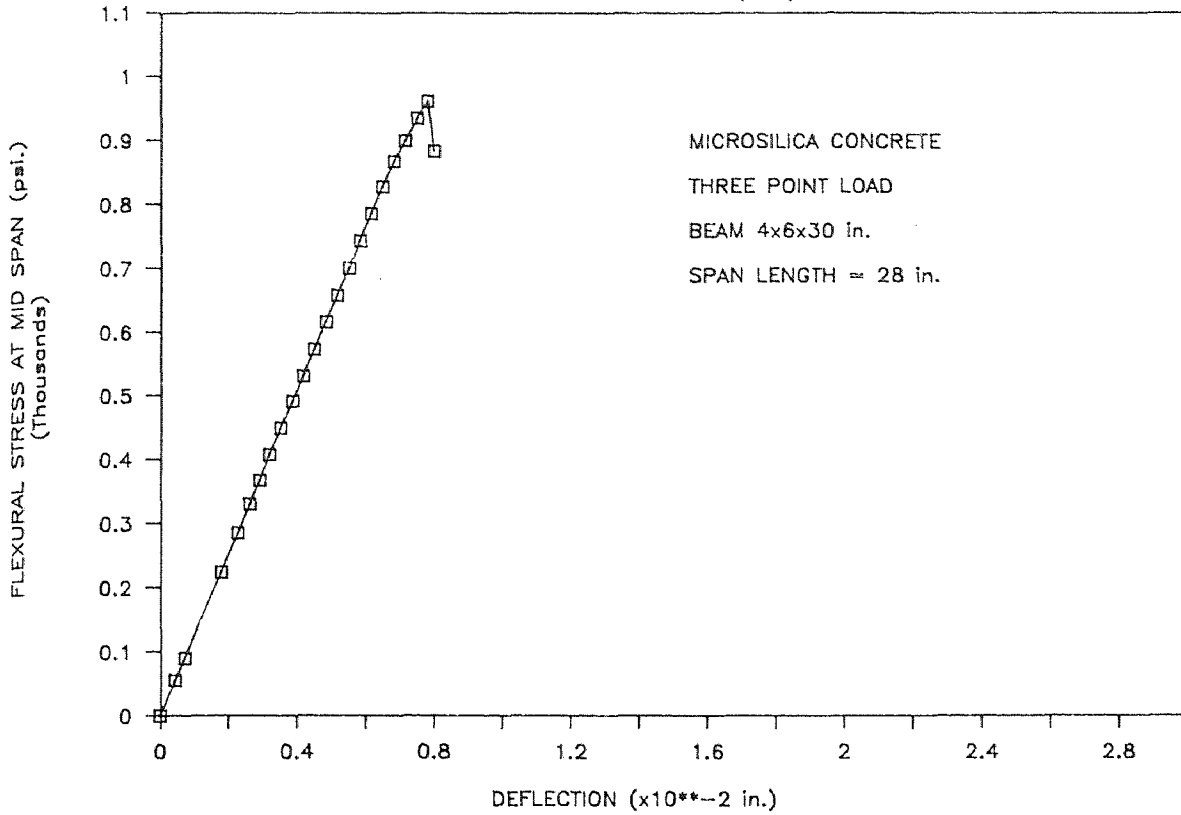
FLEXURAL STRESS VS. DEFLECTION

MICROSILICA CONCRETE (B41)



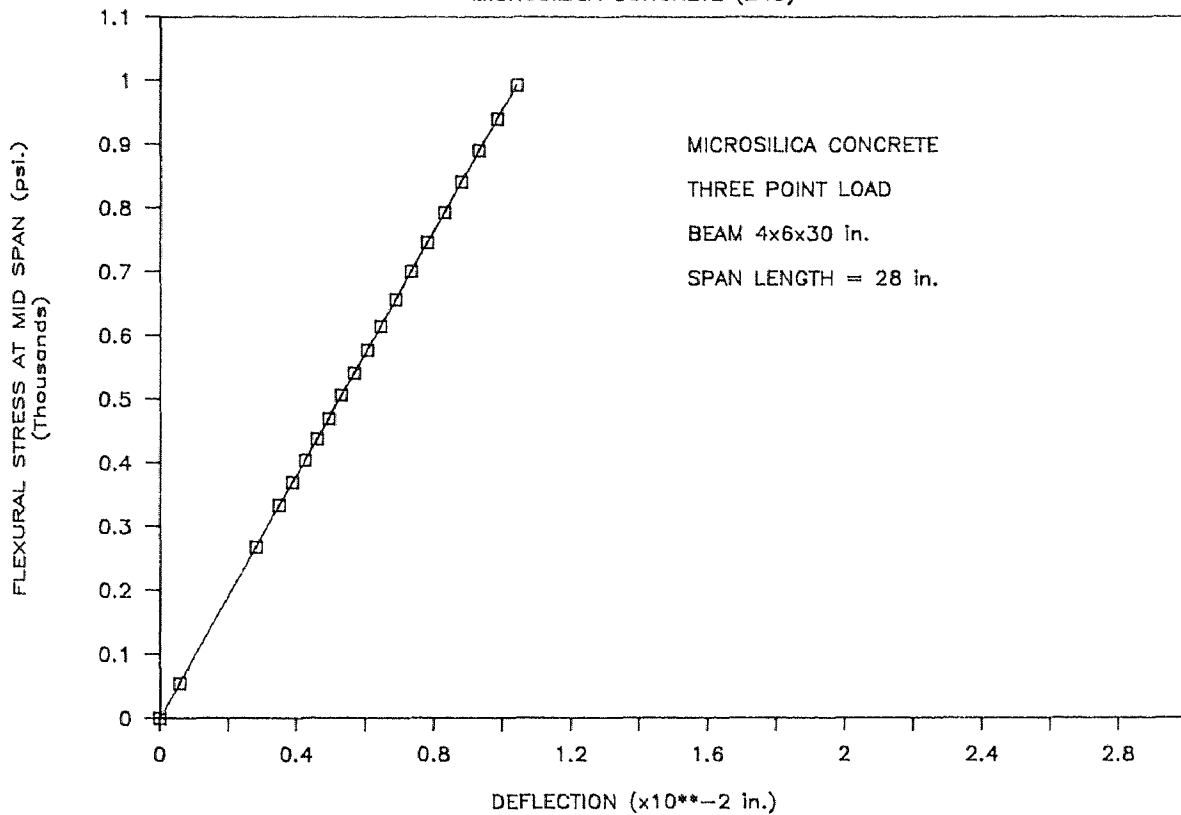
FLEXURAL STRESS VS. DEFLECTION

MICROSILICA CONCRETE (B42)



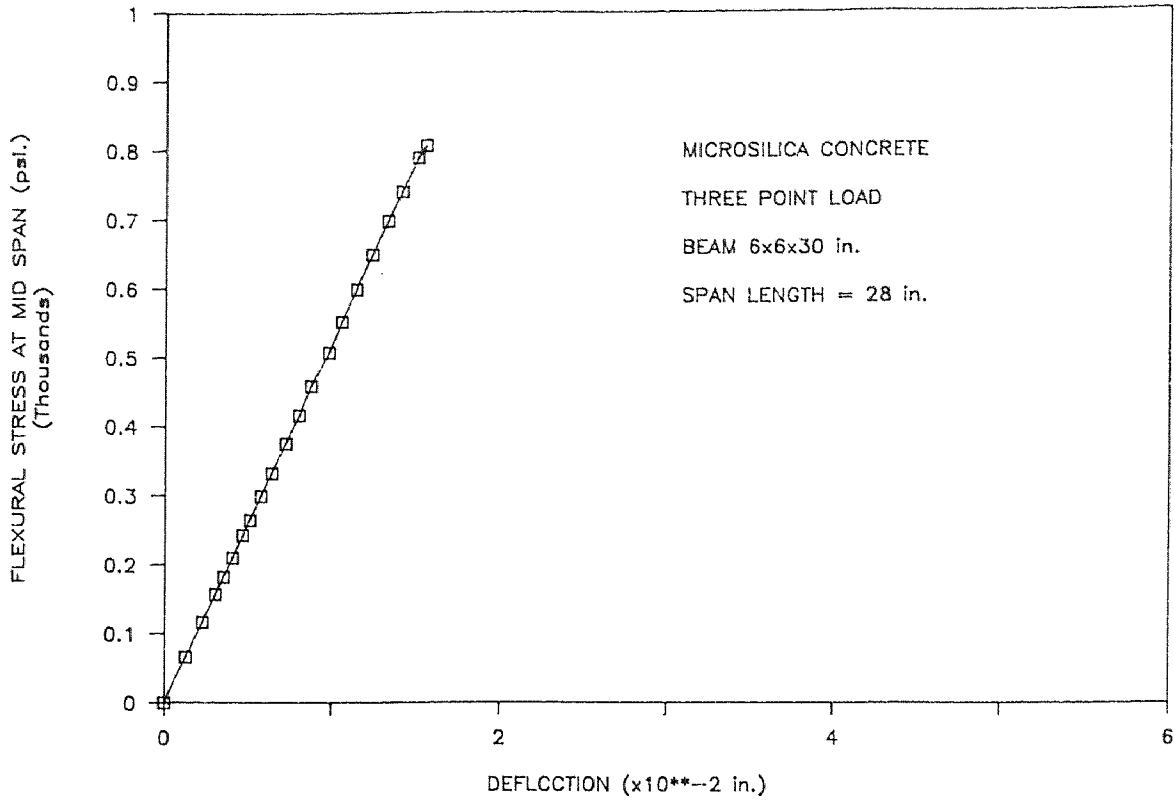
FLEXURAL STRESS VS. DEFLECTION

MICROSILICA CONCRETE (B43)



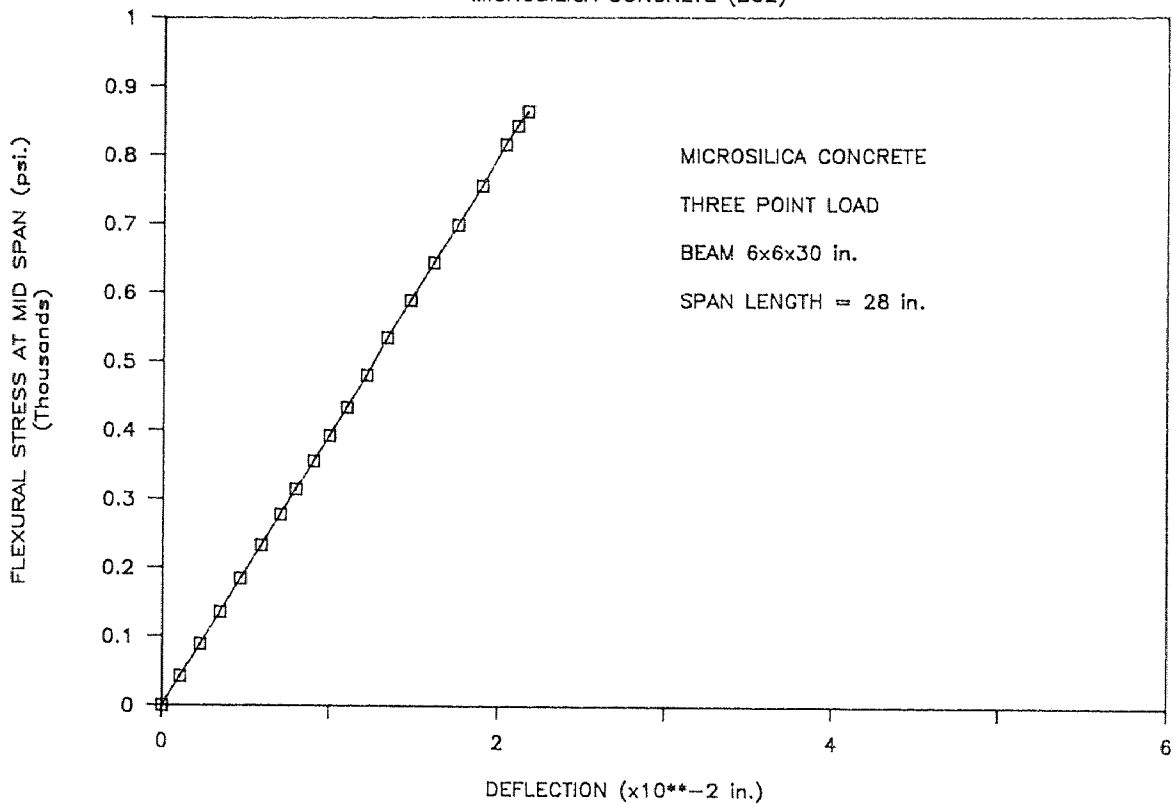
FLEXURAL STRESS — DEFLECTION

MICROSILICA CONCRETE (B61)



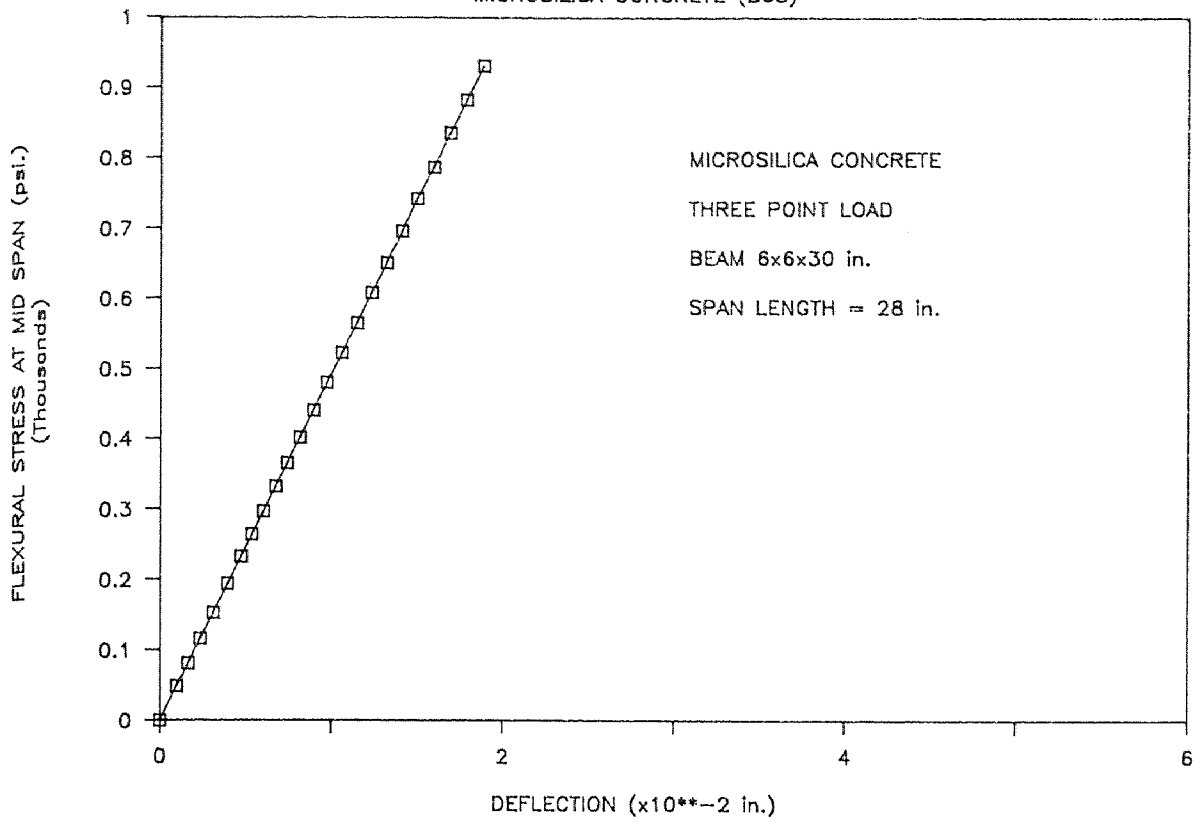
FLEXURAL STRESS VS. DEFLECTION

MICROSILICA CONCRETE (B62)



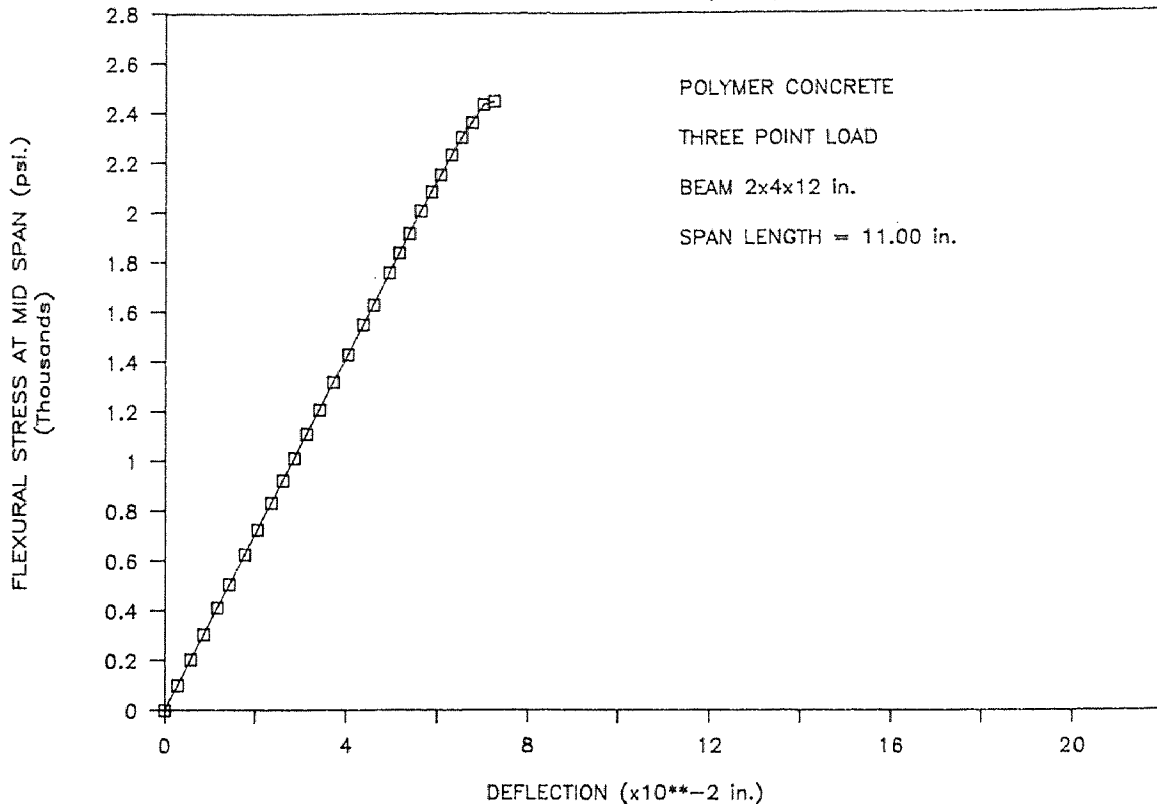
FLEXURAL STRESS VS. DEFLECTION

MICROSILICA CONCRETE (B63)



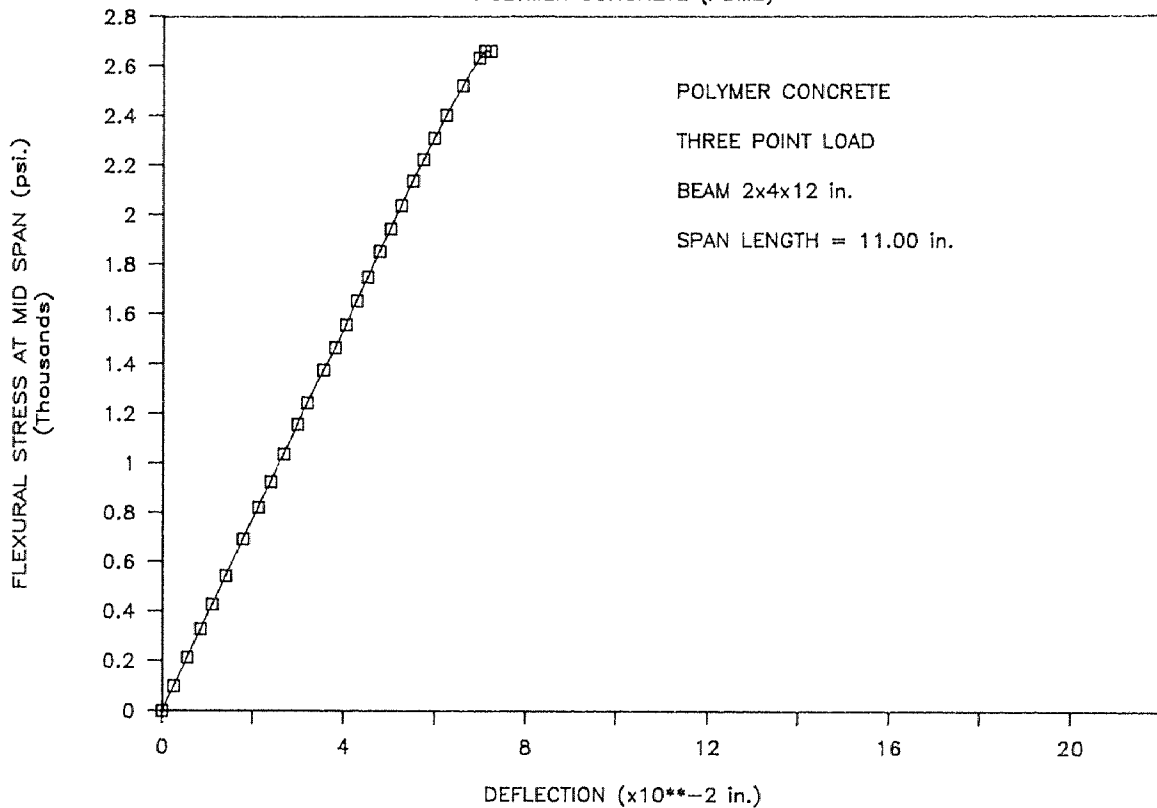
FLEXURAL STRESS VS. DEFLECTION

POLYMER CONCRETE. (PBM1)



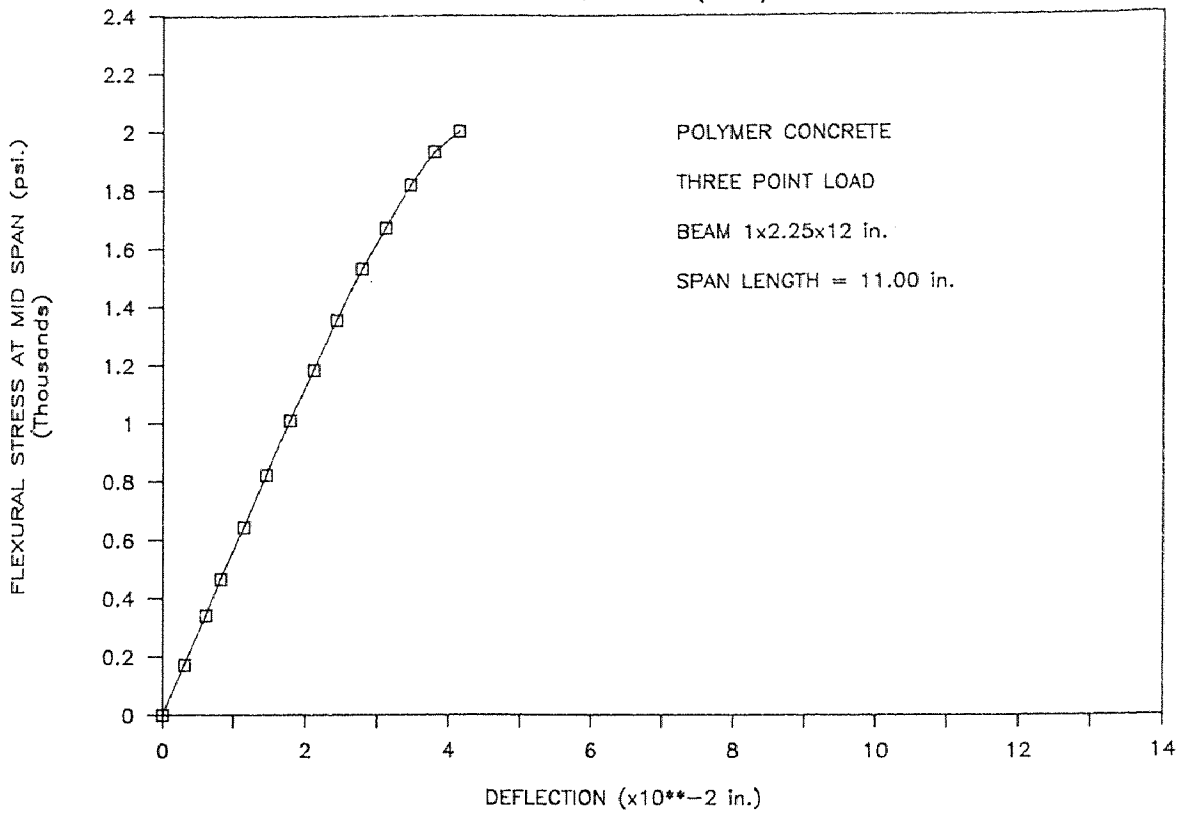
FLEXURAL STRESS VS. DEFLECTION

POLYMER CONCRETE (PBM2)



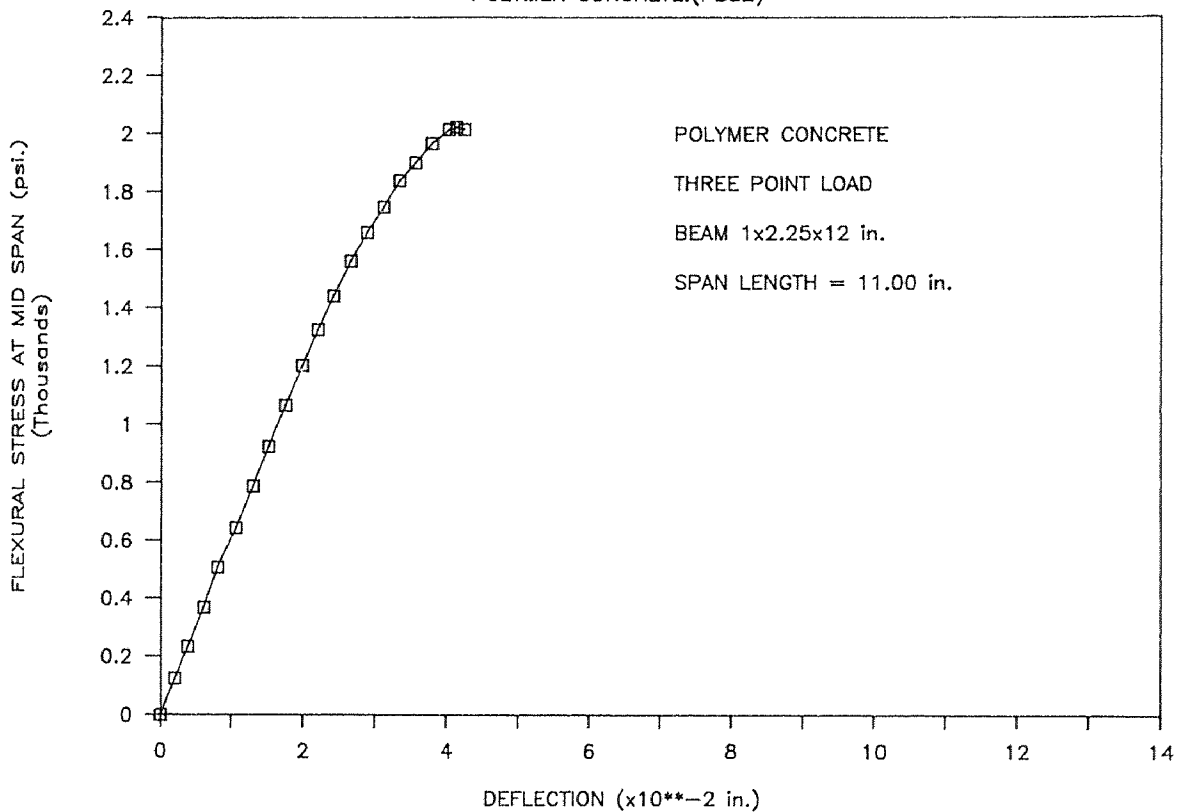
FLEXURAL STRESS VS. DEFLECTION

POLYMER CONCRETE (PBS1)



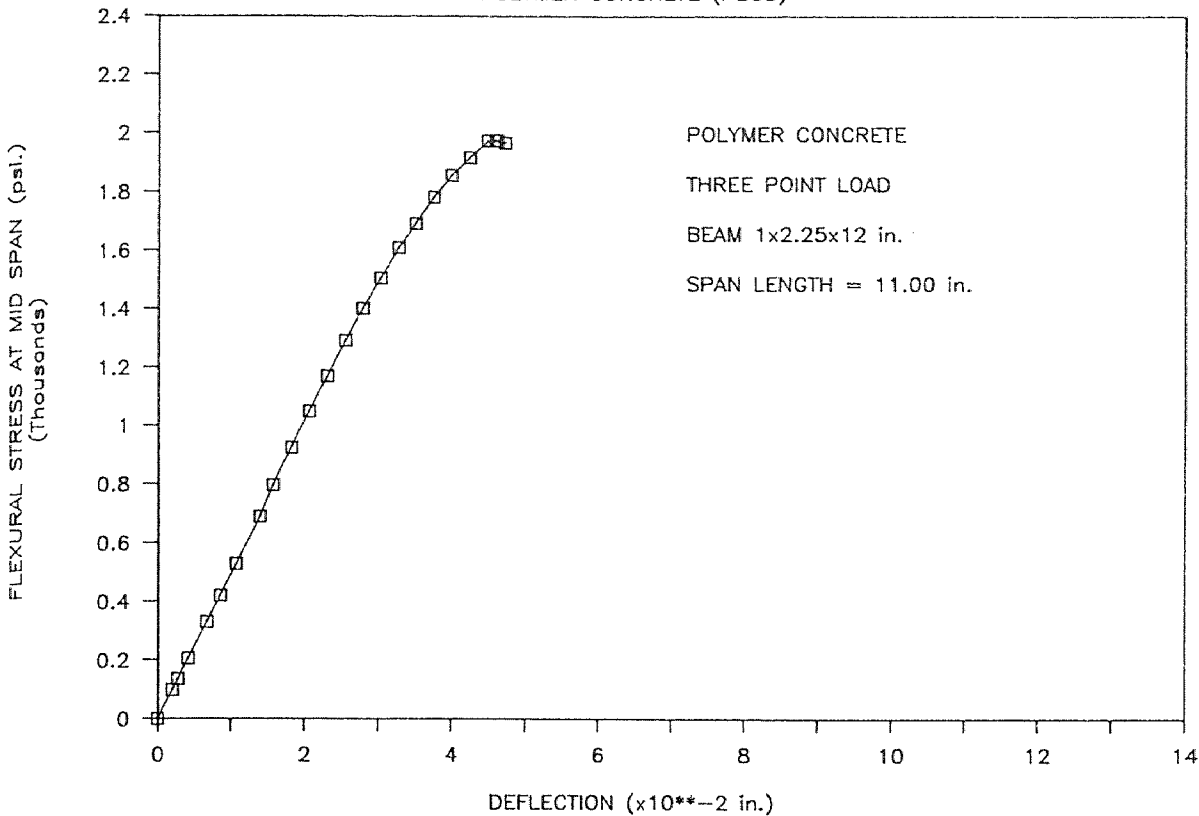
FLEXURAL STRESS VS. DEFLECTION

POLYMER CONCRETE.(PBS2)



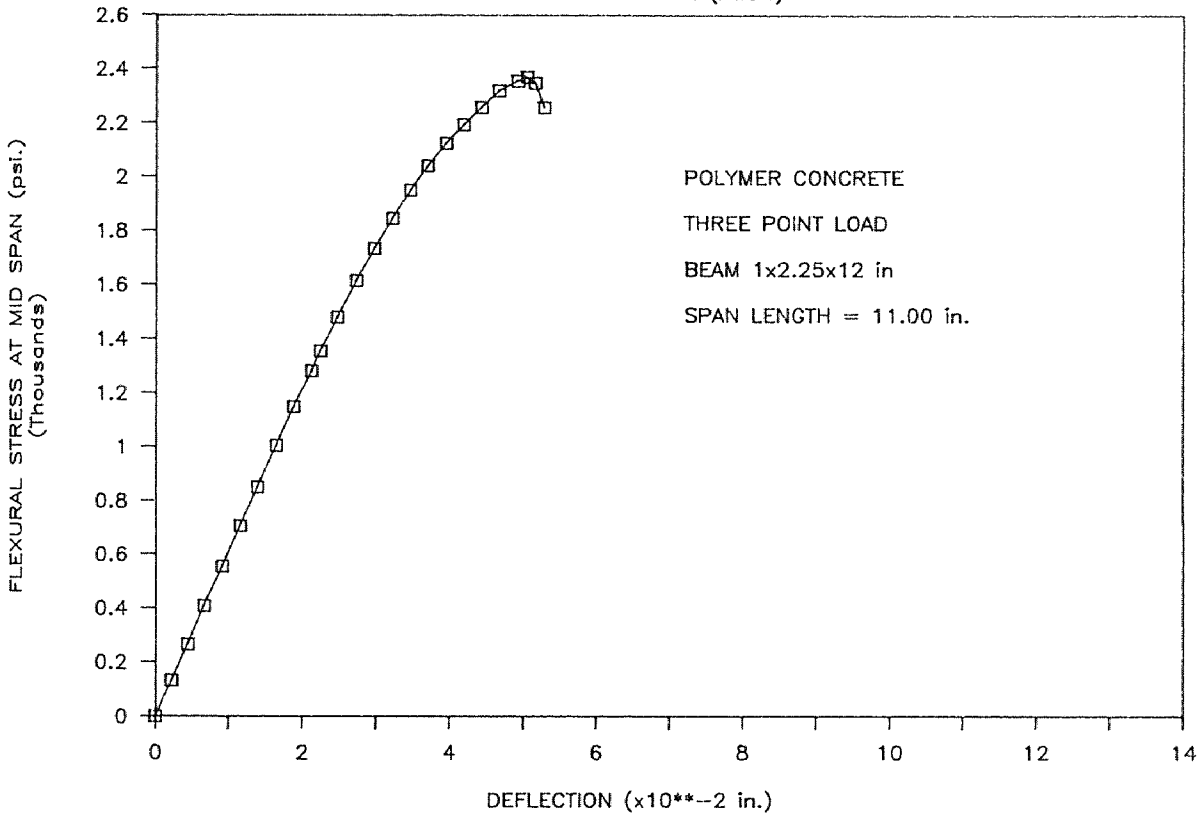
FLEXURAL STRESS VS. DEFLECTION

POLYMER CONCRETE (PBS3)



FLEXURAL STRESS VS. DEFLECTION

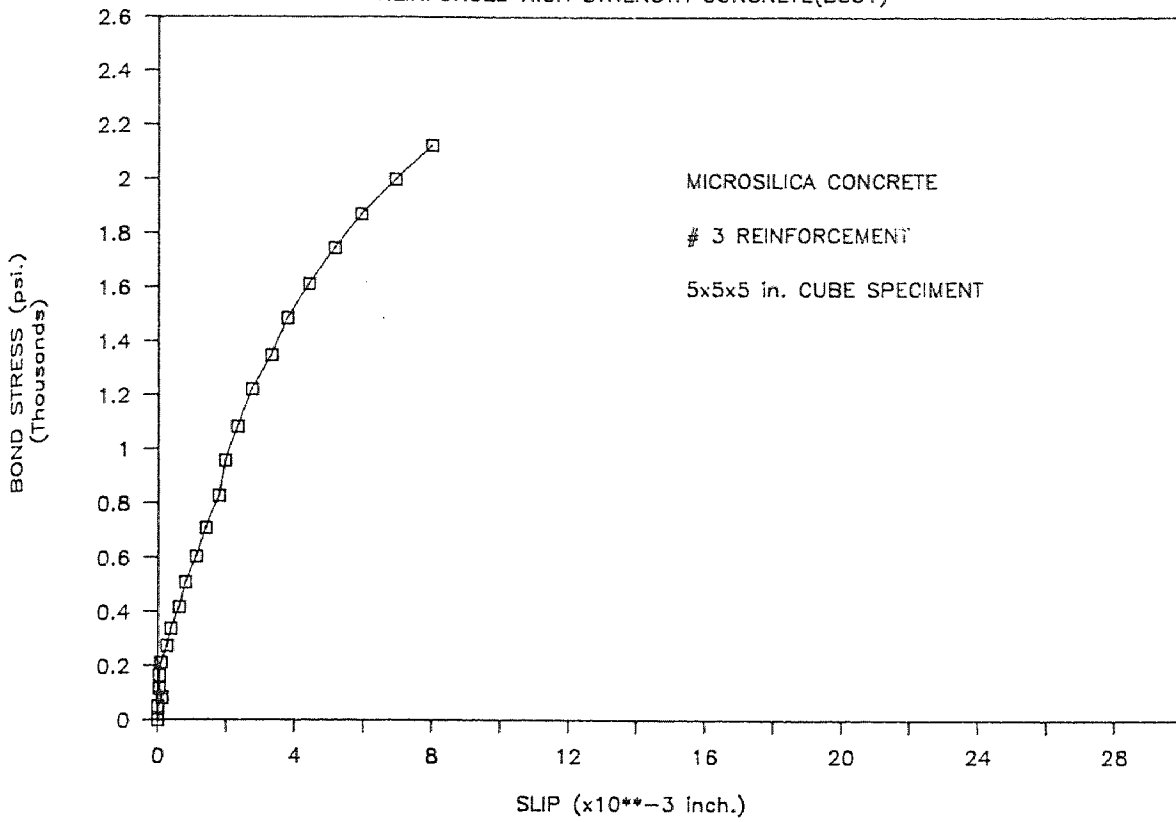
POLYMER CONCRETE (PBS4)



APPENDIX C

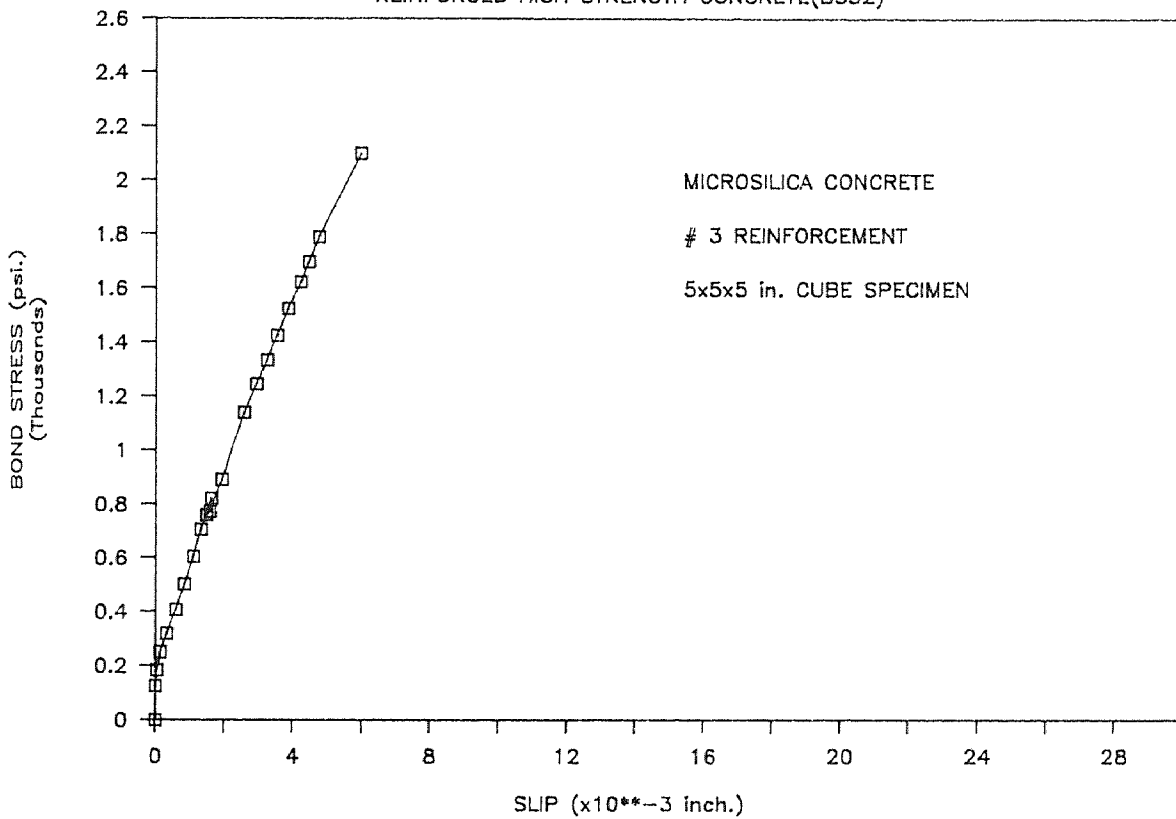
PULL-OUT TEST

REINFORCED HIGH STRENGTH CONCRETE(BS31)



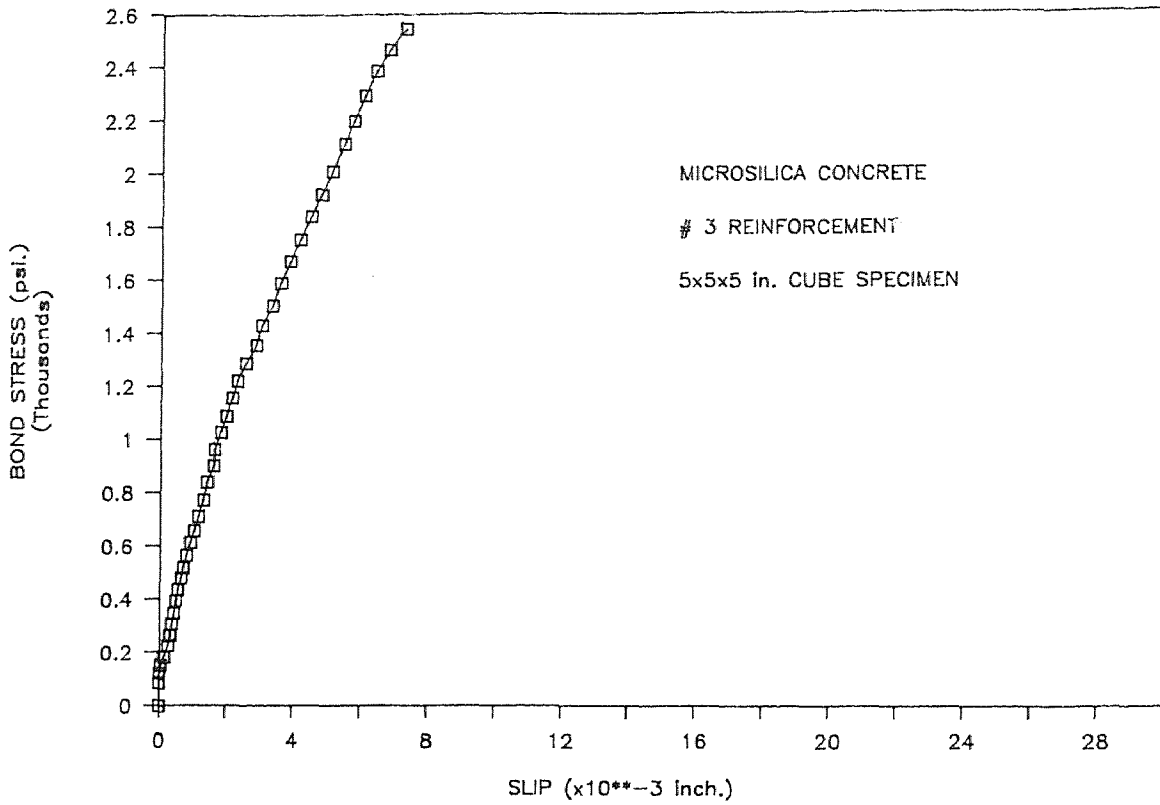
PULL-OUT TEST

REINFORCED HIGH STRENGTH CONCRETE(BS32)



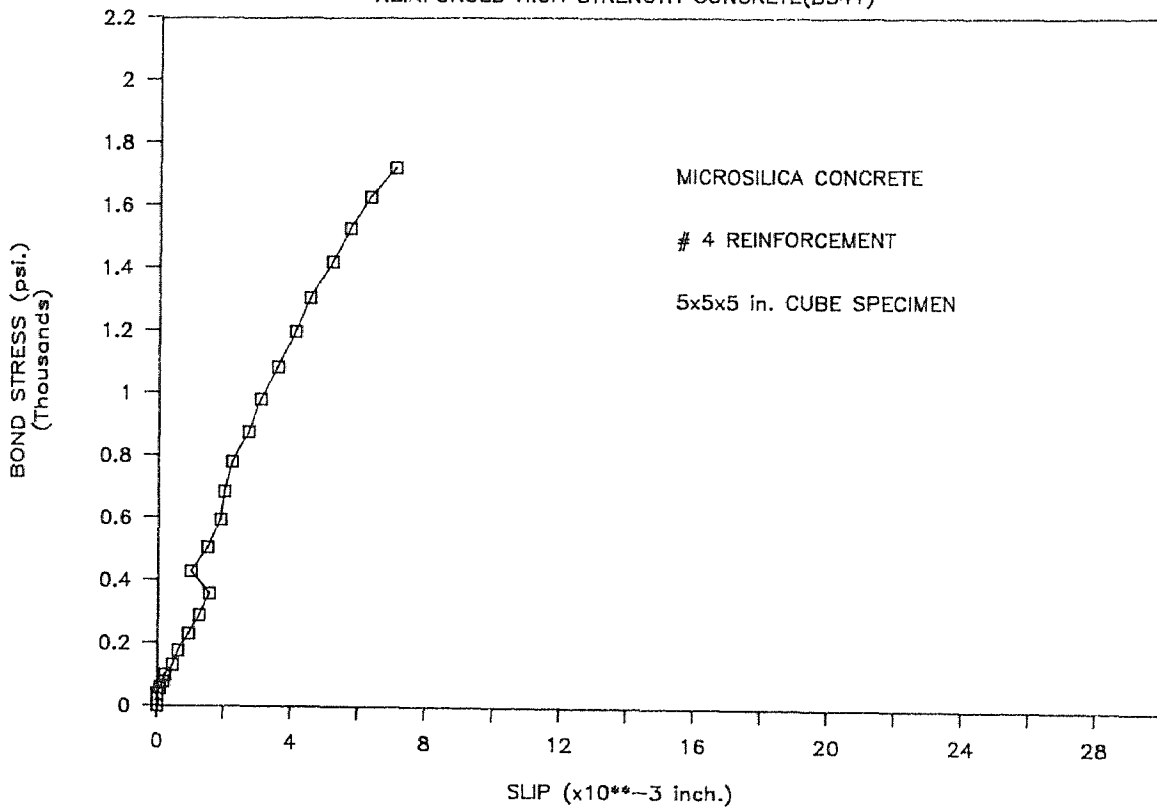
PULL-OUT TEST

REINFORCED HIGH STRENGTH CONCRETE(BS33)



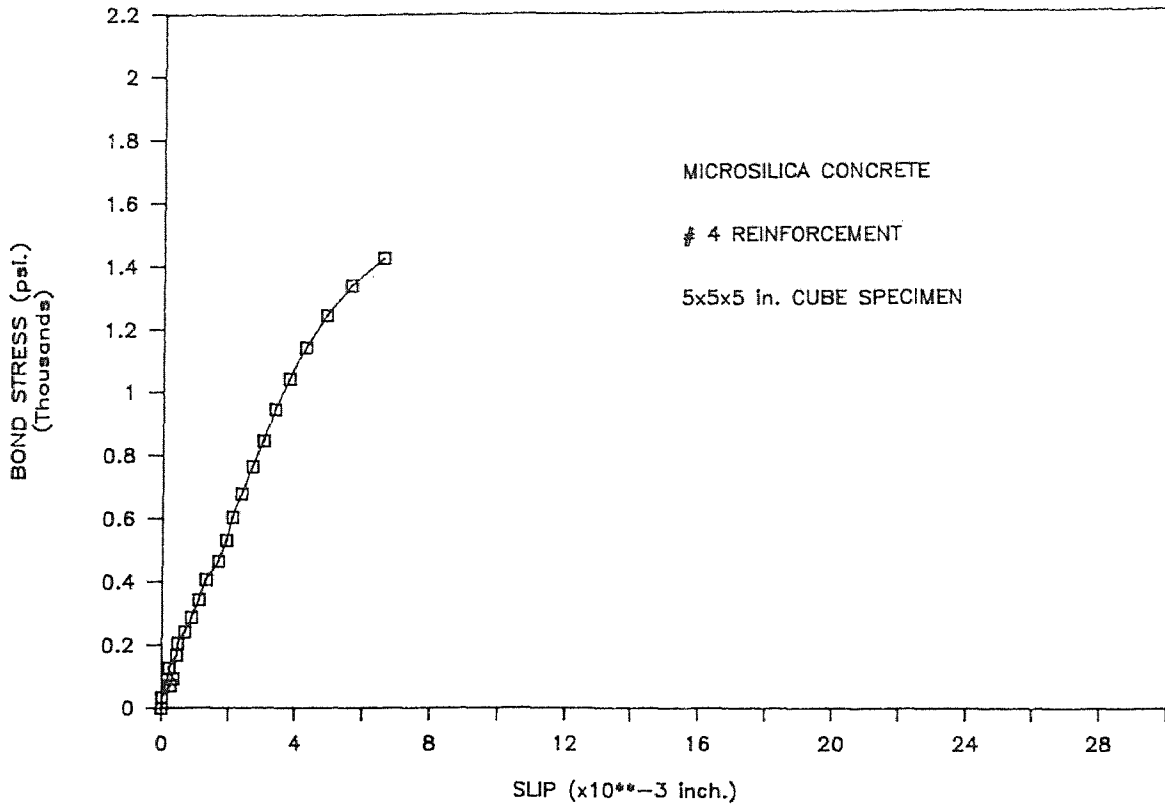
PULL-OUT TEST

REINFORCED HIGH STRENGTH CONCRETE(BS41)



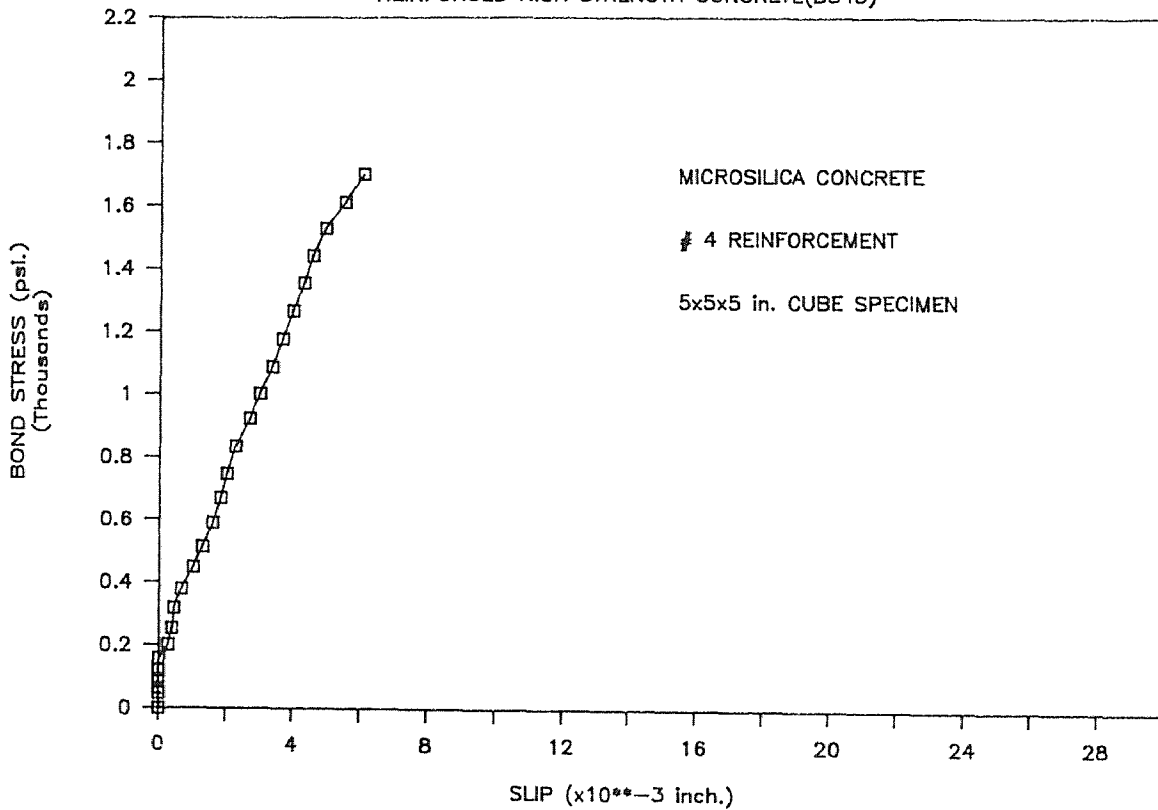
PULL-OUT TEST

REINFORCED HIGH STRENGTH CONCRETE(BS42)



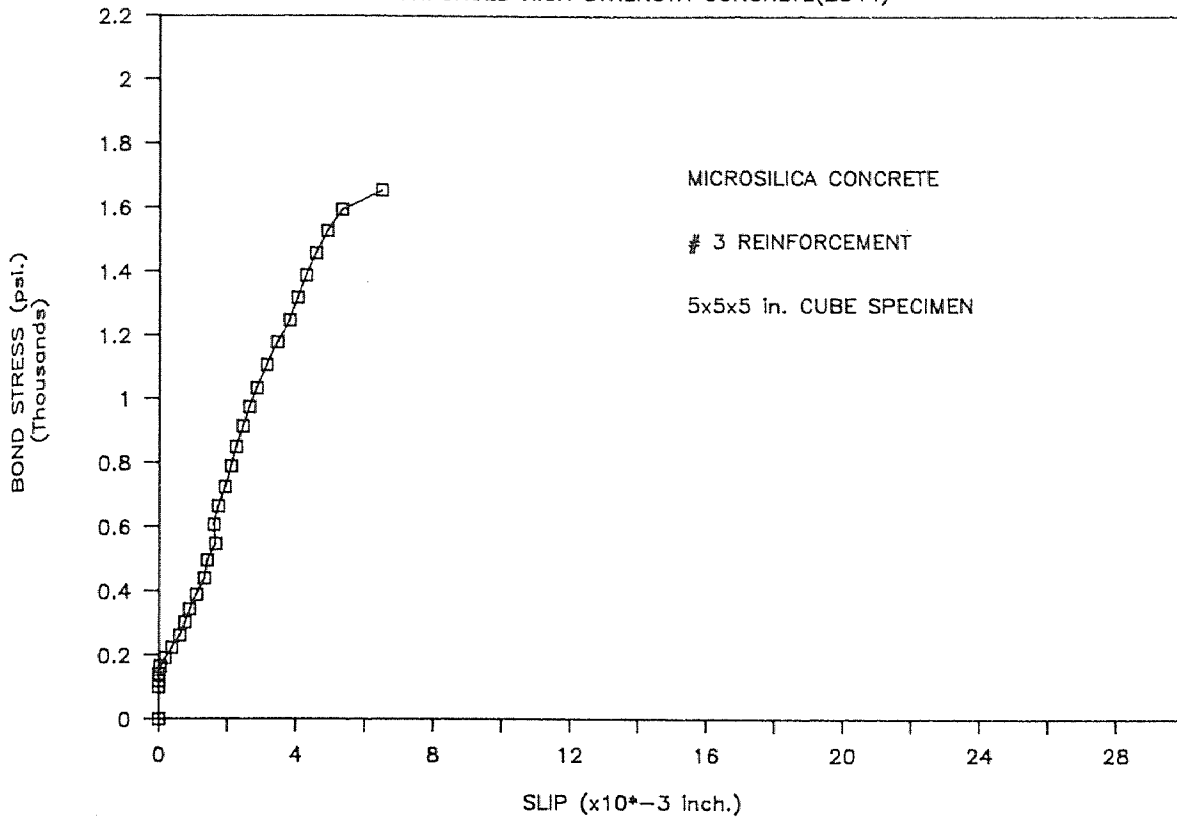
PULL-OUT TEST

REINFORCED HIGH STRENGTH CONCRETE(BS43)



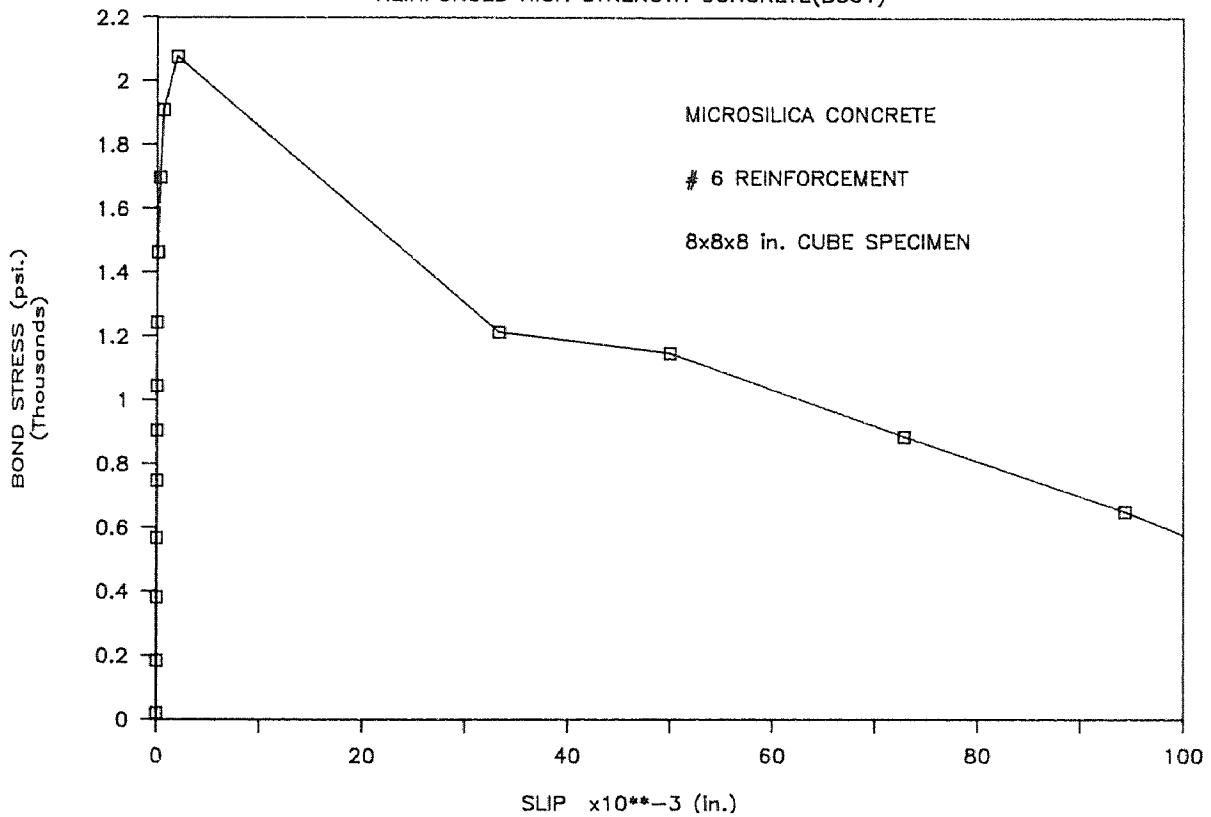
PULL-OUT TEST

REINFORCED HIGH STRENGTH CONCRETE(BS44)



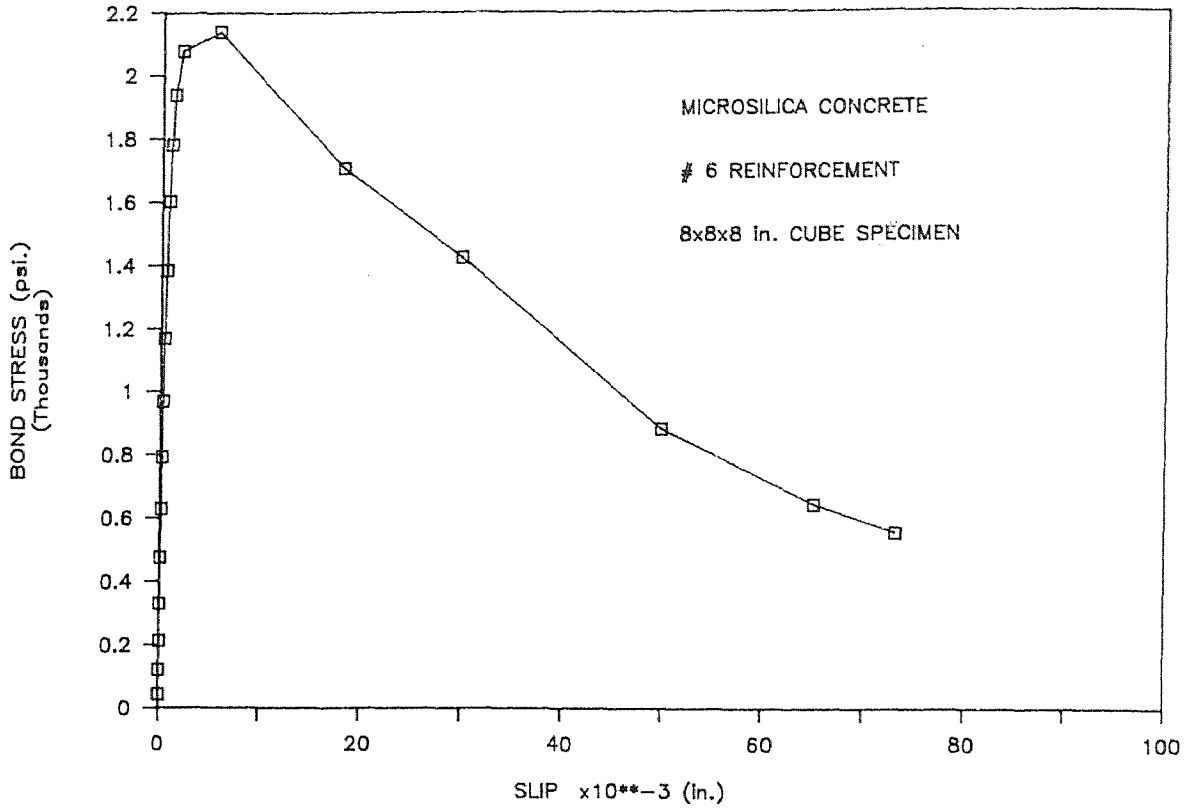
PULL-OUT TEST

REINFORCED HIGH STRENGTH CONCRETE(BS61)



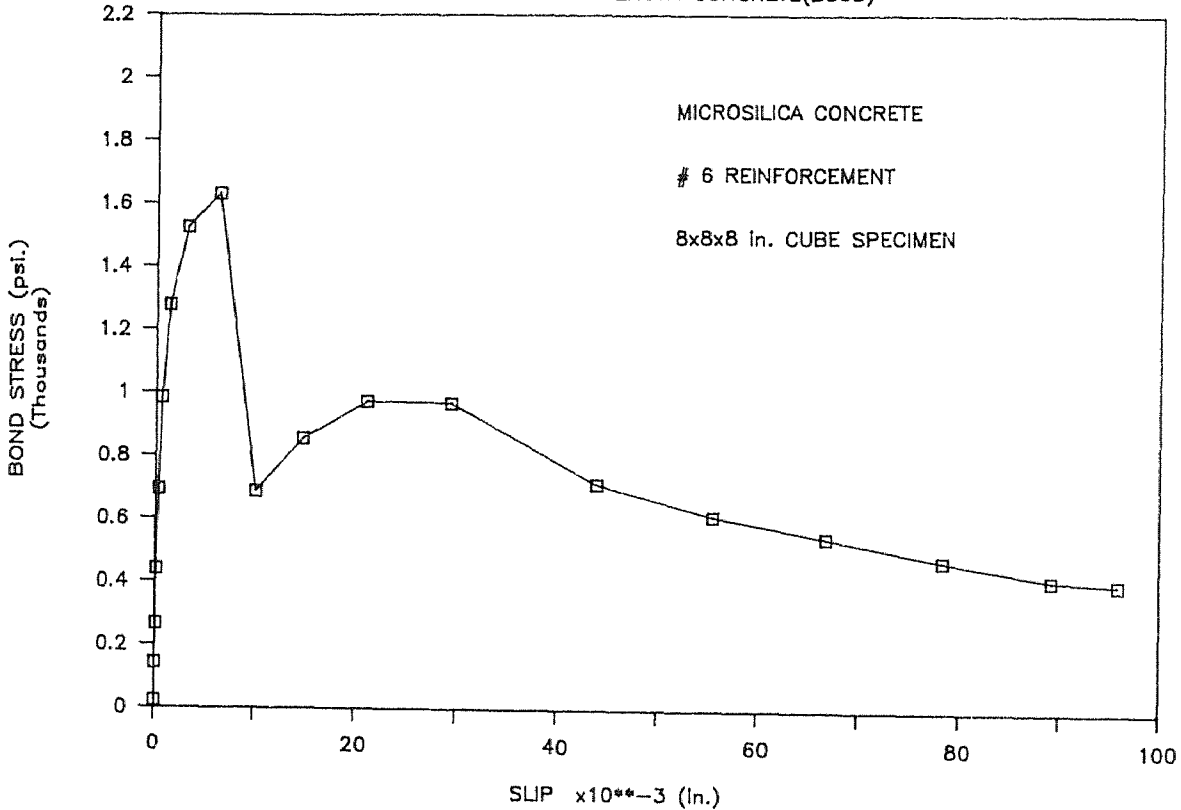
PULL-OUT TEST

REINFORCED HIGH STRENGTH CONCRETE(BS62)



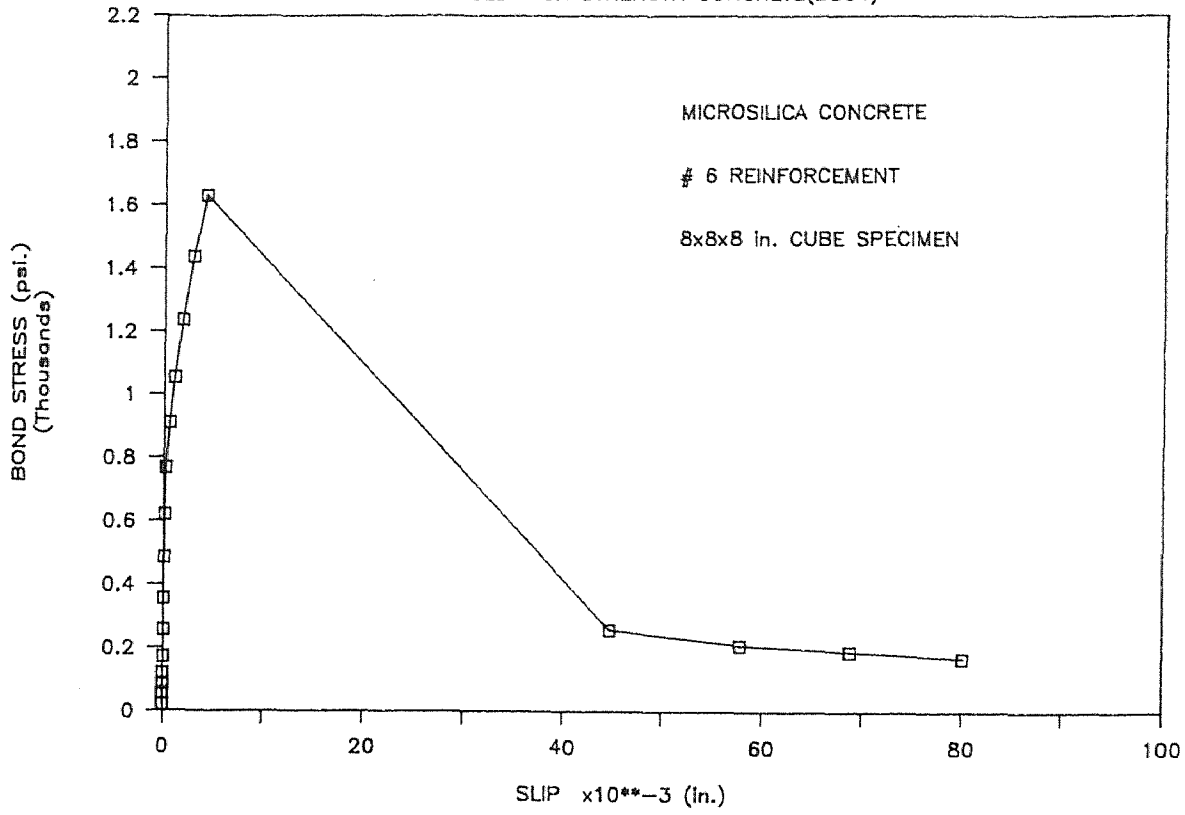
PULL-OUT TEST

REINFORCED HIGH STRENGTH CONCRETE(BS63)



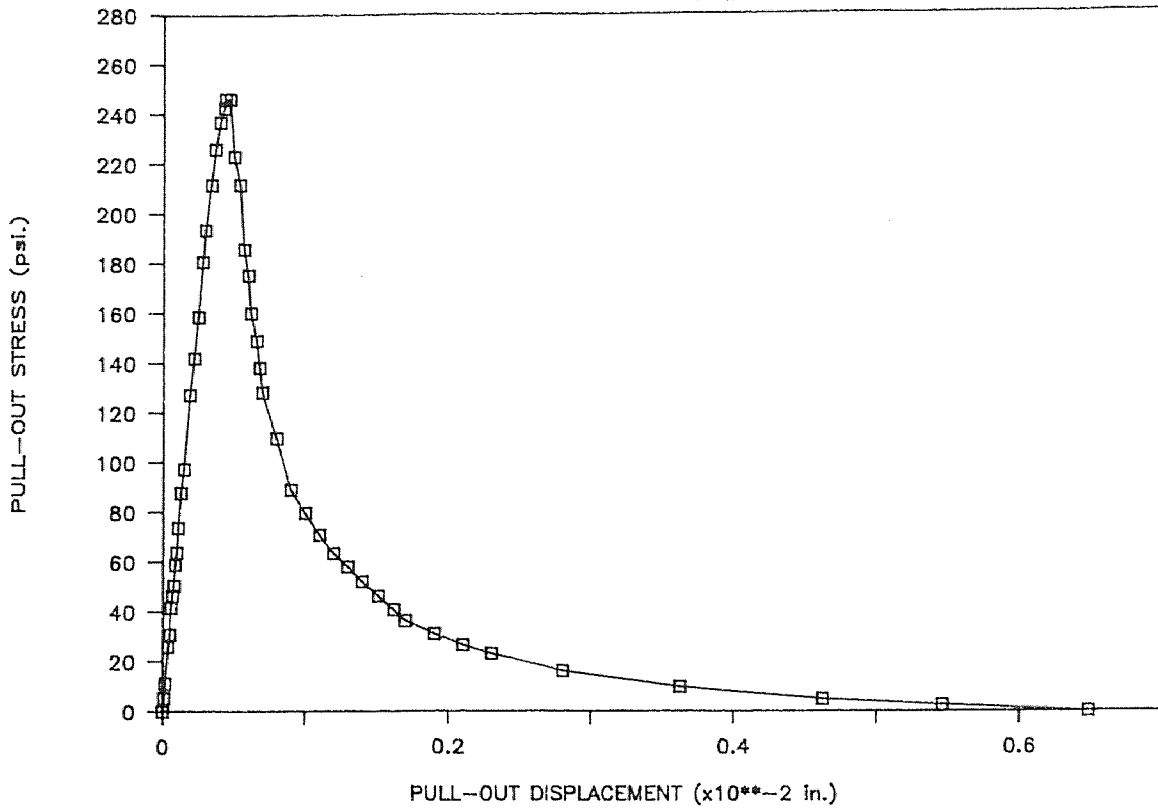
PULL-OUT TEST

REINFORCED HIGH STRENGTH CONCRETE(BS64)

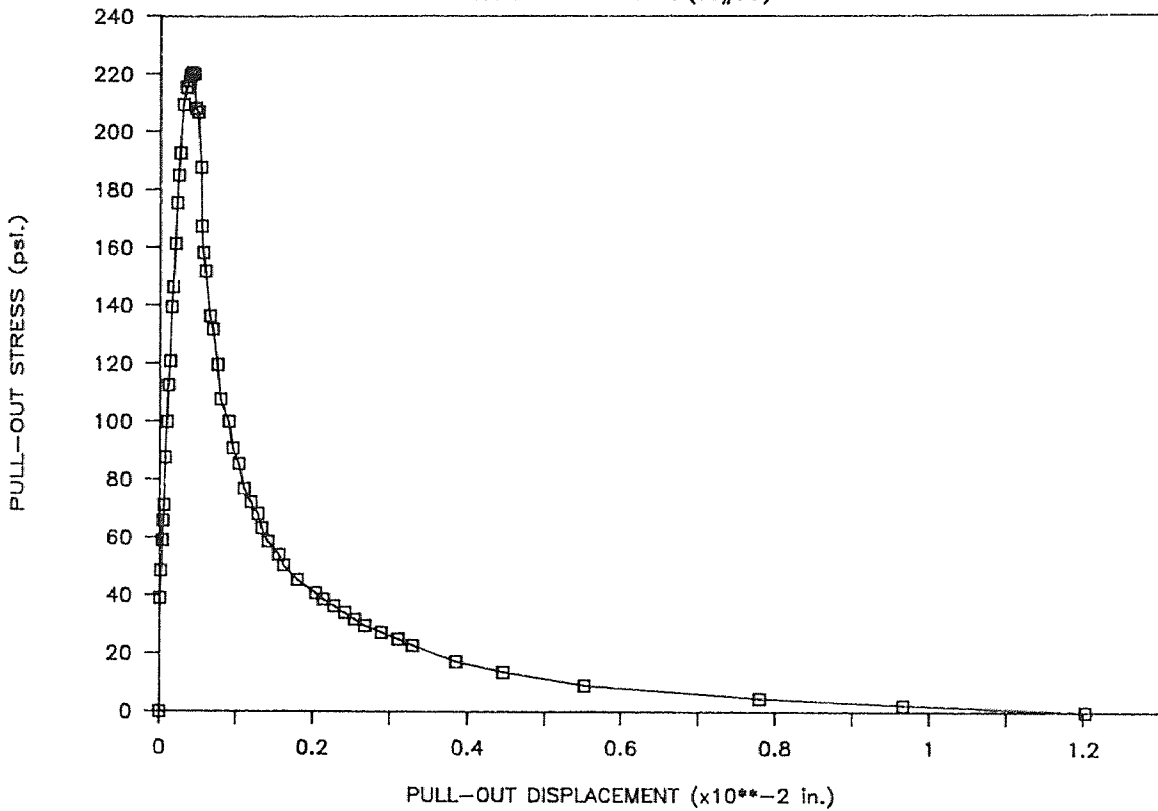


APPENDIX D

PULL-OUT TEST NORMAL CONCRETE (TC#34)

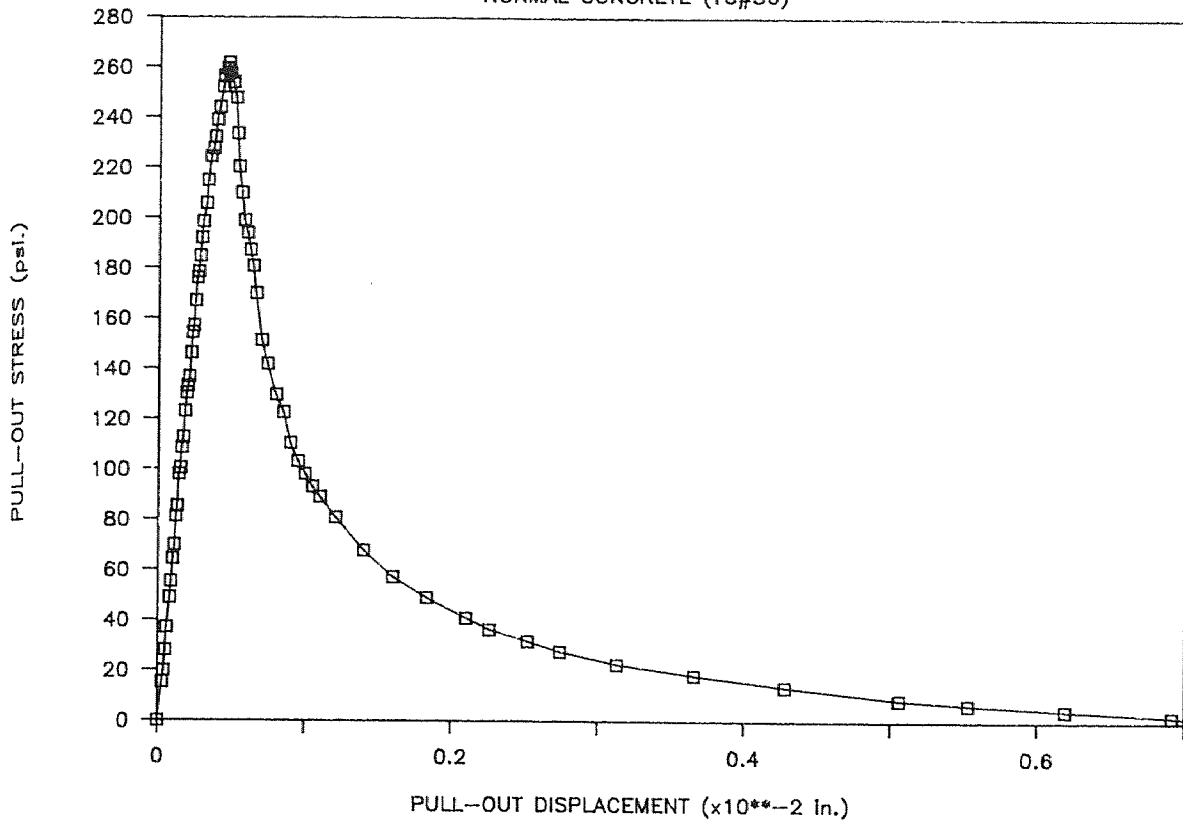


PULL-OUT TEST NORMAL CONCRETE (TC#35)



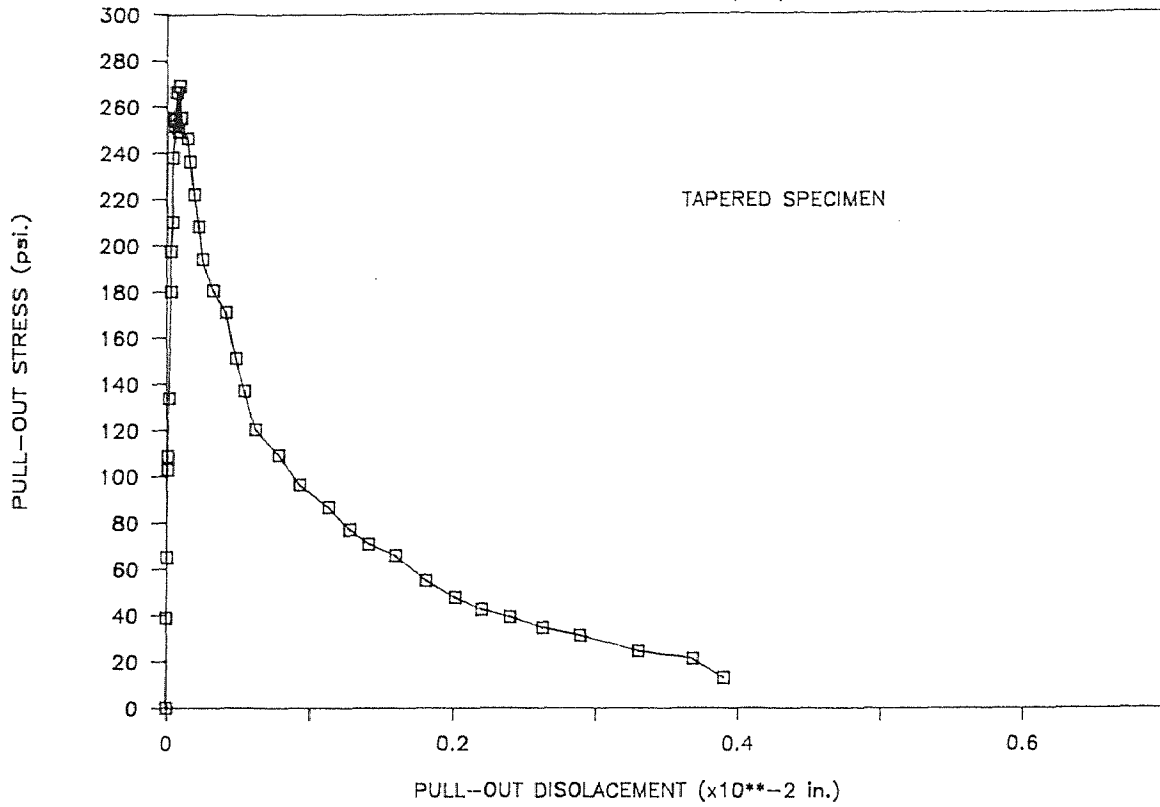
PULL-OUT TEST

NORMAL CONCRETE (TC#36)



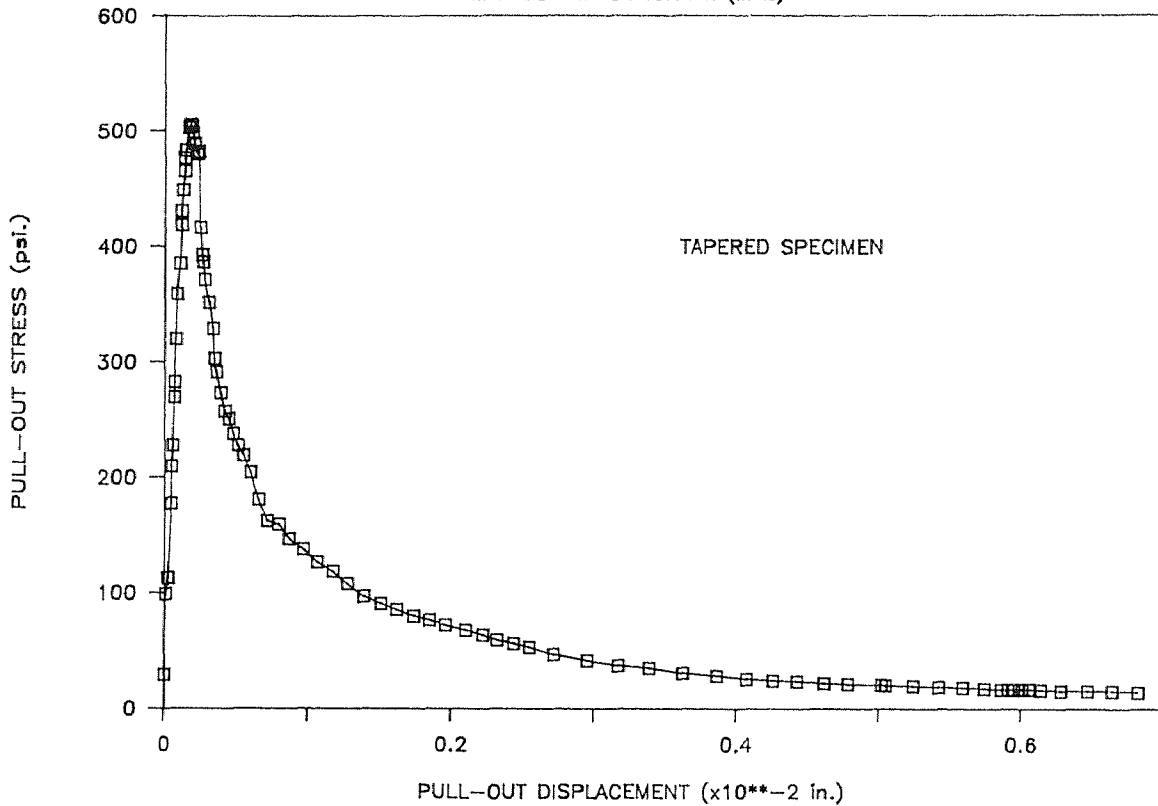
PULL-OUT TEST

MICROSILICA CONCRETE (MT1)



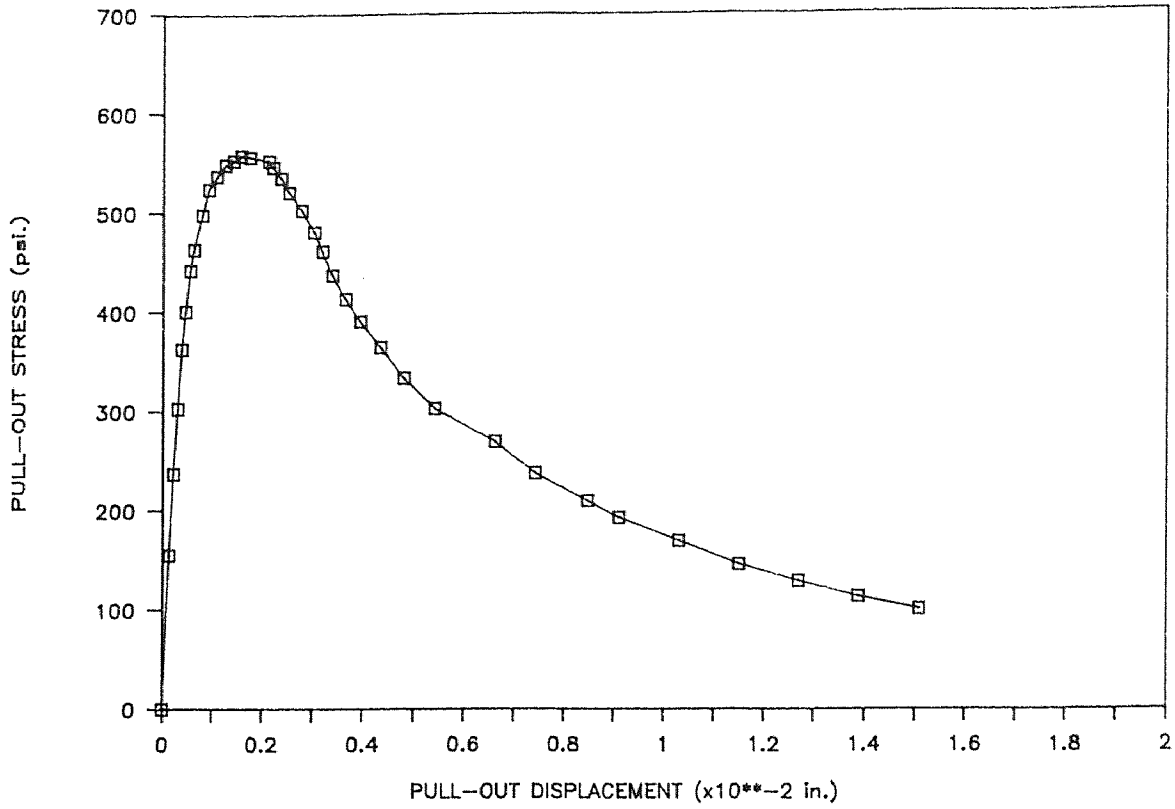
PULL-OUT TEST

MICROSILICA CONCRETE (MT2)



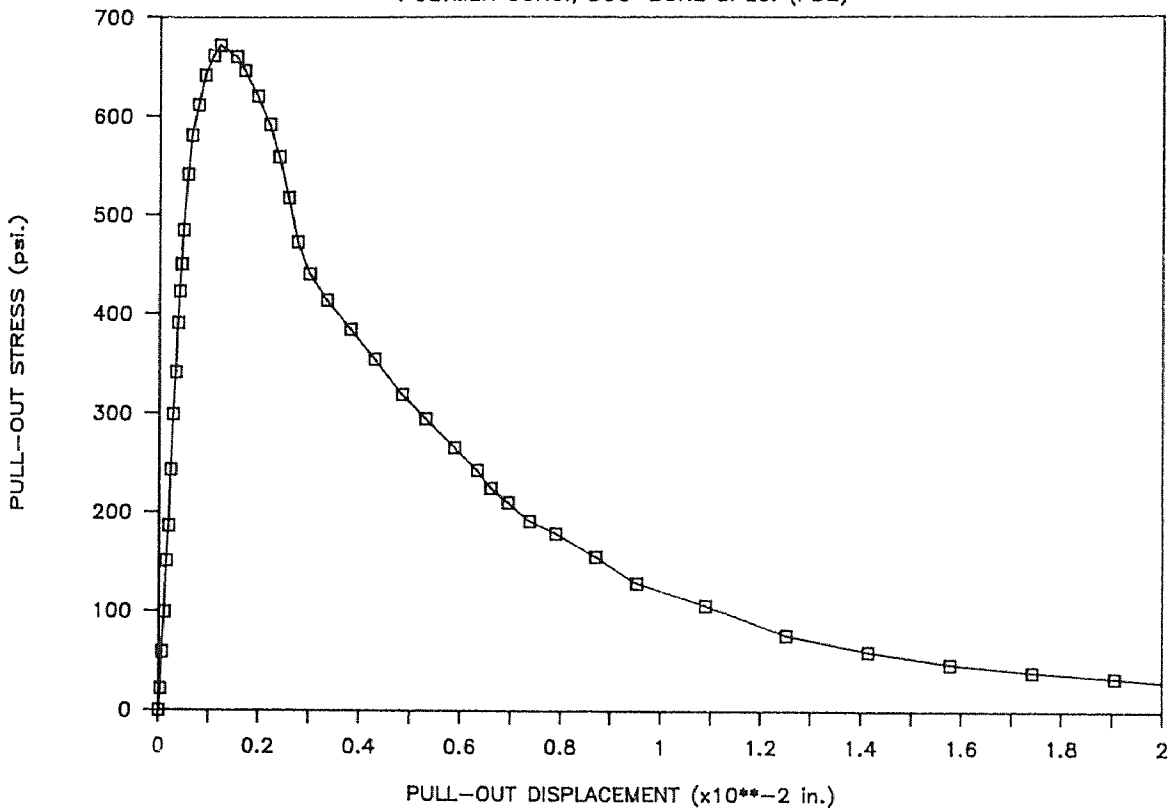
PULL-OUT TEST

POLYMER CONC., DOG-BONE SPEC. (PD1)



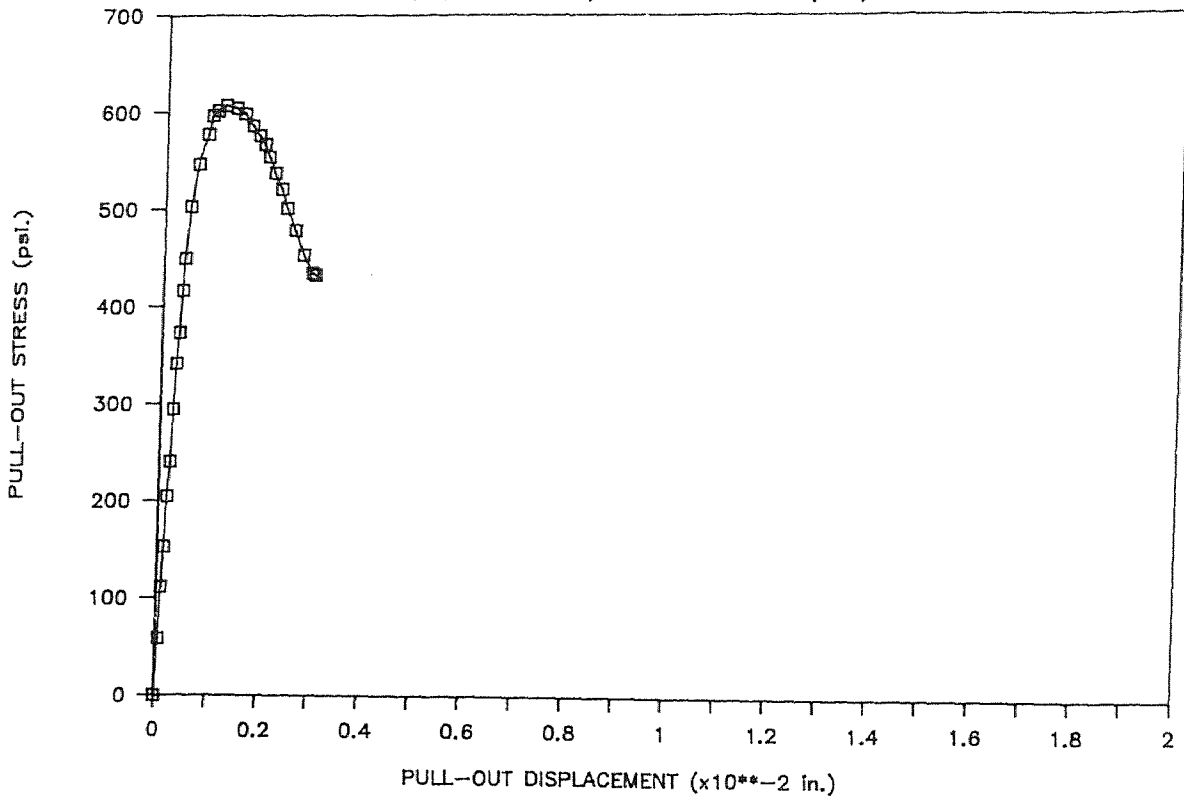
PULL-OUT TEST

POLYMER CONC., DOG-BONE SPEC. (PD2)



PULL-OUT TEST

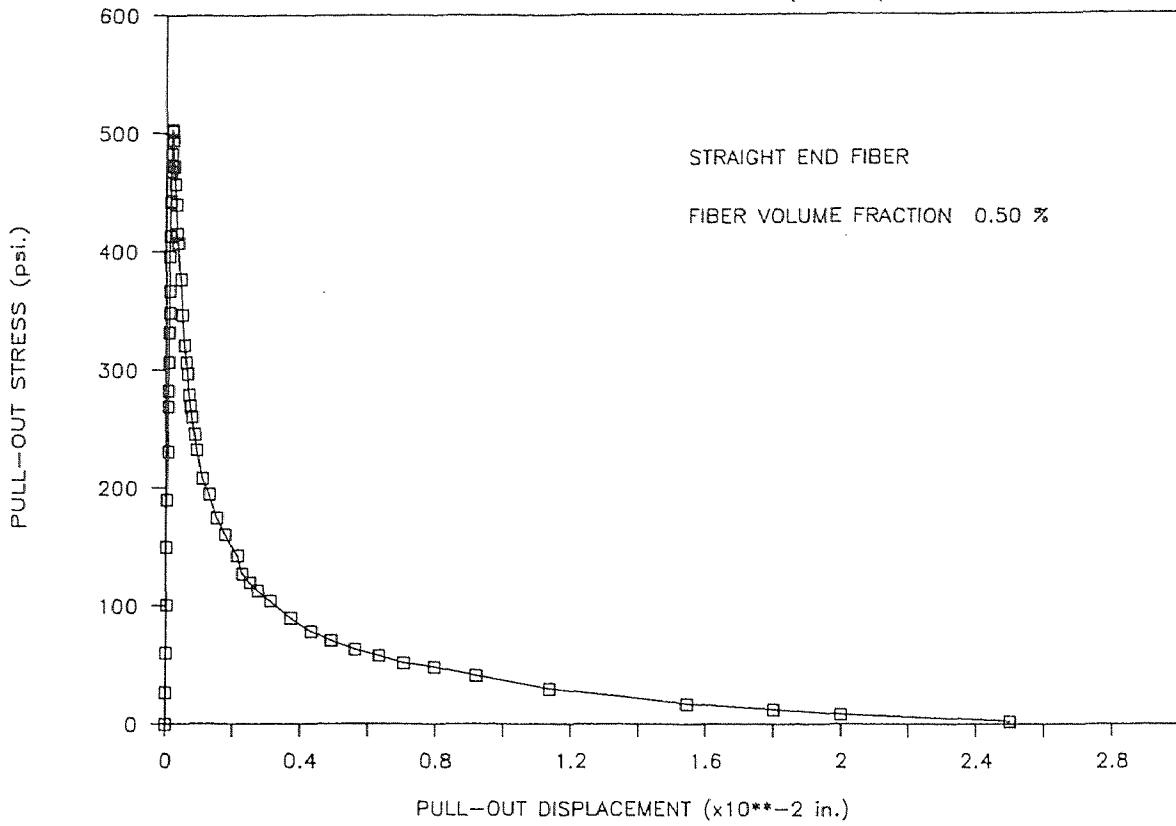
POLYMER CONC., DOG-BONE SPEC. (PD3)



APPENDIX E

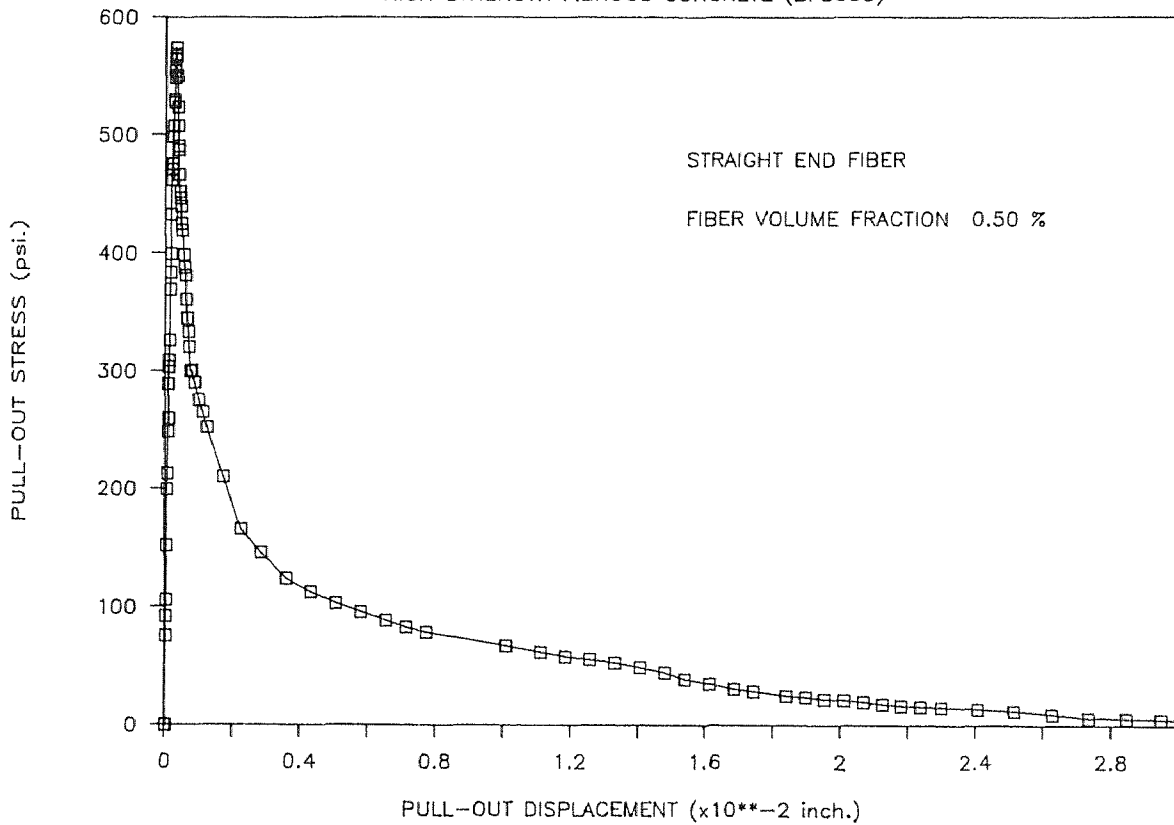
PULL-OUT TEST

HIGH STRENGTH FIBROUS CONCRETE (BFS054)



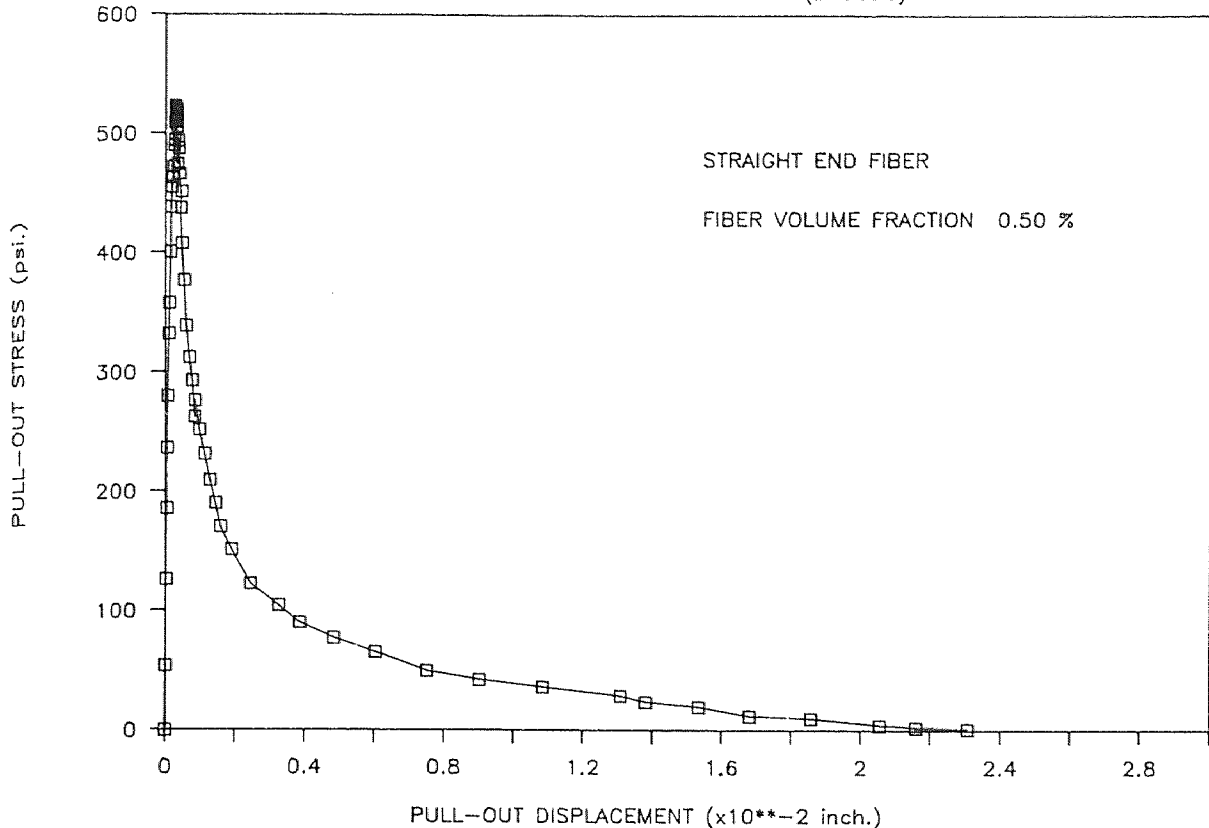
PULL-OUT TEST

HIGH STRENGTH FIBROUS CONCRETE (BFS055)



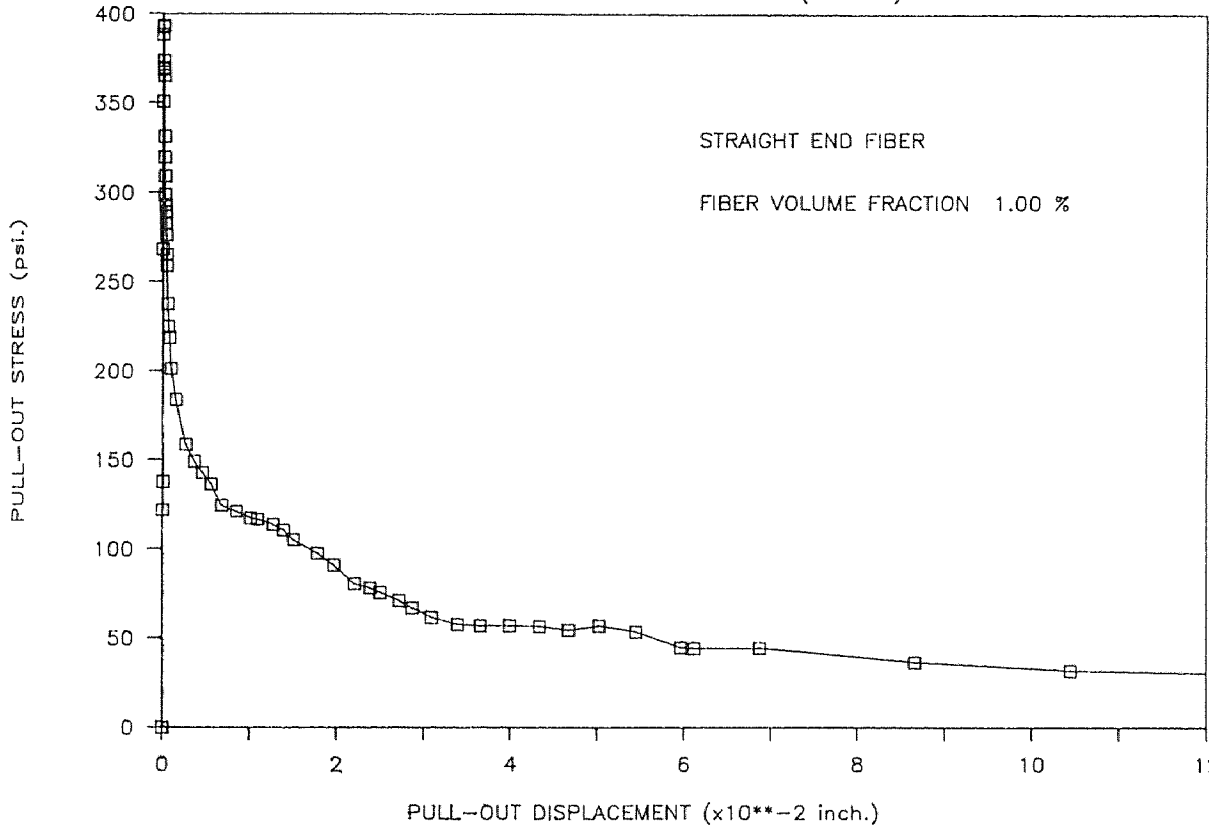
PULL-OUT TEST

HIGH STRENGTH FIBROUS CONCRETE (BFS056)



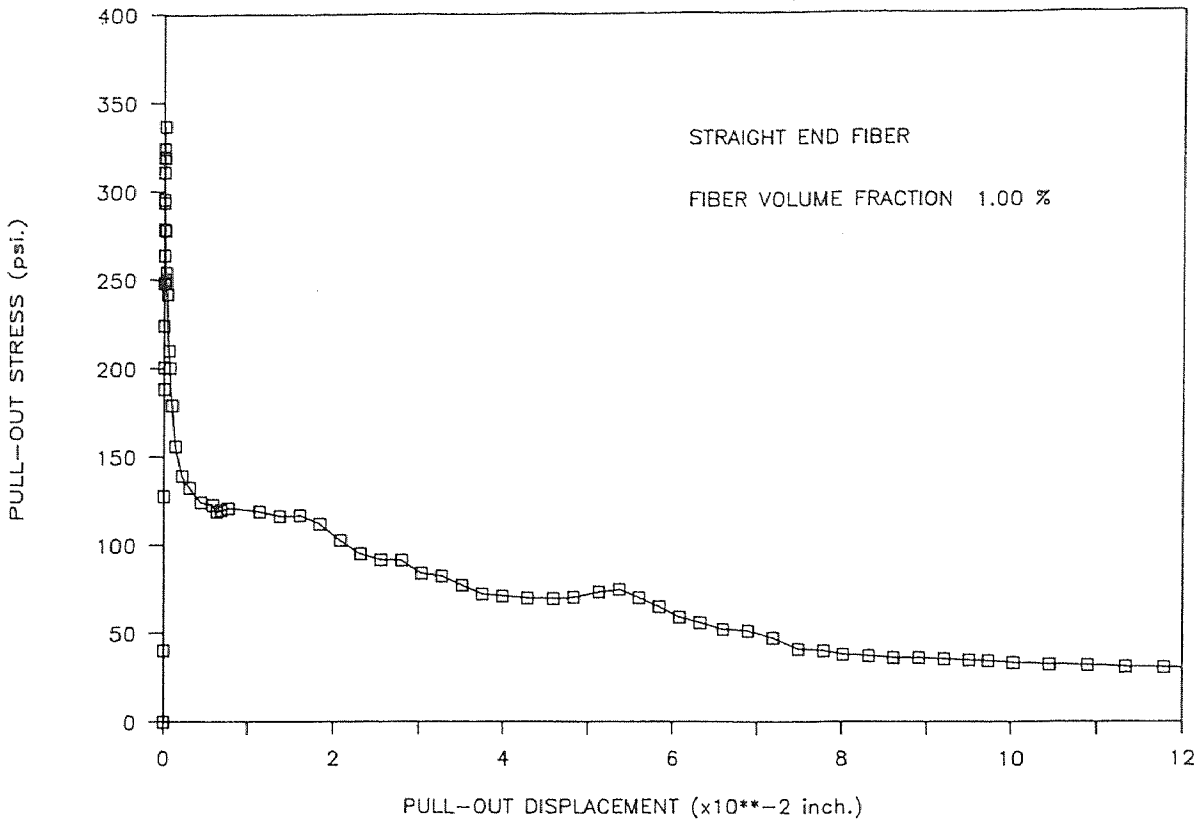
PULL-OUT TEST

HIGH STRENGTH FIBROUS CONCRETE (BFS101)



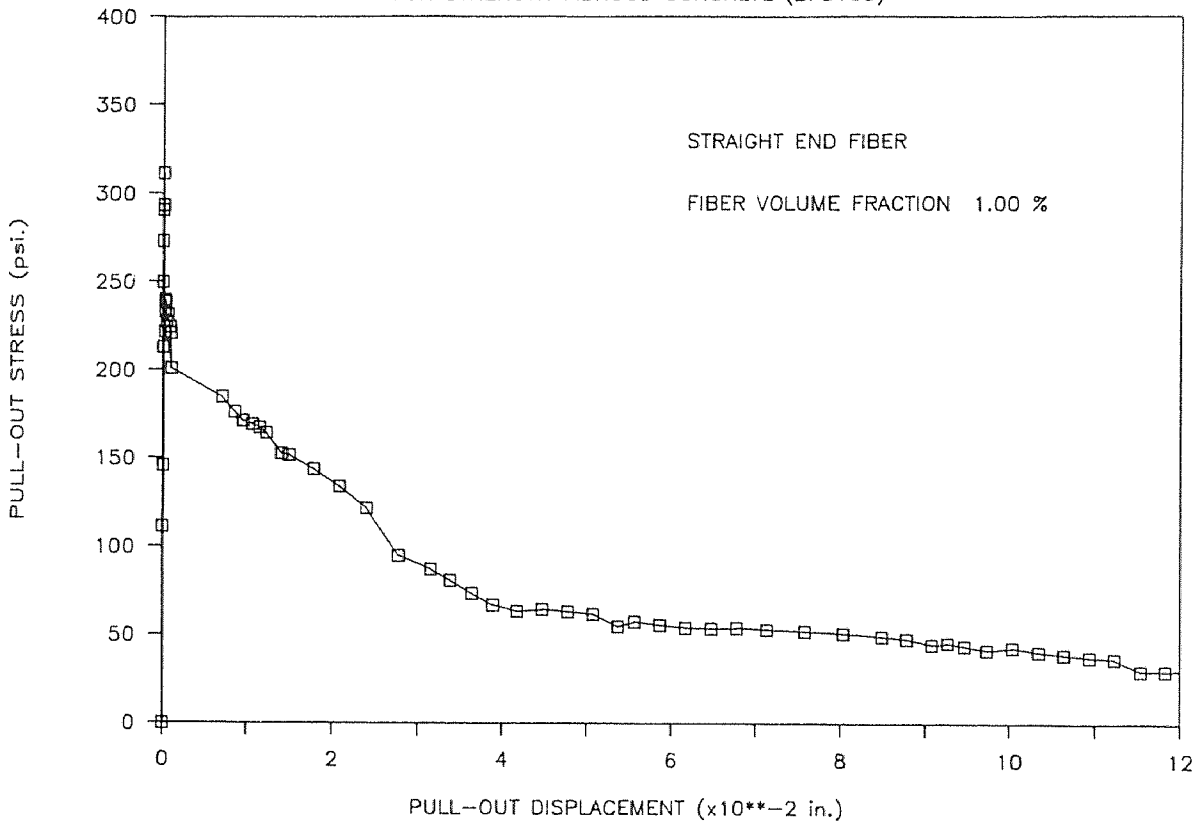
PULL-OUT TEST

HIGH STRENGTH FIBROUS CONCRETE (BFS102)



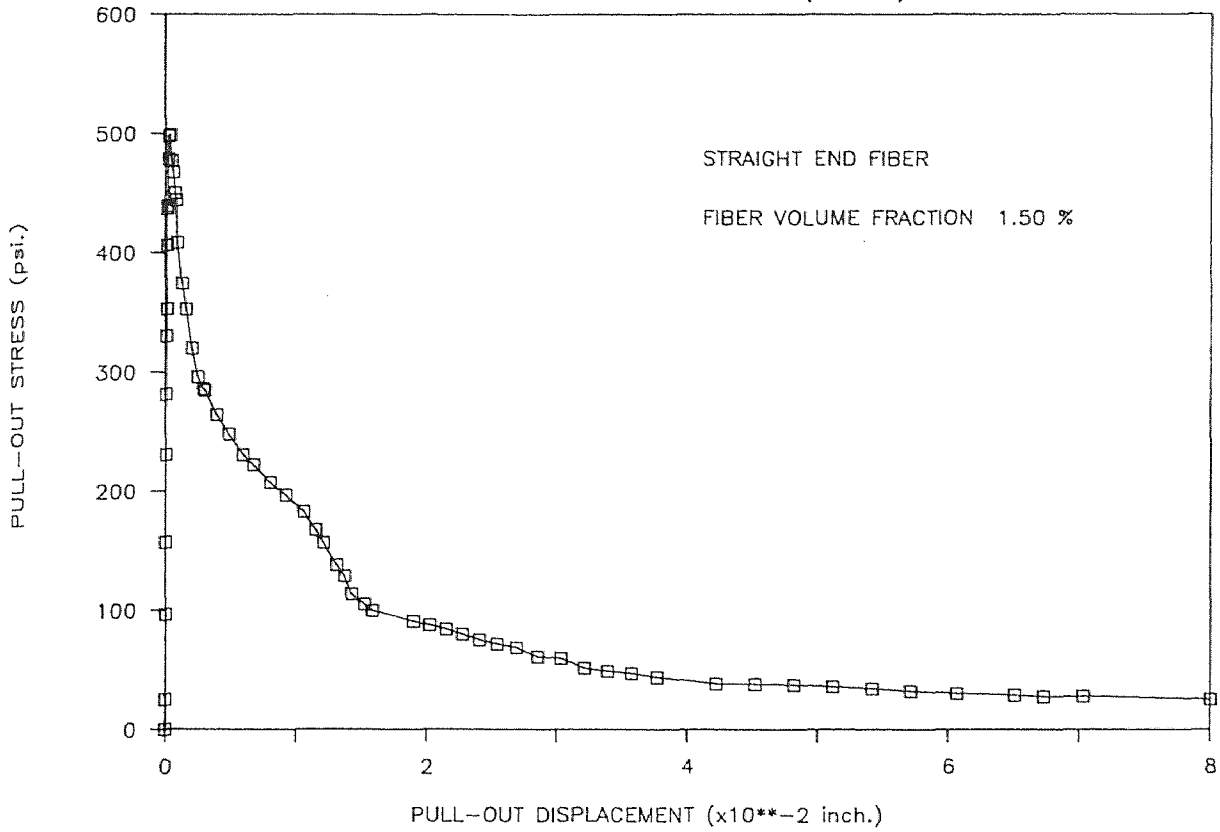
PULL-OUT TEST

HIGH STRENGTH FIBROUS CONCRETE (BFS103)



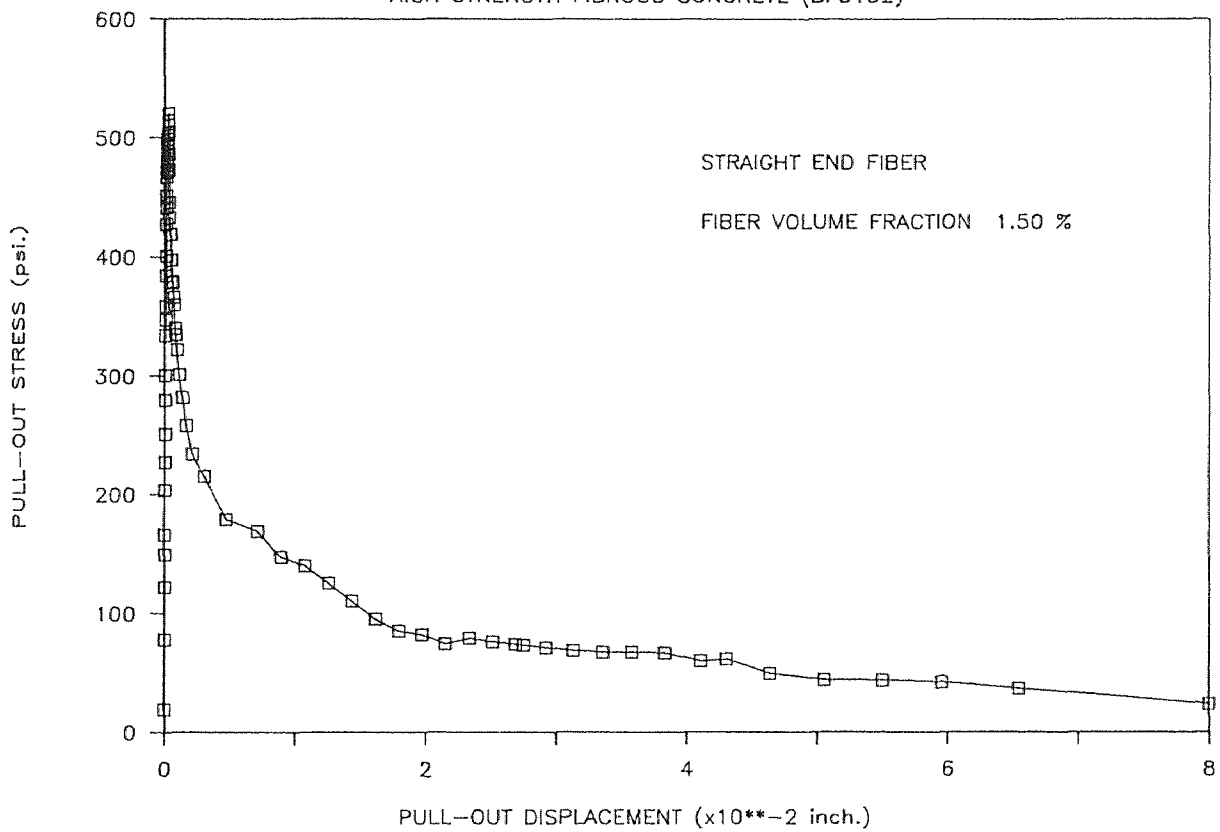
PULL-OUT TEST

HIGH STRENGTH FIBROUS CONCRETE (BFS151)



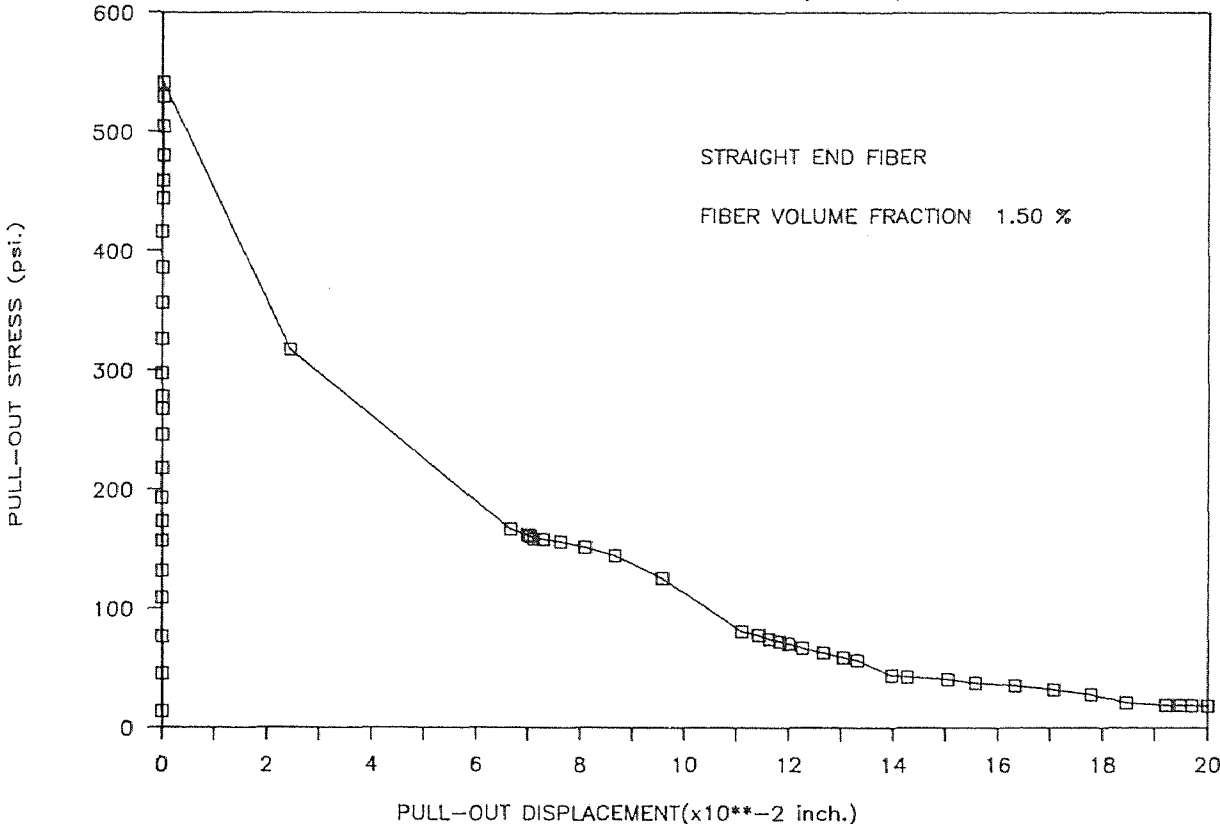
PULL-OUT TEST

HIGH STRENGTH FIBROUS CONCRETE (BFS152)



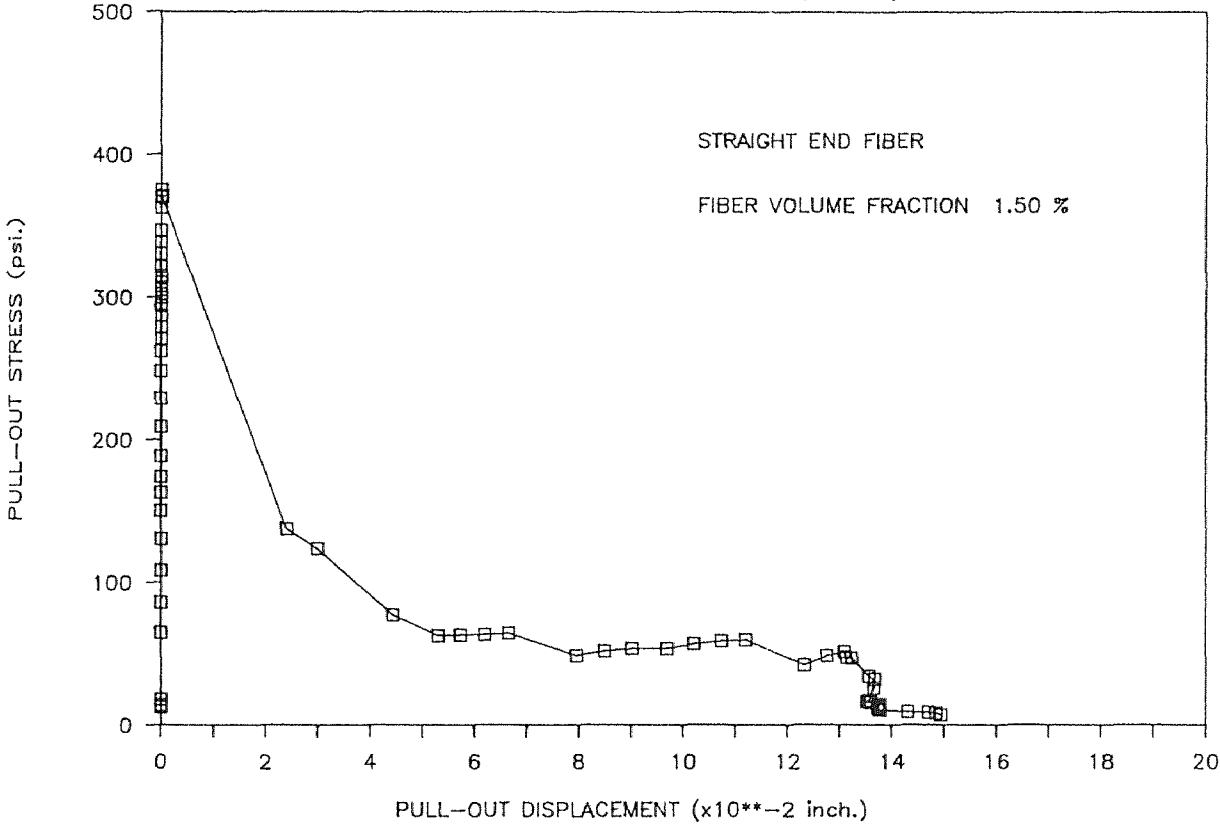
PULL-OUT TEST

HIGH STRENGTH FIBROUS CONCRETE (BFS153)



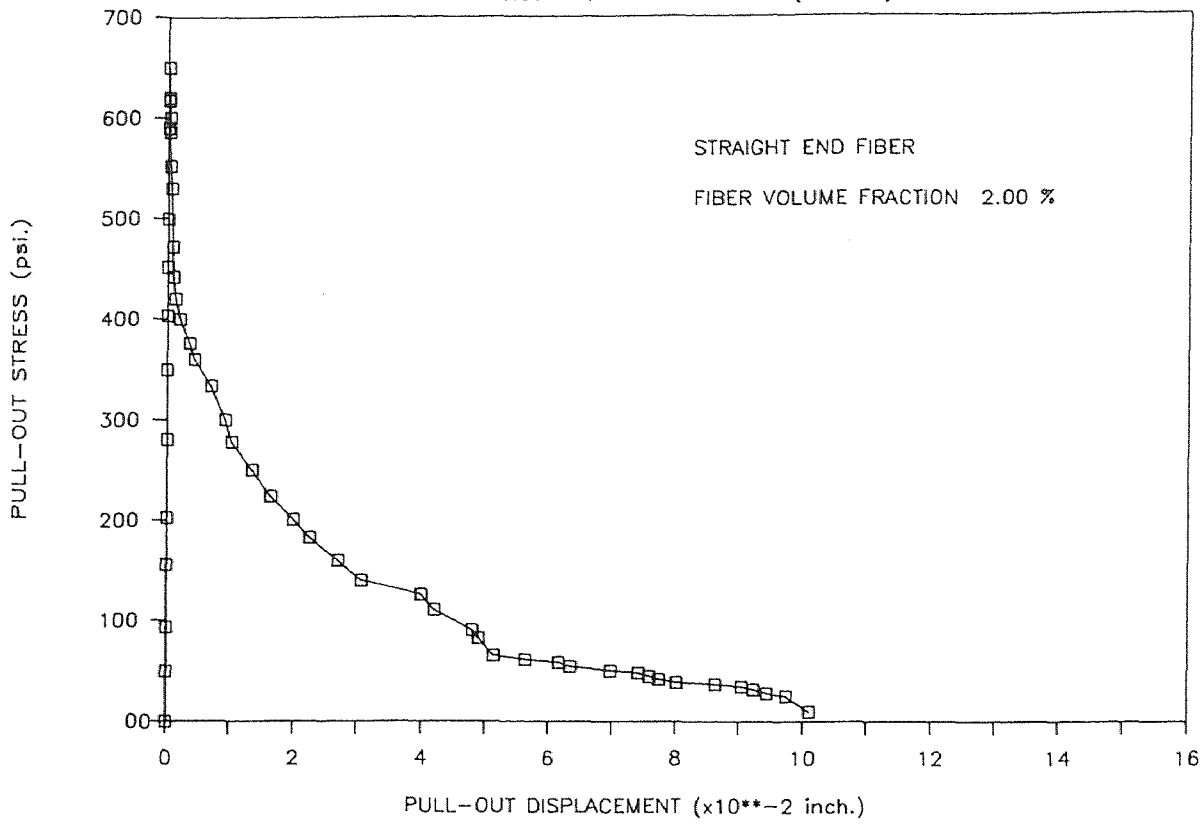
PULL-OUT TEST

HIGH STRENGTH FIBROUS CONCRETE (BFS154)



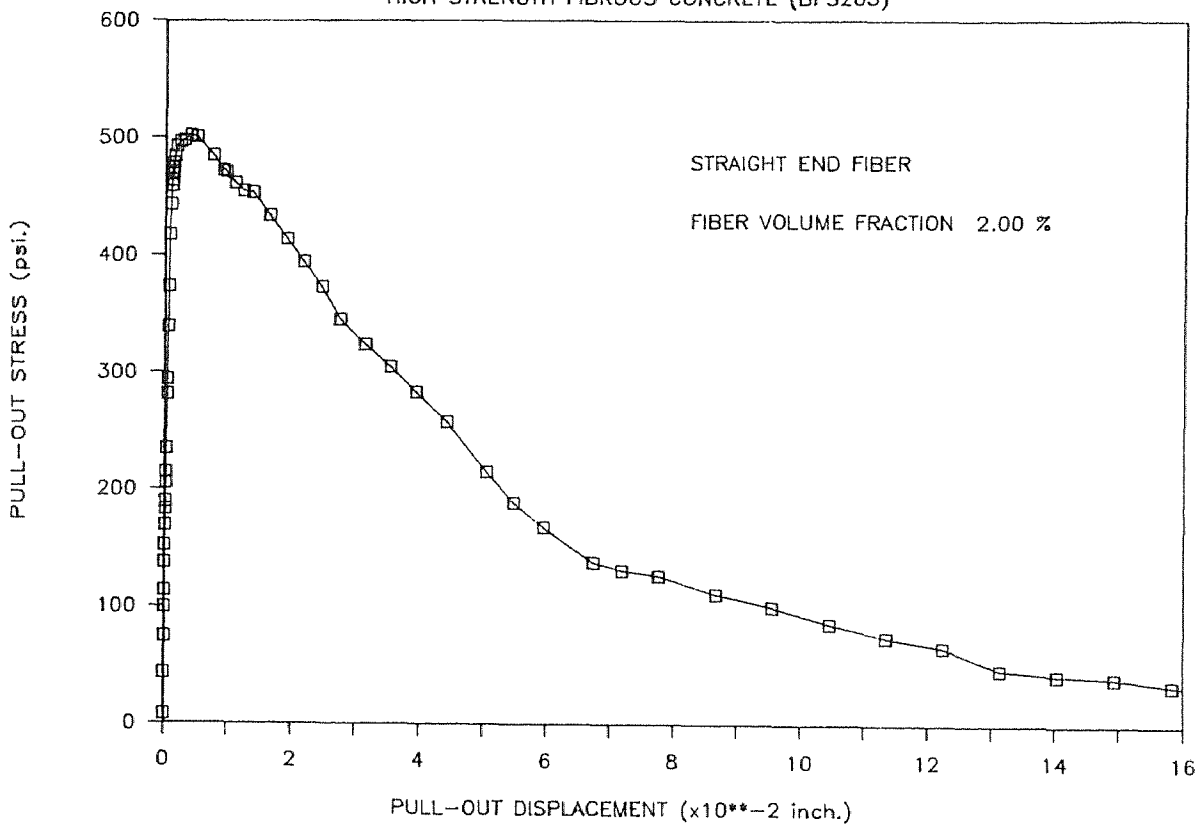
PULL-OUT STRESS

HIGH STRENGTH FIBROUS CONCRETE (BFS202)



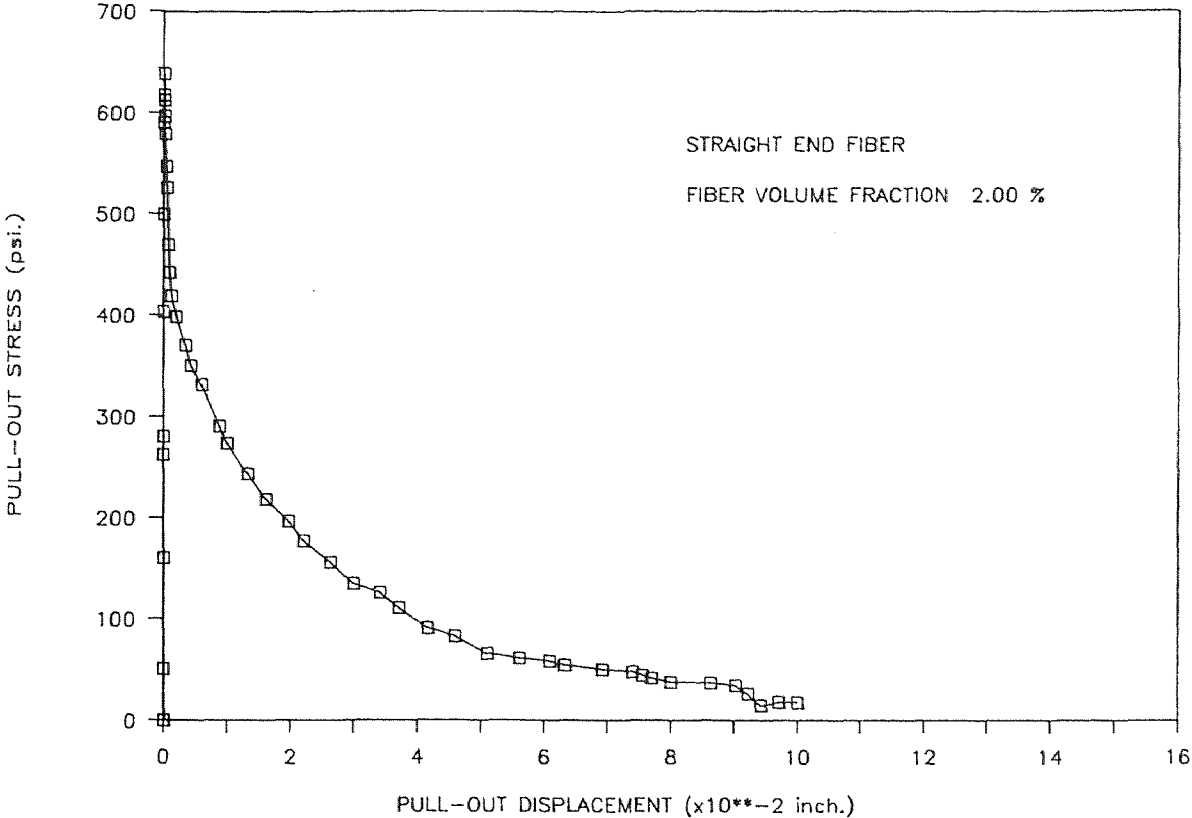
PULL-OUT TEST

HIGH STRENGTH FIBROUS CONCRETE (BFS203)



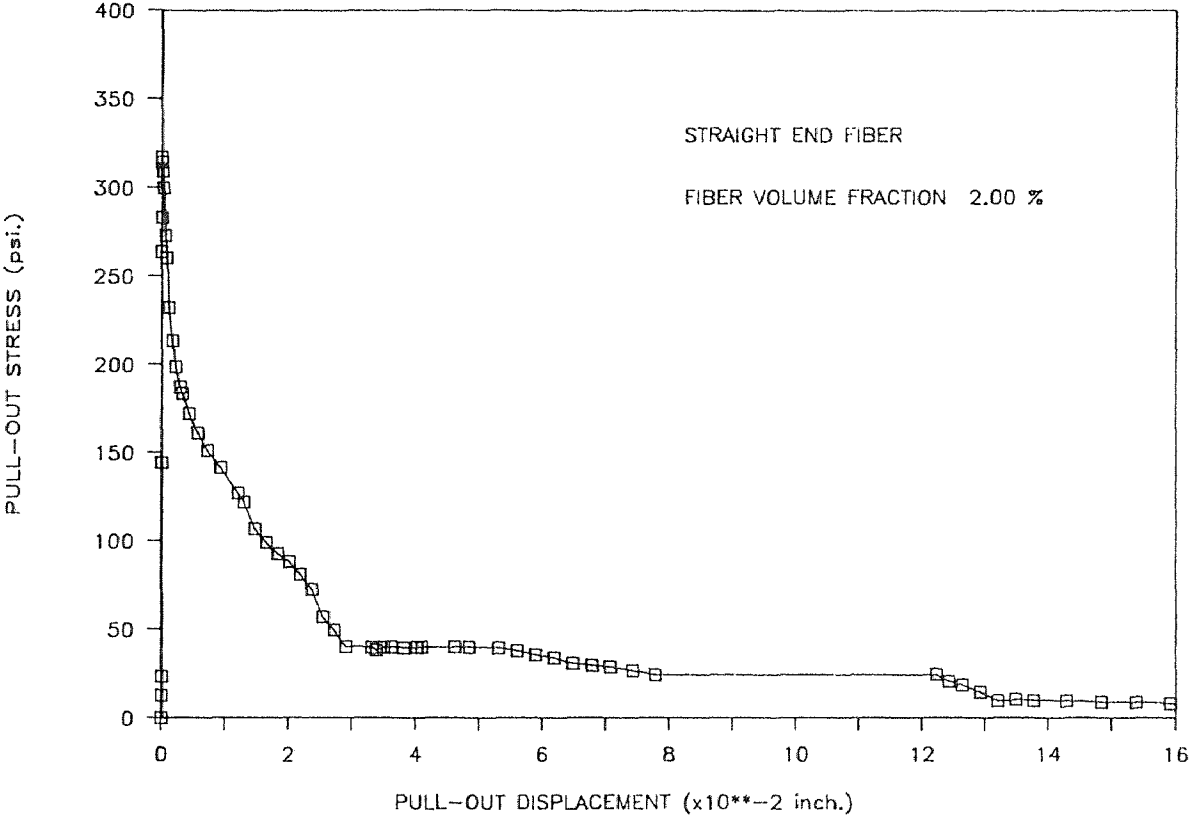
PULL-OUT TEST

HIGH STRENGTH FIBROUS CONCRETE (BFS205)



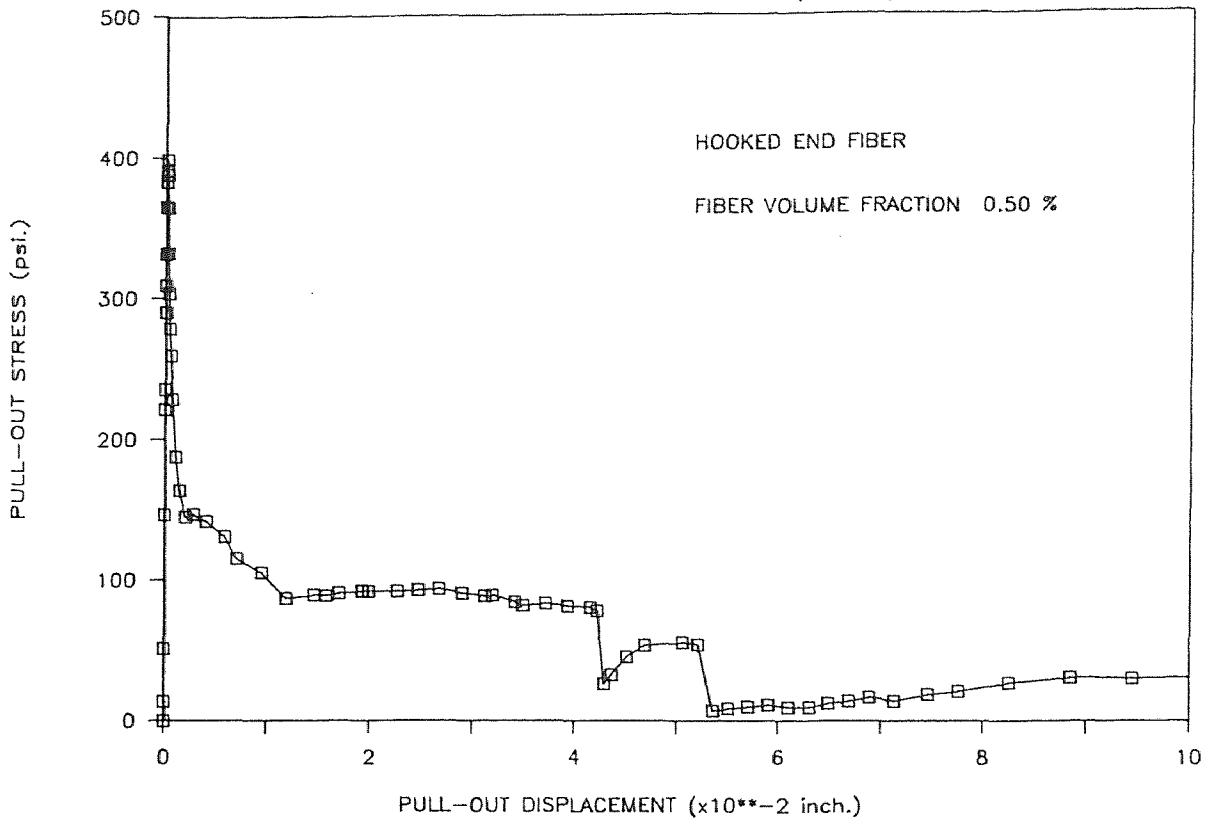
PULL-OUT TEST

HIGH STRENGTH FIBROUS CONCRETE (BFS206)



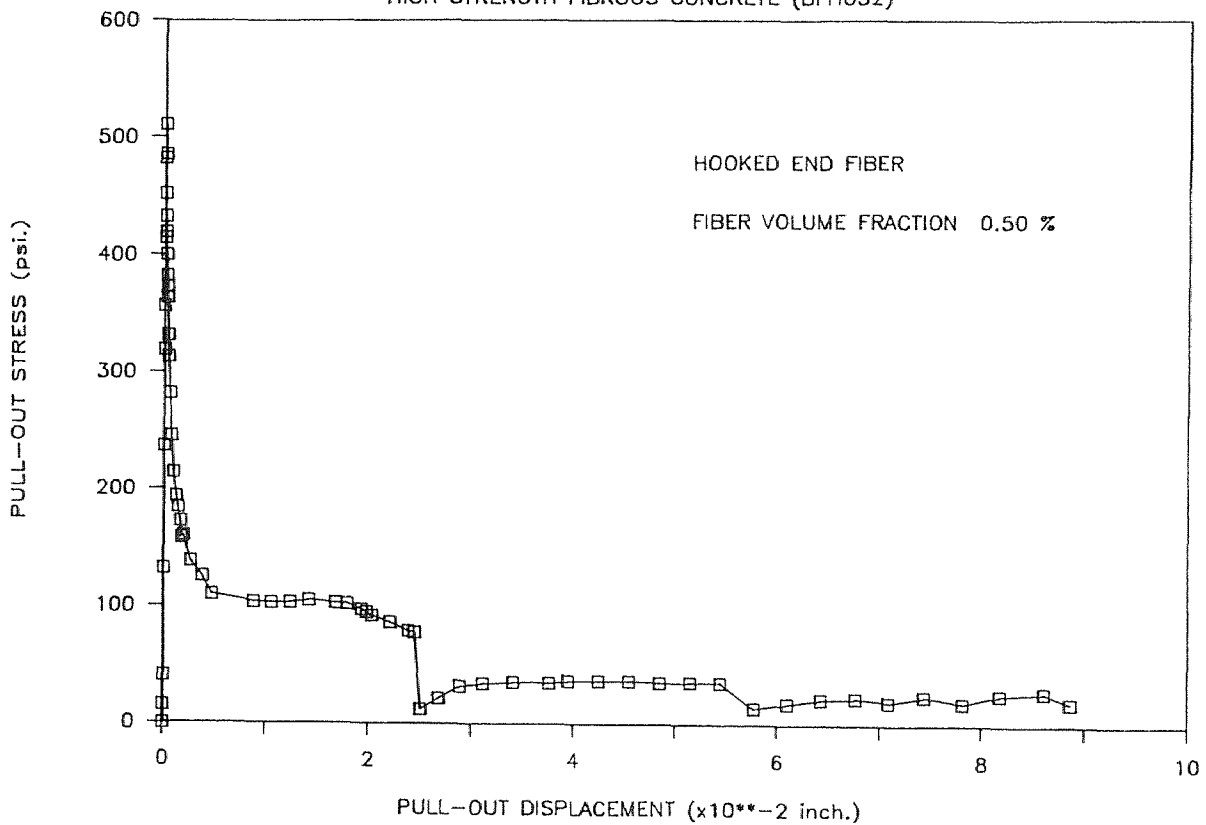
PULL-OUT TEST

HIGH STRENGTH FIBROUS CONCRETE (BFH051)



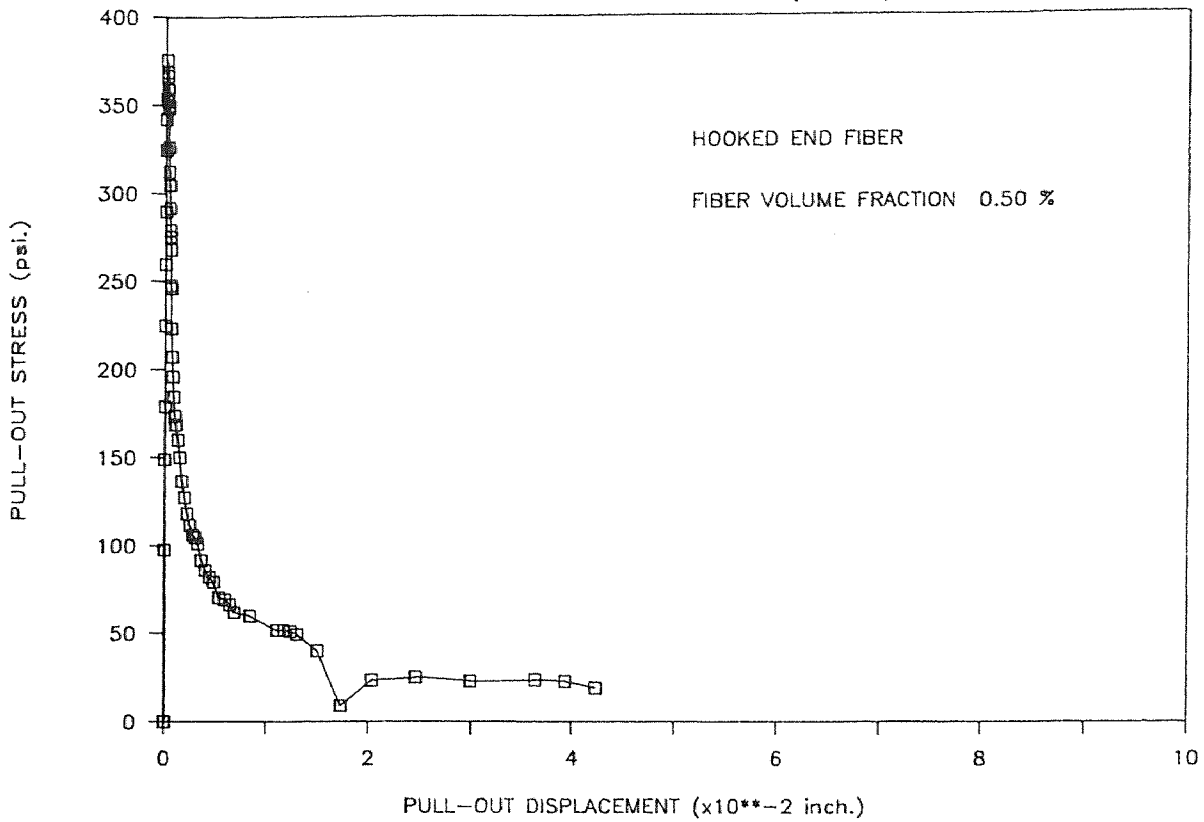
PULL-OUT TEST

HIGH STRENGTH FIBROUS CONCRETE (BFH052)



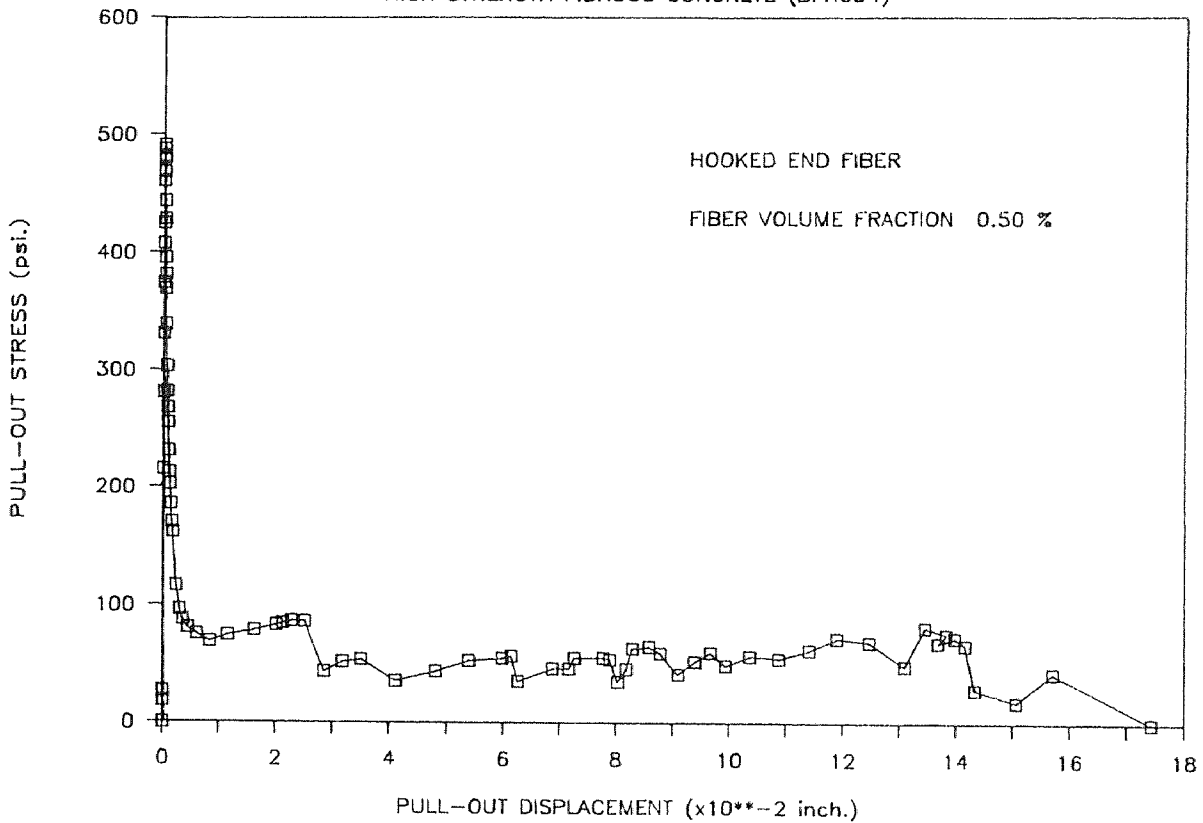
PULL-OUT TEST

HIGH STRENGTH FIBROUS CONCRETE (BFH053)



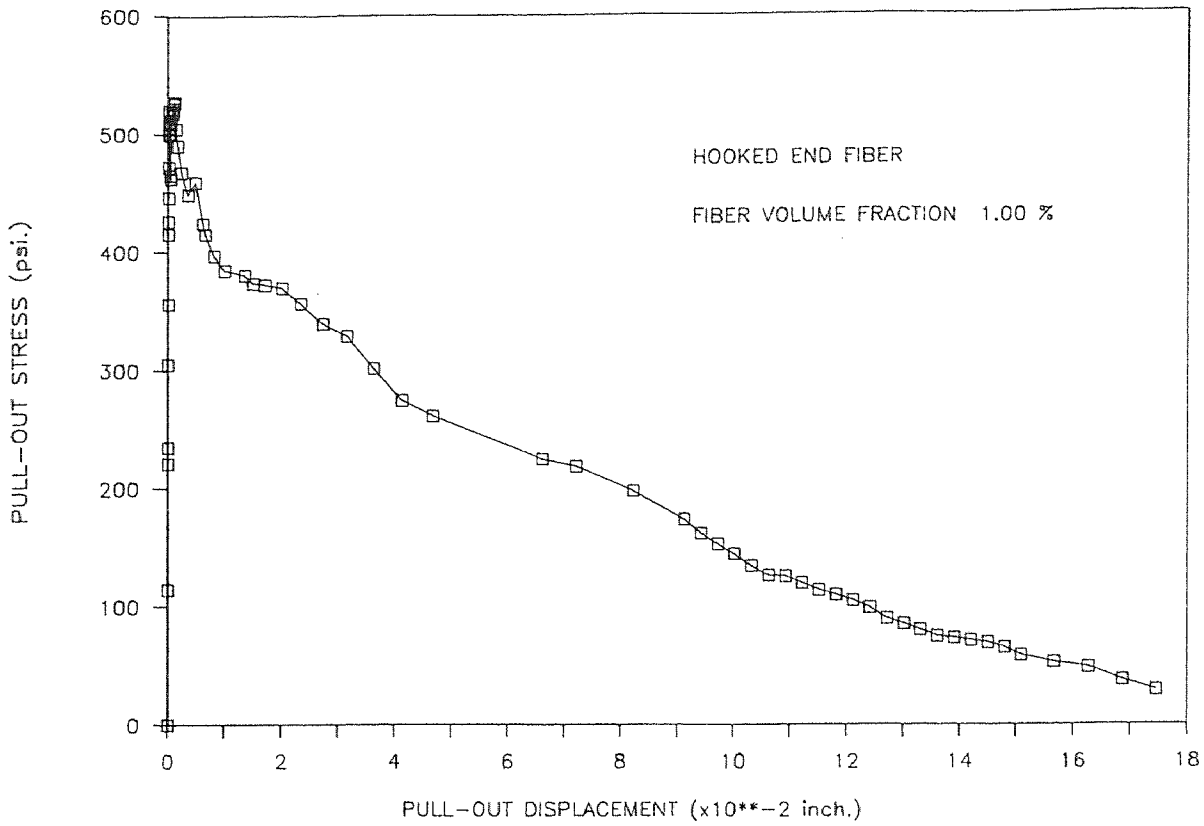
PULL-OUT TEST

HIGH STRENGTH FIBROUS CONCRETE (BFH054)



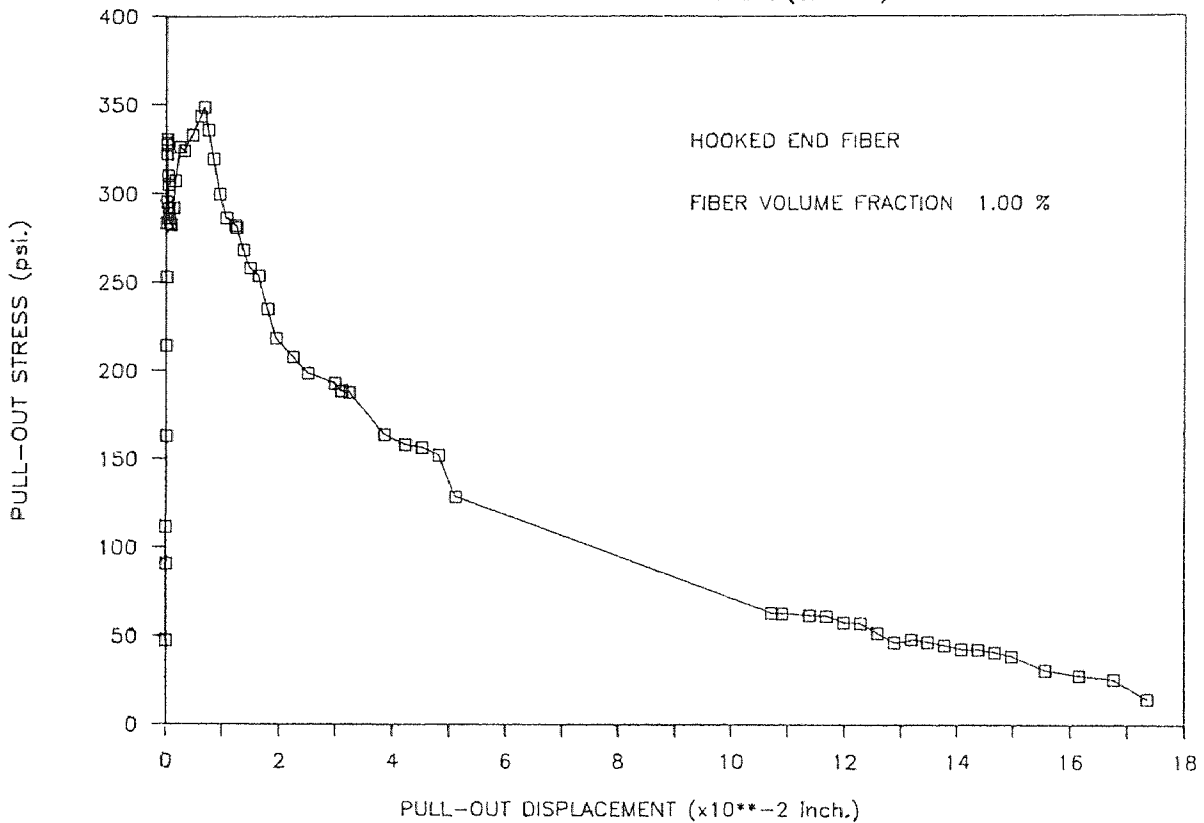
PULL-OUT TEST

HIGH STRENGTH FIBROUS CONCRETE (BFH102)



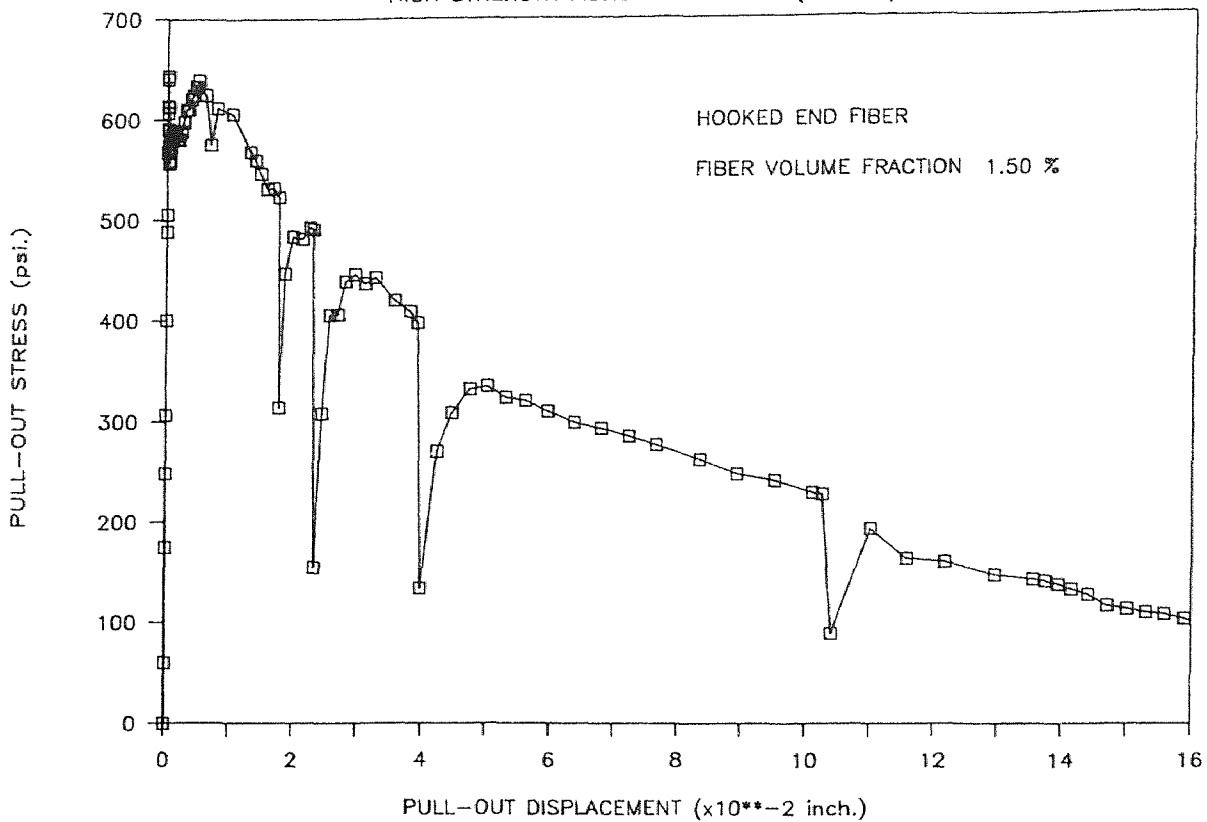
PULL-OUT TEST

HIGH STRENGTH FIBROUS CONCRETE (BFH104)



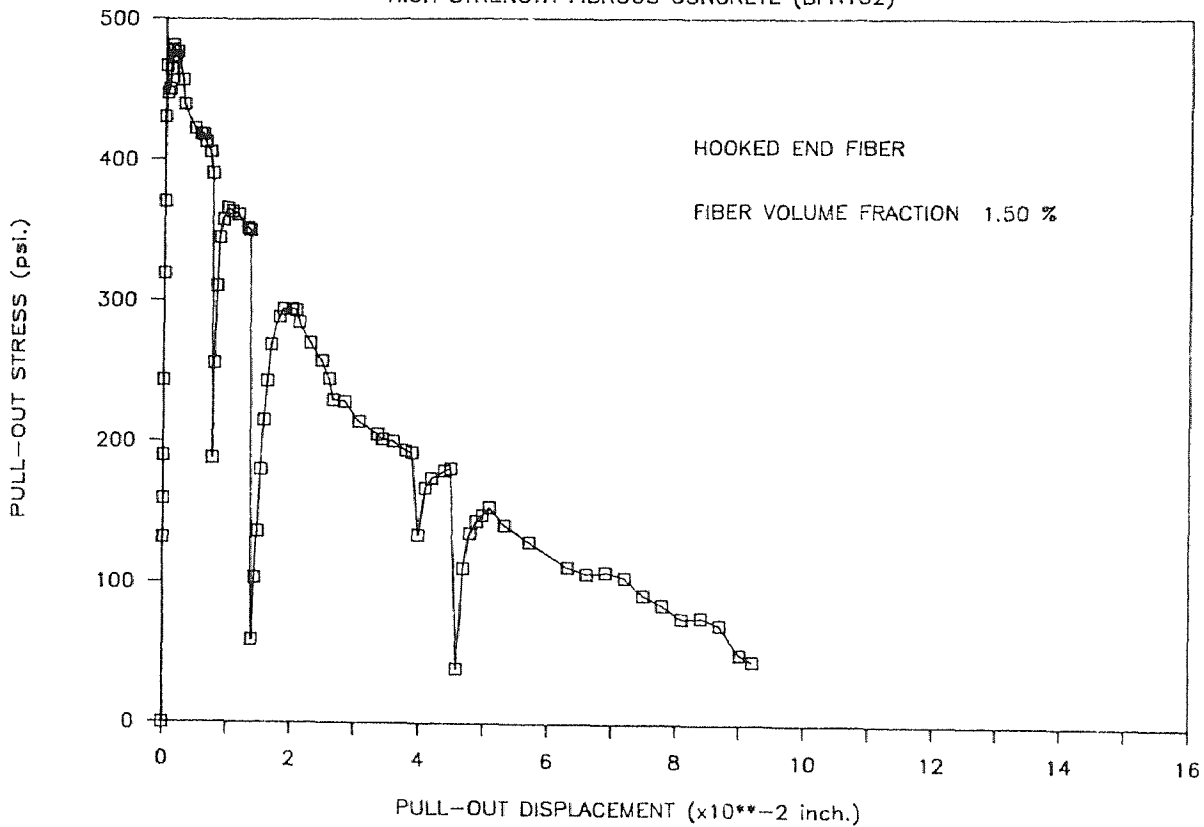
PULL-OUT TEST

HIGH STRENGTH FIBROUS CONCRETE (BFH151)

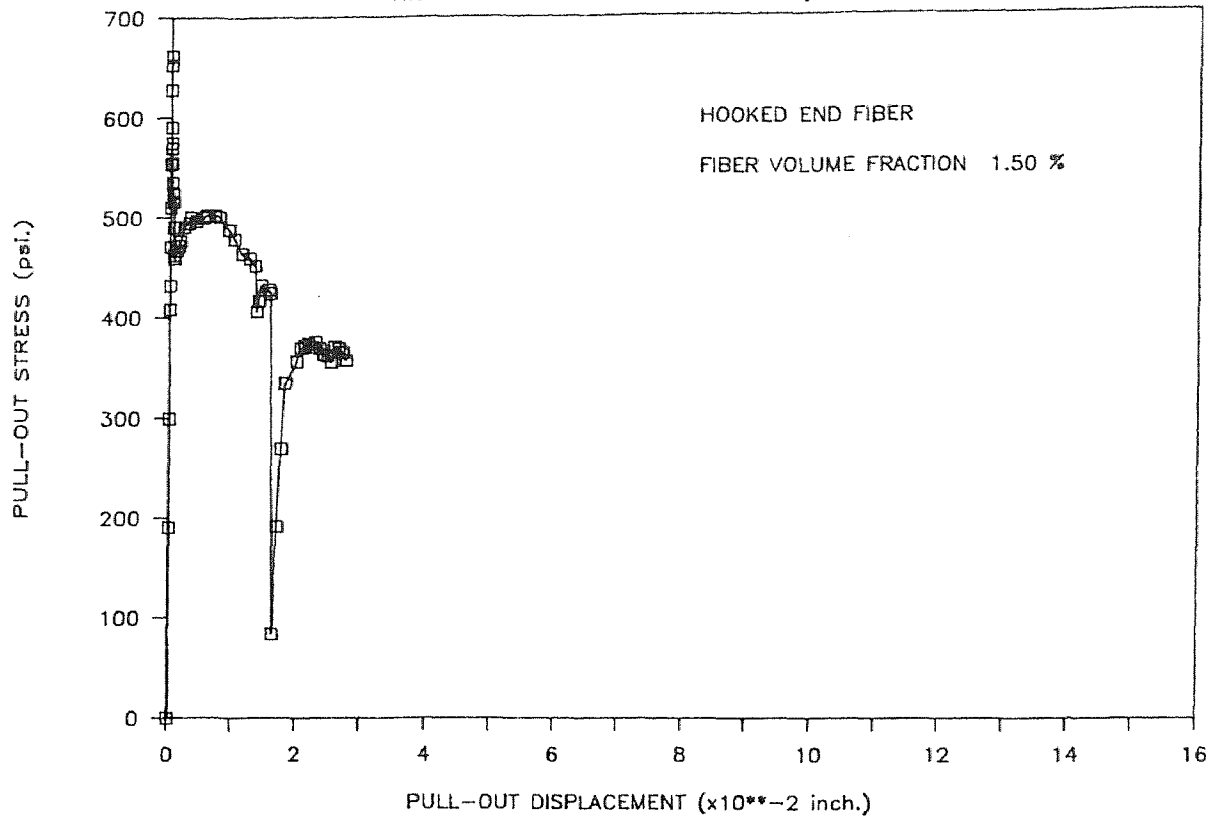


PULL-OUT TEST

HIGH STRENGTH FIBROUS CONCRETE (BFH152)

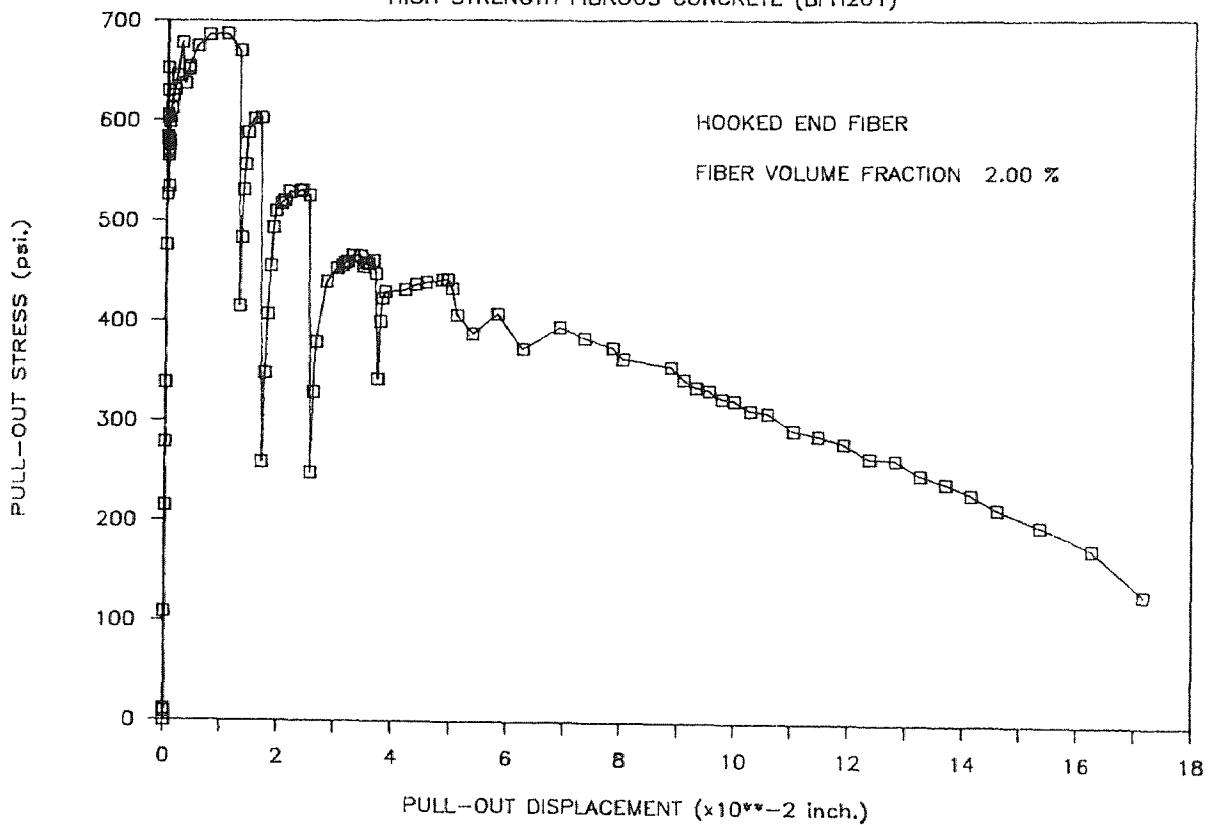


PULL-OUT TEST HIGH STRENGTH FIBROUS CONCRETE (BFH153)



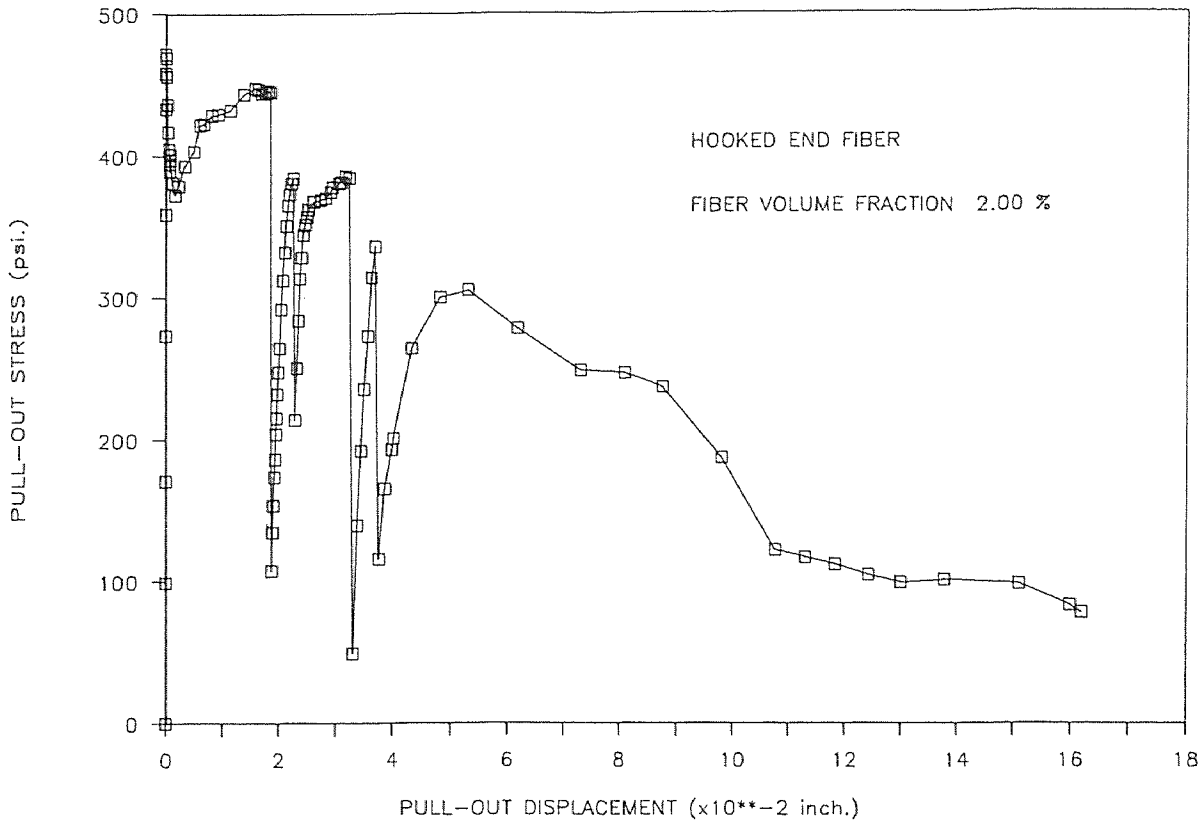
PULL-OUT TEST

HIGH STRENGTH FIBROUS CONCRETE (BFH201)



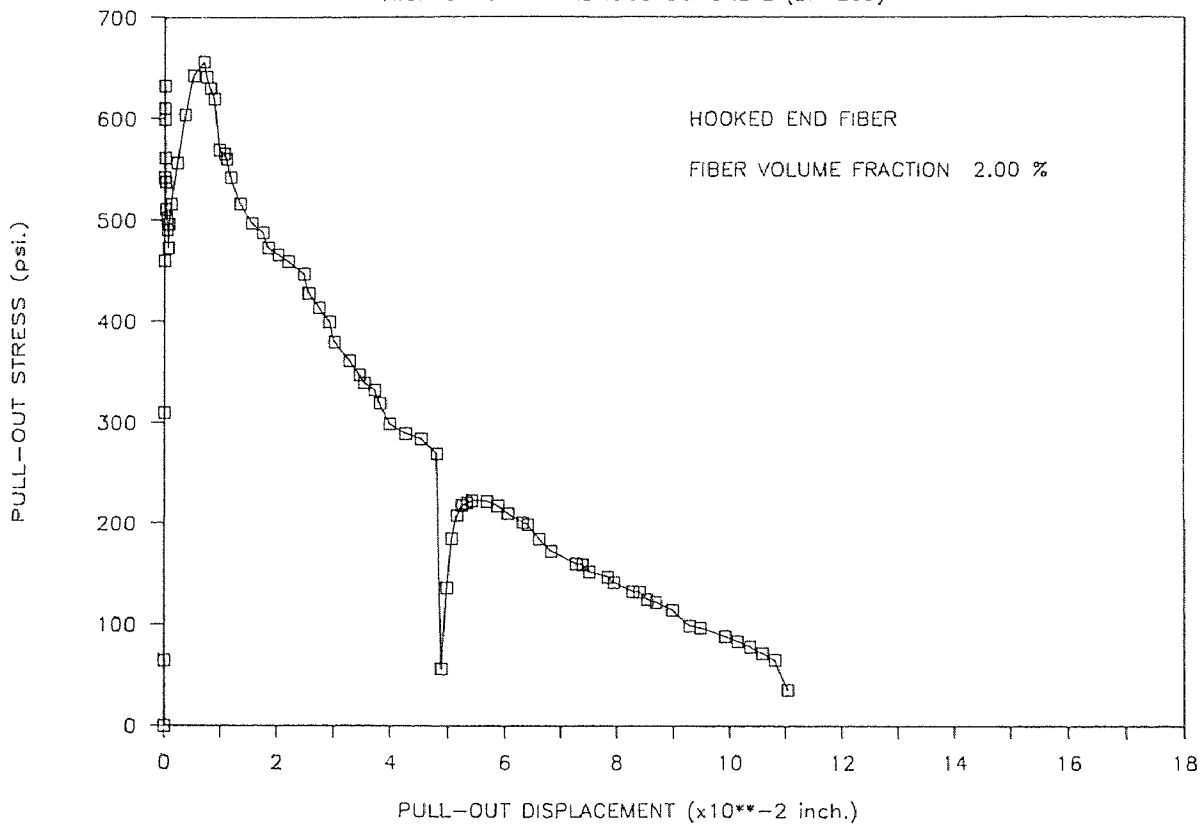
PULL-OUT TEST

HIGH STRENGTH FIBROUS CONCRETE (BFH202)



PULL-OUT TEST

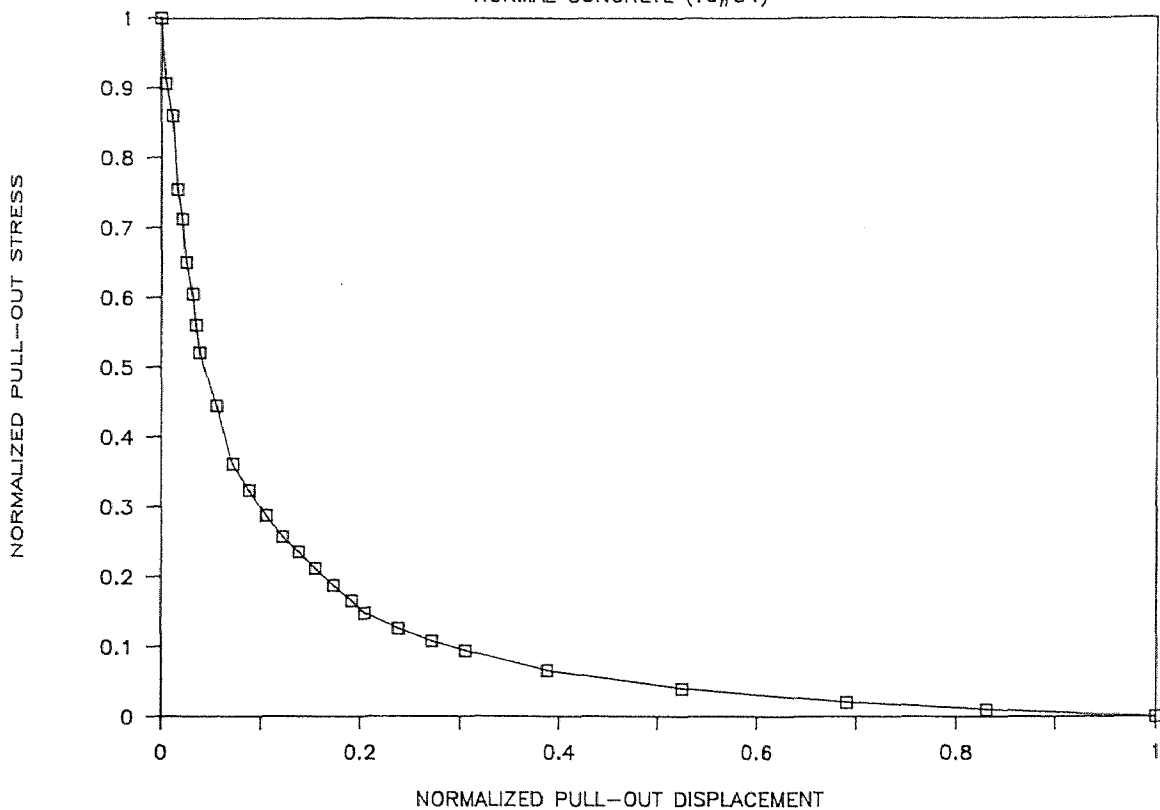
HIGH STRENGTH FIBROUS CONCRETE (BFH203)



APPENDIX F

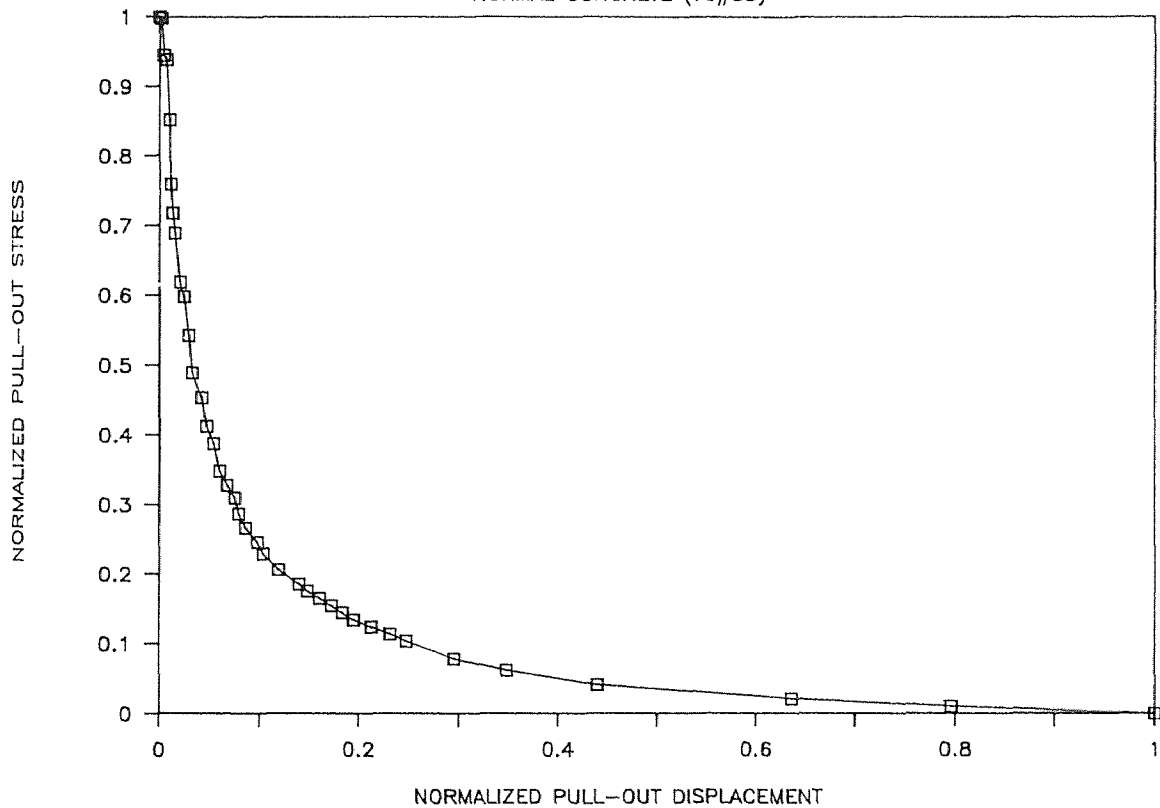
NORMALIZED STRESS VS. DISPLACEMENT

NORMAL CONCRETE (TC#34)



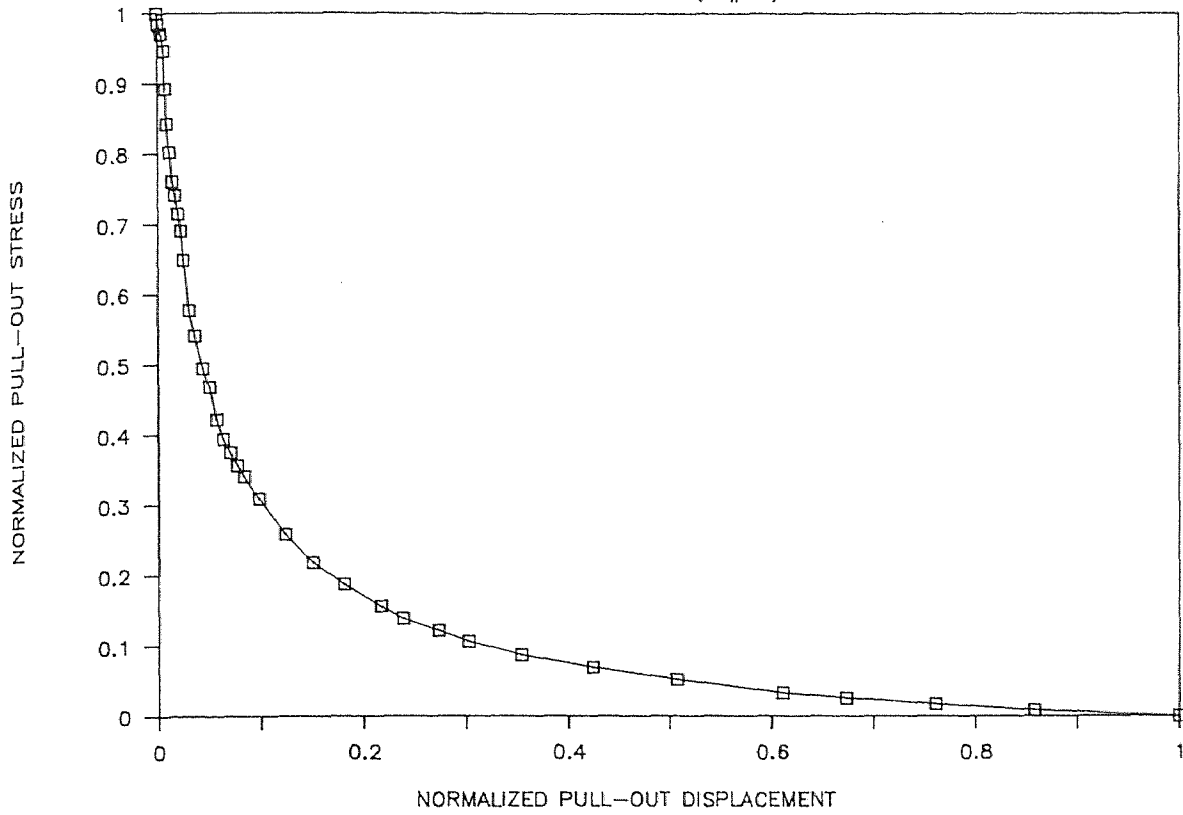
NORMALIZED STRESS VS. DISPLACEMENT

NORMAL CONCRETE (TC#35)



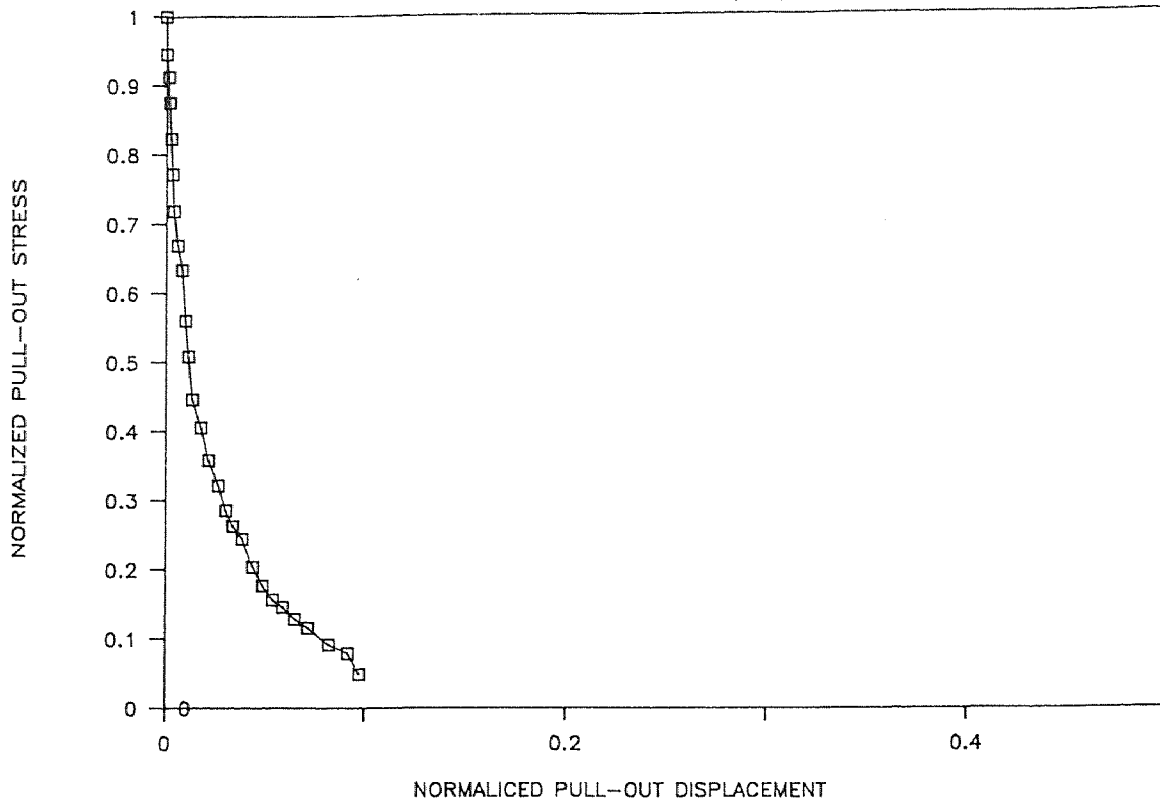
NORMALIZED STRESS VS. DISPLACEMENT

NORMAL CONCRETE (TC#36)



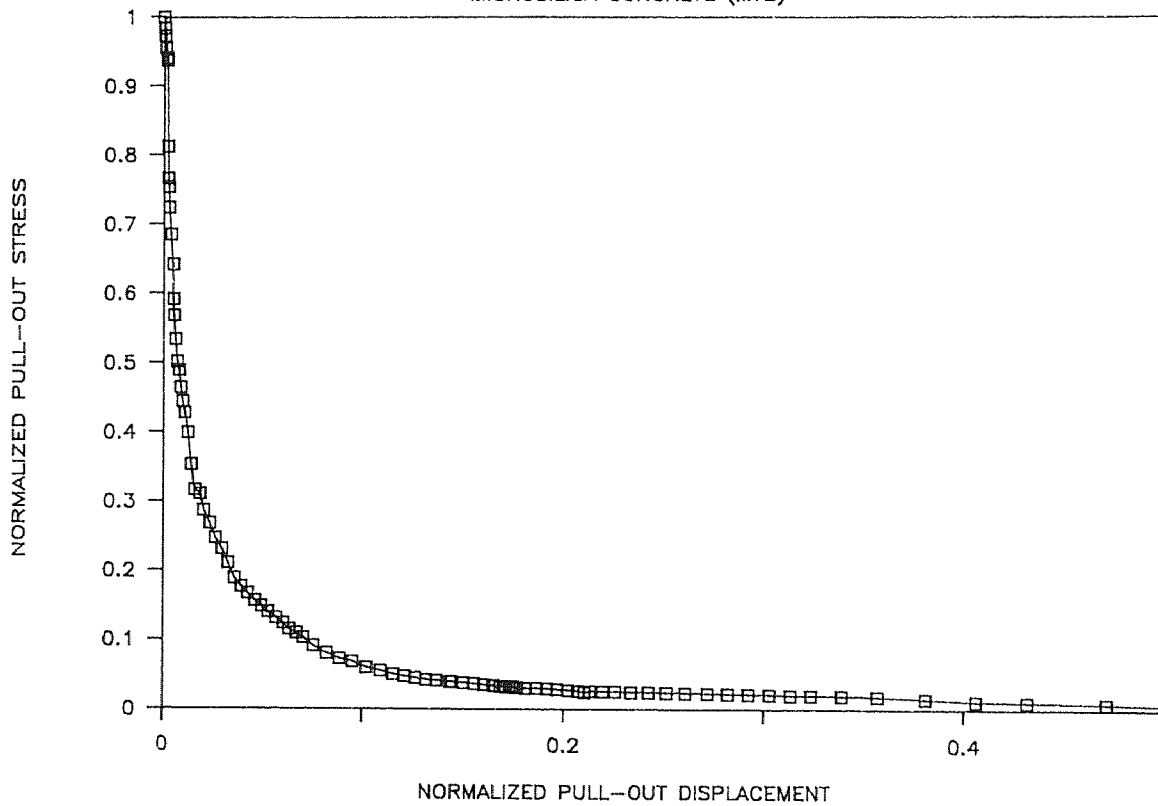
NORMALIZED STRESS VS. DISPLACEMENT

MICROSILICA CONCRETE (MT1)



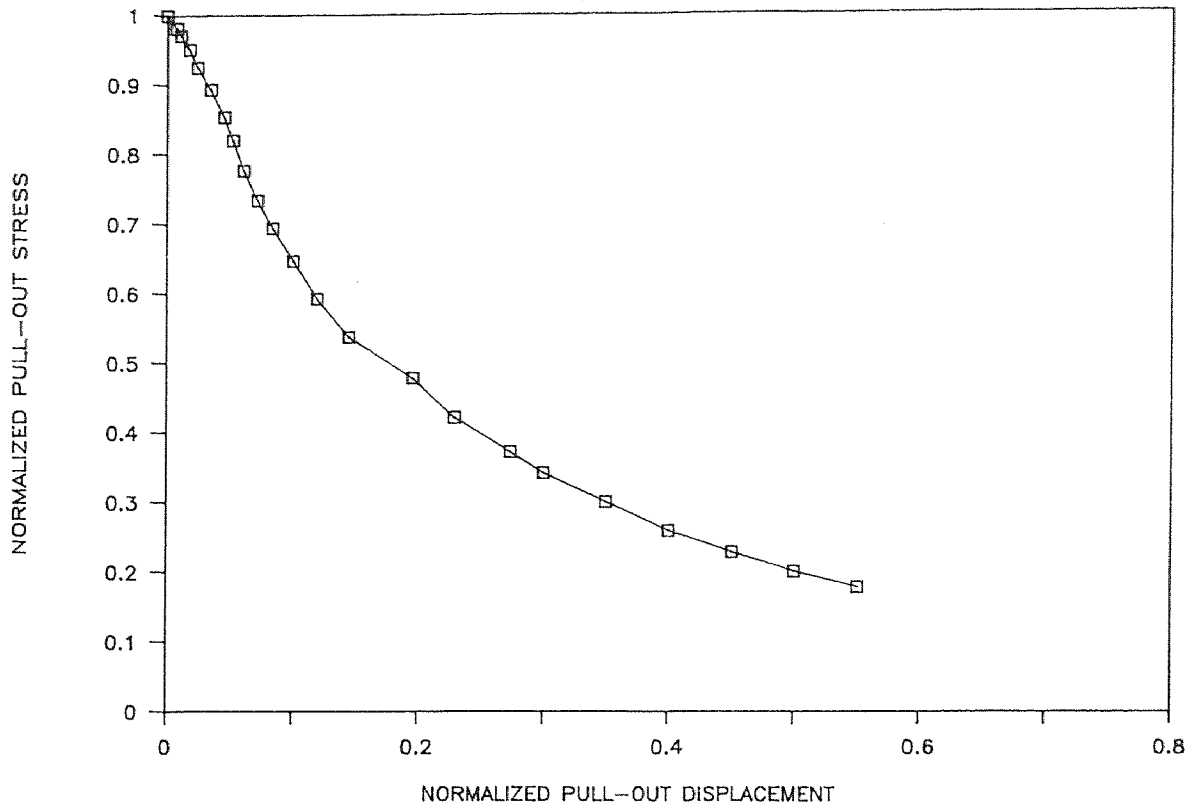
NORMALIZED STRESS VS. DISPLACEMENT

MICROSILICA CONCRETE (MT2)



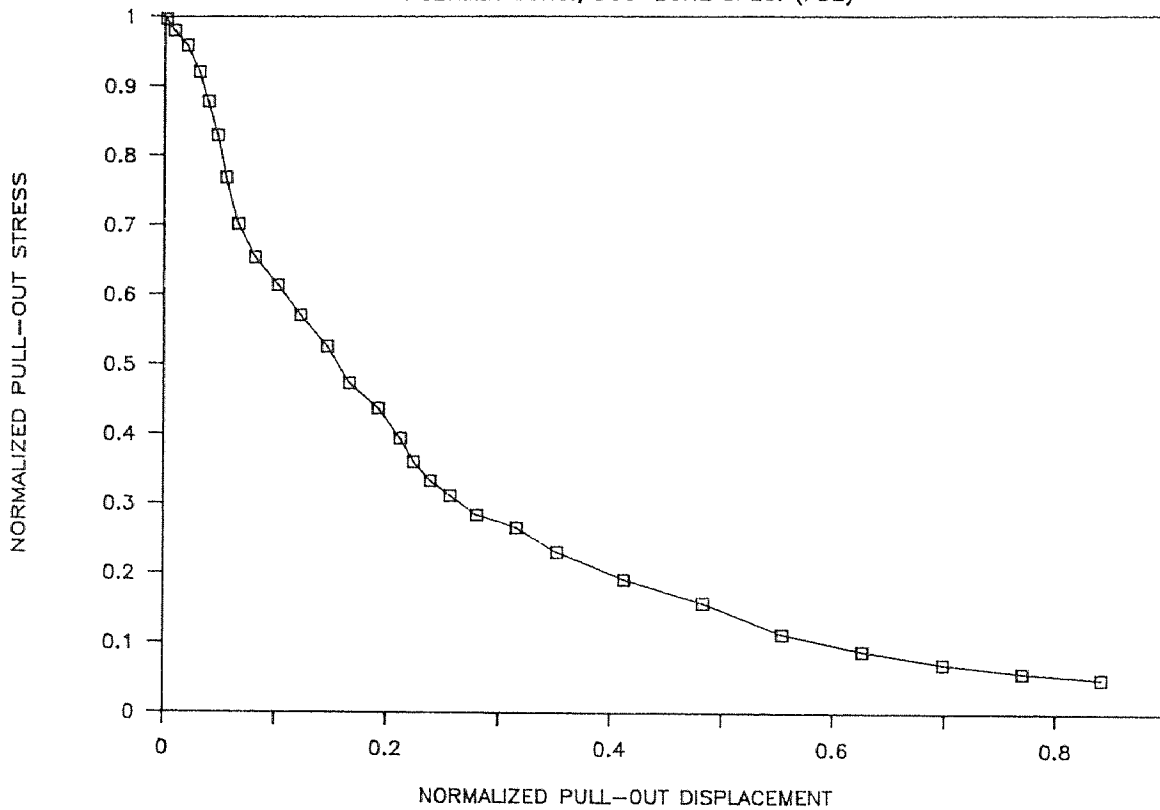
NORMALIZED STRESS VS. DISPLACEMENT

POLYMER CONC., DOG-BONE SPEC. (PD1)



NORMALIZED STRESS VS. DISPLACEMENT

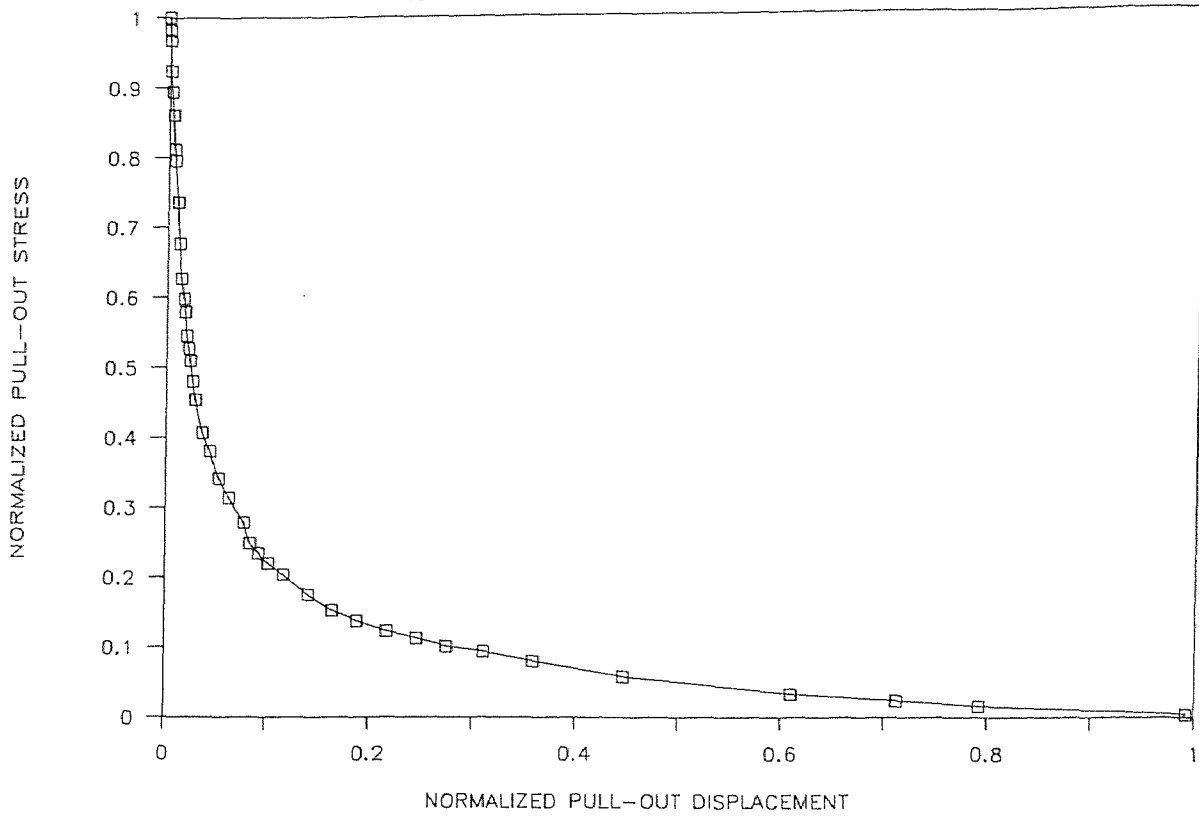
POLYMER CONC., DOG-BONE SPEC. (PD2)



APPENDIX G

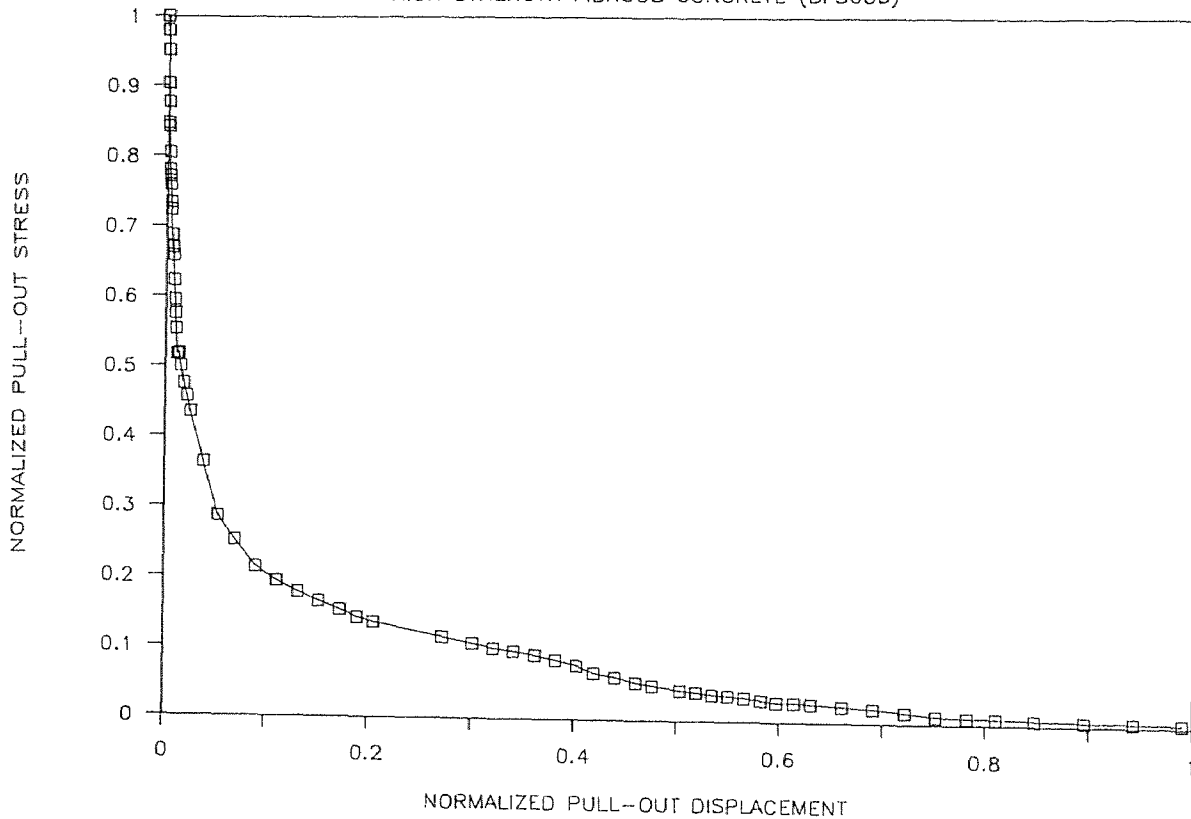
NORMALIZED STRESS VS. DISPLACEMENT

HIGH STRENGTH FIBROUS CONCRETE (BFS054)



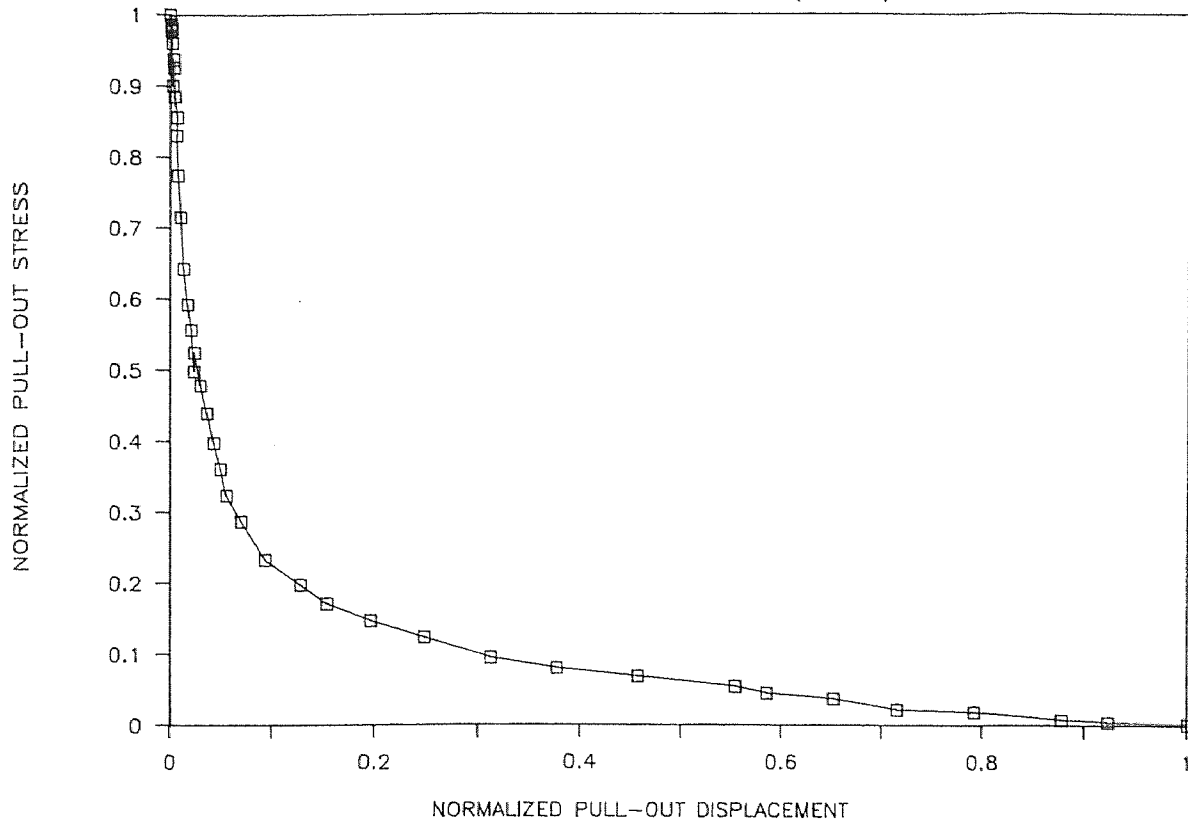
NORMALIZED STRESS VS. DISPLACEMENT

HIGH STRENGTH FIBROUS CONCRETE (BFS055)



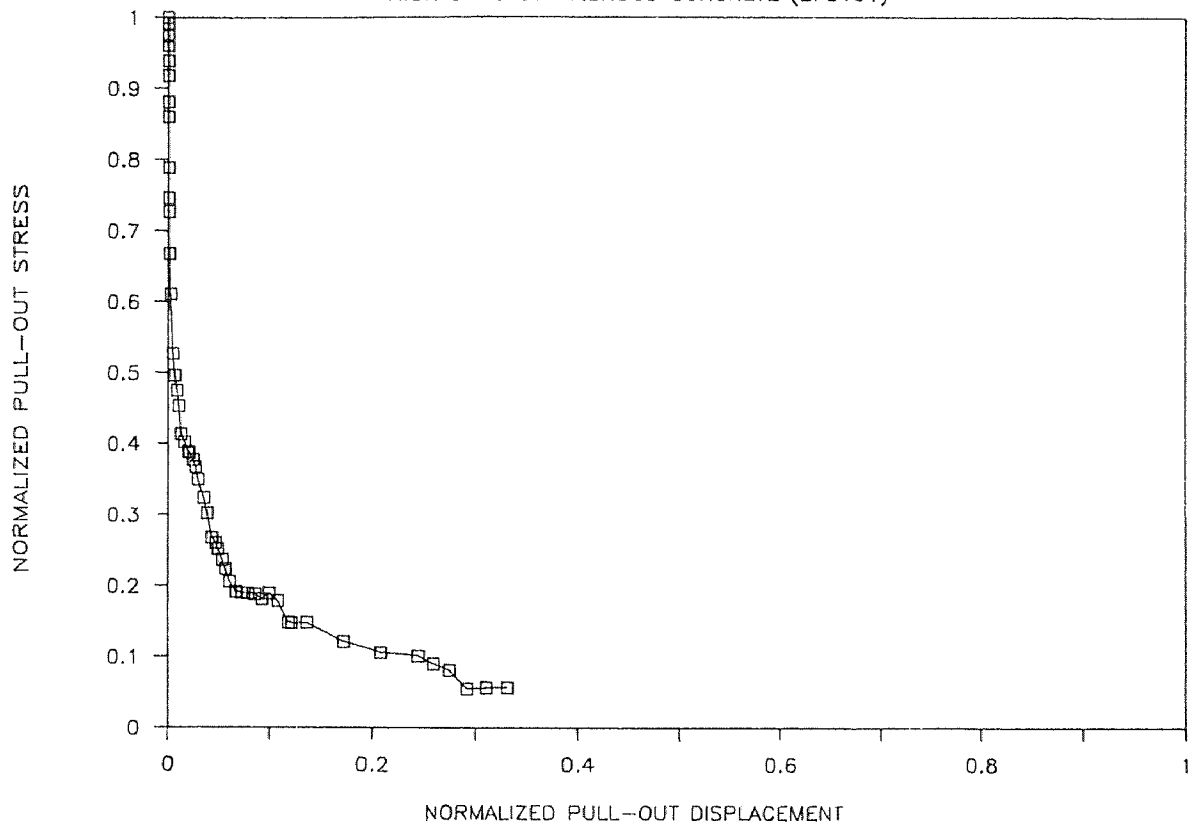
NORMALIZED STRESS VS. DISPLACEMENT

HIGH STRENGTH FIBROUS CONCRETE (BFS056)



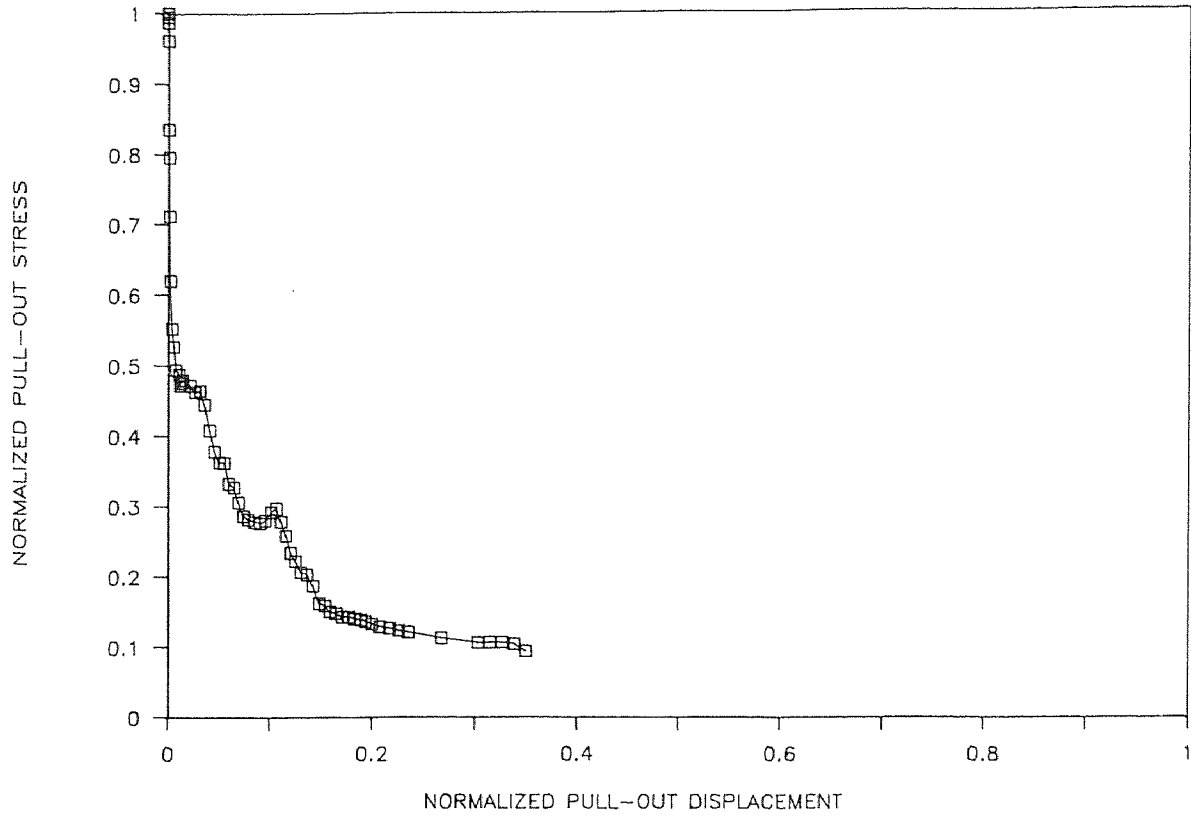
NORMALIZED STRESS VS. DISPLACEMENT

HIGH STRENGTH FIBROUS CONCRETE (BFS101)



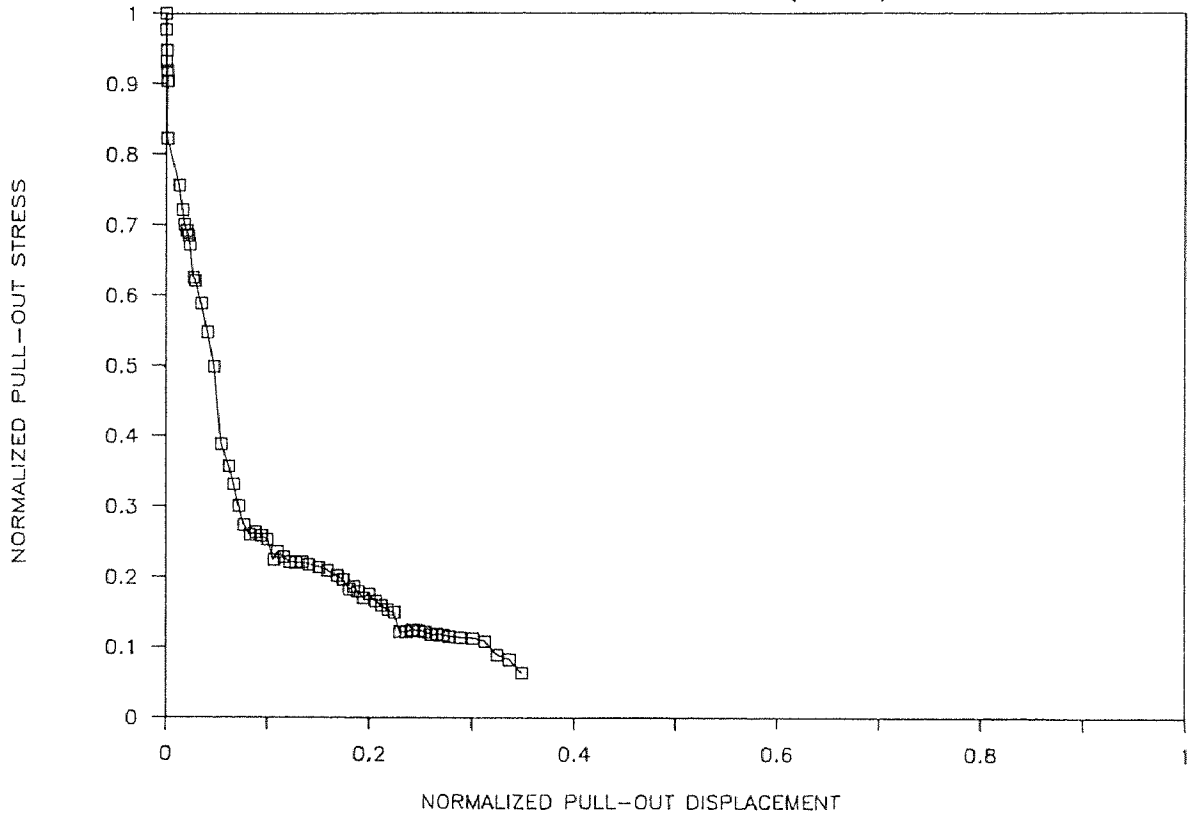
NORMALIZED STRESS VS. DISPLACEMENT

HIGH STRENGTH FIBROUS CONCRETE (BFS102)



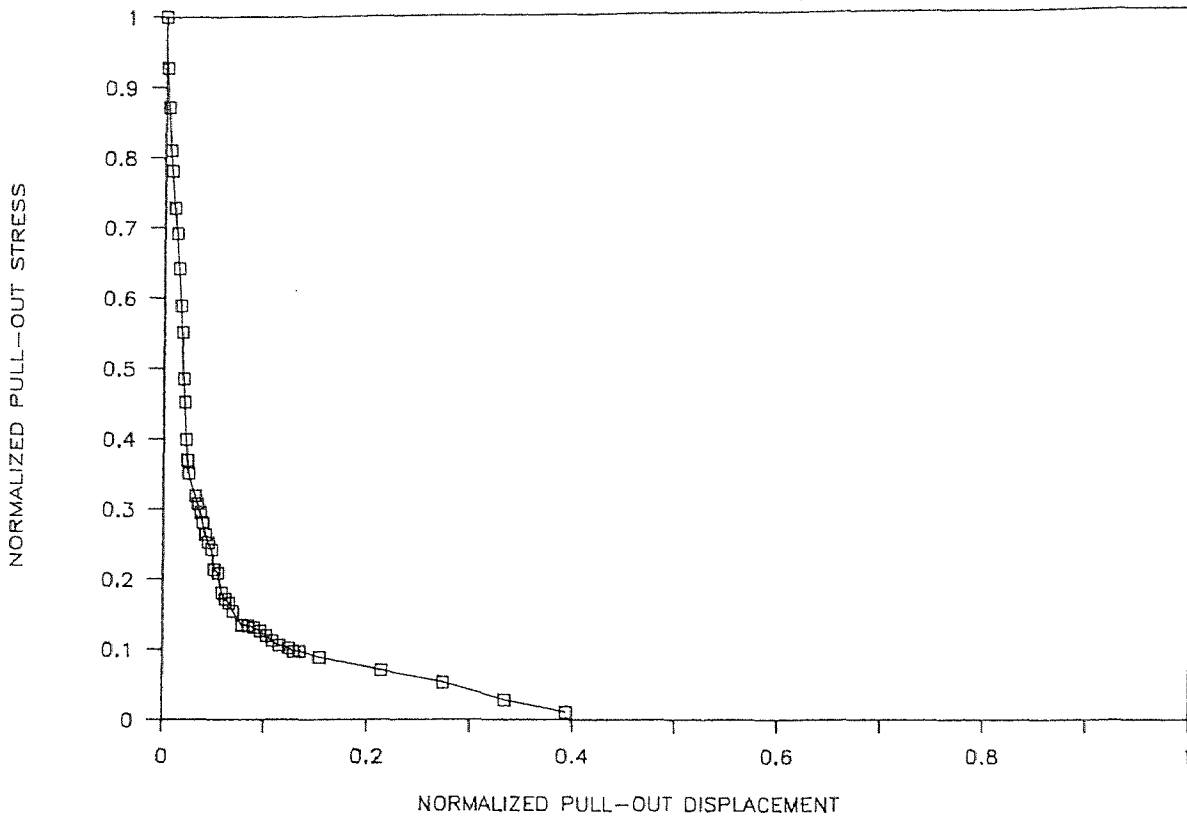
NORMALIZED STRESS VS. DISPLACEMENT

HIGH STRENGTH FIBROUS CONCRETE (BFS103)



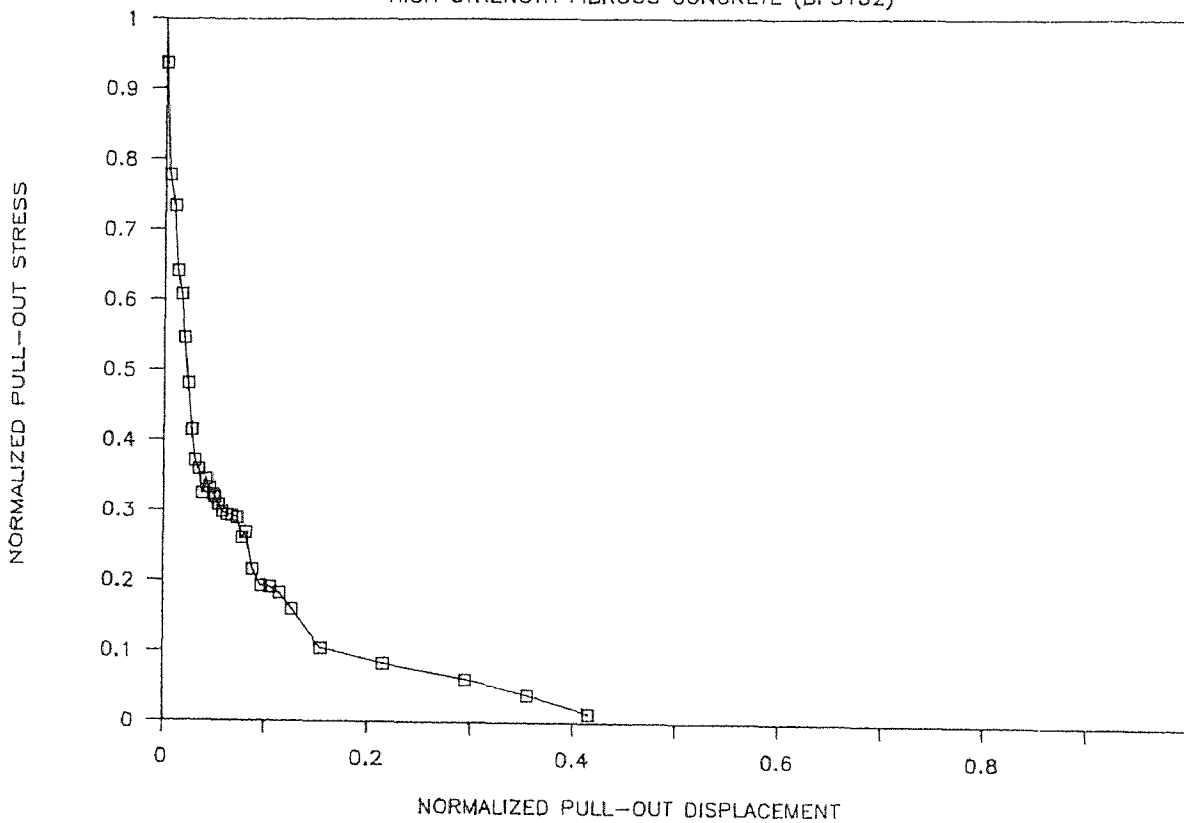
NORMALIZED STRESS VS. DISPLACEMENT

HIGH STRENGTH FIBROUS CONCRETE (BFS151)



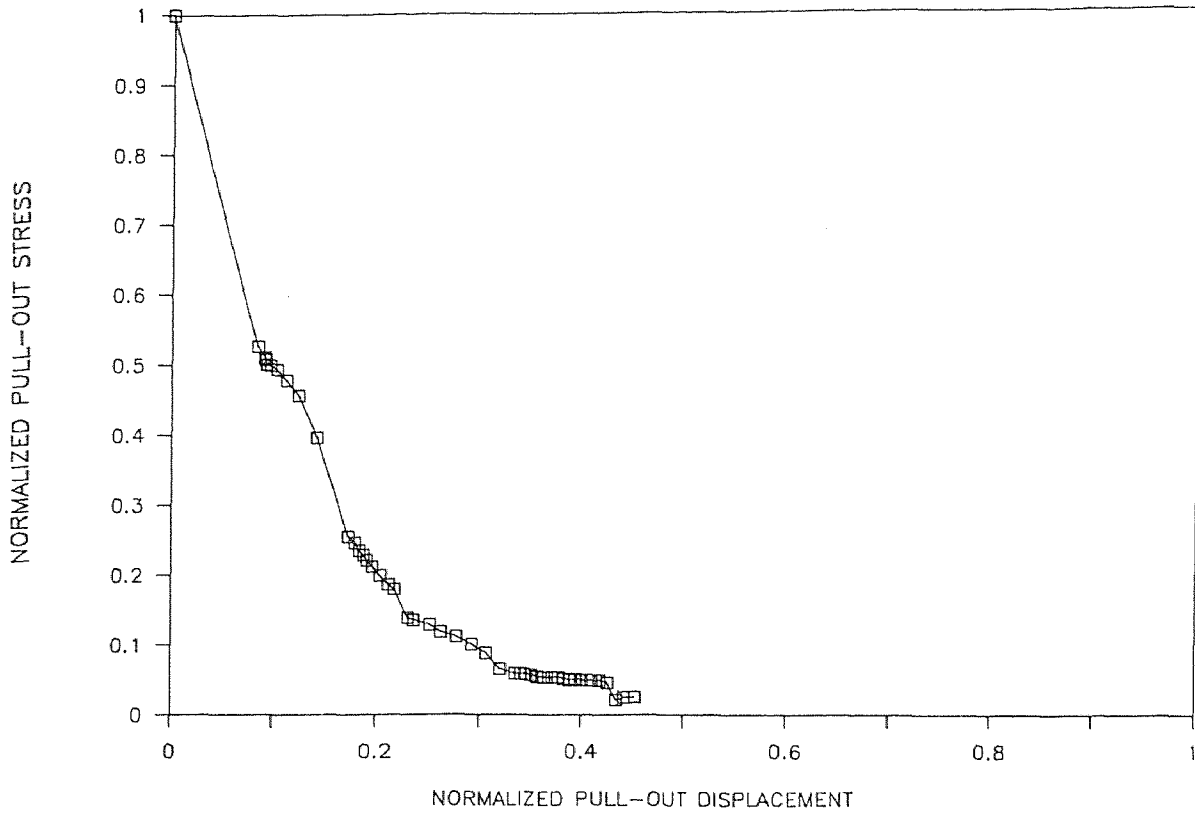
NORMALIZED STRESS VS. DISPLACEMENT

HIGH STRENGTH FIBROUS CONCRETE (BFS152)



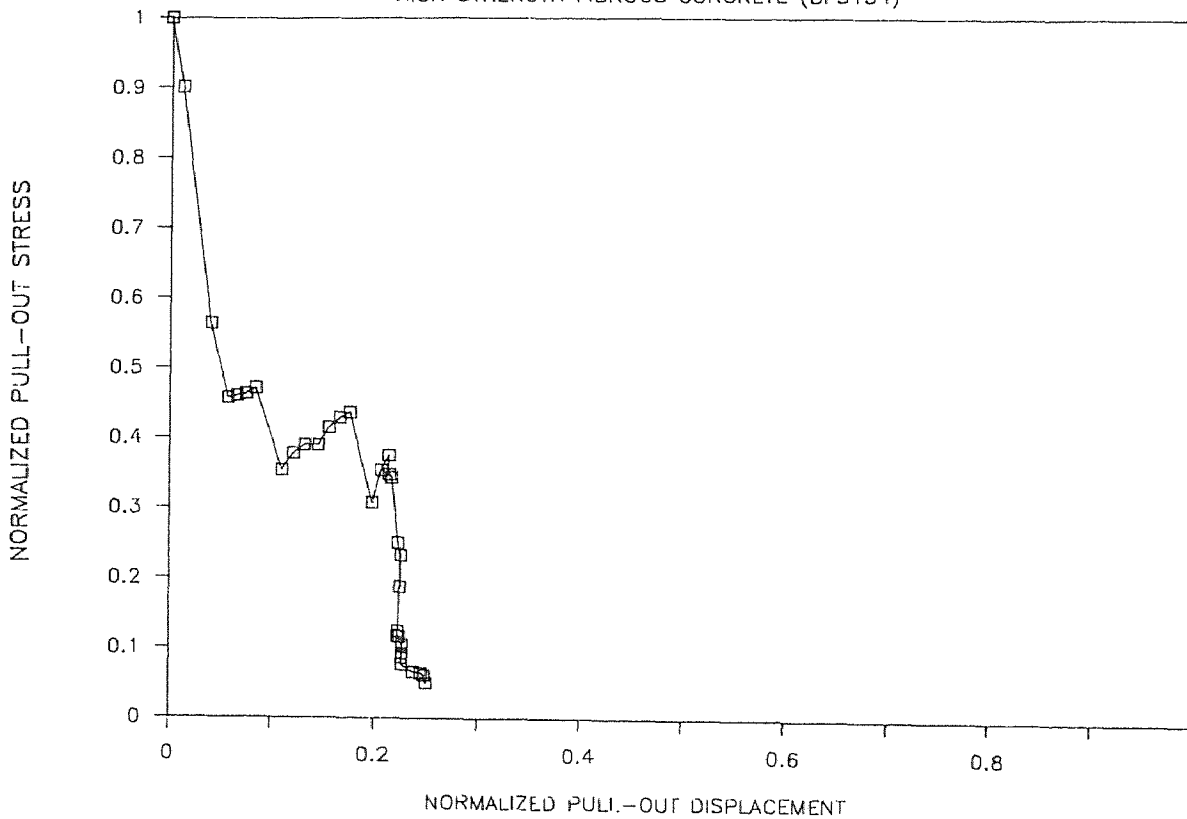
NORMALIZED STRESS VS. DISPLACEMENT

HIGH STRENGTH FIBROUS CONCRETE (BFS153)



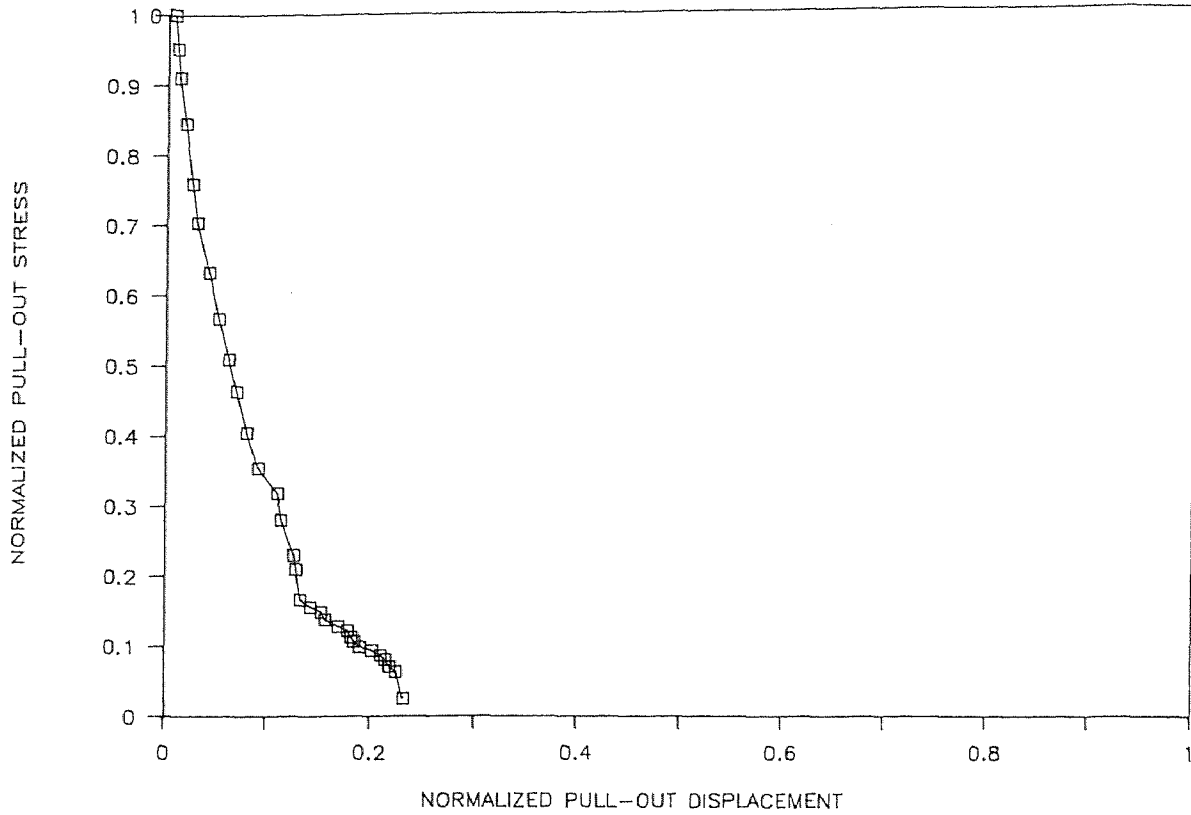
NORMALIZED STRESS VS. DISPLACEMENT

HIGH STRENGTH FIBROUS CONCRETE (BFS154)



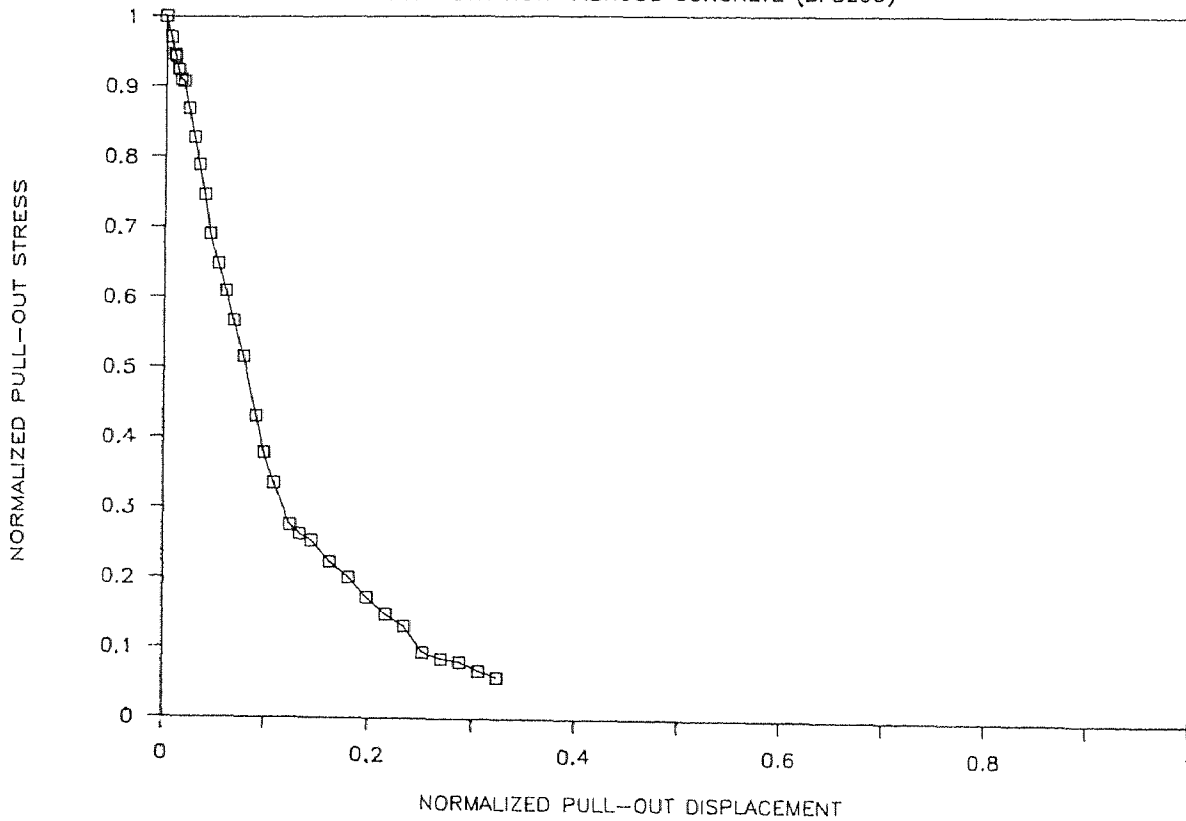
NORMALIZED STRESS VS. DISPLACEMENT

HIGH STRENGTH FIBROUS CONCRETE (BFS202)



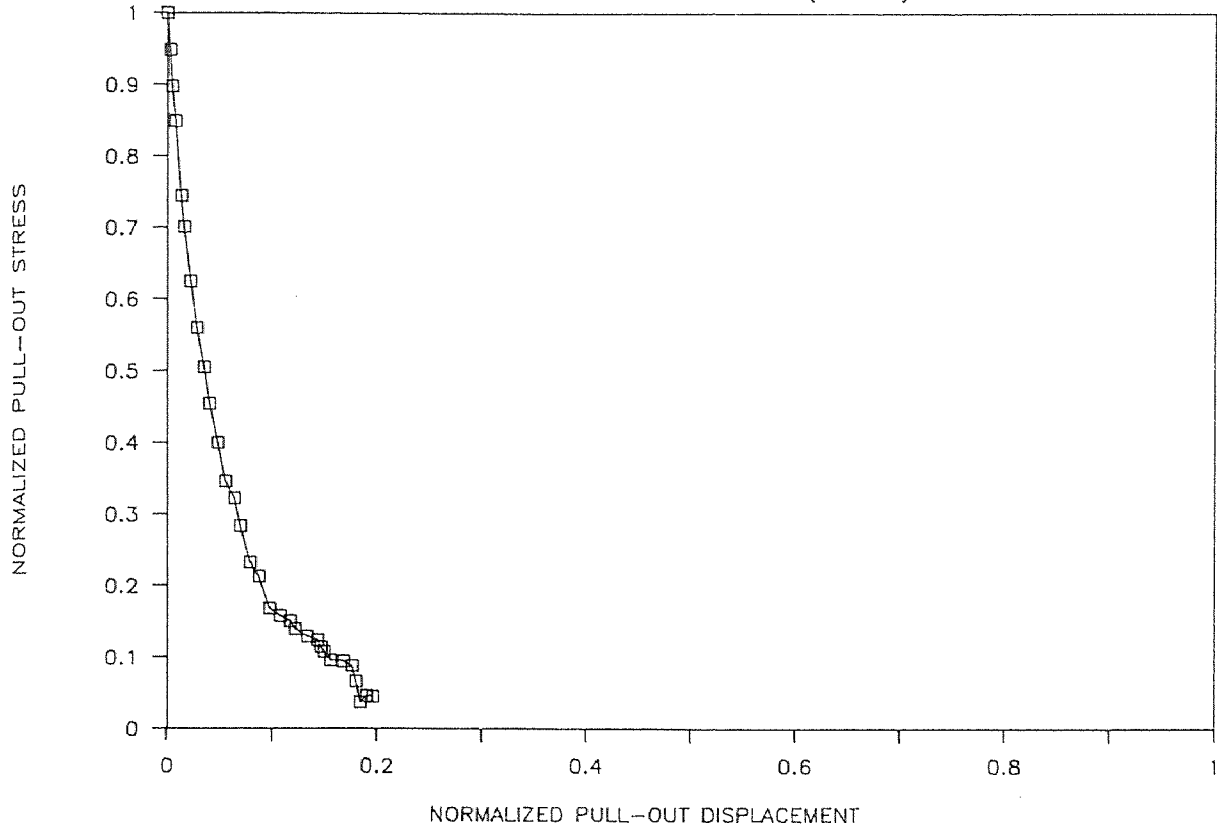
NORMALIZED STRESS VS. DISPLACEMENT

HIGH STRENGTH FIBROUS CONCRETE (BFS203)



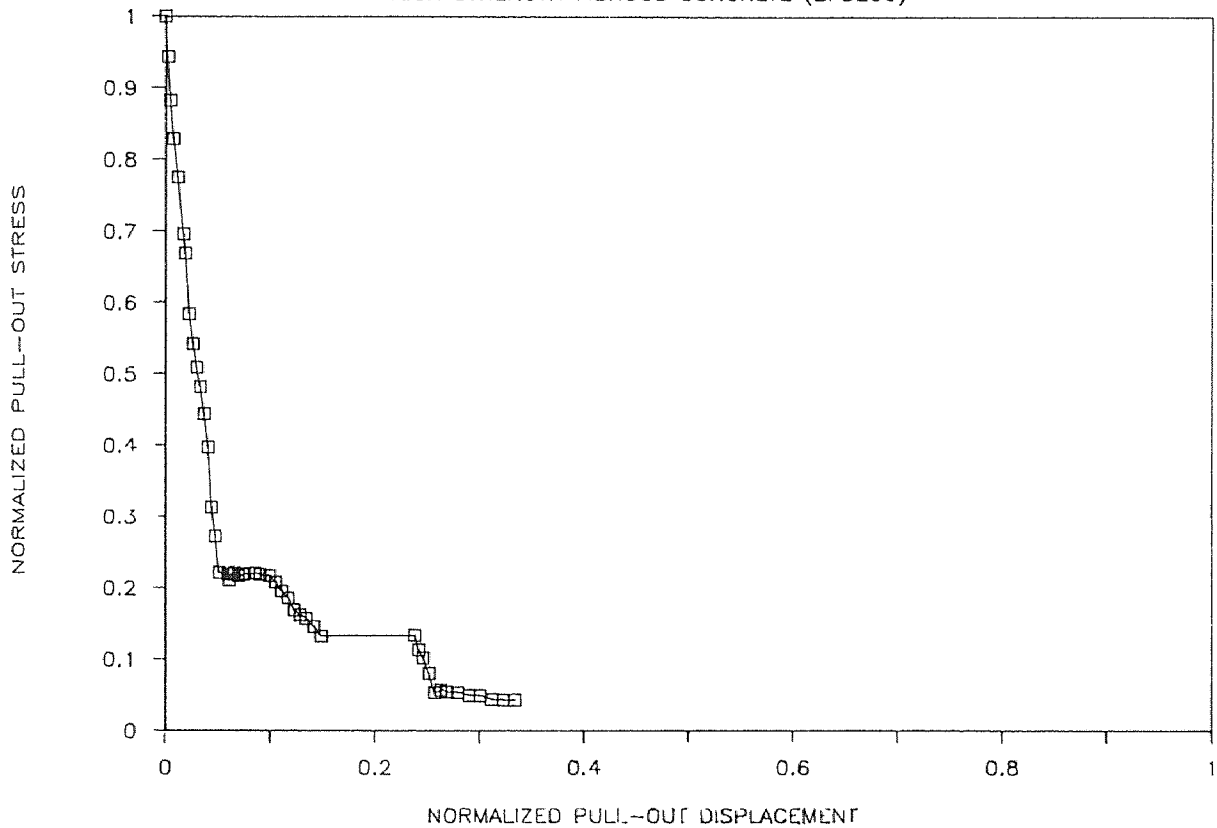
NORMALIZED STRESS VS. DISPLACEMENT

HIGH STRENGTH FIBROUS CONCRETE (BFS205)



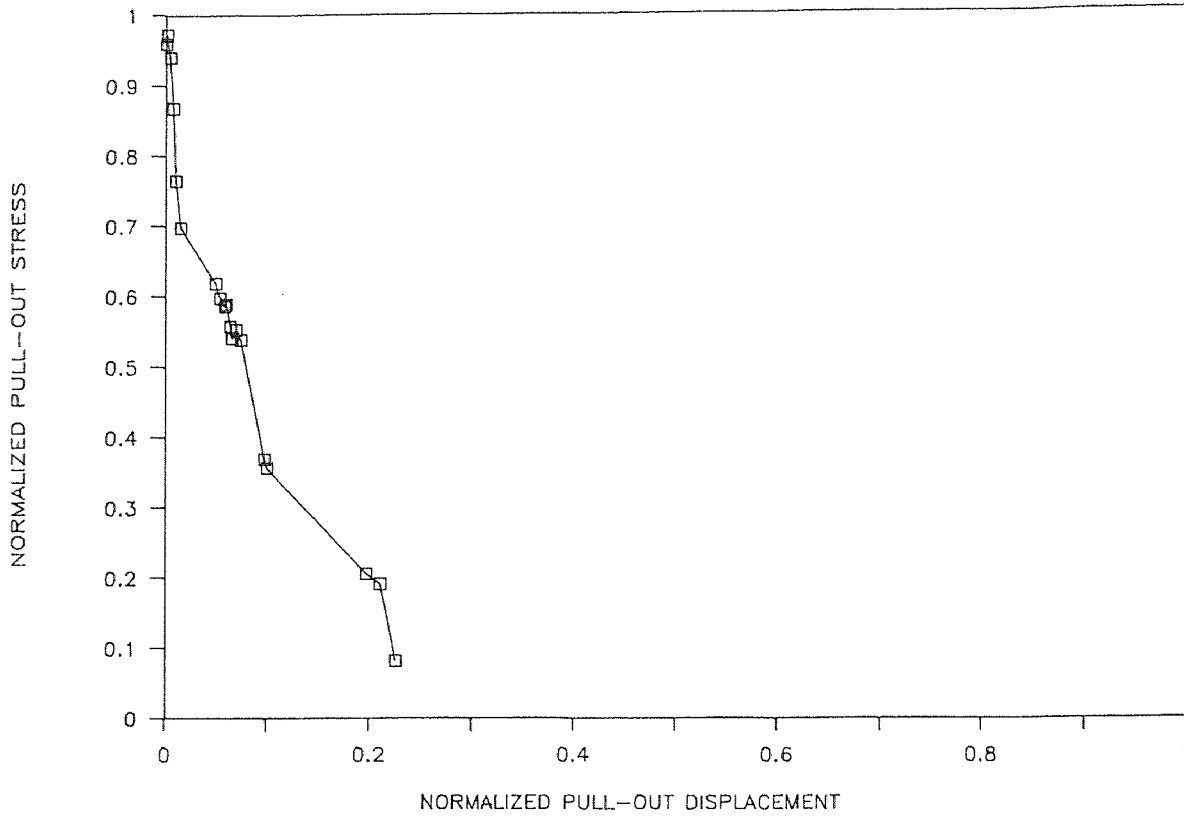
NORMALIZED STRESS VS. DISPLACEMENT

HIGH STRENGTH FIBROUS CONCRETE (BFS206)



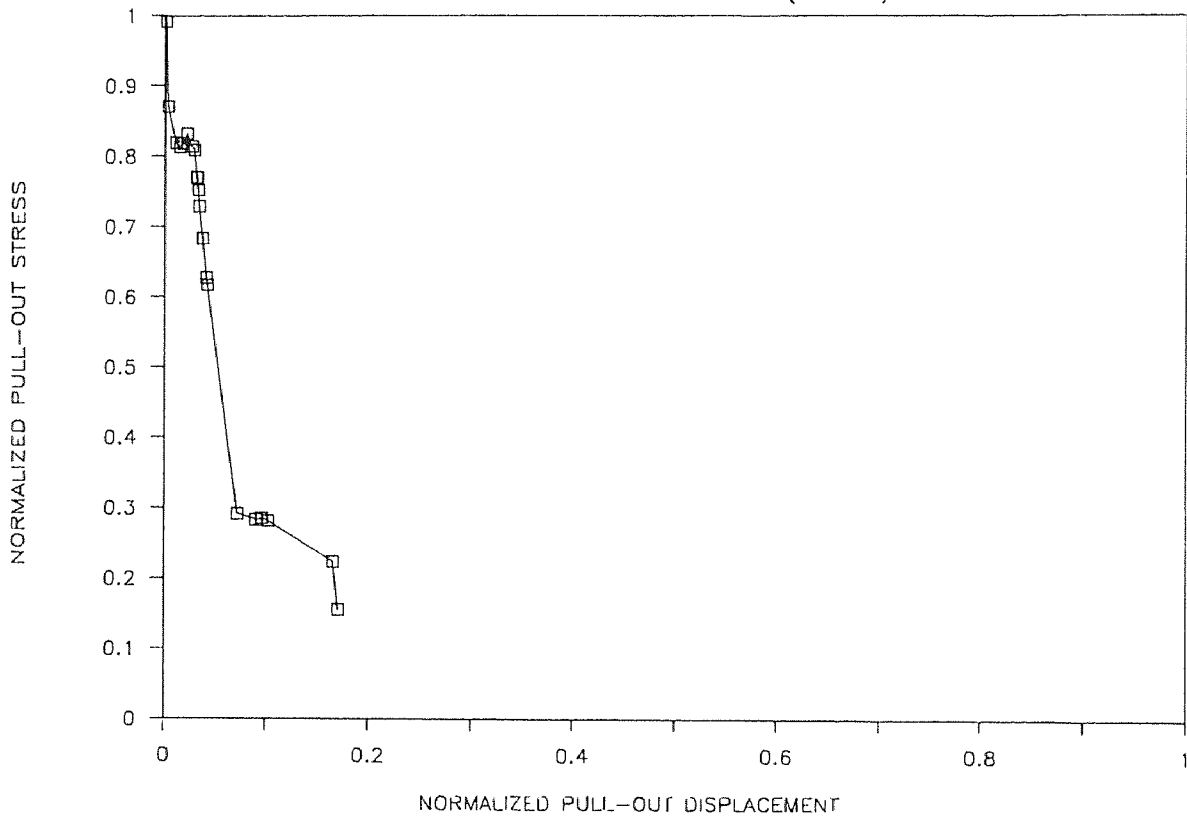
NORMALIZED STRESS VS. DISPLACEMENT

HIGH STRENGTH FIBROUS CONCRETE (BFH051)



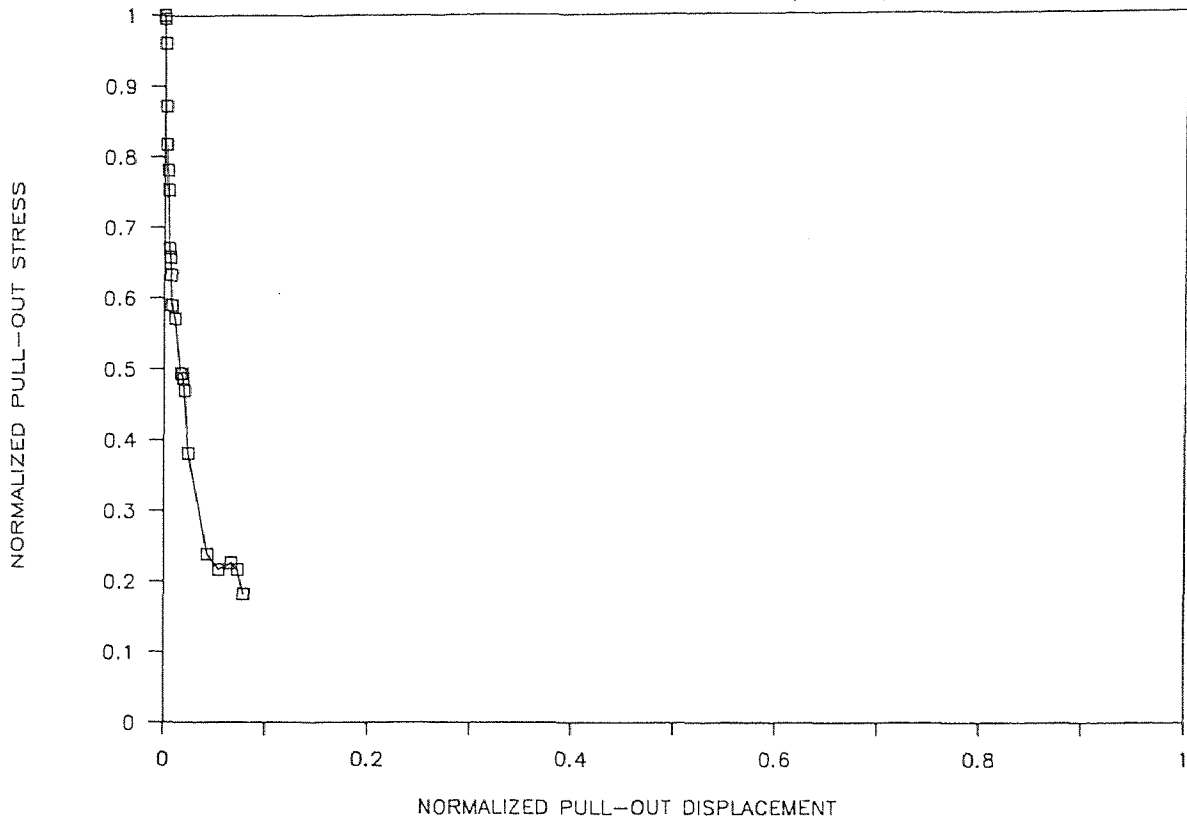
NORMALIZED STRESS VS. DISPLACEMENT

HIGH STRENGTH FIBROUS CONCRETE (BFH052)



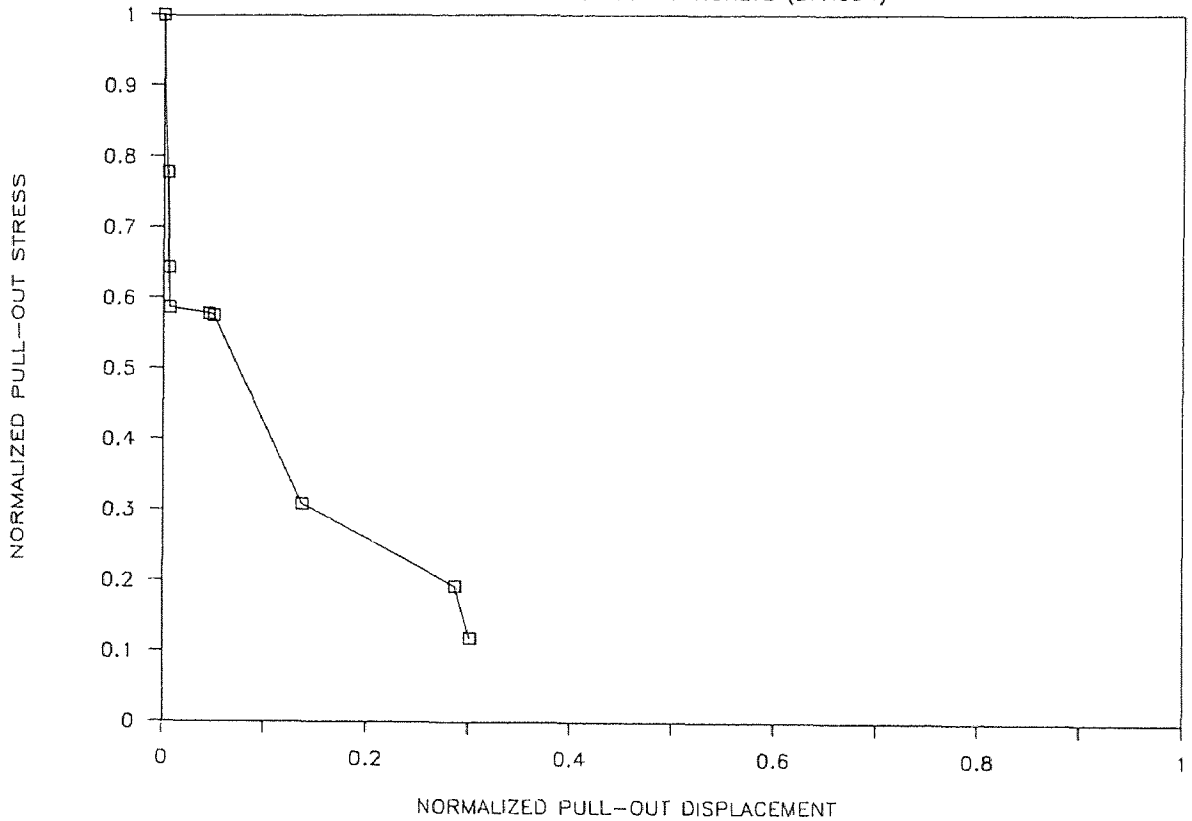
NORMALIZED STRESS VS. DISPLACEMENT

HIGH STRENGTH FIBROUS CONCRETE (BFH053)



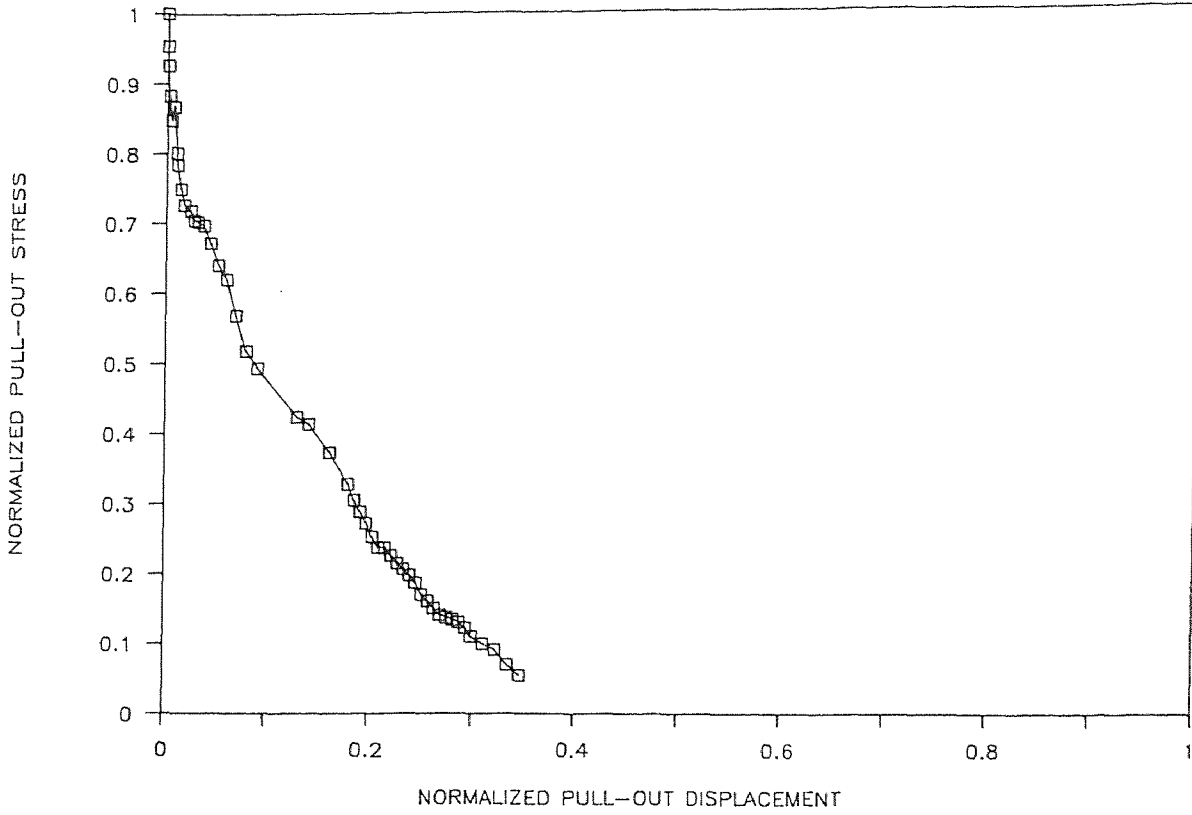
NORMALIZED STRESS VS. DISPLACEMENT

HIGH STRENGTH FIBROUS CONCRETE (BFH054)



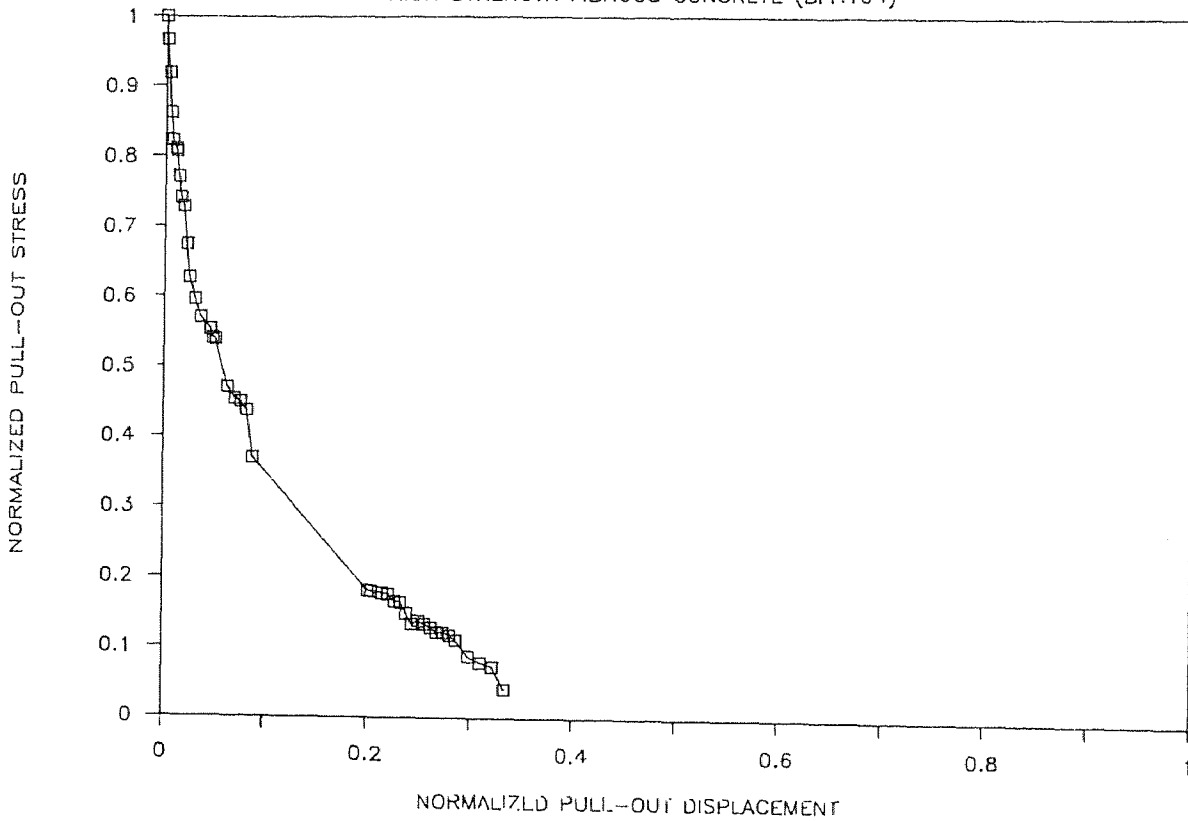
NORMALIZED STRESS VS. DISPLACEMENT

HIGH STRENGTH FIBROUS CONCRETE (BFH102)



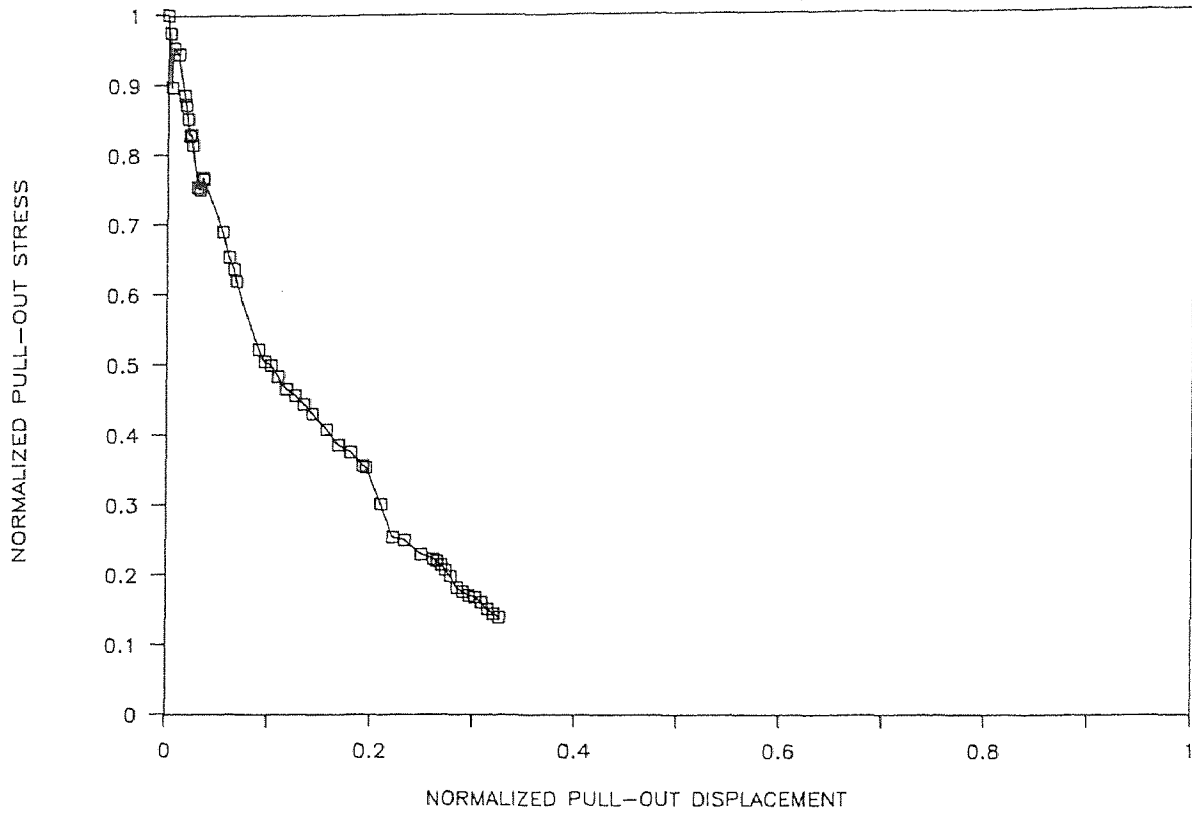
NORMALIZED STRESS VS. DISPLACEMENT

HIGH STRENGTH FIBROUS CONCRETE (BFH104)



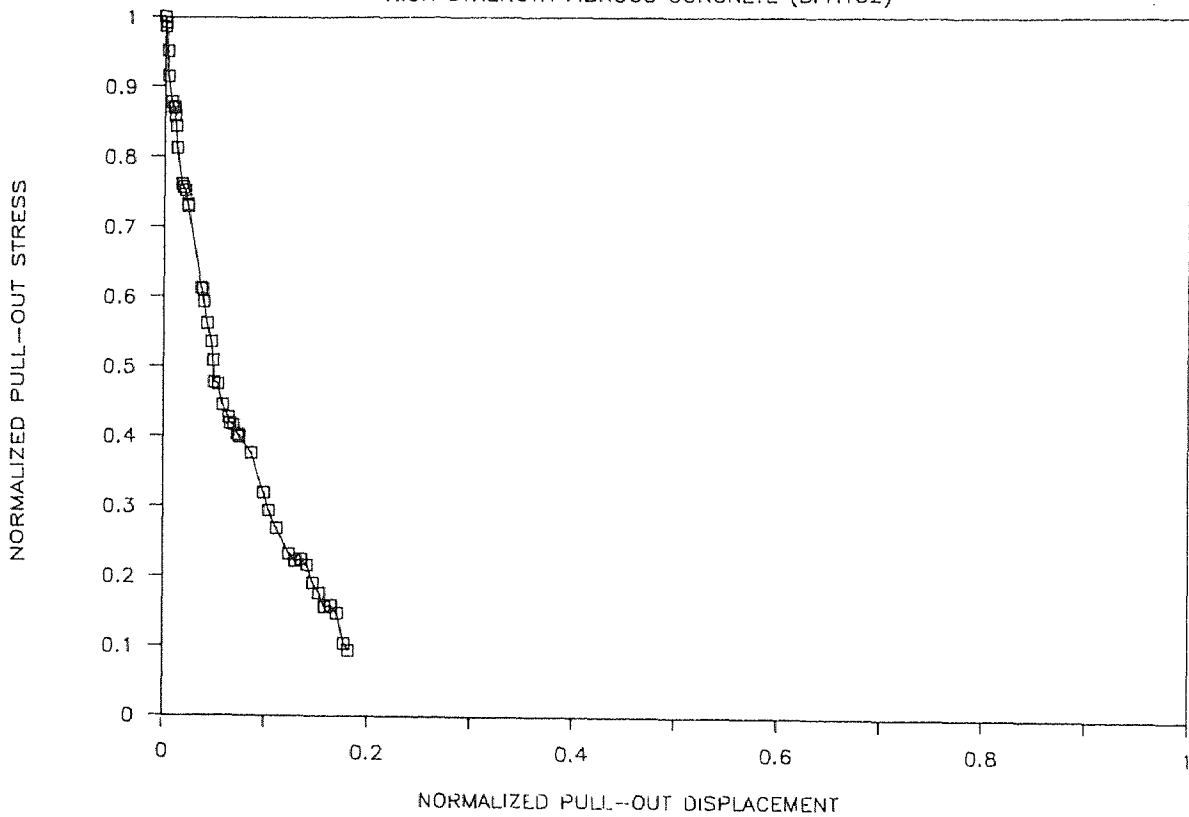
NORMALIZED STRESS VS. DISPLACEMENT

HIGH STRENGTH FIBROUS CONCRETE (BFH151)



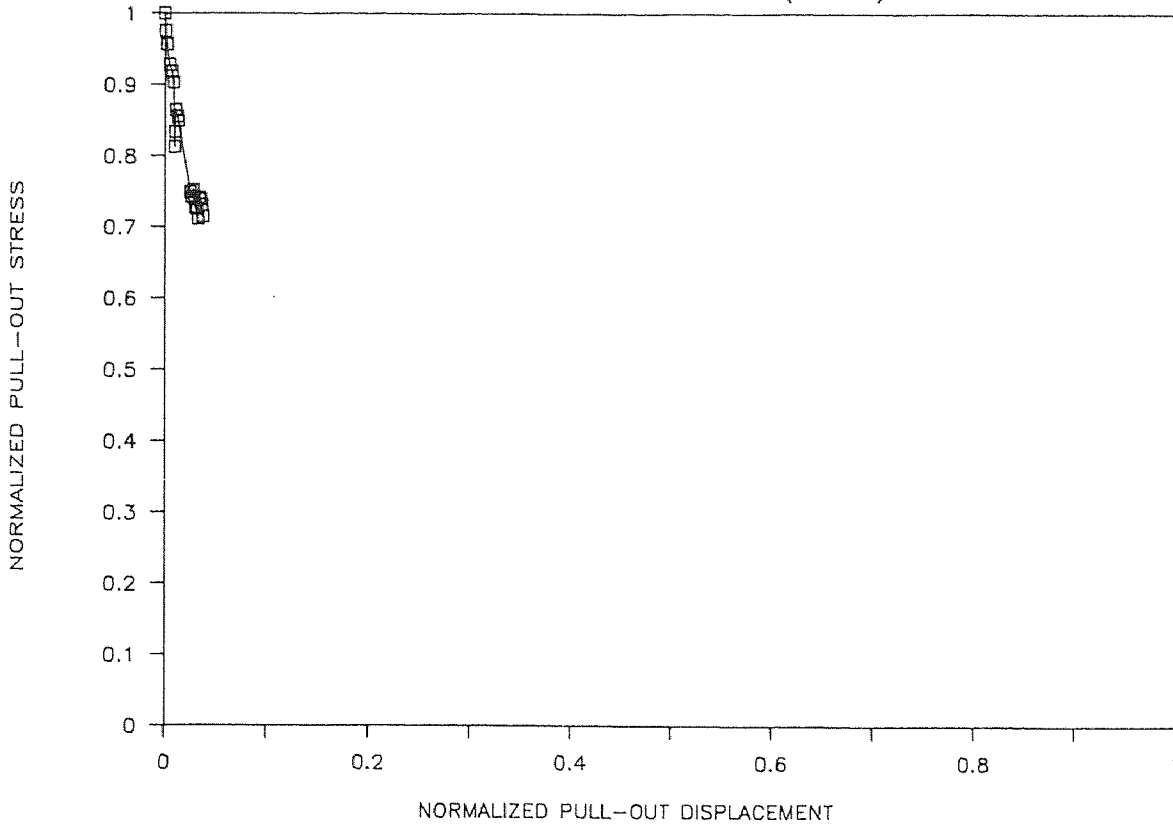
NORMALIZED STRESS VS. DISPLACEMENT

HIGH STRENGTH FIBROUS CONCRETE (BFH152)



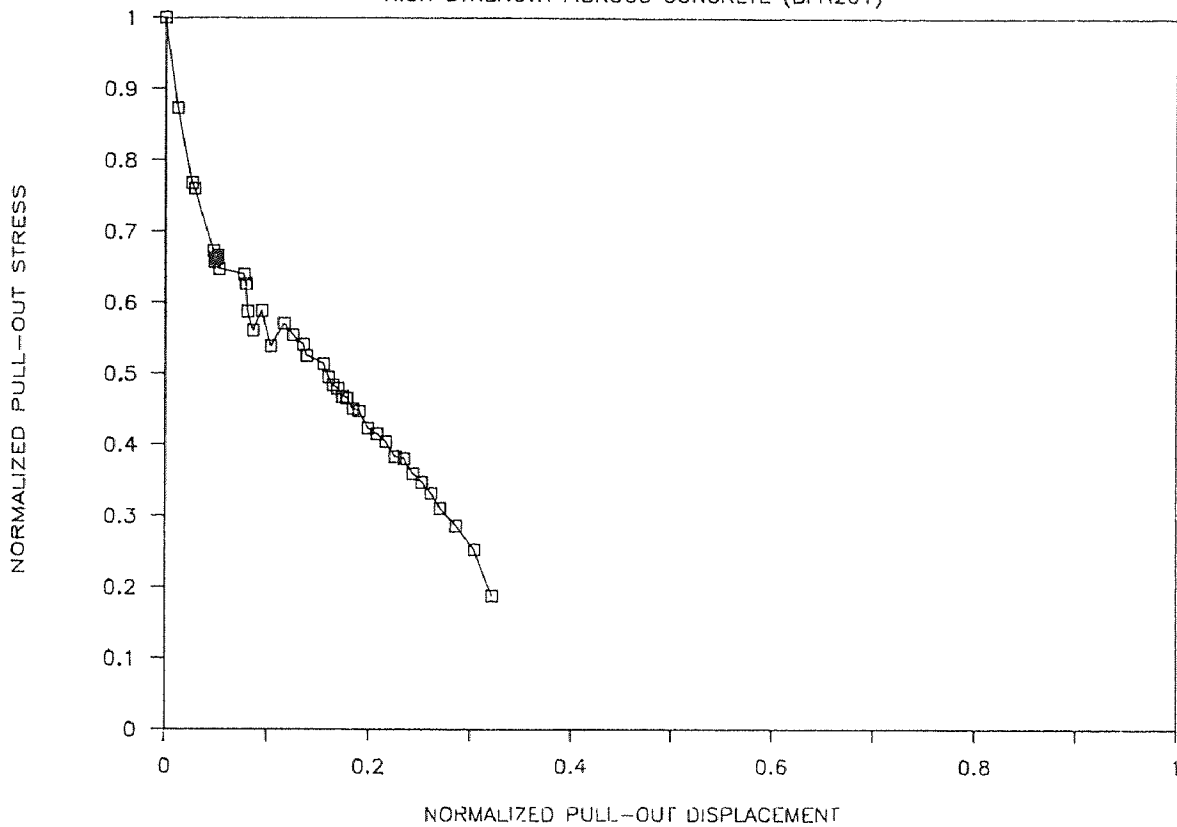
NORMALIZED STRESS VS. DISPLACEMENT

HIGH STRENGTH FIBROUS CONCRETE (BFH153)



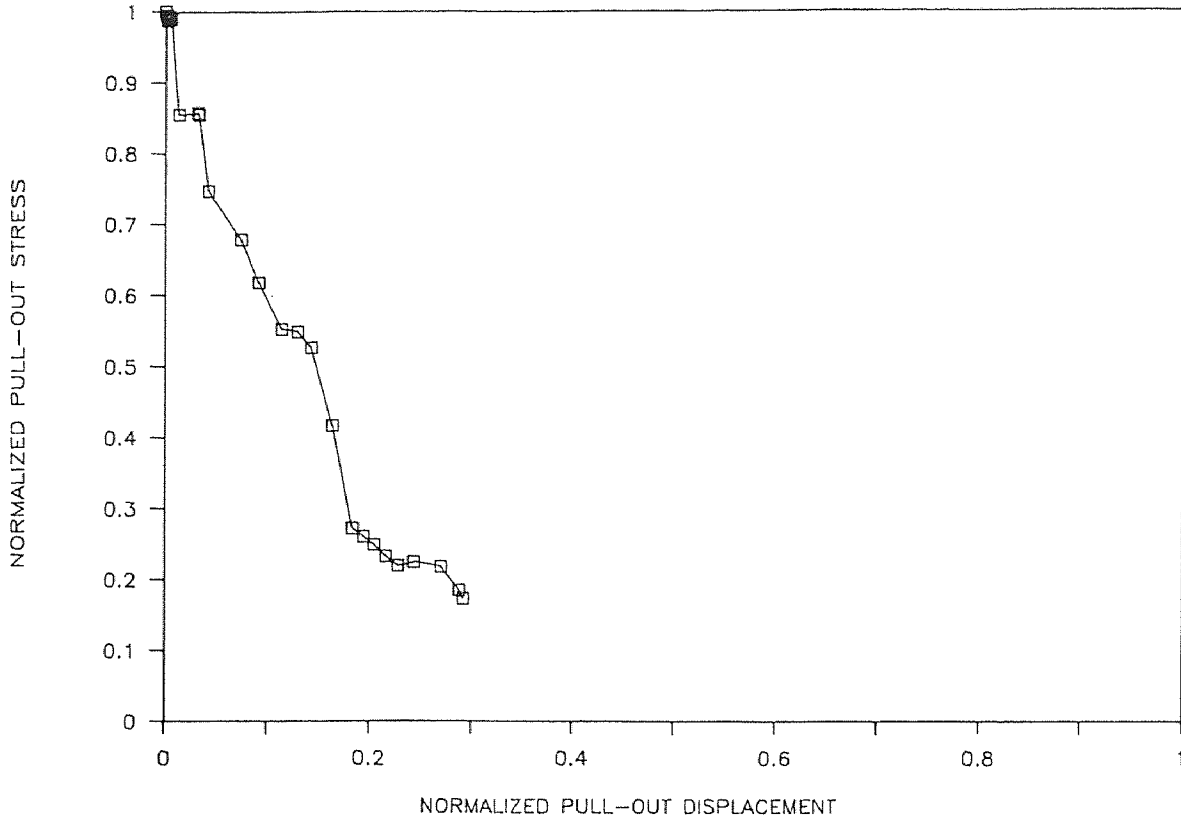
NORMALIZED STRESS VS. DISPLACEMENT

HIGH STRENGTH FIBROUS CONCRETE (BFH201)



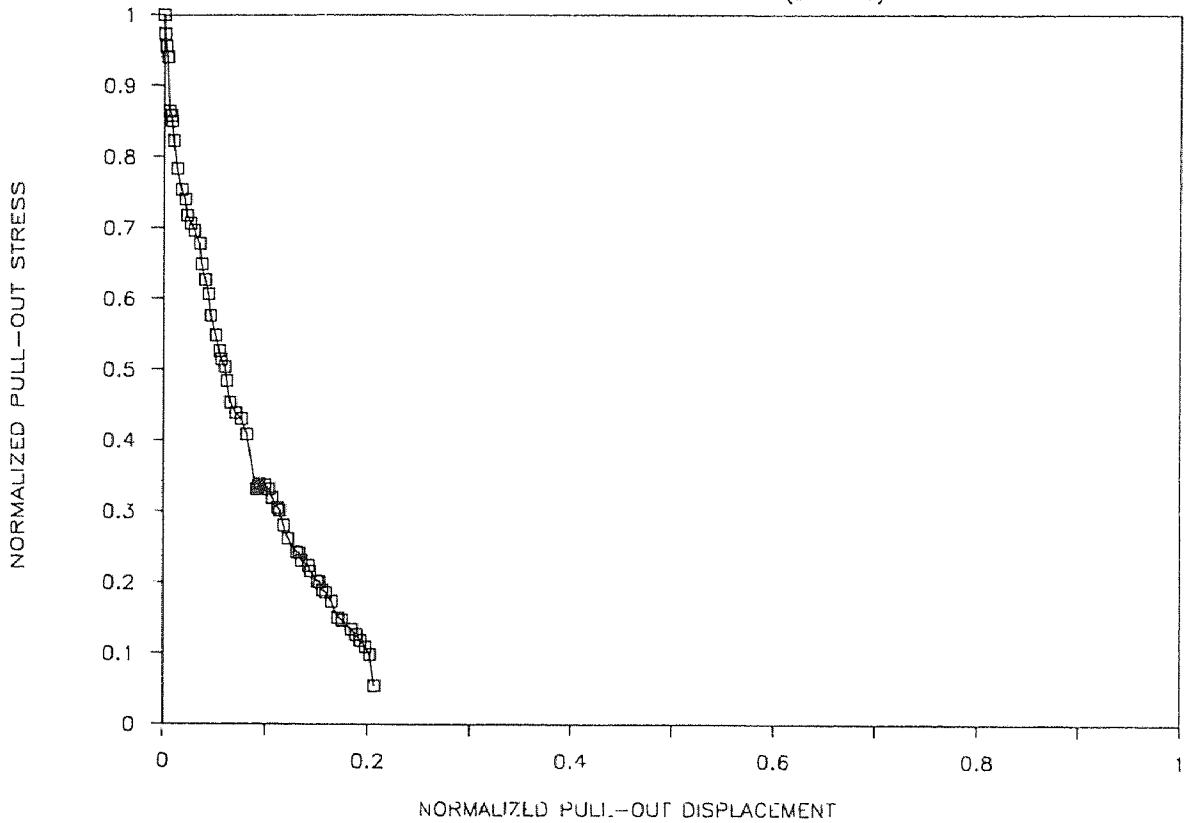
NORMALIZED STRESS VS. DISPLACEMENT

HIGH STRENGTH FIBROUS CONCRETE (BFH202)



NORMALIZED STRESS VS. DISPLACEMENT

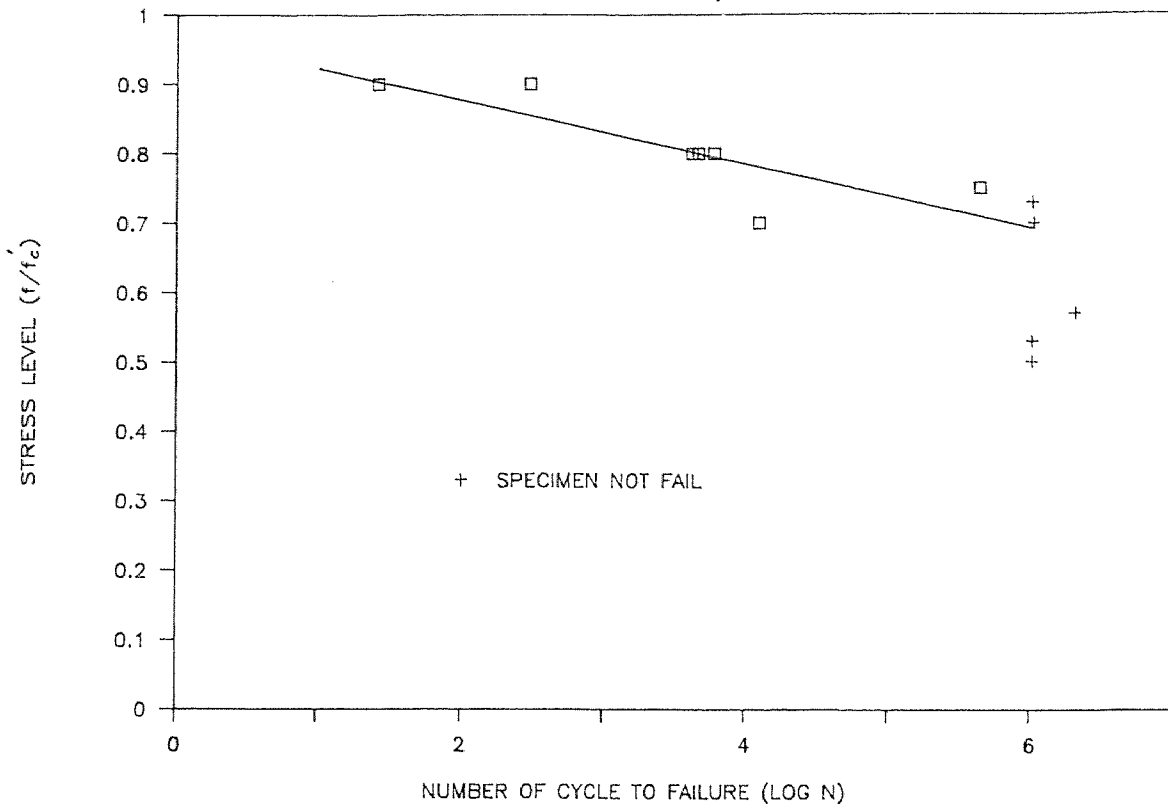
HIGH STRENGTH FIBROUS CONCRETE (BFH203)



APPENDIX H

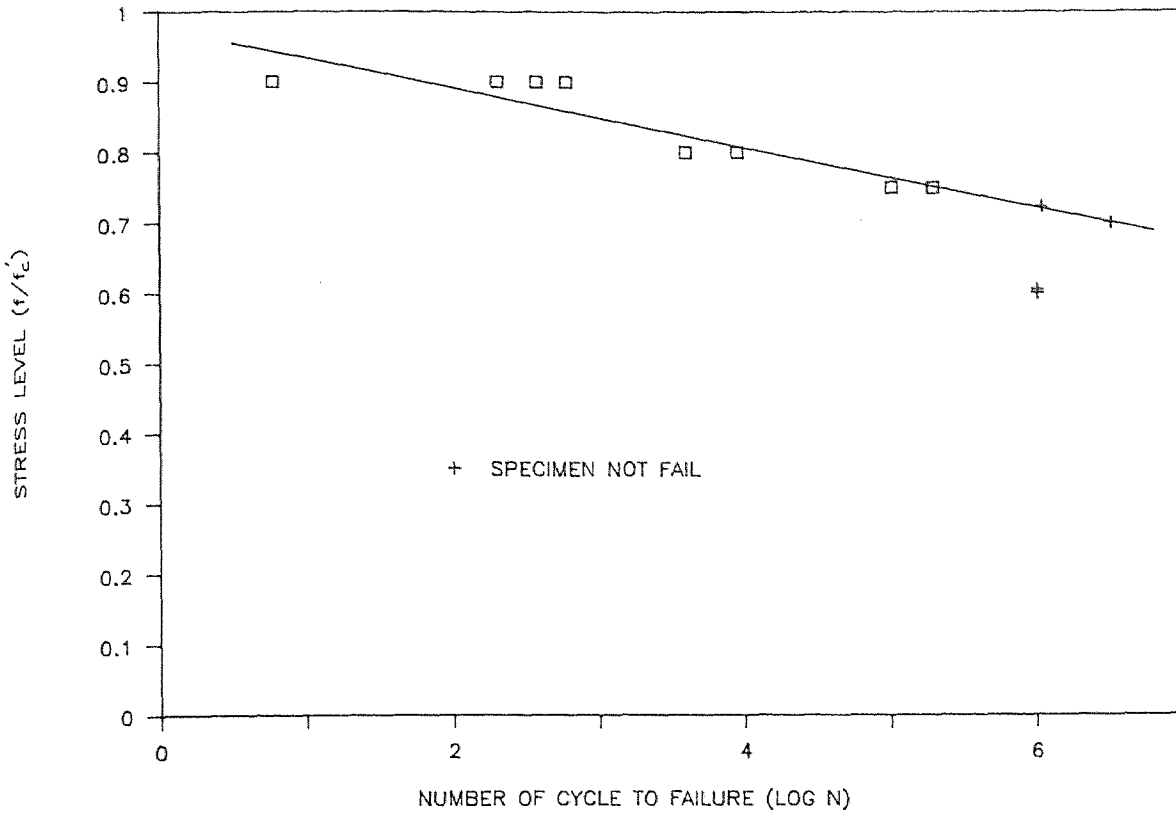
S-N CURVE

SUPERPLASTICIZER CONCRETE, RATE = 6 Hz.



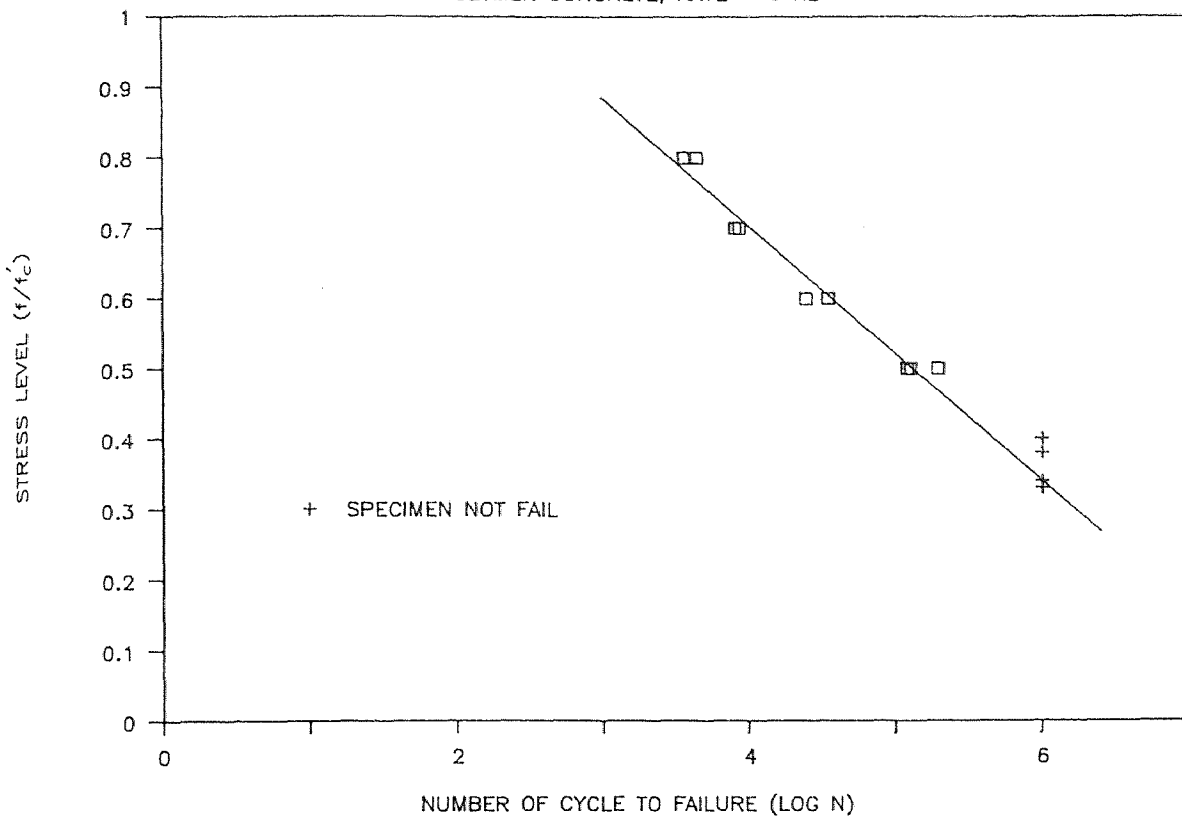
S-N CURVE

MICROSILICA CONCRETE, RATE = 6 Hz.



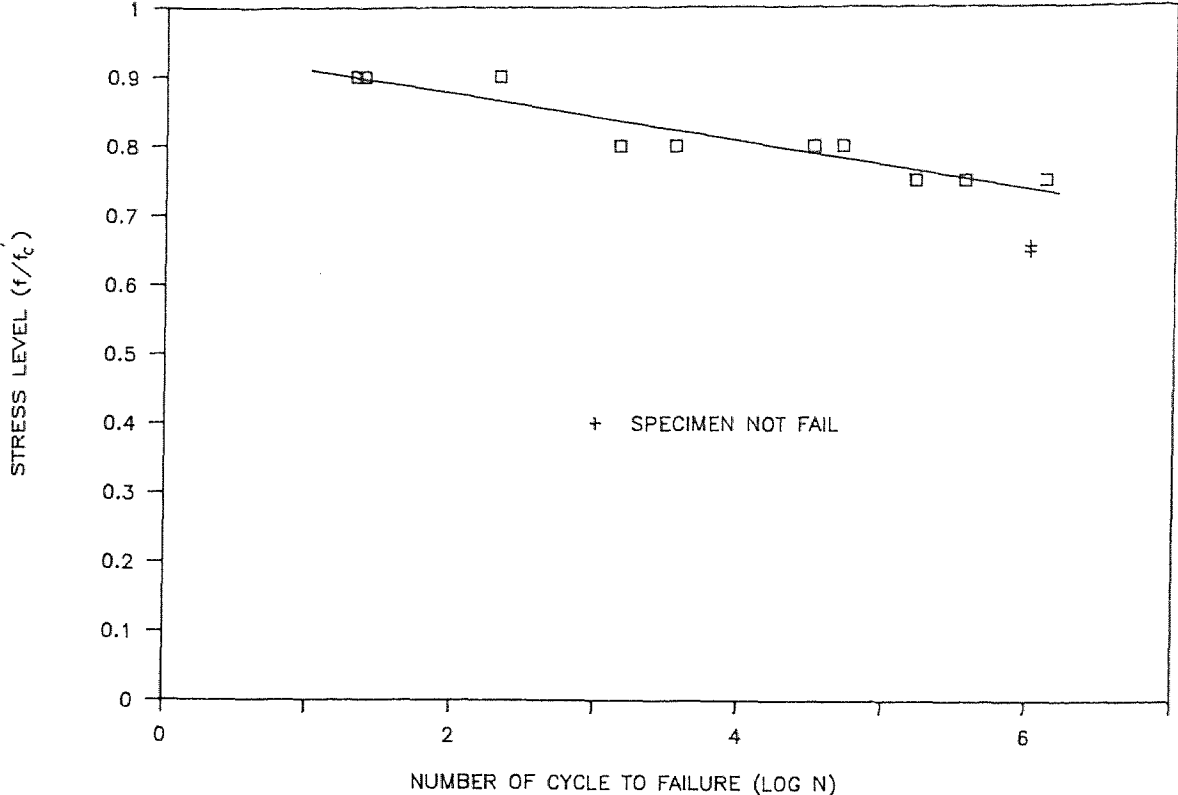
S-N CURVE

POLYMER CONCRETE, RATE = 6 Hz



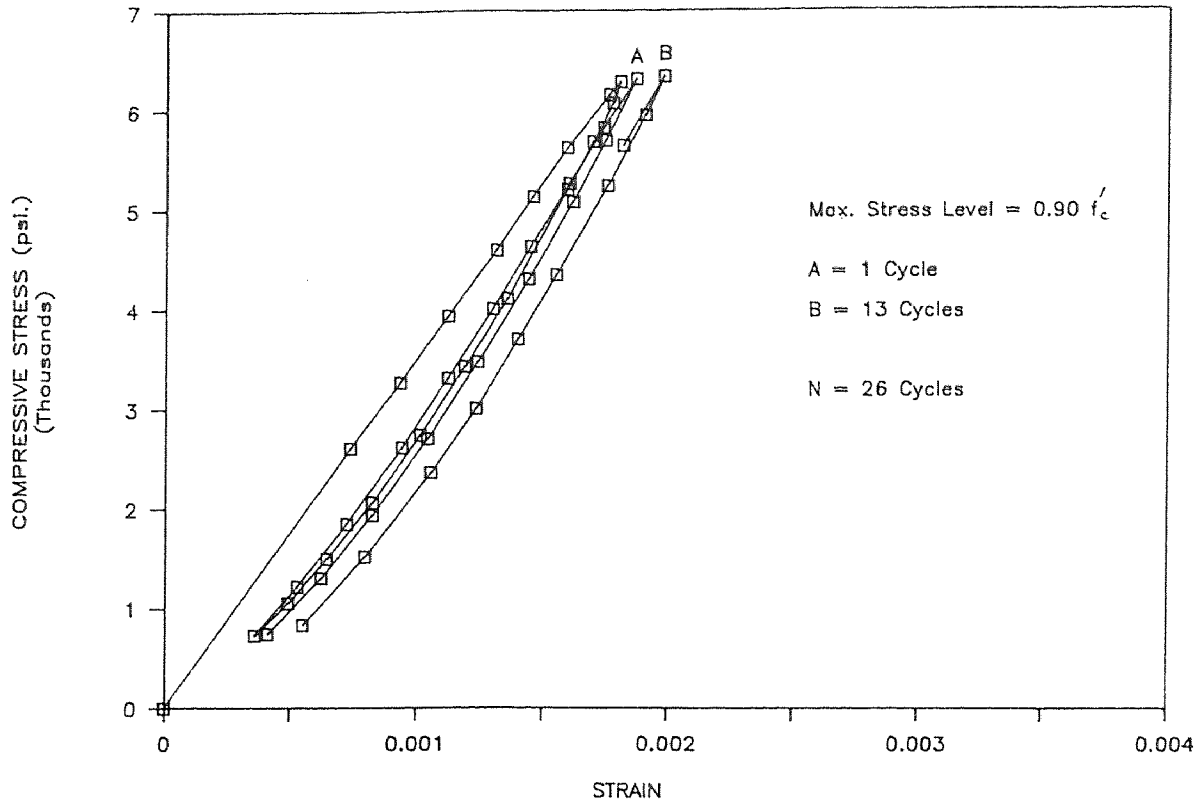
S - N CURVE

MICROSILICA CONCRETE, RATE = 12 Hz.



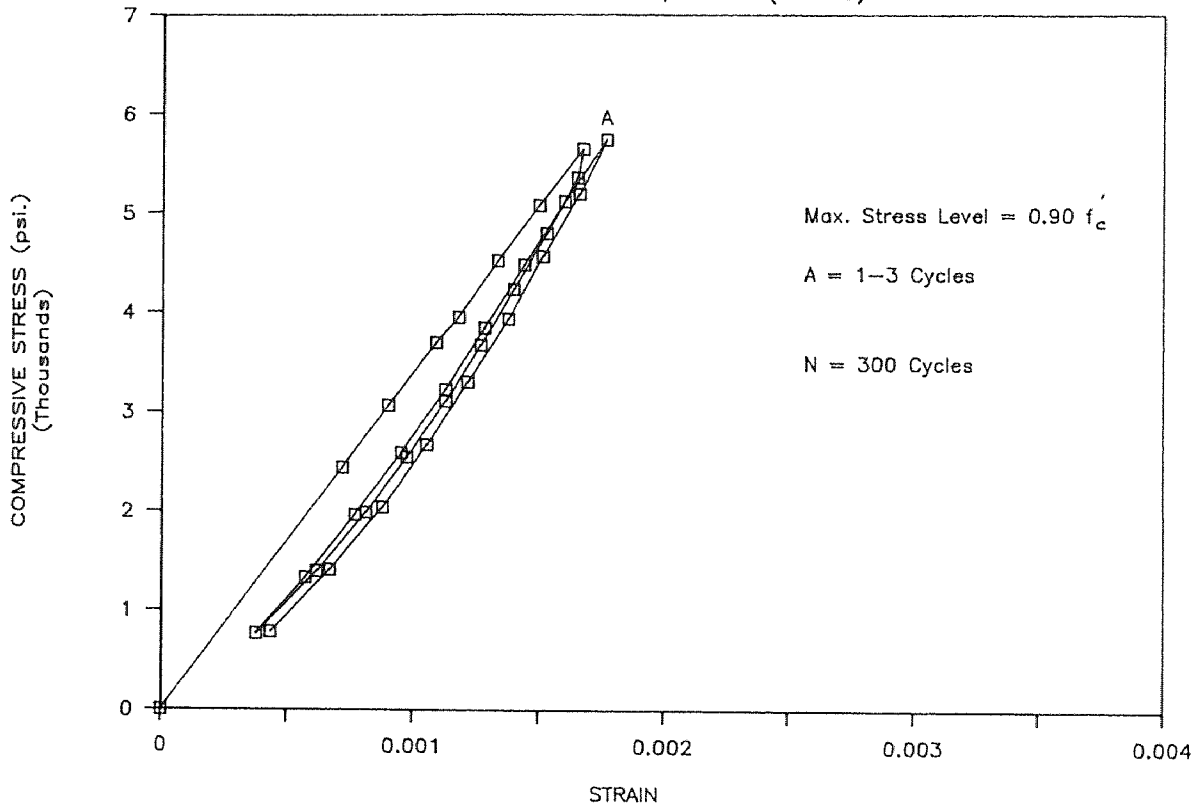
FATIGUE TEST

SUPERPLASTICIZER CONC., R=6 Hz.(S1F309)



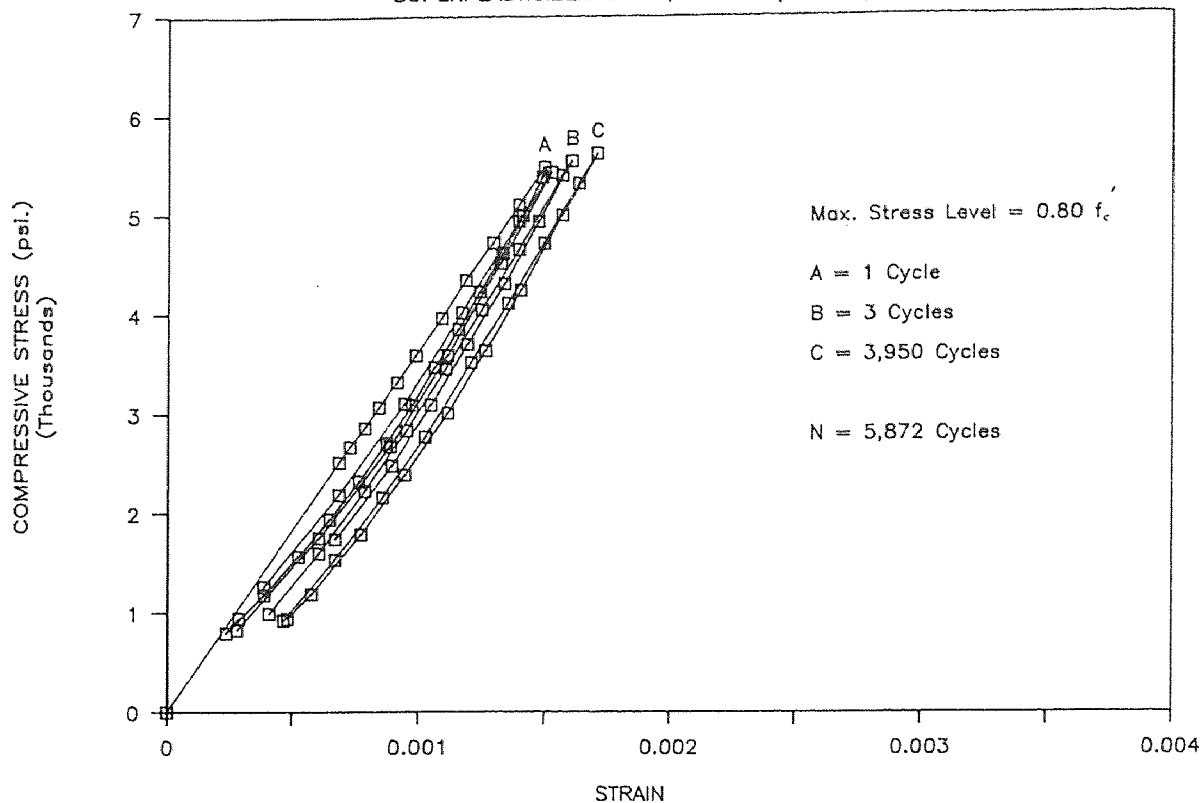
FATIGUE TEST

SUPERPLASTICIZER CONC., R=6 Hz.(S1F409)



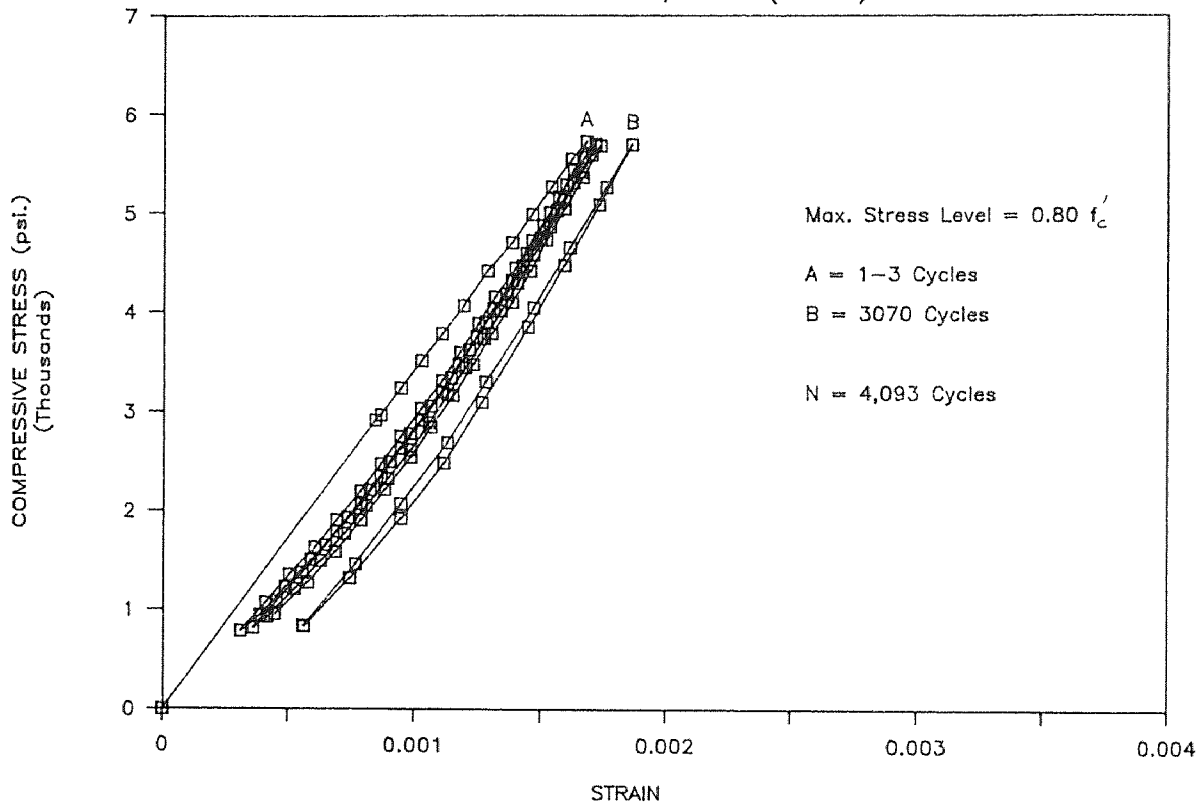
FATIGUE TEST

SUPERPLASTICIZER CONC., R=6 Hz.(S1F108)



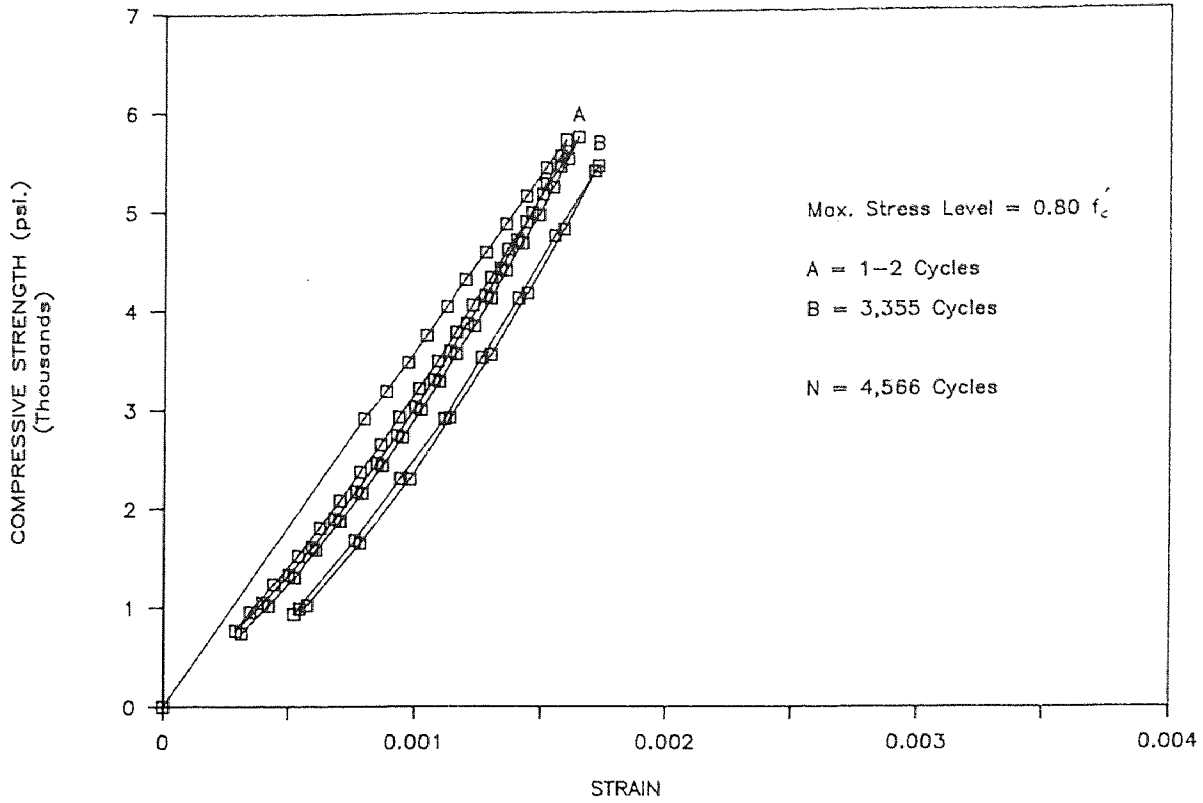
FATIGUE TEST

SUPERPLASTICIZER CONC., R=6 Hz.(S1F208)



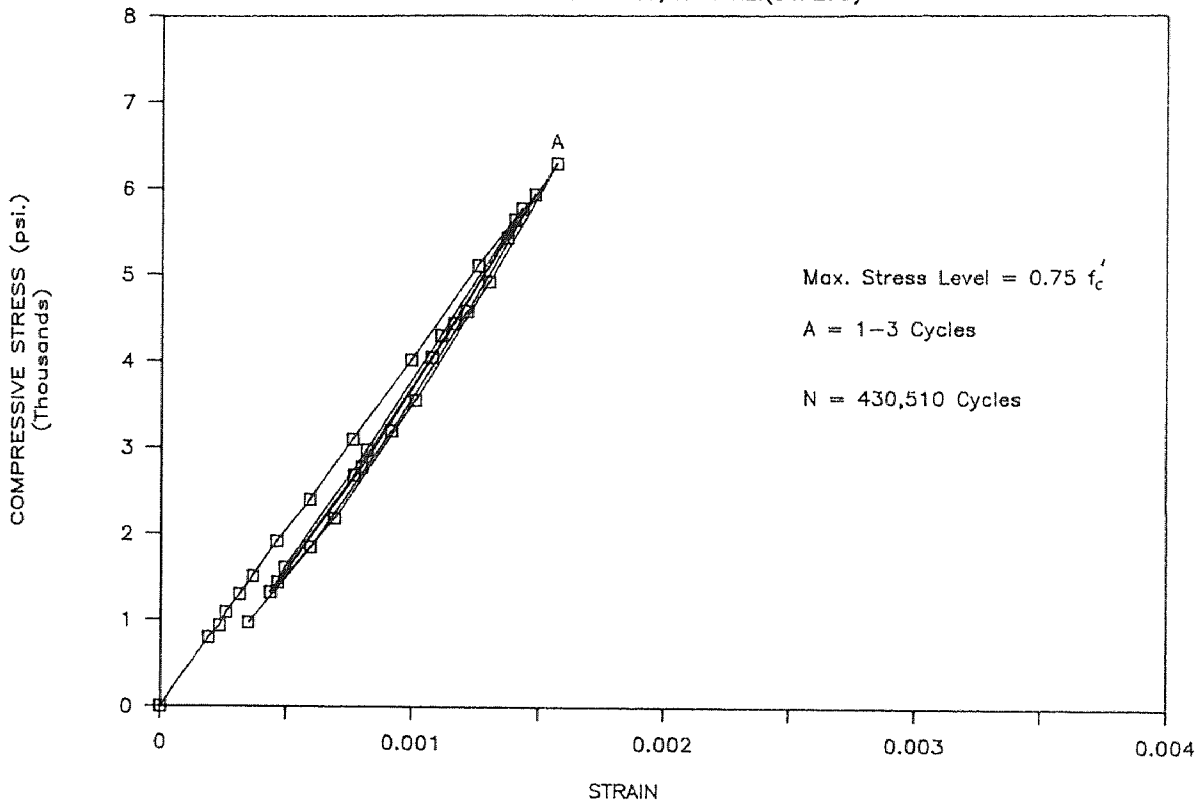
FATIGUE TEST

SUPERPLASTICIZER CONC., R=6 Hz.(S1F308)



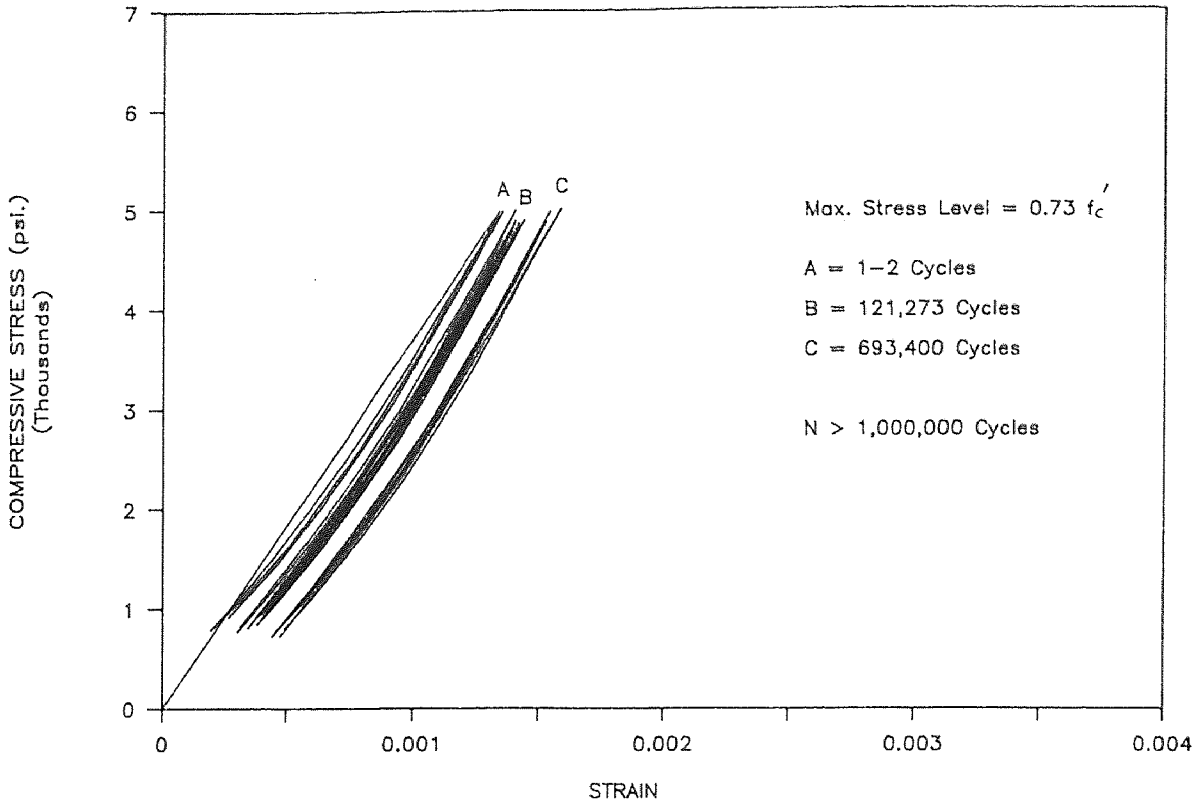
FATIGUE TEST

SUPERPLASTICIZER CONC., R=6 Hz.(S1F275)



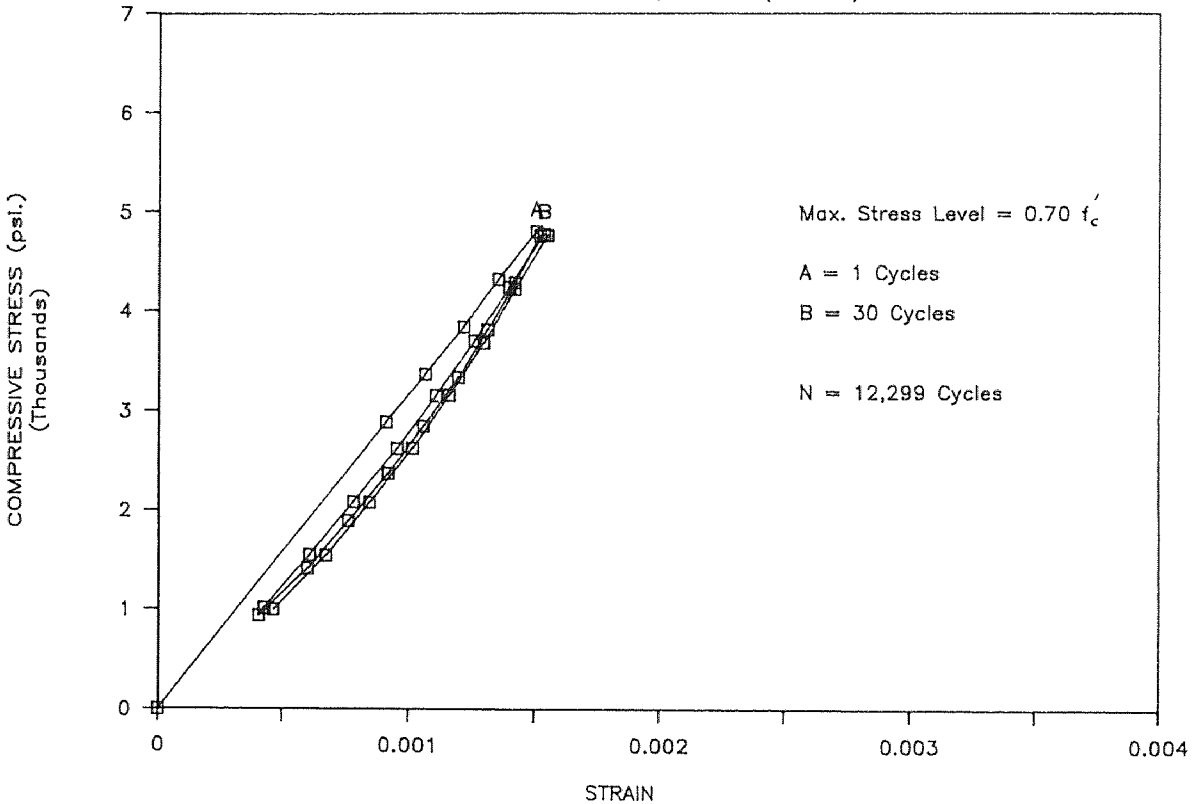
FATIGUE TEST

SUPERPLASTICIZER CONC., R=6 Hz.(S1F207)



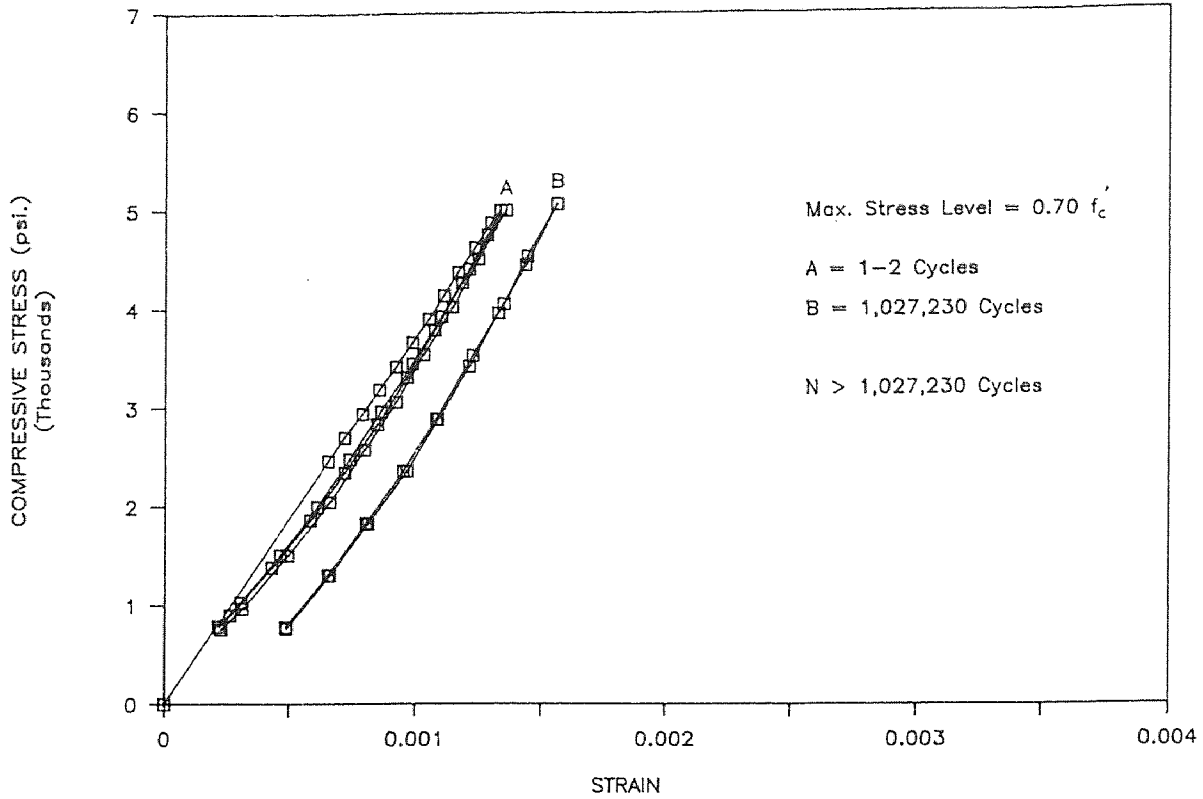
FATIGUE TEST

SUPERPLASTICIZER CONC., R=6 Hz.(S1F107)



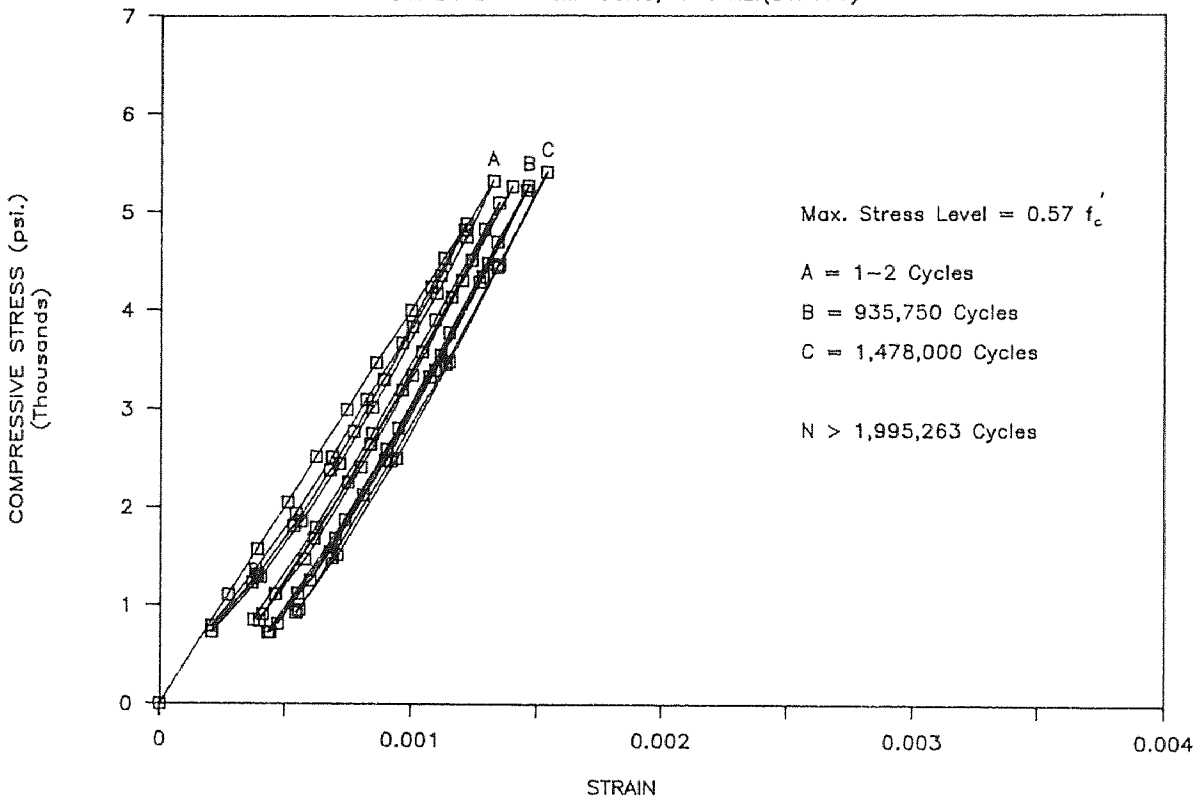
FATIGUE TEST

SUPERPLASTICIZER CONC, R=6 Hz.(S1F307)



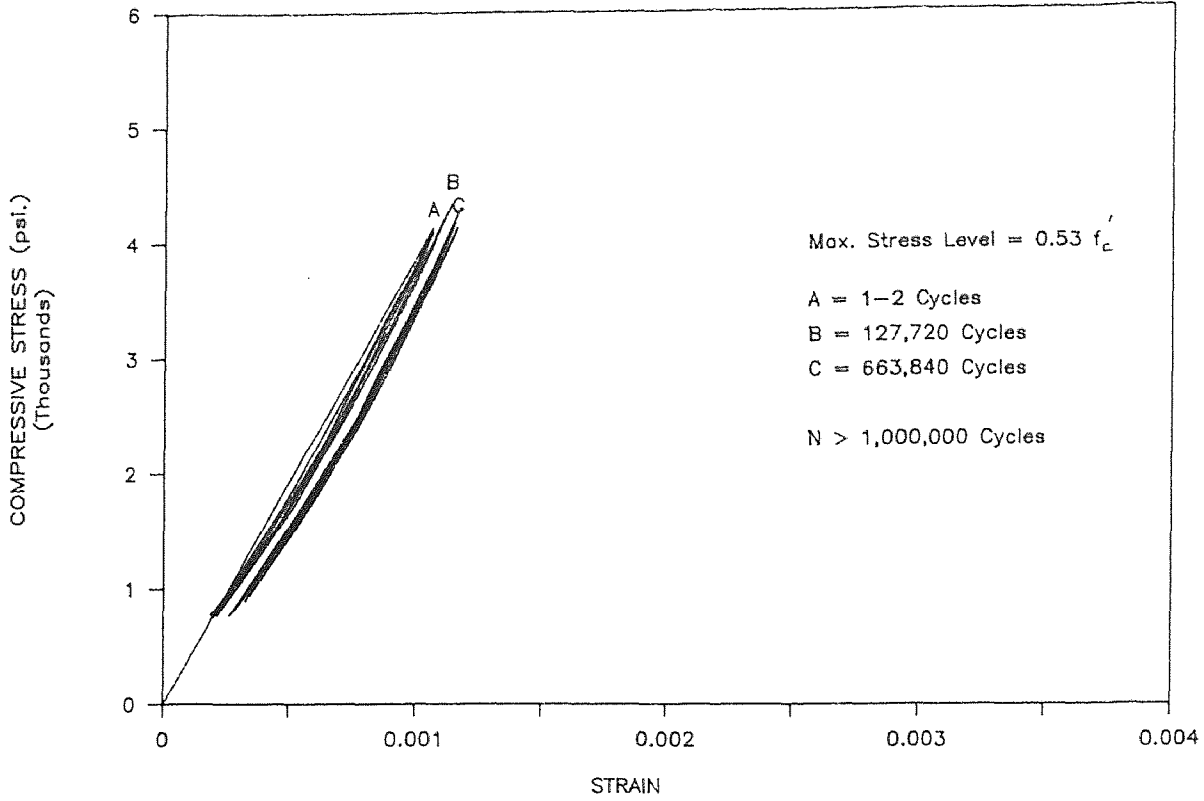
FATIGUE TEST

SUPERPLASTICIZER CONC, R=6 Hz.(S1F175)



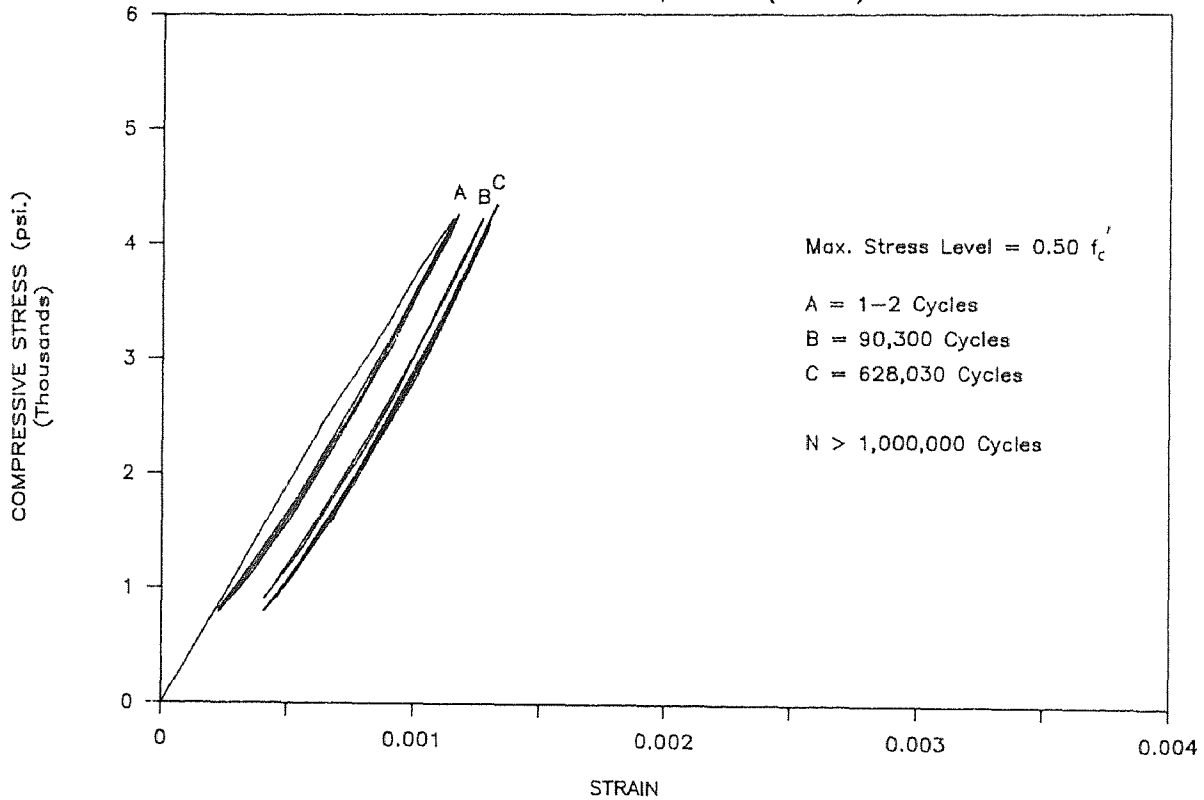
FATIGUE TEST

SUPERPLASTICIZER CONC, R=6 Hz.(S1F106)



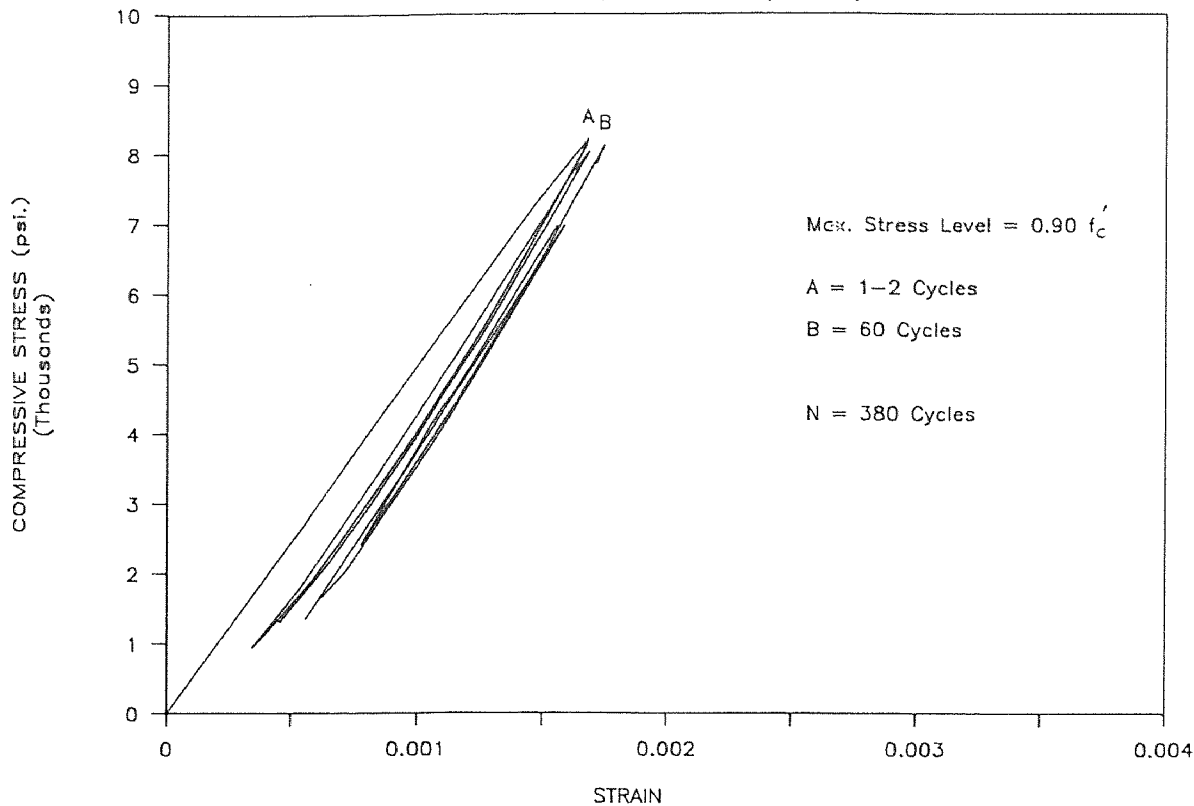
FATIGUE TEST

SUPERPLASTICIZER CONC, R=6 Hz.(S1F206)



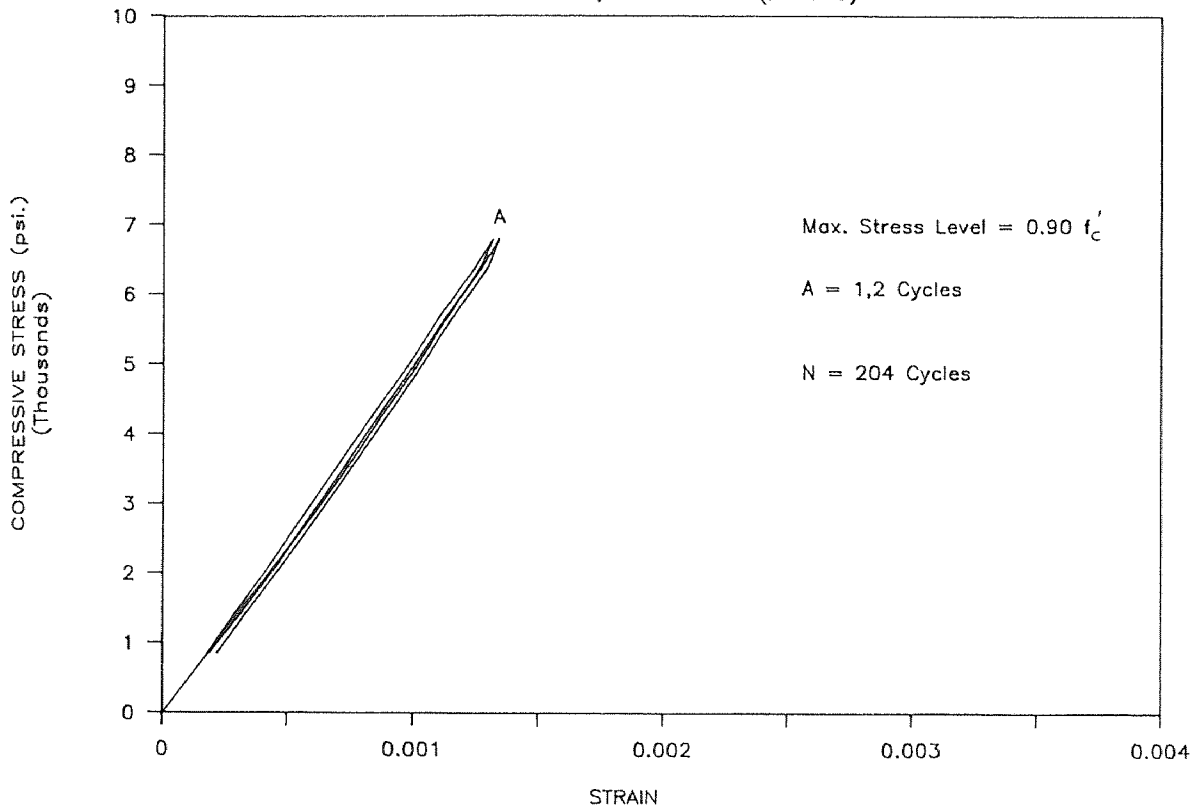
FATIGUE TEST

MICROSILICA CONC., RATE = 6 Hz.(M1F209)



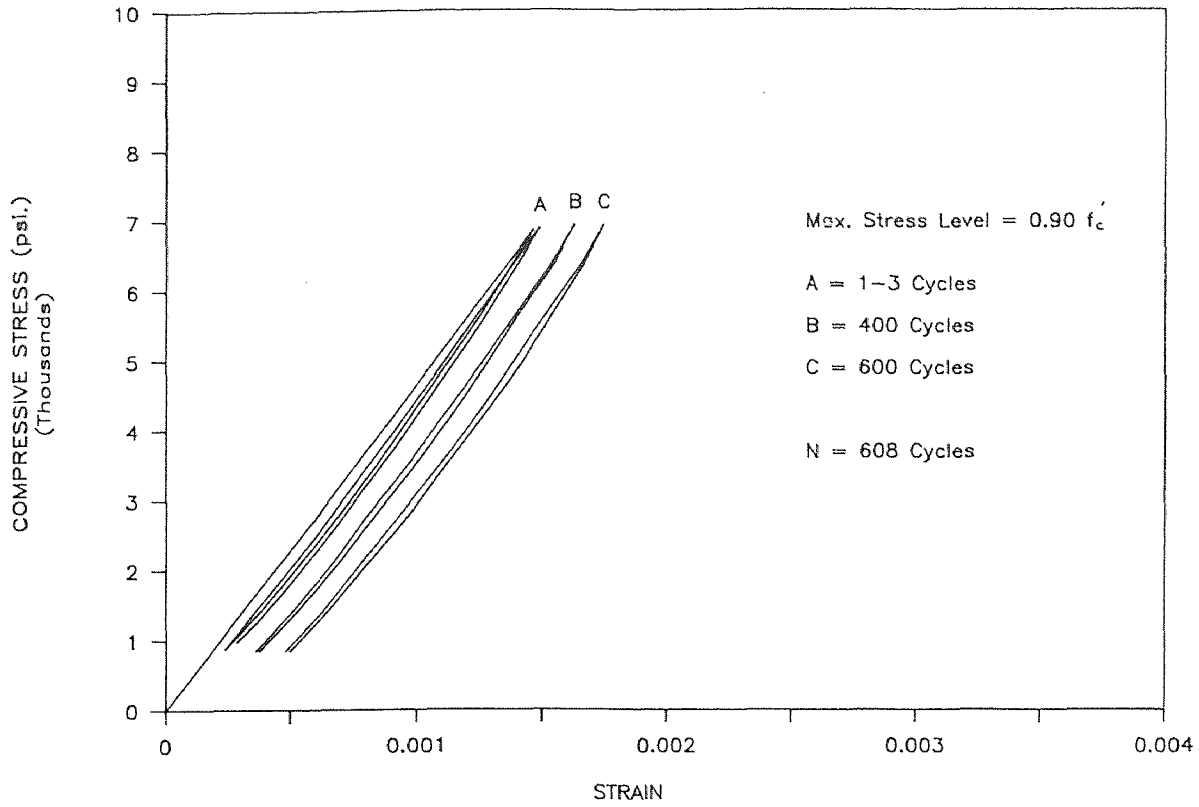
FATIGUE TEST

MICROSILICA CONC., RATE = 6 Hz.(M1F309)



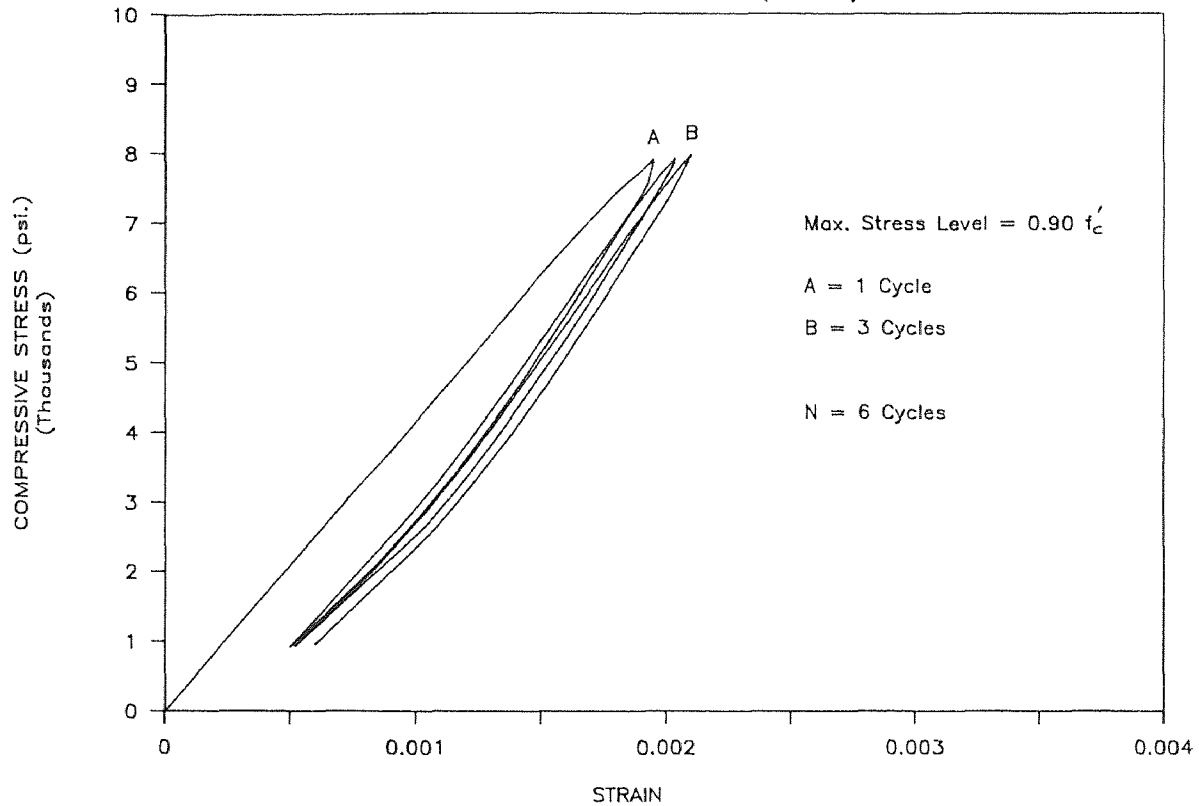
FATIGUE TEST

MICROSILICA CONC., RATE = 6 Hz.(M1F409)



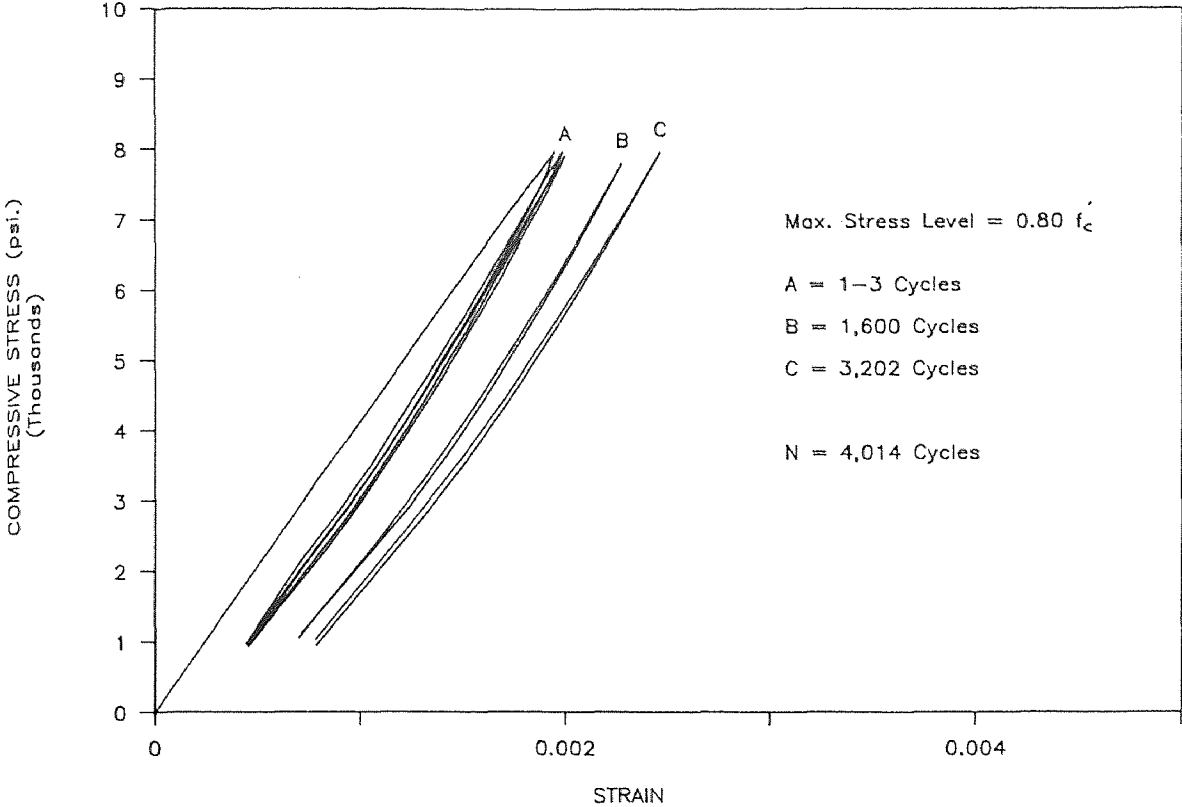
FATIGUE TEST

MICROSILICA CONC., RATE = 6 Hz.(M2F209)



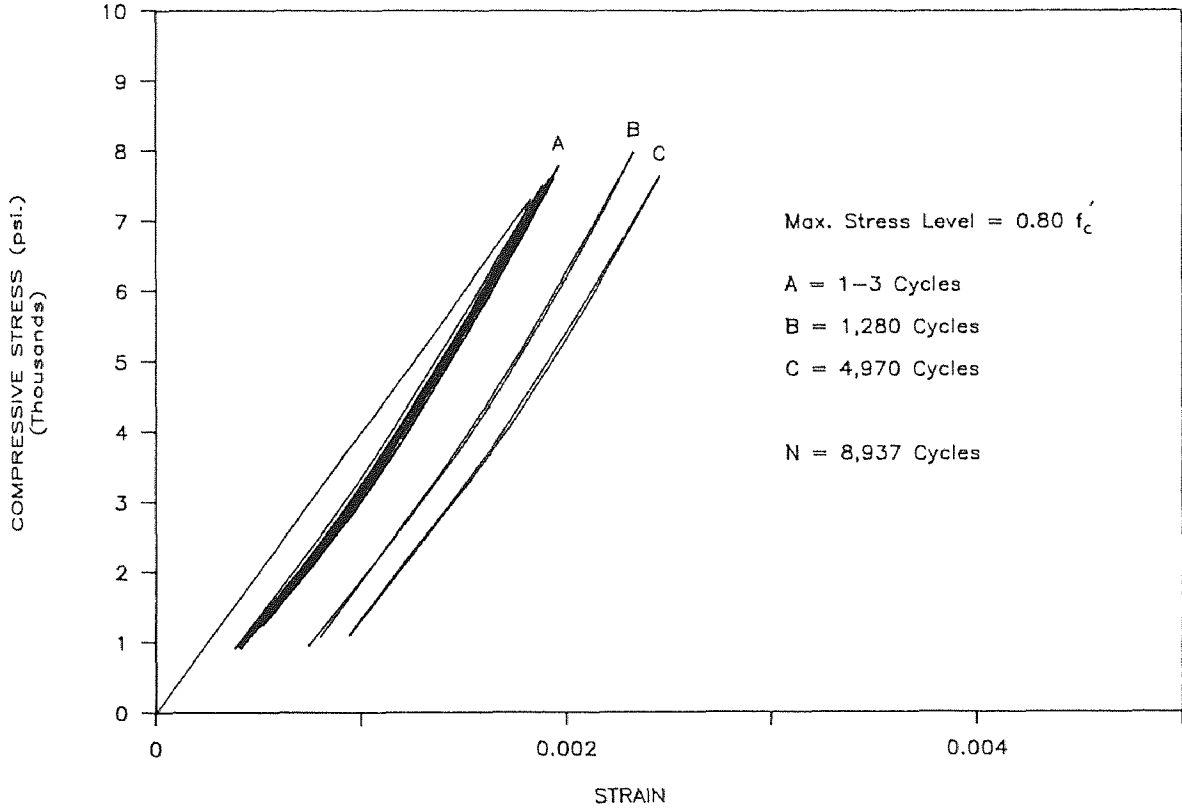
FATIGUE TEST

MICROSILICA CONC., RATE = 6 Hz.(M2F108)



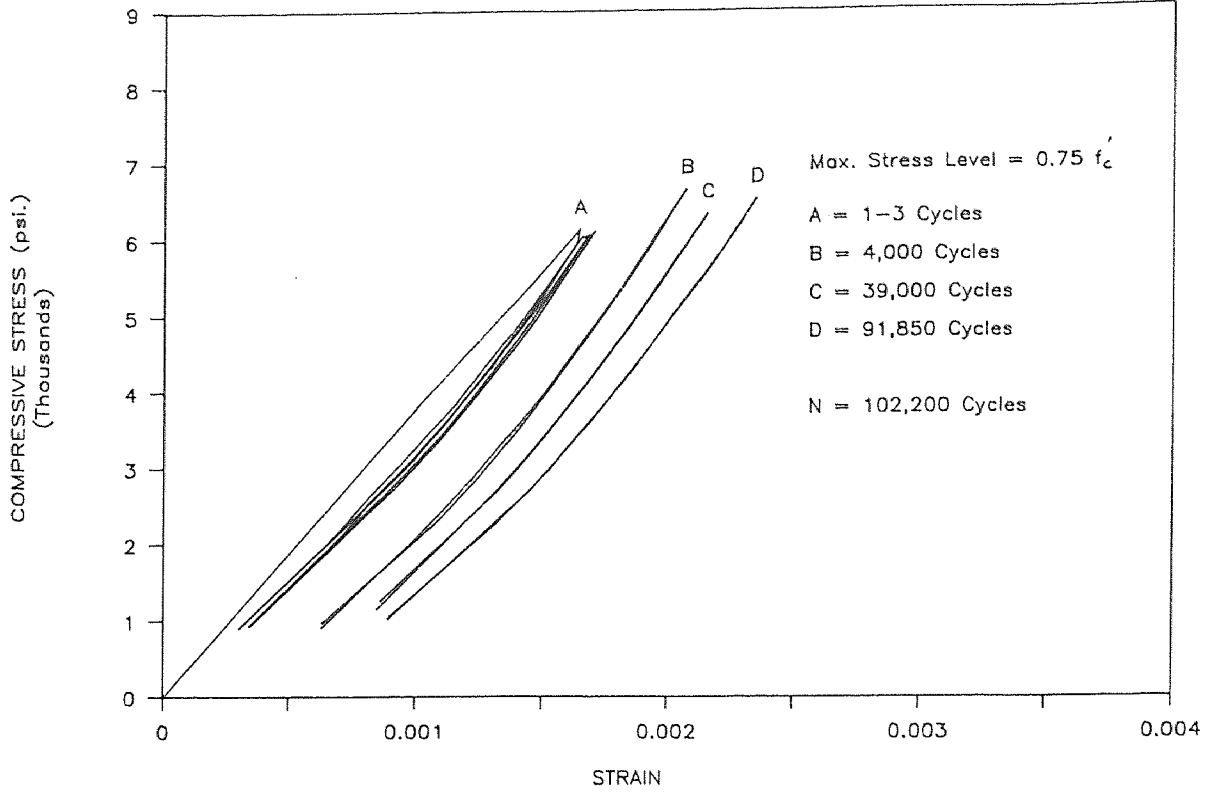
FATIGUE TEST

MICROSILICA CONC., RATE = 6 Hz.(M2F208)



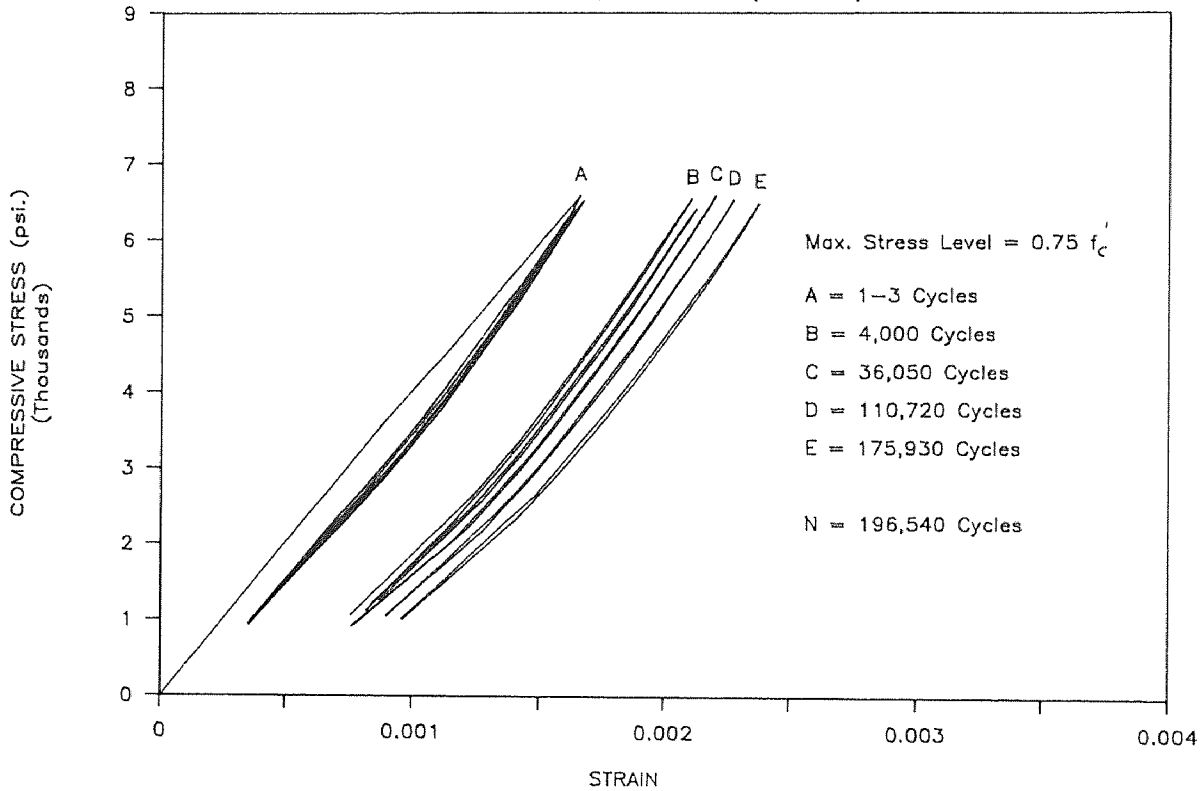
FATIGUE TEST

MICROSILICA CONC.,RATE = 6 Hz.(M2F2075)



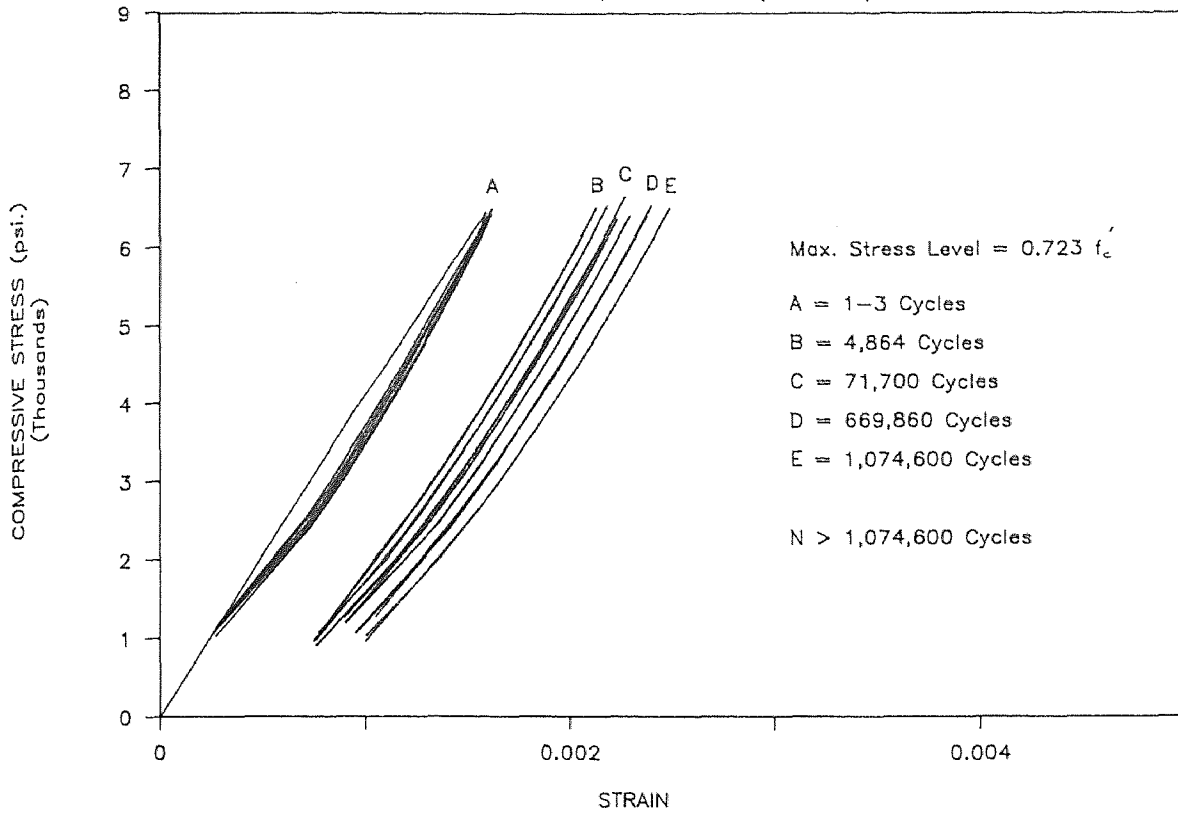
FATIGUE TEST

MICROSILICA CONC.,RATE = 6 Hz.(M2F3075)



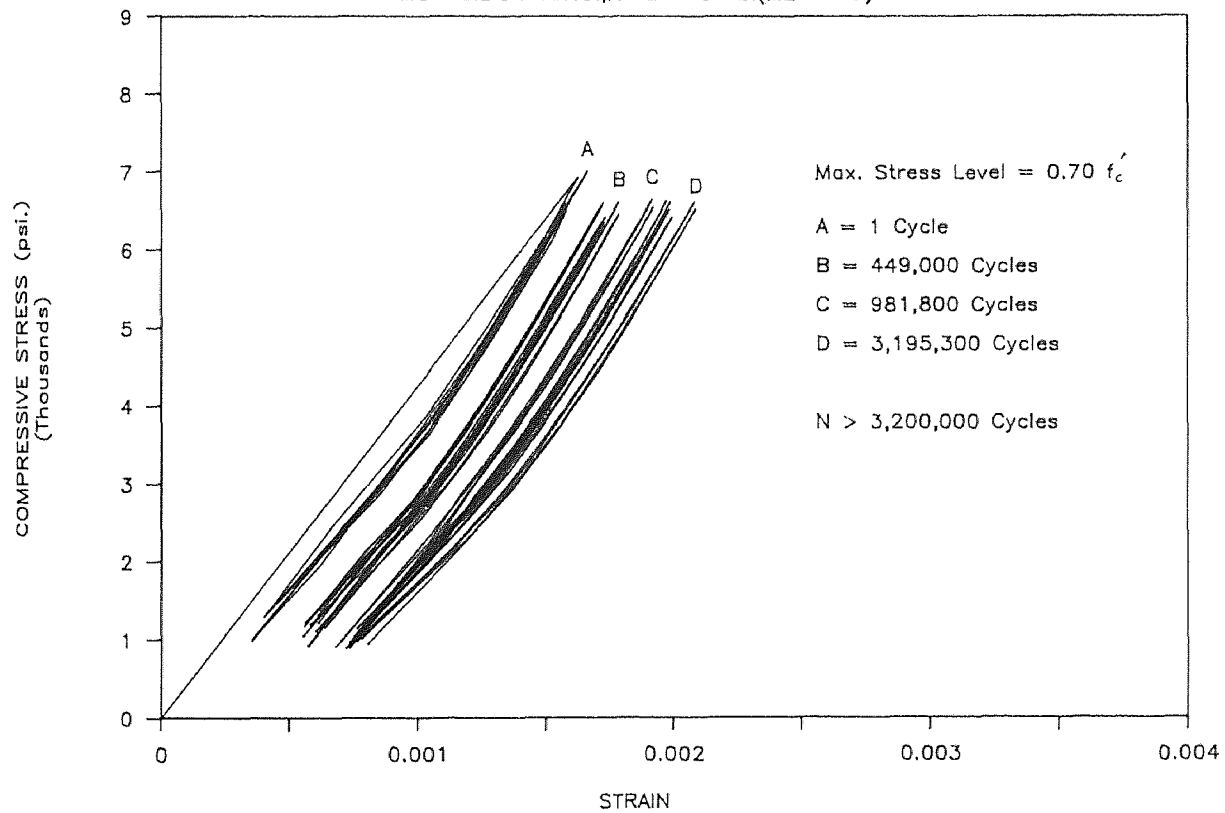
FATIGUE TEST

MICROSILICA CONC.,RATE = 6 Hz.(M2F4075)



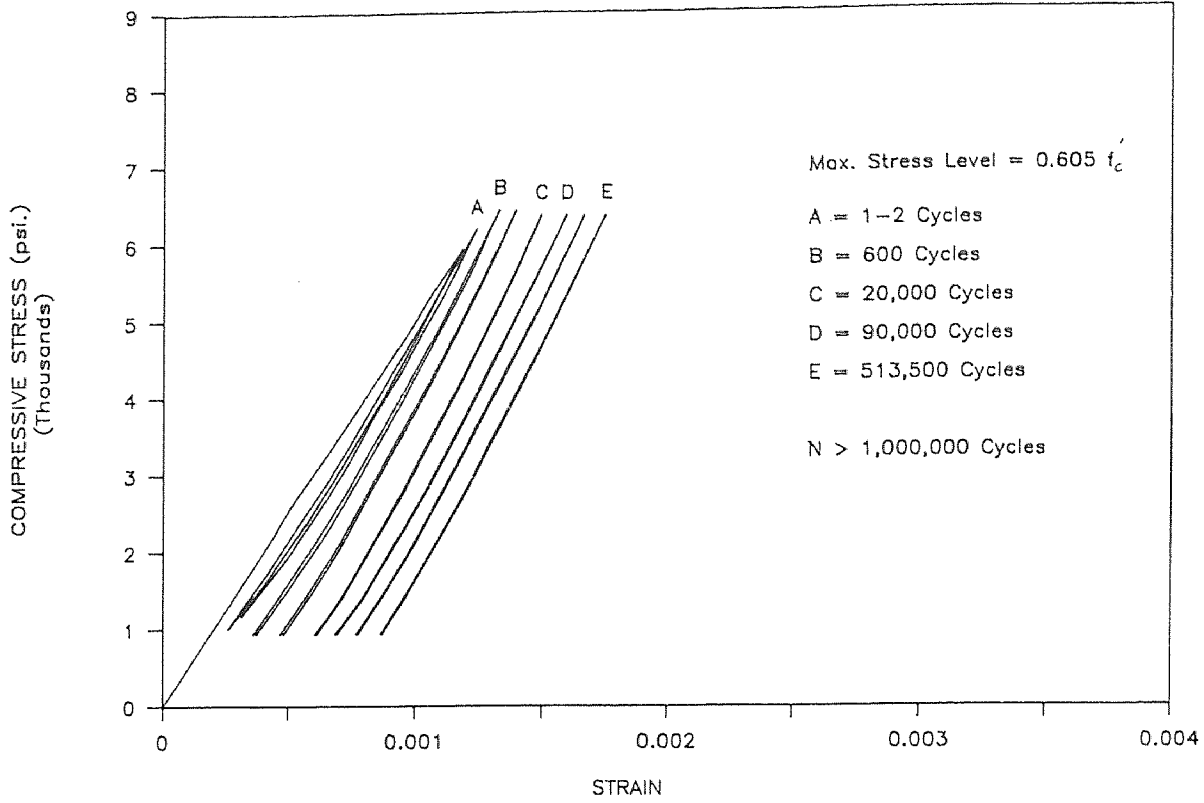
FATIGUE TEST

MICROSILICA CONC.,RATE = 6 Hz.(M2F1075)



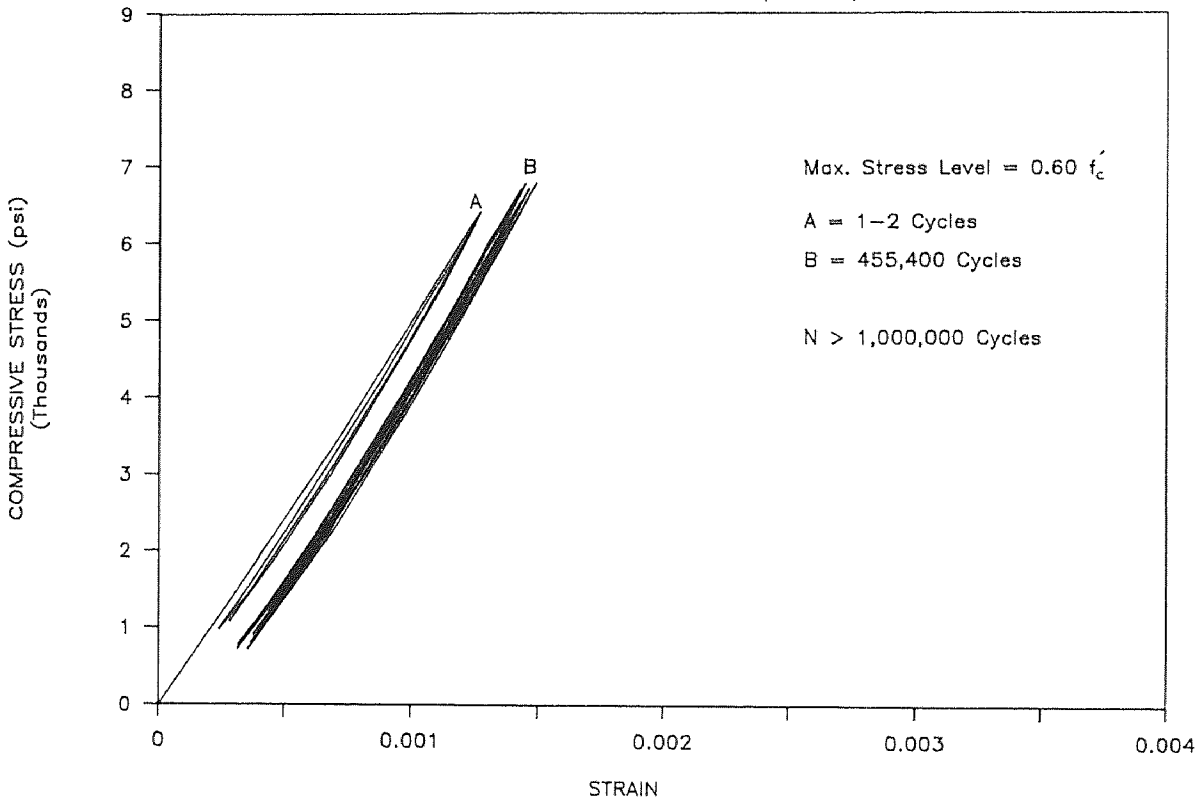
FATIGUE TEST

MICROSILICA CONC., RATE = 6 Hz.(M1F107)



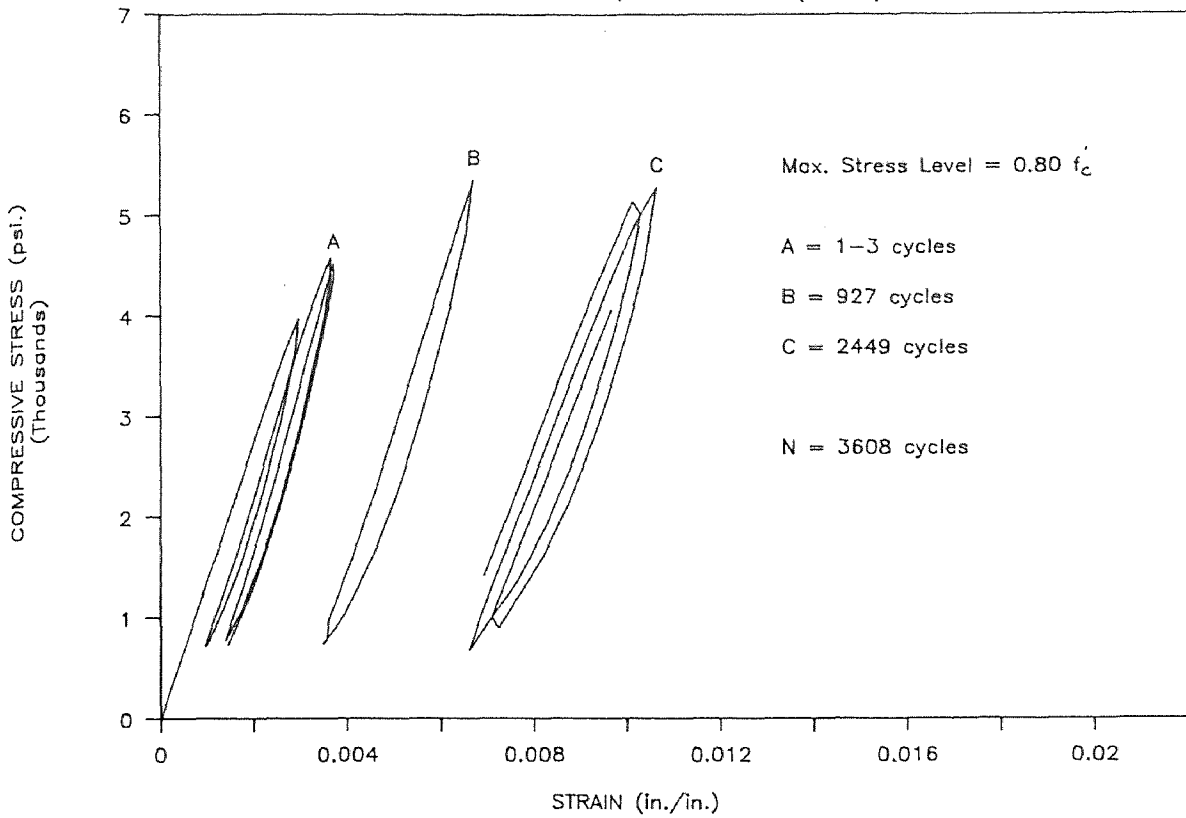
FATIGUE TEST

MICROSILICA CONC., RATE = 6 Hz.(M1F207)



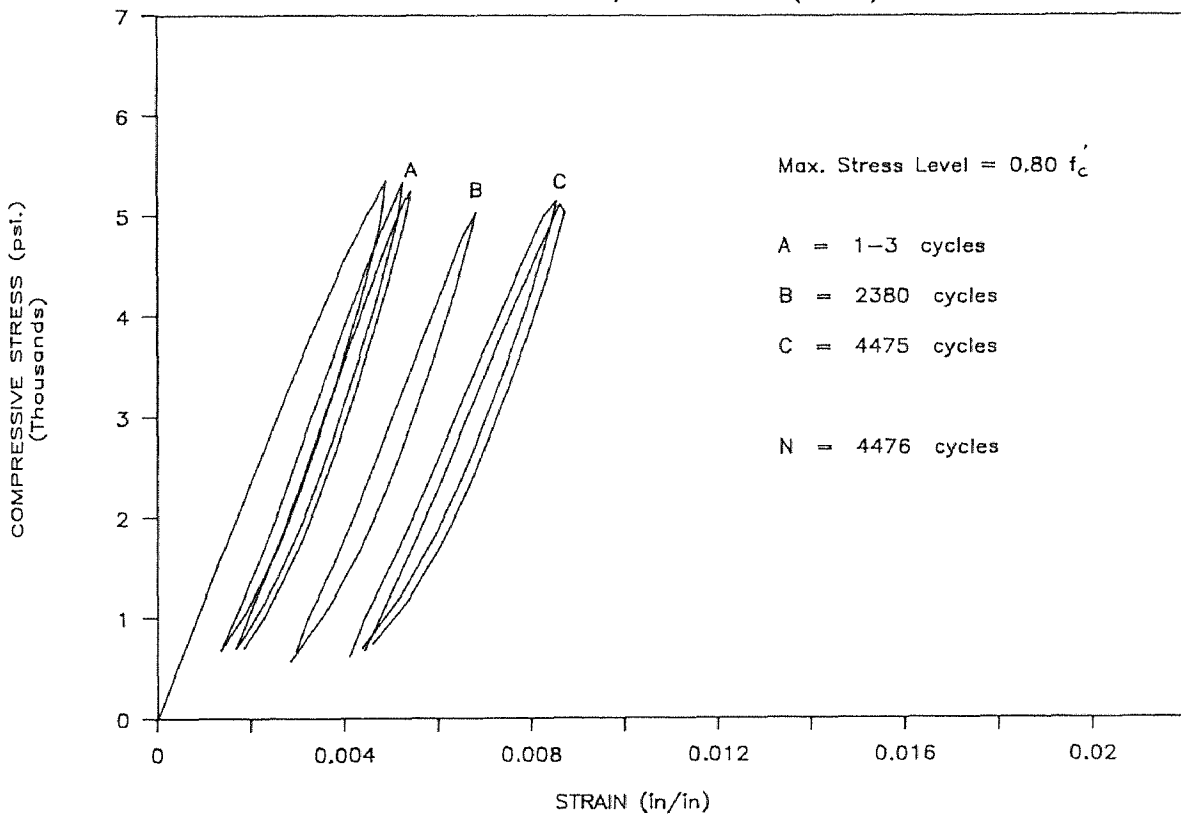
FATIGUE TEST

POLYMER CONCRETE , RATE = 6 Hz. (PF108)



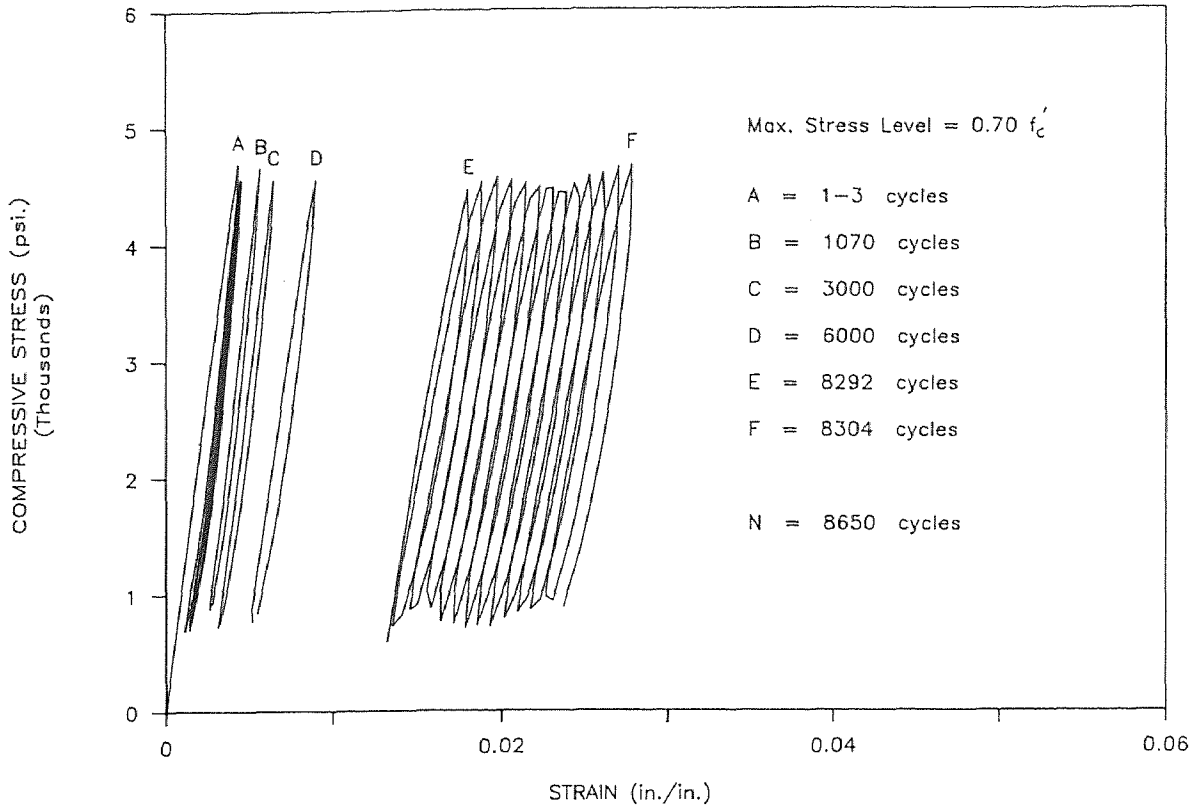
FATIGUE TEST

POLYMER CONCRETE , RATE = 6 Hz. (PF208)



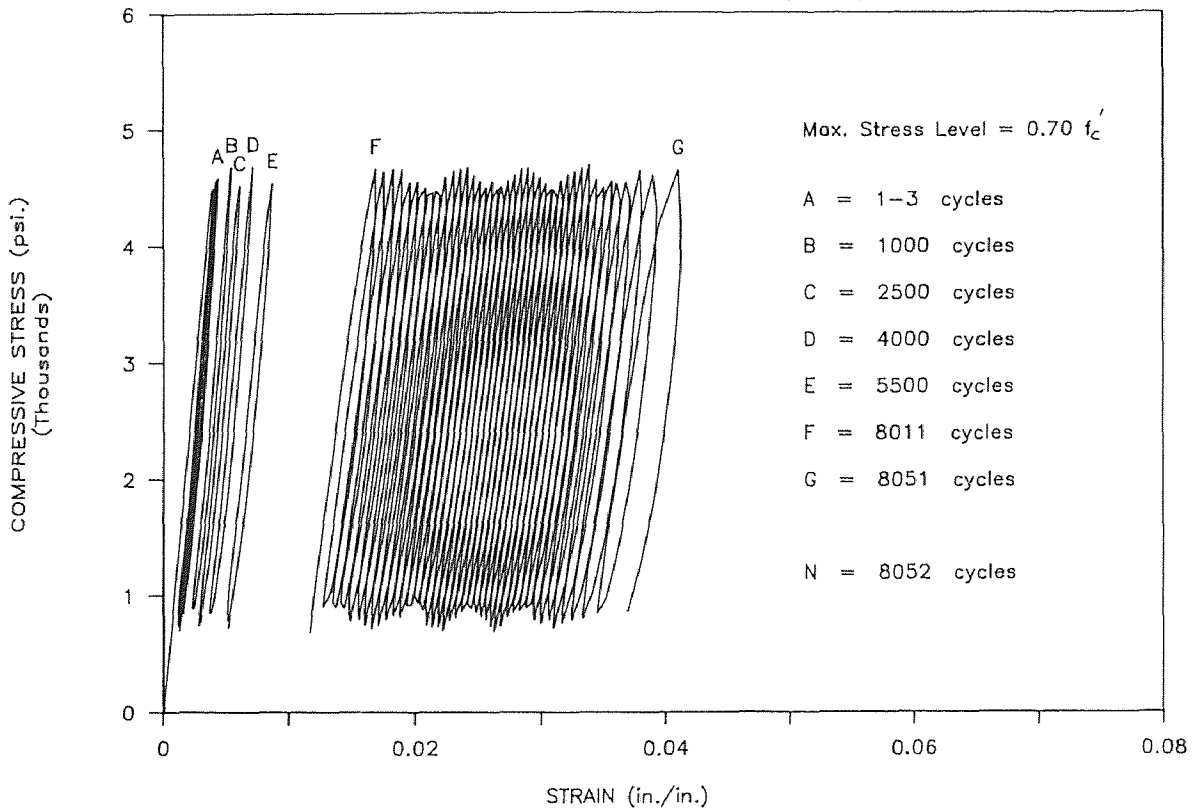
FATIGUE TEST

POLYMER CONCRETE , RATE = 6 Hz. (PF107)



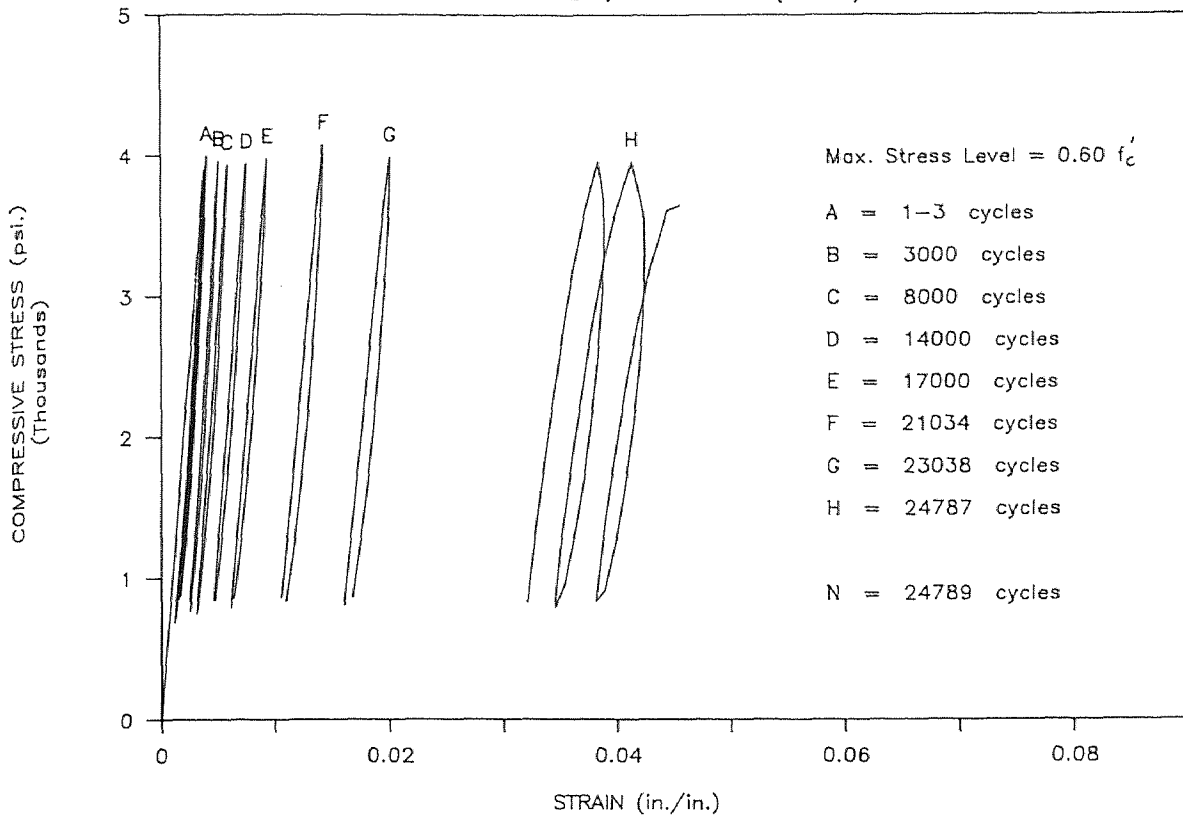
FATIGUE TEST

POLYMER CONCRETE , RATE = 6 Hz. (PF207)



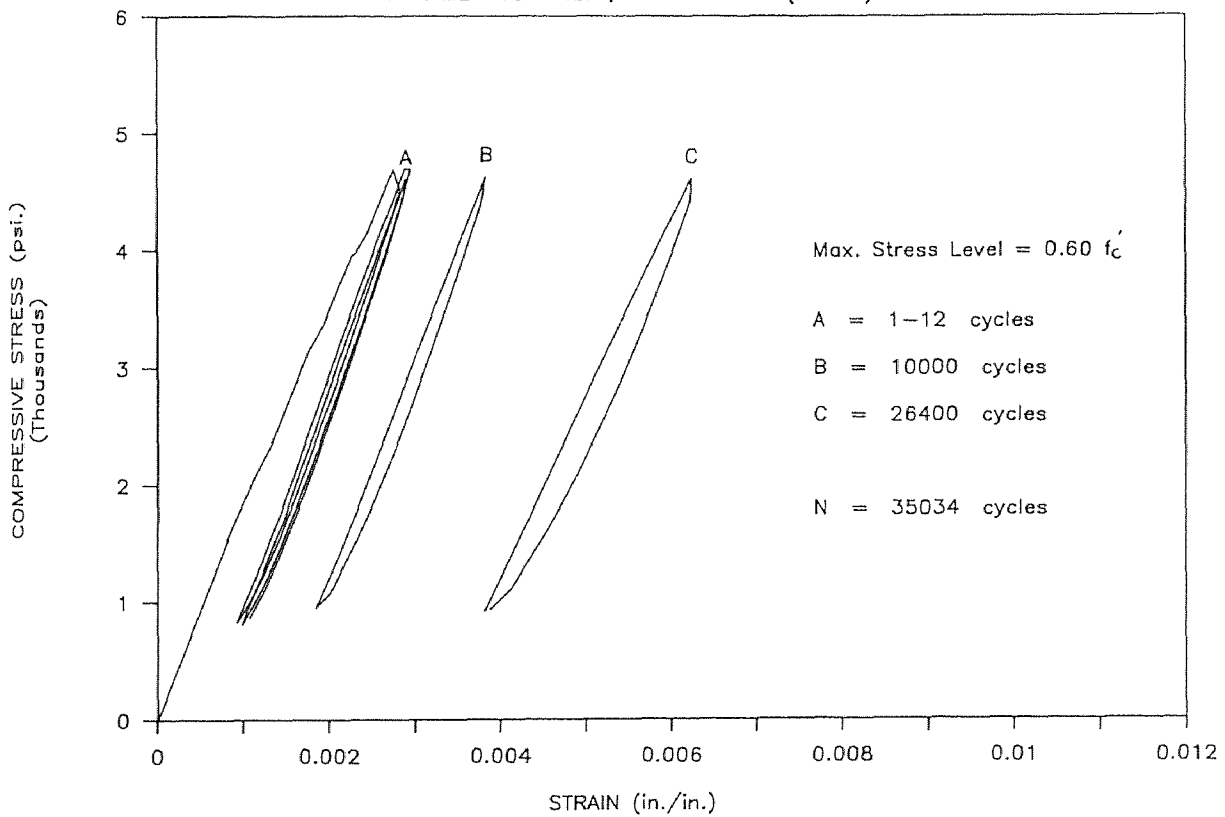
FATIGUE TEST

POLYMER CONCRETE, RATE = 6 Hz.(PF106)



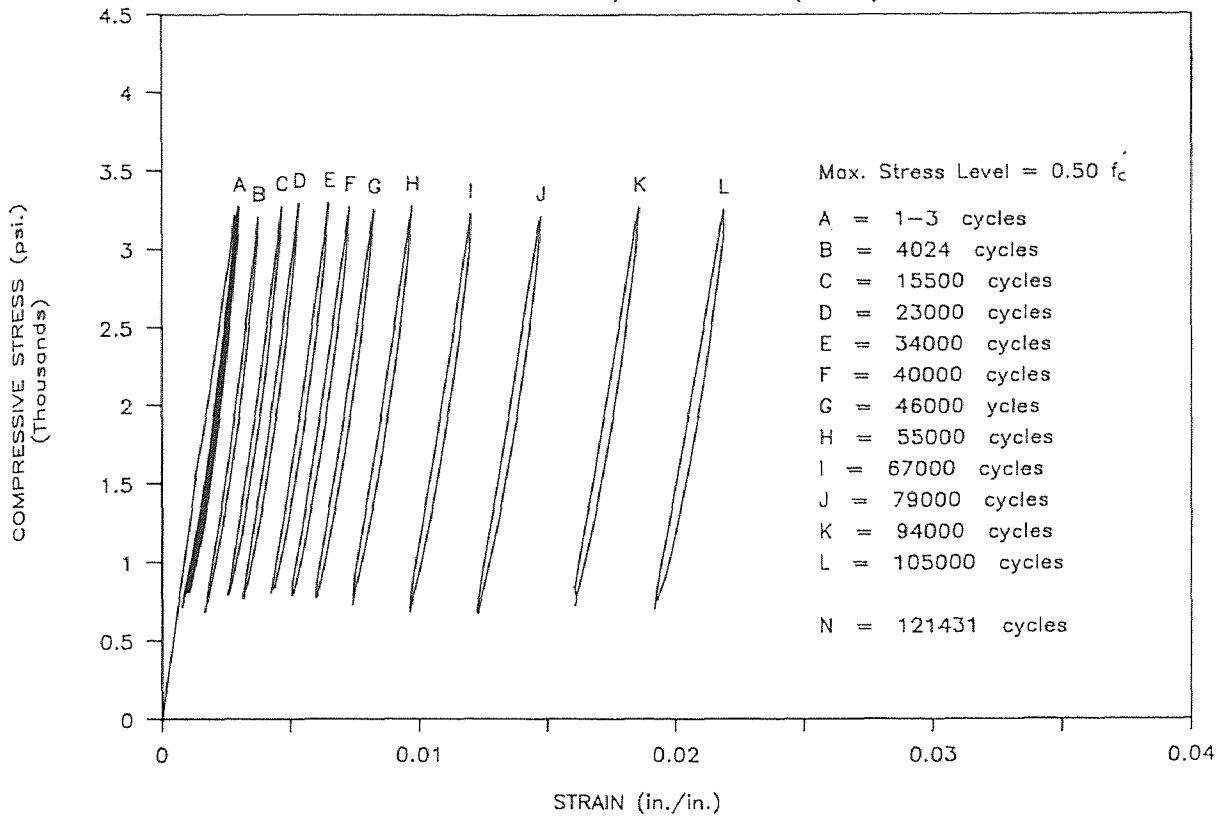
FATIGUE TEST

POLYMER CONCRETE, RATE = 6 Hz. (PF206)



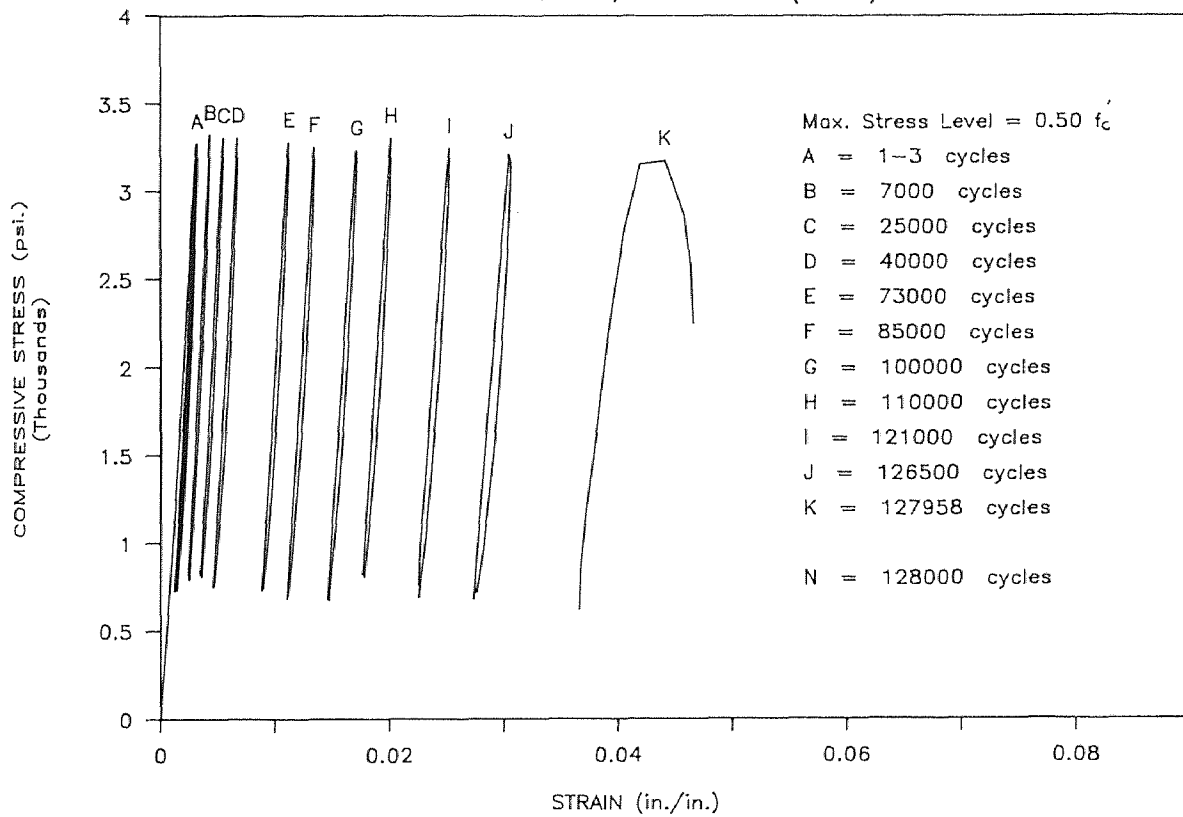
FATIGUE TEST

POLYMER CONCRETE, RATE = 6 Hz. (PF105)



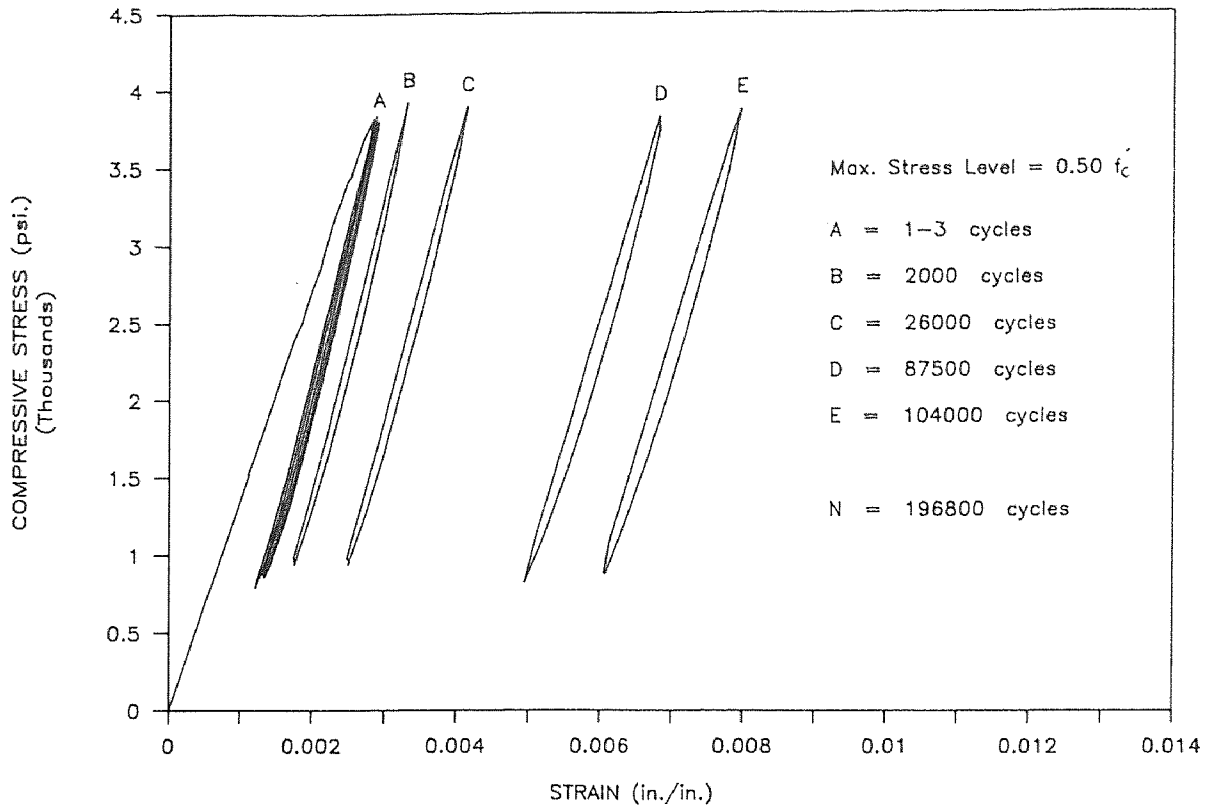
FATIGUE TEST

POLYMER CONCRETE, RATE = 6 Hz. (PF205)



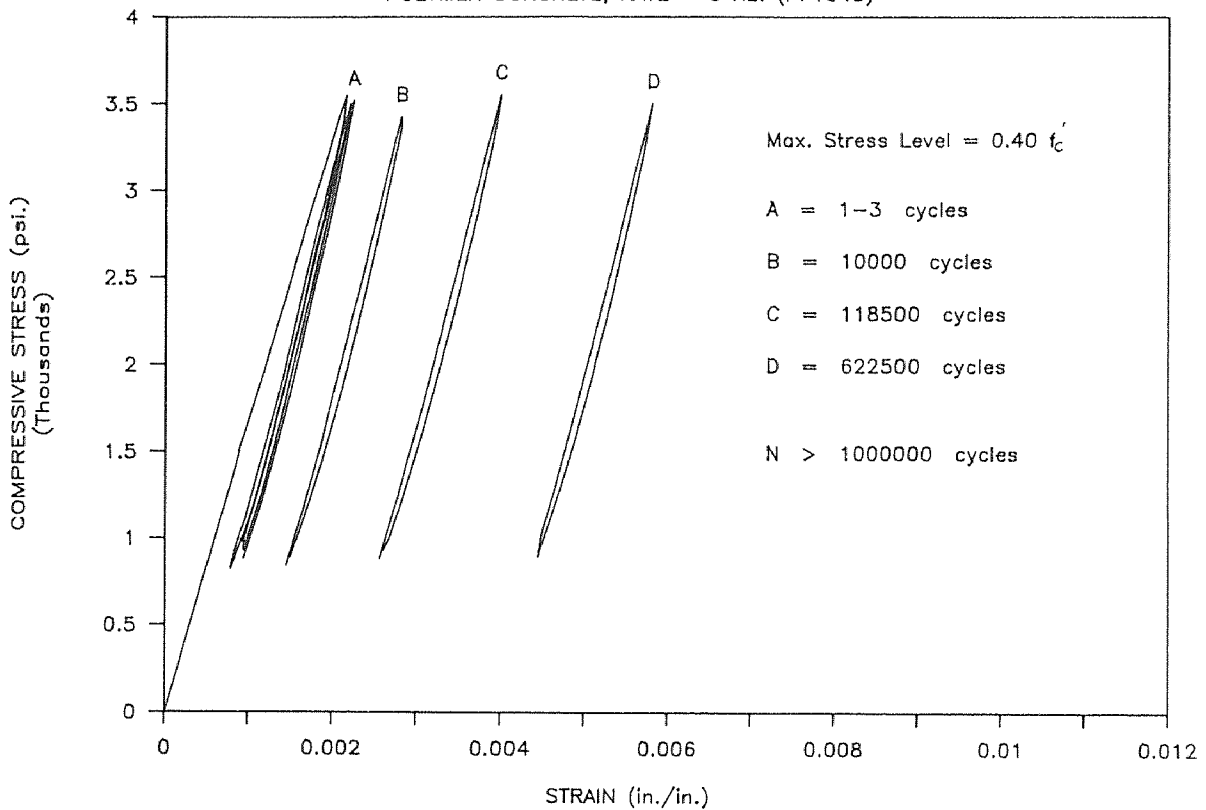
FATIGUE TEST

POLYMER CONCRETE, RATE = 6 Hz. (PF305)



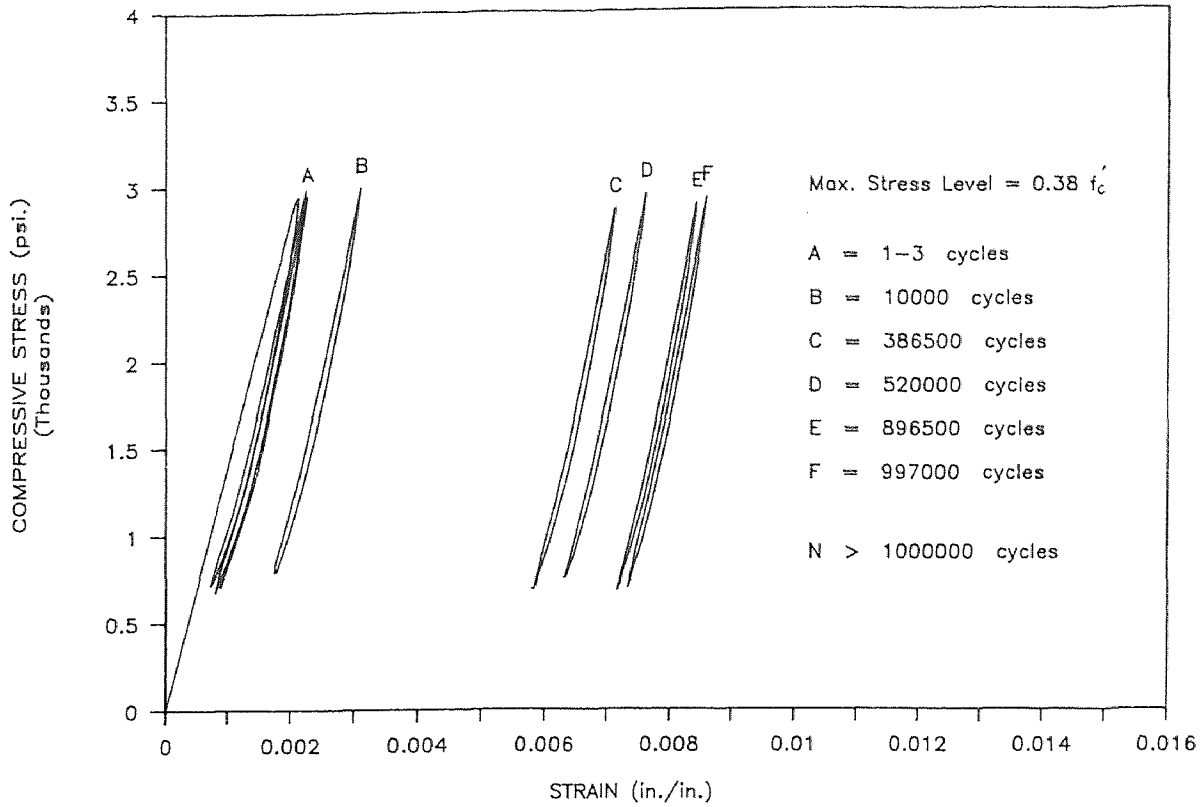
FATIGUE TEST

POLYMER CONCRETE, RATE = 6 Hz. (PF1045)



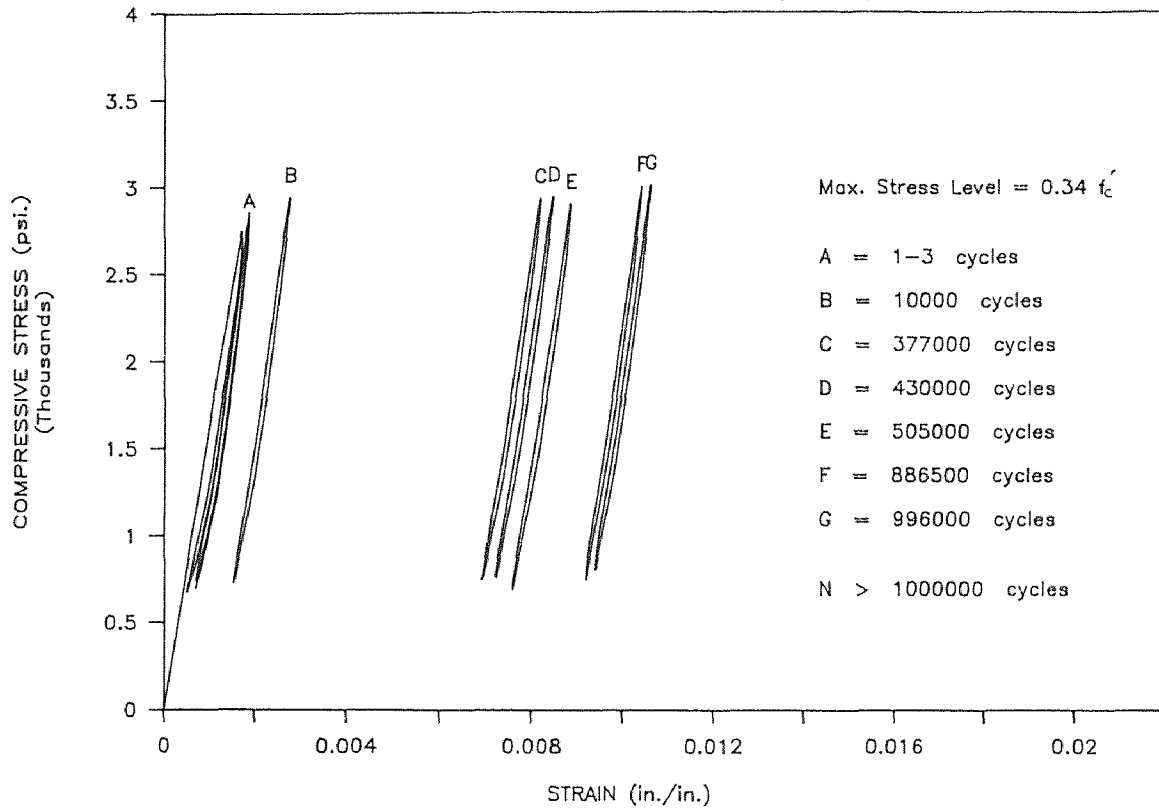
FATIGUE TEST

POLYMER CONCRETE, RATE = 6 Hz. (PF2045)



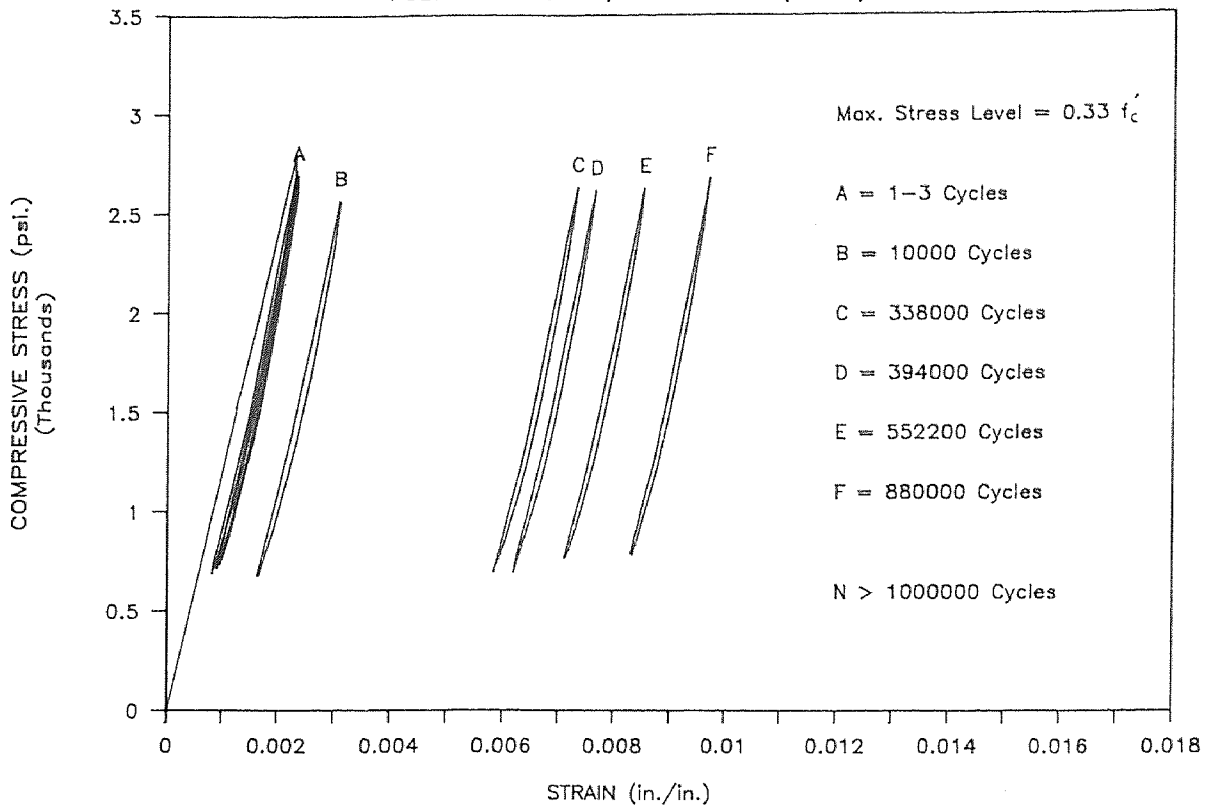
FATIGUE TEST

POLYMER CONCRETE, RATE = 6 Hz. (PF3045)



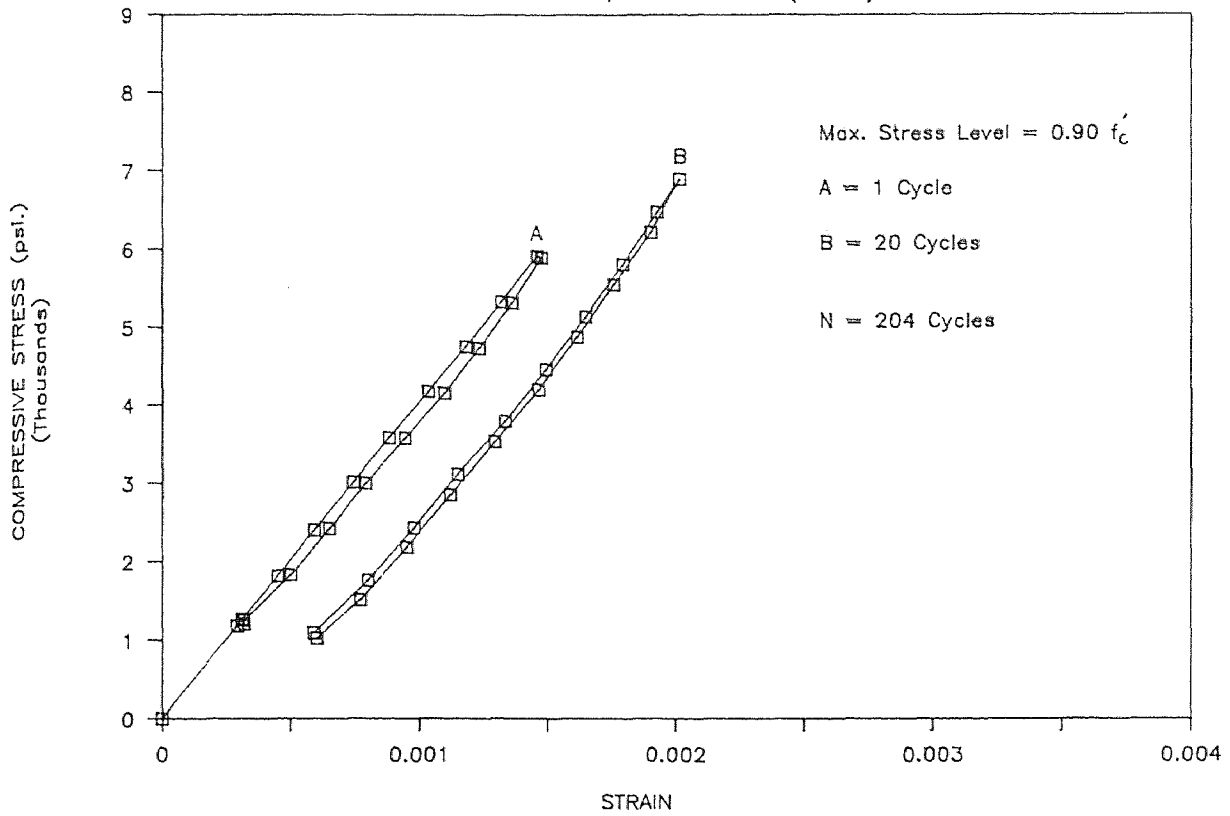
FATIGUE TEST

POLYMER CONCRETE, RATE = 6 Hz. (PF104)



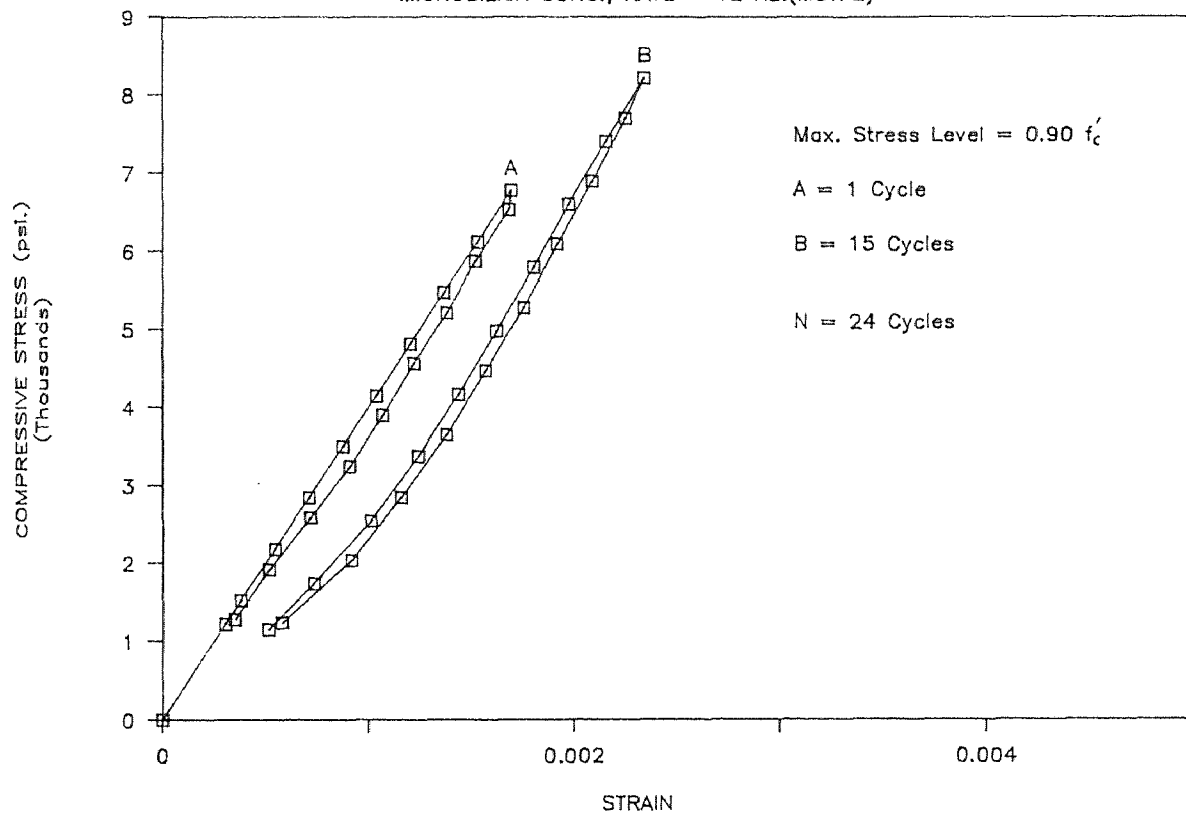
FATIGUE TEST

MICROSILICA CONC., RATE = 12 Hz.(M3TF1)



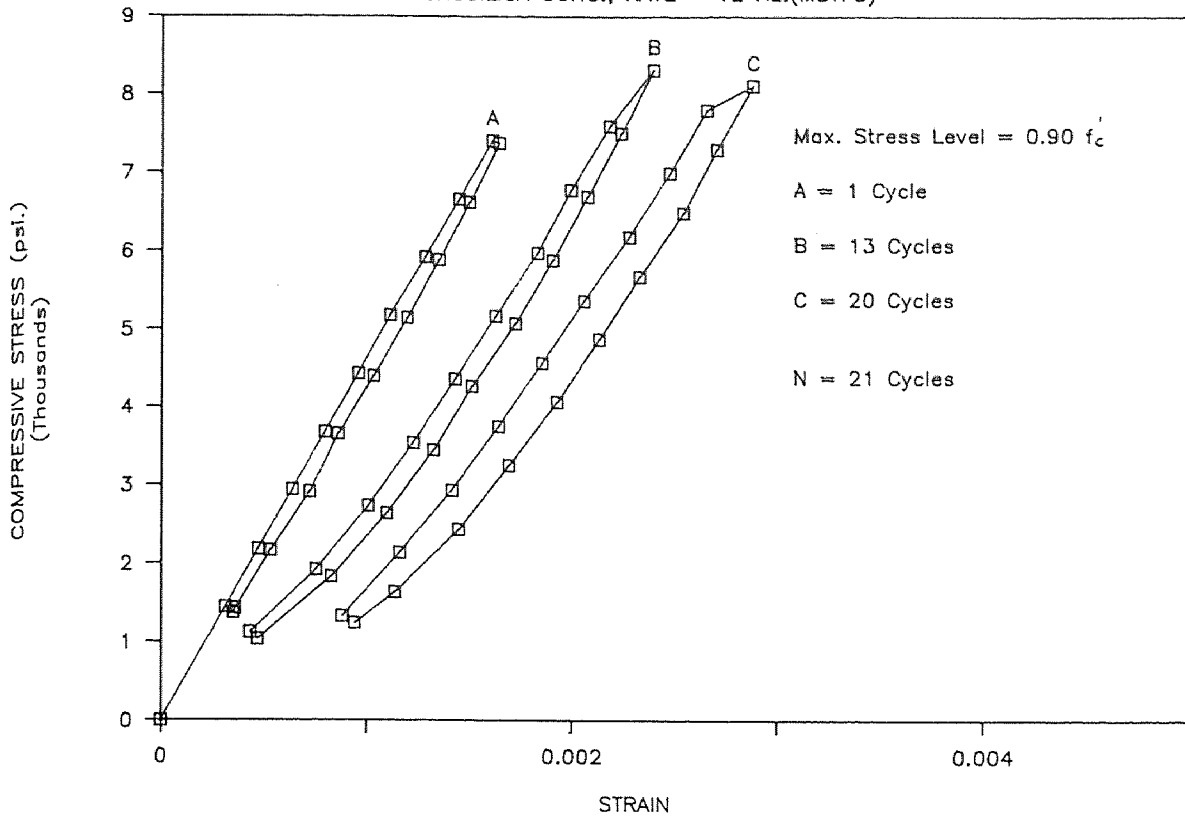
FATIGUE TEST

MICROSILICA CONC., RATE = 12 Hz.(M3TF2)



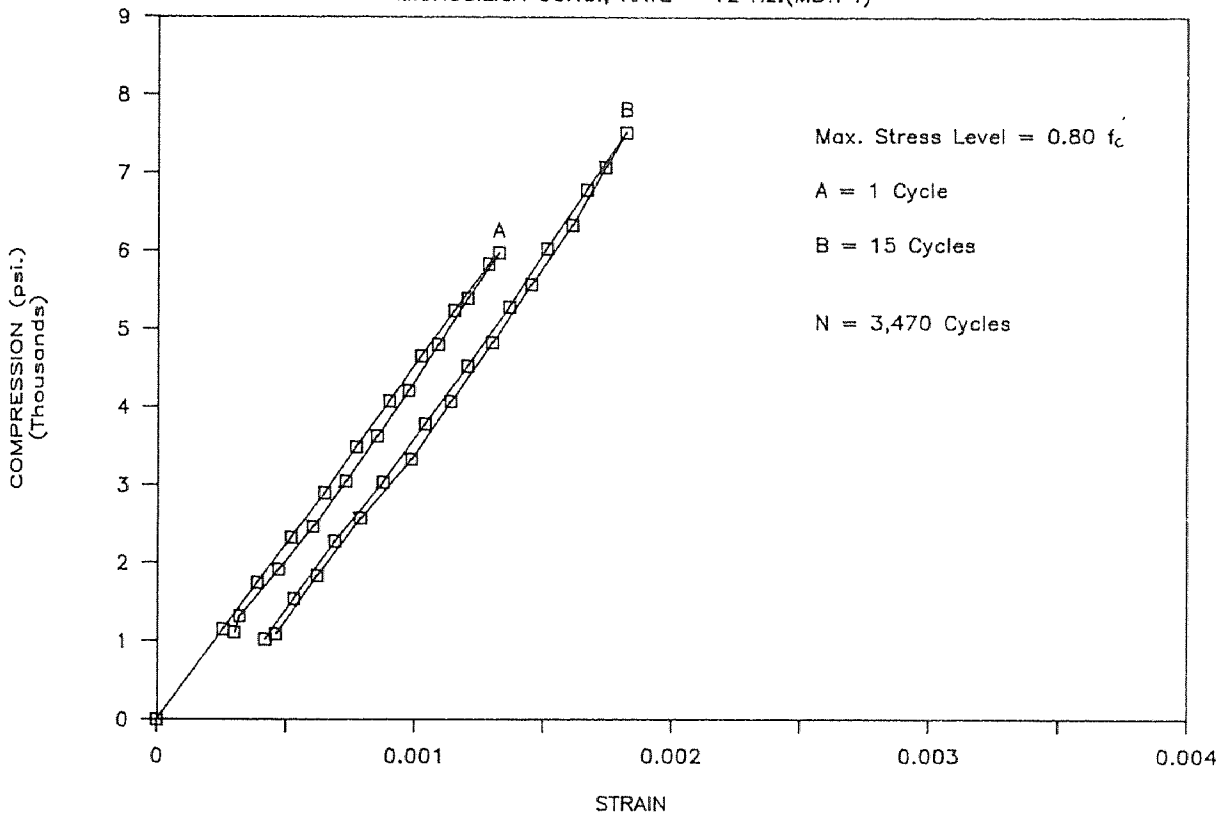
FATIGUE TEST

MICROSILICA CONC., RATE = 12 Hz.(M3TF3)



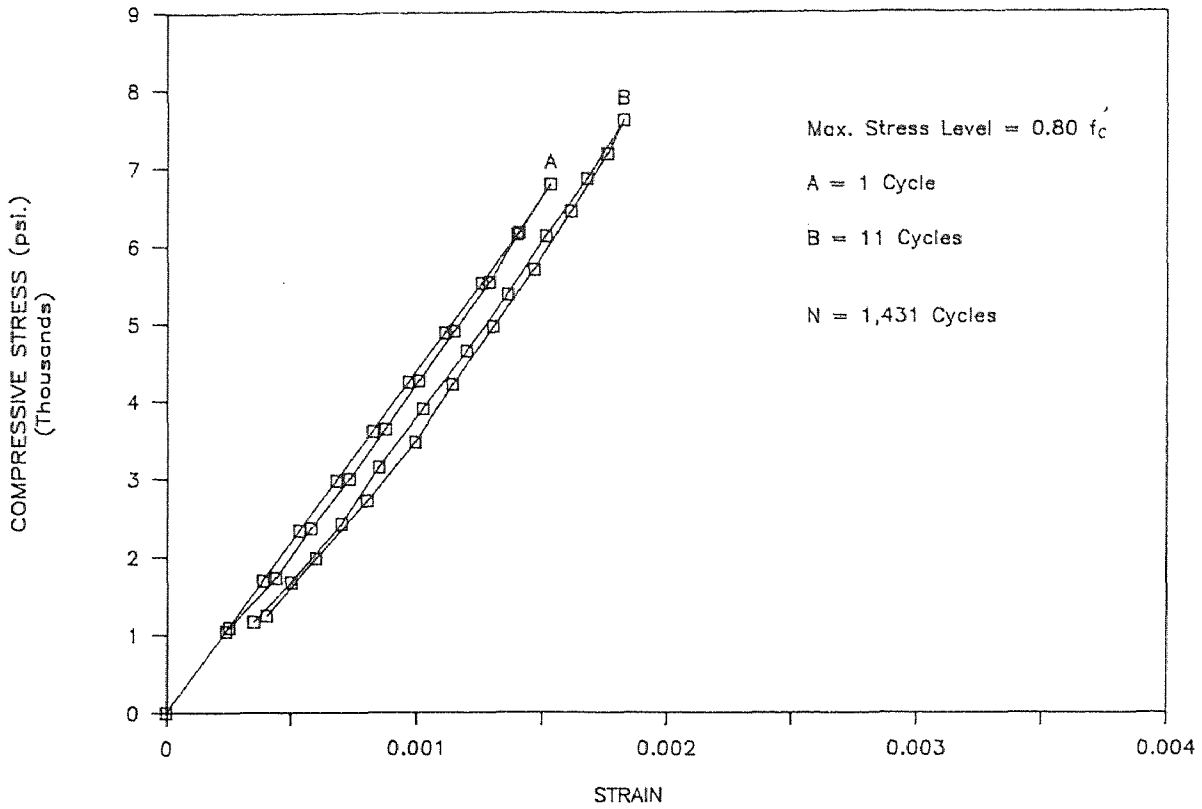
FATIGUE TEST

MICROSILICA CONC., RATE = 12 Hz.(M3TF4)



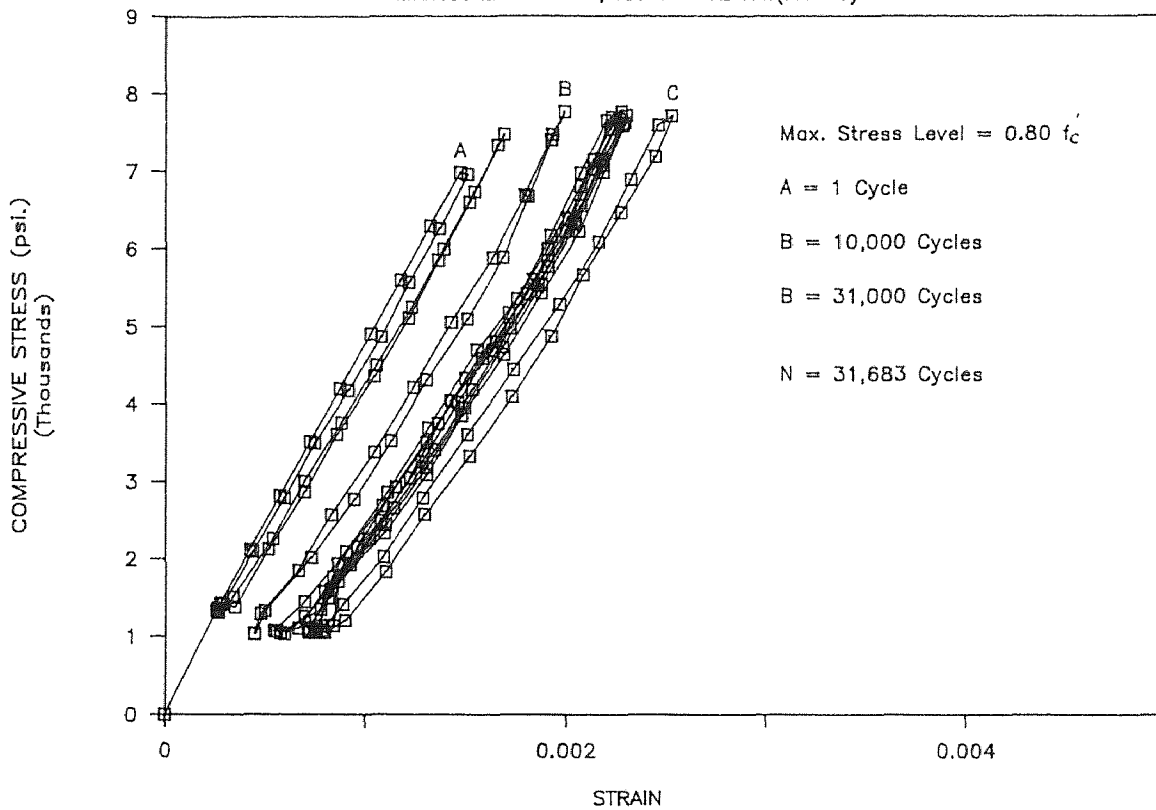
FATIGUE TEST

MICROSILICA CONC., RATE = 12 Hz.(M3TF5)



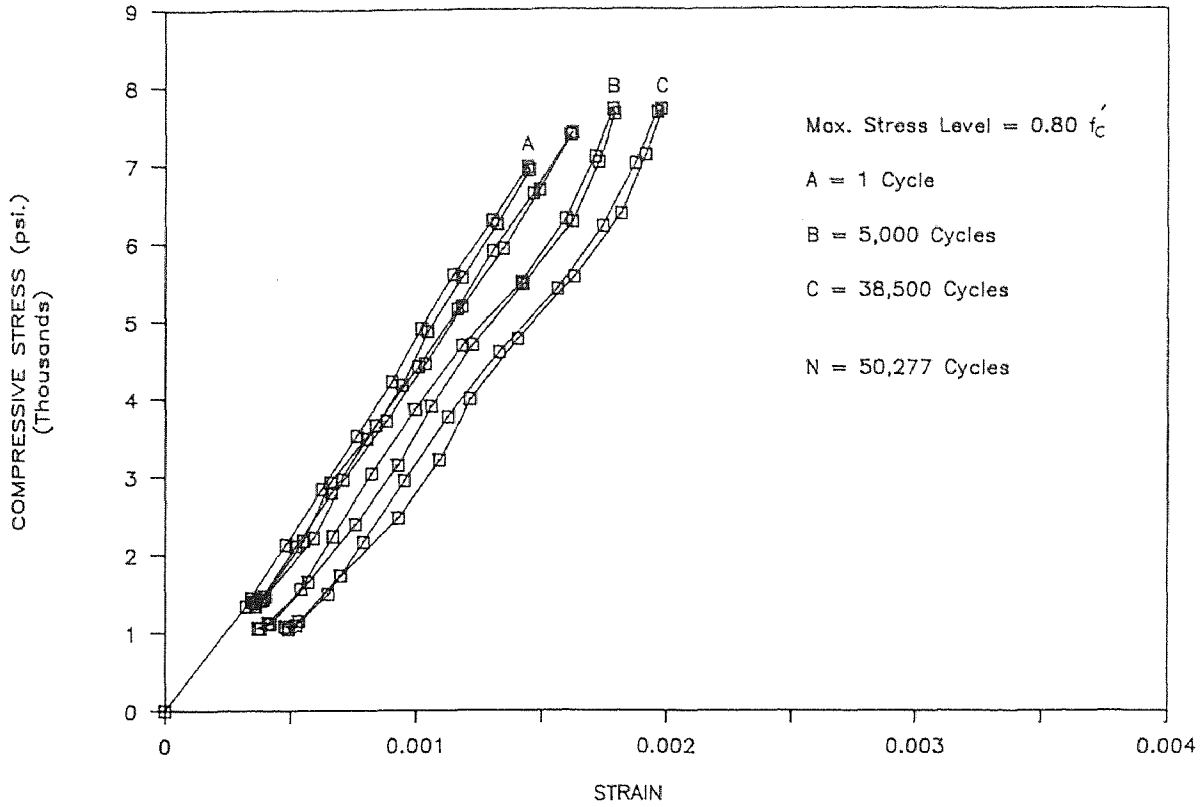
FATIGUE TEST

MICROSILICA CONC., RATE = 12 Hz.(M3TF6)



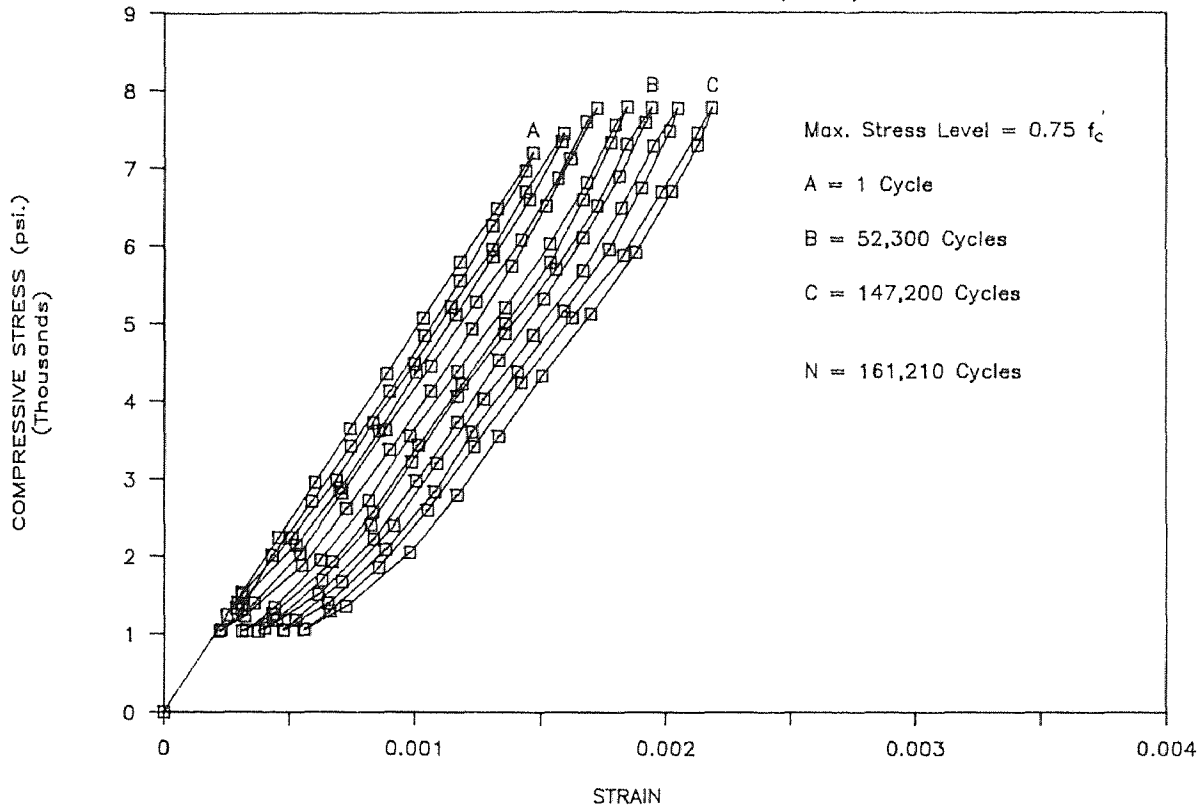
FATIGUE TEST

MICROSILICA CONC., RATE = 12 Hz.(M3TF7)



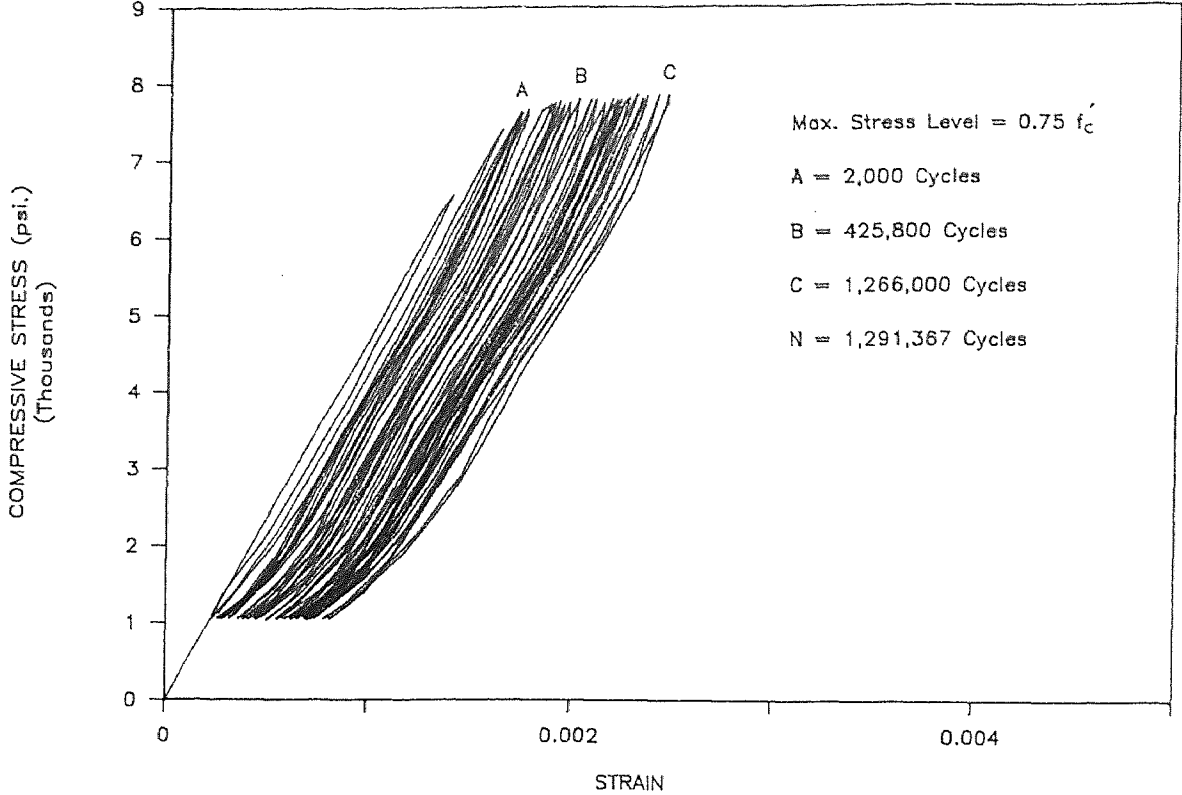
FATIGUE TEST

MICROSILICA CONC., RATE = 12 Hz (M3TF8)



FATIGUE TEST

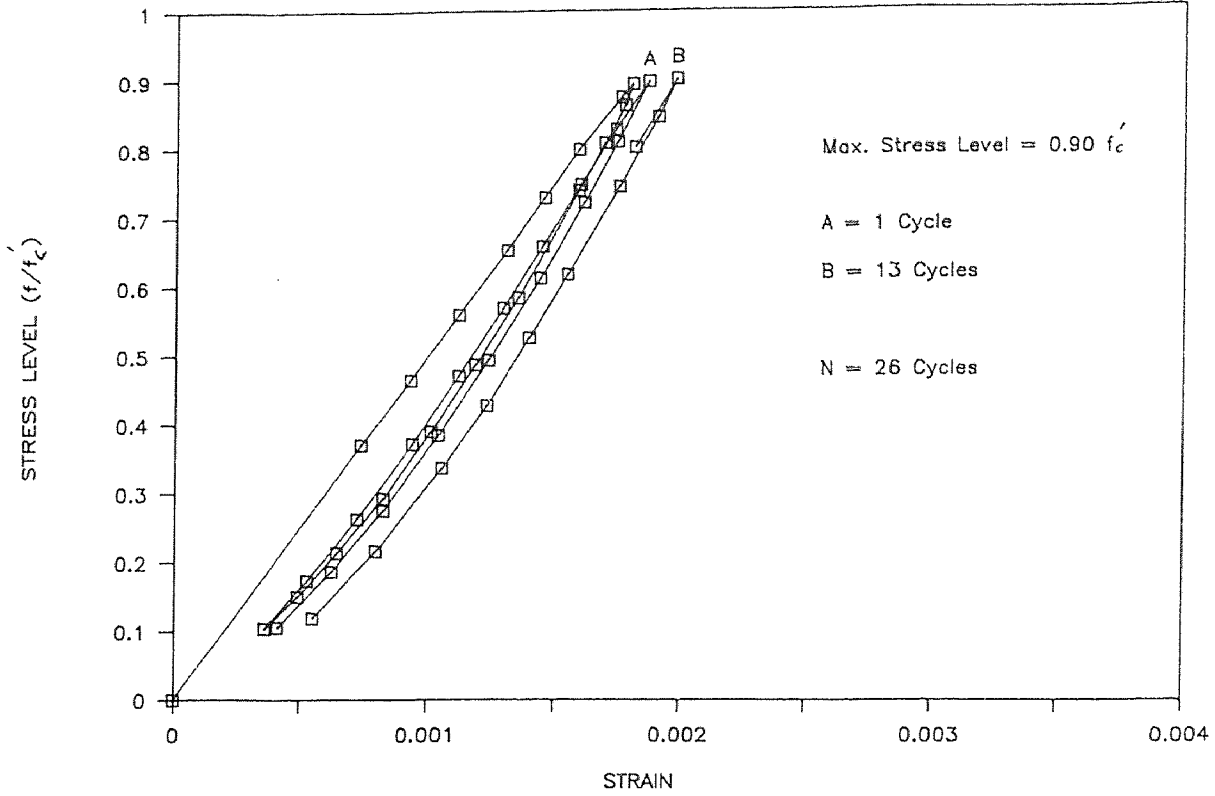
MICROSILICA CONC.,RATE = 12 Hz.(M3TF10)



APPENDIX I

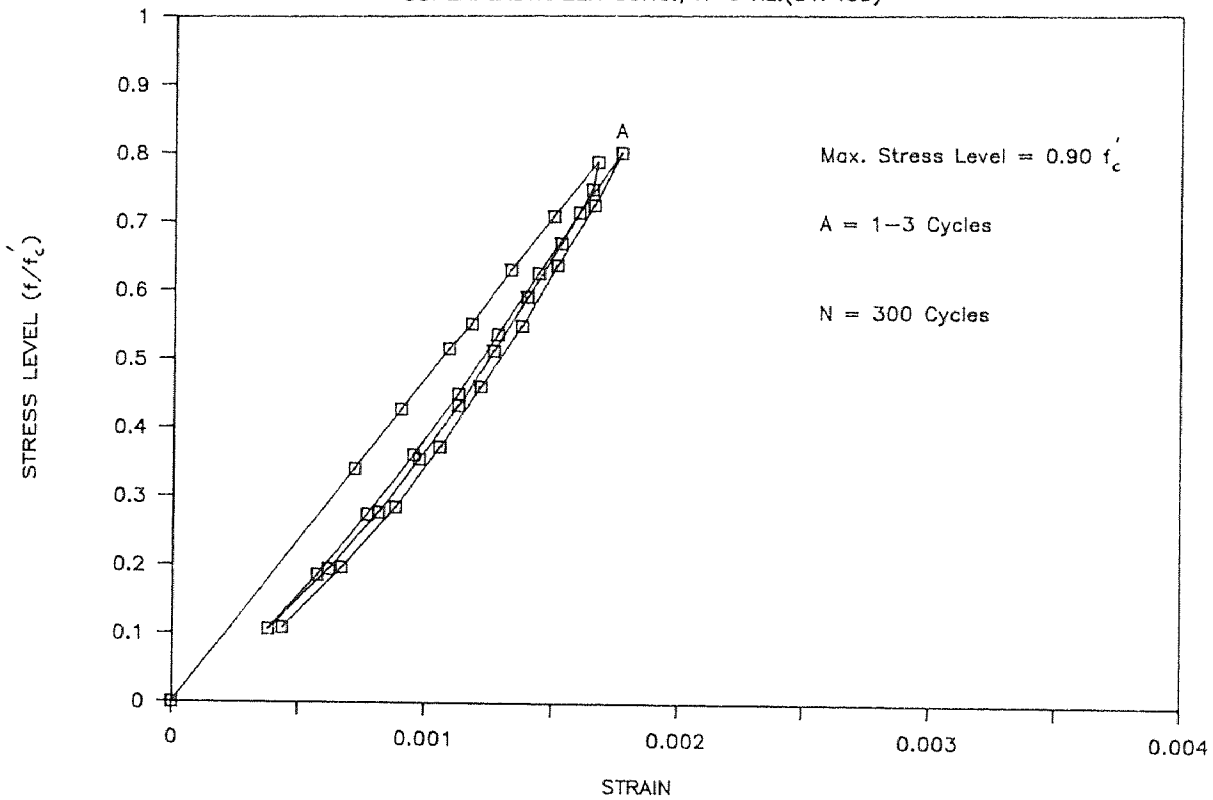
FATIGUE TEST

SUPERPLASTICIZER CONC., R=6 Hz.(S1F309)



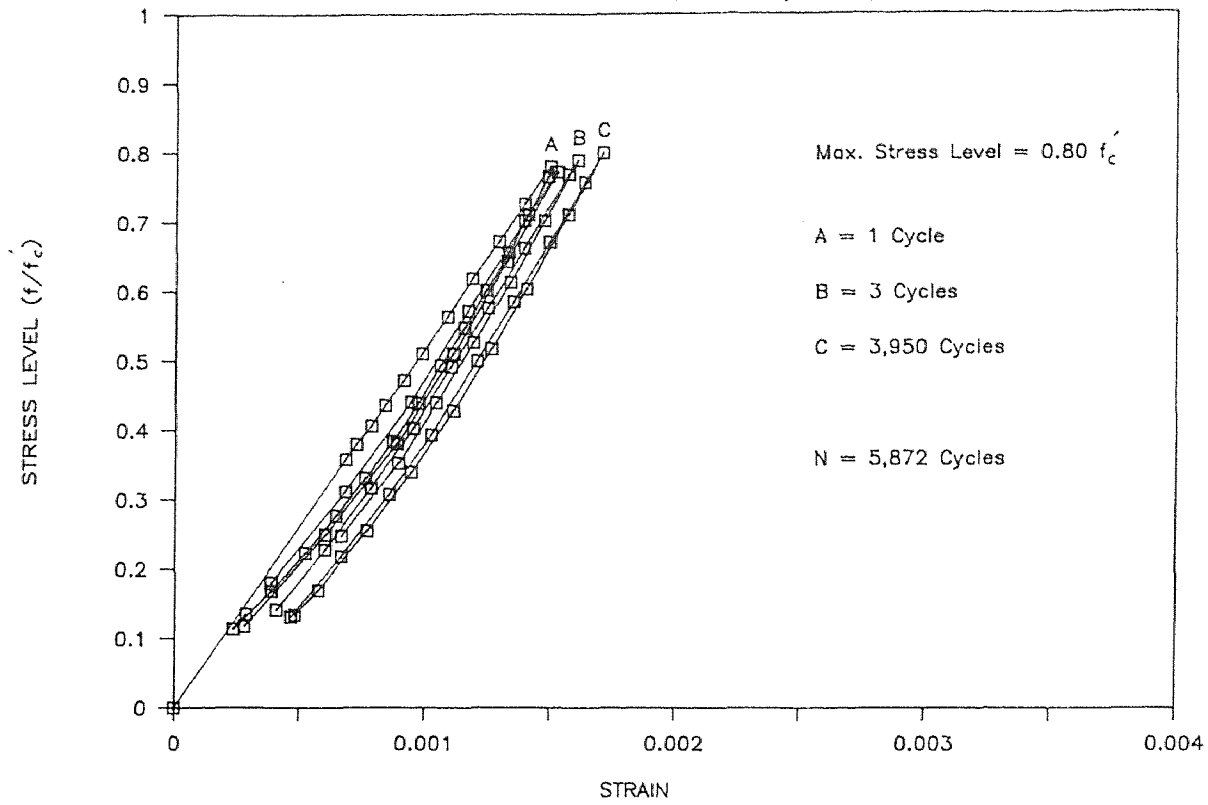
FATIGUE TEST

SUPERPLASTICIZER CONC., R=6 Hz.(S1F409)



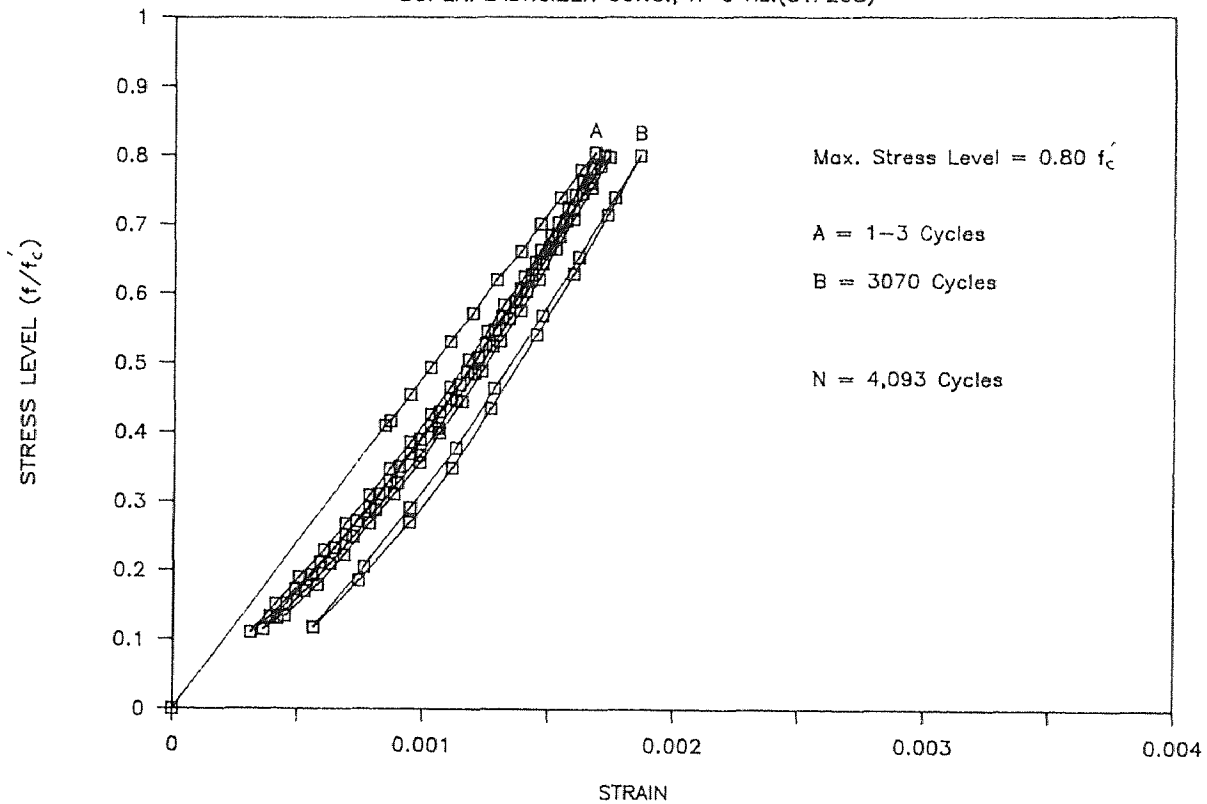
FATIGUE TEST

SUPERPLASTICIZER CONC., R=6 Hz.(S1F108)



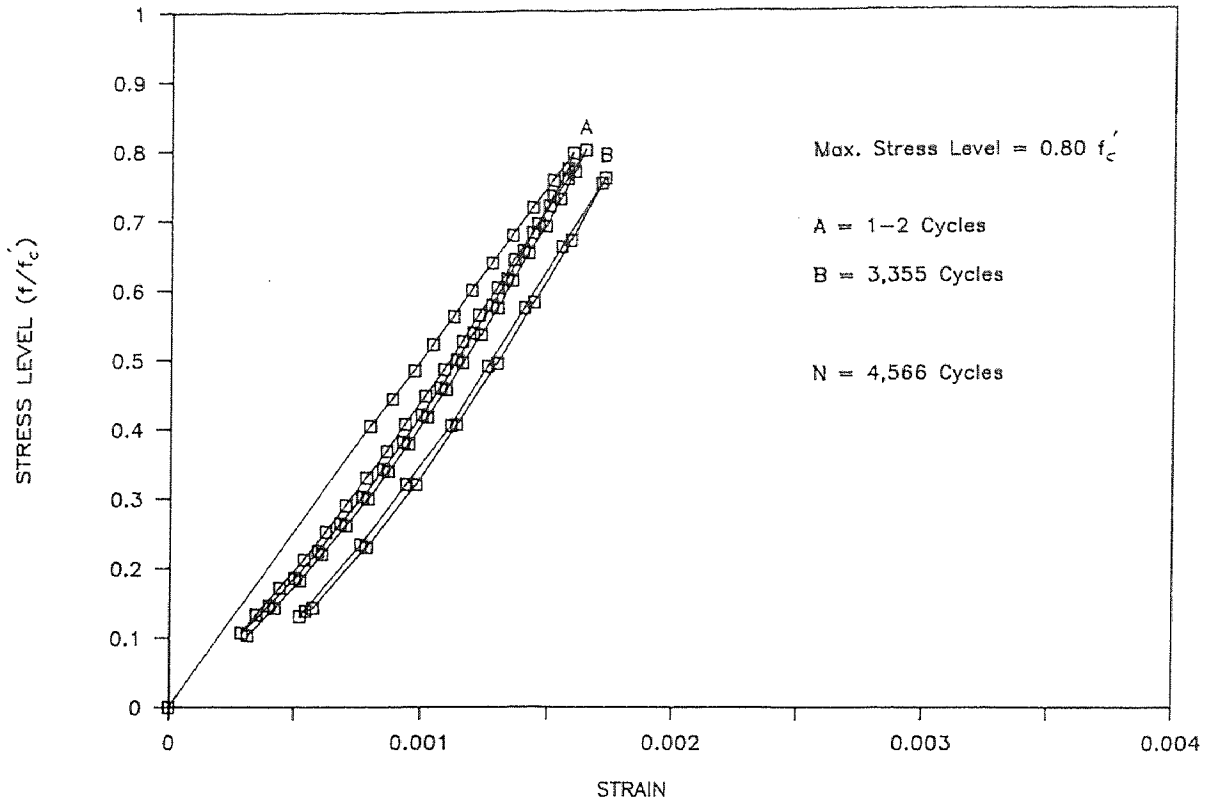
FATIGUE TEST

SUPERPLASTICIZER CONC., R=6 Hz.(S1F208)



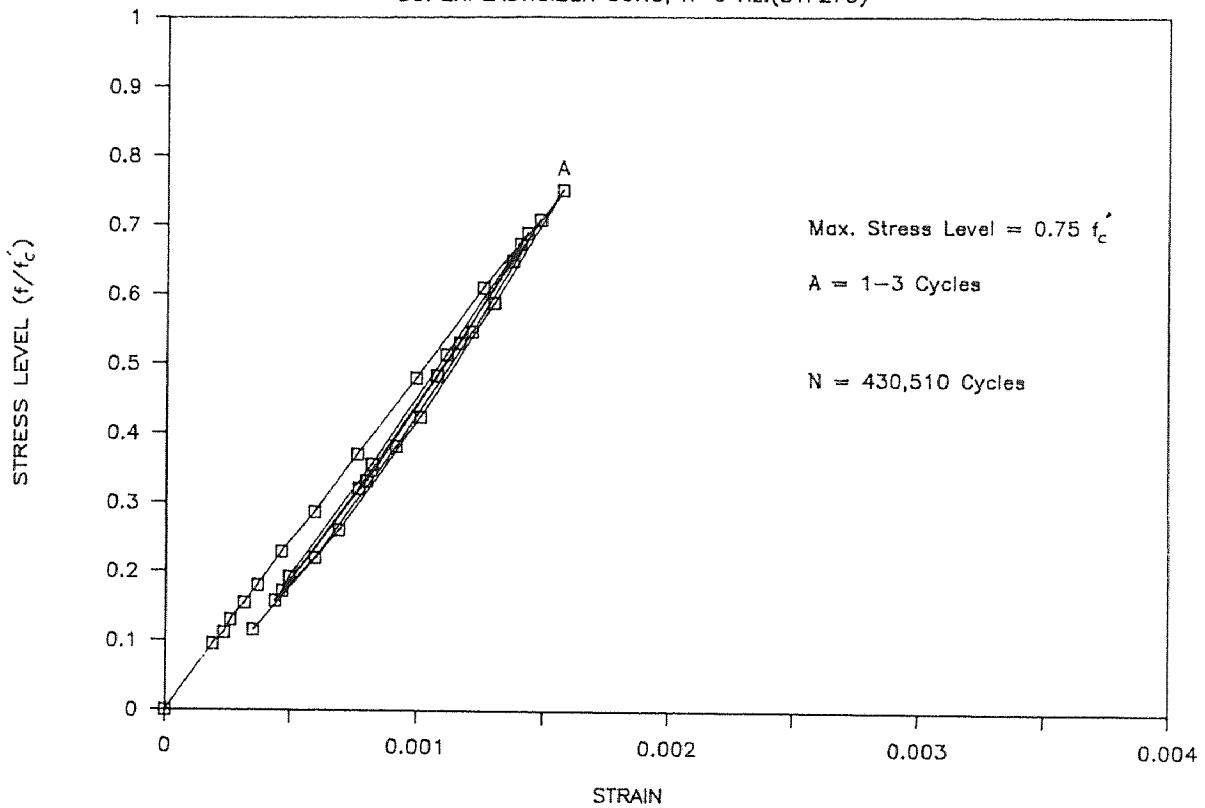
FATIGUE TEST

SUPERPLASTICIZER CONC., R=6 Hz.(S1F308)



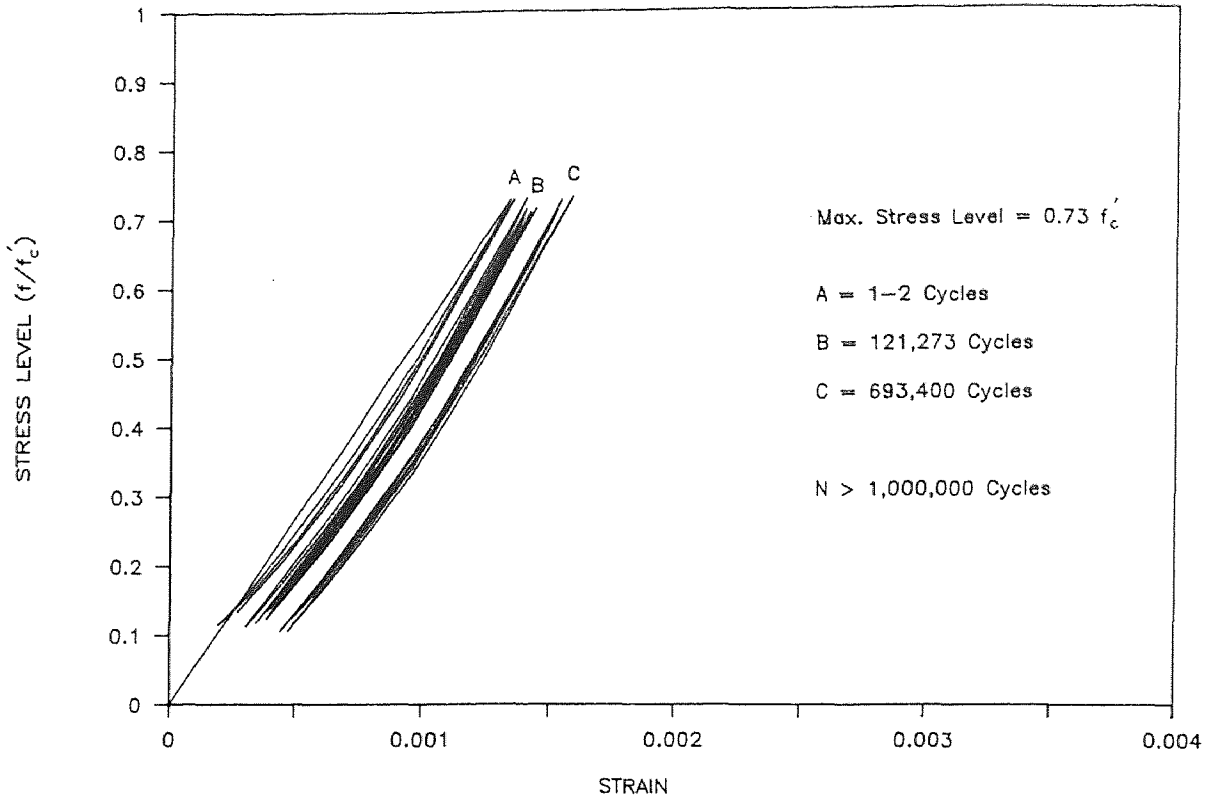
FATIGUE TEST

SUPERPLASTICIZER CONC., R=6 Hz.(S1F275)



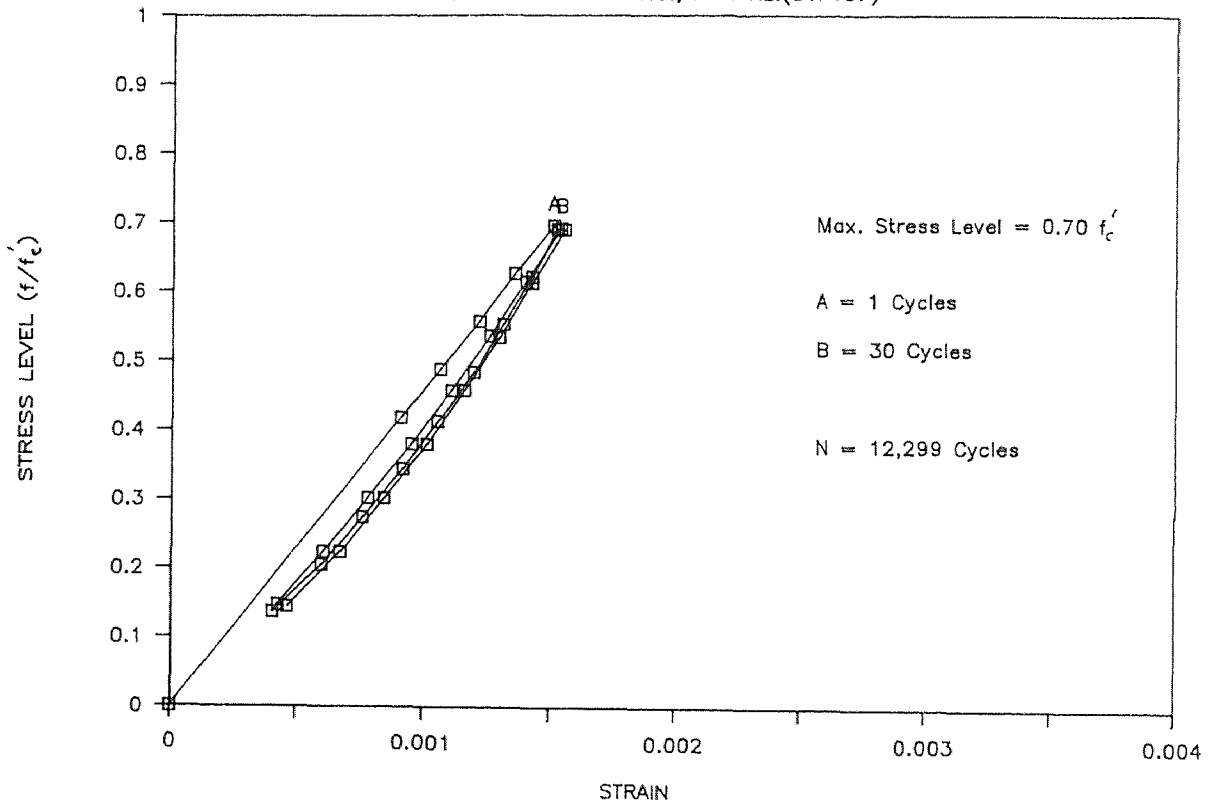
FATIGUE TEST

SUPERPLASTICIZER CONC., R=6 Hz.(S1F207)



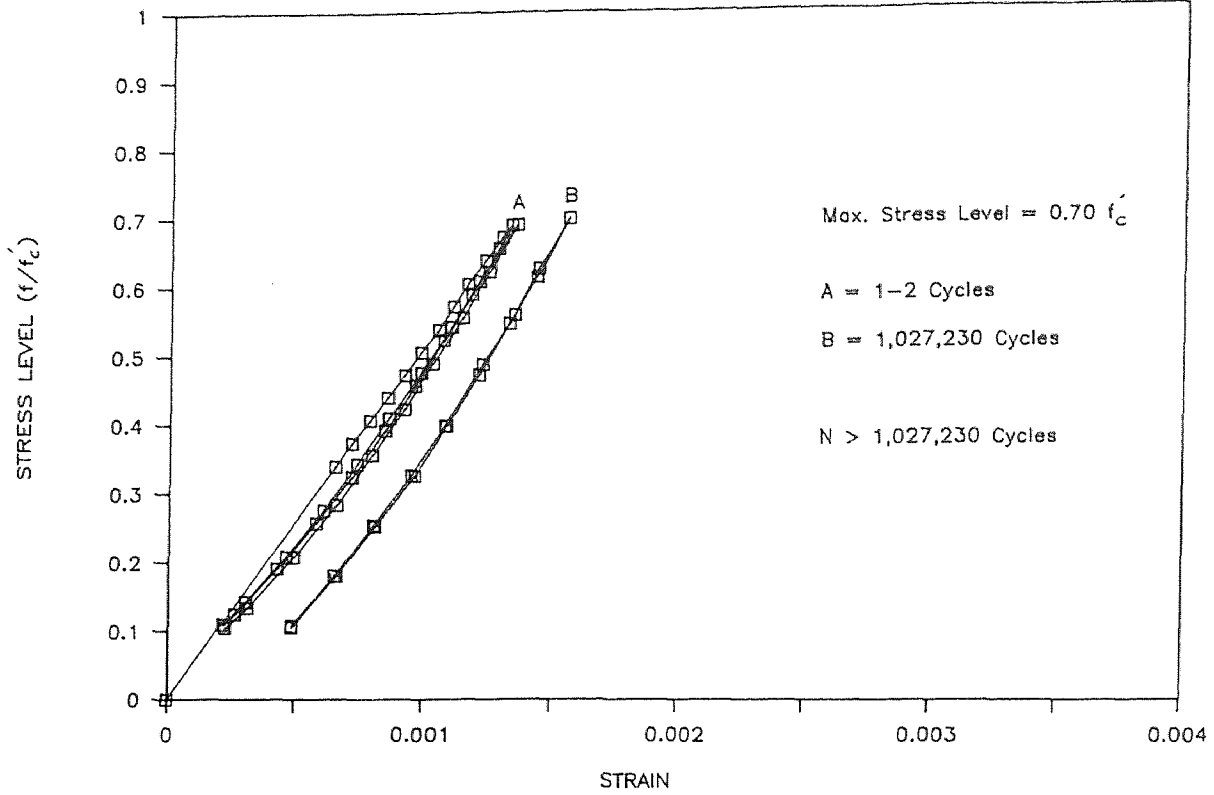
FATIGUE TEST

SUPERPLASTICIZER CONC., R=6 Hz.(S1F107)



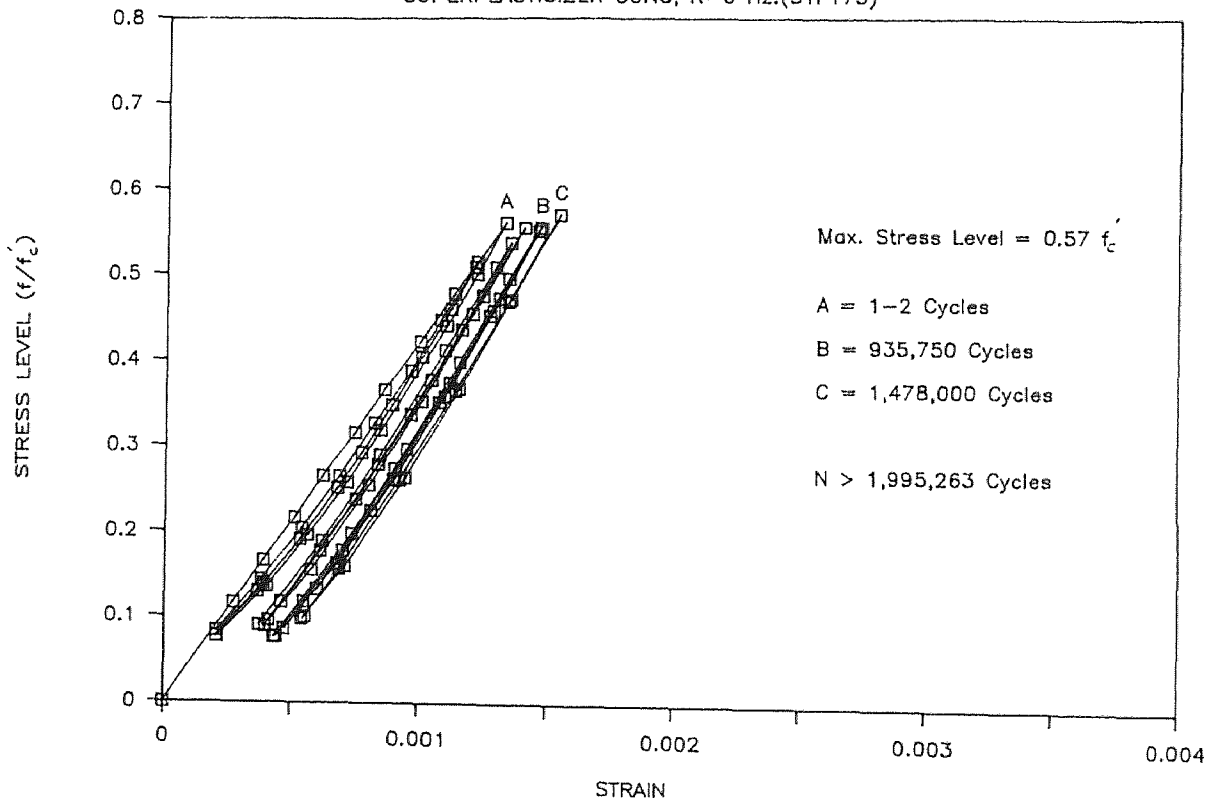
FATIGUE TEST

SUPERPLASTICIZER CONC, R=6 Hz.(S1F307)



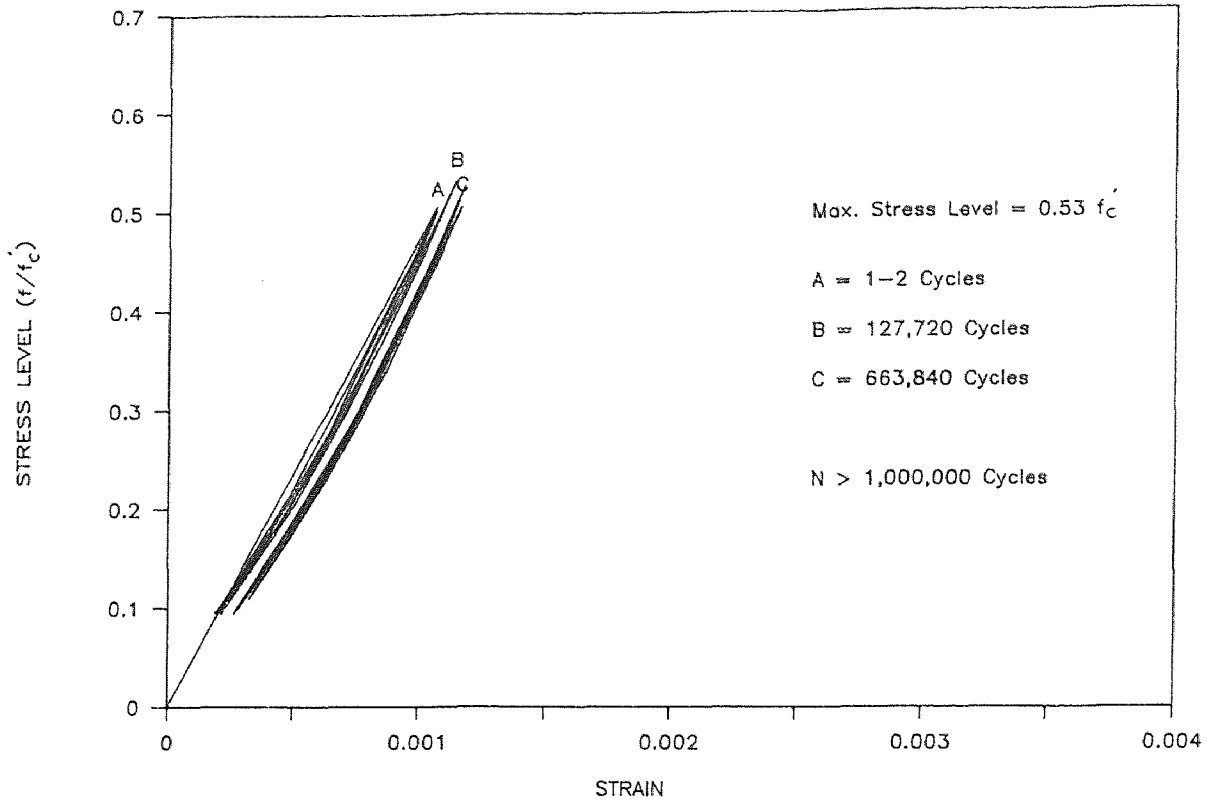
FATIGUE TEST

SUPERPLASTICIZER CONC, R=6 Hz.(S1F175)



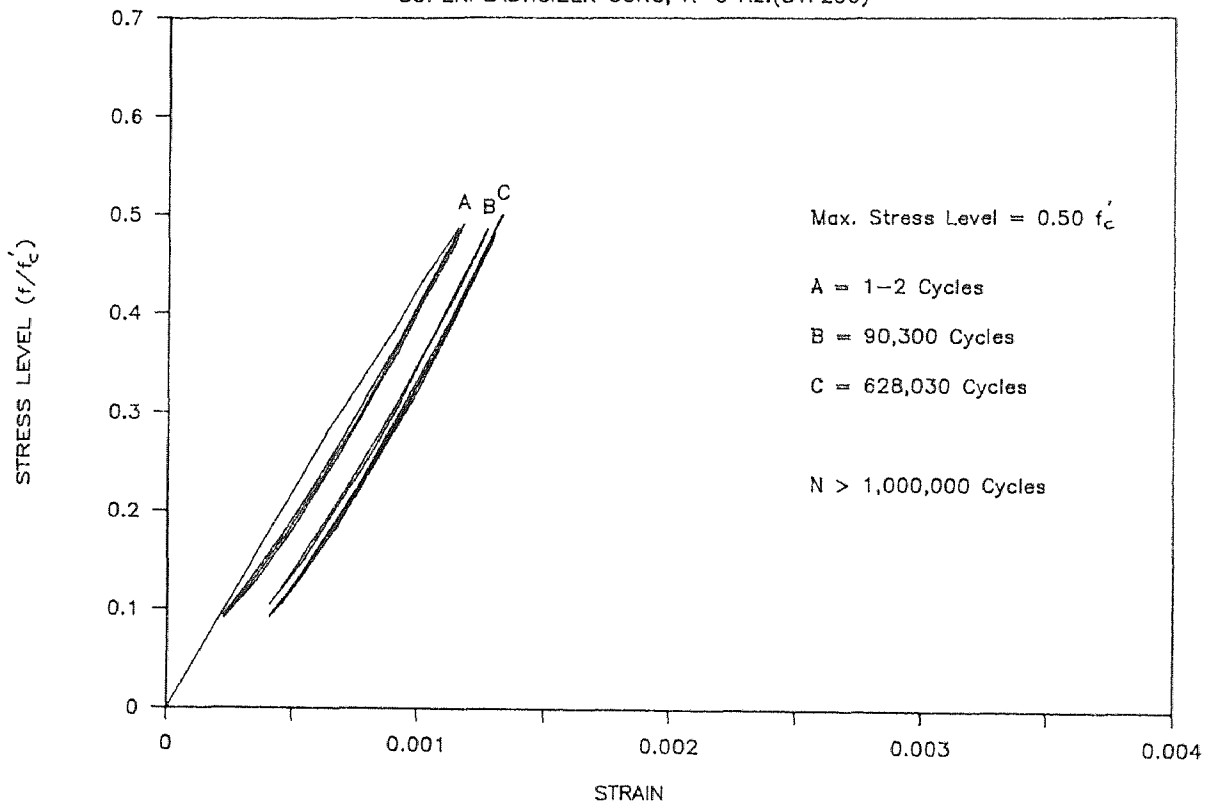
FATIGUE TEST

SUPERPLASTICIZER CONC, R=6 Hz.(S1F106)



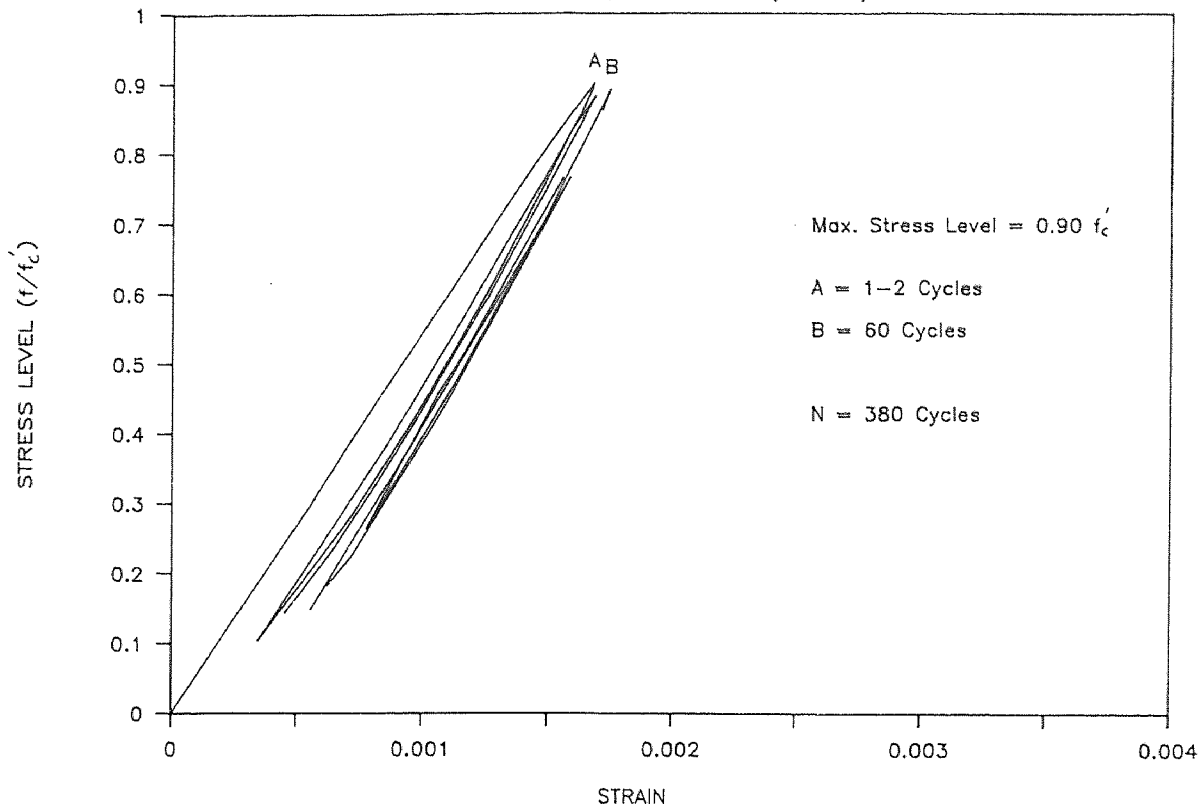
FATIGUE TEST

SUPERPLASTICIZER CONC, R=6 Hz.(S1F206)



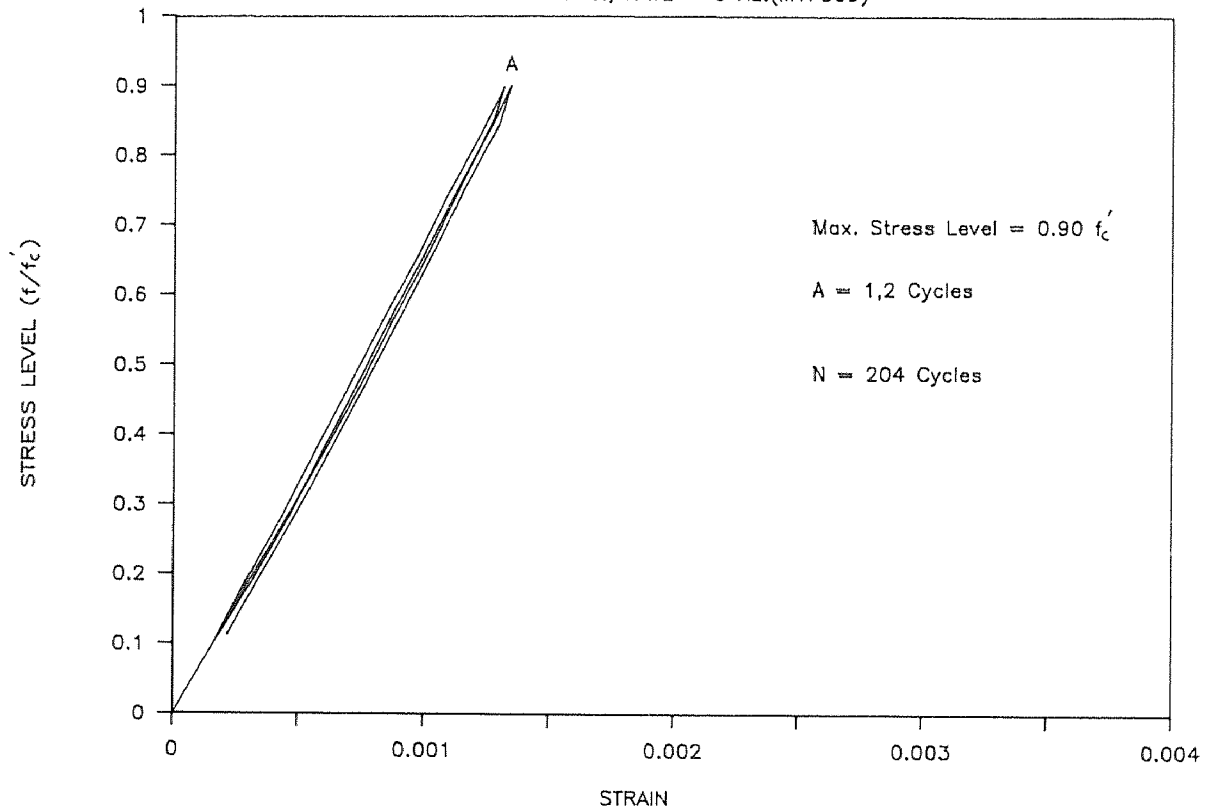
FATIGUE TEST

MICROSILICA CONC., RATE = 6 Hz.(M1F209)



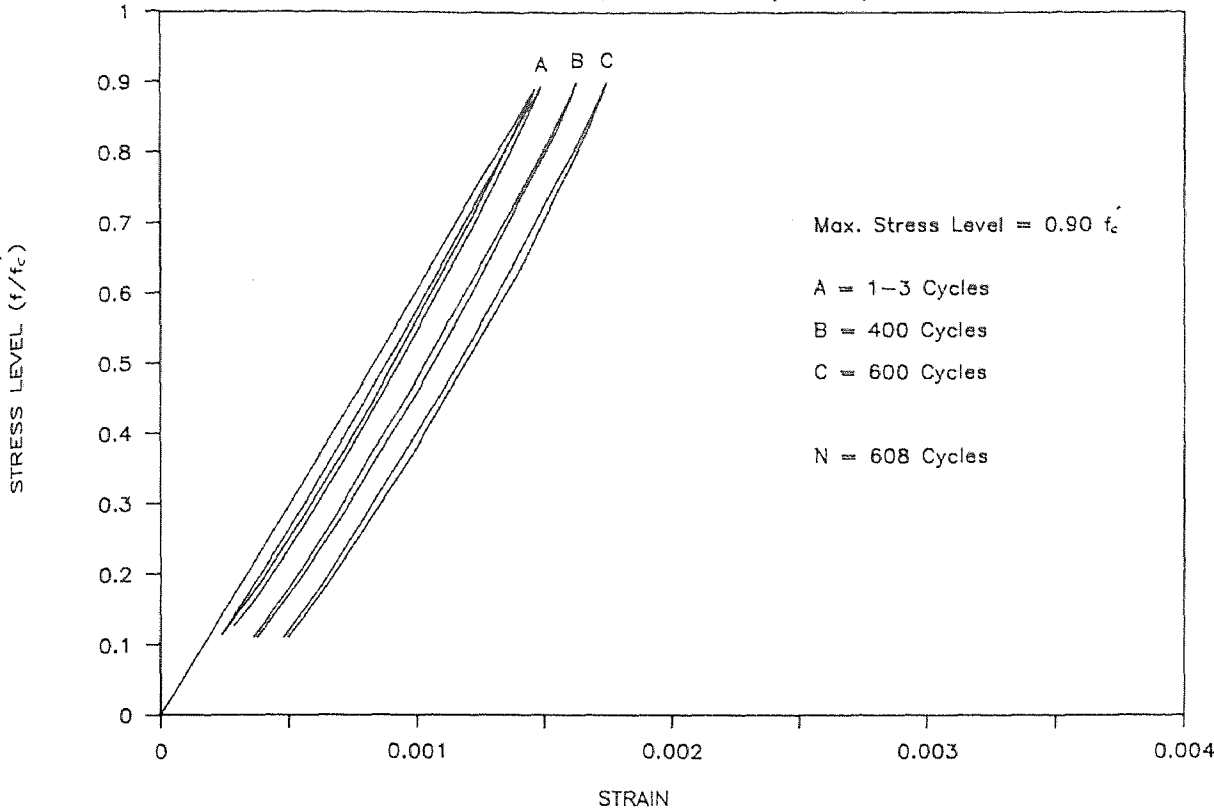
FATIGUE TEST

MICROSILICA CONC., RATE = 6 Hz.(M1F309)



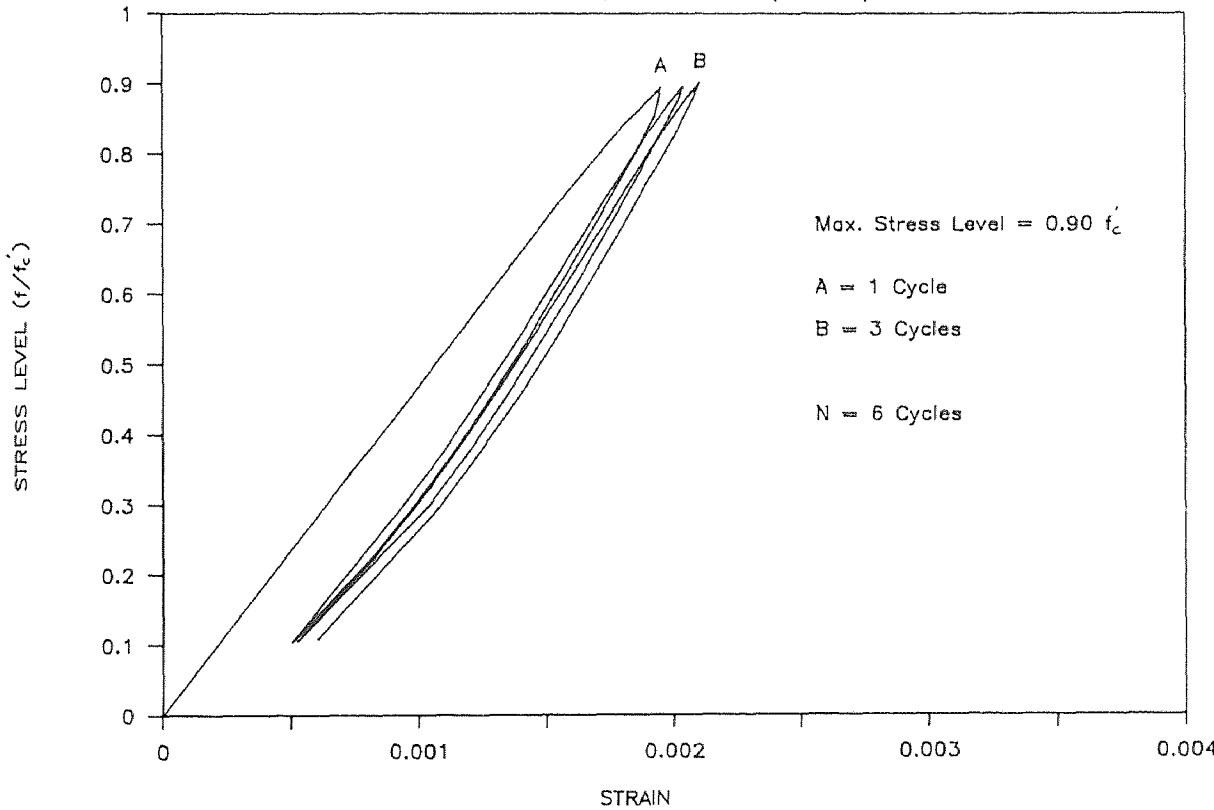
FATIGUE TEST

MICROSILICA CONC., RATE = 6 Hz.(M1F409)



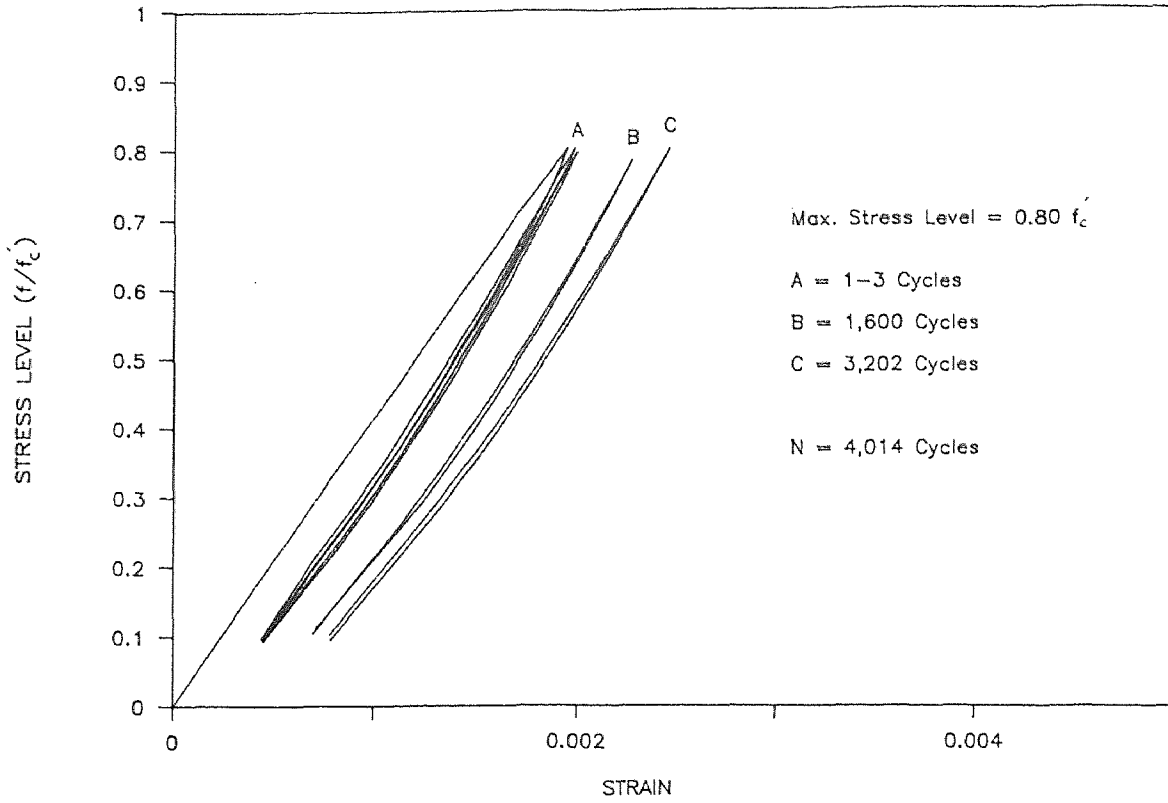
FATIGUE TEST

MICROSILICA CONC., RATE = 6 Hz.(M2F209)



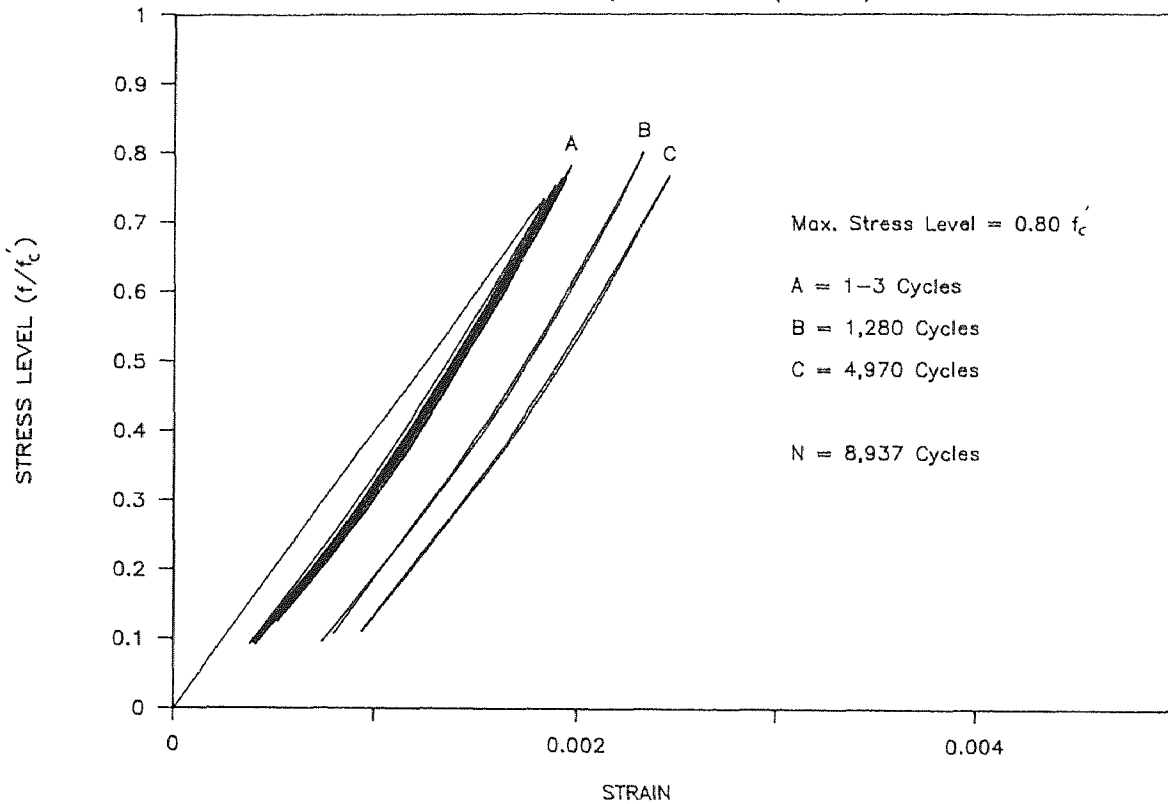
FATIGUE TEST

MICROSILICA CONC., RATE = 6 Hz.(M2F108)



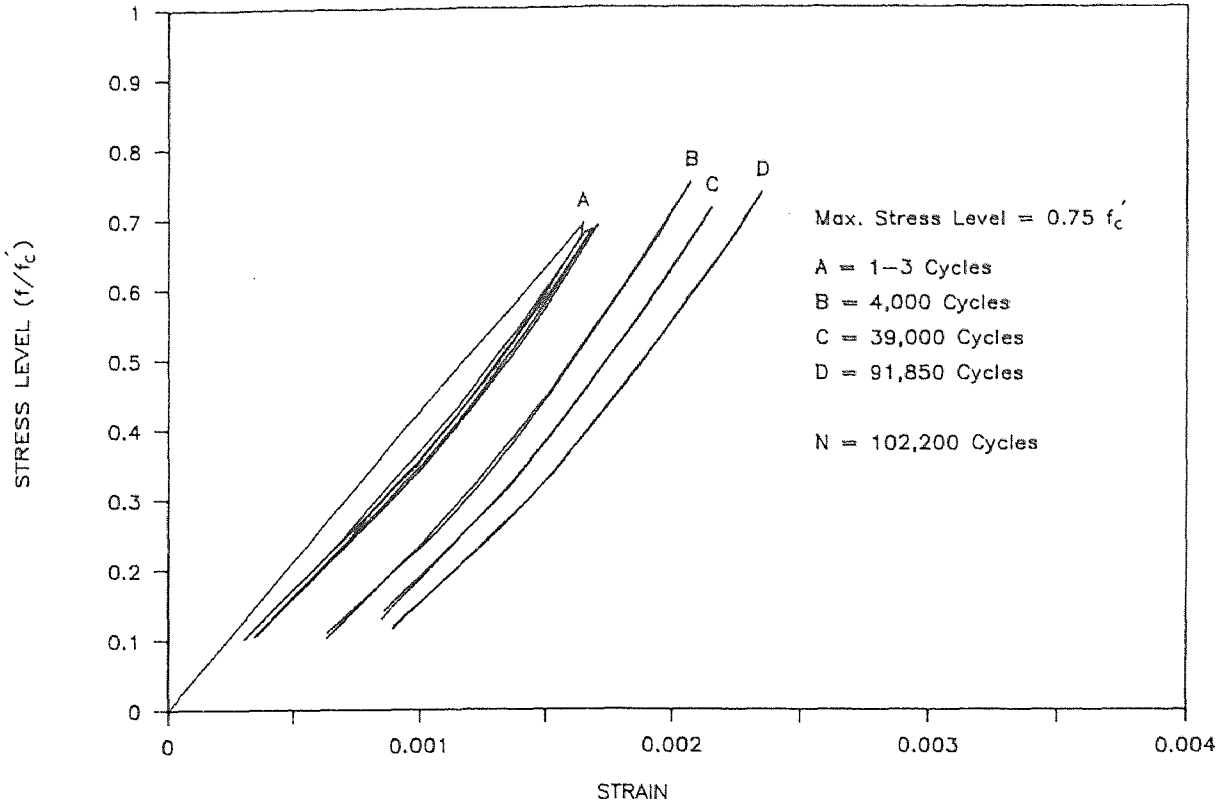
FATIGUE TEST

MICROSILICA CONC., RATE = 6 Hz.(M2F208)



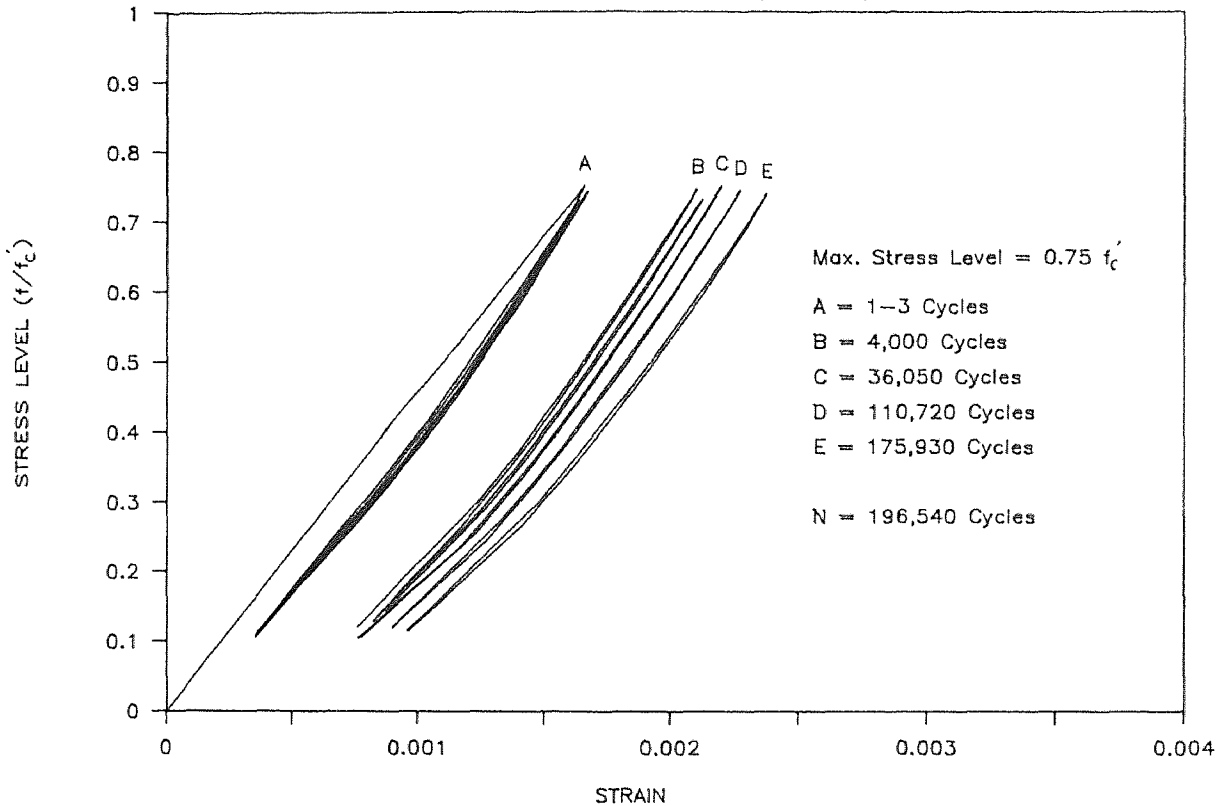
FATIGUE TEST

MICROSILICA CONC.,RATE = 6 Hz.(M2F2075)



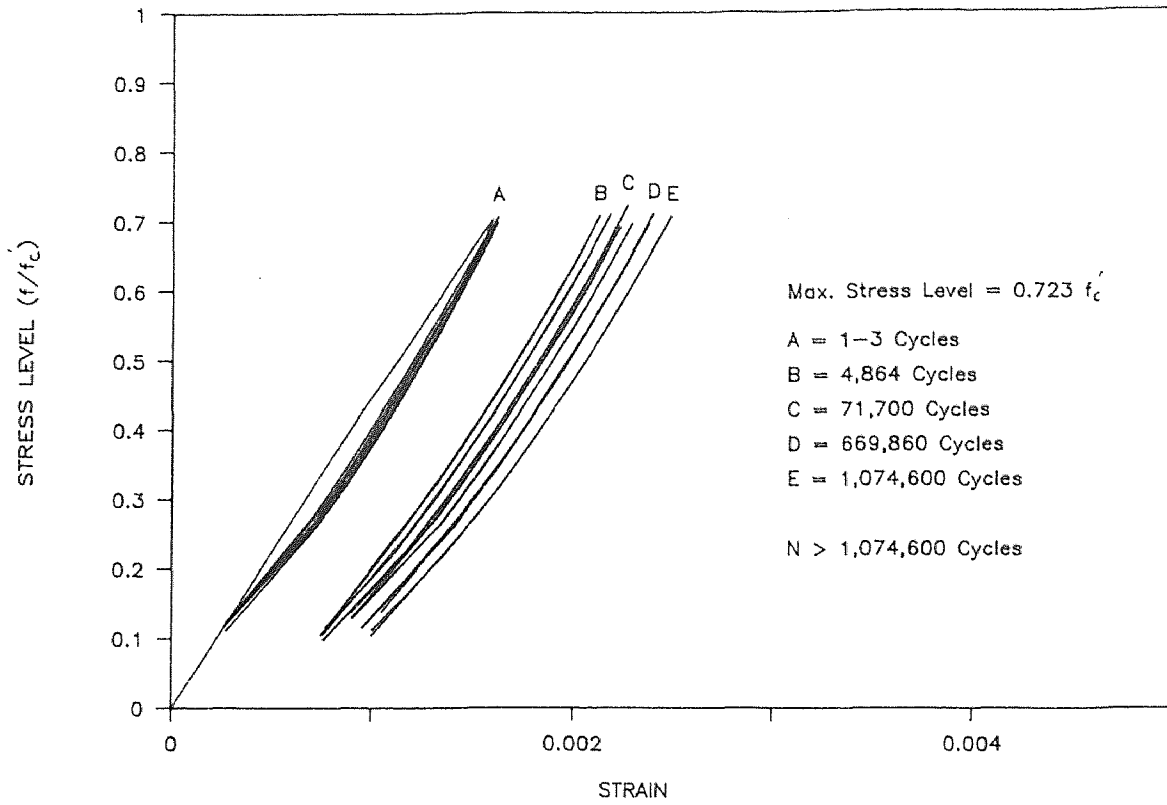
FATIGUE TEST

MICROSILICA CONC.,RATE = 6 Hz.(M2F3075)



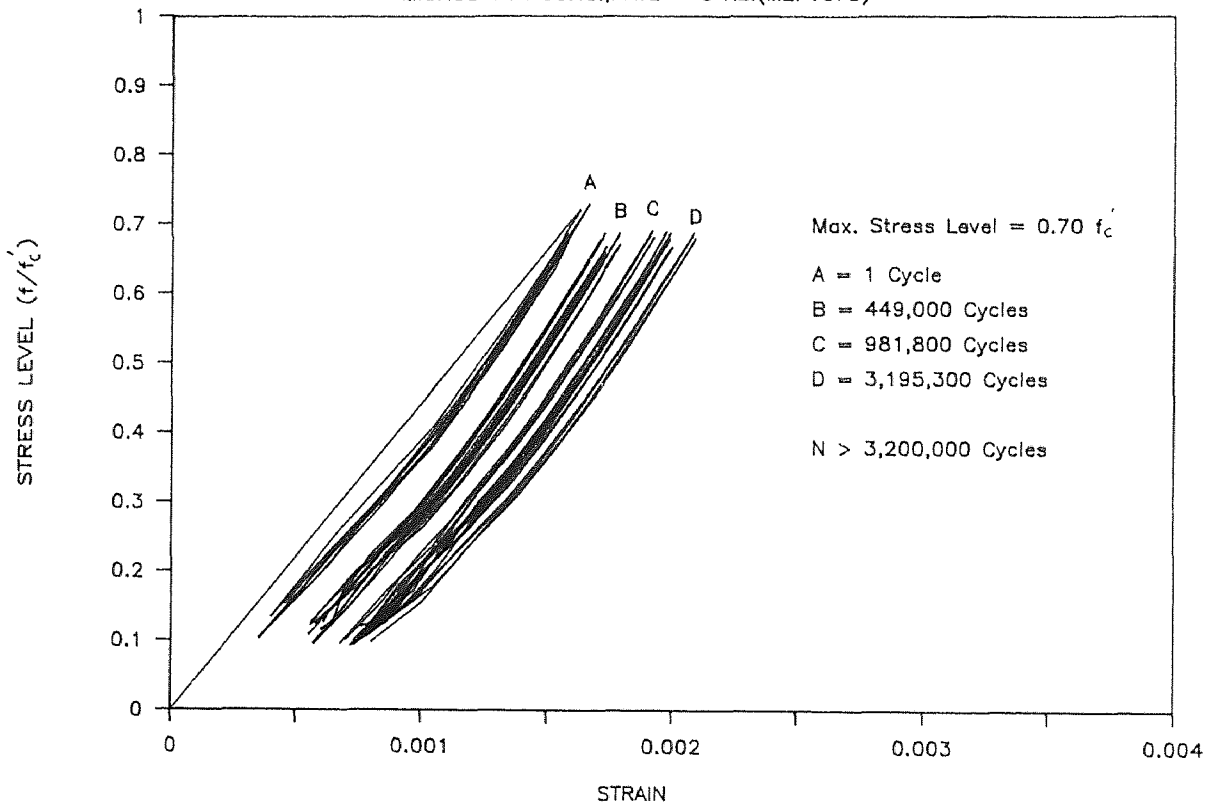
FATIGUE TEST

MICROSILICA CONC.,RATE = 6 Hz.(M2F4075)



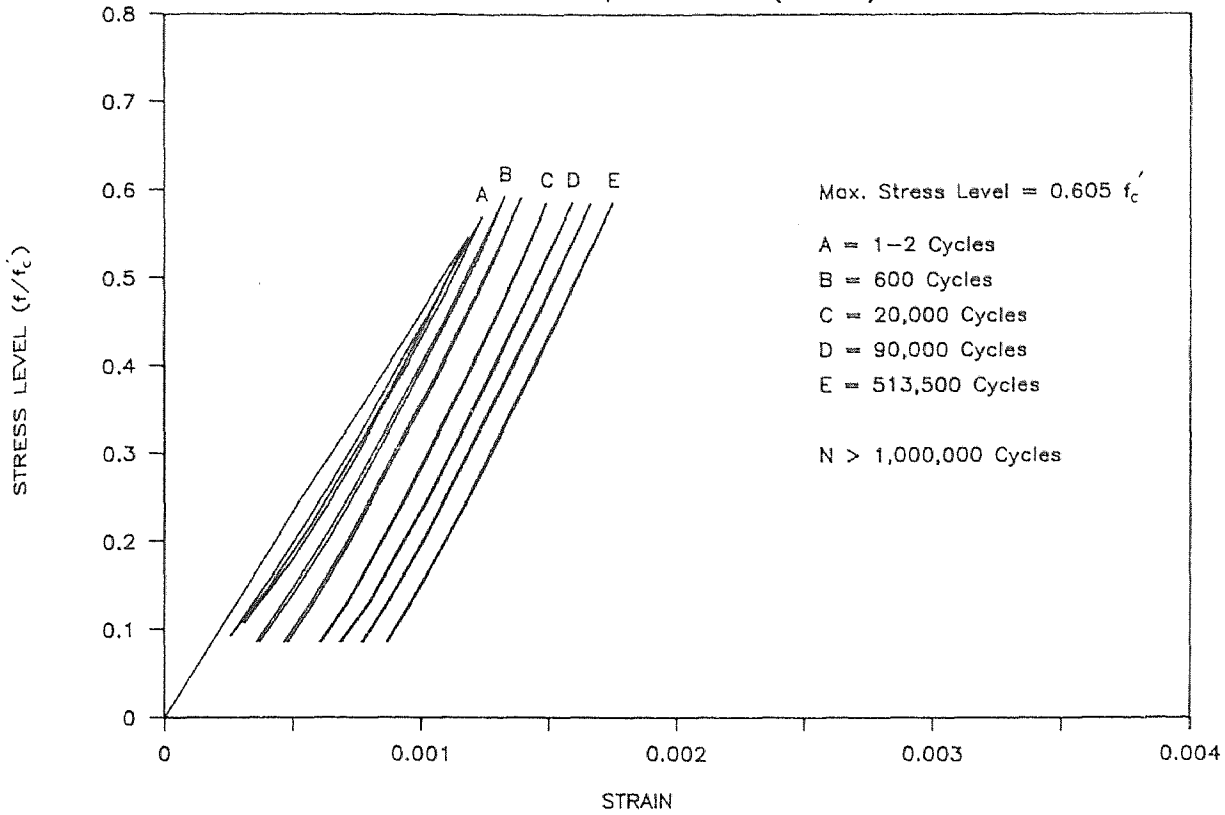
FATIGUE TEST

MICROSILICA CONC.,RATE = 6 Hz.(M2F1075)



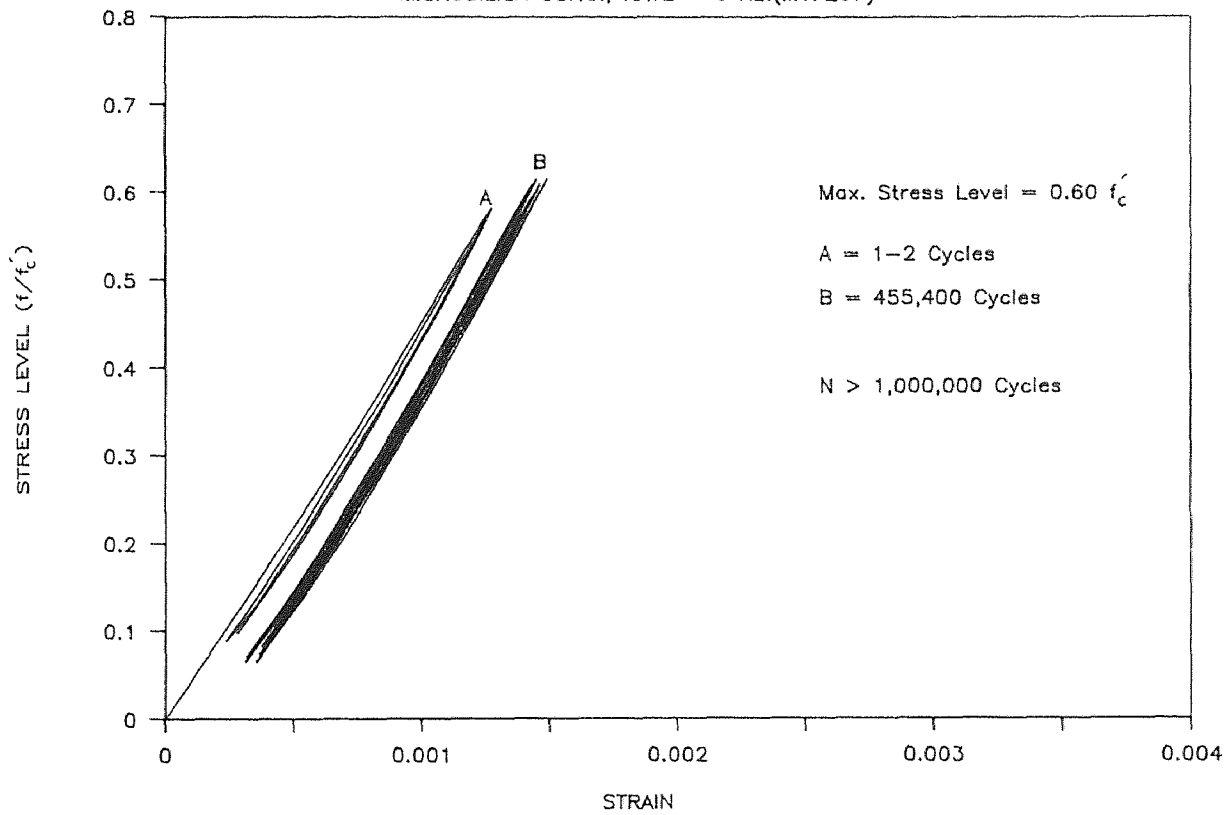
FATIGUE TEST

MICROSILICA CONC., RATE = 6 Hz.(M1F107)



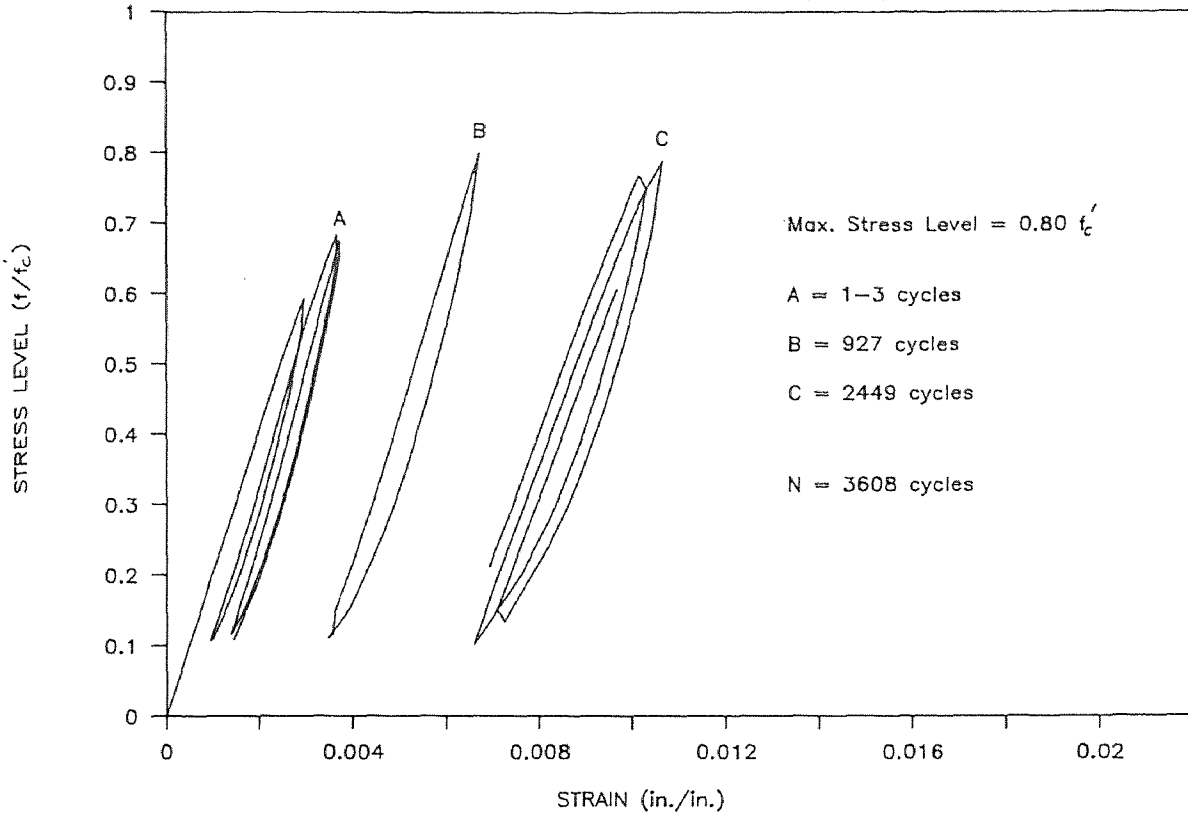
FATIGUE TEST

MICROSILICA CONC., RATE = 6 Hz.(M1F207)



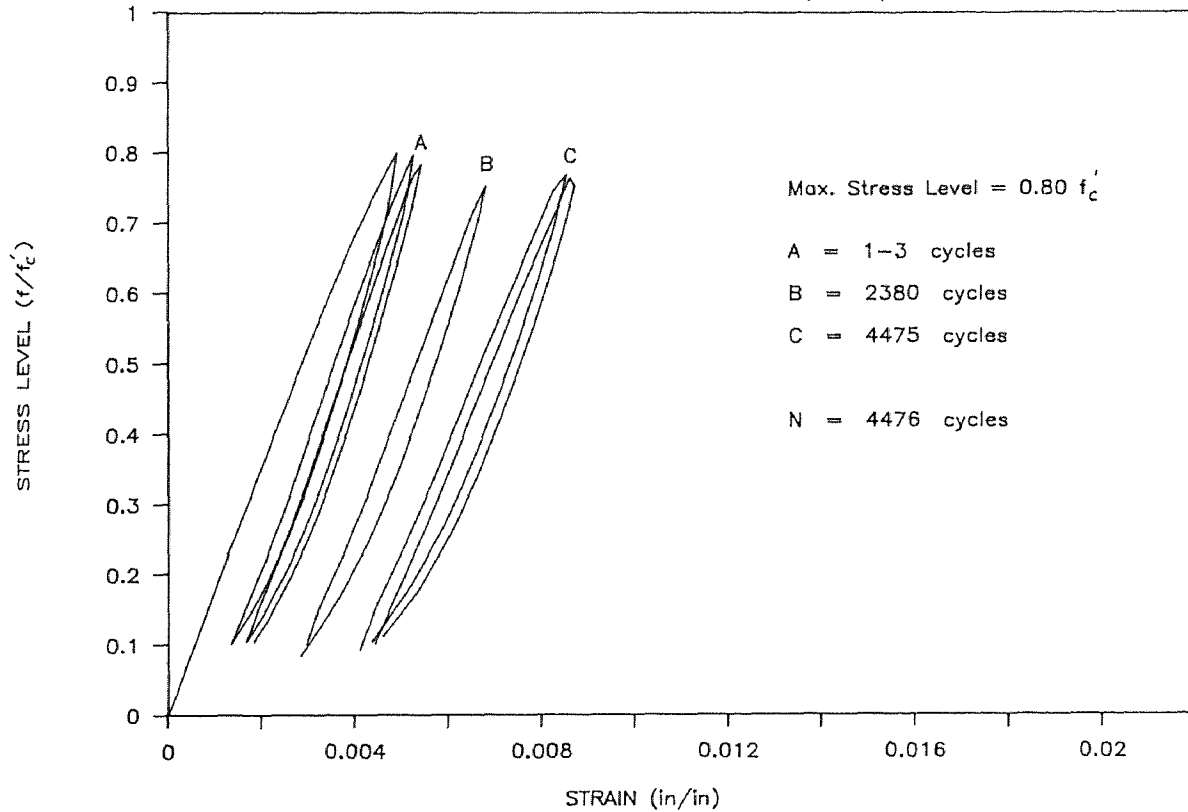
FATIGUE TEST

POLYMER CONCRETE , RATE = 6 Hz. (PF108)



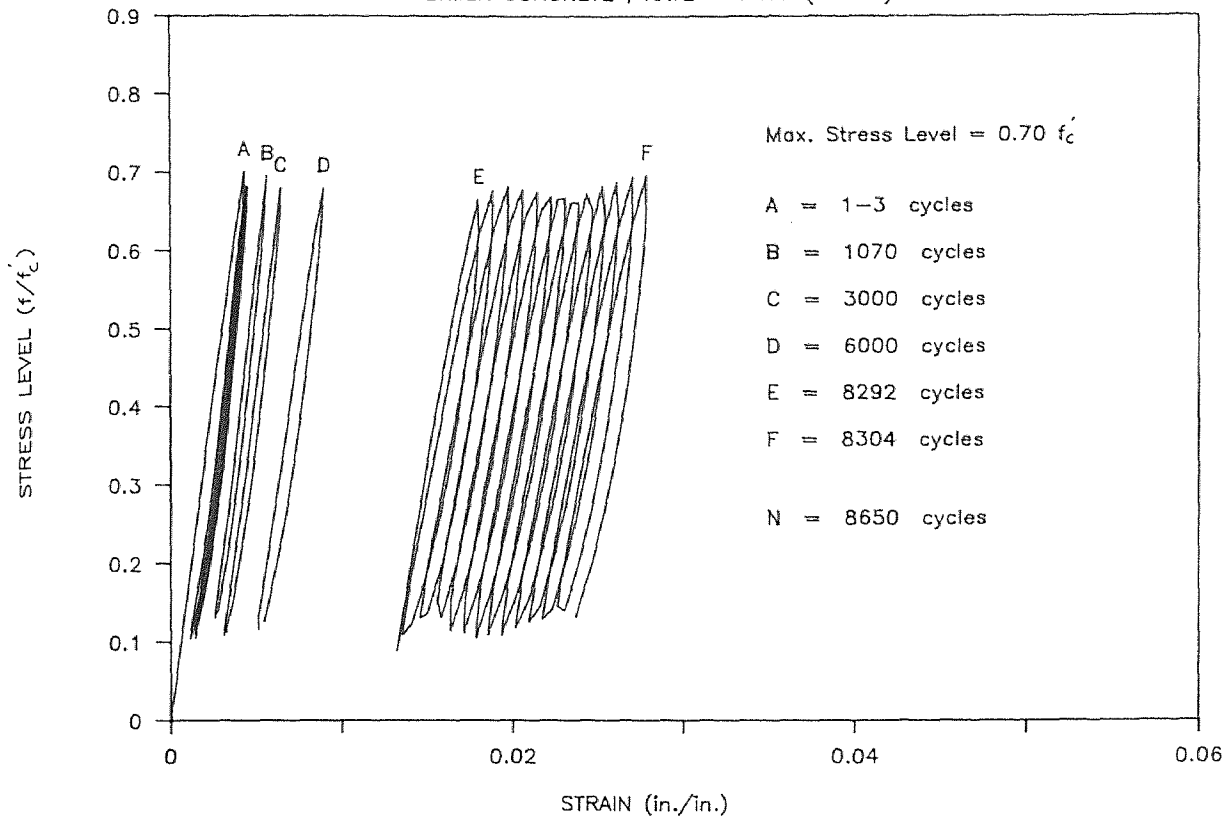
FATIGUE TEST

POLYMER CONCRETE , RATE = 6 Hz. (PF208)



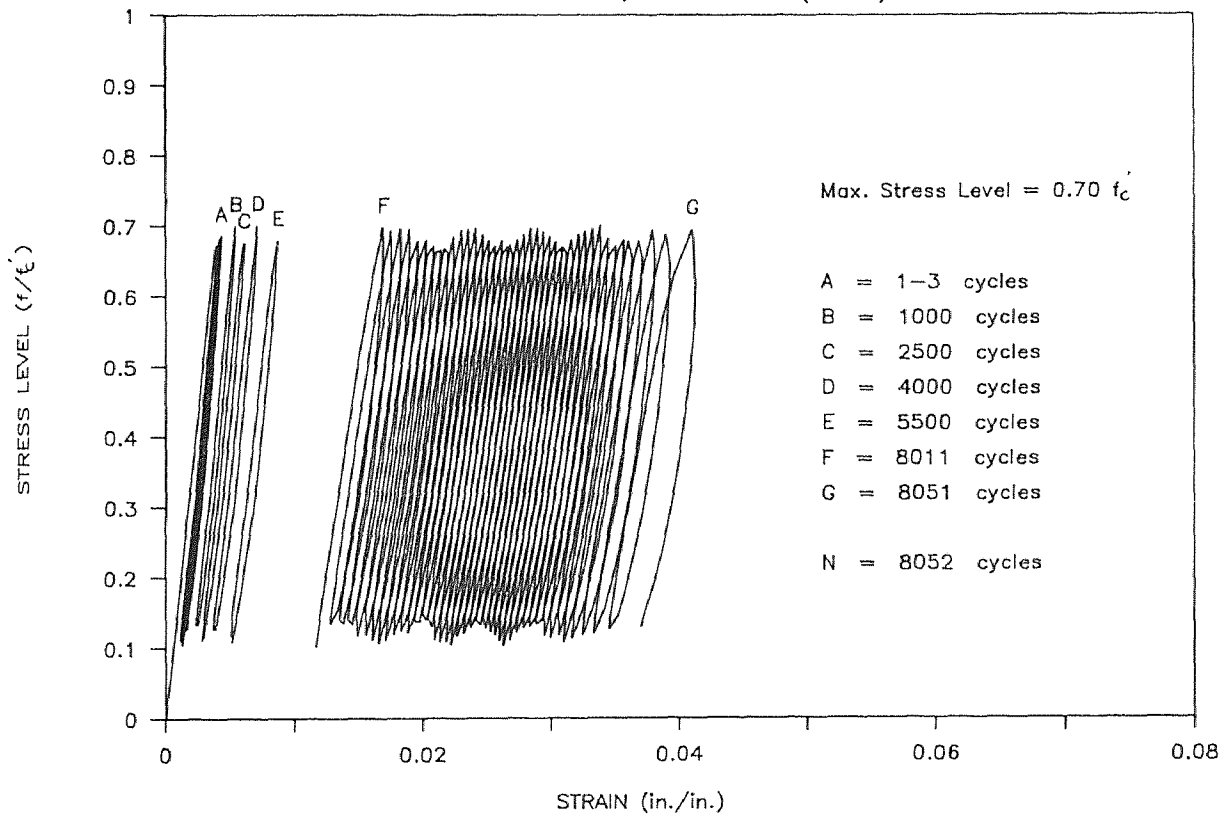
FATIGUE TEST

POLYMER CONCRETE , RATE = 6 Hz. (PF107)



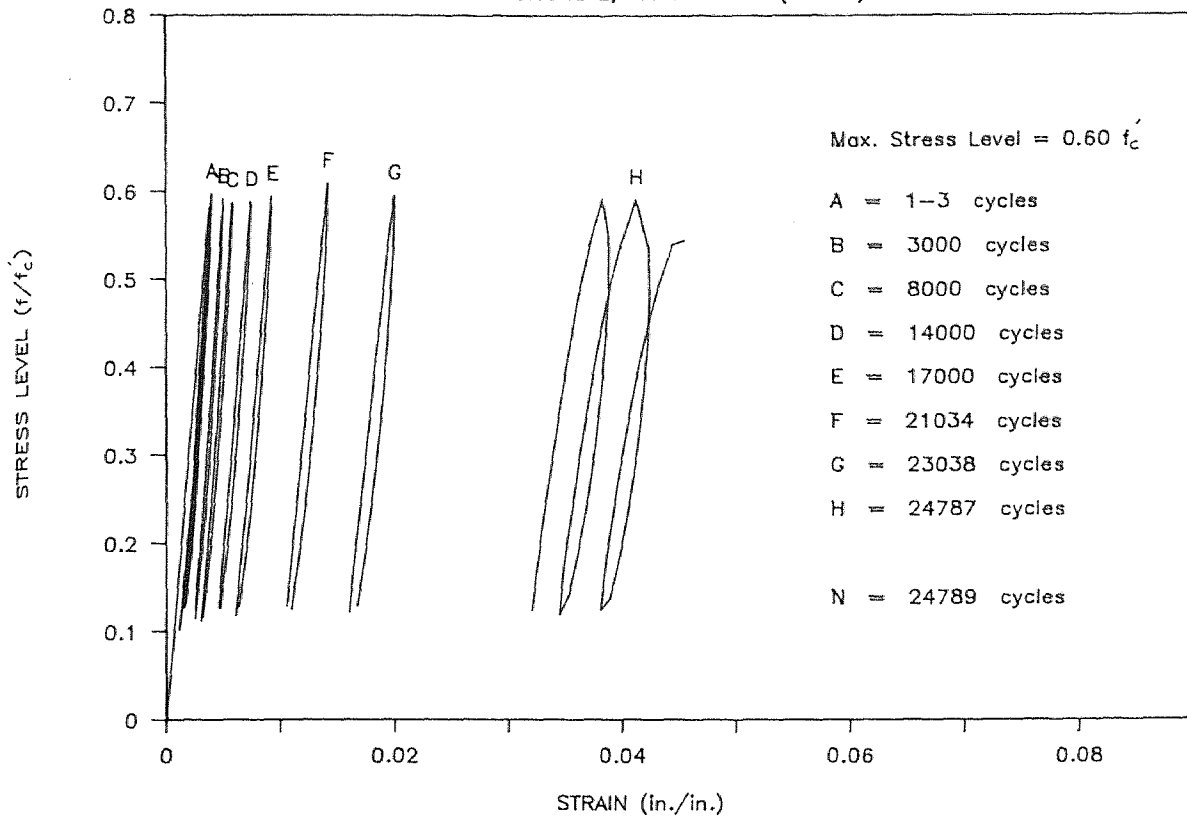
FATIGUE TEST

POLYMER CONCRETE , RATE = 6 Hz. (PF207)



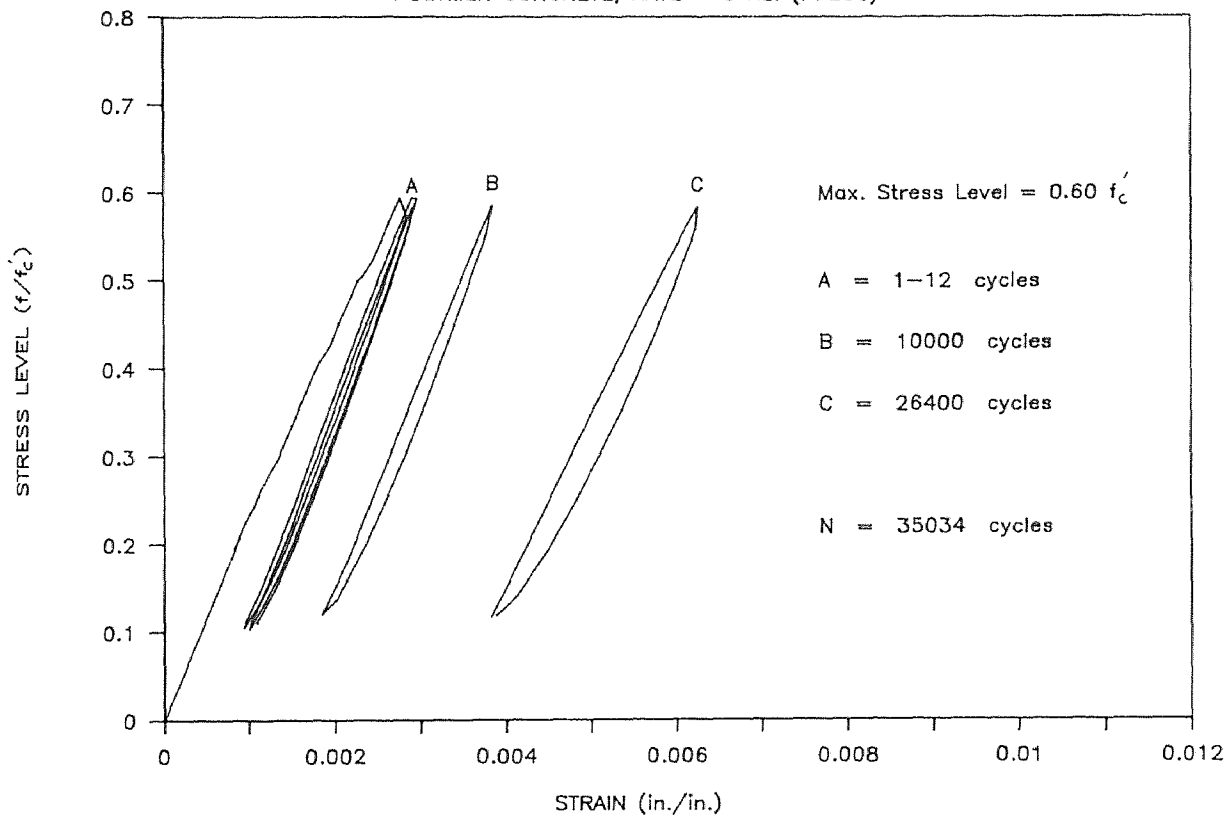
FATIGUE TEST

POLYMER CONCRETE, RATE = 6 Hz.(PF106)



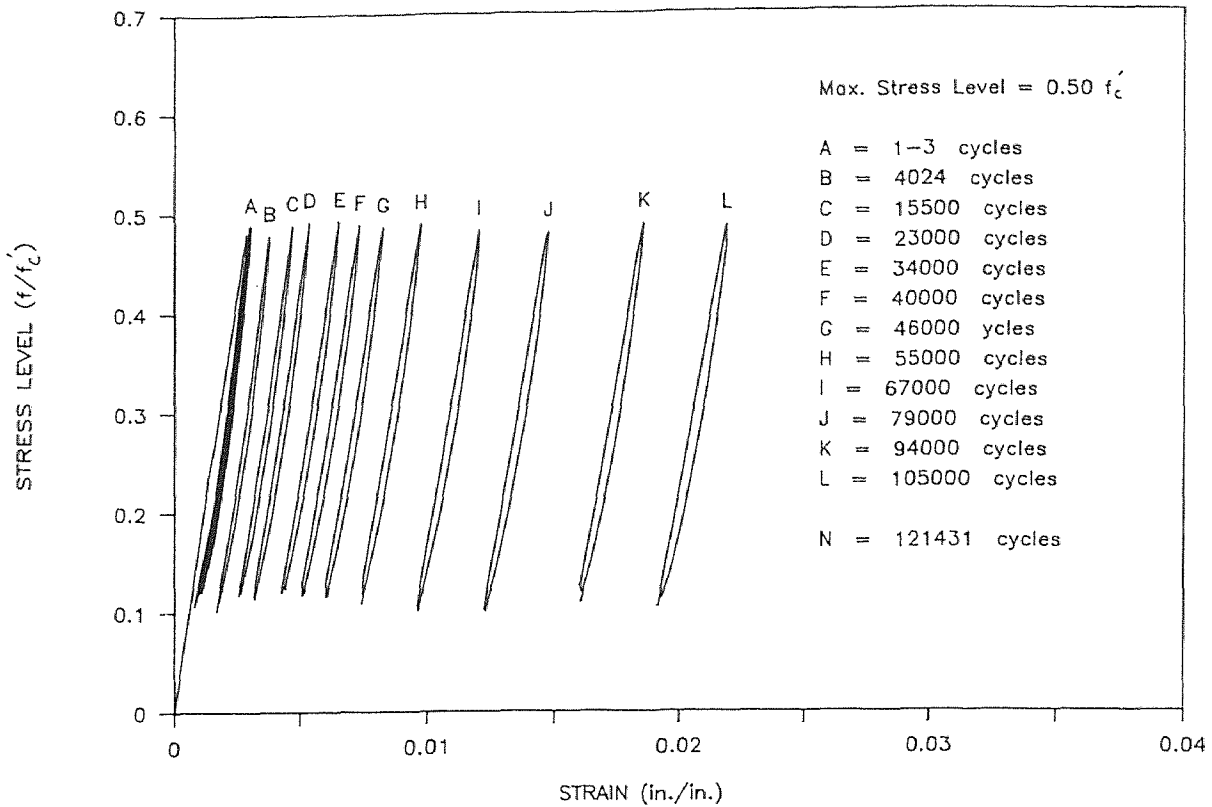
FATIGUE TEST

POLYMER CONCRETE, RATE = 6 Hz. (PF206)



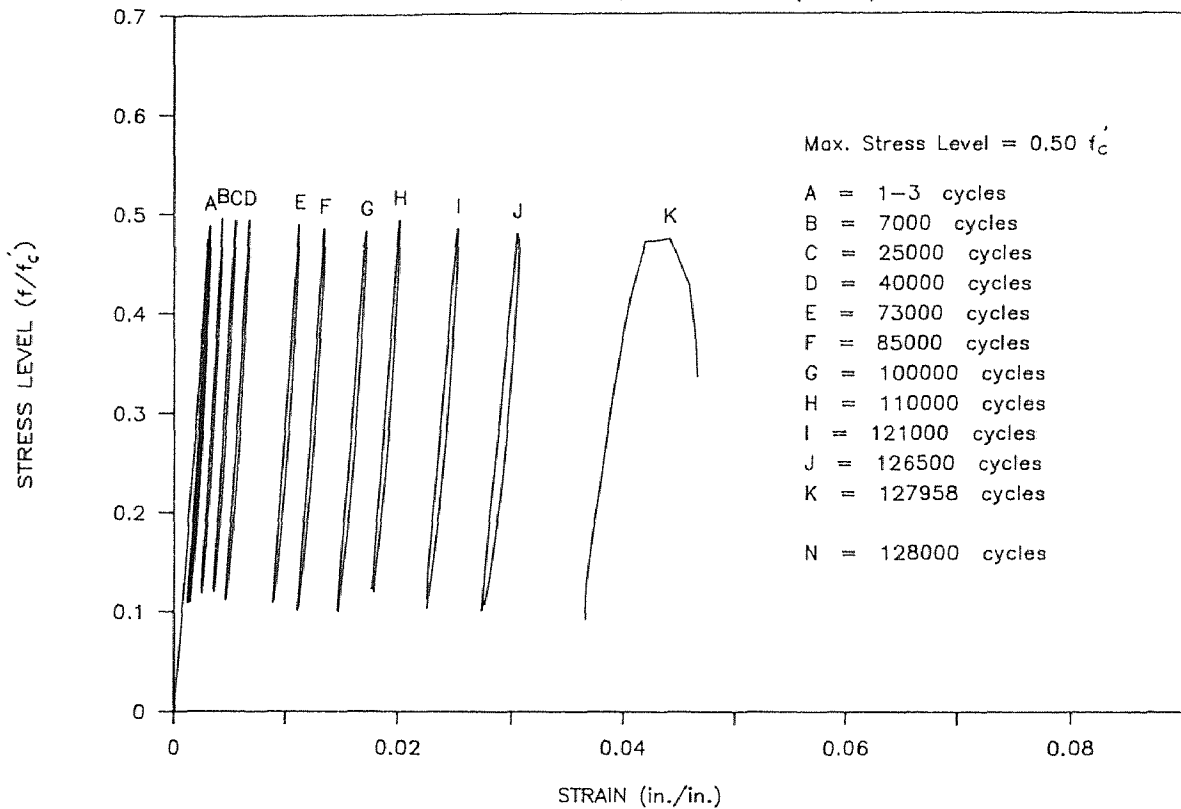
FATIGUE TEST

POLYMER CONCRETE, RATE = 6 Hz. (PF105)



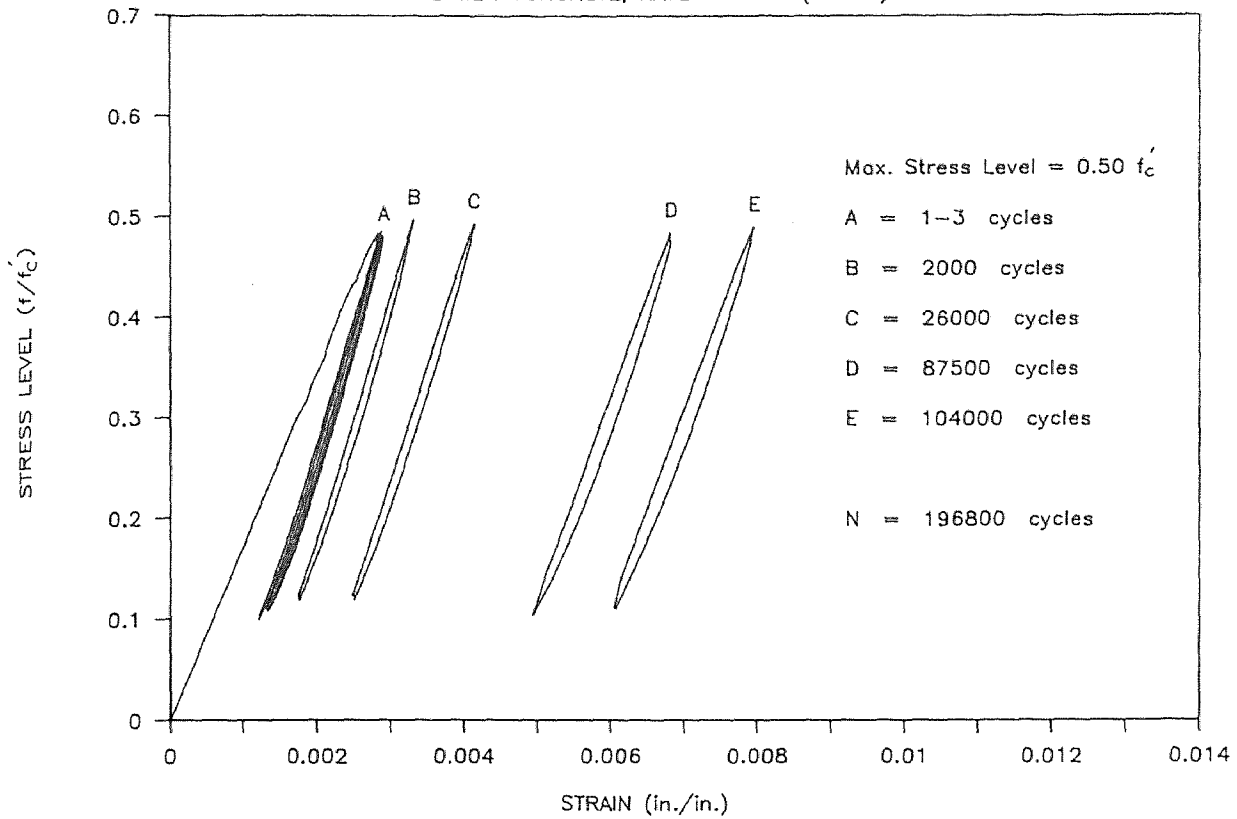
FATIGUE TEST

POLYMER CONCRETE, RATE = 6 Hz. (PF205)



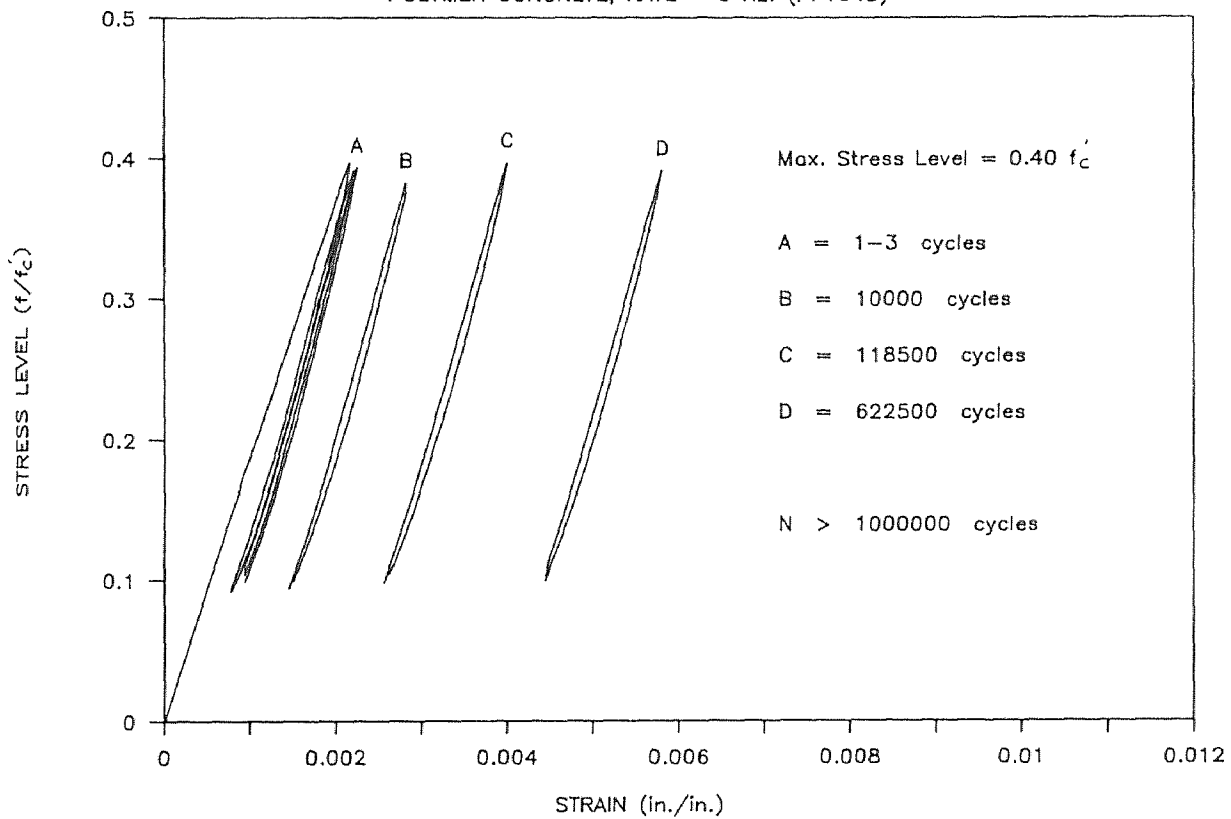
FATIGUE TEST

POLYMER CONCRETE, RATE = 6 Hz. (PF305)



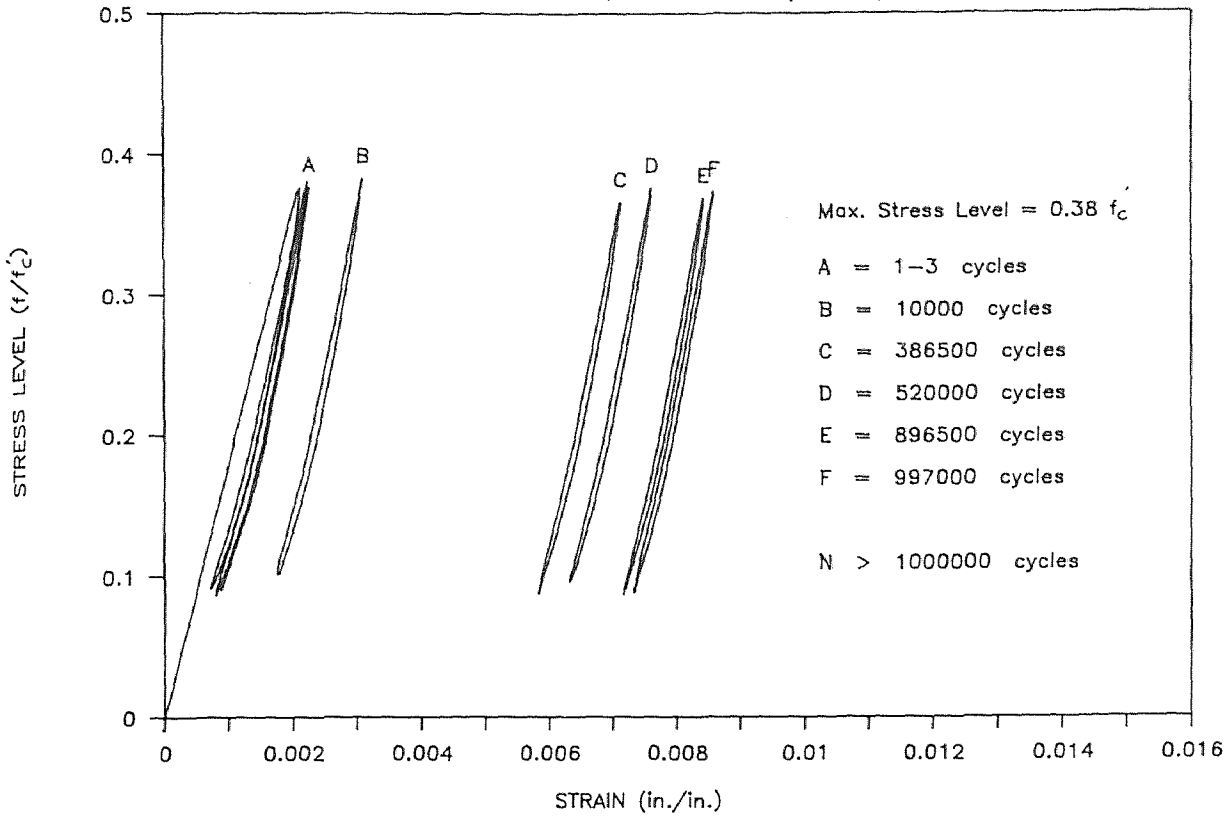
FATIGUE TEST

POLYMER CONCRETE, RATE = 6 Hz. (PF1045)



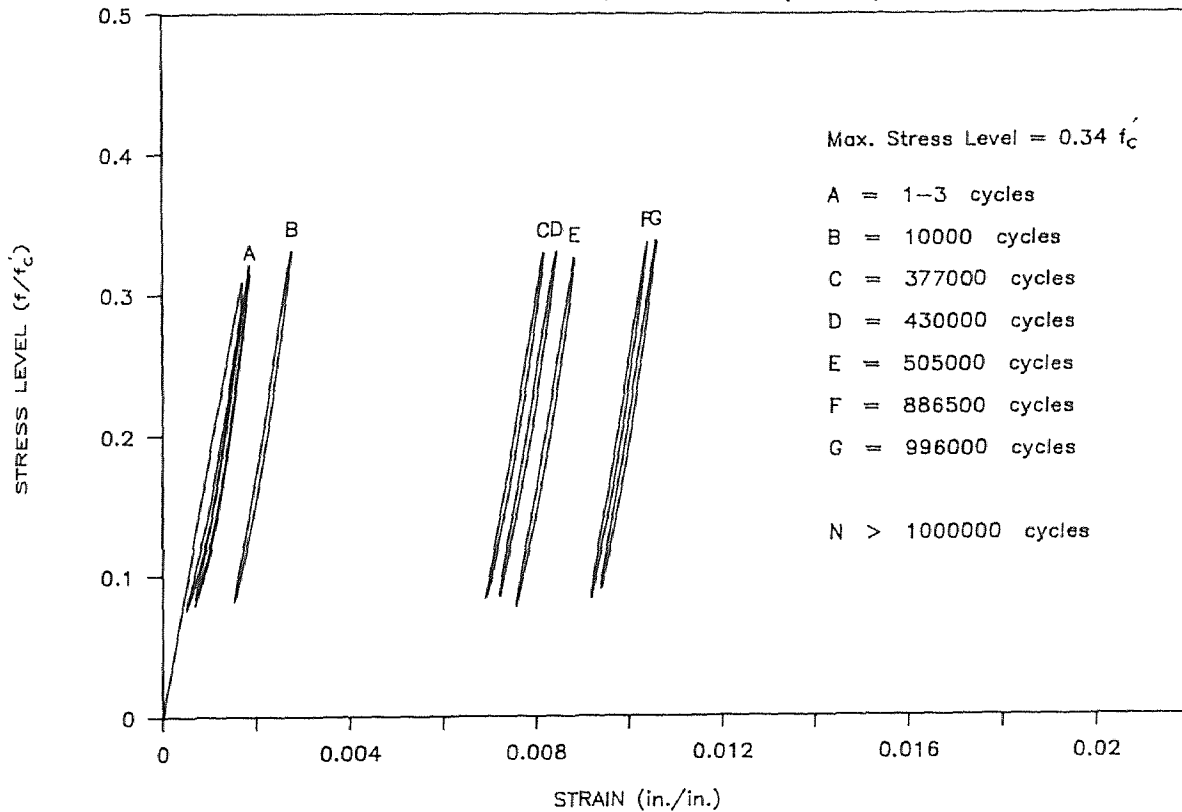
FATIGUE TEST

POLYMER CONCRETE, RATE = 6 Hz. (PF2045)



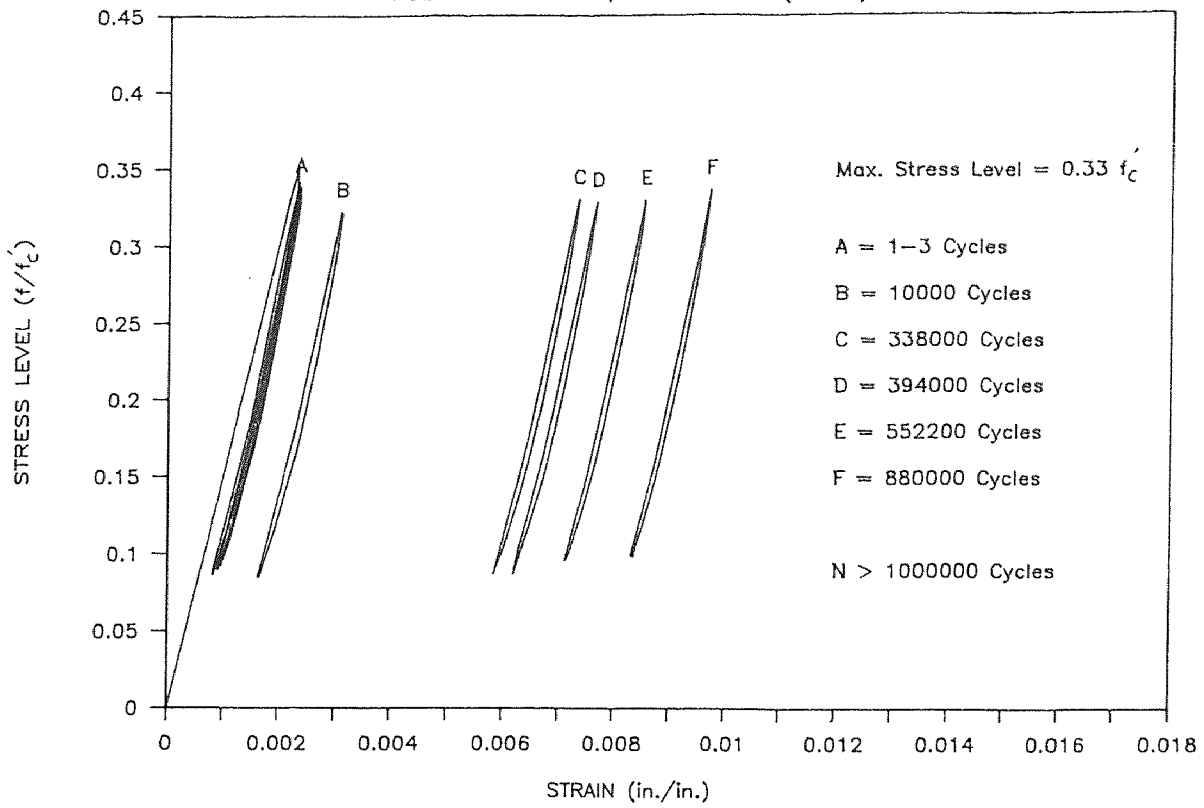
FATIGUE TEST

POLYMER CONCRETE, RATE = 6 Hz. (PF3045)



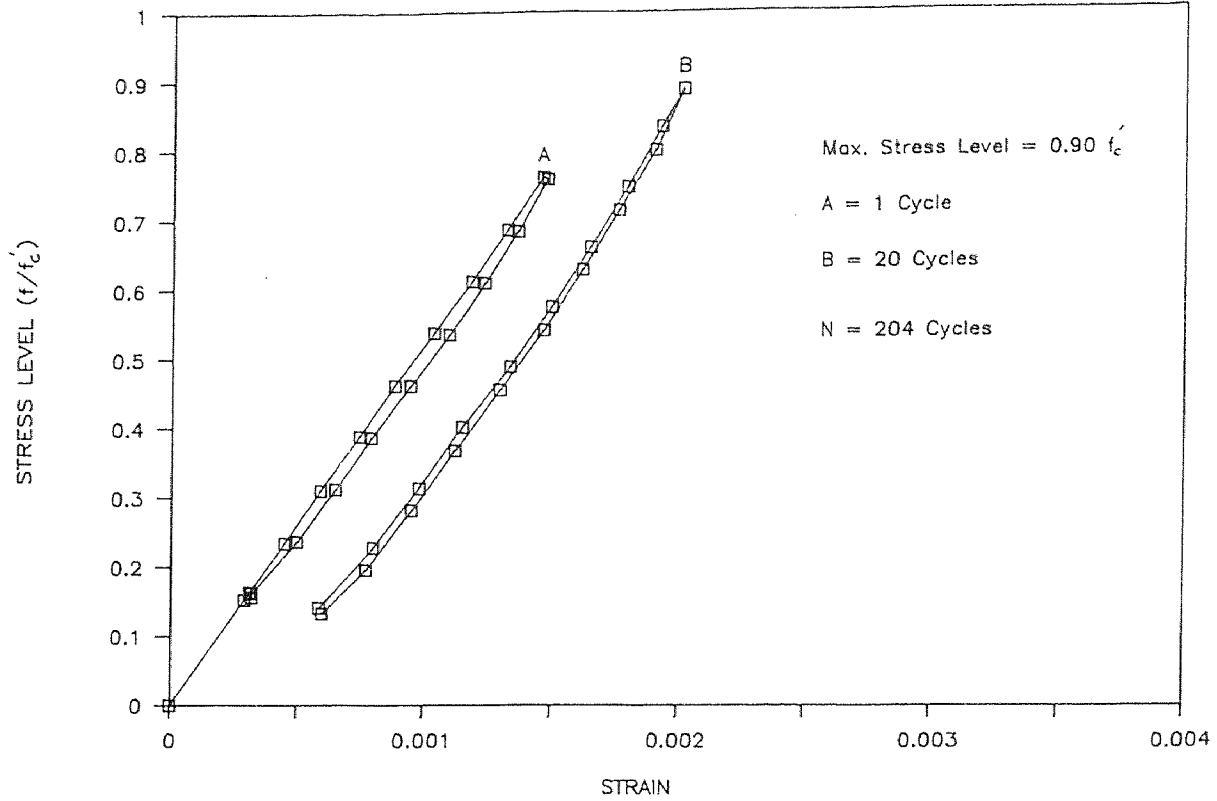
FATIGUE TEST

POLYMER CONCRETE, RATE = 6 Hz. (PF104)



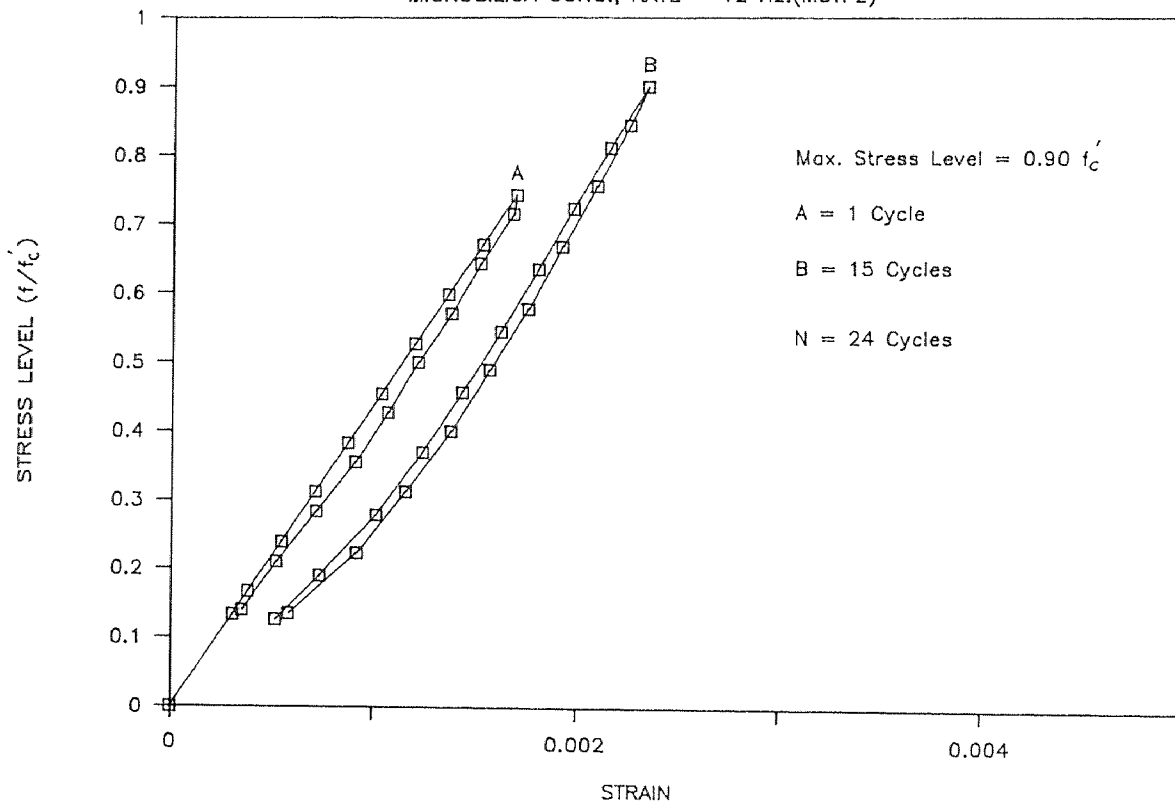
FATIGUE TEST

MICROSILICA CONC., RATE = 12 Hz.(M3TF1)



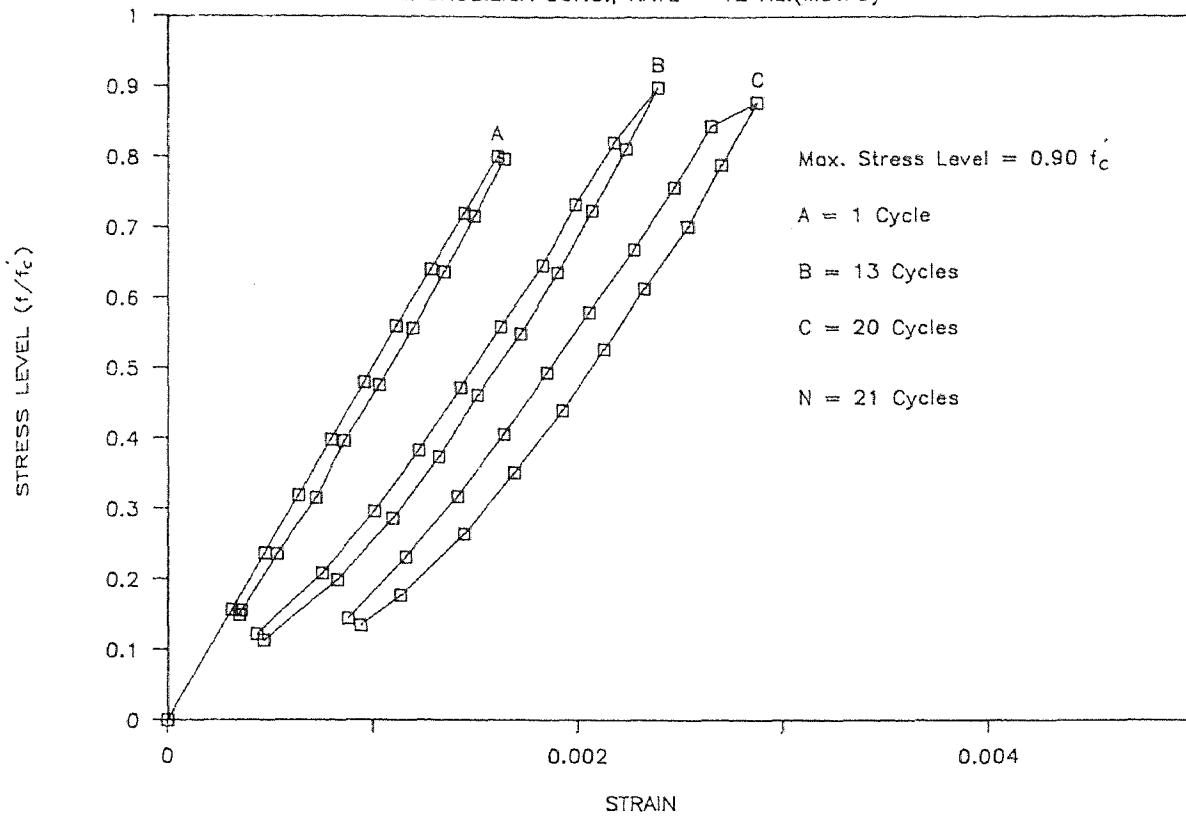
FATIGUE TEST

MICROSILICA CONC., RATE = 12 Hz.(M3TF2)



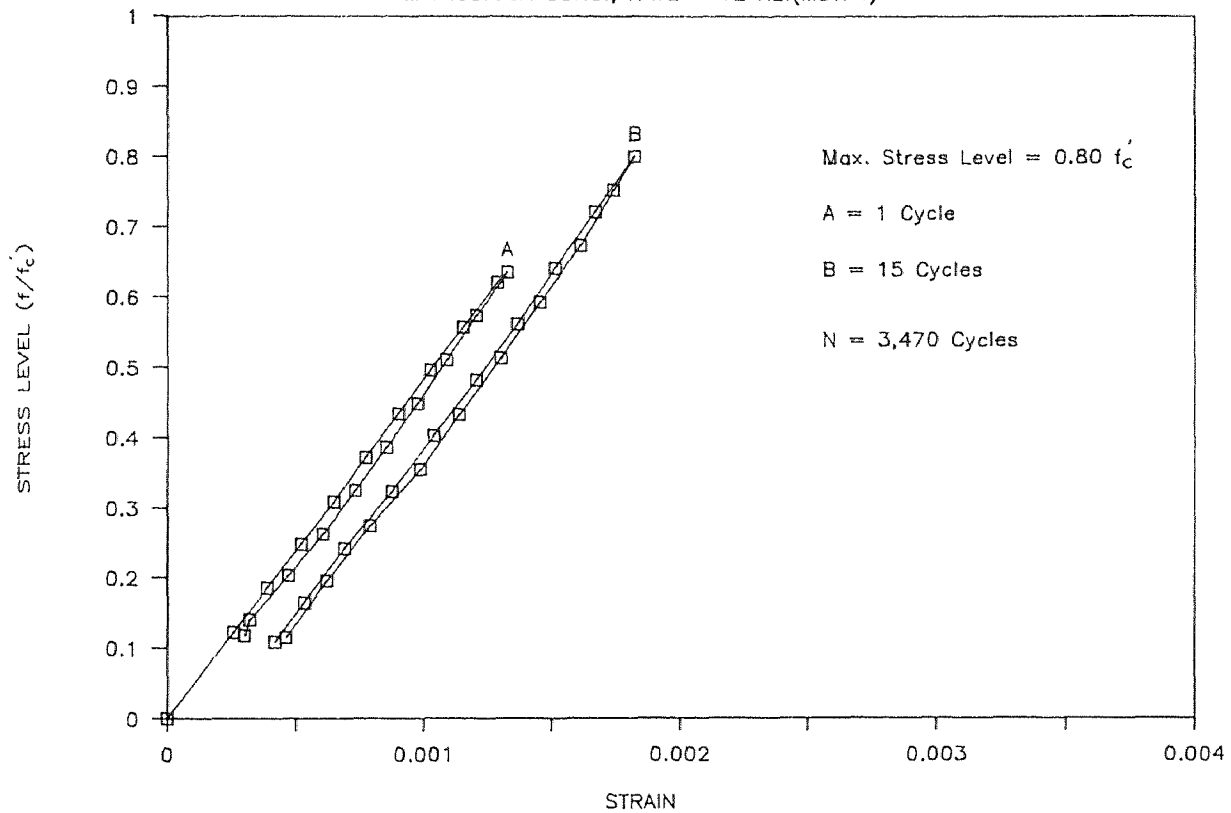
FATIGUE TEST

MICROSILICA CONC., RATE = 12 Hz.(M3TF3)



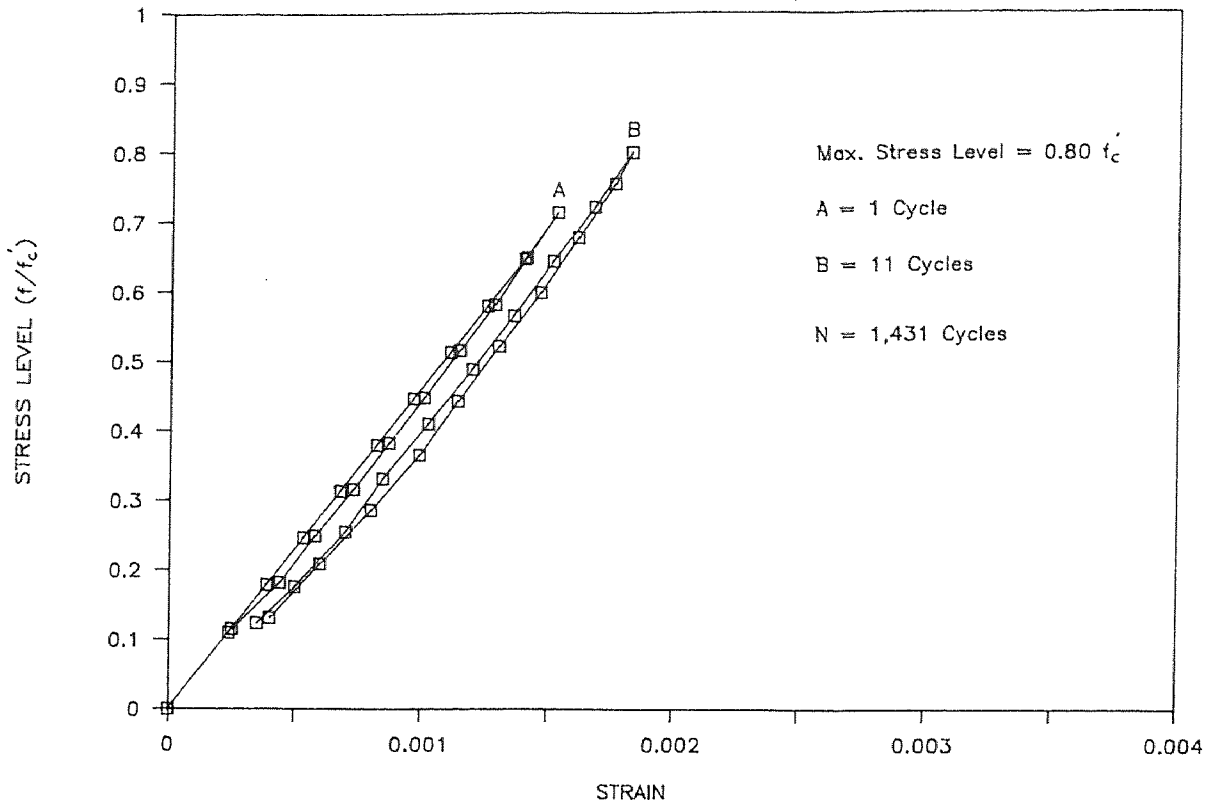
FATIGUE TEST

MICROSILICA CONC., RATE = 12 Hz.(M3TF4)



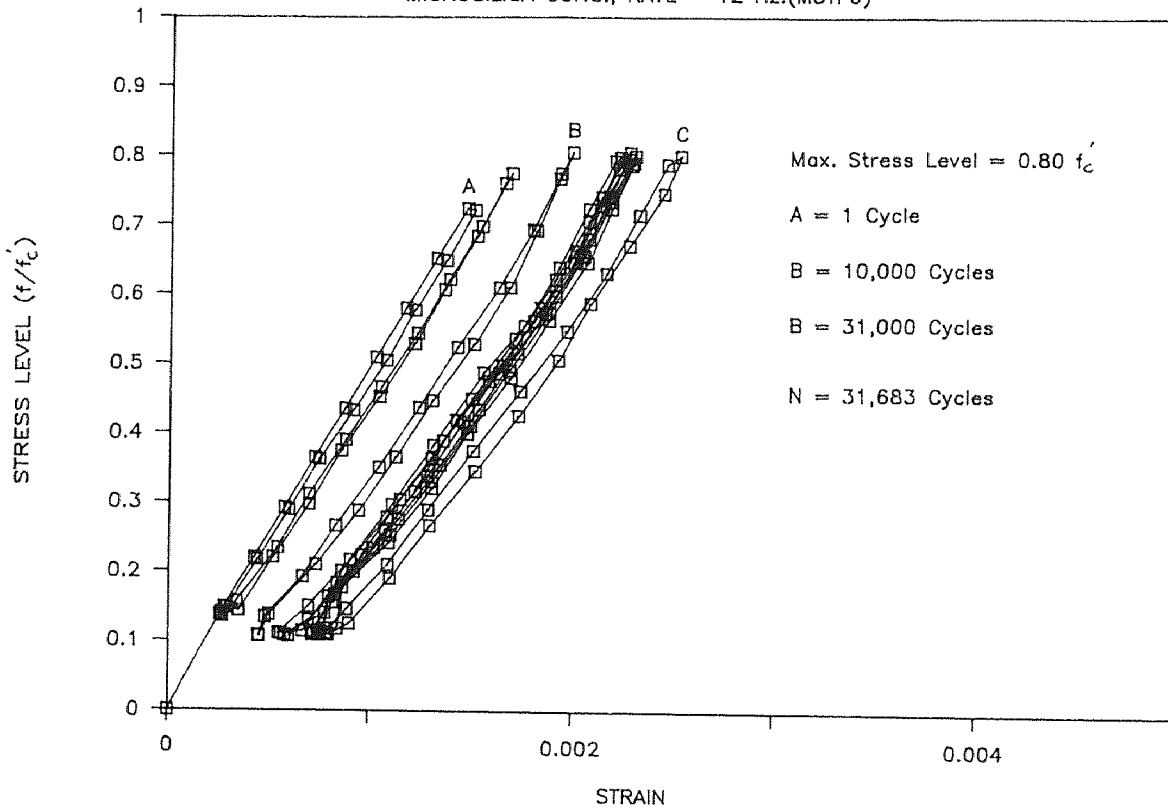
FATIGUE TEST

MICROSILICA CONC., RATE = 12 Hz.(M3TF5)



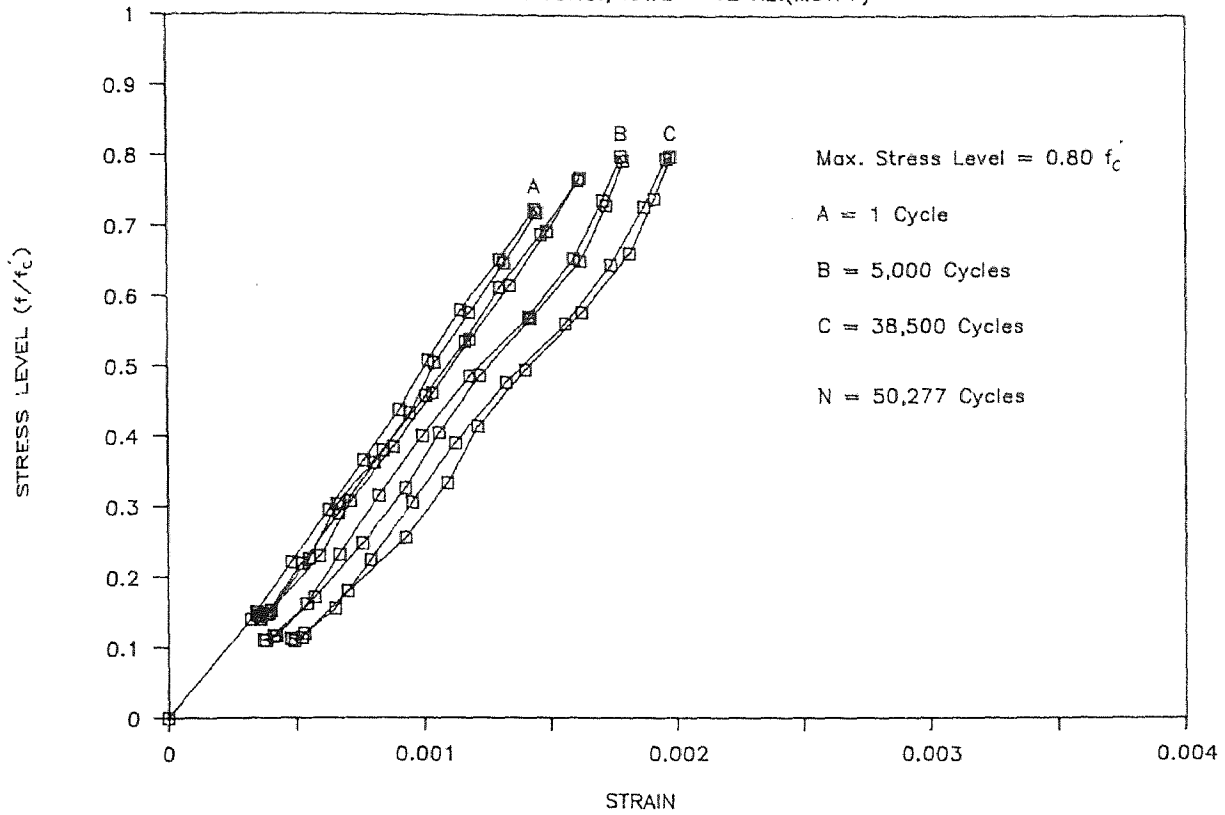
FATIGUE TEST

MICROSILICA CONC., RATE = 12 Hz.(M3TF6)



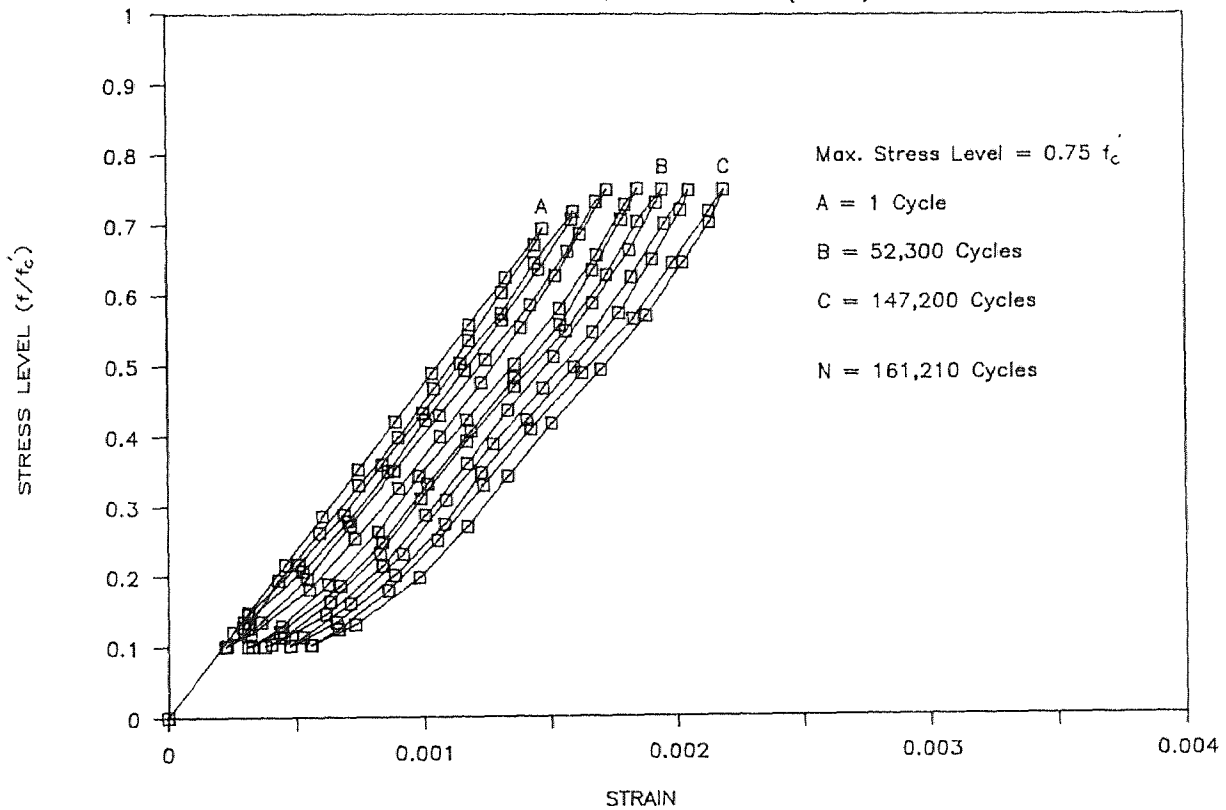
FATIGUE TEST

MICROSILICA CONC., RATE = 12 Hz.(M3TF7)



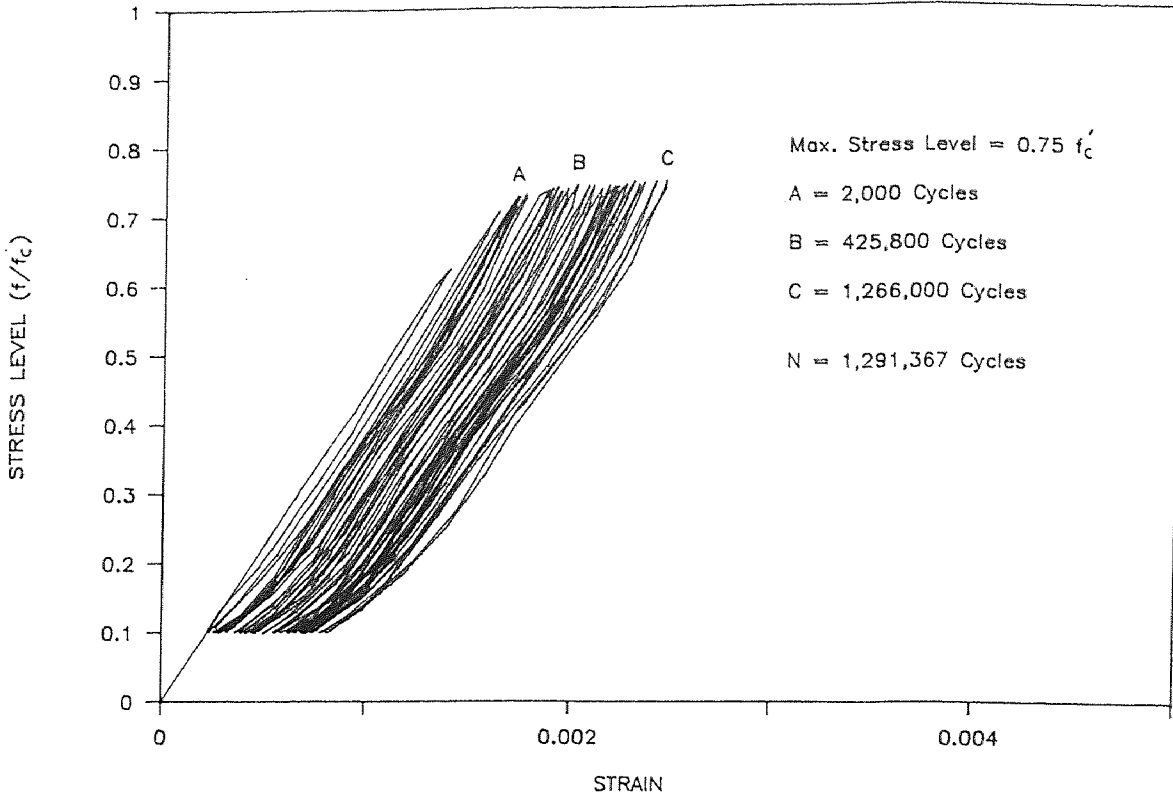
FATIGUE TEST

MICROSILICA CONC., RATE = 12 Hz (M3TF8)



FATIGUE TEST

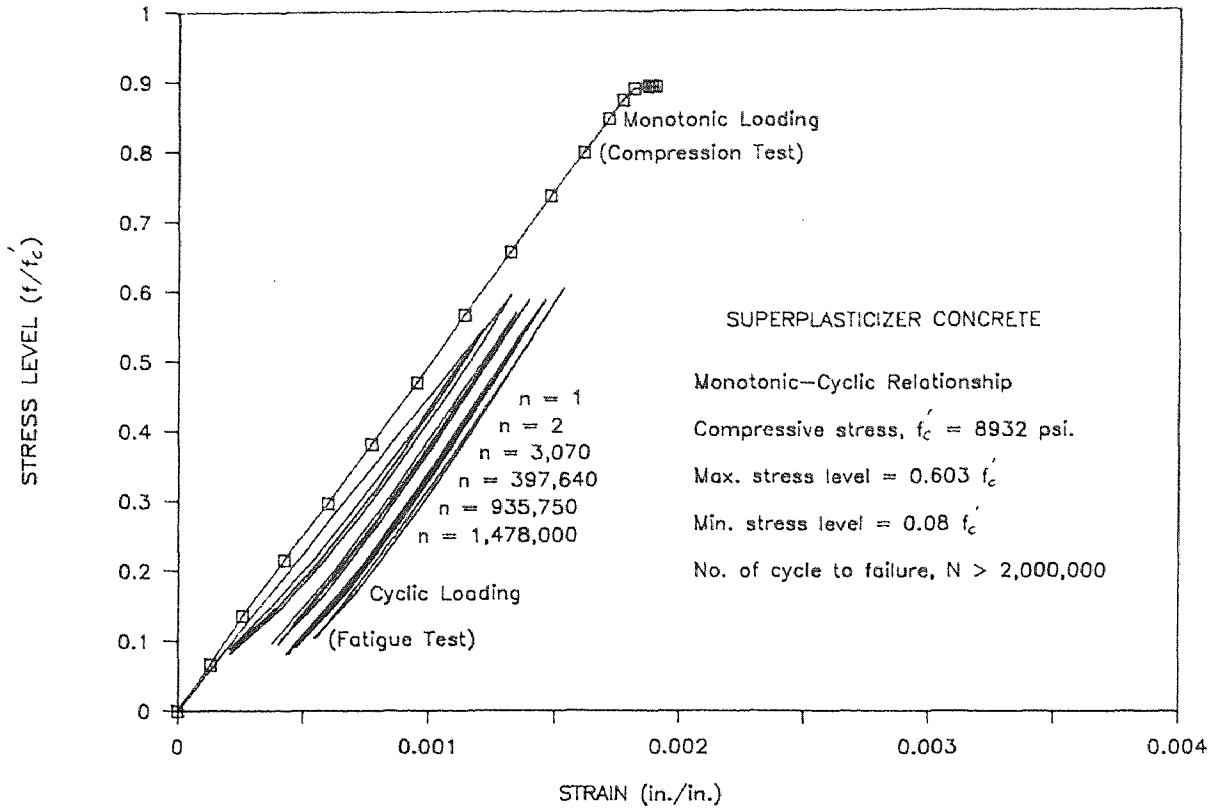
MICROSILICA CONC.,RATE = 12 Hz.(M3TF10)



APPENDIX J

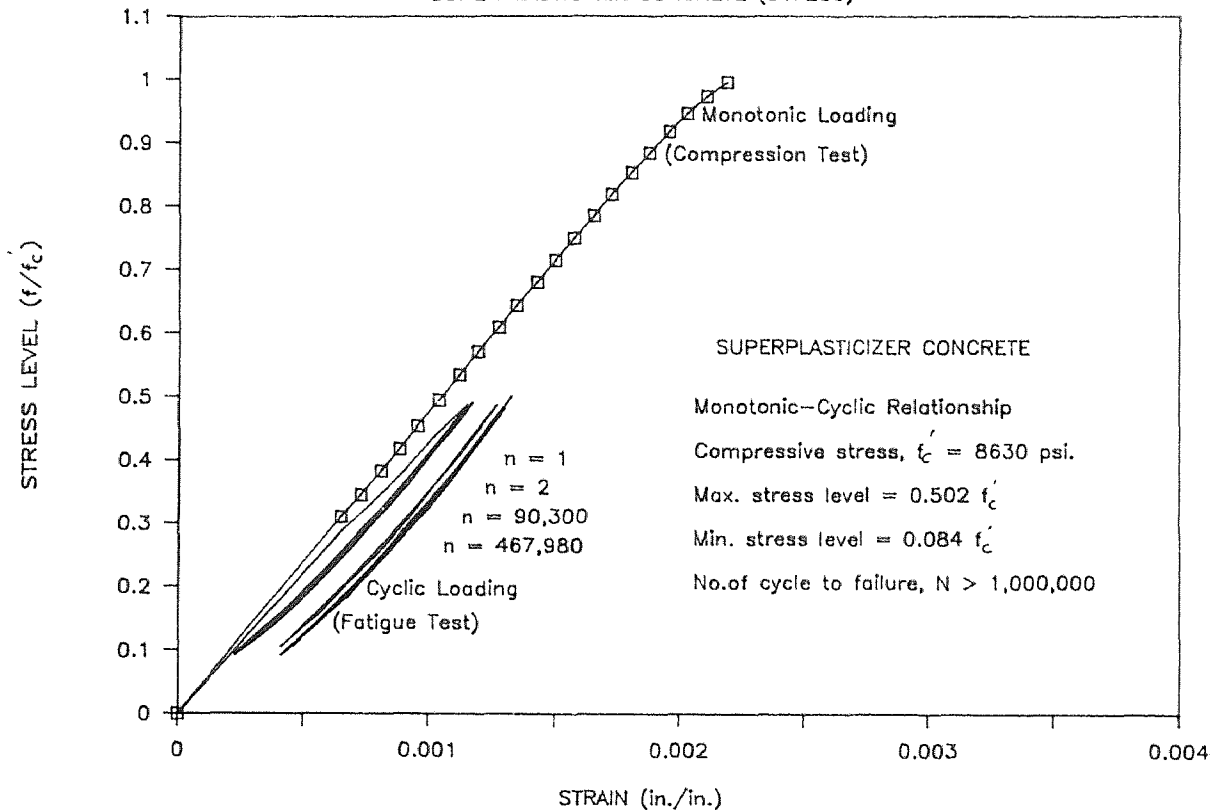
MONOTONIC VS. CYCLIC CURVE

SUPERPLASTICIZER CONCRETE (S1F175)



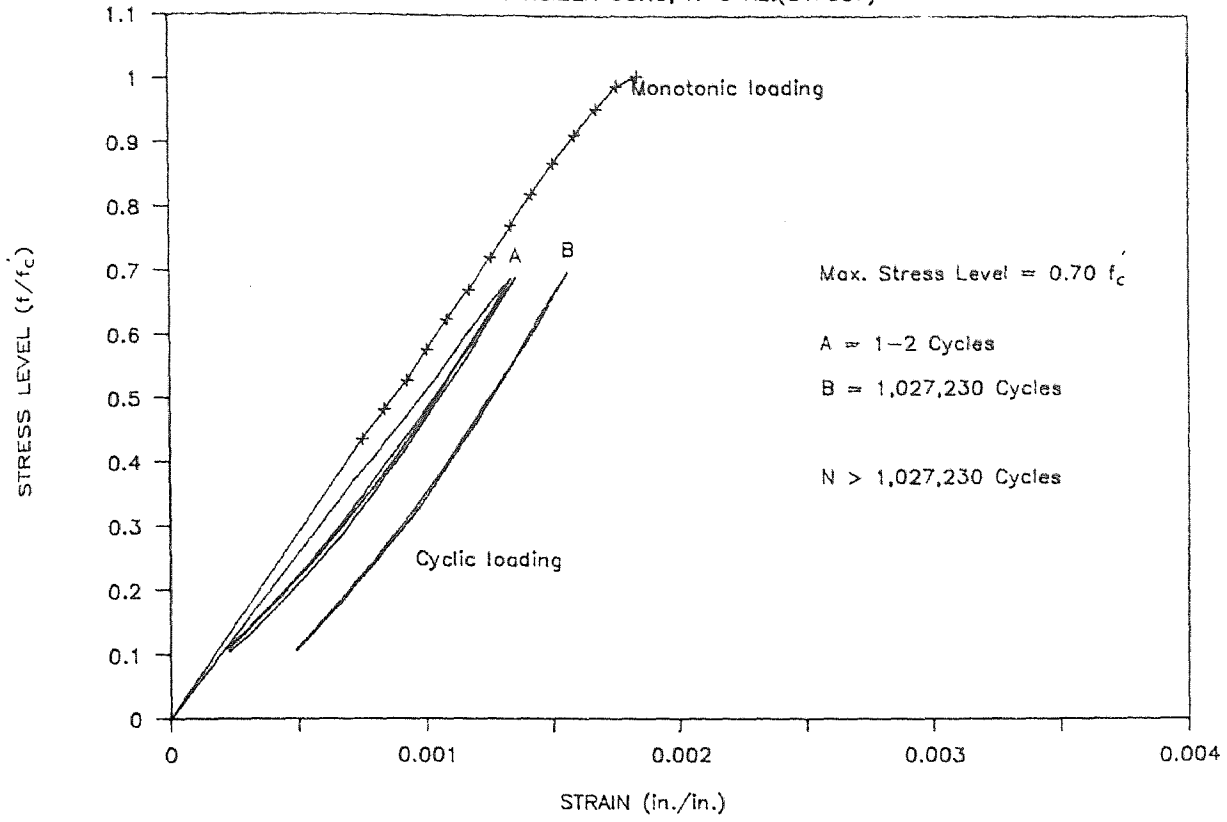
MONOTONIC VS. CYCLIC CURVE

SUPERPLASTICIZER CONCRETE (S1F206)



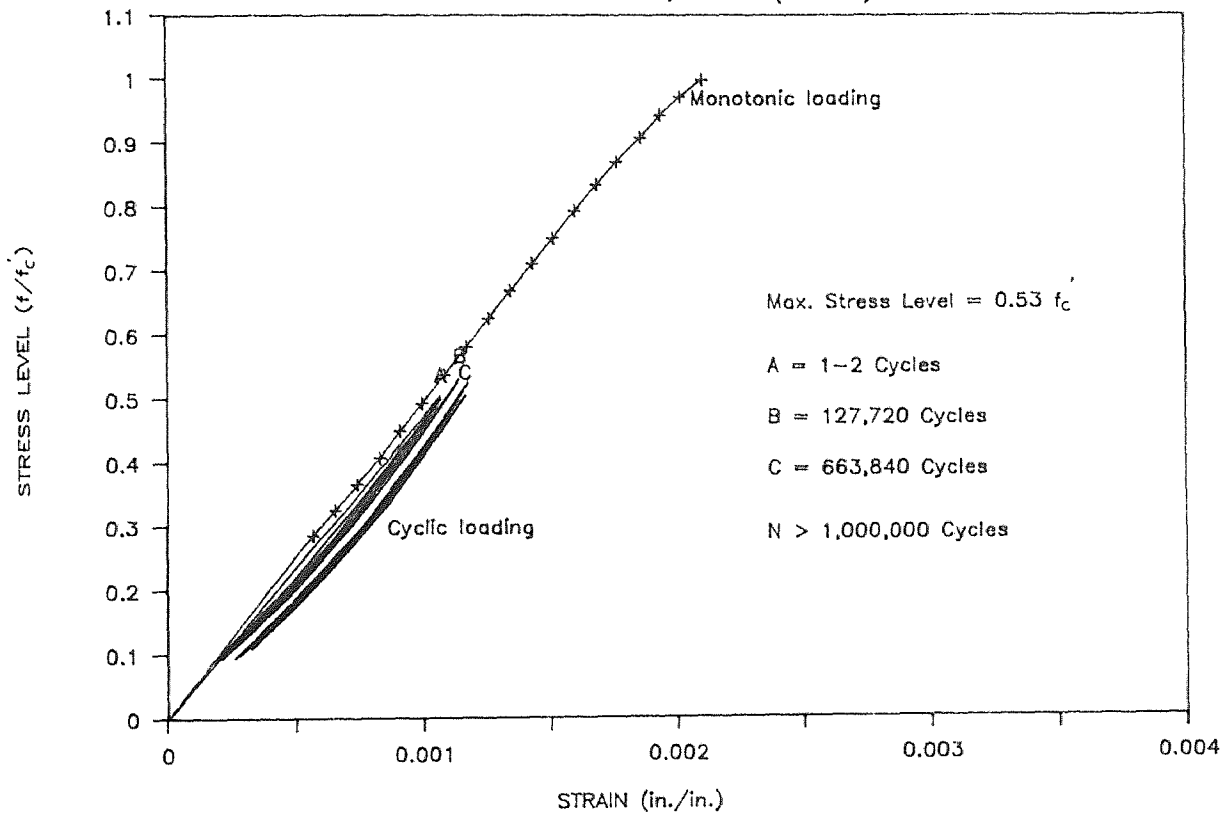
MONOTONIC VS. CYCLIC CURVE

SUPERPLASTICIZER CONC, R=6 Hz.(S1F307)



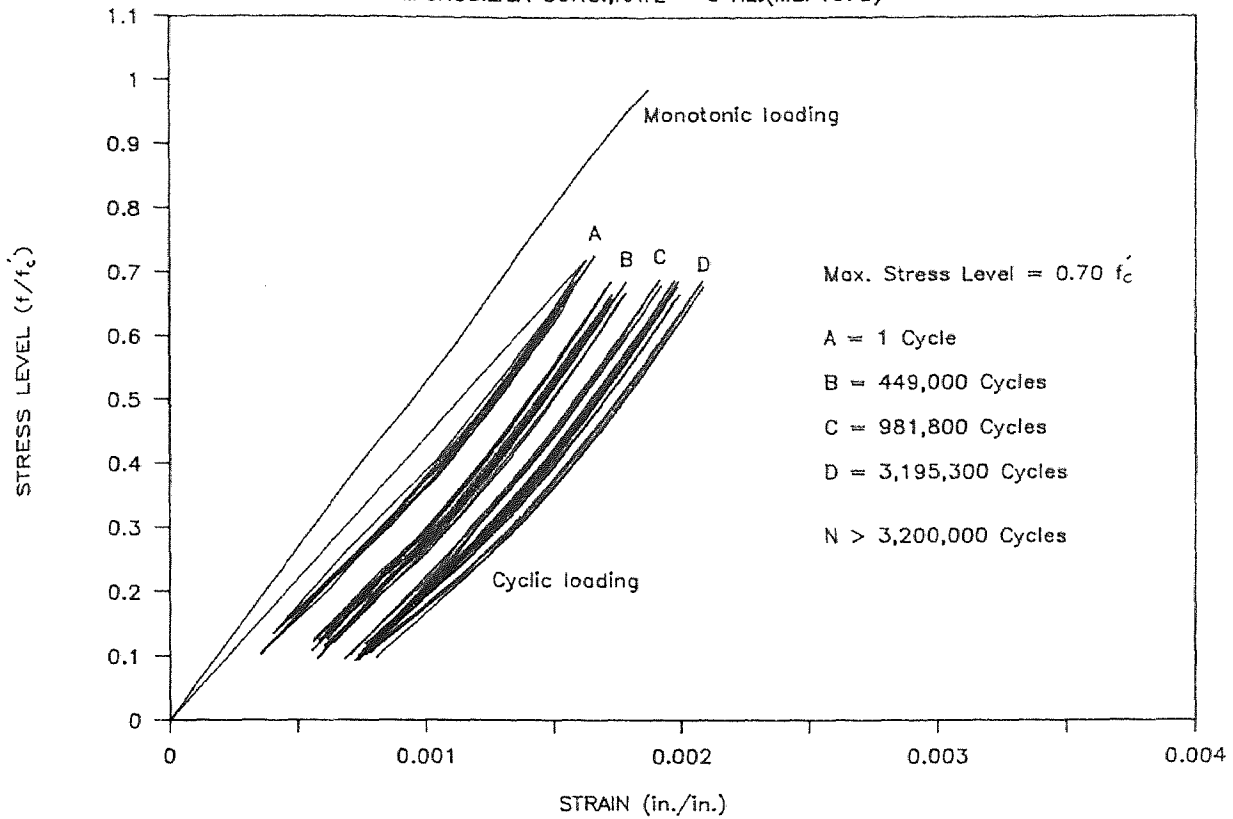
MONOTONIC VS. CYCLIC CURVE

SUPERPLASTICIZER CONC, R=6 Hz.(S1F106)



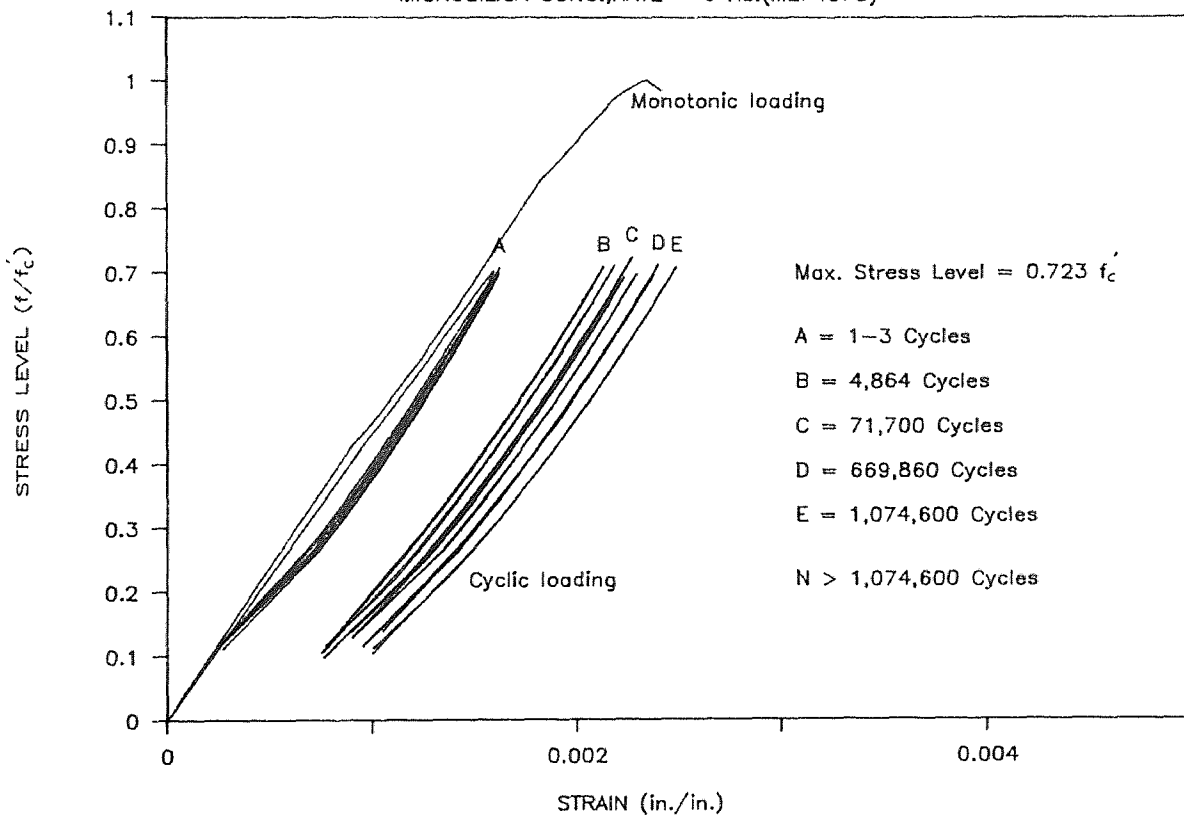
MONOTONIC VS. CYCLIC CURVE

MICROSILICA CONC.,RATE = 6 Hz.(M2F1075)



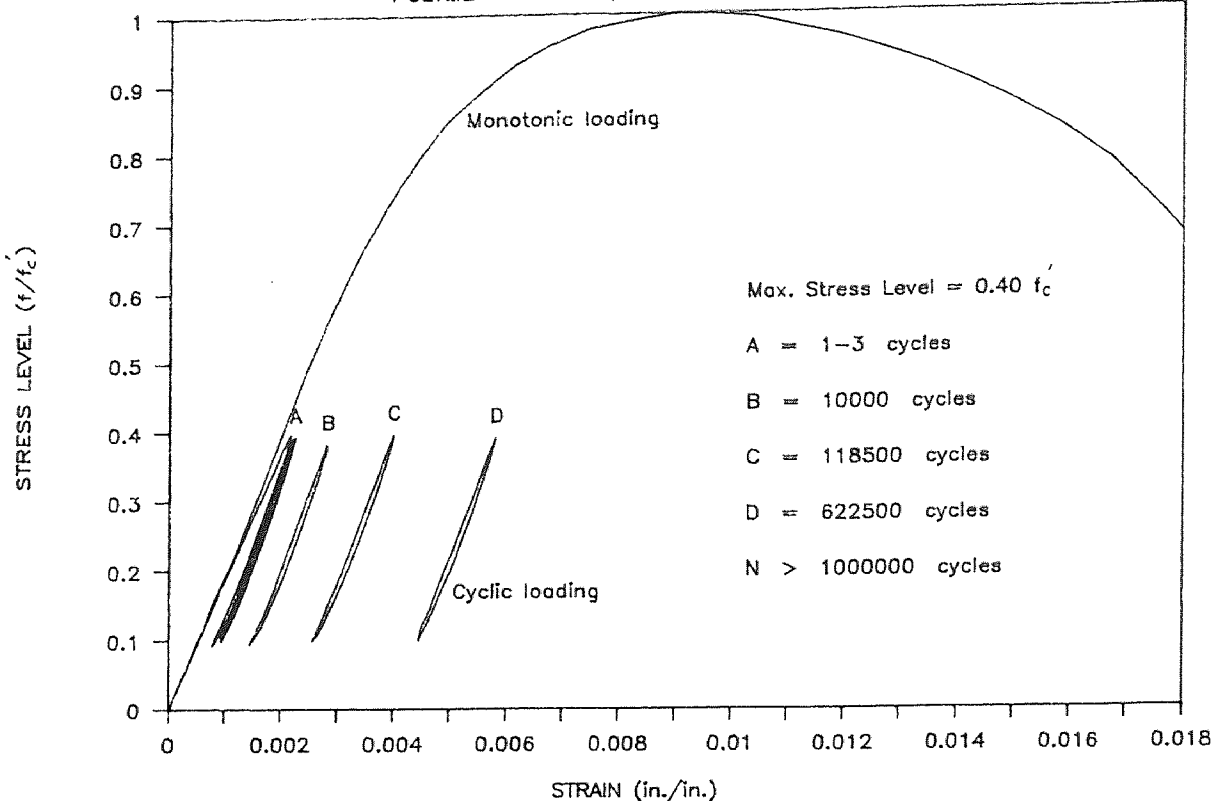
MONOTONIC VS. CYCLIC CURVE

MICROSILICA CONC.,RATE = 6 Hz.(M2F4075)



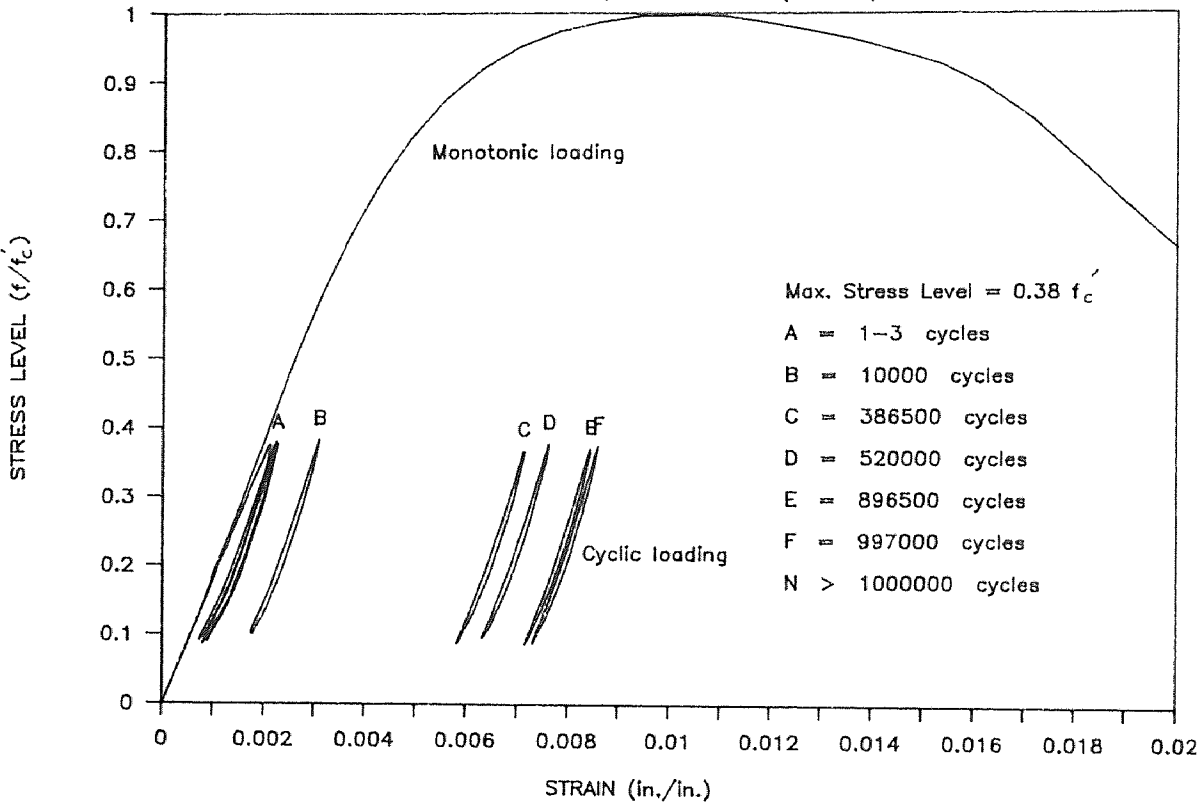
MONOTONIC VS. CYCLIC CURVE

POLYMER CONCRETE, RATE = 6 Hz. (PF1045)



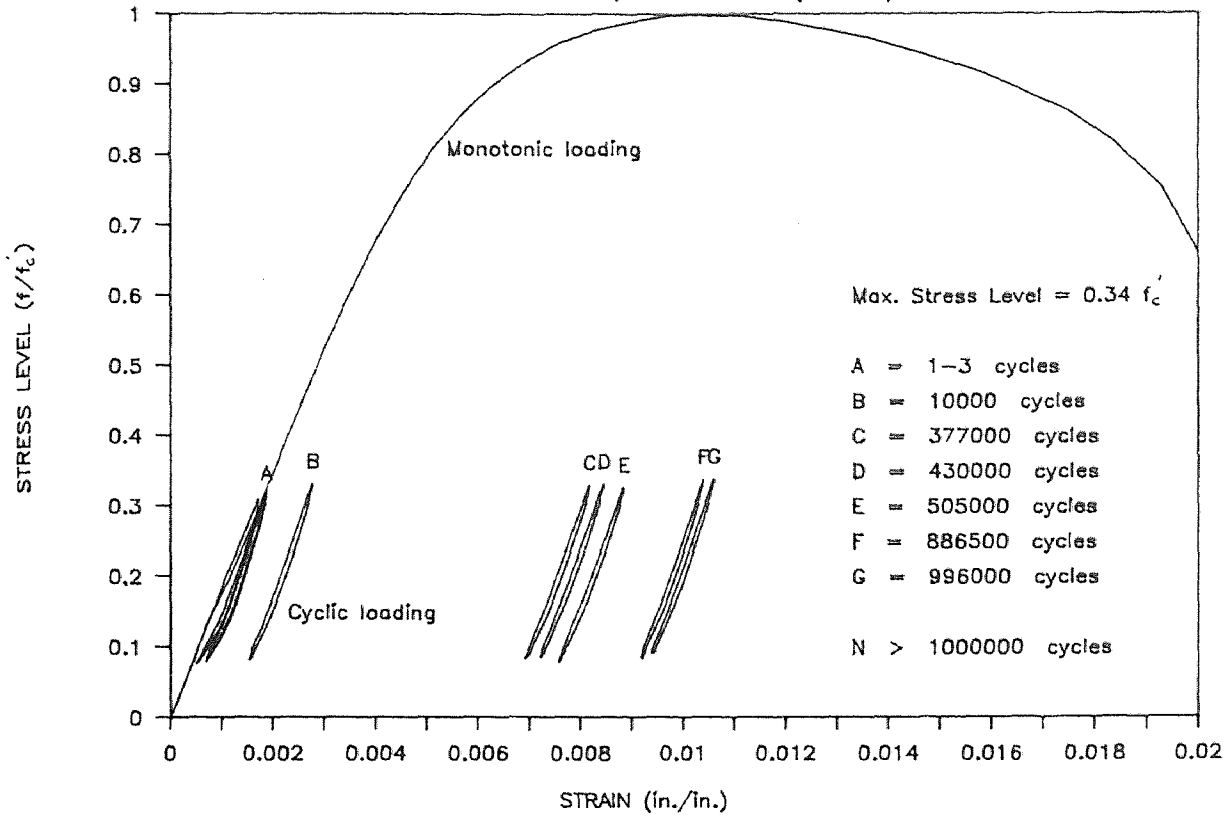
MONOTONIC VS. CYCLIC CURVE

POLYMER CONCRETE, RATE = 6 Hz. (PF2045)



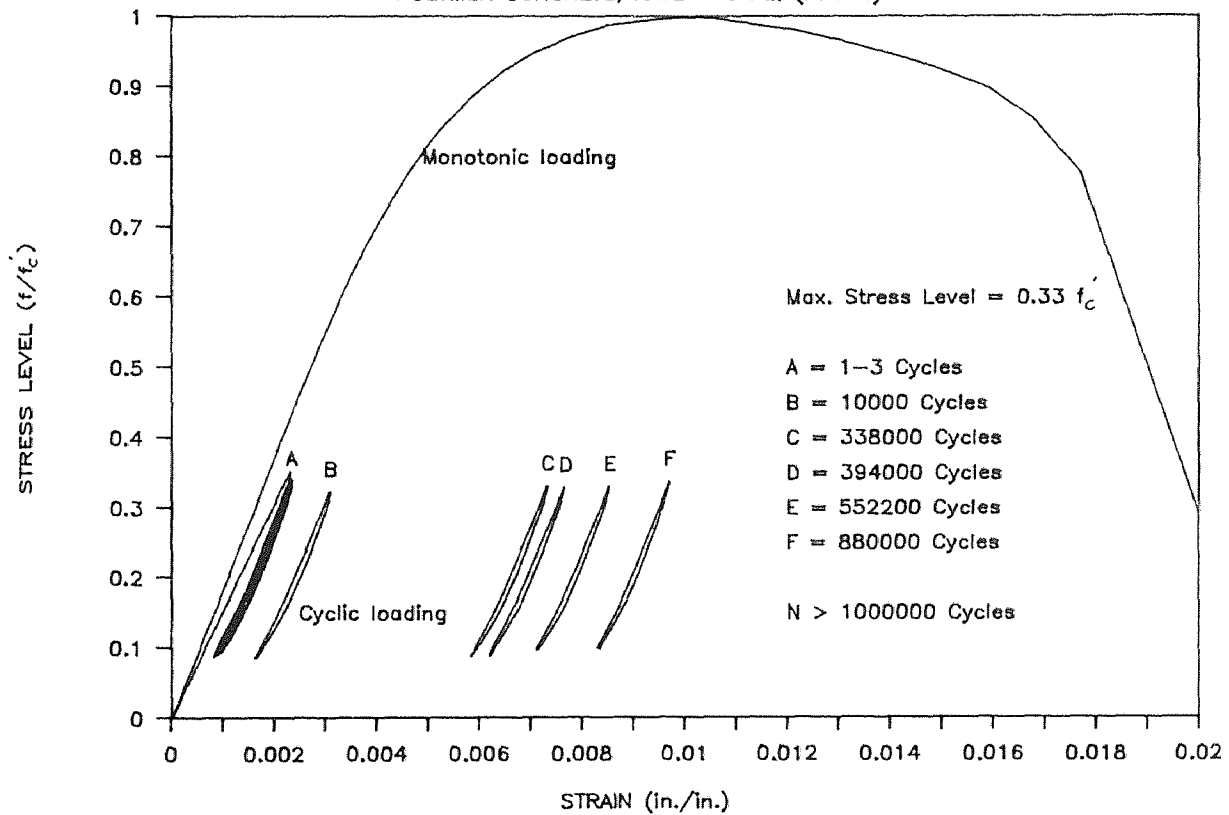
MONOTONIC VS. CYCLIC CURVE

POLYMER CONCRETE, RATE = 6 Hz. (PF3045)



MONOTONIC VS. CYCLIC CURVE

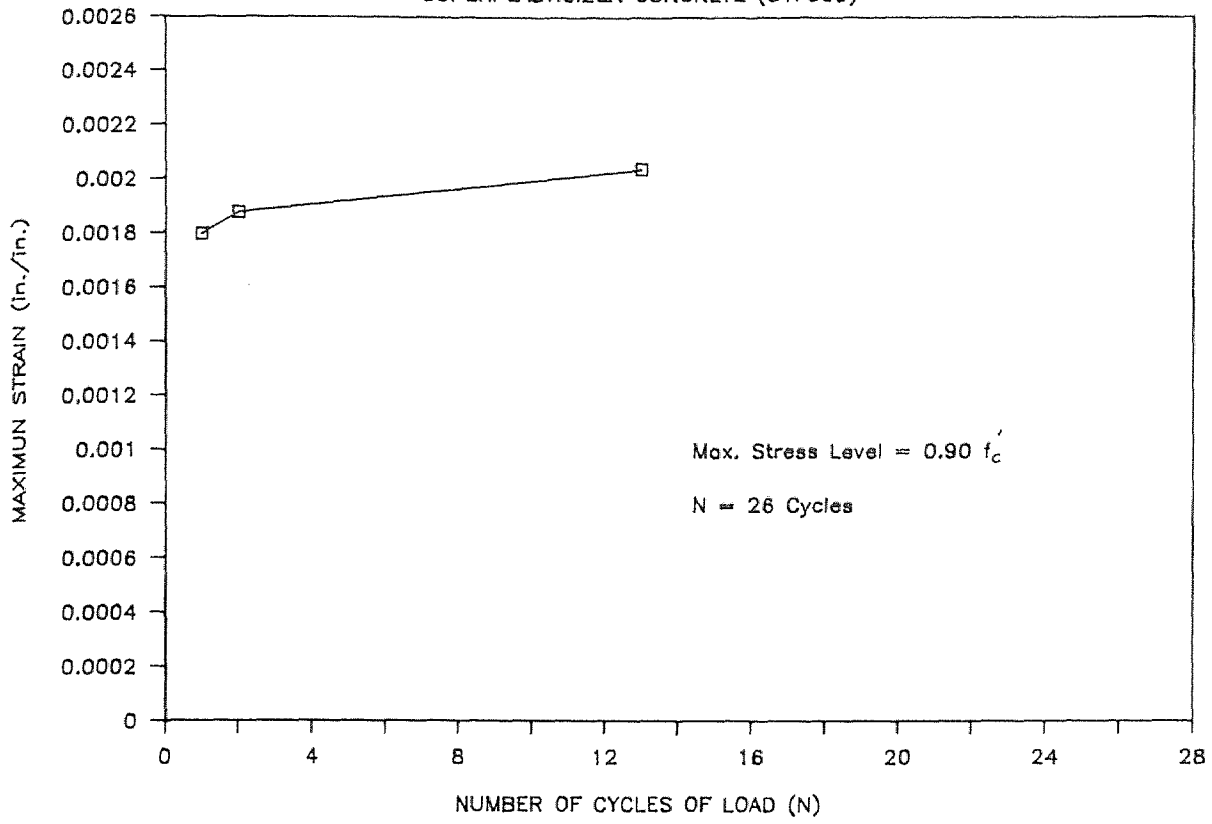
POLYMER CONCRETE, RATE = 6 Hz. (PF104)



APPENDIX K

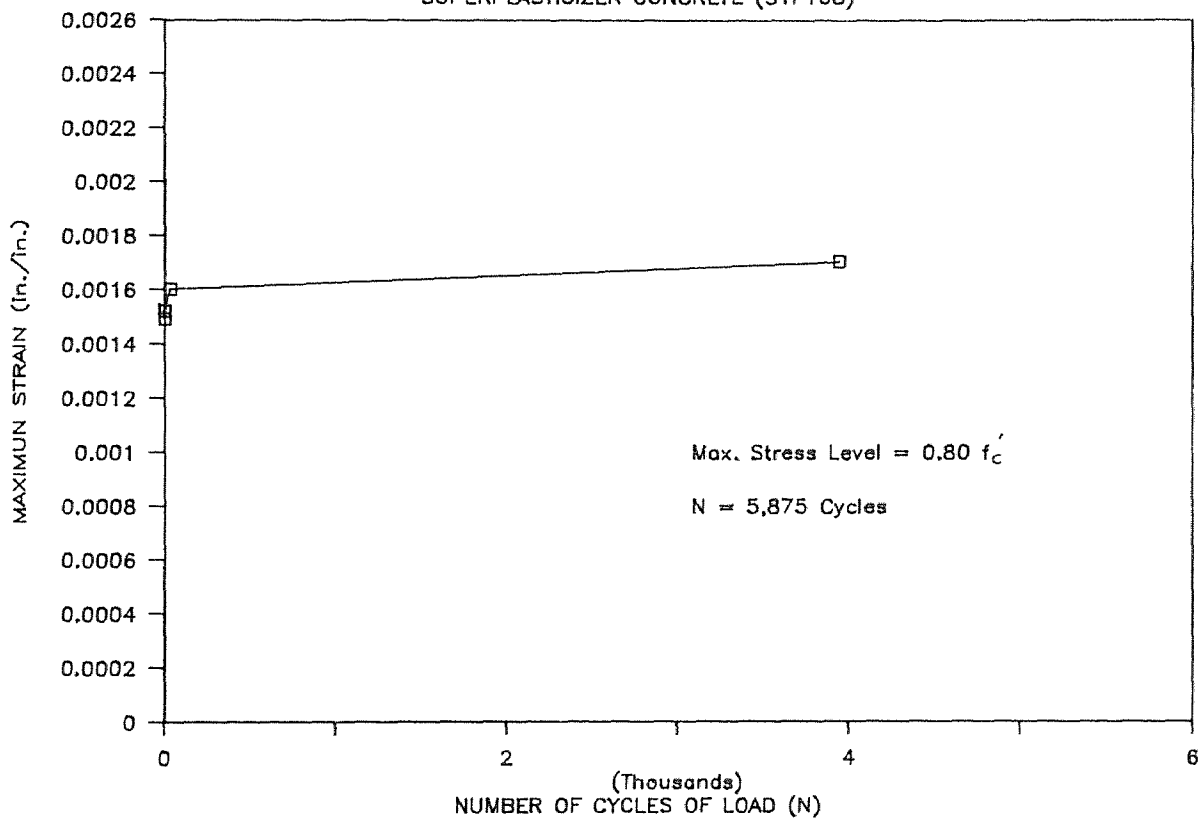
STRAIN VS. CYCLE CURVE

SUPERPLASTICIZER CONCRETE (S1F309)



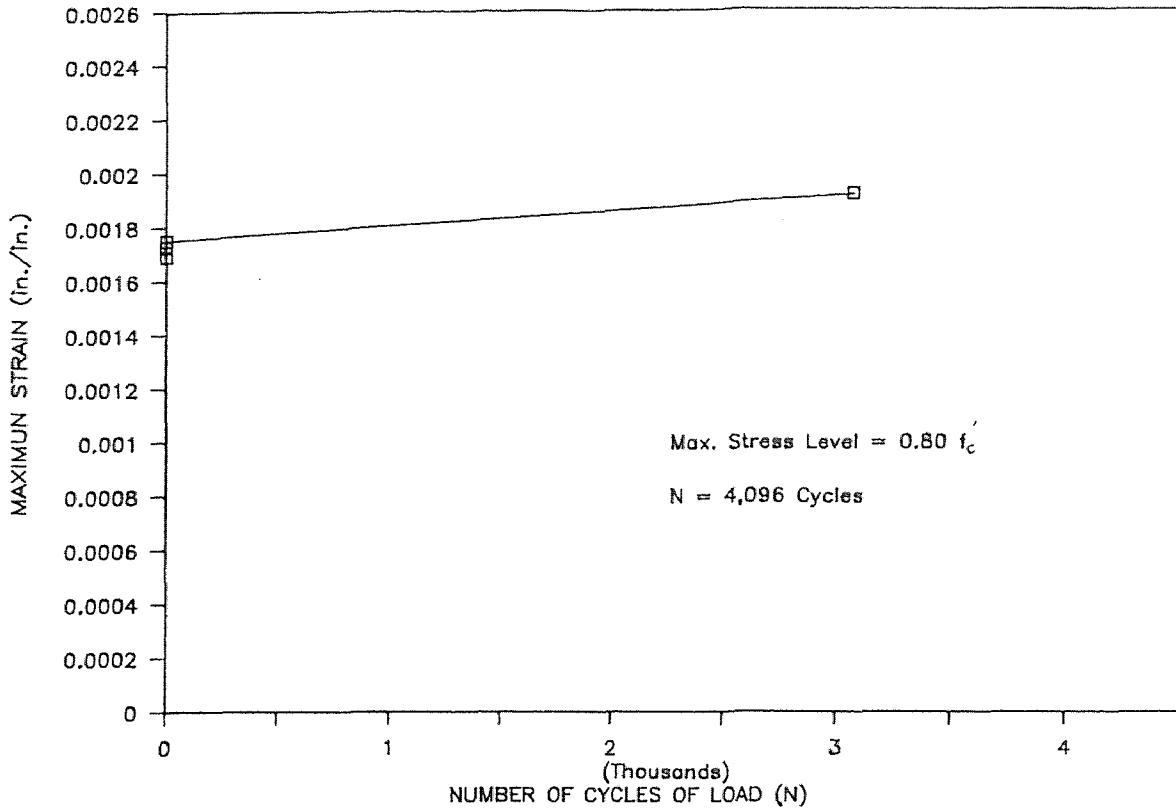
STRAIN VS. CYCLE CURVE

SUPERPLASTICIZER CONCRETE (S1F108)



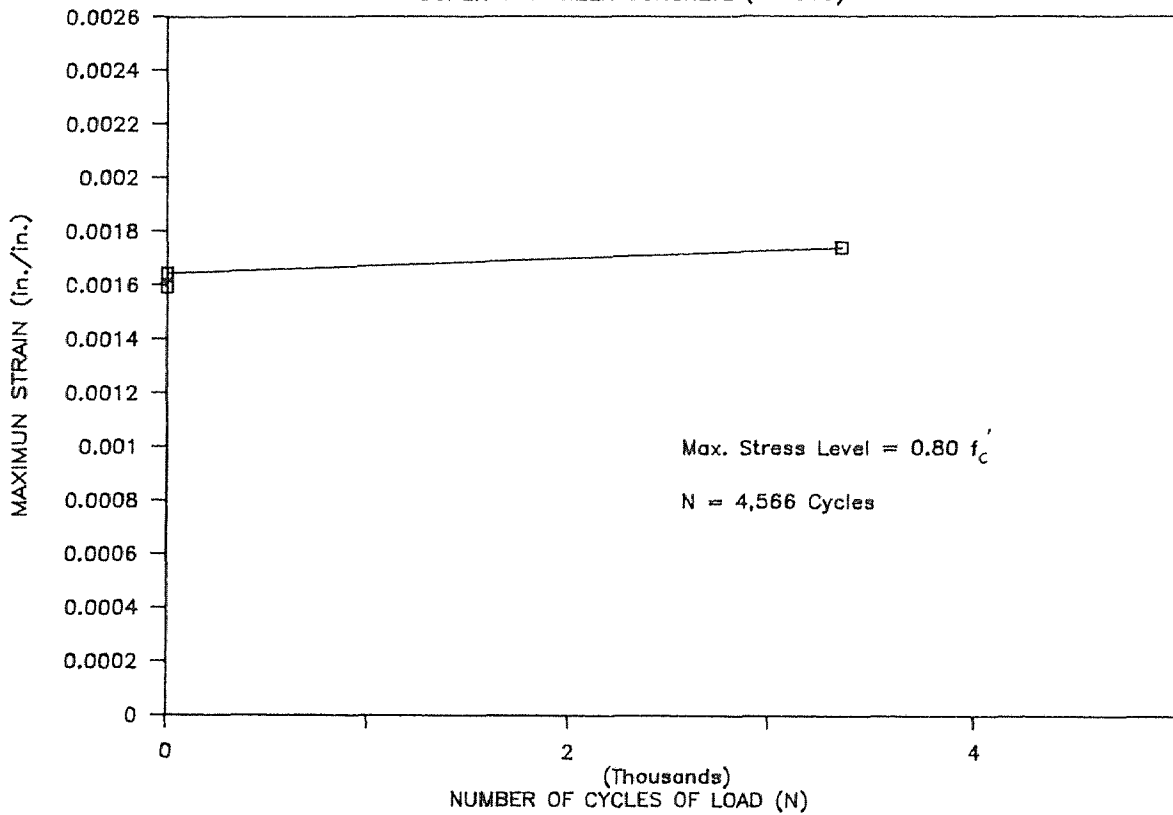
STRAIN VS. CYCLE CURVE

SUPERPLASTICIZER CONCRETE (S1F208)



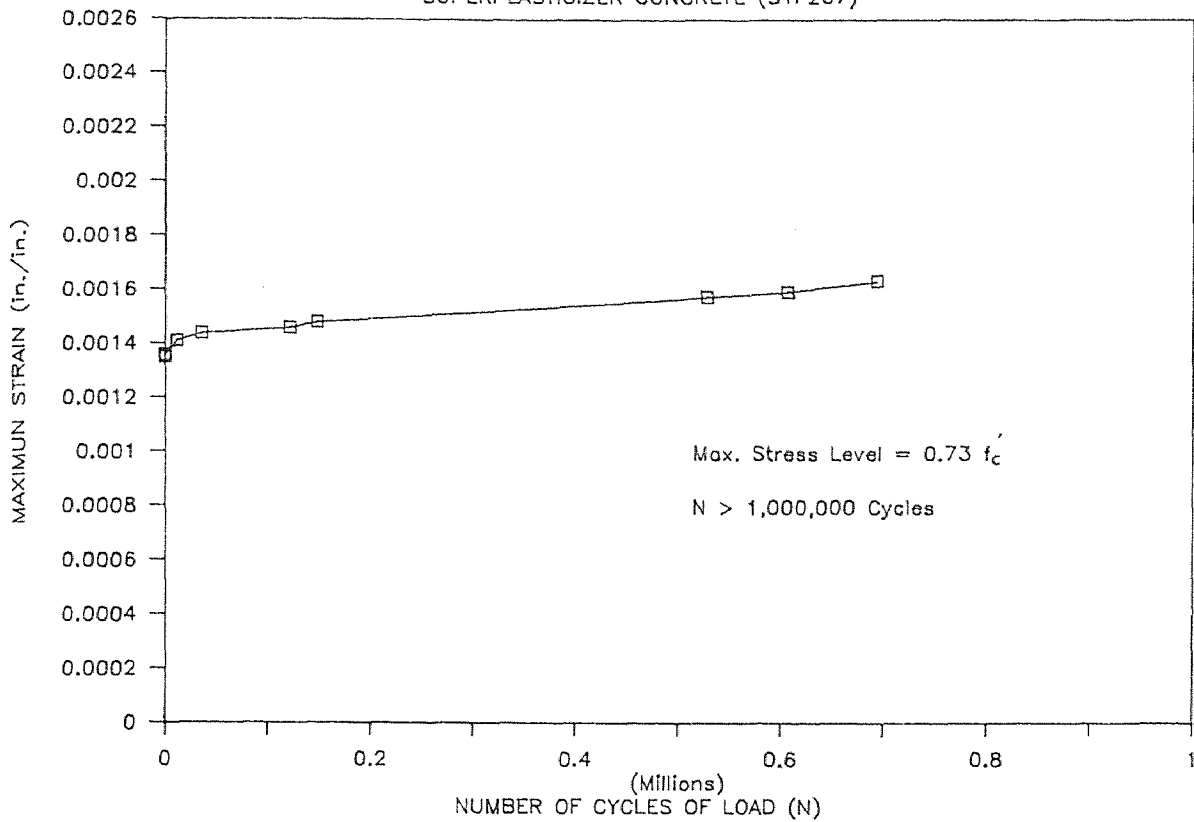
STRAIN VS. CYCLE CURVE

SUPERPLASTICIZER CONCRETE (S1F308)



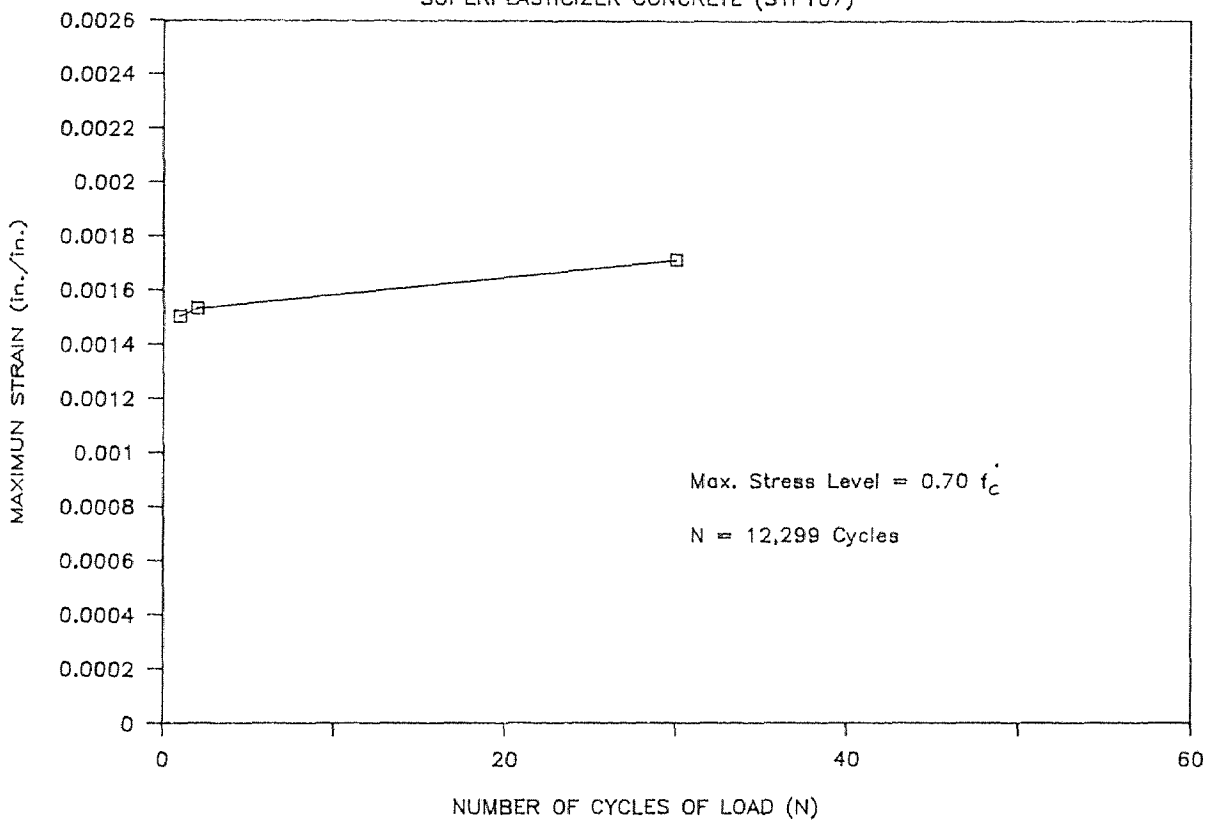
STRAIN VS. CYCLE CURVE

SUPERPLASTICIZER CONCRETE (S1F207)



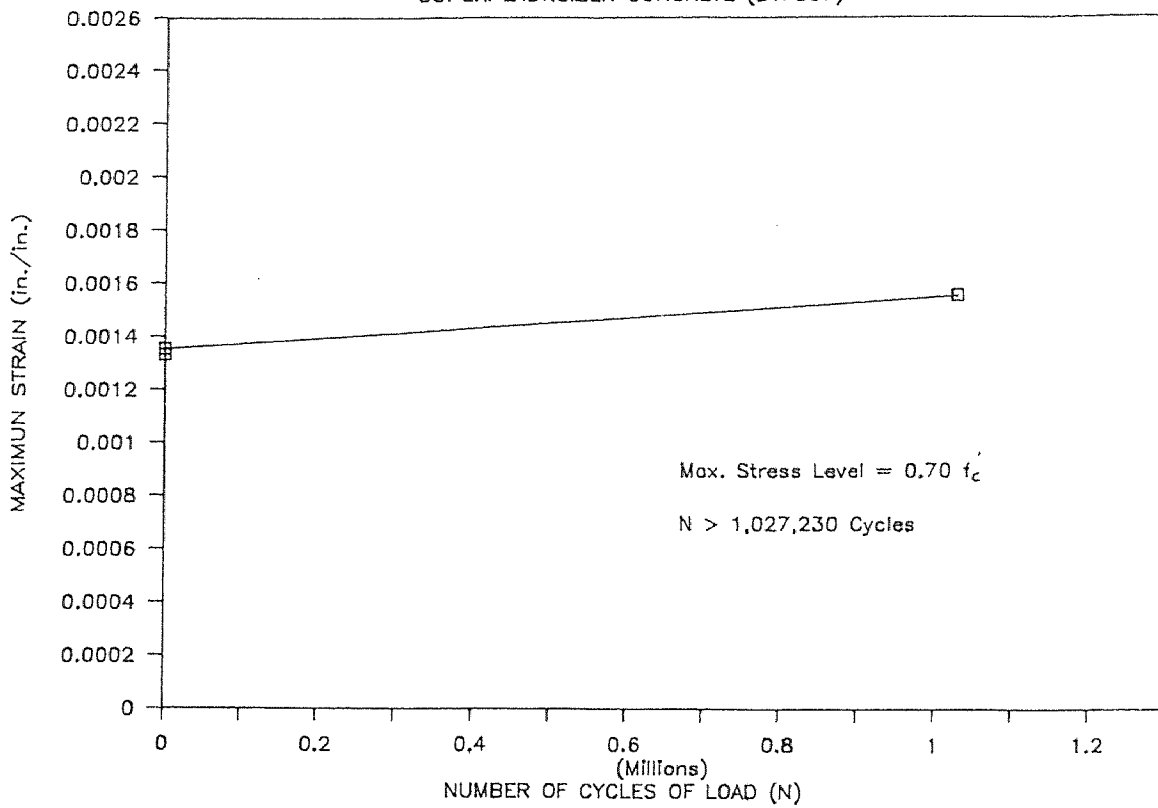
STRAIN VS. CYCLE CURVE

SUPERPLASTICIZER CONCRETE (S1F107)



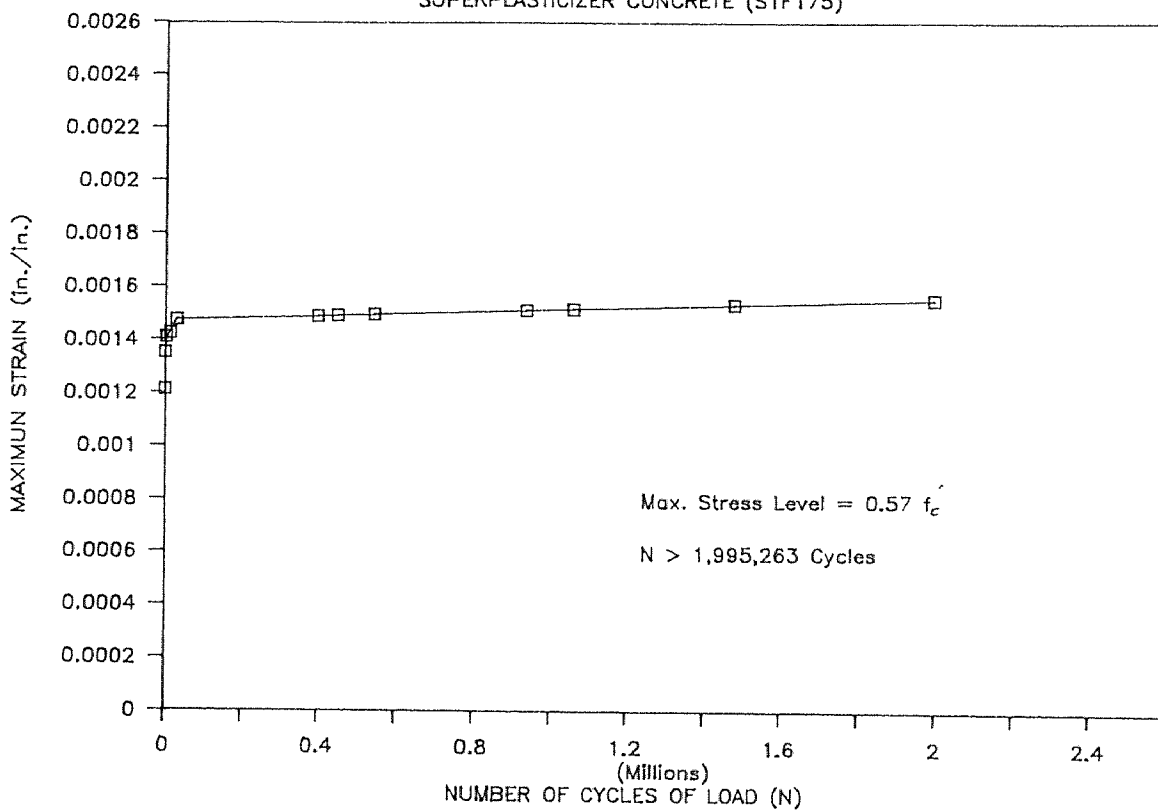
STRAIN VS. CYCLE CURVE

SUPERPLASTICIZER CONCRETE (S1F307)



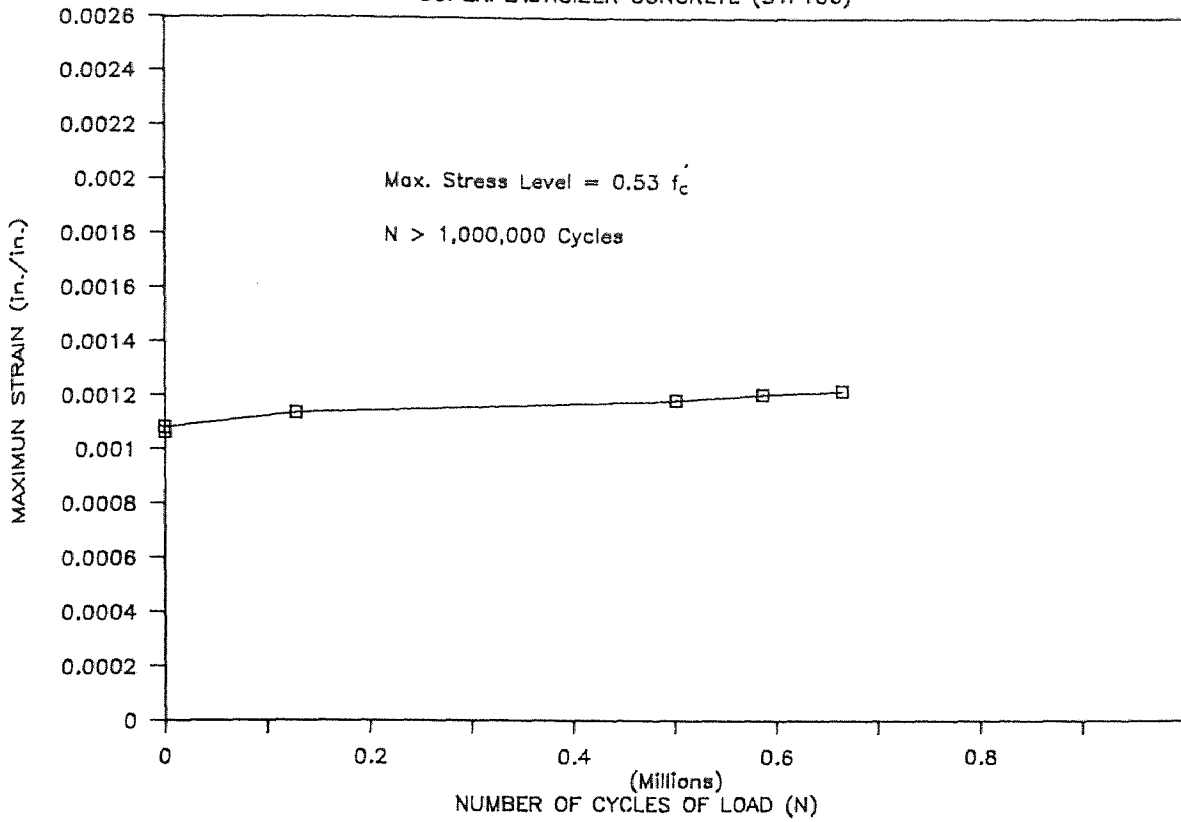
STRAIN VS. CYCLE CURVE

SUPERPLASTICIZER CONCRETE (S1F175)



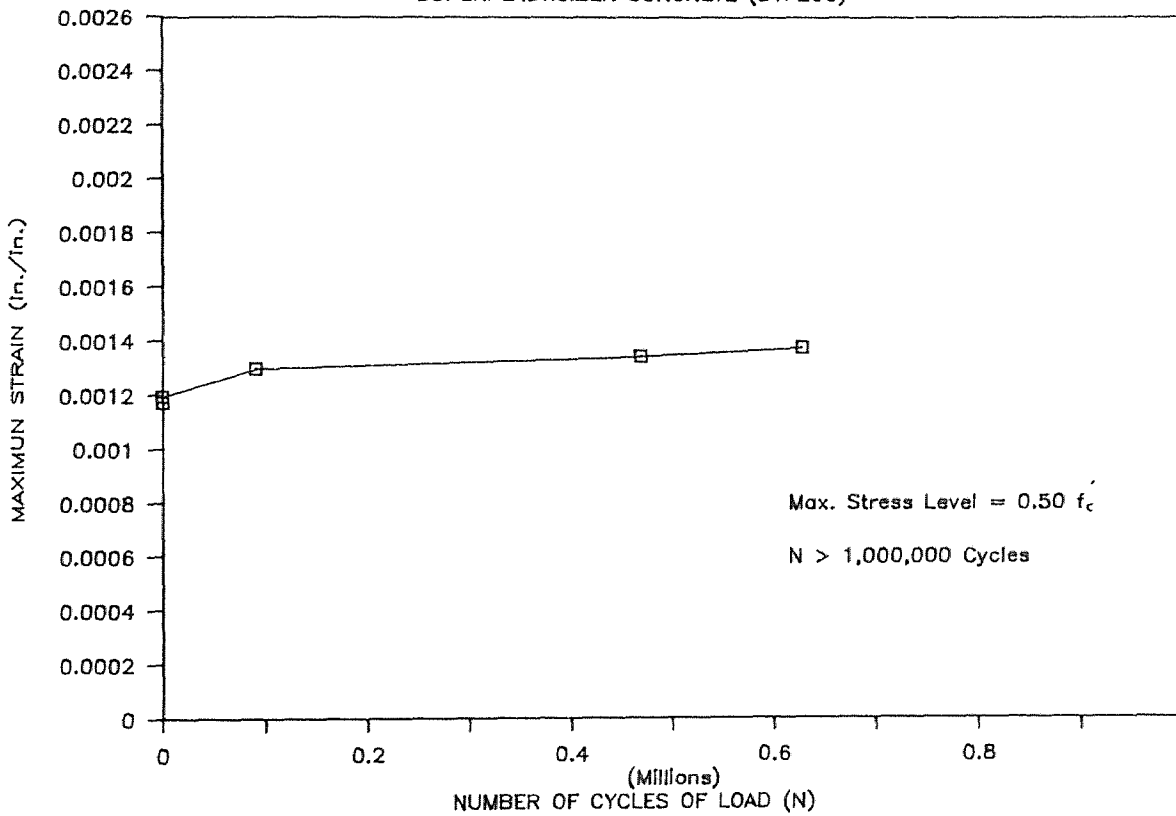
STRAIN VS. CYCLE CURVE

SUPERPLASTICIZER CONCRETE (S1F106)



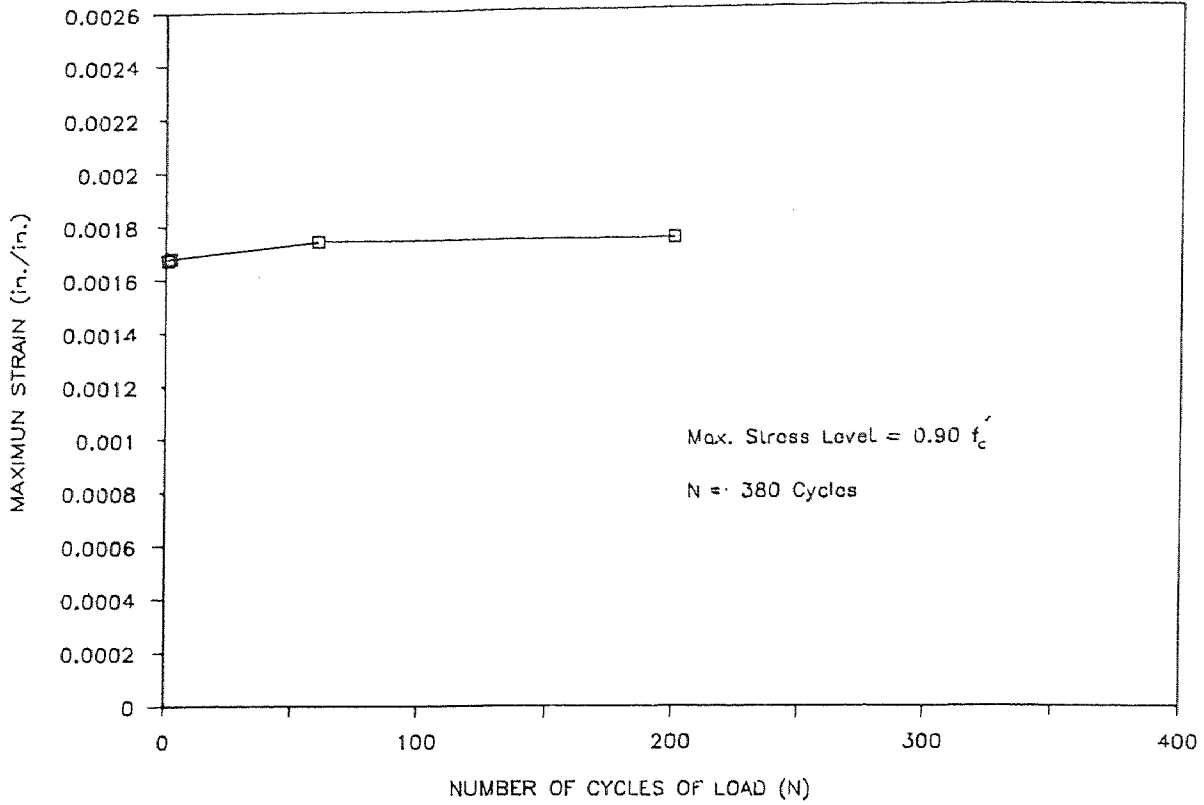
STRAIN VS. CYCLE CURVE

SUPERPLASTICIZER CONCRETE (S1F206)



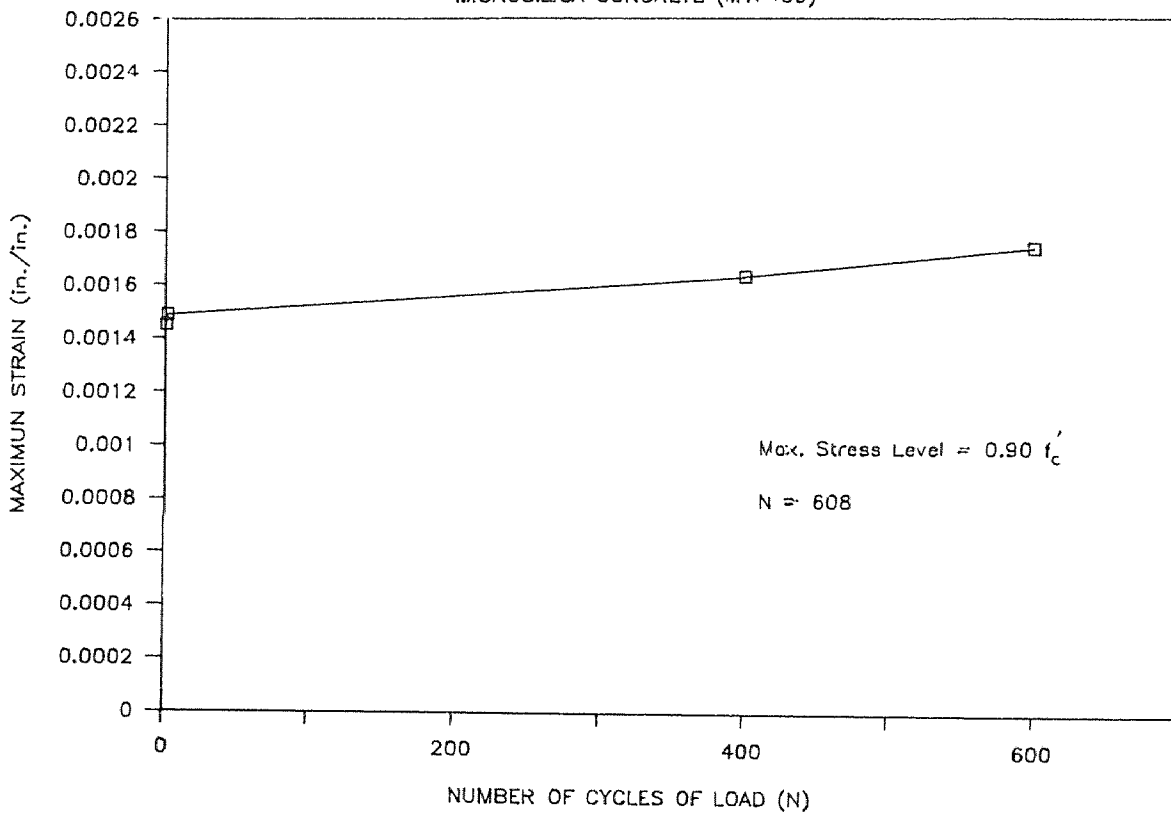
STRAIN VS. CYCLE CURVE

MICROSILICA CONCRETE (M1F209)



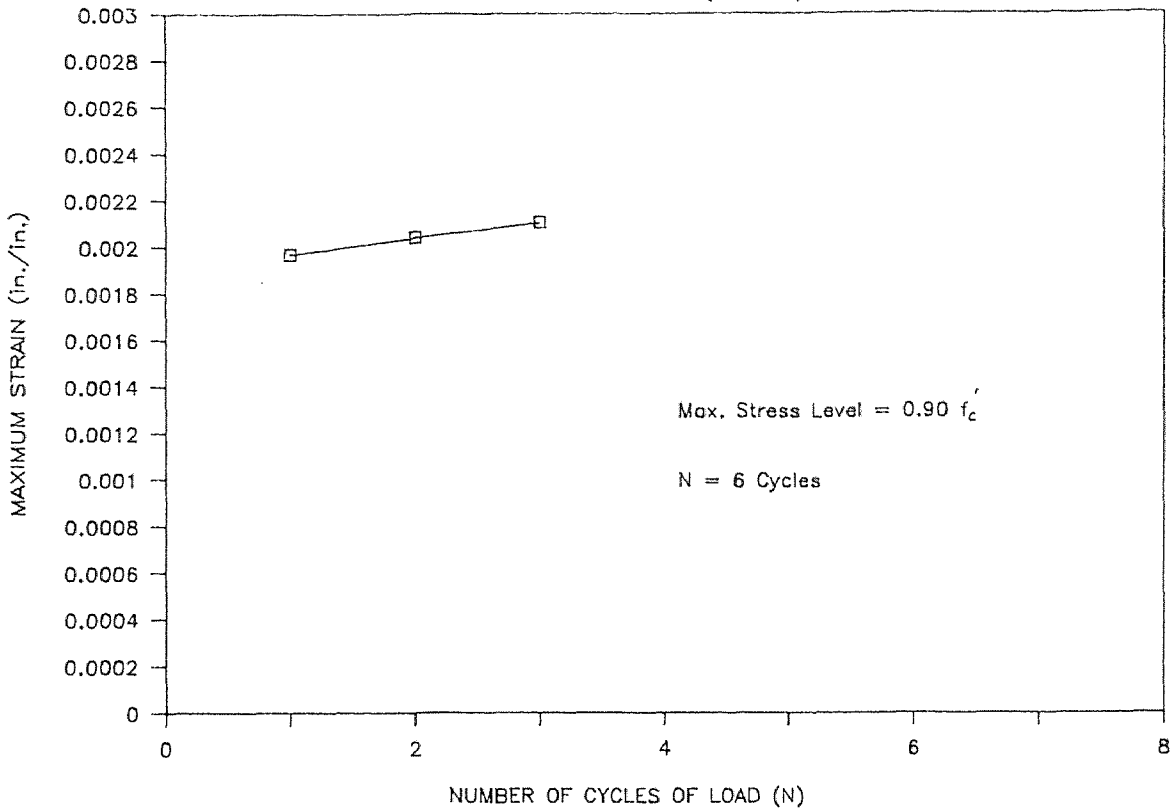
STRAIN VS. CYCLE CURVE

MICROSILICA CONCRETE (M1F409)



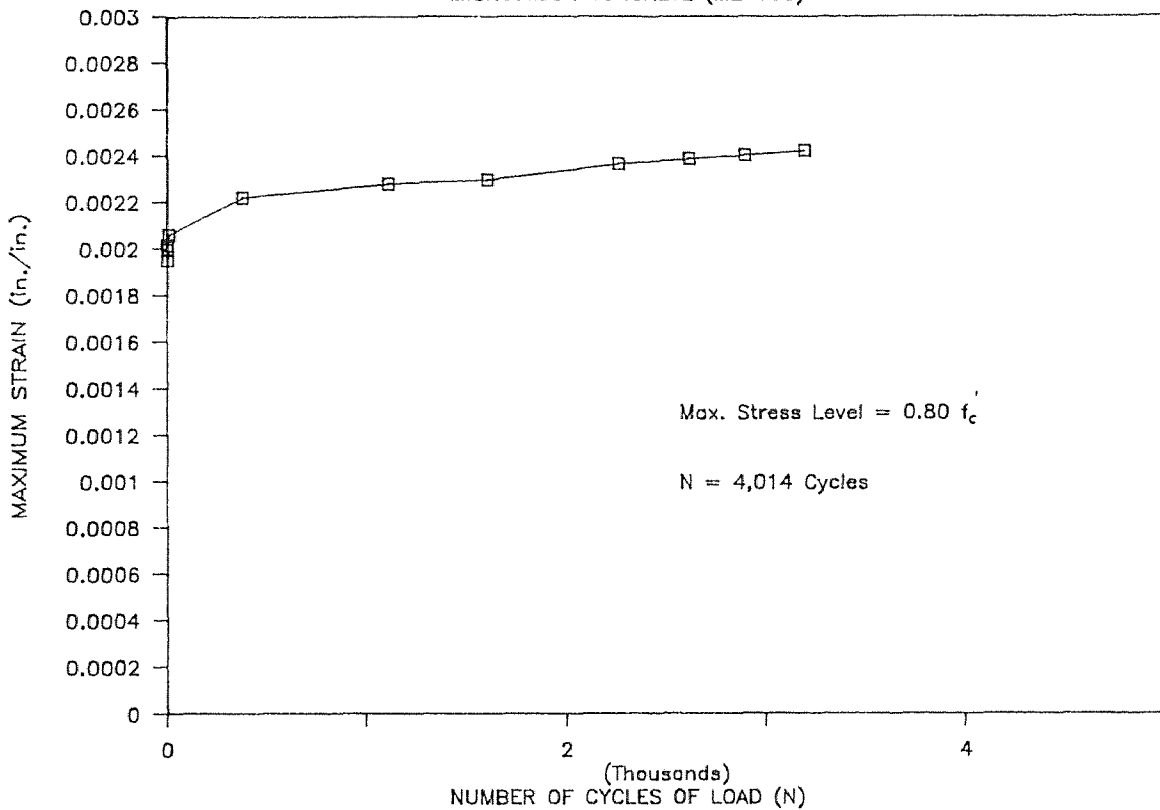
STRAIN VS. CYCLE CURVE

MICROSILICA CONCRETE (M2F209)



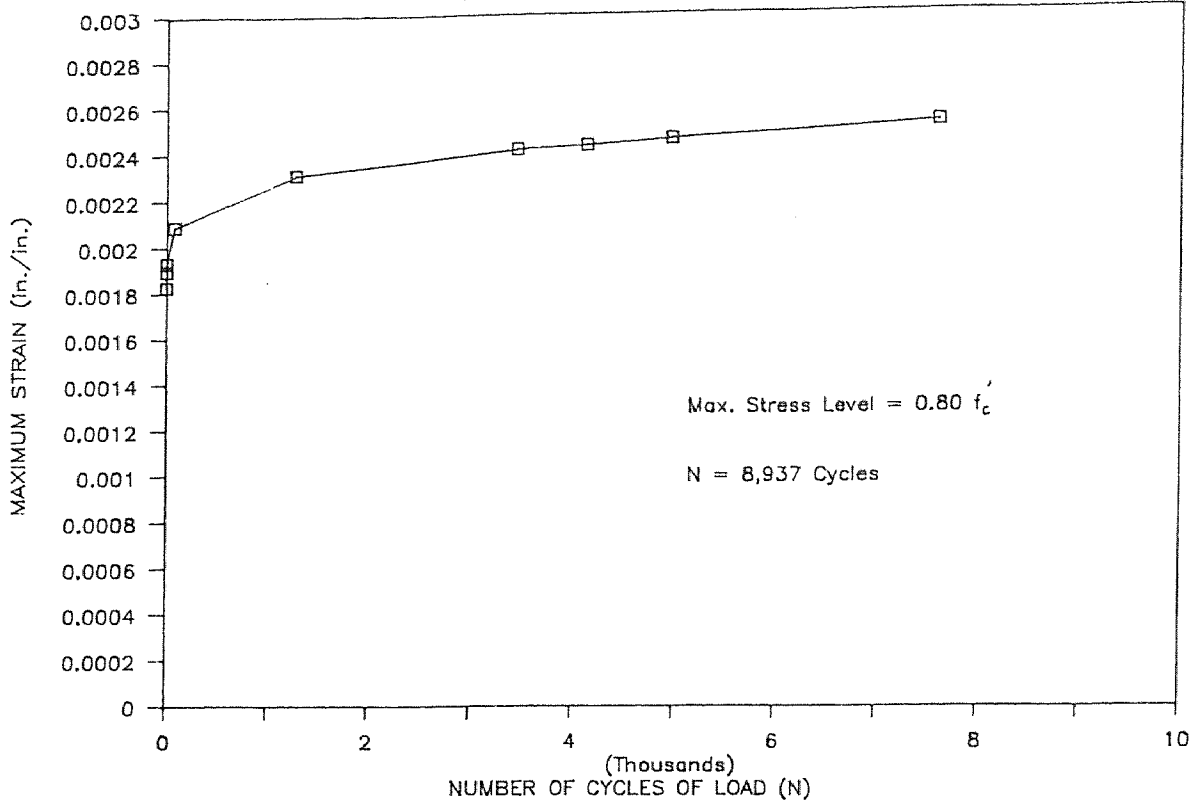
STRAIN VS. CYCLE CURVE

MICROSILICA CONCRETE (M2F108)



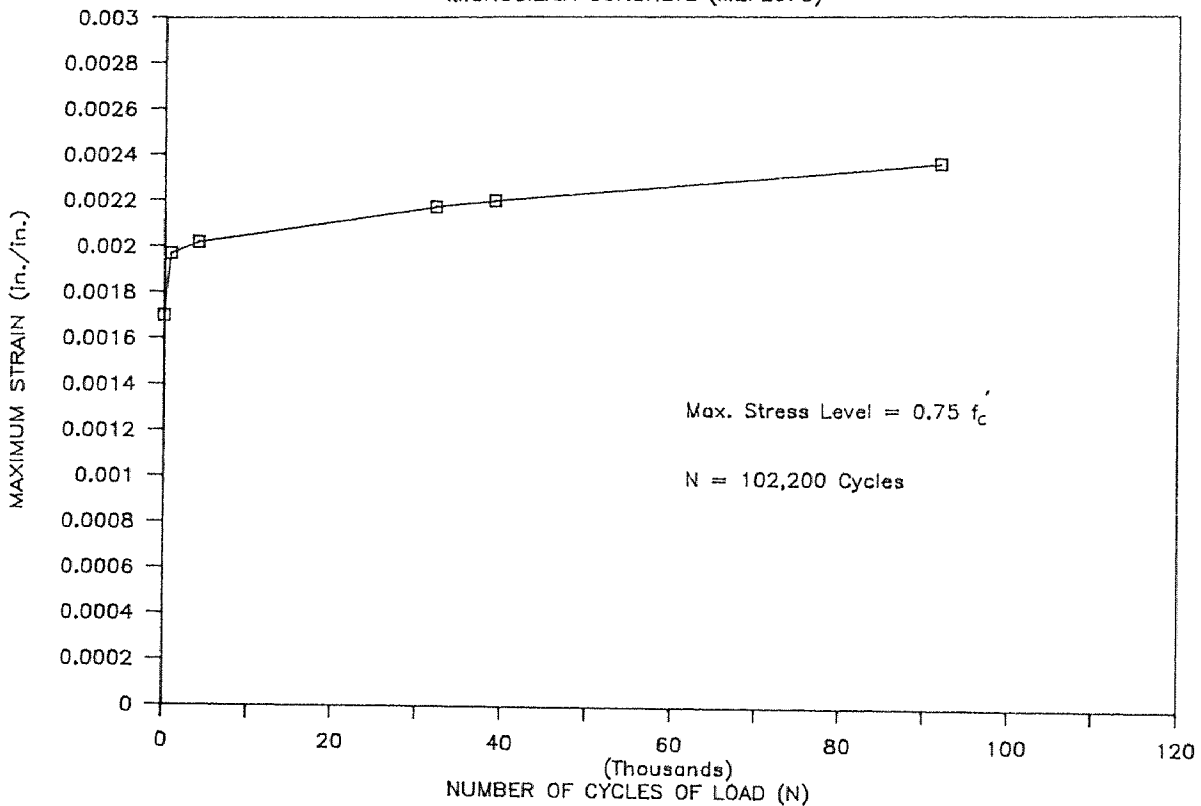
STRAIN VS. CYCLE CURVE

MICROSILICA CONCRETE (M2F208)



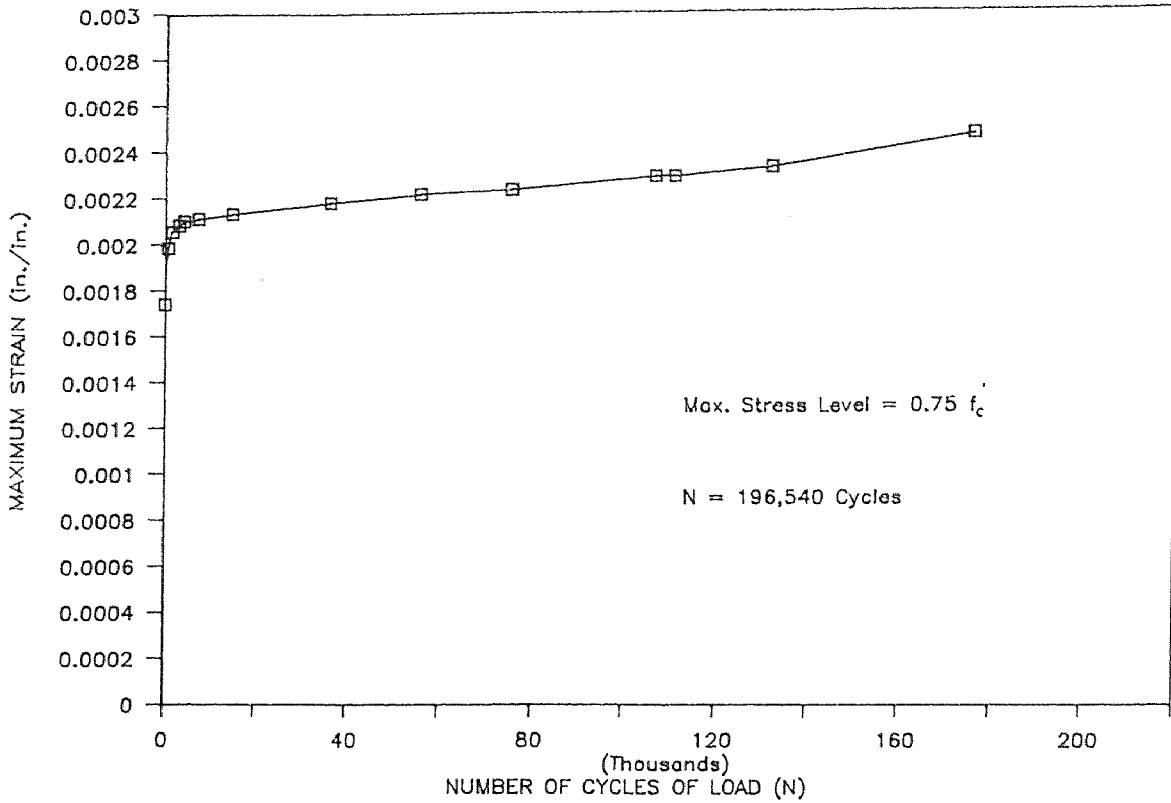
STRAIN VS. CYCLE CURVE

MICROSILICA CONCRETE (M2F2075)



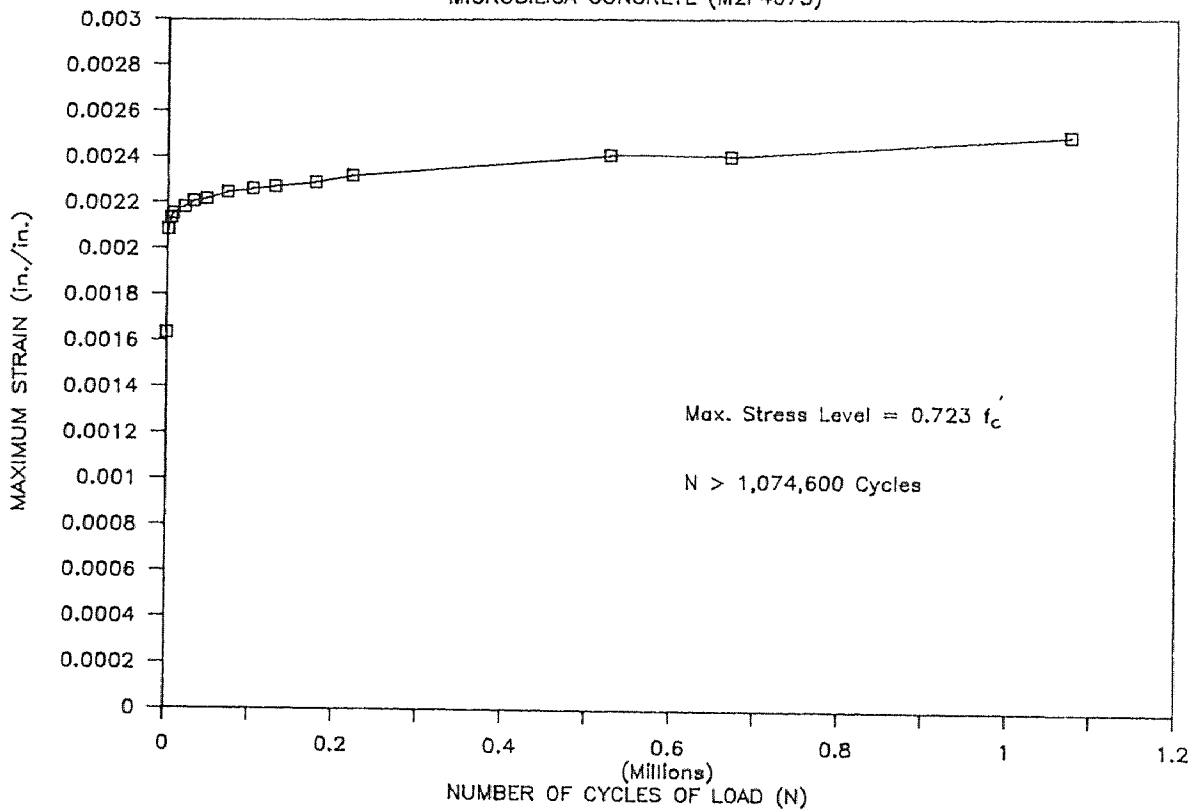
STRAIN VS. CYCLE CURVE

MICROSILICA CONCRETE (M2F3075)



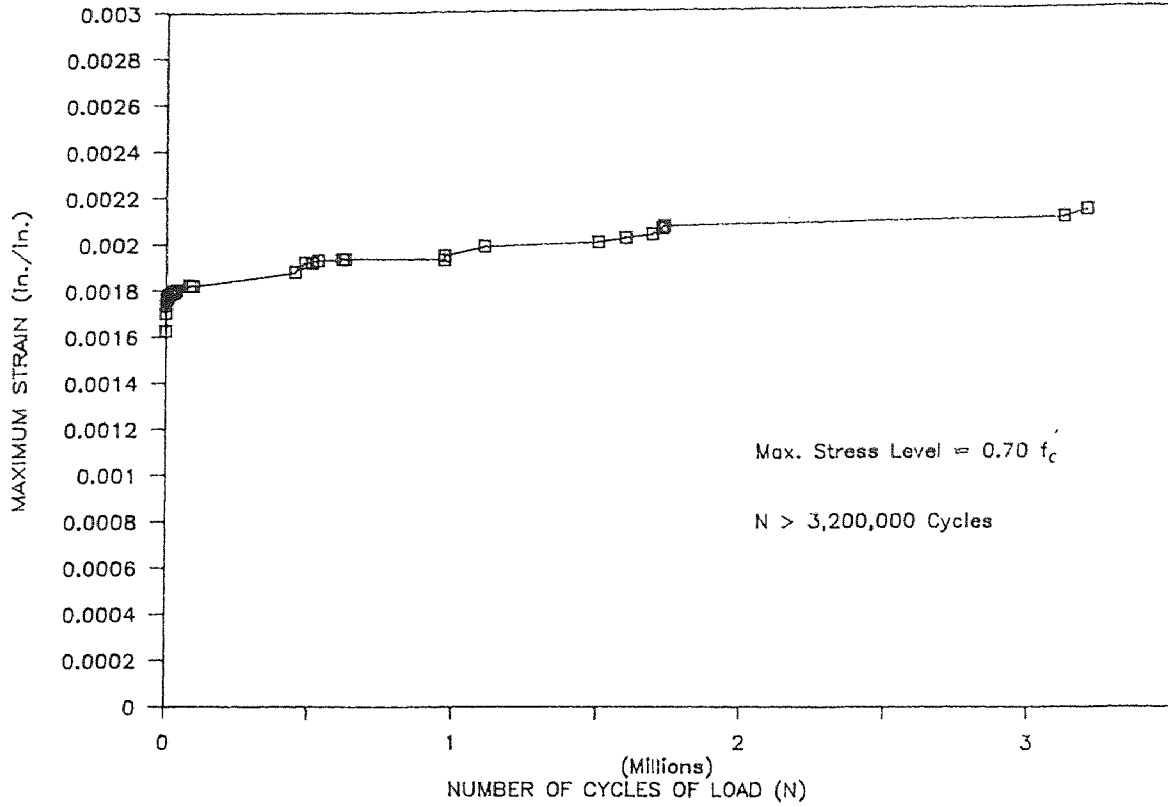
STRAIN VS. CYCLE CURVE

MICROSILICA CONCRETE (M2F4075)



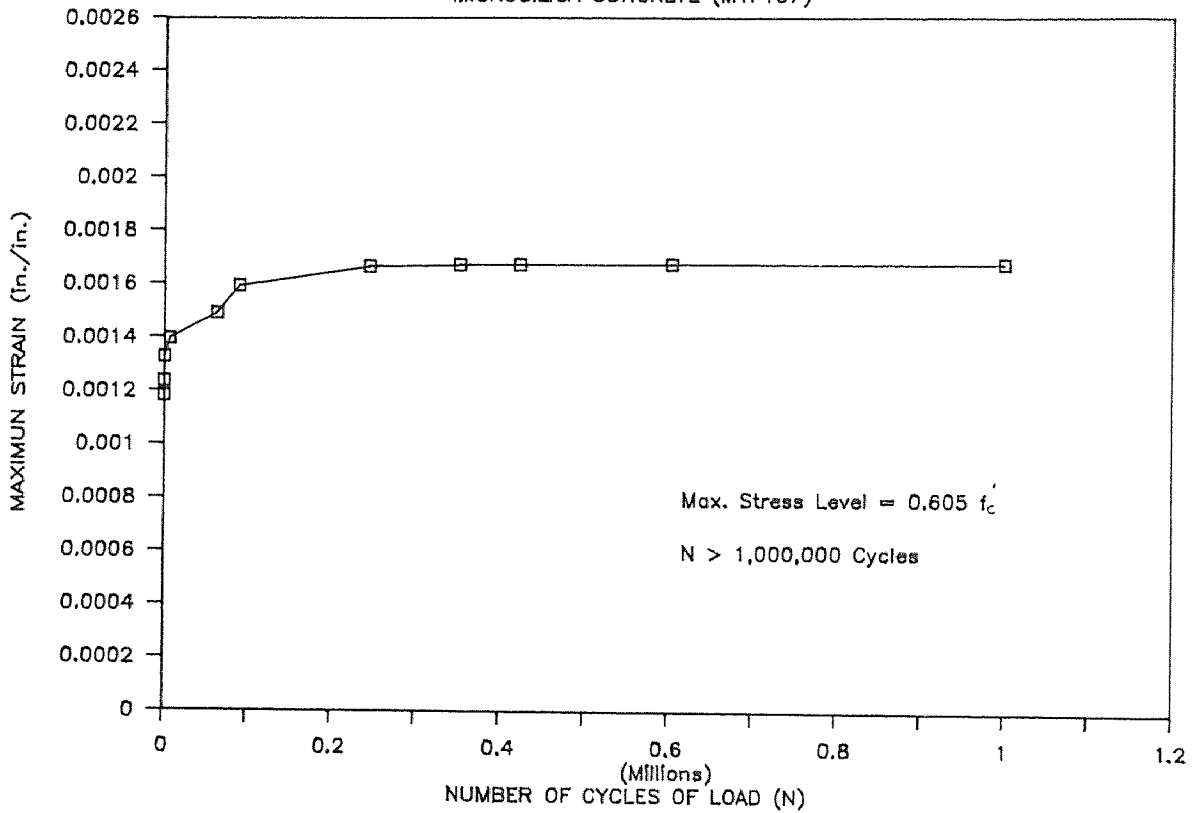
STRAIN VS. CYCLE CURVE

MICROSILICA CONCRETE (M2F1075)



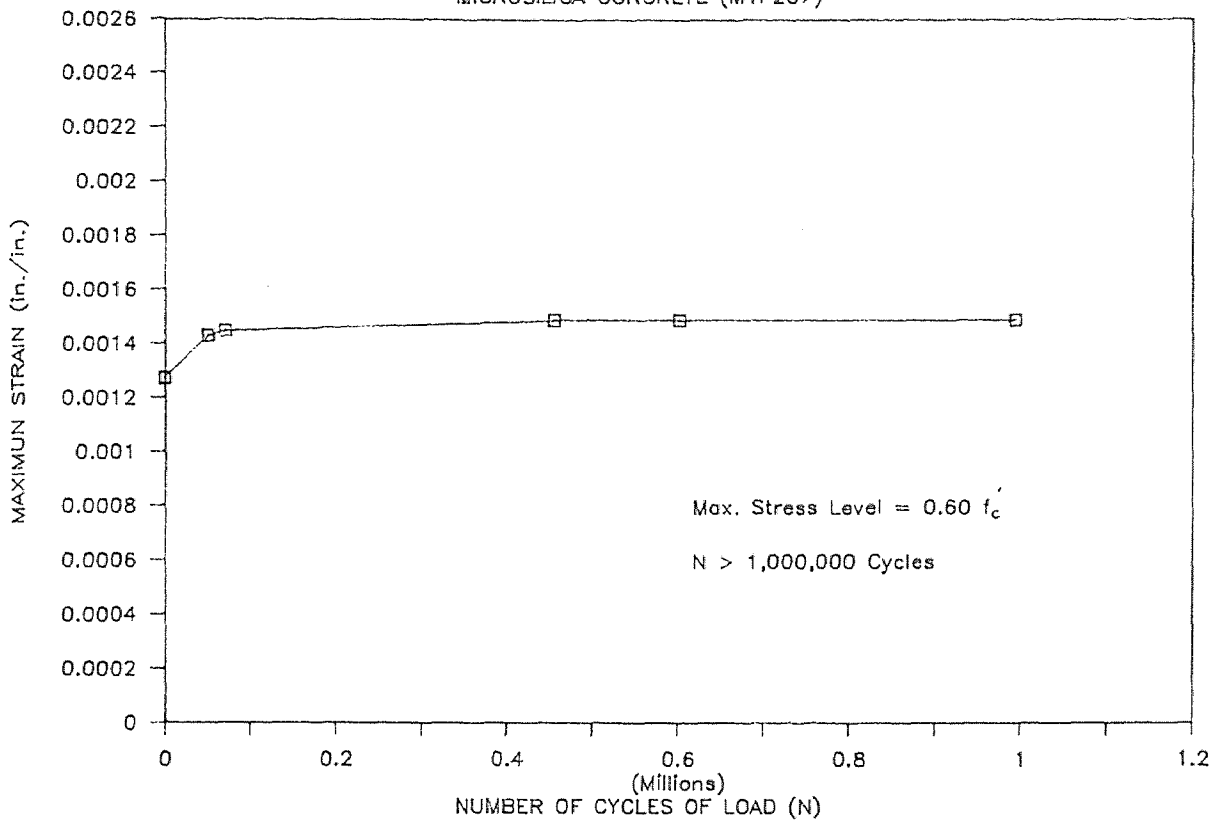
STRAIN VS. CYCLE CURVE

MICROSILICA CONCRETE (M1F107)



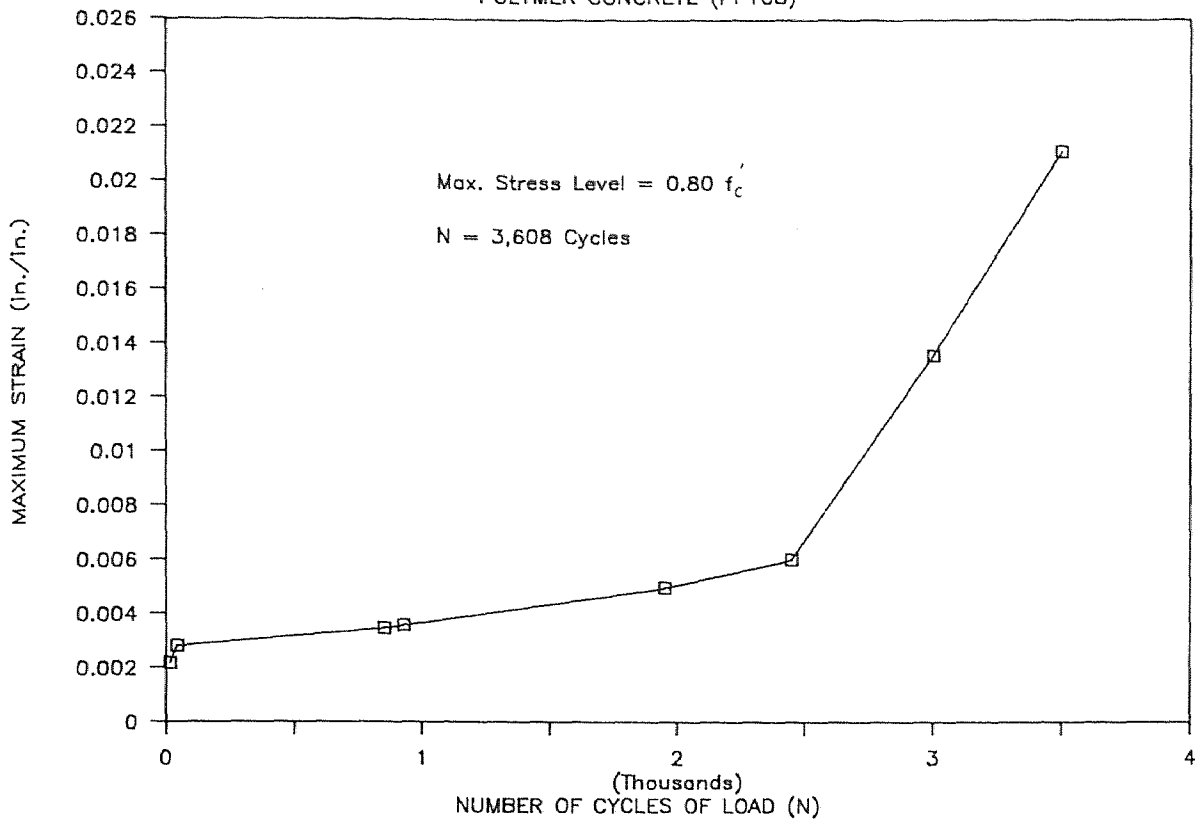
STRAIN VS. CYCLE CURVE

MICROSILICA CONCRETE (M1F207)



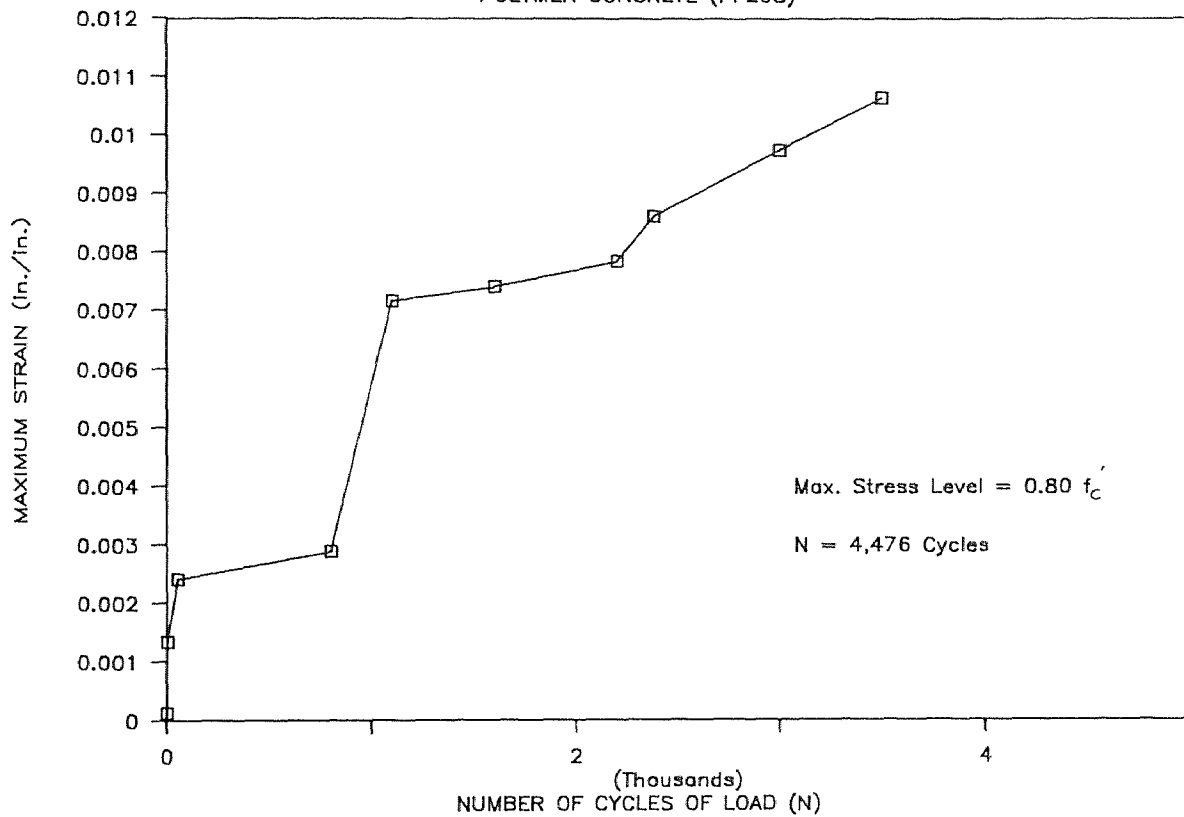
STRAIN VS. CYCLE CURVE

POLYMER CONCRETE (PF108)



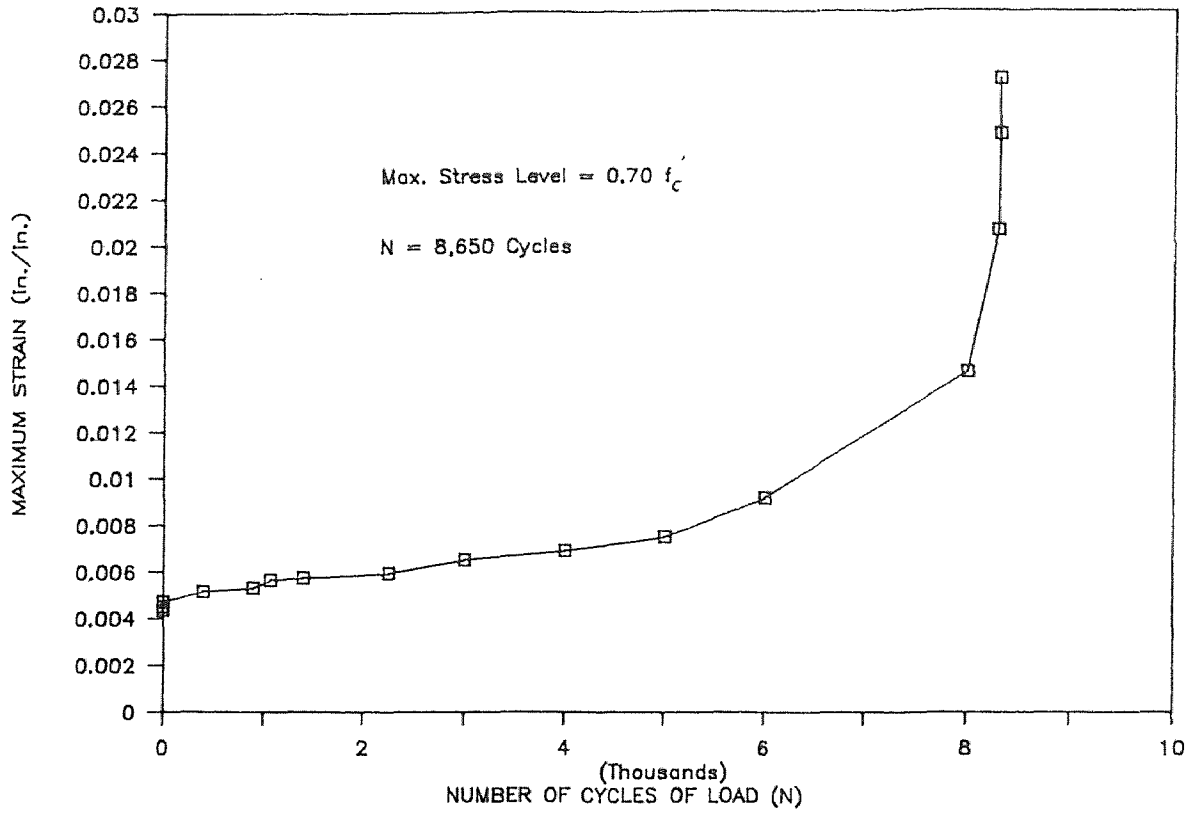
STRAIN VS. CYCLE CURVE

POLYMER CONCRETE (PF208)



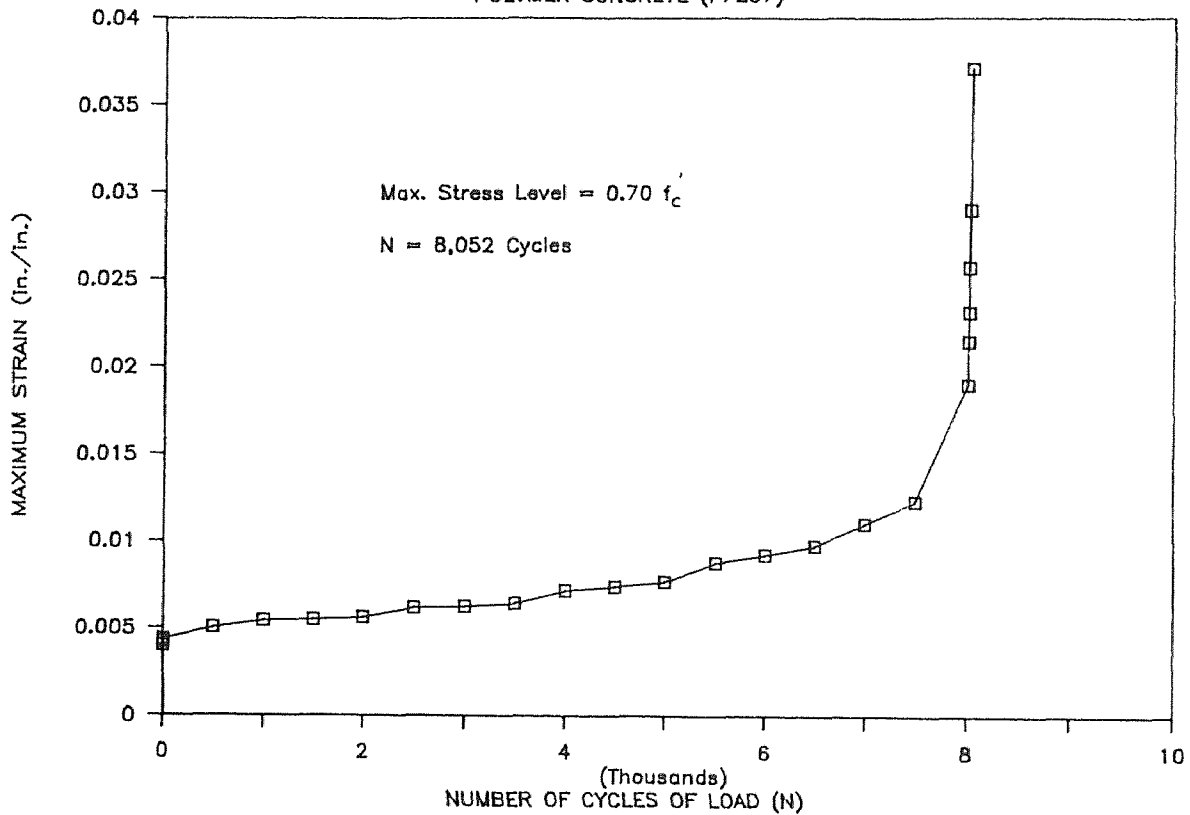
STRAIN VS. CYCLE CURVE

POLYMER CONCRETE (PF107)



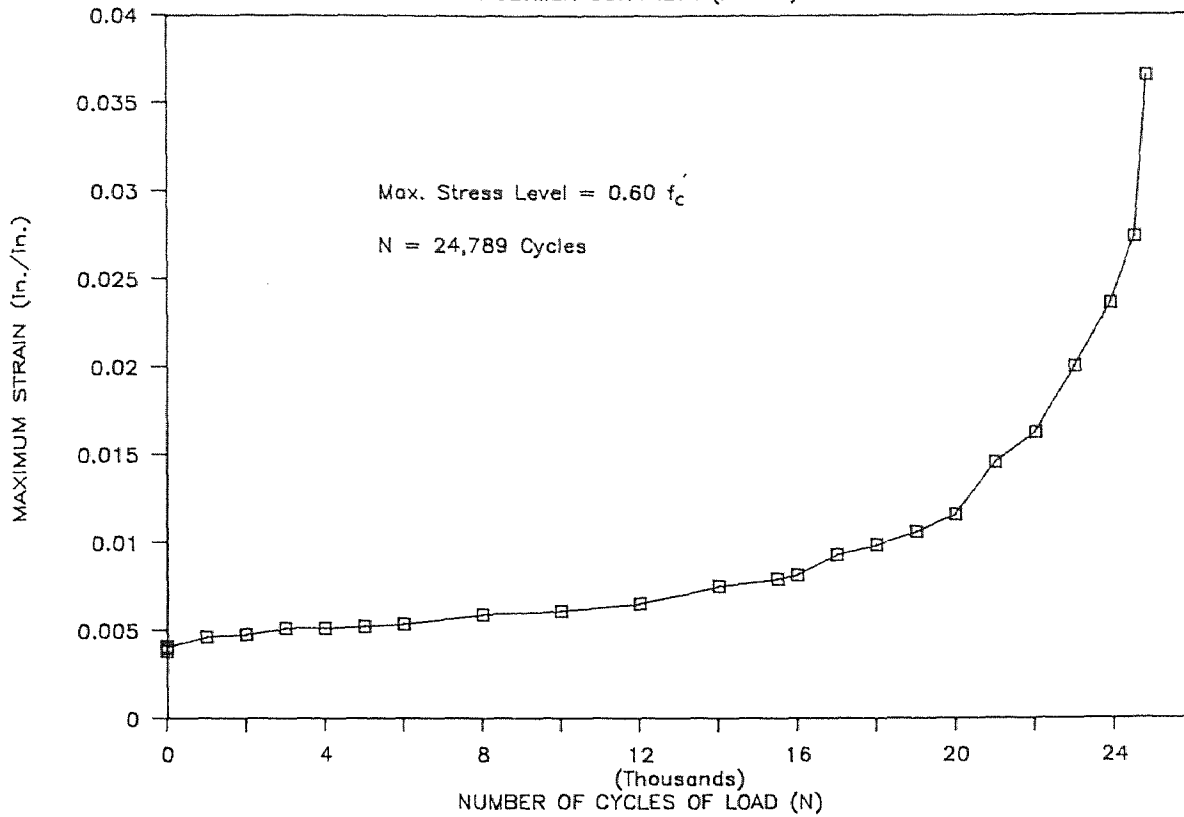
STRAIN VS. CYCLE CURVE

POLYMER CONCRETE (PF207)



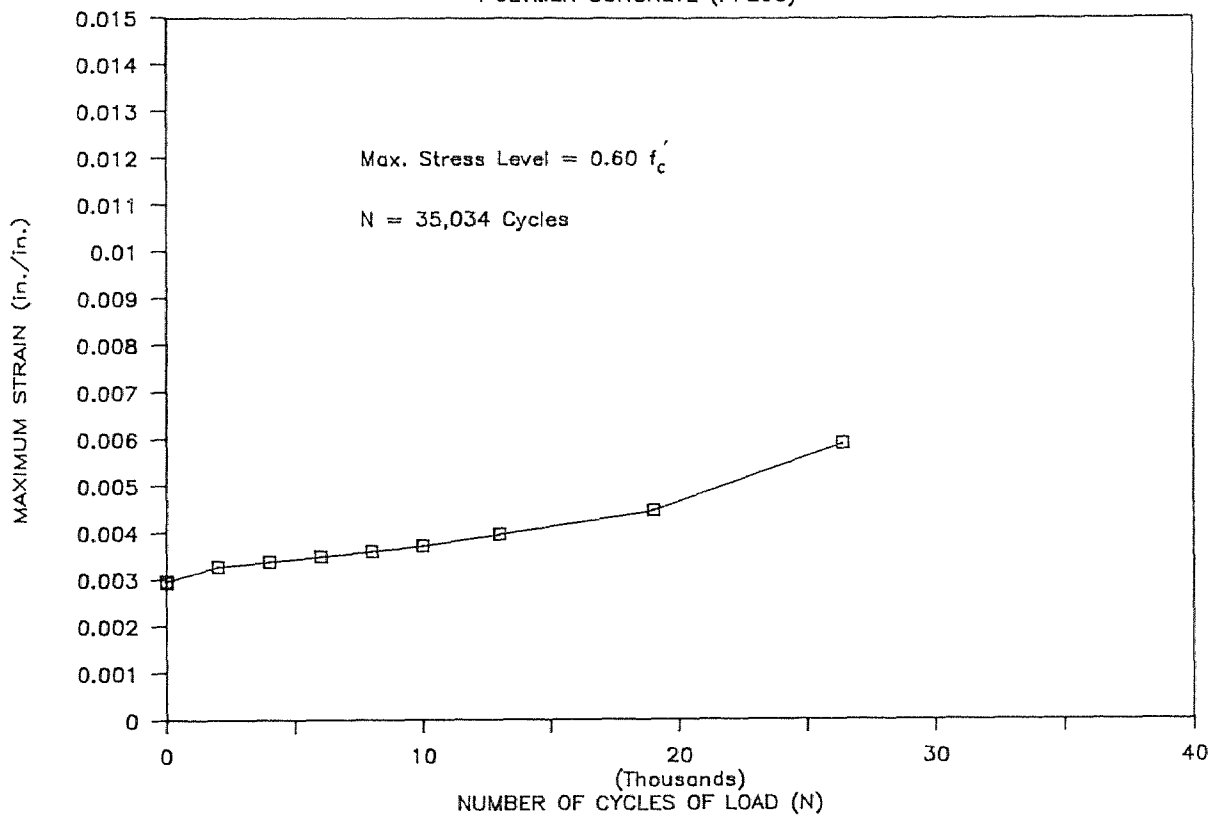
STRAIN VS. CYCLE CURVE

POLYMER CONCRETE (PF106)



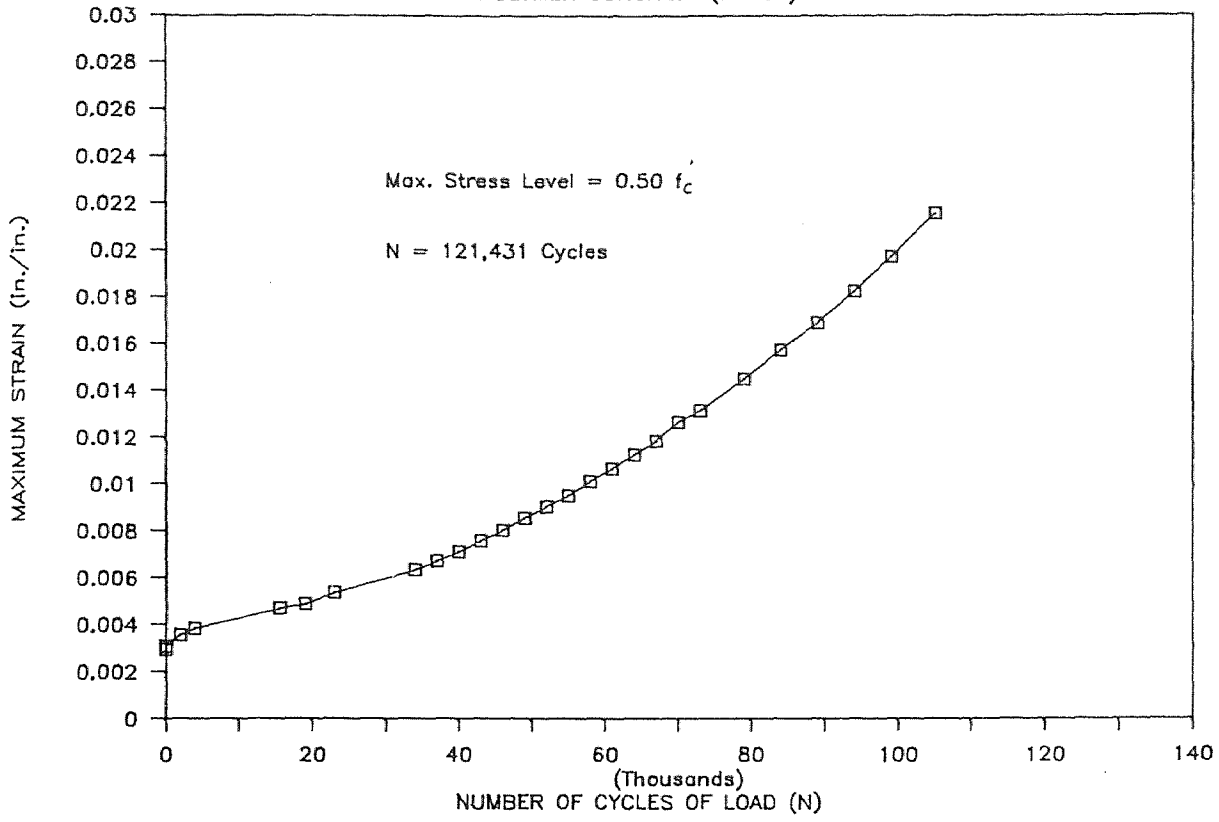
STRAIN VS. CYCLE CURVE

POLYMER CONCRETE (PF206)



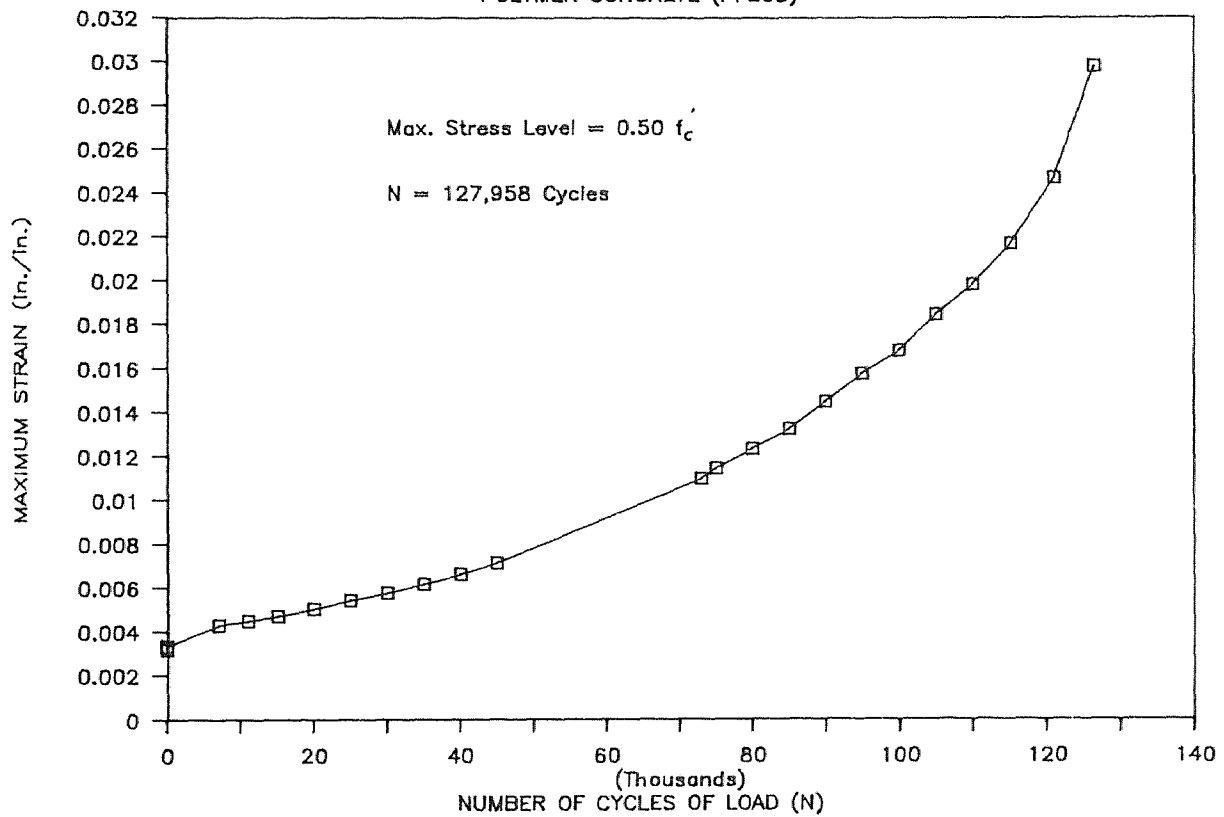
STRAIN VS. CYCLE CURVE

POLYMER CONCRETE (PF105)



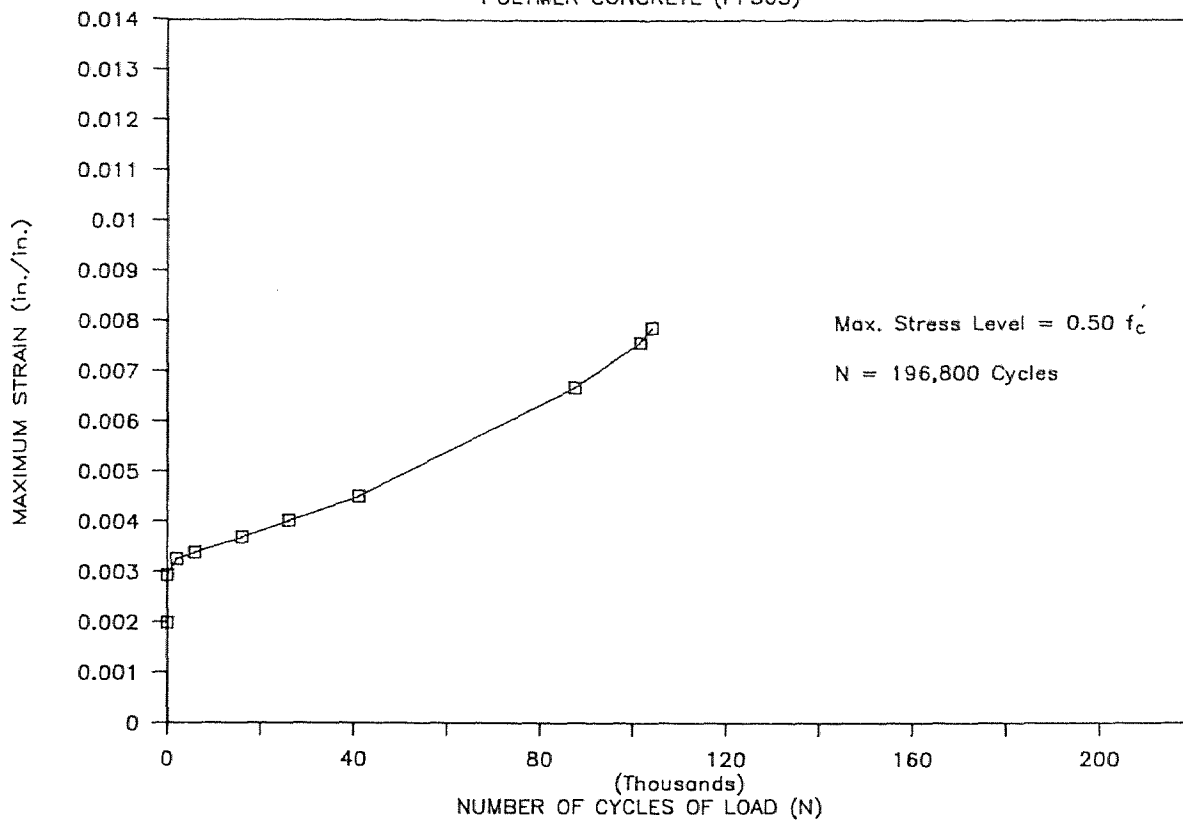
STRAIN VS. CYCLE CURVE

POLYMER CONCRETE (PF205)



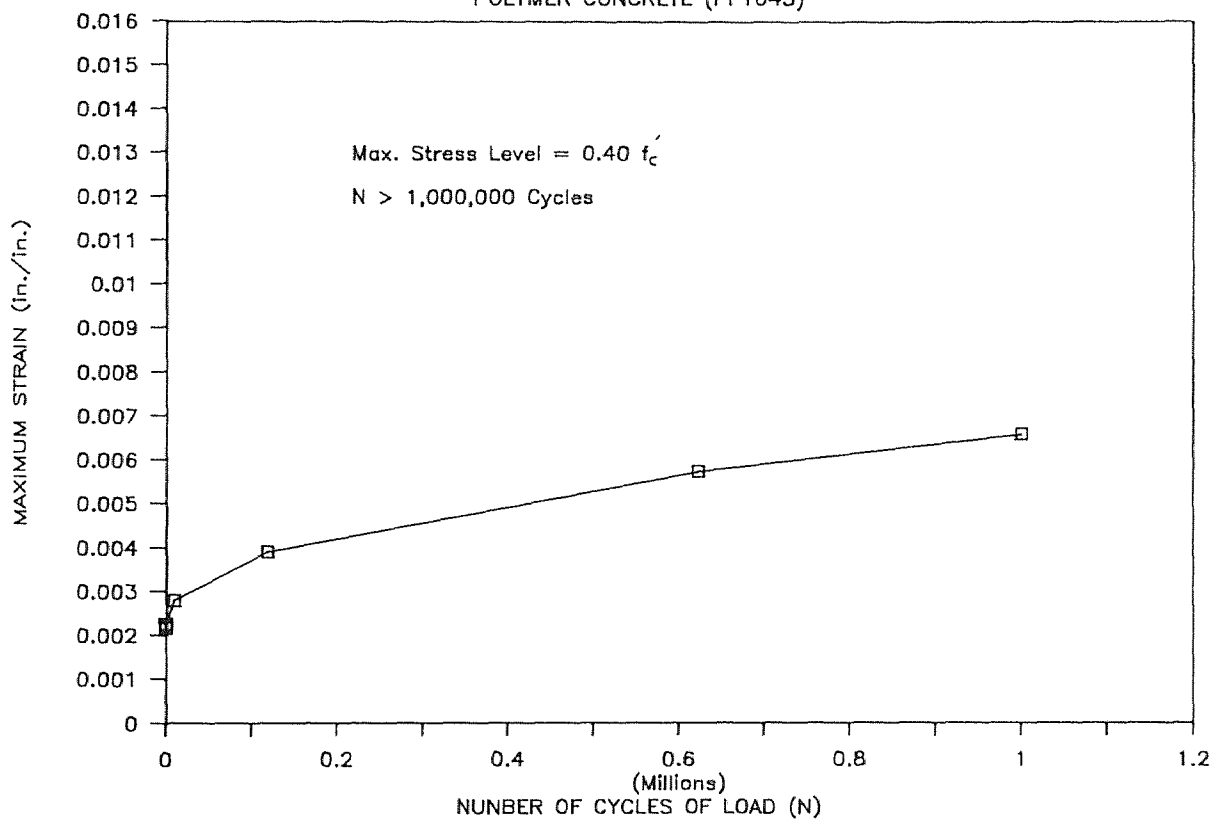
STRAIN VS. CYCLE CURVE

POLYMER CONCRETE (PF305)



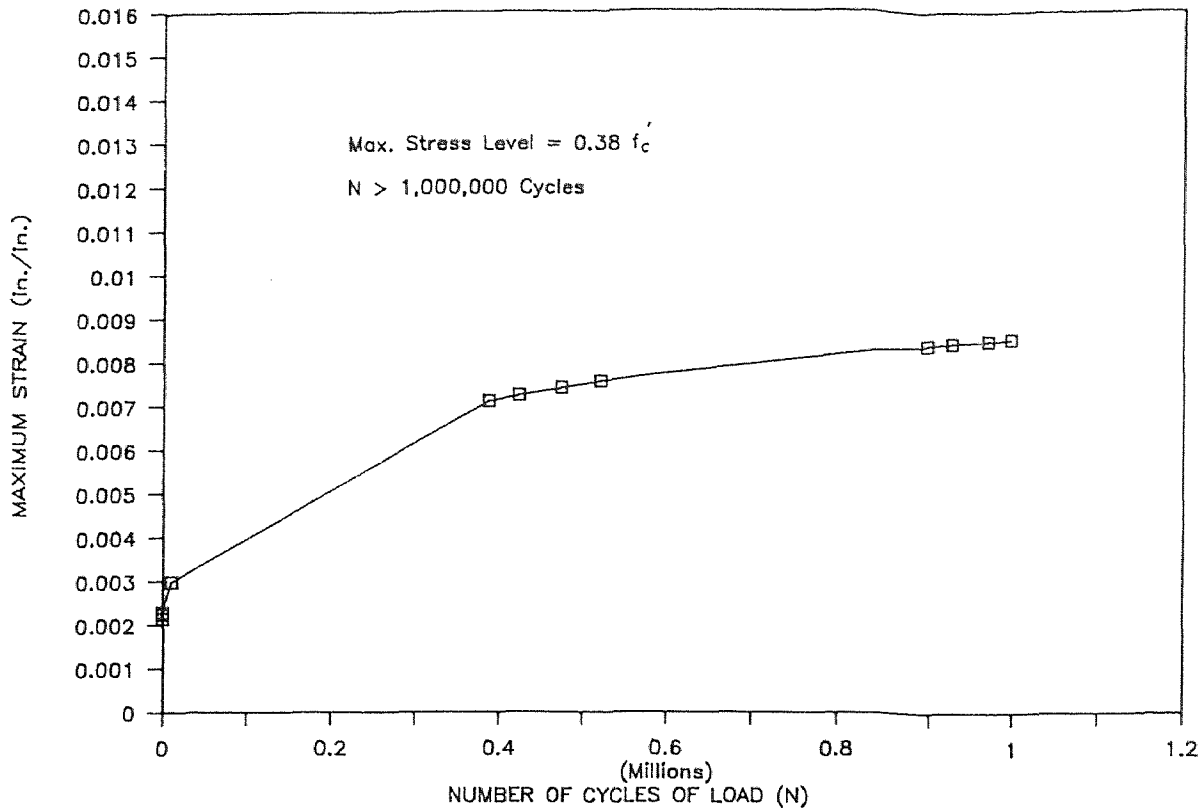
STRAIN VS. CYCLE CURVE

POLYMER CONCRETE (PF1045)



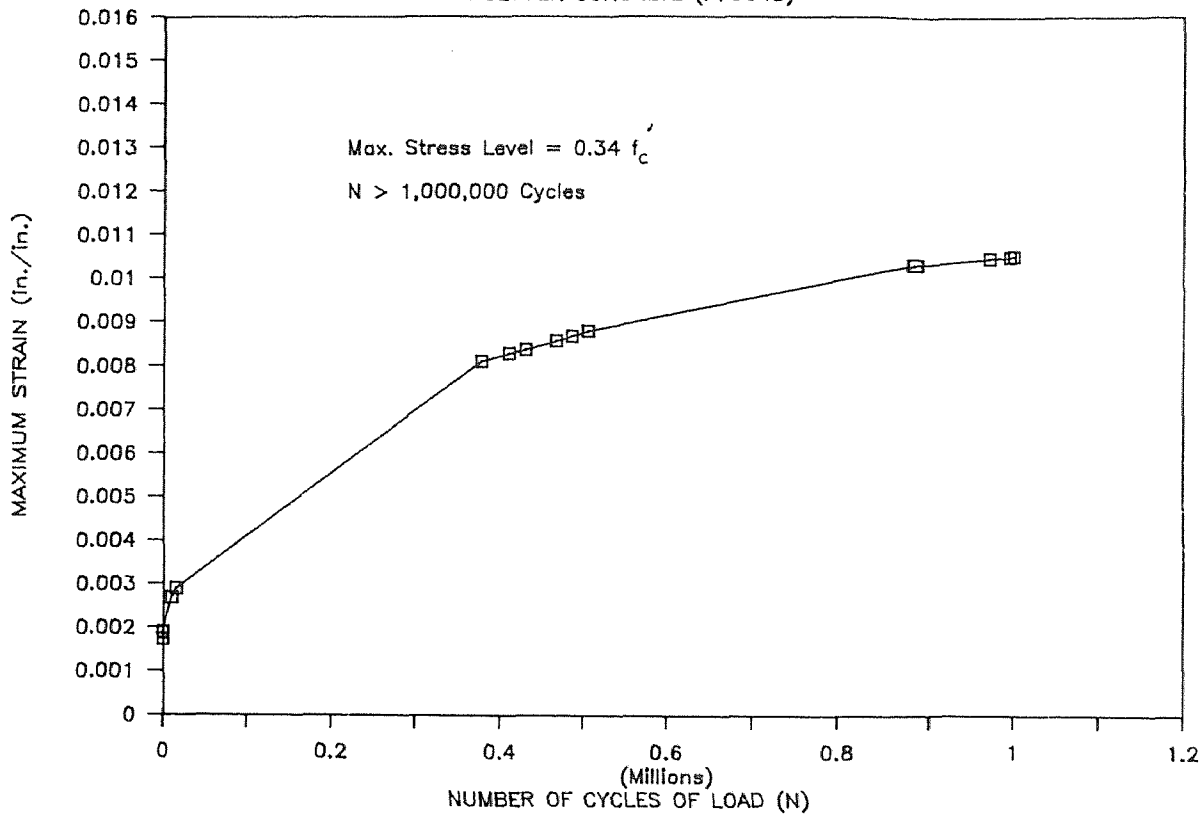
STRAIN VS. CYCLE CURVE

POLYMER CONCRETE (PF2045)



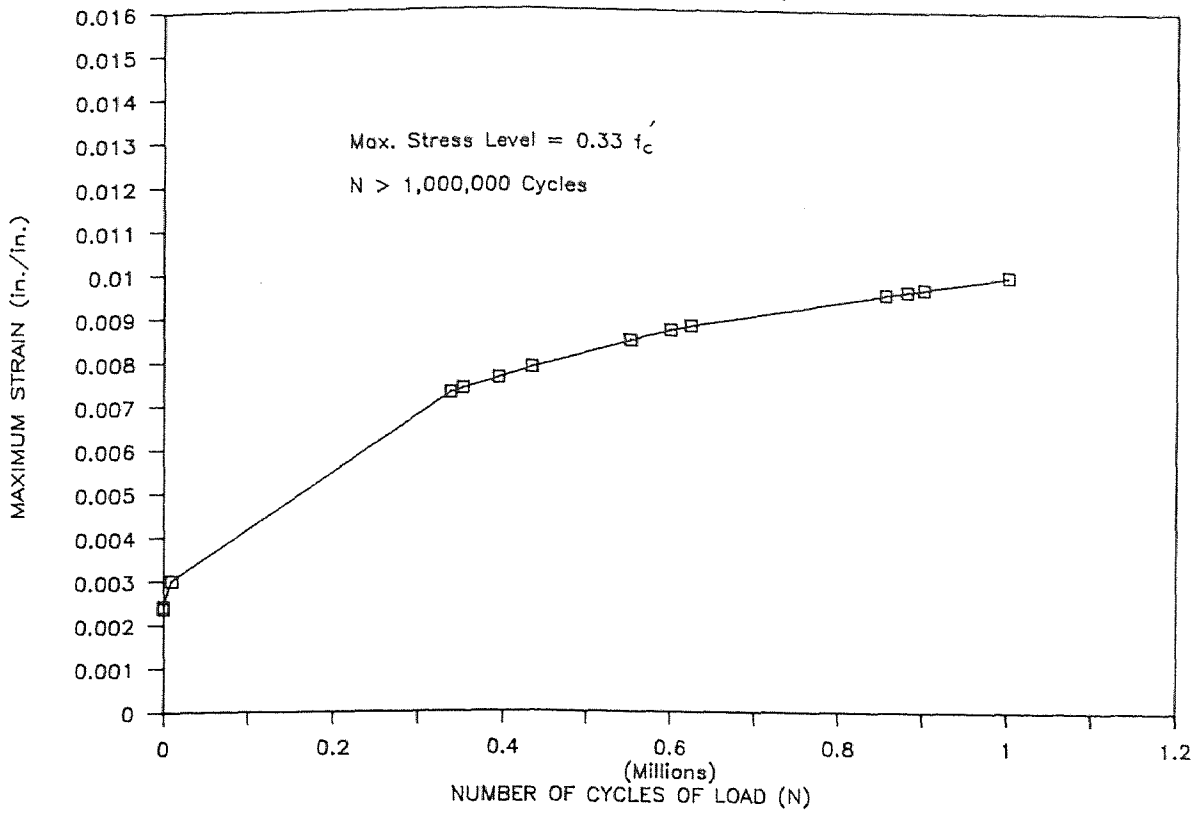
STRAIN VS. CYCLE CURVE

POLYMER CONCRETE (PF3045)



STRAIN VS. CYCLE CURVE

POLYMER CONCRETE (PF104)



APPENDIX L

COMPRESSION PROPERTIES OF
NORMAL CONCRETE

Specimen	Date Casted	Date Tested	Day	Unit wt. (lb/ft ³)	Max Load (lb)	Max Compr. Strength (psi)	Strain at Max Load x10 ⁻³ in	Modulus of Elasticity x10 ⁶ psi
SN1	9/13/87	10/3/87	21	150.00	37740	5339	3.40	2.222
SN2	9/13/87	10/3/87	21	149.50	35510	5024	3.42	2.101
SN3	9/13/87	10/3/87	21	149.20	36790	5063	3.85	1.809

COMPRESSION PROPERTIES OF
SUPERPLASTICIZER CONCRETE

Specimen	Date Casted	Date Tested	Day	Unit wt. (lb/ft ³)	Max Load (lb)	Max Compr. Streng (psi)	Strain at Max Load $\times 10^{-3}$ in	Modulus of Elasticity $\times 10^6$ psi
S1	9/22/86	10/29/86	37	150.2	39040	5521	1.910	3.250
S2	9/22/86	10/29/86	37	150.3	42190	5966	1.930	3.310
S3	9/22/86	10/29/86	37	149.6	33940	4799	1.900	3.280
S4	9/22/86	11/21/86	60	149.8	56120	7936	2.010	3.510
S5	9/22/86	11/21/86	60	150.2	51980	7351	2.100	3.430
S6	9/22/86	11/21/86	60	150.4	51380	7266	1.950	3.450
S7	9/22/86	11/21/86	60	150.3	52110	7369	2.030	3.550
S1S1	12/22/86	2/18/87	58	150.2	50280	7113	1.950	4.180
S1S2	12/22/86	2/18/87	58	150.0	50100	7074	1.910	4.150
S1S106	12/22/86	2/25/87	65	149.7	41000	5800	1.810	3.910
S1S206	12/22/86	2/25/87	65	149.8	42310	5986	1.830	3.550
S1S306	12/22/86	2/25/87	65	150.1	60460	8553	2.350	3.910
S1S406	12/22/86	2/25/87	65	150.1	47620	6737	1.922	3.840
S1S109	12/22/86	3/2/87	70	150.3	51360	7266	2.010	3.740
S1S209	12/22/86	3/2/87	70	149.9	52929	7488	2.300	3.510
S1S309	12/22/86	3/2/87	70	150.2	48942	6924	2.120	3.480
S1F106A	12/22/86	3/2/87	70	150.4	57752	8167	2.100	4.100
S1F206A	12/22/86	3/4/87	72	150.5	60757	8592	2.200	4.220
S1F207A	12/22/86	2/25/87	65	150.3	49010	6931	1.930	4.030
S1F307A	12/22/86	2/27/87	67	149.8	51621	7300	1.950	4.160
S1F175A	12/22/86	3/8/87	76	150.2	56370	7975	1.920	4.440

COMPRESSION PROPERTIES OF
MICROSILICA CONCRETE

Specimen	Date Casted	Date Tested	Day	Unit wt. (lb/ft ³)	Max Load (lb)	Max Compr. Strength (psi)	Strain at Max Load $\times 10^{-3}$ in	Modulus of Elasticity $\times 10^6$ psi
M1S1	11/5/86	12/10/86	35	150.3	59900	8471	2.070	4.260
M1S2	11/5/86	12/10/86	35	150.6	65610	9278	2.210	4.420
M1S3	11/5/86	12/10/86	35	150.3	65480	9260	2.180	4.760
M1S108	11/5/86	1/6/87	62	150.1	62450	8831	2.120	4.310
M1S208	11/5/86	1/6/87	62	150.3	57810	8175	2.010	4.260
M1S308	11/5/86	1/6/87	62	150.5	63650	9001	2.110	4.350
M1S109	11/5/86	1/9/87	65	150.7	66110	9349	2.250	4.450
M1S209	11/5/86	1/9/87	65	150.4	67400	9531	2.220	4.390
M1S309	11/5/86	1/9/87	65	150.2	65440	9254	2.160	4.390
M2S107	1/13/87	2/23/88	406	150.6	68030	9624	2.390	4.540
M2S207	1/13/87	2/23/88	406	150.1	63450	8976	2.360	4.050
M2S307	1/13/87	2/23/88	406	149.8	57080	8075	2.180	3.990
M1F107A	11/5/86	1/10/87	66	150.6	76790	10859	N/A	N/A
M1F207A	11/5/86	1/12/88	68	150.3	77980	11027	2.100	5.430
M2F175A	1/13/87	2/23/88	406	150.2	67970	9616	1.890	4.540
M2F475A	1/13/87	3/2/88	415	150.3	65220	9227	2.341	4.350
M3S1	2/18/87	10/30/88	622	150.3	59580	8429	2.183	4.611
M3S3	2/18/87	10/30/88	622	149.8	70260	9995	2.192	4.769
M3S4	2/18/87	10/30/88	622	150.3	69010	9763	2.274	4.587
M3TF11A	2/18/87	11/5/88	628	150.1	77920	11024	2.235	5.260
M3TF12A	2/18/87	11/7/88	630	150.2	78800	11148	2.563	4.829
SS31	4/20/87	6/25/87	66	150.5	78320	11080	2.110	5.061
SS32	4/20/87	6/25/87	66	150.0	52580	7439	1.950	3.810
SS33	4/20/87	6/25/87	66	150.1	55570	7862	2.110	3.830

Continued

SS41	6/23/87	10/3/87	102	150.1	56940	8055	N/A	N/A
SS42	6/23/87	10/3/87	102	150.5	70920	10033	2.680	4.260
SS43	6/23/87	10/3/87	102	149.9	59100	8361	1.960	4.230
SS61	4/27/87	8/25/87	120	150.3	67070	9488	2.080	4.360
SS62	4/27/87	8/25/87	120	150.5	86240	12200	2.490	4.710
SS63	27/87	8/25/87	120	150.4	82800	11714	2.630	4.610
SS311	7/14/87	10/3/87	82	150.4	5766	8157	N/A	N/A
SS321	7/14/87	10/3/87	82	150.2	5732	8109	2.170	3.780
SS331	7/14/87	10/3/87	82	150.4	5489	7765	2.281	4.001
S11	5/24/88	10/30/88	159	150.1	60270	8781	1.779	4.961
S12	5/24/88	10/30/88	159	150.3	52290	7398	1.723	4.278
S13	5/24/88	10/30/88	159	149.8	57840	8283	1.872	4.324
S21	5/25/88	10/30/88	159	149.9	54350	7689	1.871	4.117
S22	5/25/88	10/30/88	158	150.1	75460	10676	2.008	5.641
S23	5/25/88	10/30/88	158	150.2	51870	7338	1.653	4.396
S31	5/25/88	10/30/88	158	150.3	62790	8883	1.988	4.496
S32	5/25/88	10/30/88	158	149.8	50980	7212	1.697	4.420

COMPRESSION PROPERTIES OF
POLYMER CONCRETE

Specimen	Date Casted	Date Tested	Day	Unit wt. (lb/ft ³)	Max Load (lb)	Max Compr . Stren g (psi)	Strain at Max Load x10 ⁻² in	Modulus of Elas ticity x10 ⁶ psi
POC11	7/25/88	7/29/88	4	130.18	28230	3994	1.907	0.671
POC12	7/25/88	7/29/88	4	132.21	30120	4261	1.769	0.610
POC13	7/25/88	7/29/88	4	130.50	29470	4169	2.054	0.613
POC14	7/25/88	8/1/88	6	131.20	27910	3948	1.457	0.623
POC21	7/26/88	7/29/88	3	132.10	39800	5613	1.353	0.906
POC22	7/26/88	7/29/88	3	130.50	37930	5366	1.769	0.894
POC23	7/26/88	7/29/88	3	130.80	39410	5575	1.380	0.958
POC24	7/26/88	8/8/88	13	131.70	46860	6629	1.243	1.081
POC25	7/26/88	8/8/88	13	132.60	47800	6762	1.231	1.086
POC26	7/26/88	8/30/88	35	131.80	68950	9755	1.282	1.570
PFC13A	7/26/88	8/18/88	23	132.60	56300	7965	0.992	1.500
PFC15A	7/26/88	8/18/88	23	133.50	62850	8892	0.973	1.540
PFC16A	7/26/88	8/18/88	23	131.60	55420	7840	1.022	1.520
PFC17A	7/26/88	8/22/88	27	132.40	63300	8955	0.887	1.740

FLEXURAL PROPERTIES OF
MICROSILICA CONCRETE

Size of Specimen	Specimen	Date Casted	Date Tested	Day	Max. Load (lb)	Max. Flex. Streng (psi)	Max. Def. $\times 10^{-2}$ in	Modulus of Elasticity $\times 10^6$ psi
2x4x12	B21	5/24/88	10/28/88	157	1985	929	1.801	0.290
	B22	5/24/88	10/28/88	157	2519	1178	2.113	0.312
	B23	5/24/88	10/28/88	157	2220	1039	1.847	0.316
2x5x24	B51	5/24/88	10/28/88	157	1276	842	1.077	1.277
	B52	5/24/88	10/28/88	157	1579	1041	0.930	1.787
4x6x30	B41	5/25/88	10/27/88	155	3323	970	0.928	2.459
	B42	5/25/88	10/27/88	155	3310	967	0.784	2.785
	B43	5/25/88	10/27/88	155	3431	1002	1.050	2.076
6x6x30	B61	5/25/88	10/26/88	154	4300	836	1.611	1.129
	B62	5/25/88	10/26/88	154	4460	867	2.184	0.858
	B63	5/25/88	10/26/88	154	4820	937	1.898	1.075

FLEXURAL PROPERTIES OF
POLYMER CONCRETE

Size of Specimen	Specimen	Date Casted	Date Tested	Day	Max. Load (lb)	Max. Flex. Streng (psi)	Max. Def. $\times 10^{-2}$ in	Modulus of Elasticity $\times 10^6$ psi
1x2x12	PBS1	7/26/88	8/3/88	8	615	2005	4.148	0.720
	PBS2	7/26/88	8/3/88	8	622	2027	4.143	0.775
	PBS3	7/26/88	8/3/88	8	610	1989	4.636	0.635
	PBS4	7/26/88	8/4/88	9	728	2372	4.512	0.781
2x4x12	PBM1	7/26/88	8/4/88	9	5549	2472	7.300	0.207
	PBM2	7/26/88	8/4/88	9	5172	2673	7.255	0.195

SPLITTING TEST OF
POLYMER CONCRETE

Specimen	Date Casted	Date Tested	Dry Cured (day)	Length (in.)	Force (kip.)	Tensile Stress (psi.)
PS1	7/25/88	8/1/88	7	6.0	16.85	595.95
PS2	7/25/88	8/1/88	7	6.0	17.53	619.99
PS3	7/25/88	8/1/88	7	6.0	16.29	576.14
PS4	7/26/88	8/1/88	6	5.9	22.22	792.48
PS5	7/26/88	8/1/88	6	5.9	21.48	766.08
PS6	7/26/88	8/1/88	6	5.9	23.26	829.57

BOND STRENGTH PROPERTIES OF
REINFORCED HIGH STRENGTH CONCRETE

Specimen	Compression Test		Pull-Out Test			
	Stress (psi.)	Strain ($\times 10^{-3}$ in)	Bond Strength (psi.)	Ave. Bond Strength (psi.)	Slip ($\times 10^{-3}$ in)	Ave. Slip ($\times 10^{-3}$ in)
BS *						
31	11080	2.11	2204		8.64	
32	8150	2.22	2343		6.97	
33	8109	2.17	2577		7.41	
34	-	-	2587		N/A	
35	-	-	2567		N/A	
36	-	-	2828	2518	N/A	7.67
BS *						
41	10033	2.68	1785		7.57	
42	8361	1.96	1482		7.17	
43	8055	N/A	1749		6.39	
44	-	-	1673	1672	6.82	6.99
BS **						
61	12200	2.49	2090		2.00	
62	11714	2.63	2146		5.70	
63	9488	2.08	1631		6.3	
64	-	-	1703	1893	4.20	4.55

Remarks : * - Cube Specimen 5x5x5 in.

** - Cube Specimen 8x8x8 in.

BS 31 - Reinforced High Strength Concrete with
#3 Bar Size, Specimen No.1

DIRECT TENSION TEST OF
CEMENT-BASED COMPOSITES

Type of Concrete	Specimen	WxD (in.)	Peak Load (lb.)	Peak Stress (psi.)	Peak Displ. $\times 10^{-2}$ in	Brittleness Index (m)
Normal Concrete	TC#34	1.1x1.85	502	246.08	0.042	0.2564
	TC#35	1.1x2.00	487	221.36	0.042	0.3079
	TC#36	1.1x2.01	579	261.97	0.047	0.2788
HSC (Microsilica)	MT1	1.1x2.05	609	270.00	0.012	0.2057
	MT2	1.1x2.13	1201	513.00	0.018	0.2255
(Polymer)	PD1	1.0x0.67	377	562.84	0.165	0.3472
	PD2	1.0x0.70	472	674.57	0.132	0.4098
	PD3	1.0x0.63	388	615.08	0.125	0.3650

Remarks :

HSC : High Strength Concrete

TC#34 : Normal Concrete, Specimen No.34, reported by Terasa Cintora [90].

MT : Microsilica Concrete, Tapered Specimen

PD : Polymer Concrete, Dog-bone Specimen

PULL-OUT STRESS PROPERTIES OF
HIGH STRENGTH FIBROUS CONCRETE
(MICROSILICA CONCRETE)

Specimen	WxD (in.)	Peak Load (lb.)	Peak Stress (psi.)	Peak Displ. $\times 10^{-2}$ in	Brittle ness Index (m)	Remark
MT 001	1.1x2.05	609.00	270.00	0.012	0.206	**
002	1.1x2.13	1201.00	513.00	0.018	0.226	**
BFS 051	1.1x1.80	1112.30	561.76	N/A	N/A	* (Failed)
052	1.1x1.85	1055.50	518.67	N/A	0.260	* (Failed)
053	1.1x1.85	N/A	N/A	N/A	N/A	* (Failed)
054	1.1x1.71	961.80	511.32	0.023	0.246	**
055	1.1x1.90	1165.40	557.60	0.033	0.252	**
056	1.1x1.80	1043.40	526.97	0.031	0.248	**
BFS 101	1.1x2.05	929.20	412.10	0.012	0.262	**
102	1.1x1.88	705.49	341.10	0.023	0.261	**
103	1.1x2.00	690.00	314.00	0.018	0.263	**
BFS 151	1.1x2.07	1211.10	531.88	0.032	0.269	**
152	1.1x1.75	1004.60	532.87	0.035	0.271	**
153	1.1x1.90	1143.00	546.89	0.400	N/A	*
154	1.1x1.56	651.50	380.00	N/A	0.264	*
155	1.1x1.91	1186.20	564.50	N/A	N/A	* (Failed)
156	1.1x1.80	906.00	458.00	N/A	N/A	* (Failed)
BFS 201	1.1x1.87	1189.90	576.90	N/A	N/A	** (Failed)
202	1.1x1.91	1358.00	650.10	0.024	0.281	**
203	1.1x1.94	1476.00	692.73	0.407	0.260	**
204	1.1x2.00	1341.00	609.54	N/A	N/A	** (Failed)
205	1.1x1.78	1254.40	640.65	0.023	0.285	**
206	1.1x1.91	678.70	323.00	0.009	0.273	**
BFH 051	1.1x1.81	808.00	408.00	0.022	0.278	**

Continued

BFH 052	1.1x2.05	1172.00	520.00	0.013	0.284	**
053	1.1x2.00	837.00	380.00	0.030	0.280	**
054	1.1x1.83	1033.00	513.00	0.020	0.282	**
BFH 101	1.1x2.19	1261.00	523.00	N/A	N/A	**(Failed)
102	1.1x2.07	1195.40	520.00	0.026	0.319	**
103	1.1x2.00	950.00	432.00	N/A	N/A	**(Failed)
104	1.1x2.13	820.00	350.00	0.023	0.289	**
BFH 151	1.1x1.85	1349.50	660.00	0.022	0.305	**
152	1.1x2.00	1056.00	480.00	0.021	0.306	**
153	1.1x2.18	1600.80	668.00	0.020	0.311	**
BFH 151	1.1x2.00	1519.90	690.90	0.170	0.315	**
202	1.1x2.00	1113.40	506.10	0.012	0.306	**
203	1.1x2.05	1485.50	659.00	0.016	0.320	**
204	1.1x2.00	1419.90	645.40	N/A	N/A	**(Failed)

Remarks : * - Stroke Control

** - Strain Control

MT - High Strength Concrete

BFS - High Strength Fibrous Concrete (Straight End)

BFH - High Strength Fibrous Concrete (Hooked End)

BFH 051 - Fiber Volume Fraction = 0.05 %, Specimen No.1

PERCENTAGE OF THE LINEAR PORTION TO THE PEAK PORTION
OF THE LOAD-DISPLACEMENT CURVE UNDER DIRECT TENSION TEST

Material	Specimen	m Model	m Prop. Eq	% Linear to Peak	Average	Remark
Concrete	# 34			52.00		**
	# 35			55.10		
	# 36	0.281	0.265	49.57	52.23	
High Streng. Concrete	BT1			46.28		*
	BT2	0.216	0.200	46.60	46.44	
Polymer Concrete	PDL1			61.26		*
	PDL2			64.18		
	PDL3	0.374	0.400	60.83	62.09	
High Streng. Fibrous Conc (Straight)	BFS052			51.17		*
	054			49.50		
	055			49.85		
	056			48.12	49.66	
	BFS101			50.63		
	102			51.47		
	103			52.03	51.38	
	BFS151			52.11		
	152			52.45		
	153			52.73		
	154			55.41		
	155			43.64	51.27	
	BFS202			53.08		
	203			51.42		
	204			53.28		
	205			53.91		
206	0.264	0.259	59.38	54.21		
				51.78		

Continued

High Streng. Fibrous Conc (Hooked)	BFH051			53.88		*
	052			53.40		
	053			53.33		
	054			54.14	53.69	
	BFH102			59.05		
	104			54.24	56.65	
	BFH151			56.15		
	152			53.05		
	153			56.06	55.09	
	BFH201			56.07		
	202			55.88		
	203	0.301	0.290	56.00	55.98	
					55.11	
Steel Fiber Rein. Mortar	$V_f=1.5\%$	0.263	0.259	48.66	48.66	***

Remarks :

- * Present Study
- ** Data from T. Cintora [90]
- *** Data from V.S. Gopalaratnum and S.P. Shah [18]

FATIGUE PROPERTIES DUE TO THE EFFECT OF MAX. STRESS LEVEL OF
SUPERPLASTICIZER CONCRETE

Specimen	$S_{\max} = \frac{f_{\max}}{f_c}$	$S_{\min} = \frac{f_{\min}}{f_c}$	$R = \frac{f_{\min}}{f_{\max}}$	No. of Cycle to Failure
S1F109	0.90	0.10	0.111	Failed
S1F209	0.90	0.10	0.111	Failed
S1F309	0.90	0.10	0.111	26
S1F409	0.90	0.10	0.111	300
S1F108	0.80	0.10	0.125	5,875
S1F208	0.80	0.10	0.125	4,096
S1F308	0.80	0.10	0.125	4,566
S1F275	0.75	0.10	0.133	430,510
S1F207	0.73	0.087	0.114	>1,000,000
S1F107	0.70	0.10	0.143	12,299
S1F307	0.70	0.083	0.118	>1,027,230
S1F306	0.63	0.105	0.167	>1,000,000
S1F175	0.57	0.081	0.142	>1,995,263
S1F106	0.53	0.09	0.170	>1,000,000
S1F206	0.50	0.084	0.168	>1,000,000

Remarks :

* : Rate of Loading = 6.0 Hz (cycle/sec)

S1 : Superplasticizer Concrete, Batch 1

F1 : Fatigue Test, Specimen No.1

09 : Maximum Stress Level, $0.90 f_c$

FATIGUE PROPERTIES DUE TO THE EFFECT OF MAX. STRESS LEVEL OF
MICROSILICA CONCRETE

Specimen	$S_{\max} = \frac{f'_{\max}}{f'_c}$	$S_{\min} = \frac{f'_{\min}}{f'_c}$	$R = \frac{f'_{\min}}{f'_{\max}}$	No. of Cycle to Failure
M1F109	0.90	0.10	0.111	Failed
M1F209	0.90	0.10	0.111	380
M1F309	0.90	0.10	0.111	204
M1F409	0.90	0.10	0.111	608
M2F209	0.90	0.10	0.111	6
M2F108	0.80	0.10	0.125	4,014
M2F208	0.80	0.10	0.125	8,937
M2F2075	0.75	0.10	0.133	102,200
M2F3075	0.75	0.10	0.133	196,540
M2F4075	0.723	0.096	0.133	>1,074,600
M2F1075	0.70	0.092	0.131	>3,200,000
M1F107	0.605	0.086	0.142	>1,000,000
M1F207	0.60	0.085	0.142	>1,000,000

Remarks :

- * : Rate of Loading = 6.0 Hz (cycle/sec)
- M1 : Microsilica Concrete, Batch 1
- F1 : Fatigue Test, Specimen No.1
- 09 : Maximum Stress Level, $0.90 f'_c$

FATIGUE PROPERTIES DUE TO THE EFFECT OF MAX. STRESS LEVEL OF
POLYMER CONCRETE

Specimen	$S_{\max} = \frac{f'_{\max}}{f'_c}$	$S_{\min} = \frac{f'_{\min}}{f'_c}$	$R = \frac{f'_{\min}}{f'_{\max}}$	No. of Cycle to Failure
PF108	0.80	0.10	0.125	3,608
PF208	0.80	0.10	0.125	4,476
PF107	0.70	0.10	0.143	8,650
PF207	0.70	0.10	0.143	8,052
PF106	0.60	0.10	0.167	24,789
PF206	0.60	0.10	0.167	35,034
PF105	0.50	0.10	0.200	121,431
PF205	0.50	0.10	0.200	127,800
PF305	0.50	0.10	0.200	196,800
PF1045	0.40	0.088	0.220	>1,000,000
PF2045	0.38	0.085	0.224	>1,000,000
PF3045	0.34	0.075	0.221	>1,000,000
PF104	0.33	0.084	0.255	>1,000,000

Remarks :

* : Rate of Loading = 6.0 Hz (cycle/sec)

P : Polymer Concrete

F1 : Fatigue Test, Specimen No.1

08 : Maximum Stress Level, $0.80 f'_c$

FATIGUE PROPERTIES DUE TO THE EFFECT OF RATE OF LOADING
MICROSILICA CONCRETE

Loading Rate 6 Hz.					Loading Rate 12 Hz.				
Spec.	S _{max}	S _{min}	R	N	Spec.	S _{max}	S _{min}	R	N
M1F209	0.90	0.10	0.111	204	M3TF1	0.90	0.10	0.111	204
M1F309	0.90	0.10	0.111	380	M3TF2	0.90	0.10	0.111	24
M1F409	0.90	0.10	0.111	608	M3TF3	0.90	0.10	0.111	21
M2F109	0.90	0.10	0.111	6					
M2F108	0.80	0.10	0.125	4,014	M3TF4	0.80	0.10	0.125	3,470
M2F208	0.80	0.10	0.125	8,937	M3TF5	0.80	0.10	0.125	1,431
					M3TF6	0.80	0.10	0.125	31,683
					M3TF7	0.80	0.10	0.125	50,277
M2F1075	0.75	0.10	0.133	102,200	M3TF8	0.75	0.10	0.133	161,210
M2F2075	0.75	0.10	0.133	196,540	M3TF9	0.75	0.10	0.133	353,502
M2F3075	0.723	0.10	0.096	>1,074,600	M3TF10	0.75	0.10	0.133	1,291,367
M2F107	0.70	0.092	0.131	>3,200,000	M3TF11	0.655	0.085	0.130	>1,000,000
M2F207	0.605	0.086	0.142	>1,000,000	M3TF12	0.647	0.084	0.130	>1,000,000
M2F307	0.60	0.085	0.142	>1,000,000					

Remarks :

$$S_{\max} = \frac{f_{\max}}{f_c}$$

$$S_{\min} = \frac{f_{\min}}{f_c}$$

$$R = \frac{f_{\min}}{f_{\max}}$$

N = Number of cycles to failure

	Brittleness Index	Fiber Type	% Fiber
	Y ₁	X ₁	X ₂
1	.260	St End	A
2	.246	St End	A
3	.252	St End	A
4	.248	St End	A
5	.262	St End	B
6	.261	St End	B
7	.263	St End	B
8	.269	St End	C
9	.271	St End	C
10	.264	St End	C
11	.281	St End	D
12	.260	St End	D
13	.285	St End	D
14	.273	St End	D
15	.278	Hk End	A
16	.284	Hk End	A
17	.280	Hk End	A
18	.282	Hk End	A
19	.319	Hk End	B
20	.289	Hk End	B
21	.305	Hk End	C
22	.306	Hk End	C
23	.311	Hk End	C
24	.315	Hk End	D
25	.306	Hk End	D
26	.320	Hk End	D

Two-Factor Analysis of Variance

Anova table for a 2-factor Analysis of Variance on Y₁: Brittleness Index

Source:	df:	Sum of Squares:	Mean Square:	F-test:	P value:
Fiber Type (A)	1	.009	.009	142.166	.0001
% Fiber (B)	3	.003	.001	17.488	.0001
AB	3	1.562E-4	5.207E-5	.853	.4833
Error	18	.001	6.106E-5		

There were no missing cells found.

1

The AB Incidence table on Y₁: Brittleness Index

% Fiber:		A	B	C	D	Totals:
Fiber Type	St End	4 .252	3 .262	3 .268	4 .275	14 .264
	Hk End	4 .281	2 .304	3 .307	3 .314	12 .3
Totals:		8 .266	5 .279	6 .288	7 .291	26 .28

2

Two-Factor Analysis of Variance

Multiple Regression Y₁:Brittleness Index 2 X variables

DF:	R:	R-squared:	Adj. R-squared:	Std. Error:
25	.941	.886	.876	.008

Analysis of Variance Table

Source	DF:	Sum Squares:	Mean Square:	F-test:
REGRESSION	2	.011	.006	89.512
RESIDUAL	23	.001	6.265E-5	p = .0001
TOTAL	25	.013		

No Residual Statistics Computed

Note: 6 cases deleted with missing values.

1

Multiple Regression Y₁:Brittleness Index 2 X variables

Beta Coefficient Table

Parameter:	Value:	Std. Err.:	Std. Value:	t-Value:	Probability:
INTERCEPT	.205				
Fiber Type	.036	.003	.823	11.687	.0001
% Fiber	.009	.001	.487	6.921	.0001

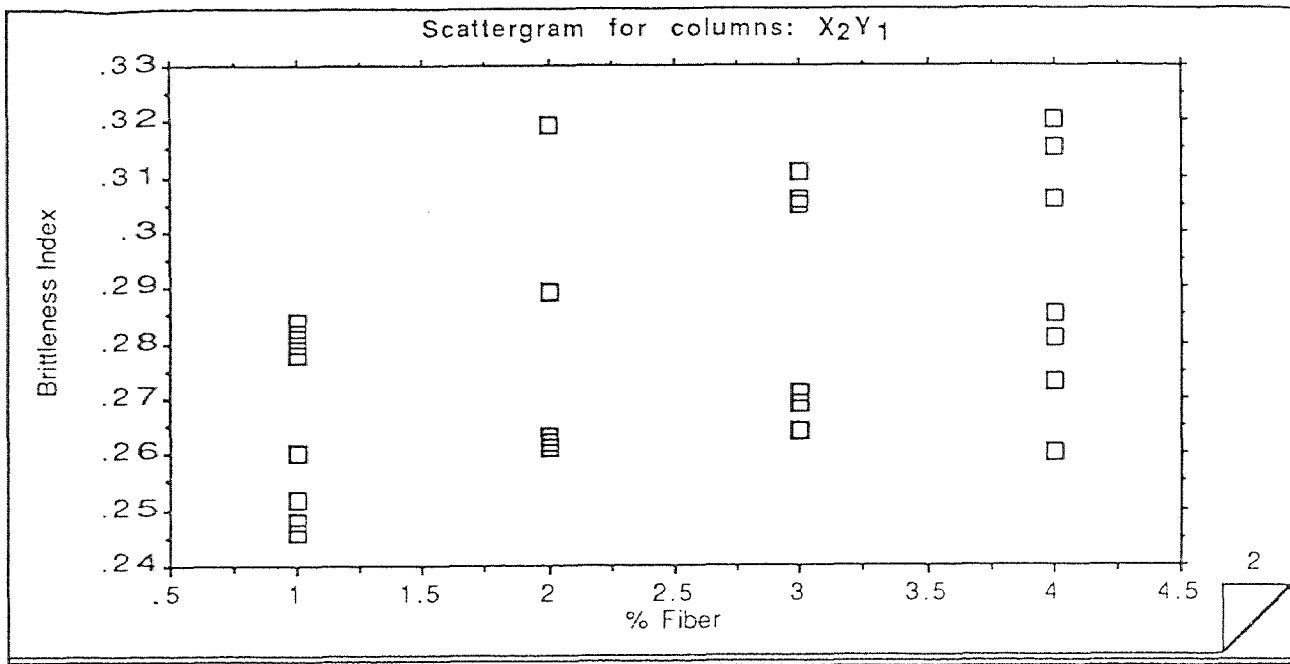
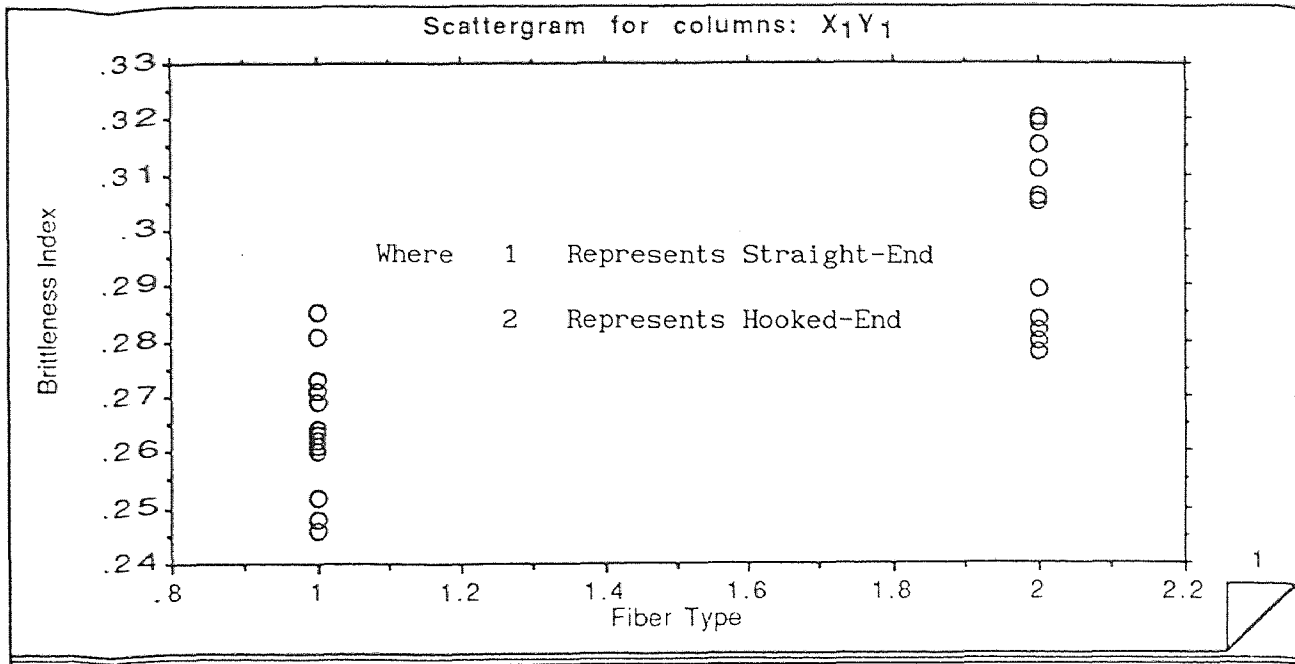
2

Multiple Regression Y₁:Brittleness Index 2 X variables

Confidence Intervals and Partial F Table

Parameter:	95% Lower:	95% Upper:	90% Lower:	90% Upper:	Partial F:
INTERCEPT					
Fiber Type	.03	.043	.031	.042	136.576
% Fiber	.006	.012	.007	.011	47.903

3



Two-Factor Analysis of Variance